

**PROBING THE BIOSYNTHESIS AND
MODE OF ACTION OF AZINOMYCIN B**

A Dissertation

by

GILBERT THOMSON KELLY

Submitted to the Office of Graduate Studies of
Texas A&M University
in partial fulfillment of the requirements for the degree of

DOCTOR OF PHILOSOPHY

August 2009

Major Subject: Chemistry

**PROBING THE BIOSYNTHESIS AND
MODE OF ACTION OF AZINOMYCIN B**

A Dissertation

by

GILBERT THOMSON KELLY

Submitted to the Office of Graduate Studies of
Texas A&M University
in partial fulfillment of the requirements for the degree of

DOCTOR OF PHILOSOPHY

Approved by:

Chair of Committee,
Committee Members,

Head of Department,

Coran M. H. Watanabe
Frank M. Raushel
Daniel A. Singleton
Michael D. Manson
David H. Russell

August 2009

Major Subject: Chemistry

ABSTRACT

Probing the Biosynthesis and
Mode of Action of Azinomycin B. (August 2009)
Gilbert Thomson Kelly, B.S., Centre College
Chair of Advisory Committee: Dr. Coran M. H. Watanabe

Since the isolation of azinomycins A and B in 1954 from the soil bacterium, *Streptomyces sahachiroi*, these natural products have been synthetic targets. Both compounds exhibit *in vitro* cytotoxic activity at submicromolar levels and demonstrate anti-tumor activities comparable to that of mitomycin C *in vivo*. Unique to this class of natural products is the presence of an aziridine [1,2-*a*] pyrrolidine ring system. Coupled with an epoxide moiety, these structural functionalities impart the ability to form interstrand cross-links with DNA via the electrophilic C10 and C21 carbons of azinomycin and the N7 positions of suitably disposed purine bases.

This dissertation investigates the global impact of azinomycin B treatment in a yeast model with special emphasis on DNA damage response, the resulting cell cycle effects, and cellular localization of the compound. The results provide the first demonstration of the *in vivo* actions of azinomycin B and are consistent with the proposed role of the drug as a DNA cross-linking agent. Biosynthesis of azinomycin B was investigated and appears to have polyketide, non-ribosomal peptide synthetase and alkaloid origins. In pursuit of elucidating the biosynthetic origin we developed both a cell culturing system and a cell-free extract procedure capable of supporting azinomycin synthesis; we used these. These were employed with labeled metabolites to probe the biosynthetic origins of the molecule. Investigations with this enzyme preparation imparted important information regarding the substrate and cofactor requirements of the pathway. These results supported the premise of a mixed origin for the biosynthesis of the molecule and paved the way for expansive stable isotope labeling studies, which largely revealed the biosynthetic precursors and probable construction of the azinomycins. Some of these studies corroborate while other results conflict with initial proposed biosynthetic routes based upon the azinomycin biosynthetic gene cluster sequence.

Future azinomycin biosynthetic gene cluster enzyme characterization, mechanistic investigations, and genetic modifications will ultimately provide definitive proof for the intermediacy of proposed biosynthetic precursors and the involvement of specific cofactors. Better understanding of how nature constructs unique molecule may provide insight into eventual chemoenzymatic/gene therapy based approaches toward cancer therapy.

DEDICATION

To:

My Family, Friends, and God

ACKNOWLEDGMENTS

I thank my second family, the Watanabe group, beginning from the days of Coran and myself to the current members, especially including those who have persisted with me for the last several years: Dr. Scott Angell, B.J. Bench, Eunjin Kim, Jennifer Foulke-Abel, and of course Dr. Vasudha Sharma with whom I had such a successful, collaborative relationship as this dissertation reveals. I particularly acknowledge B.J., whose constant friendship, encouragement, advice and company (while putting in “crazy hours”) have no doubt sustained me during the most difficult times in and out of the laboratory.

To the new members, Dr. Hutiu Zhang, Victor Suarez, Hillary Agbo, and the rest of the current crew, I bid farewell and suggest you take control of your projects and stay current with the literature. It is a long fight to the finish and the game changes often. Do not stagnate.

I also thank my large group of friends whom I have counted on for laughs, love, and encouragement. Daniel Miller, Peter McPherson, Vladimir Kuznetsov, and Katherine Popelka have been essential friends at critical times in this process.

I am indebted to Dr. Coran M. H. Watanabe for allowing me the freedom to work in her group, to explore my own ideas, and most importantly to do the science that has enabled me to produce this dissertation.

I appreciate and gladly acknowledge Dr. Daniel Singleton’s advice, mentoring, and service on my committee. For service on my committee and helpful suggestions, I thank Dr. Frank Raushel, Dr. Michael Kladde, Dr. Michael Manson, and the late revered Dr. A. Ian Scott.

The professionalism, courtesy, and efficiency experienced during my time at Texas A&M has been enjoyed and will be long remembered, particularly when I hear “howdy”. Particular help on projects must be recognized: Dr. Shane Tichy for significant mass spectrometry help and guidance, and Dr. Roger Smith III for considerable flow cytometry experimental time and analysis on projects that did and did not pan out.

I am probably most indebted to my family and particularly my parents, Lyle and Anne Kelly, whose expectations and support for me always have been high. Your hopes for my future have come true. I will finally become “Dr. G. Thomson Kelly!”

TABLE OF CONTENTS

	Page
ABSTRACT.....	iii
DEDICATION.....	v
ACKNOWLEDGMENTS.....	vi
TABLE OF CONTENTS.....	vii
LIST OF FIGURES.....	xi
LIST OF SCHEMES.....	xvii
LIST OF TABLES.....	xviii
 CHAPTER	
I INTRODUCTION.....	1
Introduction.....	1
Man, Natural Products, and Streptomyces.....	1
Carzinophillin/Azinomycins.....	2
Streptomyces and Biosynthesis.....	5
Natural Product Pathways.....	6
The Terpenes.....	9
The Alkaloids.....	9
Fatty Acid Biosynthesis.....	12
The Phosphopantetheine Arm.....	13
The Polyketides.....	14
Neocarzinostatin.....	18
Modular PKS Model.....	19
The Non-Ribosomal Peptides.....	21
Calcium Dependent Antibiotic.....	23
Modifications of CDA Reflecting NRPS Construction.....	25
PKS-NRPS Hybrid Pathways.....	28
Traditional Methods of Biosynthetic Investigation.....	29
Statement of Purpose.....	30
 II CELLULAR EFFECTS INDUCED BY THE ANTITUMOR AGENT AZINOMYCIN B.....	31
Introduction.....	31
Results and Discussion.....	34
Cellular Localization of Azinomycin B.....	34
DNA Damaging Effect of Azinomycin B.....	36
Transcriptional Response and Cell Cycle Analysis.....	37
Cell Cycle Effects.....	46

CHAPTER	Page
Confirmation of Selected Gene Changes by RT-PCR.....	50
Significance	51
Experimental Procedures.....	52
Instrumentation and General Methods	52
Organisms.....	52
Culture Conditions	52
Azinomycin B Isolation.....	53
Nuclear Localization Experiments	53
Genomic Analysis	54
Yeast Sample Preparation and GeneChip Evaluation	54
GeneChip Evaluation by (RT)-PCR.....	55
Primers	55
Cell Cycle Analysis by Flow Cytometry.....	56
Naphthoate Synthesis	57
III <i>IN VITRO</i> BIOSYNTHESIS OF THE ANTITUMOR AGENT AZINOMYCIN B.....	58
Introduction	58
Results and Discussion.....	59
Development of the Cell Free Extract System	59
Inhibitors	62
Cofactor Requirements.....	67
Substrate Requirements.....	69
Significance	71
Experimental Procedures.....	72
General	72
Instrumentation.....	72
Organism	73
Culture Conditions	73
Cell-Free Extract Preparation.....	73
Enzyme Activity Assays	73
HPLC Coinjection Assays.....	74
Protein Inhibition Assays	75
Naphthoate Synthesis	75
IV AN IMPROVED METHOD FOR CULTURING <i>STREPTOMYCES</i> <i>SAHACHIROI</i> FOR THE PRODUCTION OF AZINOMYCIN B	76
Introduction	76
Results and Discussion.....	77
Development of the Culture System.....	77
Solid Media Evaluation	78
Dehydrated Plates.....	78
Liquid Media Evaluation.....	80
Water Source	81
Bio-availability	81

CHAPTER	Page
Large Scale Fermentation System	833
Significance	84
Experimental Procedures	85
Instrumentation and General Methods	85
Organism	85
Spore Stocks	85
Media Conditions	86
Solid Plates	87
Dehydrated Plates	87
First Stage Culture	87
Second Stage Culture	87
Fermentation	87
Isolation and Purification of Azinomycin B	88
Azinomycin B	88
 V	
STABLE ISOTOPE FEEDING STUDIES	90
Introduction	90
Metabolism in Streptomyces	934
Results and Discussion	95
System for Studies	95
Incorporation of Methionine	96
Incorporation of Acetate	97
Biosynthetic Route to the Epoxide Moiety	99
Biosynthetic Route to the Enol Fragment	106
Biosynthetic Route to the End Fragment of Azinomycin A	109
Incorporation of Molecular Oxygen into Azinomycin B	118
Cytochrome P450 Monooxygenase	119
Heavy Oxygen Introduction	120
Analysis of ¹⁸ O ₂ /O ₂ Exposed Azinomycin B	125
Biosynthetic Route to the Aziridino[1,2a]pyrrolidine Moiety	129
The Substrates	133
Ornithine	134
Glycine	134
Proline	136
Carbohydrates	136
Aspartate, Asparagine, Lysine, Arginine, and Serine	138
Synthetic Precursor Series for the Discrete Formation of the 1- azabicyclo[3.1.0]hexane Ring	140
Glutamic Acid	146
Significance	148
Experimental Procedures	149
Instrumentation and General Methods	149
Materials	149
Organism	149
Culture Conditions	149
General Feeding Conditions	150

CHAPTER	Page
Isolation and Purification of Azinomycin B.....	150
Azinomycin A	151
Azinomycin B.....	152
VI CONCLUSION.....	153
REFERENCES.....	158
APPENDIX.....	181
VITA.....	302

LIST OF FIGURES

		Page
Figure 1.	Azinomycin B.	1
Figure 2.	Suggested Structures for Carzinophilin A/Azinomycin B.	3
Figure 3.	Corrected Structures for Carzinophilin A/Azinomycin B.	4
Figure 4.	<i>Streptomyces sahachiroi</i> Mycelia.	6
Figure 5.	Typical Examples of Natural Product Structures from the Polyketide, Alkaloid, NRPS, Terpene, and Shikimate Pathway Families.	8
Figure 6.	The Building Blocks, Arrangement, and Nonmevalonate Biosynthesis of Terpenes.	9
Figure 7.	The Biosynthesis of the Plant Derived Alkaloid Cocaine.	10
Figure 8.	The Biosynthesis of the <i>Streptomyces refuineus</i> Derived Alkaloid Anthramycin.	11
Figure 9.	An Outline of Potential Alkaloid-type Biosyntheses of Aziridinopyrrolidine Moiety of the Azinomycins.	12
Figure 10.	Fatty Acid Biosynthesis.	13
Figure 11.	Structure of Coenzyme A and Phosphopantetheine Arm Attached to the Acyl Carrier Protein/Thiolation Domain.	14
Figure 12.	Selected Examples of Aromatic, Macrolactone, and Polyene Polyketides.	15
Figure 13.	Comparing PKS and FAS Biosynthesis.	16
Figure 14.	PKS Model Diagrams.	17
Figure 15.	Possible PKS Origins for the Azinomycin Naphthoate.	17
Figure 16.	Structural Similarity in Neocarzinostatin and Azinomycin B.	18
Figure 17.	Type 1 Iterative PKS Producing 6-methylsalicylic Acid and Chlorothricin.	18
Figure 18.	Type 1 Iterative PKS Producing the Neocarzinostatin Naphthoate Moiety.	19
Figure 19.	Modular Structure of DEBS (6-Deoxyerythronolide) Synthetase.	20
Figure 20.	Possible Modular Structures of a Naphthoate PKS Synthase.	21

	Page
Figure 21. NRPS Chemistry.	22
Figure 22. Structure of CDA, the Calcium Dependent Antibiotic(s), Produced by <i>Streptomyces coelicolor</i> A3(2).	24
Figure 23. Modular Structure of the NRPS Portions of <i>Streptomyces coelicolor</i> Calcium Dependent Antibiotic Biosynthesis.	25
Figure 24. Modifications found in CDA.	26
Figure 25. Diagram of the Gene Cluster Responsible for the Biosynthesis of CDA.	27
Figure 26. Possible Arrangement for the NRPS Portion of Azinomycin B.	27
Figure 27. Key Domains Found in the NRPS-PKS Biosynthesis Which May be Involved in Azinomycin B Biosynthesis.	28
Figure 28. Examples of NRPS-PKS Natural Product Molecules.	28
Figure 29. Structures of Azinomycin A and B.	31
Figure 30. Azinomycin B DNA Cross-linking Preference.	32
Figure 31. Neocarzinostatin and Azinomycin B.	33
Figure 32. Molecules Used in Cellular Localization Experiments.	35
Figure 33. Cellular Localization of Azinomycin B in Yeast Cells.	35
Figure 34. Yeast DNA Damaged Observed on an Agarose Gel.	37
Figure 35. GeneChip DNA Microarray Gene Expression Monitoring.	39
Figure 36. DNA Damaging Agents Used in Previous Studies with Affymetrix Oligonucleotide Microarrays, GeneChip® Yeast Genome S98 Array.	42
Figure 37. Diagram of Gene Changes Observed from Azinomycin B Treatment.	44
Figure 38. Illustration of the Damage and Induction of Observed Gene Expression in Response to Azinomycin B Exposure in an Example Yeast Cell in S Phase.	45
Figure 39. Diagram of the Yeast Cell Cycle and the Observed Impact of Azinomycin B Treatment.	46
Figure 40. Flow Cytometry Analysis of Azinomycin B Treated Yeast Cultures.	48

	Page
Figure 41. Closer Inspection of Flow Cytometry Data Analysis of 12hr Azinomycin B Treatment Set.	49
Figure 42. Semi-quantitative Reverse Transcriptase (RT)-PCR Analysis of the Selected Genes: HUG1, RAD51, PLM2, and TOM1.	51
Figure 43. Structures of Azinomycin A and B.	58
Figure 44. Preparation and Analysis of the Cell Free Extract (CFE).	60
Figure 45. Demonstration of <i>In Vitro</i> Biosynthesis.	61
Figure 46. Structures of Biosynthesis Inhibitors Used in this Study.	63
Figure 47. Mono-oxygenases.	63
Figure 48. Naphthoate Compound Series Fed by Lowden, <i>et al.</i>	64
Figure 49. Hydroxylation of the Naphthoate Involving the NIH Shift Associated with Mono-oxygenases.	64
Figure 50. Effect of Enzyme Inhibitors on Naphthoate Production.	65
Figure 51. Effect of Enzyme Inhibitors on Azinomycin B Production.	66
Figure 52. Cofactors Used in Probing Cofactor Requirements of Azinomycin B Biosynthetic Pathway (Conversion to Azinomycin B).	67
Figure 53. Cofactor Requirements of Azinomycin B Biosynthetic Pathway (Conversion to Azinomycin B).	68
Figure 54. Substrates Used to Probe Azinomycin B Biosynthesis.	68
Figure 55. Investigation of the Principle Building Blocks of the Azinomycin B Pathway.	69
Figure 56. Possible Formation of the Azabicyclic Ring from Lysine.	71
Figure 57. Diagram Depicting Possible Substrate Requirements of Azinomycin B Biosynthetic Pathway.	71
Figure 58. Structures of Azinomycin A and B.	76
Figure 59. Making Effective Spore Stocks.	80
Figure 60. Evaluation of Fermentation System.	84
Figure 61. Azinomycin A and B.	90

	Page
Figure 62. Azinomycin B Proton Spectrum.....	92
Figure 63. Azinomycin B Carbon Spectrum and Assignment.....	93
Figure 64. Scrambling of Carbons in Metabolism.....	95
Figure 65. Incorporation of [¹³ C-methyl] L-methionine.....	96
Figure 66. Incorporation of [1- ¹³ C] Sodium Acetate into Azinomycin B.....	98
Figure 67. Incorporation of [1- ¹³ C], [2- ¹³ C], and [1, 2- ¹³ C] Sodium Acetate into Azinomycin B.....	98
Figure 68. Incorporation of Labeled Acetate into the Citric Acid Cycle Byproducts.....	99
Figure 69. Biosynthesis of the Amino Acid L-valine as Determined from Analyzed Streptomyces Species Sequence Information.....	99
Figure 70. Incorporation of [1- ¹³ C] L-valine into Azinomycin B.....	100
Figure 71. Possible Paths of Valine Modifications to Produce the Azinomycin Epoxide.....	101
Figure 72. Incorporation of a Modified Valine Substrate into Cereulide.....	101
Figure 73. Incorporation of [1- ¹³ C] Sodium Allylketocarboxylate into Azinomycin B.....	102
Figure 74. Stability Profile of V3-V12.....	105
Figure 75. Biosynthetic Route to the Epoxide Moiety in the Azinomycins.....	105
Figure 76. Incorporation of Labeled Acetate into the Krebs Cycle Byproducts Oxaloacetate (and Subsequently Threonine then the Enol Moiety).....	106
Figure 77. Summary of Feeding Studies Targeting Enol Fragment.....	107
Figure 78. Proposed Biosynthetic Routes to the Enol Fragment of Azinomycin B.....	108
Figure 79. Proposed Biosynthetic Routes for Production of the Aminoacetone Moiety of Azinomycin A.....	110
Figure 80. Biosynthetic Pathways Linking Conversion of Glycine and Threonine to L-2-amino-3-ketobutyrate, Which Decarboxylates to Form Aminoacetone.....	111
Figure 81. ¹⁵ N-L-threonine Incorporation into the Azinomycin B Detected by ¹ H NMR.....	113

	Page
Figure 82. Dosage Profile for Aminoacetone (AA5) within the Optimized Range for Production of Azinomycins.....	116
Figure 83. Production of Azinomycin A as a Function of the Amount of Aminoacetone, AA5 Fed Per 10 Liter Culture.....	117
Figure 84. Proposed Biosynthetic Route for the Formation of Aminoacetone and Its Subsequent Direct Incorporation into Azinomycin A.....	118
Figure 85. Origin of Oxygen Atoms in Azinomycin B.....	119
Figure 86. Active Site of a Cytochrome P450 Monooxygenase During Oxygen Insertion.....	119
Figure 87. Oxygen Insertion by a Monooxygenase to Produce the C3' Methoxy Oxygen.....	120
Figure 88. A Standard Oxygen Recirculation System.....	121
Figure 89. Our Fermenter Culture Based Oxygen Recirculation System.....	122
Figure 90. Improvements to the Fermenter Culture Based Oxygen Recirculation System.....	123
Figure 91. ¹³ C Signals Displaying a Shift from ¹⁸ O ₂ Incorporation.....	126
Figure 92. Positional Incorporation of Heavy Oxygen Atoms from ¹⁸ O ₂	127
Figure 93. A Proposed Mechanism for the Insertion of a Heavy Oxygen Atom Via a Monooxygenase for the Formation of the Epoxide Moiety.....	128
Figure 94. Proposed Mechanisms for the Hydroxylation of the Pyrrolide Ring at C12 and C13.....	128
Figure 95. Biosynthetic Routes to the Aziridino[1,2a]pyrrolidine Fragment of Azinomycin B Indicated by Results from the Cell Free Extract Experiments.....	130
Figure 96. Possible Mechanism for the Formation of Aziridino-pyrrolidine Containing Amino Acid.....	130
Figure 97. Potential Routes for the Formation of the 1-azabicyclo[3.1.0]hexane Ring Involving Formation of the Pyrrolidine Ring Before Attachment to the Natural Product Backbone.....	131
Figure 98. Potential Routes for the Formation of the 1-azabicyclo[3.1.0]hexane Ring from a Glutamate Derivative, Two Carbon Sugar Derivative, Sulfotransferase, and Formation of the Diol from Molecular Oxygen.....	132
Figure 99. Stable Isotope Substrates Employed in Exploring the Biosynthesis of the Azirinopyrrolidine Moiety.....	133

	Page
Figure 100. Observed Incorporation of Various Isotopically Labeled Glycines into Azinomycin B.	135
Figure 101. Formation of Aminoacetone from [2,2-D ₂] Glycine.	135
Figure 102. Possible Formation of the 1-azabicyclo[3.1.0]hexane Ring from D-arabinose and Glycine.	138
Figure 103. Possible Formation of the 1-azabicyclo[3.1.0]hexane Ring from [3- ¹³ C] L-aspartate.	138
Figure 104. Possible Formation of the 1-azabicyclo[3.1.0]hexane Ring from [2- ¹³ C] L-serine.	140
Figure 105. Possible Scaffolds Contributing towards Origin of Azabicycle, AZ3.	140
Figure 106. Proposed Aza-sugars AZ15a, AZ15b and Dihydroxy Glutamic Acids AZ16a and AZ16b.	143
Figure 107. ¹³ C labeled Substrates Synthesized for Feeding to <i>S. sahachiroi</i> Cultures for Potential Incorporation into Azinomycin B.	145
Figure 108. Possible Formation of the 1-azabicyclo[3.1.0]hexane Ring from [1- ¹³ C] DL-glutamic Acid.	147
Figure 109. Biosynthesis of the Azinomycins as Indicated by Stable Isotope Feeding Studies.	148

LIST OF SCHEMES

	Page
Scheme 1. Synthesis of Aminoacetone Hydrogen Chloride.....	113
Scheme 2. Synthesis of D-glutamic acid, AZ6.....	141
Scheme 3. Synthesis of the Azabicycle AZ4.....	142
Scheme 4. Ring Opening of Azabicycle AZ4.....	143
Scheme 5. Synthesis of 2-(hydroxymethyl) 3, 4- dihydroxy Pyrrolidinone Unit.....	144
Scheme 6. Synthesis of AZ15a, AZ15b, AZ16a, AZ16b.....	145

LIST OF TABLES

		Page
Table 1.	Up-regulated Gene Expression in Response to Azinomycin B Treatment.....	40
Table 2.	Down-regulated Gene Expression in Response to Azinomycin B Treatment.....	41
Table 3.	Effect of Enzyme Inhibitors on Naphthoate Production.	64
Table 4.	Effect of Enzyme Inhibitors on Azinomycin B Production.	66
Table 5.	Investigation of the Principle Building Blocks of the Azinomycin B Pathway.	70
Table 6.	HPLC Conditions for the Separation of Naphthoate and Azinomycin B.....	74
Table 7.	Evaluation of Solid Media for Growth and Production of Azinomycin B.....	79
Table 8.	Liquid Culture and Fermentation Conditions.....	82
Table 9.	Percent Incorporation of [1- ¹³ C] acetate (1g) into azinomycin B.....	97
Table 10.	Percent Incorporation at C-17 of Azinomycin B and the Epoxyamide.....	103
Table 11.	Percent Incorporation at C-2 of Azinomycin A and B.....	112
Table 12.	Feeding Results for [¹⁵ N] –threonine and [¹⁵ N]- glycine.....	112
Table 13.	Feeding Details and Conditions of All Compounds Fed for Biosynthetic Route to the End Fragment of Azinomycin A Section.	115
Table 14.	Production of Azinomycin A as a Function of Amount of Aminoacetone Fed Per 10 Liters of Culture.....	116
Table 15.	Oxygen Consumption Trials with the Recirculation System.	124
Table 16.	¹³ C Shifts Observed in Carbons Next to Oxygen in Azinomycin B.....	127
Table 17.	Percent Incorporation into Azinomycin B for ¹³ C Labeled L-proline and Glycine.....	136
Table 18.	Percent Incorporation into Azinomycin B for ¹³ C Labeled D-arabinose, D-xylose, and D-glucose.....	137
Table 19.	Percent Incorporation into Azinomycin B for ¹³ C Labeled Aspartate, Lysine, Arginine, and Serine.....	14039
Table 20.	Positional Percent Incorporation of Labeled Precursors into Azinomycin B....	14546

CHAPTER I

INTRODUCTION

INTRODUCTION

Azinomycin B is a naturally produced secondary metabolite produced by two species of *Streptomyces* bacteria, *S. sahachiroi* [1] and *S. griseofuscus* [2]. This molecule (**Figure 1**) is of particular interest to the scientific community because of its proven ability as an anticancer and antibacterial agent [1, 3]. This ability is attributed to the DNA cross linking action from the epoxide and aziridine moieties in the molecule. The unique structure of the aziridino[1,2-a]pyrrolidine (1-azabicyclo[3.1.0]hexane) ring system and functionality of the molecule have made this natural product a popular topic of research. Mode of action, total synthesis of azinomycin and derivatives, and investigation of the molecule's biosynthesis have comprised the focus of recent research. Accessing the unique functionality in this molecule via synthesis, elucidation of its biosynthesis, and biosynthetic gene cluster manipulation could eventually lead to more effective antibiotic and cancer treatments.

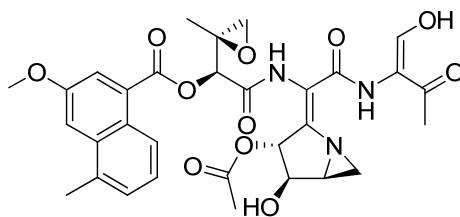


Figure 1. Azinomycin B.

MAN, NATURAL PRODUCTS, AND STREPTOMYCES

Since antiquity, people have used natural sources for pharmacological benefit. Plants have long been a resource for medicinal treatment for a myriad of ailments as well as a source of poisons. Microorganisms have also been a resource and a problem for the same reason. As scientific,

This dissertation follows the style of Chemistry and Biology.

medicinal, and industrial knowledge have increased, so have the numbers and types of natural products available for pharmaceutical use. In the mid-20th century, the search for new sources of drugs was investigated with industrial vigor and scale. *Streptomyces* species, which are primarily terrestrial soil bacteria, were of particular interest to screeners looking for unique natural products due to their renowned ability to produce diverse secondary metabolites. Collecting and screening these microorganisms reached a fevered pitch in the late 1960s. Investigators' efforts ranged from local collections of rural soil, soil samples collected while on vacation [4], and industrial scale collection and screening by pharmaceutical companies.

Although the rate at which new and effective pharmaceuticals strictly isolated from nature has decreased, natural products still provide a significant source of inspiration to the drug industry. According to a 2007 report by Newman and Cragg, over the past 25 years 47% of new drugs in the US marketplace were natural products or their derivatives [5]. However, 73% of these new drugs were derivatives or were based upon the basic skeleton of natural products previously discovered [5]. Many of these drugs are aimed at cancer treatment. In addition, antibacterial/antifungal activity is another prized property, especially with the rise of multi-drug resistant microorganisms [6].

CARZINOPHILLIN/AZINOMYCINS

It was during one of the aforementioned soil screens that the initial activities of the "carzinophilins" were first described along with the previously unnamed producing organism, *Streptomyces sahachiroi* [1]. The strain was isolated from a soil sample collected in Tokyo in January 1951. The initial culture broth of *S. sahachiroi* was shown to have a pronounced inhibitory effect on Gram positive and Gram negative bacteria, but not fungi. The culture broth was screened against a Yoshida sarcoma, a malignant rat tumor, and showed an inhibitory growth effect. Culture broth treatment resulted in prolonged life for the treated rat. These encouraging results led to further investigation and isolation of the "causative agent." From subsequent investigations, only indirect evidence of the structure was gained: the substance was white, and acidic; it was susceptible to change in pH and temperature; it formed salts with sodium, potassium, calcium, etc.; it was soluble in water, alcohols, acetone, butyl acetate, chloroform, but not petroleum ether.

In 1955, improvements in purification, characterization, and tests upon live rats and mice with tumor cells demonstrated the effectiveness of azinomycin B and helped to establish it as a

molecule of interest [7]. In 1956, reports on the effect of carzinophilin on malignant tumors [8] and the clinical and histological studies on the cases treated by carzinophilin [9] were published.

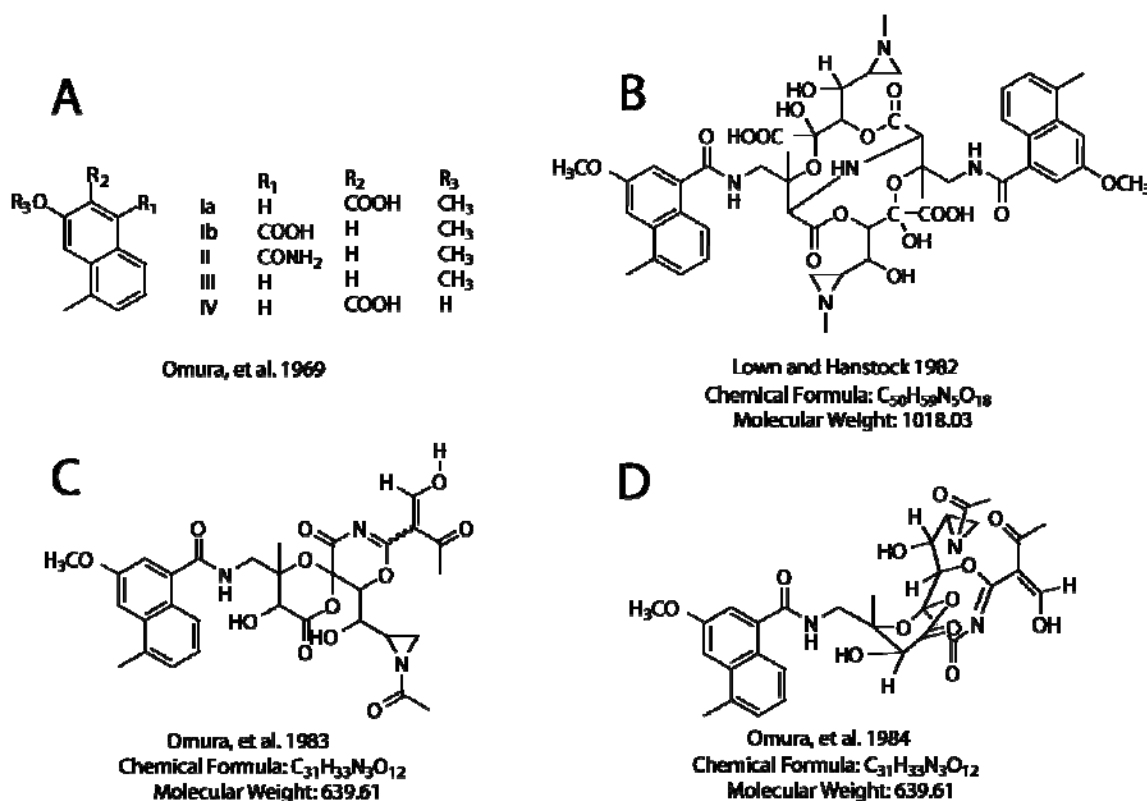


Figure 2. Suggested Structures for Carzinophilin A/Azinomycin B.

Characterization of azinomycin B/carzinophilin A has been an ongoing process with several suggested structures based on chemical and spectroscopic investigations (**Figure 2**). The original report suggested a molecular formula C₆₀H₆₀O₂₁N₆ [7] but Tanka *et al.* [10, 11] suggested it should actually be C₅₀H₅₈O₁₈N₅. The authors further reported alkaline hydrolysis of carzinophilin that yielded 3-methoxy-5-methylnaphthalene-2-carboxylic acid. Additional reports by Hata and others in 1969 [12] clarified the structure of naphthoate portion of the molecule resulting in the assignment indicated in **Figure 2A Ib** and asserted that the related primary amide had the structure indicated in **Figure 2A II**. Lown and Hanstock reported further characterization of the molecule in a 1982 report [13] claiming a dimeric arrangement of the molecule (**Figure 2B**). This claim is based largely upon proton and carbon NMR, nuclear

Overhauser effect (NOE) experiments previously reported molecular mass, and chemical degradation experiments [13]. The 1982 report, in addition to a 1977 report by Lown [14], indicated the DNA alkylating and fluorescence properties of carzinophilin A [14], suggesting a molecule containing two aziridine moieties. Shortly thereafter, another report [15] suggested a different structure (**Figure 2C**) with a molecular formula $C_{31}H_{33}O_{12}N_3$. A subsequent report by the same authors [16] suggested the stereochemistry seen in **Figure 2D**.

The structure's true conformation was determined in 1986 and reported by Yokoi *et al.* [17]. This analysis reassigned the designation of carzinophilin A to azinomycin B. They reported structures with a corrected molecular formula $C_{31}H_{33}O_{11}N_3$. In addition, the investigators reported finding azinomycin A, which contains a methylene (CH_2) group instead of the enol group found in azinomycin B (**Figure 3A&B**). Naphthoate derivatives were also isolated, including one that contained the epoxide portion (**Figure 3C**) seen in azinomycin A, azinomycin B, methoxy-naphthoate (**Figure 3D**), naphthamide (**Figure 3E**), and the 3-methoxy-5-methylnaphthalene-carboxylic acid (**Figure 3F**).

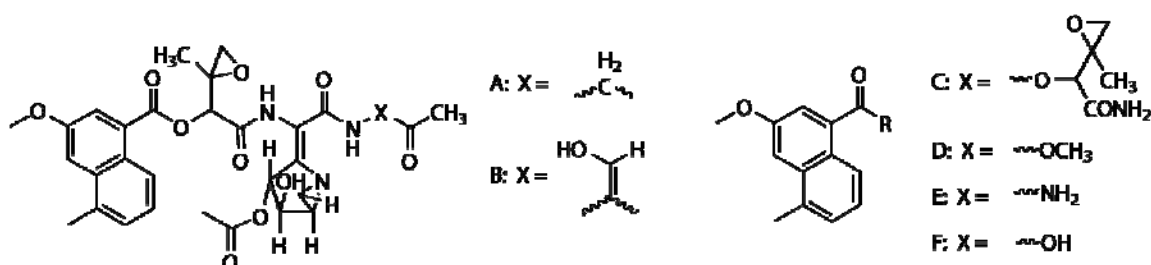


Figure 3. Corrected Structures for Carzinophilin A/Azinomycin B.

Compounds isolated from *Streptomyces sahachiroi* culture broths and identified: (A) azinomycin A (B) azinomycin B and naphthoate group derivatives (C-F) adapted from Yokoi *et al.* 1986 [17].

After complete structural characterization, research interest in the azinomycins and derivatives turned toward total synthesis and mode of action. Efforts towards synthesizing azinomycin B were unsuccessful. However, in 2001 Coleman *et al.* reported the total synthesis of azinomycin A [18]. Several derivatives and portions of the azinomycin skeleton have been synthesized and investigated for structure activity relationship [19-29]. Despite interest in the unique synthetic challenge, investigations of the biosynthetic origin of these molecules were not reported until 2004 [30, 31], fifty years after the molecule's discovery.

STREPTOMYCES AND BIOSYNTHESIS

Streptomyces species have a well established reputation as a source for many pharmacological compounds. The *Streptomyces* are primarily soil dwelling bacteria, with the exception of a few; largely eradicated species and related mycobacteria: *Mycobacterium tuberculosis* and *Mycobacterium leprae*, the causative agents in tuberculosis and leprosy, respectively [4]. The *Streptomyces* bacteria were long considered to be an evolutionary link between bacteria and fungus. Their filamentous appearance, differential morphology producing roots, branches, spores similar in structure to fungi, and resistance to many antibiotics contributed to this misunderstanding. Further research, aided by advances in genetics, led to the recognition of their distinct identity. The bacteria seem to have evolved to suit their exact situation both morphologically and chemically. The soil environment puts selective pressure upon its inhabitants to be versatile in adapting to environmental changes and to competitors. Its ability to consume simple and complex nutrient sources, adapt to drought and deluge and to cold and heat, in addition to its ability to compete with all the other forms of life, has enabled *Streptomyces* species to occupy a unique niche in soil. The *Streptomyces* are mostly non-motile, but eminently adaptable. They grow in contiguous segments sharing cell walls with neighboring cells. It has been speculated that the contiguous nature of *Streptomyces* colony growth is a particularly useful adaptation for the soil environment, allowing for the ability to span gaps, and the stability to provide attachment to other cells [4]. The growth of these colonies, especially in liquid media, results in a macroscopic appearance of irregular spheres and a microscopic appearance of tangled filaments (**Figure 4**). On solid media, the *Streptomyces* colonies pass through several developmental stages and variations during on the maturation of the colony, ultimately leading to the production of aerial spores. Although the differentiation in *Streptomyces* colonies gives it the appearance of a multi-cellular organism, any portion of the “mycelia” may be removed to give rise to new colonies. Multiple signaling pathways result in cascades of gene expression changes both spatially and temporally in the entire mycelia bunch. Tied to the growth and differentiation of the mycelia is the production of a variety of secondary metabolites. *Streptomyces*’ complex ability to adjust expression of genes in concert with, or in response to, environmental conditions is thought to be a result of a very sensitive and complex system of sigma and transcription factors. The microorganism’s ability to adjust of gene expression enables it to adapt to a variety of different environmental conditions and to exploit a wide range of available resources. Production of secondary metabolites in *Streptomyces* is known to be largely tied to the formation of spores.

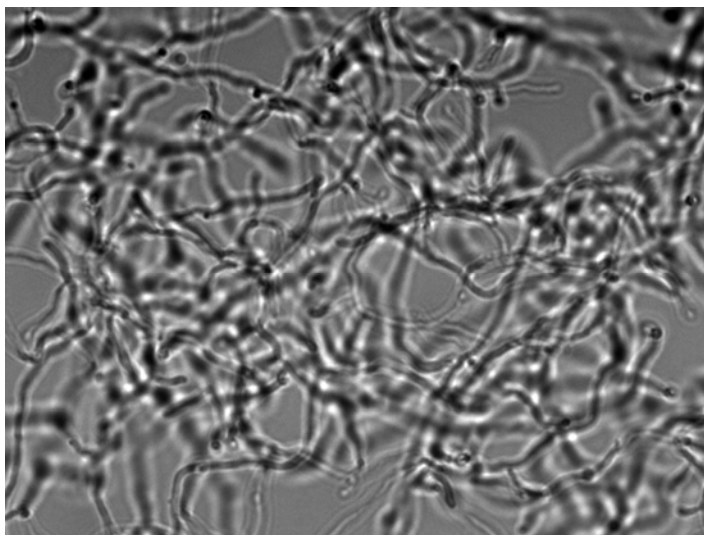


Figure 4. *Streptomyces sahachiroi* Mycelia.

S. sahachiroi mycelia branches in liquid media (seen here at 1000X magnification) grown from spores. Picture taken by the author.

Streptomyces tend to dominate the conversation on natural products because of their proven performance as “the antibiotic producers.” Over the past 70 years, the genus of *Streptomyces* has been the predominant source of readily discoverable antibiotics and other natural products. The true richness of *Streptomyces* species was further disclosed in 2002 with the public revealing of the *Streptomyces coelicolor* A3 (2) genome sequence [32]. Since this date, *Streptomyces avermitilis* (2003) [33], an industrial microorganism producing the macrolide avermectins, *Streptomyces scabies* (2007), and *Streptomyces griseus* (2008) [34] have had their genome sequence published. Many more genomes have been sequenced but have not been publicly released. A significant number of sequences for biosynthetic pathways or key proteins have been available. The full complexity of *Streptomyces* and the nature of the production of their secondary metabolites is being revealed slowly. Genome sequencing increases the accessibility of *Streptomyces* species as a source of cryptic or silent metabolic pathways. The advent of cheaper genome sequencing has led to a revolution in the analysis of natural product biosynthesis.

NATURAL PRODUCT PATHWAYS

A survey of isolated natural products will yield a menagerie of varied and distinct molecules, yet the origin of these molecules flows from basic pathways related to primary metabolism. Primary

metabolites include amino acids, nucleotides, fatty acids, and vitamin complexes which produce proteins, nucleic acids, and cell membranes. Secondary metabolites are typically classified upon the basic origin of their construction from both the metabolic building blocks and the molecular machinery that assembles the units. Natural products, also known as secondary metabolites, are by definition not required for the survival of the organism. These natural products are produced by a few pathways including the non-ribosomal peptide synthetase (NRPS), alkaloid, shikimate, isoprenoid, fatty acid synthase (FAS), and polyketide synthase (PKS) pathways. Polyketide synthases (PKS) are similar to fatty acid synthases (FAS), producing carbon chains of repeating units in various states of oxidation. PKS pathways are constructed with structurally diverse starting units with subsequent 2 or 3 carbon extension units. NRPS pathways provide a route for the formation of polypeptide units from natural and unnatural amino acids. Alkaloids are organic, nitrogenous bases found mostly in plants, but also to some extent in microorganisms. Shikimate derivatives are often aromatic amino acids as they are from variations on the biosynthesis of L-phenylalanine, L-tyrosine, and L-tryptophan. Terpenes are constructed from 5 carbon isoprene starting units.

Figure 5 illustrates some proto-typical molecular examples of products derived from different natural product pathway classes. Aflatoxin B₁, a highly toxic compound produced by *Aspergillus* fungi, is a polyketide, having been constructed from acetate building blocks (**Figure 5A**) [35-41]. Cocaine, an addictive analgesic drug, is an alkaloid made by the coca plant, *Erythroxylon coca* (**Figure 5B**) [42]. Vancomycin, a glycopeptide antibiotic used in the prophylaxis and treatment of infections caused by Gram-positive bacteria shown in **Figure 5C** [43, 44], is NRPS derived [35]. The drug Taxol, isolated from the bark of the Pacific yew tree, is a common pharmaceutical used in cancer treatment, due to its terpenoid skeleton (**Figure 5D**) [45]. Chloramphenicol, a bacteriostatic antimicrobial produced by *Streptomyces venezuelae*, is a shikimate pathway derived (**Figure 5E**) [46]. Although the origin, producing organisms, and effects of these molecules are quite different, the construction of these molecules share common characteristics.

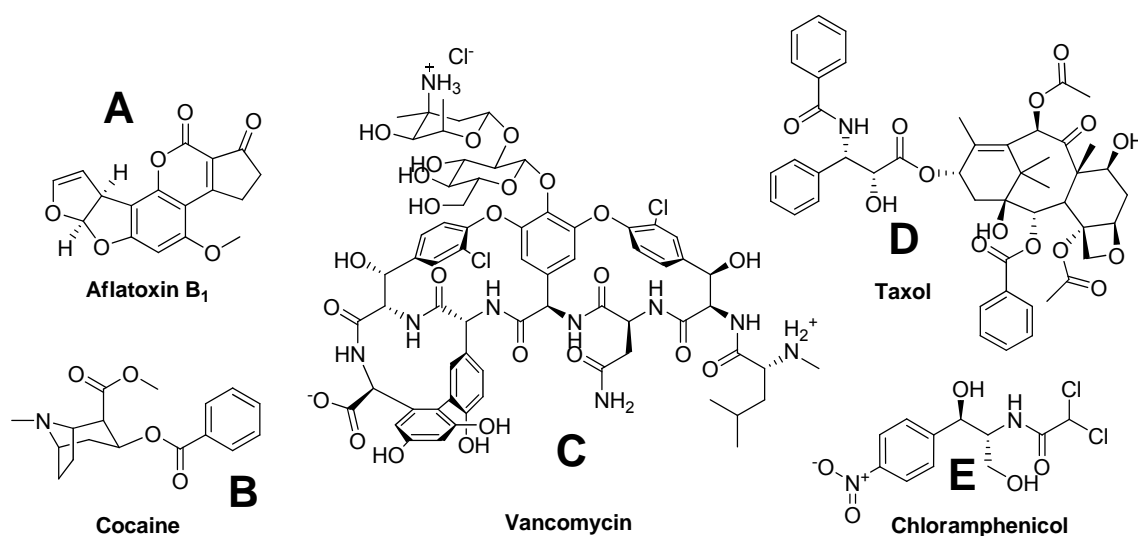


Figure 5. Typical Examples of Natural Product Structures from the Polyketide, Alkaloid, NRPS, Terpene, and Shikimate Pathway Families.

(A) Aflatoxin B₁, a polyketide, (B) Cocaine, an alkaloid, (C) Vancomycin, a non-ribosomal peptide. (D) Taxol, a terpene, and (E) Chloramphenicol, a shikimate pathway derived natural product.

Often in microorganisms, but not in plants, the genes coding for the biosynthesis of a natural product tend to be clustered in the same region of the genome. Consequently, when they are transcribed all appropriate components are produced. These genes work in *cis*. The large multi-domain enzymes produced are also accompanied with efflux proteins or other resistance proteins, and modifying enzymes. Some genes or related elements of natural product biosynthesis are not clustered, but work in *trans* requiring coordination of several distantly located genes or in conjunction with primary metabolic pathways. The pathways are defined by the origin of their primary building blocks. While some significant types of pathways include fatty acid synthesis, polyketide synthases, non-ribosomal peptide synthetases, terpenes, alkaloids, or modifications of shikimate biosynthesis, the end product skeleton is rarely unmodified. Synthases use acyl-CoA subunits while synthetases require ATP in the biosynthetic process. Oxidation/reduction (changing of the oxidative state), glycosylation (addition of sugar substituents), transamination (the removal or addition of an amino group), alkylation (such as addition of a methyl group), and acylation (such as addition of an acetyl group) are among the standard modifications. Some natural products have portions of their skeletons from completely different pathway types. This leads to the hybrid origin of many natural product molecules, including azinomycin B.

THE TERPENES

Terpene biosynthesis resembles that of a simple metabolic pathway (**Figure 6**). Unlike PKS and NRPS pathways, there is no multi-active site and no megasynthase assembly-line; each enzyme acts independently [47]. Most terpenes undergo oxidation by various oxidases to generate alcohols and ketones. In addition, they are frequently acylated, glycosylated, and alkylated. Terpenes are most often associated with plant natural product biosynthesis, where terpene biosynthesis is related to the mevalonate pathway [47]. In *Streptomyces*, most terpenes are derived from the nonmevalonate pathway [47, 48]. The structure of azinomycin B is not consistent with the standard, 5 carbon isoprene unit patterns associated with terpene natural products and is not isoprenoid derived.

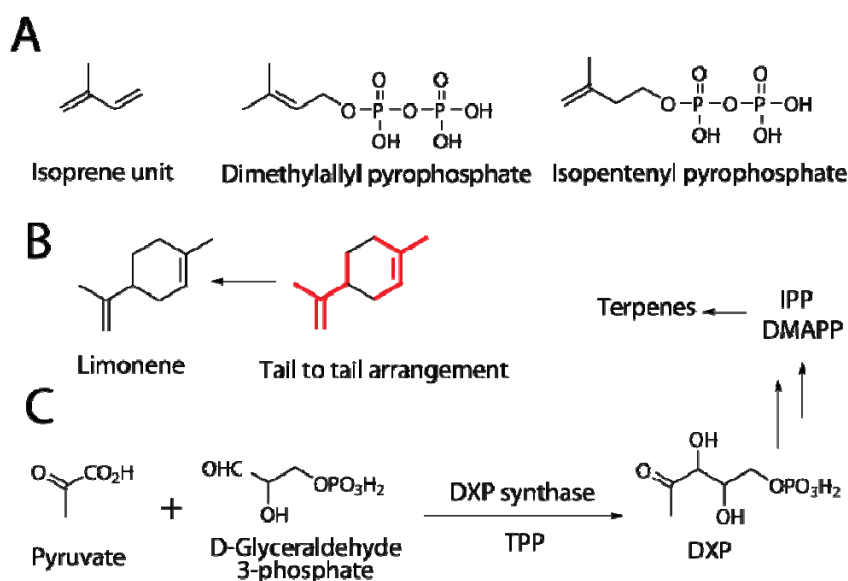


Figure 6. The Building Blocks, Arrangement, and Nonmevalonate Biosynthesis of Terpenes. (A) 5 carbon Isoprene unit, starting unit include dimethylallyl pyrophosphate and isopentenyl pyrophosphate. (B) Typical patterning, in red, seen in a limonene, a terpene. (C) The biosynthesis of terpenes from the nonmevalonate pathway [47].

THE ALKALOIDS

The alkaloids are a group of natural products that contain basic nitrogen atoms having earned their name from the term alkaline which used to refer to any nitrogen containing base. Alkaloids are often identified by the skeletal nitrogenous base from which they are most closely related. The amino acid building blocks of alkaloids are modified by decarboxylation, aldol

condensation, reductive amination or methylation. Successive alterations using these relatively few biosynthetic transformations lead to alkaloids in which the original amino acid building block is often hard to identify. Cocaine is an example of an L-ornithine derived tropane alkaloid [49]. **Figure 7** illustrates the modification to the original L-ornithine (methylation, transamination, addition of two carbon acetate units, oxidation, and cyclization) to ultimately biosynthetically produce cocaine.

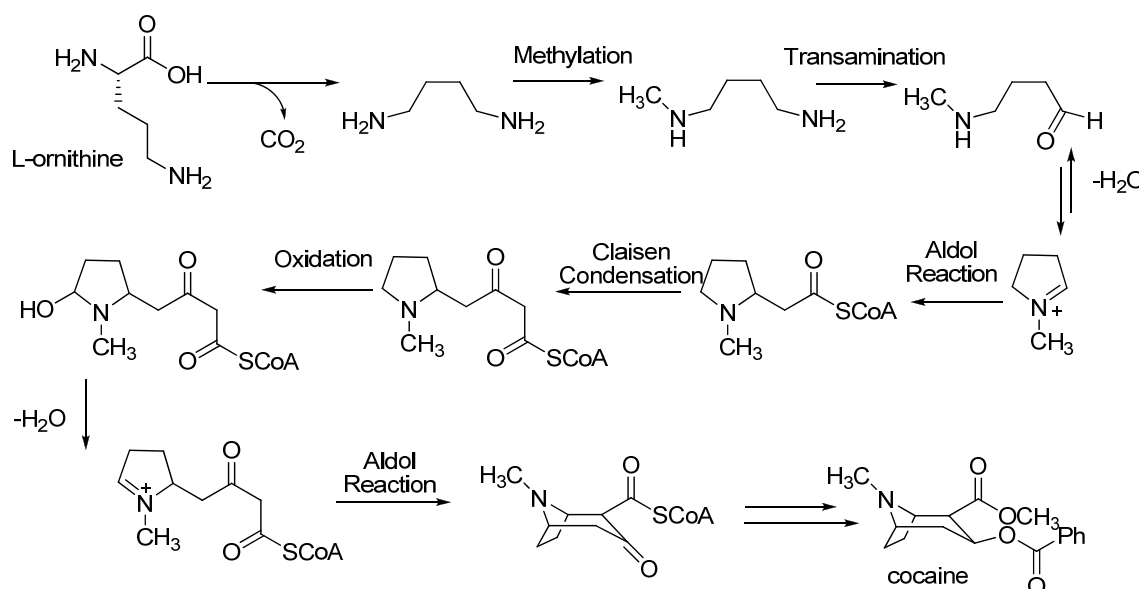


Figure 7. The Biosynthesis of the Plant Derived Alkaloid Cocaine. The biosynthesis of cocaine from the coca plant, *Erythroxylon coca* [49].

Production of modified amino acids or subunits which undergo further modification is an alternate description of the alkaloids. Several alkaloid type natural products produced by *Streptomyces* species have been reported such as the benzodiazepine antramycin in *Streptomyces refuineus* [50] (**Figure 8**). L-tryptophan, L-tyrosine, and the methyl group from L-methionine are modified by enzymes in the antramycin biosynthetic gene cluster to produce antramycin and related natural products.

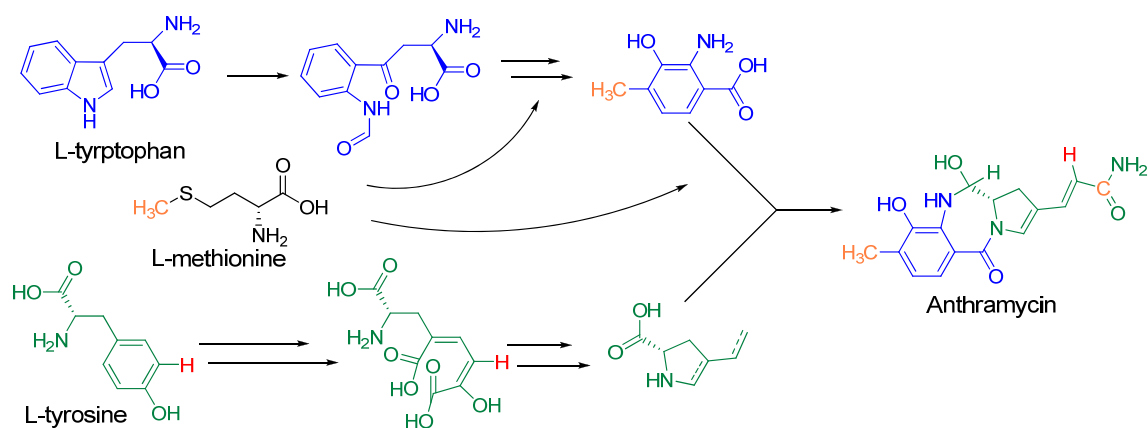


Figure 8. The Biosynthesis of the *Streptomyces refuineus* Derived Alkaloid Anthramycin.

The biosynthesis of the alkaloid natural product anthramycin as determined by isotopic feeding experiments. Figure after Hu *et al.* [50].

It is possible to envision the production of a modified unit for attachment to the azinomycin backbone to produce the main portion of the aziridinopyrrolidine ring from L-ornithine. **Figure 9 path A** envisions the main aziridinopyrrolidine ring forming from the five carbons and the primary nitrogen of L-ornithine, after biosynthetic modifications. **Figure 9 path B** envisions modification of L-ornithine to produce part of the backbone of azinomycin with two additional carbon units and a nitrogen being added to complete the pyrrolidine and aziridine rings. **Figure 9 path C** envisions modification of L-tyrosine, similar to that which helped form anthramycin in **Figure 8**, where decarboxylation, transamination, and other modification reactions could lead to the formation of an aziridinopyrrolidine amino acid. Whereas most of the azinomycin molecule does not appear to be alkaloid derived, it is likely that a portion of the molecule could have alkaloid biosynthetic origins before incorporation into the larger natural product.

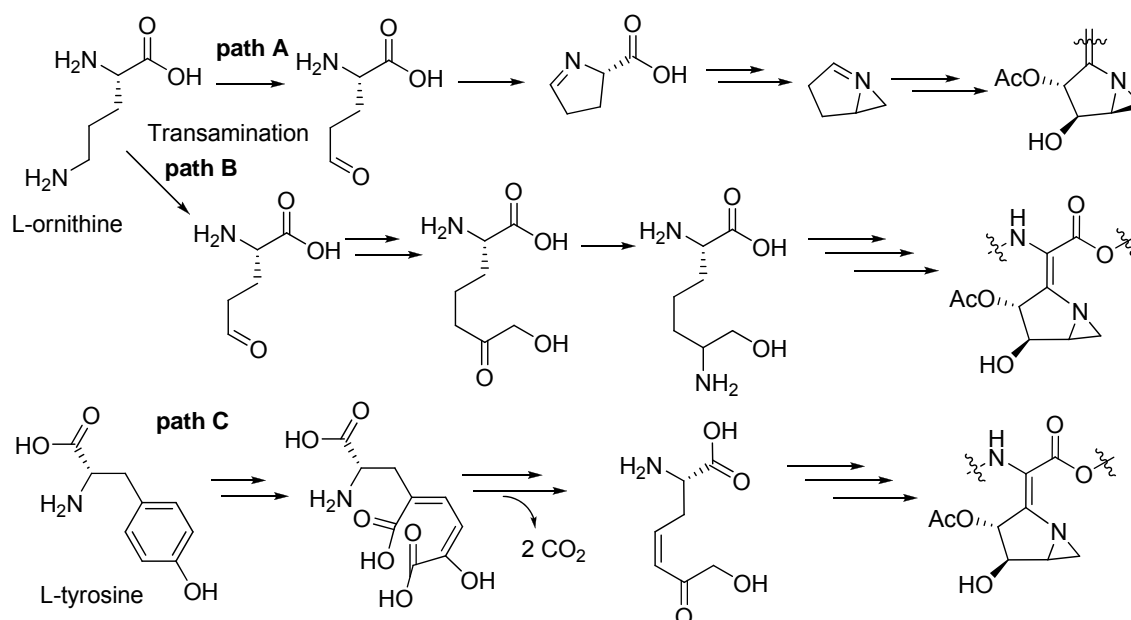


Figure 9. An Outline of Potential Alkaloid-type Biosyntheses of Aziridinopyrrolidine Moiety of the Azinomycins.

FATTY ACID BIOSYNTHESIS

Fatty acid biosynthesis is part of the primary metabolism responsible for the synthesis of lipids. Fatty acid construction begins with a keto starting unit, often acetate, attached to the fatty acid synthase (FAS) enzyme. A unit is added by the keto synthase (KS) when the malonyl unit decarboxylates, leading to the attack of the carbonyl carbon on the starter unit, resulting in detachment from the enzyme. Next, the unit that has been extended then undergoes a reduction via the ketoreductase (KR) to the resulting alcohol. Next the alcohol is turned into an alkene via the dehydratase (DH) and finally is reduced by the enoylreductase to the alkane. If the unit is further extended, the process is repeated after transfer of the molecule to the enzyme from the phosphopantetheinyl arm. This cycle is illustrated in **Figure 10**. Chain extension proceeds until a native limit, when the acyl thioester is released or, in the case of some fatty acid synthesis, terminated by a thioesterase (TE) domain.

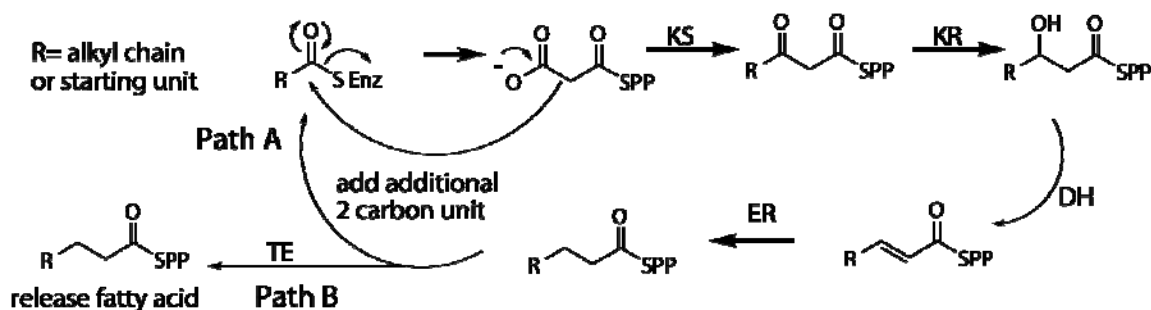


Figure 10. Fatty Acid Biosynthesis.

Fatty acid biosynthesis proceeds through a cyclic mechanism, beginning with a Claisen condensation-like carbon-carbon bond forming reaction, then proceeding through a reduction, dehydration, and a second reduction to generate a saturated chain. KS - ketosynthase, KR - ketoreductase, DH - dehydratase, ER - enoyl reductase, SPP - phosphopantetheine thiol, SEnz - enzyme bound cysteine. Path A adds additional 2 carbon units to the growing chain. Path B releases the fatty acid by way of the TE – thioesterase domain. Adapted from Dewick, 2002 [35].

THE PHOSPHOPANTETHEINE ARM

The phosphopantetheine arm is a common and essential feature in the biosynthesis found in fatty acid biosynthesis, non-ribosomal peptides, and often polyketide biosynthesis. 4'-Phosphopantetheine, derived from coenzyme A, is an essential prosthetic group in biosynthetic pathways. Domains carrying the molecule under construction, including the acyl carrier protein (ACP), peptidyl carrier proteins (PCP), and aryl carrier proteins (ArCP), all contain this prosthetic group. These carrier domains are referred to as thiolation domains (T) (**Figure 11B**) once the prosthetic group is attached (**Figure 11A**).

The phosphopantetheine arm fulfills two demands: First, the intermediates remain covalently linked to the synthases (or synthetases) in an energy-rich thiol ester linkage; Secondly, the flexibility and length of phosphopantetheine chain (approximately 2 nm) allows the covalently tethered intermediates to have access to spatially distinct enzyme active sites. Phosphopantetheine is covalently linked *via* a phosphate ester to a serine hydroxyl of the acyl carrier protein, also known as the thiolation domain of Fatty Acid Synthase.

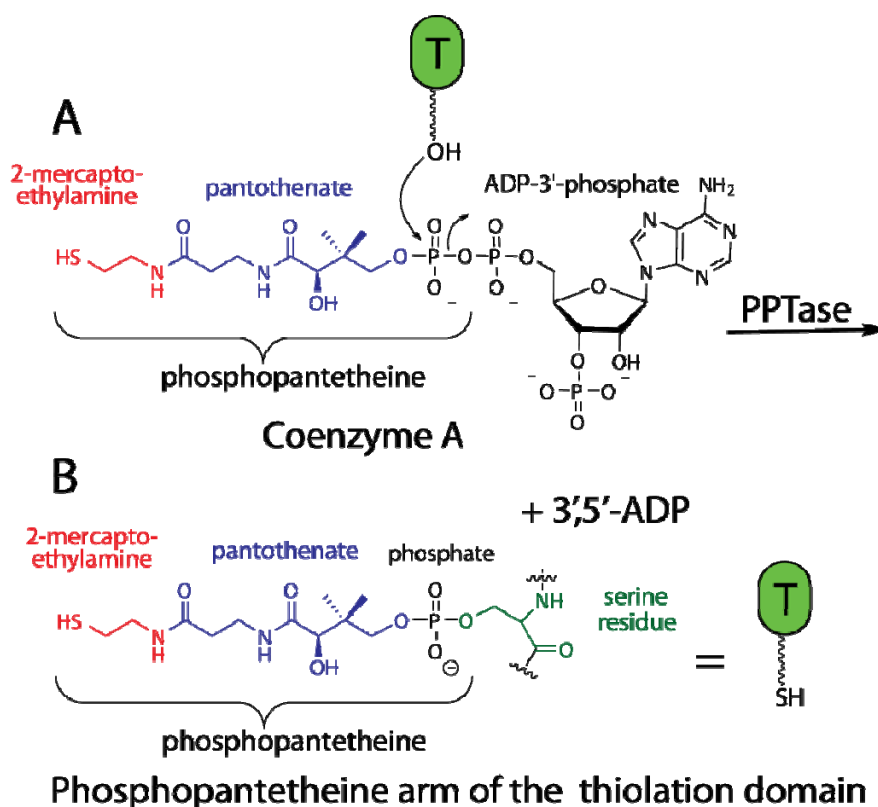


Figure 11. Structure of Coenzyme A and Phosphopantetheine Arm Attached to the Acyl Carrier Protein/Thiolation Domain.

Adapted from Figures after Dewick, 2002 and Walsh et al., 2006, [35, 51].

THE POLYKETIDES

The wide varieties of compounds that share the polyketide origin share a common skeletal design. The differences in these compounds result from the flexibility of their construction and modifications. Polyketide compounds have several major categories such as aromatic, macrolactone, and polyene molecules. Examples of each of these different types are seen in **Figure 12**. These differences reflect the construction of the molecules. Polyketide synthase genes for most polyketides are organized in a single operon in bacteria or in gene clusters in eukaryotes. From an initial analysis, it would appear that the naphthoate group of azinomycin B could be derived from an aromatic polyketide pathway.

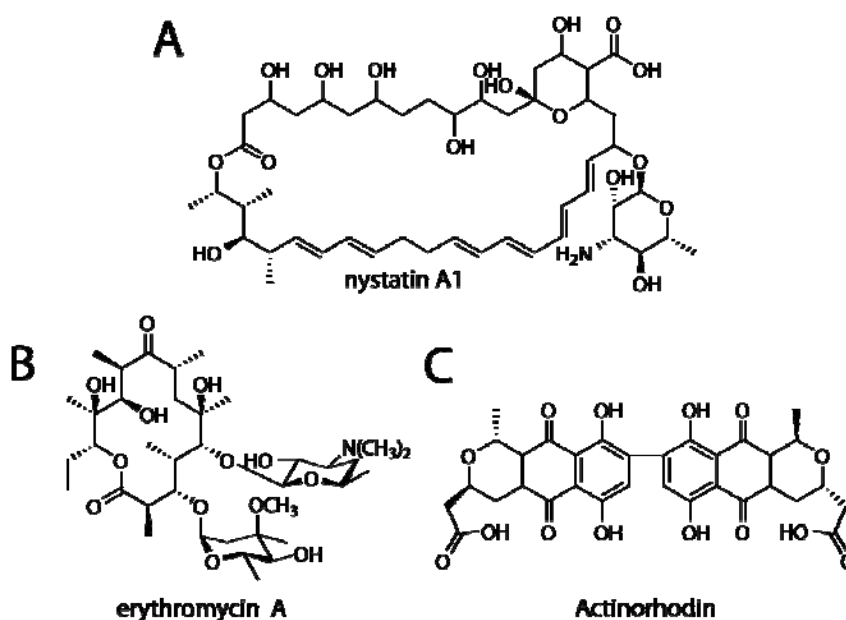


Figure 12. Selected Examples of Aromatic, Macrolactone, and Polyene Polyketides. (A) Nystatin A1, a polyene produced by *Streptomyces noursei* [52]. (B) Erythromycin A, a macrolactone is produced from a strain of the actinomycete *Saccharopolyspora erythraea*, formerly known as *Streptomyces erythraeus* [53]. (C) Actinorhodin an aromatic polyketide from *Streptomyces coelicolor* A3(2) [54].

Polyketide construction is most clearly understood to parallel fatty acid biosynthesis. In fatty acid biosynthesis, smaller units like malonyl CoA units are added stepwise onto a growing chain and are subsequently reduced from keto form to an alkane. The first step in this process is the loading of malonate onto a coenzyme A molecule. The next step involves the addition of the malonyl-CoA unit onto the fatty acid biosynthesis enzyme's phosphopantetheine arm. The differences between PKS and FAS biosynthesis diverge after this point upon the degree to which the units are processed (**Figure 13**). Polyketide construction differs from the FAS model in the degree of reduction and the repetitive nature of the process. Some polyketides are simply modular for each step while others are iterative, like the FAS model. Instead of being fully processed each time, the process may be cut short. Polyketide biosynthesis also differs from fatty acid biosynthesis in that the starting units in polyketides vary widely. PKS are also commonly extended by methyl malonate units, rather than malonate units, which results in a branched natural product chain. Although FAS produce straight chain fatty acids in an iterative process, PKS construction is not always iterative. PKS is often modular, with different enzymes processing each additional unit to the molecule.

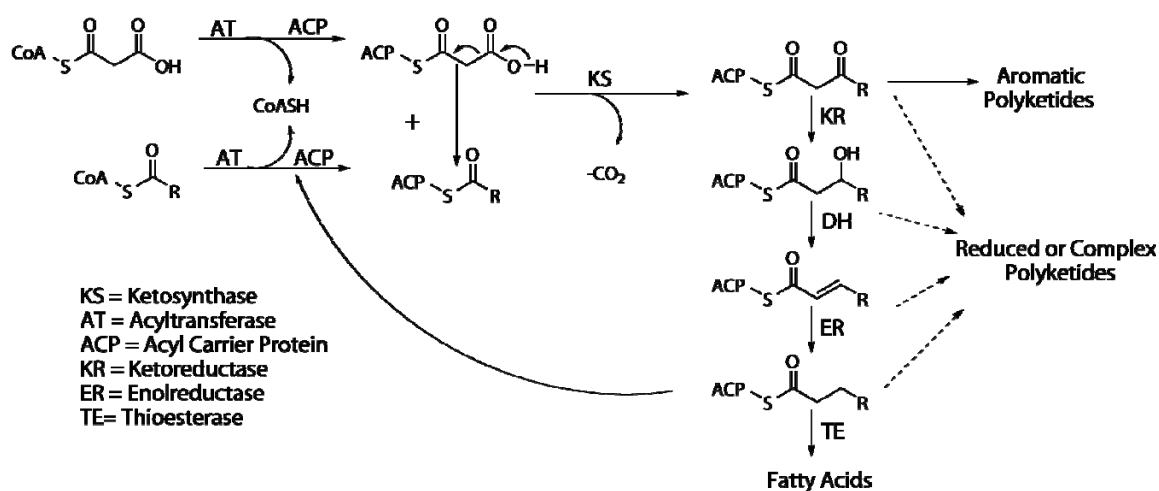


Figure 13. Comparing PKS and FAS Biosynthesis.

There are different classes of polyketides: type I, type II, and type III (**Figure 14A**). Type I polyketide synthases are large, highly modular proteins. Type II polyketide synthases are aggregates of monofunctional proteins. Type III polyketide synthases lack ACP domains; they are iterative, homodimeric enzymes that directly catalyze the condensation of the acyl-CoA unit [55], and are highly divergent from either type I or type II synthases. Type I PKSs are further subdivided: iterative PKSs, which reuse domains in a cyclic fashion, and modular PKSs, which contain a sequence of separate modules and do not repeat domains. Aromatic PKSs consist of iteratively used active sites that are on a group of separate proteins encoded by clustered genes (bacterial PKS) or on a single protein (fungal PKSs) [56]. Although PKS starting units can be quite structurally diverse (propionate, acetate), the extending units are predominantly malonyl-CoA or methylmalonyl-CoA (**Figure 14B**). After incorporation onto a growing chain powered by decarboxylation, these extension units effectively add acetate or propionate units (**Figure 14C**).

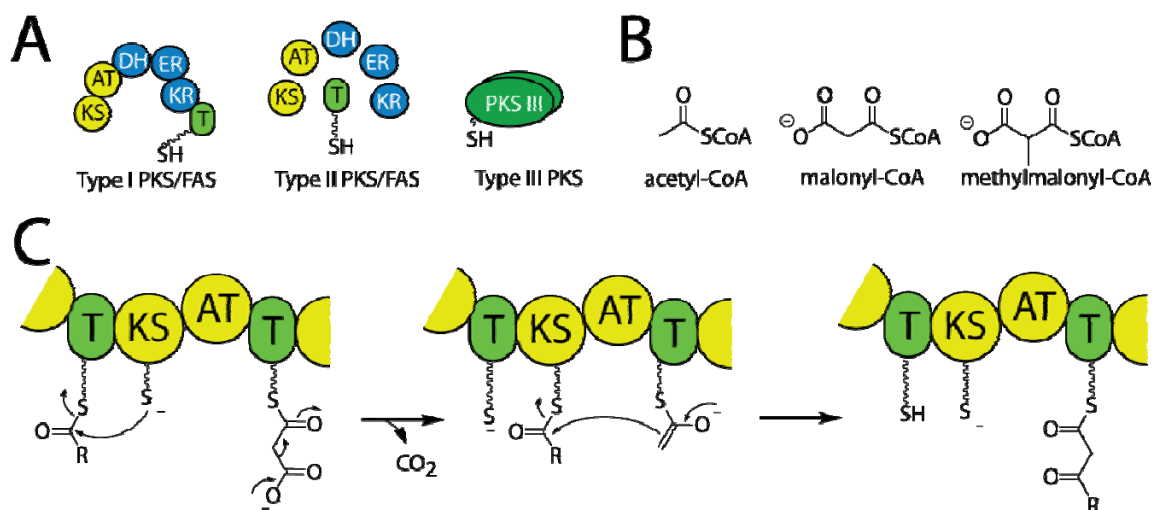


Figure 14. PKS Model Diagrams.

(A) Fatty acid synthase/ Polyketide synthase models. (B) Common starter and extender units in PKS systems. Starter units are variable in structure. (C) Loading and elongation of PKS type 1 models occur in the minimal model. Figures after Walsh *et al.*, 2006 [51].

Evaluation of the naphthoate group of azinomycin B suggests that the 12 carbon skeleton of the naphthoate could result from the condensation of 5 malonyl-CoA units with a starting acetate unit. This hexaketide could undergo an intramolecular aldol condensation with the resulting aromatization yielding the naphthoate skeleton (**Figure 15**). Such a construction could be attributed to a number of PKS types. The closest parallel found is the similarly structured naphthoate group in neocarzinostatin (**Figure 16**) [57, 58]. The neocarzinostatin naphthoate was determined to originate from a type I iterative pathway [57, 58].

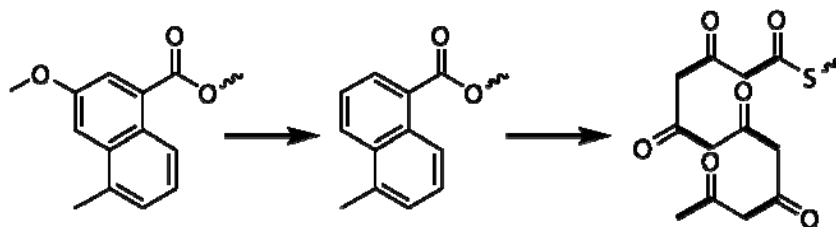


Figure 15. Possible PKS Origins for the Azinomycin Naphthoate.

Analysis of the naphthoate structure would indicate that it could originate from a PKS hexaketide product.

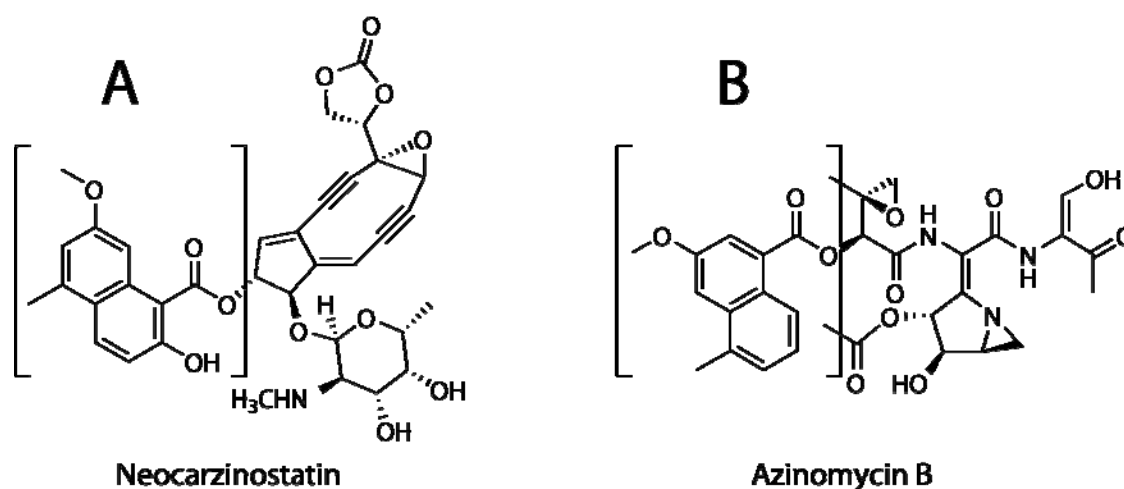


Figure 16. Structural Similarity in Neocarzinostatin and Azinomycin B.
 (A) Neocarzinostatin and (B) azinomycin B share a similarly structured naphthoate group (in brackets).

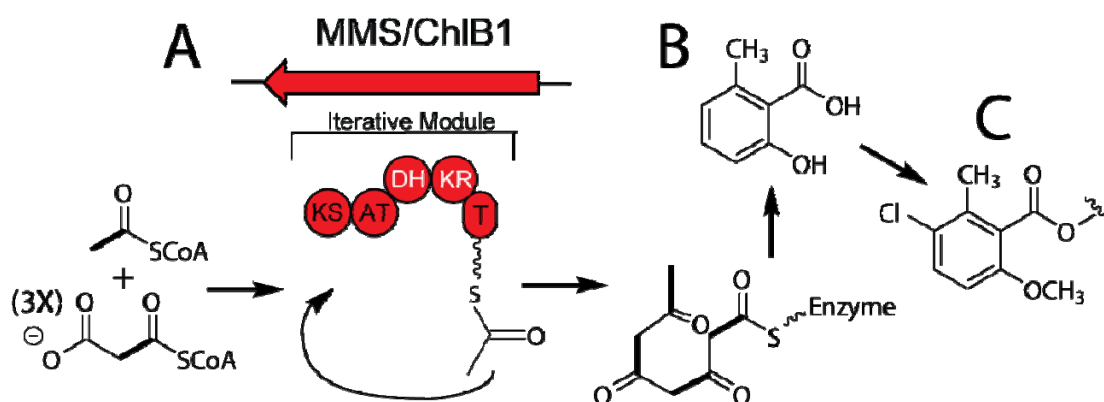


Figure 17. Type 1 Iterative PKS Producing 6-methylsalicylic Acid and Chlorothricin.
 (A) 6-methylsalicylic acid synthase (ChlB1) involved in the biosynthesis of (B) 6-methyl salicylic acid in *Penicillium patulum* and (C) chlorothricin from *S. antibioticus* [59].

NEOCARZINOSTATIN

Neocarzinostatin (**Figure 16A**) is a potent DNA-damaging bicyclic dienediyne antibiotic produced by *Streptomyces carzinostaticus* [57, 58]. Attached to the bicyclic dienediyne “warhead” portion of the molecule is a naphthoate moiety. Its biosynthesis has been determined to include a type 1 iterative polyketide synthase with high homology to the most investigated type 1 iterative PKS, the multifunctional 6-methylsalicylic acid synthase gene from the fungus *Penicillium patulum* [56, 57, 60, 61]. A 6-methylsalicylic acid synthase has also been isolated from *Streptomyces antibioticus* involved in the chlorothricin biosynthesis [59] (**Figure 17**). The

genes responsible for neocarzinostatin's naphthoate are a single PKS gene, NNS, flanked by an O-methyl transferase gene (O-MT) and a gene for an ATP-dependent adenylate/thioester-forming enzyme (A) in **Figure 18** [57]. Presumably there would be an oxygenase that would produce the two hydroxyl groups, one of which gets methylated in neocarzinostatin. The similarity to the azinomycin naphthoate moiety cannot be overlooked. There are, however, alternative models to consider.

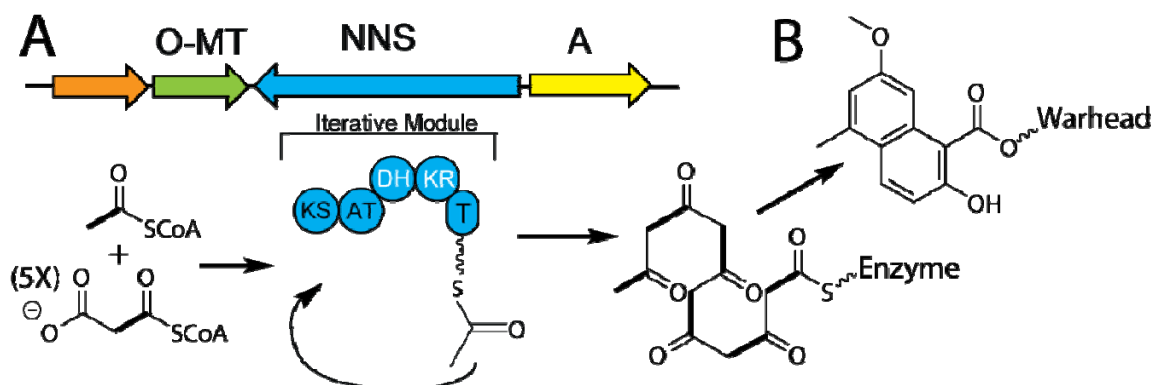


Figure 18. Type 1 Iterative PKS Producing the Neocarzinostatin Naphthoate Moiety. (A) Type 1 iterative PKS and flanking genes involved in the biosynthesis of (B) the naphthoate of neocarzinostatin in *Streptomyces carzinostaticus*.

MODULAR PKS MODEL

It is reasonable to consider the non-iterative type I PKS biosynthesis in relation to azinomycin B. Construction of 6-deoxyerythronolide B is the best-characterized example of PKS construction. The construction of 6-deoxyerythronolide B, essentially the skeleton of the effective antibiotic erythromycin, exemplifies variations seen in molecules with polyketide origin. Methylmalonyl Co-A units are used to construct this molecule and are subsequently reduced to varying degrees. The entire 7-unit molecule then undergoes a cyclization via macrolactonization. Analysis of the biosynthetic genes for the production of 6-Deoxyerythronolide B revealed the three DEBS PKS genes, each containing the distinct modules seen in **Figure 19**. Other types of multimodular PKS enzymes contain non-functioning domains, disabling the particular unit reduction. If azinomycin B would follow the type I format, the construction of the hexaketide would occur using five successive modules using an acetate unit as a starting unit.

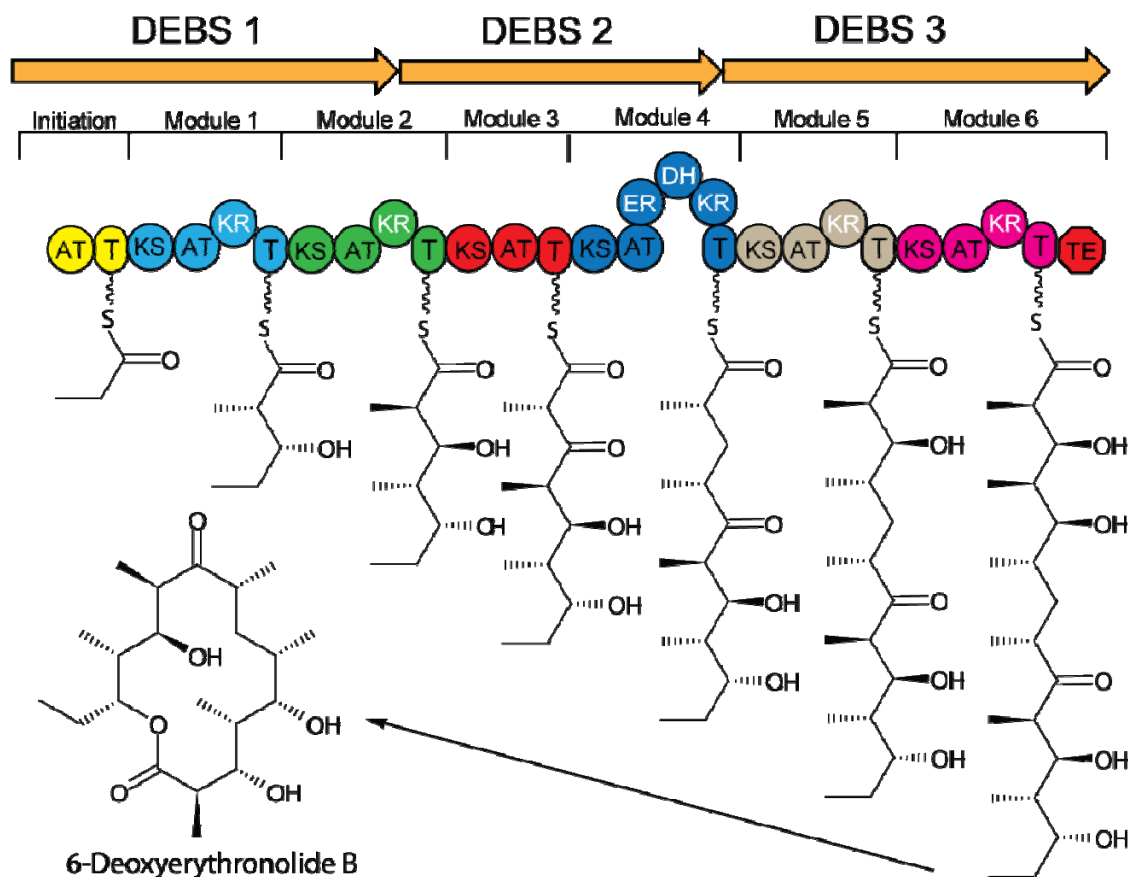


Figure 19. Modular Structure of DEBS (6-Deoxyerythronolide) Synthetase. After Khosla, et al., 2007 [53].

Considering the known biosynthetic structure of DEBS synthetases, we could postulate what the biosynthetic design for the naphthoate construction would entail. As mentioned previously, the naphthoate could originate from any type of PKS. It is most likely that the naphthoate originates from either a traditional type I or type I iterative PKS similar to that discovered in neocarzinostatin's naphthoate biosynthesis (**Figure 20**).

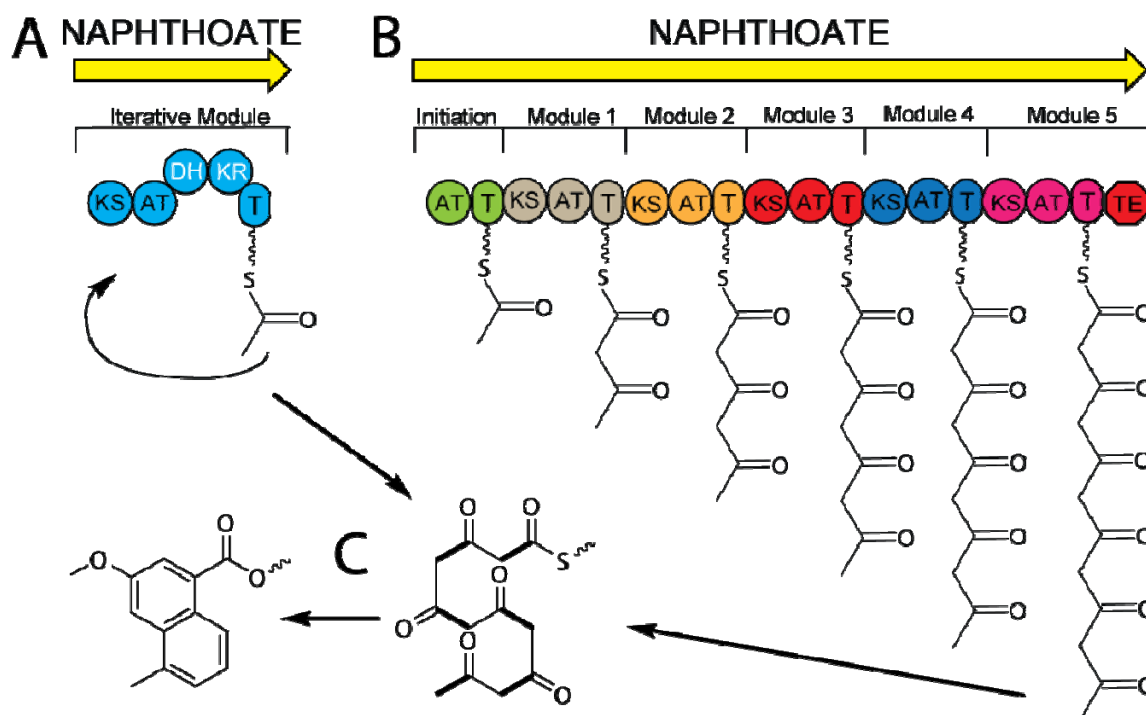


Figure 20. Possible Modular Structures of a Naphthoate PKS Synthase. Possibilities for PKS involvement in construction of the naphthoate include (A) an iterative type I PKS like the iterative type I from neocarzinostatin or (B) minimal modular type I, 5 module PKS producing (C) the hexaketide proposed intermediate of the naphthoate.

THE NON-RIBOSOMAL PEPTIDES

Non-ribosomal peptides are produced through a series of acylation reactions on a large, multifunctional protein complex [62]. NRPS pathways incorporate amino acids and aryl acids onto a growing chain. This process largely mimics the PKS paradigm. There are three different classes of NRPS pathways: types A, B, and C. Type A are linear, containing the three core domains; the sequence of the peptide produced depends on the number and order of the modules. This is much like the PKS pathway seen in the production of 6-Deoxyerythronolide B. Type B are iterative, using domains or modules more than once for a single peptide and often using the TE domain as a tether domain for the growing peptide. Type C is non-linear, containing at least one unusual arrangement of the core domains and often incorporating small molecules. Evaluation of azinomycin B indicates that it is likely to have NRPS origins.

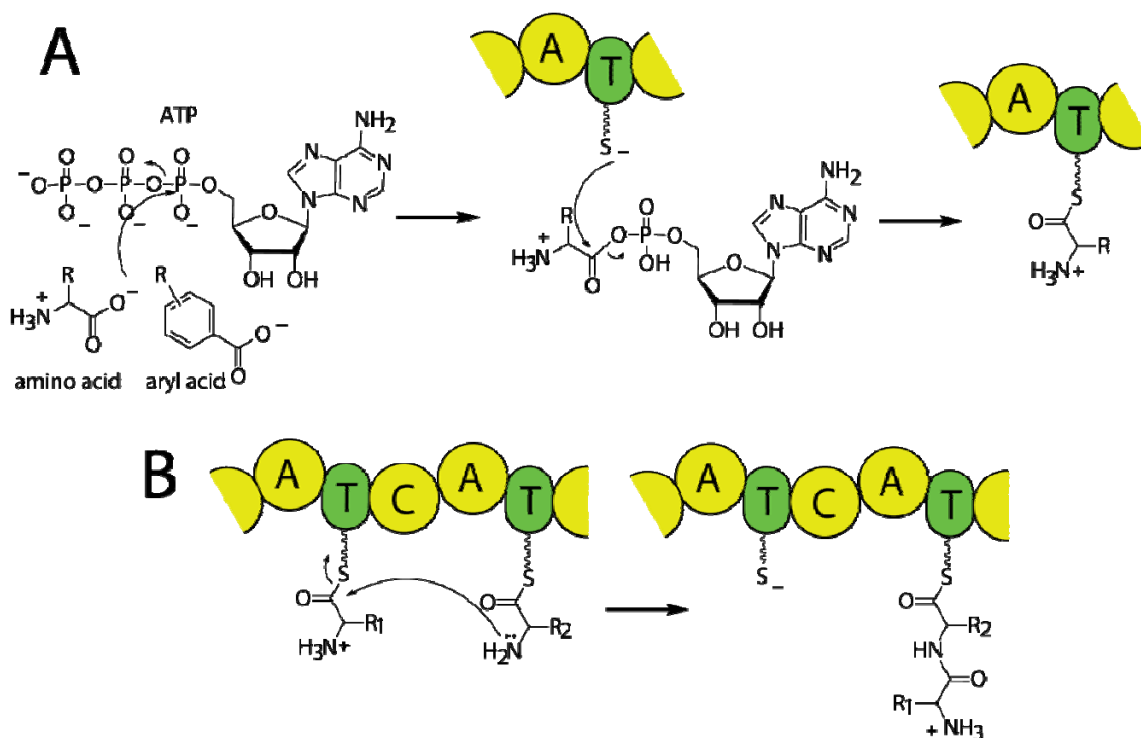


Figure 21. NRPS Chemistry.

(A) Chemistry of amino acid activation and loading a modular NRPS with starter units for NRPS construction, amino and aryl acids [35, 51]. (B) Chemistry of chain elongation on a modular NRPS.

Differences with the PKS model include the use of amino acids or aryl acids as units (**Figure 21A**), the peptidyl carrier protein (PCP) or thiolation (T) domain instead of the ACP, and ATP as the loading molecule for the unit in lieu of coenzyme A resulting in an AMP ester amino acid. A core NRPS module is comprised of three principle domains: the adenylation domain (A), the condensation domain (C), and the thiolation (T) domain. The initiation of the peptide begins in the A domain. The A domain is responsible for recognizing the appropriate amino acid and subsequently activating it with an ATP molecule to form the AMP ester, which is added to the T domain *via* a thioester linkage to the attached pantetheinyl arm (**Figure 21A**).

The elongation is catalyzed by the C domain. The amino group nucleophile of the neighboring aminoacyl thioester attacks the carbonyl group, resulting in a new peptide bond (**Figure 21B**). The molecule may finally be cut loose or cyclized by a terminal thioesterase (TE) or cyclization (Cy) domain, respectively. Nonribosomal peptides are often dimers or trimers of identical sequences chained together, cyclized, or even branched.

Additional modifying domains are found in NRPS biosynthesis for modification of or production of unnatural amino acids. These domains include epimerization (E) into D-amino acids, internal cyclization (Cy), oxidation (Ox), formylation (F), reduction (Red), and reduction (R) to terminal aldehyde or alcohol. The A domain is not limited to the proteinogenic amino acids, allowing for diverse NRPS products. Non-proteinogenic amino acids include D-amino acids, carry modifications like *N*-methyl and *N*-formyl groups, or are glycosylated, acylated, halogenated, or hydroxylated. Additionally aryl acids are also incorporated. The variety of NRPS products possible is quite large. Azinomycin B appears to involve the incorporation of at least 3 amino acids, although one could consider the naphthoate group as an aryl acid starting group. To understand this construction we turn to a well characterized NRPS based natural product with type A construction, the calcium dependent antibiotic.

CALCIUM DEPENDENT ANTIBIOTIC

A direct example of the type A NRPS model can be found in the biosynthesis of the calcium dependent antibiotic(s) (CDA) (**Figure 22**) produced by *Streptomyces coelicolor* A3(2). As one of the three main antibiotic products (the others being actinorhodin and undecylprodigiosin from this prototypical *Streptomyces*) CDA and its biosynthesis has been thoroughly investigated [63]. The production of the molecule(s) involves many common steps in NRPS-containing pathways, including, presumably azinomycin B. CDA is comprised of a cyclic lactone undecapeptide with an N-terminal 2,3-epoxyhexanoyl fatty acid side chain. CDA contains several D-configured and unusual amino acids including D-4-hydroxyphenylglycine, D-3-phosphohydroxyasparagine, and L-3-methylglutamic acid. Evaluation of azinomycin B indicates all 3 amino acids are unusual. The amino acids required for biosynthesis are tyrosine, aspartate, asparagines, tryptophan, threonine, glycine, serine, glutamate, and oxoglutarate [63]. Several modifications are necessary to produce various alterations found within CDA molecules. The combination of the possibilities at these positions results in the variation seen in CDA (**Figure 22**).

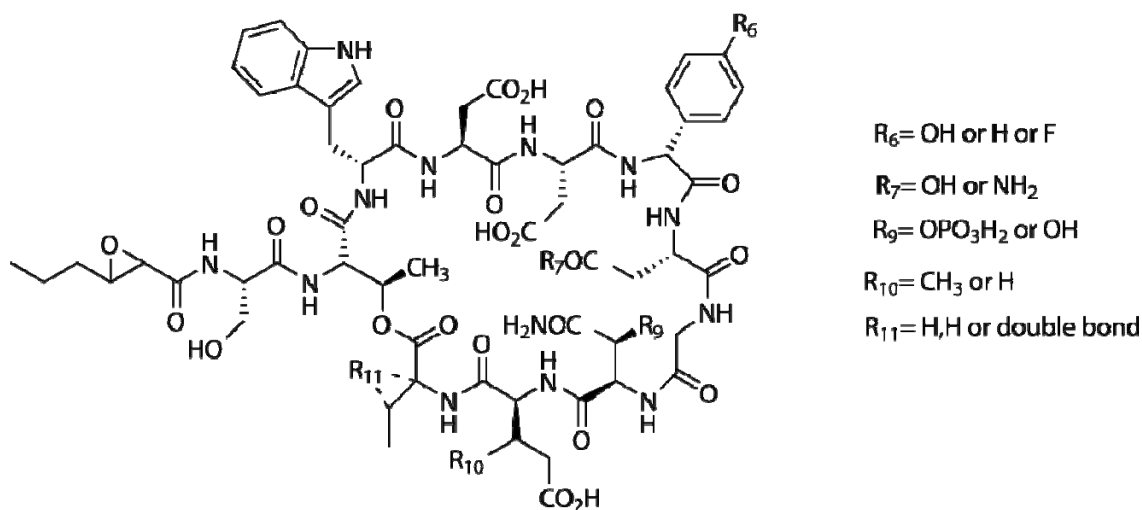


Figure 22. Structure of CDA, the Calcium Dependent Antibiotic(s), Produced by *Streptomyces coelicolor* A3(2).

Adapted from Micklefield *et al.* [64].

The construction of the NRPS portion of CDA begins with an unusual starter unit. The 2,3-epoxyhexanoyl fatty acid is initially condensed with the first amino acid, L-serine. The next amino acid added is L-threonine. Subsequent amino acids (D-tryptophan, L-aspartic acid, D-4-hydroxyphenylglycine) are added via the large multi-domain NRPS gene product of *cdaPS1*. L-aspartic acid, glycine, and D-asparagine are then incorporated by the NRPS gene product of *cdaPS2*. The subsequent incorporation of L-3-methylglutamic acid, and finally L-tryptophan, is guided by *cdaPS3*. This is illustrated in **Figure 23**. The epimerization units change the stereochemistry of three incorporated amino acids. The molecule is subsequently cyclized into a macrolactone.

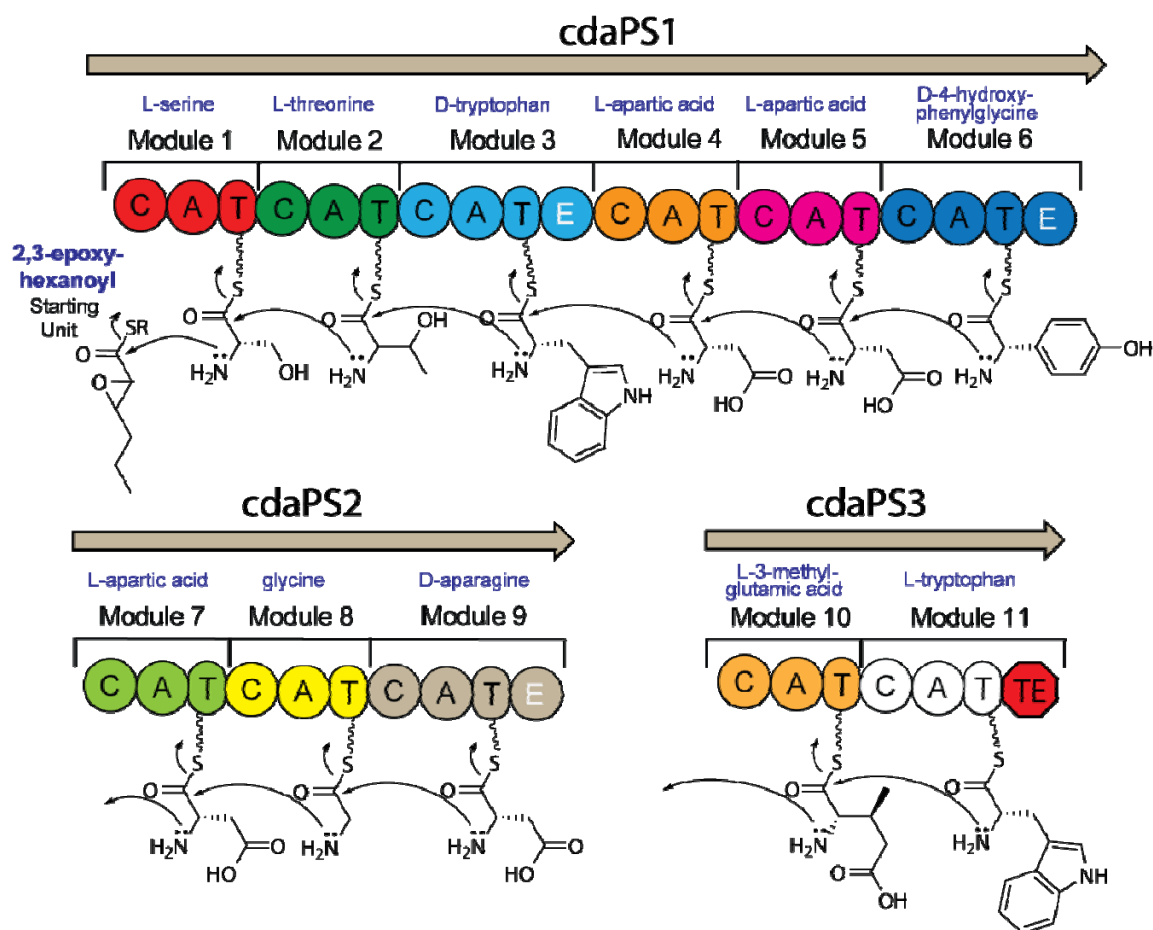


Figure 23. Modular Structure of the NRPS Portions of *Streptomyces coelicolor* Calcium Dependent Antibiotic Biosynthesis.

Adapted from Micklefield *et al.* [64].

MODIFICATIONS OF CDA REFLECTING NRPS CONSTRUCTION

Alterations and nonproteogenic amino acids enable NRPS natural products to evade the natural peptidases and may be at the very core of their activities. The nonproteogenic amino acids in CDA include 4-hydroxyphenylglycine and 3-methyl-glutamic acid (**Figure 24A** and **B**). These two amino acids are specifically produced by genes found in the CDA biosynthetic cluster [64]. Additional modifications occur after the decapeptide is produced, including oxidation of the asparagine residue, and subsequent phosphorylation (**Figure 24C**) [64].

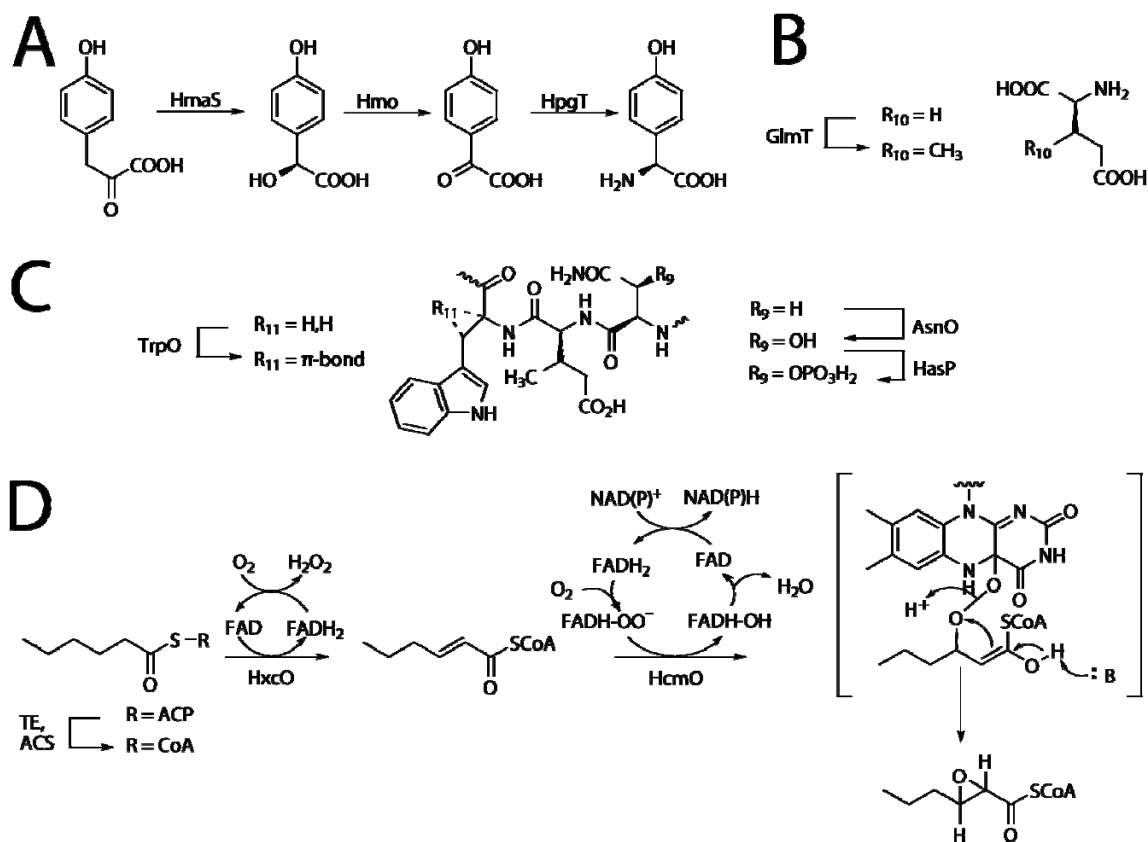


Figure 24. Modifications found in CDA.

(A) Biosynthesis of nonproteogenic amino acids 4-hydroxyphenylglycine and (B) 3-methyl-glutamic acid. (C) Modification of l-tryptophan and d-asparagine residues in CDA. (D) Formation of the trans-2,3-epoxyhexanoyl-coA CDA starting unit. Adapted from Micklefield *et al.*, 2002 [64].

The trans-2,3-epoxyhexanoyl-coA starting unit is produced specifically by genes in the gene cluster. The production of the six carbon chain results from fatty acid genes. These are then transferred from an ACP to the coenzyme A and subsequently oxidized to the enone by the FAD assisted HxcO seen in **Figure 24D**. The molecule is then epoxidized by HcmO, a monooxygenase [64].

Analysis of the gene cluster reveals groups of related genes, such as those for amino acid biosynthesis, fatty acid biosynthesis, regulation, resistance, as well as three NRPS genes, and several genes of unknown function (**Figure 25**) [64]. This clustering reflects the common arrangement of natural product genes.

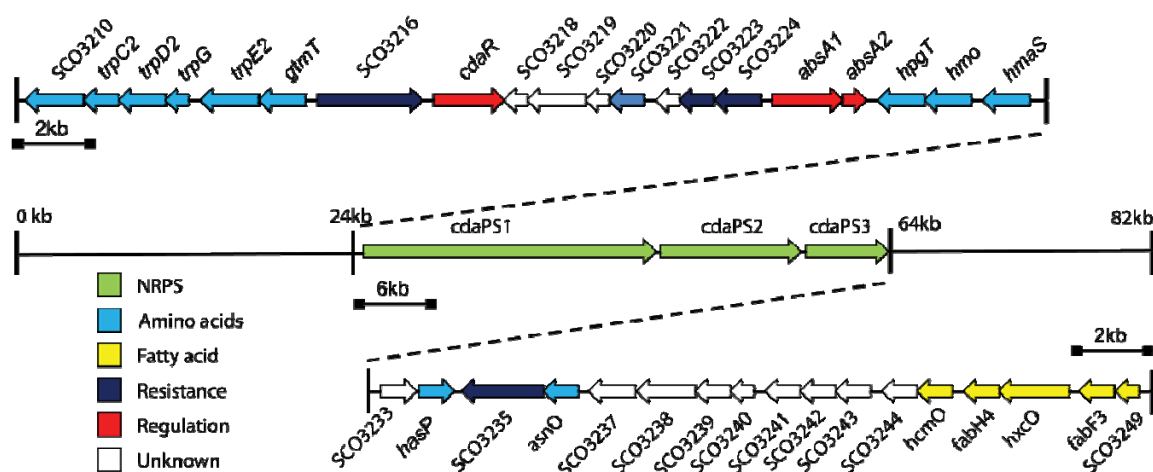


Figure 25. Diagram of the Gene Cluster Responsible for the Biosynthesis of CDA. Adapted from Micklefield *et al.* [64].

Additional modifications involved in the production of *Streptomyces coelicolor* A3(2)'s calcium dependent antibiotic offer an example of prototypical modifications in the production of natural products of hybrid origin. Azinomycin B also appears to have a similar composition, containing a non-PKS starting unit plus additional units with a modified amino acid appearance. Like CDA, the unit may be modified before or after incorporation into the growing chain. The curious azabicyclic unit is of particular interest as there are few parallels in natural product chemistry. **Figure 26** presents one possible arrangement of modules for the construction of the NRPS portion of azinomycin B.

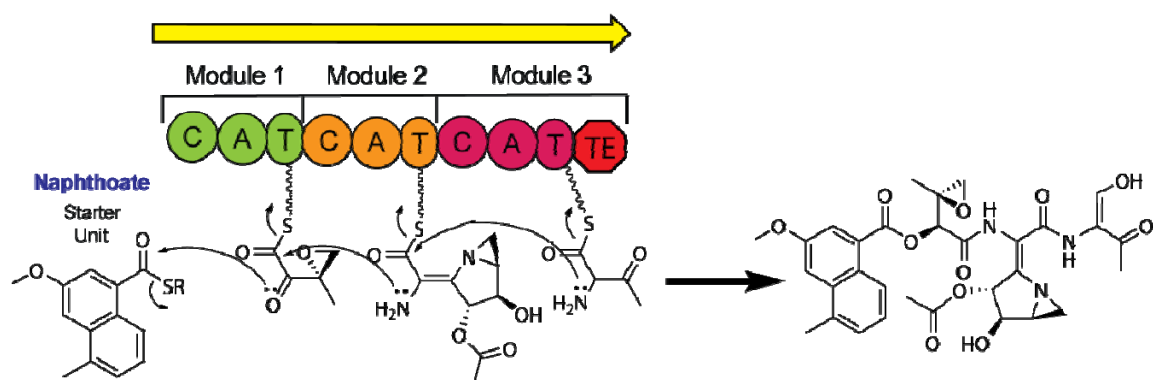


Figure 26. Possible Arrangement for the NRPS Portion of Azinomycin B.

PKS-NRPS HYBRID PATHWAYS

Considering the similarities involved in PKS and NRP biosynthesis, it is possible for the two systems to interact. In fact, the two may be viewed with the same basic logic. The individual units or domains within modules in the pathway may be viewed as “pearls on a string,” reflecting the PKS type 1 model. **Figure 27** illustrates the several types of domains that are found in either NRPS or PKS systems. Evaluation of azinomycin B would indicate that its biosynthesis likely has hybrid origins, with the left half portion reflecting PKS origins and the right half NRPS origins. There are many examples of such hybrid pathways.

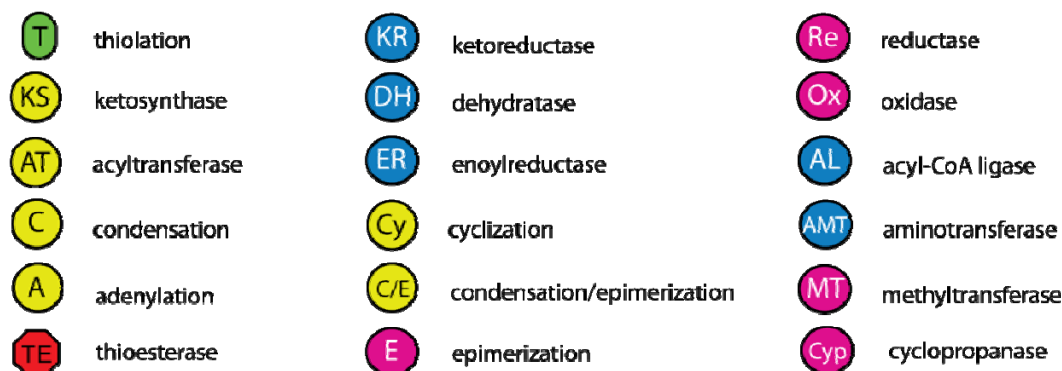


Figure 27. Key Domains Found in the NRPS-PKS Biosynthesis Which May be Involved in Azinomycin B Biosynthesis.

Adapted from Walsh *et al.* [51]. Core domains are seen in yellow, green, and red with dark letters. The additional modifying domains are seen in blue and pink with light colored letters.

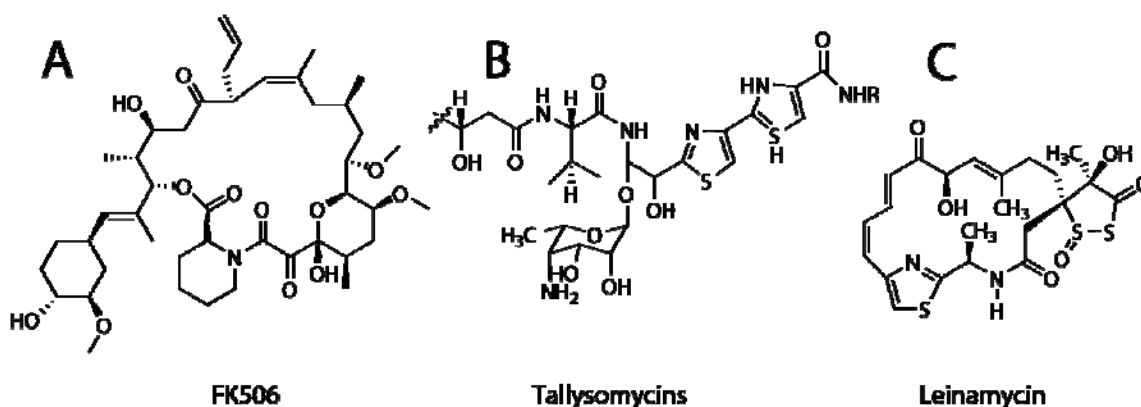


Figure 28. Examples of NRPS-PKS Natural Product Molecules.

(A) FK506 (B) Tallysomycins (C) Leinamycin. Adapted from Shen *et al.* 2005 [65].

Hybrid NRPS-PKS molecules include FK506, Tallysomycins, and leinamycin (**Figure 28**). FK506 is an immunosuppressive drug whose primary function is to reduce the risk of organ rejection following a transplant [66]. It was discovered from a soil bacteria fermentation screen, performed with *Streptomyces tsukubaensis* [66]. Tallymycins A and B are antibiotic/anticancer natural products [65]. Leinamycin, produced by *Streptomyces atroolivaceus* S-140, is a DNA alkylating agent [65].

TRADITIONAL METHODS OF BIOSYNTHETIC INVESTIGATION

There are several methods for approaching and deciphering the biosynthesis of a natural product such as azinomycin B. Isolation and characterization of the compound of interest is of paramount importance. Isolation and characterization usually occur as a result of a screen for biological activity. Once the active component is isolated, other components are also analyzed. This can be an important step in understanding the biosynthesis, as biosynthesis of many natural products is “leaky,” resulting in a number of molecules of related structure. This is attributed to evolutionary bet-hedging. The various molecules produced may have different positive attributes making the metabolic expenditure worth the price. Variation on molecular structure were shown earlier with the calcium dependent antibiotic’s variable structure. However, the very “leakiness” of the pathway yields insights into the biosynthesis of the molecule. Following isolation of the compound(s), a next logical step is to optimize culture conditions to achieve maximal metabolite production. With microorganisms this involves variations in media, temperature, oxygenation, and other factors. Once these conditions are firmly established, it sets the stage for direct inquiry of the pathway with isotopically labeled precursors (^2H , ^{13}C , ^{14}C , ^{15}N , ^{18}O , etc.). Stable isotopes, often ^{13}C or ^2H , can be employed to investigate molecules spectroscopically, usually with nuclear magnetic resonance (NMR) spectroscopy. If higher sensitivity is required, radioactive isotopes, often ^3H or ^{14}C , are used. Incorporation of “labeled” metabolic precursors or synthetic derivatives into the molecule yield greater insight into the molecule’s biosynthetic origin. Additionally, inhibitors can also be employed to query pathways.

Another approach to accessing biosynthetic pathways includes “fishing” experiments to isolate the proteins involved in the biosynthesis. These experiments use compounds attached to a solid support that mimic a portion of the natural product or molecule of interest to extract associated proteins from a cellular preparation of the producing organism. This technique is similar to a nickel affinity column to trap proteins with histidine tags. Isolation of these enzymes enables one to study the mechanisms of the biosynthesis in greater detail. In addition, one can

sequence the proteins involved, and reverse engineer a DNA probe to search for the original sequence in a genomic library of the targeted organism. Advances in gene sequencing and analysis have identified sequence commonalities in biosynthetic gene pathways. These sequence patterns enable investigators to search for similar unidentified pathways by design of degenerate DNA primers to probe genomic libraries for the desired pathway (PKS, NRPS, terpene, etc.). These probes are used to screen a prepared genomic library, often a library of substantial size such as a bacterial artificial chromosome (BAC), fosmid (FOS), or cosmid (COS) library. Additionally, with the recent reduction in cost of genome sequencing, a new option to researchers is to simply get the organism sequenced commercially. From the sequence information, in addition to known public databases, the sequence for the desired biosynthetic pathway may be discerned. This approach will increasingly be a starting point, but will not replace the previously mentioned techniques for elucidating the biosynthesis of the natural product of interest. This approach is currently being used in Dr. Coran Watanabe's group to investigate not only the azinomycin B biosynthesis, but myriad marine and terrestrial microorganisms producing natural products of interest.

STATEMENT OF PURPOSE

Natural products have long been of interest for a multitude of reasons. The azinomycins have been a target for total synthesis and have been evaluated for their mode of action due to the attractive anti-tumor and anti-biotic effects that these compounds exhibit. Interest in this molecule has now been redirected towards its biosynthesis. In parallel, the field of biosynthetic research in natural product chemistry has slowly shifted from a focus on the chemical characterization and synthesis towards the genes that result in the natural product's production. Analysis of the biosynthesis of the azinomycins and their unique construction may yield insights that allow access to an additional set of modules for the production of custom or combinatorially produced natural products. Ultimately, manipulation of the biosynthetic genes involved with azinomycin biosynthesis increases the available tools to apply towards medicinal ends.

CHAPTER II

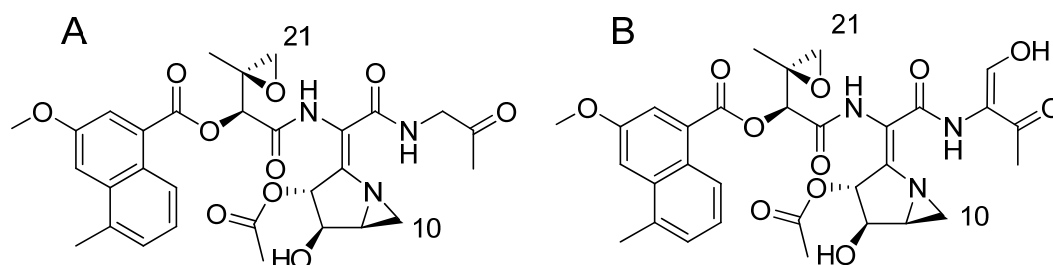
CELLULAR EFFECTS INDUCED BY THE ANTITUMOR AGENT
AZINOMYCIN B *

Figure 29. Structures of Azinomycin A and B.

INTRODUCTION

Azinomycins A and B (**Figure 29**) are naturally occurring anti-tumor agents that are among a small set of molecules that interact with DNA in the major groove [67]. Azinomycin B was originally isolated from *Streptomyces sahachiroi* in 1954 as carzinophilin A [1] and subsequently re-isolated from another *Streptomyces* strain, *S. griseofuscus*, in 1986, along with the related natural product azinomycin A [2]. The total synthesis of azinomycin A was achieved in 2001 [18], and numerous reports on synthetic approaches to these natural products have been reported [27, 68].

The seminal discovery that azinomycin B interacts with DNA, forming interstrand cross-links without prior activation, was achieved by Lown and Majumdar in 1977 [14]. Since this initial demonstration, a substantial number of *in vitro* studies have revealed both the regioselectivity and apparent sequence selectivity of the compound [69-73]. Azinomycin B interacts with the duplex DNA sequence 5'-d(PuNPy)-3' [71, 74], forming covalent interstrand

*Reprinted with permission from "Cellular Effects Induced by the Antitumor Agent Azinomycin B" by Kelly, G. T., Liu, C., Smith, R., 3rd, Coleman, R.S., and Watanabe, C. M. H., 2006. *Chemistry and Biology*, 13, 485-492, Copyright [2006] by Cell Press and Elsevier.

cross-links via the electrophilic C10 and C21 carbons of azinomycin and the N7 positions of suitably disposed purine bases [69] (**Figure 30**). Kinetic assays together with synthetic work further suggested that the monoalkylated product is formed first through reaction with the aziridine, followed by cross-linking with the epoxide. The highest levels of cross-linked product are attained with the DNA recognition sequence 5'-d(GGC·CCG)-3' [69] (**Figure 30**).

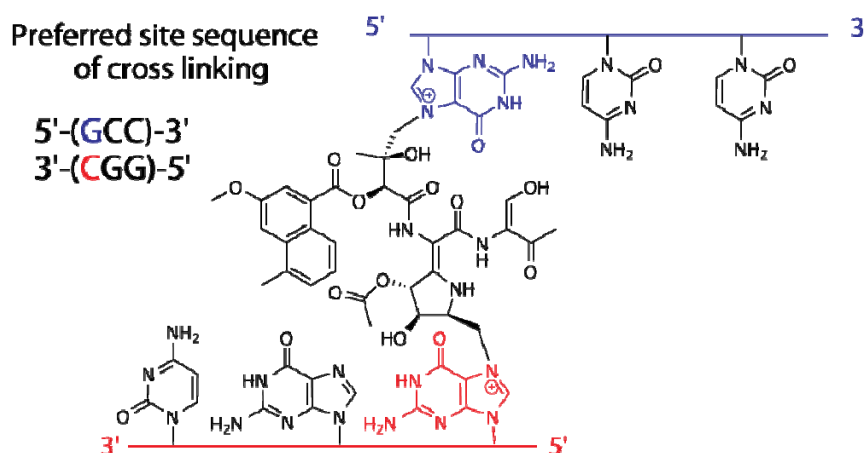


Figure 30. Azinomycin B DNA Cross-linking Preference.

In vitro incubations of azinomycin B with 15 base pair (bp) strands of double stranded DNA (here colored red and blue) revealed a preferred site of cross-linking as reported by Coleman, *et al.* [69].

Viscometry, fluorescence contact energy transfer, and DNA unwinding experiments to probe the role of the azinomycin naphthoate point to a non-intercalative binding (not stacking between DNA bases) mode for this group [69]. This is in contrast to the neocarzinostatin naphthoate, which despite structural similarity with the azinomycin naphthoate seen in **Figure 31**, has been demonstrated to exhibit an intercalative binding mode [75]. In support of these results, computer-modeling studies point to a non-intercalative binding mode for azinomycin B [74, 76]. These results, however, still leave unanswered the question of whether DNA is the relevant cellular target of this agent.

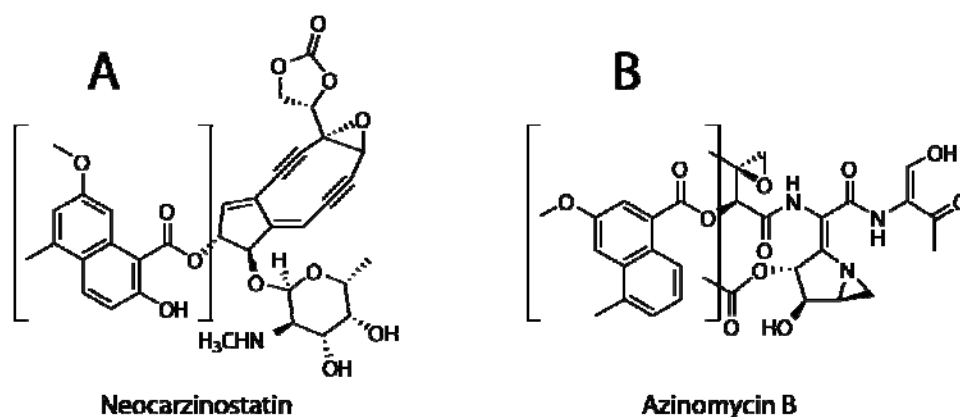


Figure 31. Neocarzinostatin and Azinomycin B. Two DNA alkylating agents that contain a naphthoate group (A) neocarzinostatin and (B) azinomycin B. The brackets highlight the naphthoate portions of the molecules.

Despite extensive work to characterize the interaction of azinomycin B with its DNA receptor *in vitro*, data on the *in vivo* actions of the molecule are limited to the initial description of its cytotoxicity in microorganisms [1, 7] and in early phase clinical investigations in Japan [3, 77]. In Ishizeki *et al.*'s report, the natural products were shown to exhibit potent cytotoxic activity with a half maximal inhibitory concentration, IC₅₀, of 0.07 $\mu\text{g/mL}$ for azinomycin A (**Figure 29A**) and 0.11 $\mu\text{g/mL}$ for azinomycin B (**Figure 29B**) against the leukemia cell line L5178Y. Azinomycin B (**Figure 29B**) provided a 193% increased life span, ILS, at 32 $\mu\text{g/kg/d}$ (3/7 survivors) against an intraperitoneal, IP, implanted P388 leukemia mouse model. In the same system, mitomycin C exhibited a 204% ILS, but at 1 mg/kg/d. This reinforced interest in this compound as a legitimate pharmaceutical target. A preliminary clinical investigation by Shimada, *et al.* with carzinophilin (azinomycin B (**Figure 29B**)) gave favorable results in 36 cases of malignant neoplasms [3]. Intravenous injection of a solution of azinomycin B resulted in a better treatment mode than subcutaneous or intramuscular injection due to side effects including induration, a hardening of an area of the body as a reaction to inflammation, hyperemia, or neoplastic infiltration, necrosis, and ulcer. Remarkable efficacy was observed in a case of squamous cell carcinoma (a form of skin cancer). Local administration of azinomycin B led to rapid reduction of the ulcer surface and eventual disappearance of the tumor cells [3].

In this chapter, the first evidence for *in vivo* DNA damage by azinomycin B using cellular localization studies and transcriptional profiling experiments across the yeast (*Saccharomyces cerevisiae*) genome is presented. The results suggest that the well-established

DNA alkylation and cross-linking exhibited by this agent *in vitro* is likely the biologically relevant lesion *in vivo*.

RESULTS AND DISCUSSION

In the original 1987 report, azinomycin B was found to have no biological effect against yeast [77]. We have examined azinomycin B against cultures of *Saccharomyces cerevisiae* and observed cytotoxic activity at moderate concentrations ($ED_{50} = 10 \mu\text{g/mL}$). In pharmacology, effective dose is the minimal dose that produces the desired effect of a drug. The effective dose is often determined based on analyzing the dose-response relationship specific to the drug. The dosage that produces a desired effect in half the test population is referred to as the ED_{50} , for “effective dose, 50%.” In this chapter, yeast, as a eukaryote, is used as a model organism to establish the cellular origin of cytotoxicity exhibited by this agent.

CELLULAR LOCALIZATION OF AZINOMYCIN B

(THE AUTHOR)*

In efforts to substantiate the purported biological role of azinomycin B as a DNA cross-linking agent, we initially examined the localization pattern of the agent in yeast using fluorescence microscopy. In earlier work, Coleman and co-workers reported the following Ultraviolet/visual spectrum for the azinomycin naphthoate: λ_{max} (MeOH/H₂O, 1:1) 240 (ϵ 34,000), 298 (ϵ 6,300), 338 nm (ϵ 7,400); and described fluorescence contact energy transfer experiments where emission by the naphthoate was observed at 435 nm [69]. This fluorescence range is comparable to that exhibited by the fluorescent stain DAPI, which has excitation and emission wavelengths of 345 nm and 455 nm, respectively.

Evaluation of cellular localization in live cells required controls to ensure reliable results in addition to simply treating with azinomycin B (**Figure 32A**). Since azinomycin B is dissolved in ethanol for treatment, treatment with ethanol only (**Figure 32B**) was used as a negative control. To ensure specificity, the naphthoate fragment of azinomycin (**Figure 32C**) was synthesized by Dr. Chaomin Liu as a second control. Propidium iodide (PI) (**Figure 32D**) binds to DNA by intercalating between the bases with little or no sequence preference and with a stoichiometry of one dye per 4–5 base pairs of DNA. As propidium iodide is not taken in by live cells, treatment is used upon killed or membrane compromised cells.

* Denotes major contributor(s) to each section.

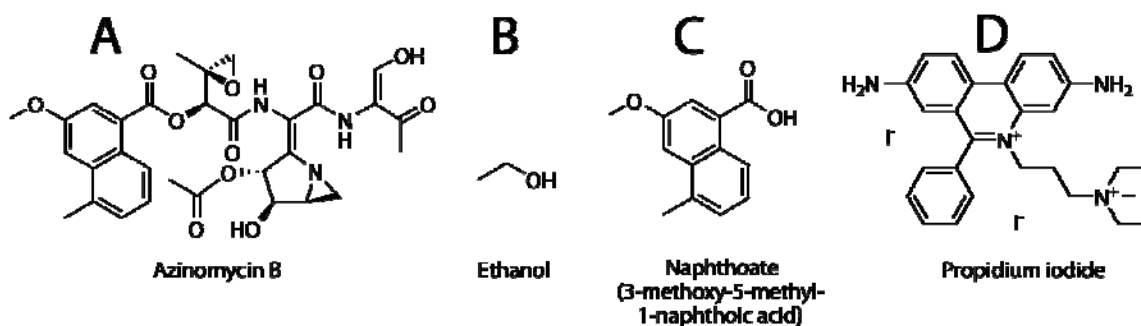


Figure 32. Molecules Used in Cellular Localization Experiments.

In addition to (A) azinomycin B a treatment of (B) ethanol (negative control) and (C) fluorescent naphthoate group of azinomycin were used to evaluate cellular localization. (D) Propidium iodide was used as a control to identify patterning of nuclear staining in ethanol fixed (killed) yeast cells.

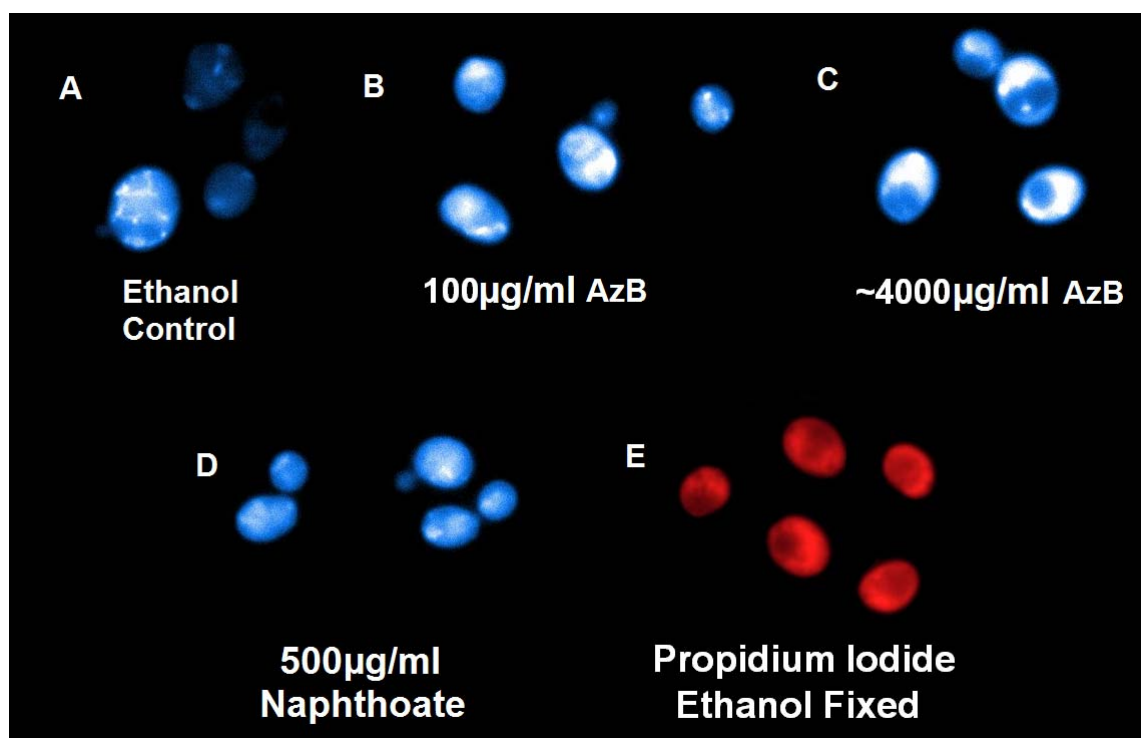


Figure 33. Cellular Localization of Azinomycin B in Yeast Cells.

Evaluation of cellular localization of azinomycin B included: (A) ethanol at 50 $\mu\text{g}/\text{mL}$ (B) azinomycin B at 100 $\mu\text{g}/\text{mL}$ (C) higher treatment of ~4000 $\mu\text{g}/\text{mL}$ ethanol (negative control) and (D) fluorescent naphthoate group at 500 $\mu\text{g}/\text{mL}$ (E) Propidium iodide staining in ethanol fixed (killed) yeast cells treated. Yeast cells are seen here at 1000X magnification.

At 1000X amplification, yeast treated with azinomycin B exhibited localized binding and fluorescence (**Figure 33**). *Saccharomyces cerevisiae* were treated with azinomycin B (100

$\mu\text{g/mL}$ and a blast treatment of $4000 \mu\text{g/mL}$; **Figure 33A and B**, respectively) or the naphthoate core of azinomycin (DNA non-binder; $500 \mu\text{g/mL}$; **Figure 33D**), and were compared to ethanol-fixed yeast cells (**Figure 33C**), and fixed cells stained with the DNA intercalator propidium iodide (1 ng/mL ; **Figure 33E**). After incubation for 4 h, cells were centrifuged and re-suspended in phosphate buffered saline. Cells were viewed with a Zeiss fluorescence microscope and the images captured digitally, under constant image capture conditions.

The pattern of fluorescence exhibited by azinomycin B paralleled that exhibited by propidium iodide, where staining of the nuclear region of the cell was observed (*i.e.*, the area of the cell that surrounds the central body or vacuole storage organelle of yeast). In contrast, control cells treated with ethanol showed diffuse background fluorescence (**Figure 33C**), as did yeast cells treated with the azinomycin naphthoate (a DNA non-binder; **Figure 33D**). These results provide evidence that azinomycin B is concentrated in the cell nucleus, which would be expected for an agent that interacts covalently with duplex DNA.

DNA DAMAGING EFFECT OF AZINOMYCIN B

(COLLABORATION BETWEEN DR. CORAN M. H. WATANABE AND THE AUTHOR)

The targeting of nucleic acids, in particular DNA, by azinomycin B in live yeast cells was further corroborated by evaluation of yeast DNA damage that resulted with azinomycin exposure. Genomic DNA isolated from yeast treated with the natural product demonstrated increased shearing of the DNA as compared to yeast cells incubated with ethanol alone (**Figure 34**). In this gel, a dose dependent response in DNA damage and shearing was observed. This damaged or increasingly fragile DNA isolated from treated yeast cells indicates clear effects attributable to azinomycin B treatment.

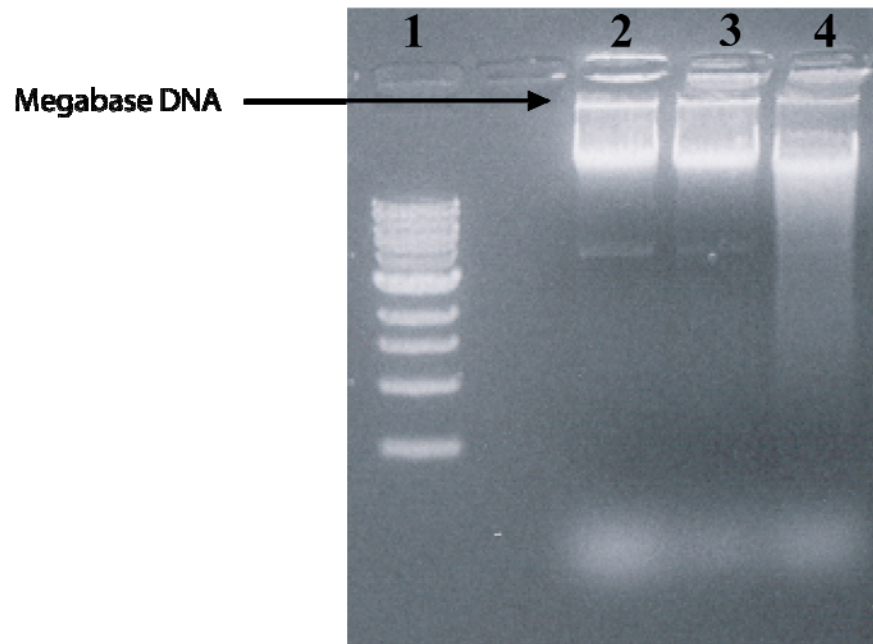


Figure 34. Yeast DNA Damaged Observed on an Agarose Gel.
Analytical 1% agarose gel stained with SYBR green DNA dye visualized using ultraviolet backlight: (1) 1kb DNA ladder, (2) ethanol control, (3) 10µg/mL azinomycin B, and (4) 100µg/mL azinomycin B.

TRANSCRIPTIONAL RESPONSE AND CELL CYCLE ANALYSIS

(COLLABORATION BETWEEN DR. CORAN M. H. WATANABE AND THE AUTHOR)

Transcriptome analysis, essentially monitoring the expression of mRNA produced by a cell population or tissue sample, has been a recent innovation only possible with the sequencing of the genome of target organisms. The principle behind microarray analysis is based upon using sets of arrays containing hundreds of thousands of chemically synthesized oligonucleotides that have homology (match) or non-specific homology (mismatch) to specific gene transcripts. The match refers to a 25 nucleotide oligomer that is directly homologous to sequence in the gene of interest. The mismatch is identical to the match, except for a single base pair difference at the 13th position. Total RNA is isolated from the sample of interest using a hot phenol method and reverse transcription used to make cDNA, which is subsequently made into biotin labeled cRNA via *in vitro* transcription (**Figure 35**). The biotinylated cRNA is fragmented and subsequently hybridized to the microarray plate where the fragmented, biotinylated cRNA hybridizes with the probe sets or DNA imprinted upon the chip surface. The use of sets of oligonucleotides for each open reading frame (ORF) provides redundancy in detection and analysis of data, helps alleviate false positives by cross hybridization, and ensures that all probes do not have to bind identically

to obtain quantitative information. The light intensity of the streptavidin fluorescent stain, which binds tightly to the biotinylated cRNA, highlights areas of cRNA hybridization to the gene chip probes. The intensities of the match and mismatch are compared to ensure proper true hybridization. The data for the sets are evaluated and intensity levels compared to control levels. It is important to note that, while a high correlation between the relative levels of transcripts of particular genes often corresponds to higher expression of the end product, what we are able to measure using transcriptional array profiling gives us insight only to the level of mRNA expression.

The effect of azinomycin B on the yeast transcriptome was examined using Affymetrix oligonucleotide microarrays (Yeast S98 Array). The GeneChip® Yeast Genome S98 Array contains probe sets for approximately 6,400 *Saccharomyces cerevisiae* (S288C strain) genes identified in the Saccharomyces Genome Database by December 1998. This array also contains approximately 600 additional probe sets representing putative ORFs identified by SAGE analysis, mitochondrial proteins, TY proteins, plasmids, and a small number of ORFs for strains other than S288C. ORFs recognized are detailed on both SGD (*Saccharomyces* Genome Database) and MIPS (Munich Information center for Protein Sequences) databases. The current Affymetrix oligonucleotide microarrays for yeast is the yeast Genome 2.0 Array which contains probe sets to detect transcripts from both *Saccharomyces cerevisiae* and *Schizosaccharomyces pombe*, the two most commonly studied species of yeast.

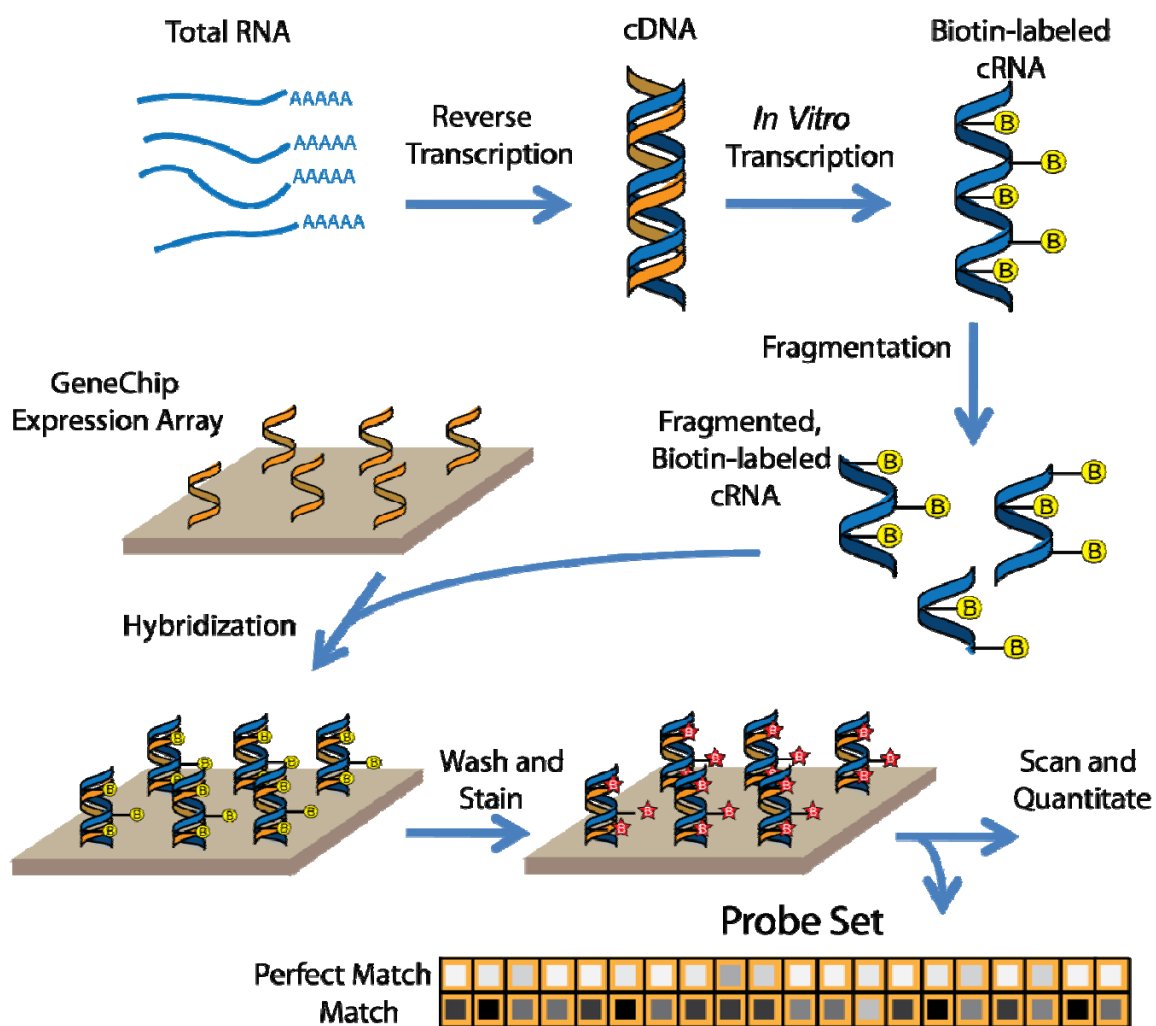


Figure 35. GeneChip DNA Microarray Gene Expression Monitoring.

Data were obtained at two concentrations of azinomycin B (**Table 1** and **Table 2**). Drug treatment was carried out in duplicate at the ED_{50} concentration (10 $\mu\text{g}/\text{mL}$) and 10-fold higher concentration (100 $\mu\text{g}/\text{mL}$) for 6 H. The data in **Table 1** and **Table 2** are remarkably consistent with the proposed mode of action of azinomycin B as a DNA-damaging agent. Differential mRNA gene expression (≥ 2 -fold) was observed in 47 transcripts out of approximately 6200 genes that comprise the yeast genome. Approximately 57% of those differentially expressed transcripts were nuclear-related, including genes involved in DNA repair, DNA maintenance, cell cycle control, and genes for transposons. The remaining genes included ribosomal proteins, mitochondrial genes, transporter proteins, and a few unclassified genes.

Table 1. Up-regulated Gene Expression in Response to Azinomycin B Treatment.

Up-Regulated Genes				Fold Change	
Probe Set	Gene Name	Common Name	Gene Description	Treatment	
				10	100
				µg/mL	µg/mL
Nuclear/DNA Damage					
4045_s_at	YIL066C	RNR3	Ribonucleotide reductase, one of two large subunits	2.5	-
5643_at	YER070W	RNR1	Ribonucleotide reductase, one of two large regulatory subunits	-	3
5626_at	YER095W	RAD 51	RecA homolog, RAD 51, involved in recombinational repair	-	3
5970_at	YDR501W	PLM2	PLM2 plasmid maintenance	2.6	9
3262_at	YGLCTAU3	Ty4 LTR	YGLCTAU3 Ty4 LTR	-	14.6
3200_l_at	YHLWDELTA2	Ty1 LTR	YHLWDELTA2 Ty1 LTR	-	23.7
10222_at	YLR103C	CDC45	Chromosomal DNA replication protein	-	6.3
7352_at	YBL009W	ALK2	Protein kinase; phosphorylated in response to DNA damage	-	4.1
3058_s_at	YHR015W	MIP6	DNA helicase and DNA dependent ATPase involved in DNA repair	-	3.2
8639_at	VOL104C	NDJ1	Involved in meiotic chromosome segregation, might stabilize homologous DNA interactions at telomeres	-	4.3
5365_at	YFR023W	PES4	Poly(A) binding protein, suppressor of DNA polymerase epsilon mutation, similar to Mip6p	-	3.5
6293_at	YDR191W	HST4	Homolog of SIR2	-	9.08
Cell Signaling/Cell Cycle					
9293_at	YML058W-A	HUG1	Protein involved in the Mec1p-mediated checkpoint pathway that responds to DNA damage or replication arrest, transcription is	16	73
5108_at	YGL089C	MF(ALPHA)2	α-mating factor	2.1	5.7
8028_at	YPL267W	ACM1	Cell cycle regulated protein of unknown function	-	4.18
6021_f_at	YDR461W	MFA1	a-factor mating pheromone precursor	-	10.3
6585_at	YDL101C	DUN1	Cell-cycle checkpoint serine-threonine kinase required for DNA damage-induced transcription of certain target genes	-	3.7
10164_at	YLR183C	TOS4	Transcription factor induced in G1, binds to promoter in the cell cycle	-	21.6
Ribosomal Proteins					
7190_l_at	YBR189W	RPS9B	Ribosomal protein S9B (S13)(rp21)YS11)	-	8.6
7191_f_at	YBR189W	RPS9B	Ribosomal protein S9B (S13)(rp21)YS11)	-	7.1
6069_l_at	YDR418W	RPL12B	Ribosomal protein L 12B (L15B)(YL23)	-	3.3
5076_f_at	YGL076C	RPL7A	Ribosomal protein L7 A(L6A)(rp11)(YL8)	-	4.1
11237_at	YJL189W	RPL39	Ribosomal protein L39(L46)(YL40)	-	4.7
11235_at	YJL191W	RPS14B	Ribosomal protein S14B (rp59B)	-	6.4
10068_l_at	YLR264W	RPS28B	Ribosomal protein S28B(S33B)(YS27)	-	8.3
9497_l_at	YMR143W	RPS16A	Ribosomal protein S16A (rp61R)	-	4.5
9006_s_at	YNL162W	RPL42A	Ribosomal protein L42A(YL27)(141A)	-	4.5
9075_at	YNL227C	JJJ1	Co-chaperone that stimulates the ATPase activity of Ssa1p, required for a late step of Co-chaperone that stimulates the ATPase activity of Ssa1p, required for a late step of ribosome	-	6.6
Transport					
7792_at	YPL051W	ARL3	GTPase of the Ras superfamily required to recruit Arl1p to the	-	3.8
Unclassified Genes					
7697_l_at	YPR077C		Questionable ORF, gene function unknown	-	4.3
4854_at	YGR153W		Hypothetical protein, uncharacterized	-	4.4
49R1_at	YGR035C		Hypothetical protein, potential Cdc28p substrate	-	6.1

Table 2. Down-regulated Gene Expression in Response to Azinomycin B Treatment.

Down-Regulated Genes				Fold Change	
Probe Set	Gene Name	Common Name	Gene Description	Treatment	
				10	100
				$\mu\text{g/mL}$	$\mu\text{g/mL}$
Nuclear/DNA Damage					
3310_s_at			YERWDELTA18 Ty1 LTR	-	-5.8
4692_f_at			TY element transposition	-	-5.9
7513_f_at			TY element transposition	-	-4.7
8752_f_at			TY element transposition	-	-5.7
11323_at	YAL001C	TFC3	Transcription factor tau (TFIIIC) subunit 138	-3.2	-
3248_s_at	YGR109W-B	TYA Gag TYB Pol	TYA Gag and TYB Pol genes, DNA and RNA binding, RNA dependent DNA replication, transferase activity	-3	-
3712_s_at	YNRCTY1-3		Full length Ty1, transposon	-3.9	-
3913_s_at	YARCTY1-1		Full length Ty1, transposon	-3.6	-
Cell Signaling/Cell Cycle					
2350_s_at	YDR457W	TOM1	Ubiquitin ligase, required for G2/M transition	-3.2	-
Transport					
4842_at	YGR142W	BTN2	Involved in intracellular protein transport	-3.6	-
2642_s_at	YOR153W	PDR5	Transporter, exhibits nucleoside triphosphatase activity	-3.9	-
2643_s_at	YOR153W	PDR5	Transporter, exhibits nucleoside triphosphatase activity	-4	-
Mitochondrial					
10934_at	YJR095W	SFC1	Mitochondrial succinate-fumarate transporter, transports succinate into and fumarate out of the mitochondrion; required	-	7.8
5679_at	YER024W	YAT2	Similarity to carnitine O-acetyltransferase Yat1p	-	4
4005_at	Q0045	COX1	Cytochrome C oxidase subunit I	-	7.2

The transcriptional array results were compared with transcriptional array results from other known DNA damaging agents calicheamicin γ_1^1 and methyl methanesulfonate (MMS). Transcriptional array profile studies involving yeast and calicheamicin γ_1^1 were performed by the author's primary research advisor as reported in Watanabe *et al.*, 2002 [78]. Calicheamicin γ_1^1 is an antibiotic including an unprecedented enediyne "warhead" region with a safety catch trisulfide region to prevent premature misfiring of the warhead. The adjacent oligosaccharide/aromatic portion of the molecule serves as a guide for the high sequence selectivity of this agent for DNA, similar to azinomycin B. After reductive cleavage of the polysulfide and formation of a dihydrothiophene anchor, the enediyne moiety reorganizes itself following the dicta of Bergman cyclization, to produce C2 from C1 (**Figure 36**) [79]. The 1,4-diyl in C2 cleaves double stranded DNA through a radical process.

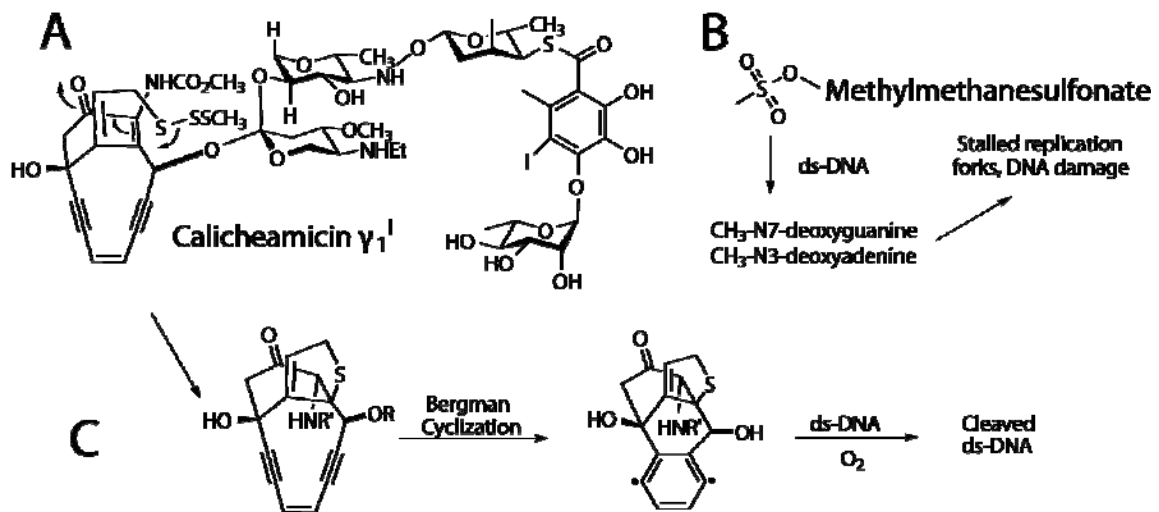


Figure 36. DNA Damaging Agents Used in Previous Studies with Affymetrix Oligonucleotide Microarrays, GeneChip® Yeast Genome S98 Array.

(A) Calicheamicin γ_1^I and (B) methyl methanesulfonate (MMS) are DNA damaging agents that showed similar DNA damage response, but not similar TY element gene changes observed with azinomycin B treatment. MMS is a DNA methylating agent. (C) Calicheamicin γ_1^I acts via a “warhead” to result in a radical induced double strand cleavage of DNA. Adapted from Wilson and Danishefsky, 2007 [79].

MMS methylates DNA on N7-deoxyguanine and N3-deoxyadenine. Originally, this action was believed to directly cause double-stranded DNA breaks, because homologous recombination-deficient cells are particularly vulnerable to the effects of MMS [80]. However, it is now believed that MMS stalls replication forks, and cells that are homologous recombination-deficient have difficulty repairing the damaged replication forks [80]. Comparing results of previous mode of action studies of these DNA damaging agents will yield further information about the *in vivo* actions of azinomycin B.

Among the nuclear effects, Ty elements were largely affected with azinomycin treatment. Another example of a eukaryotic transposable element is the Ty element of yeast. This element has several features that are unique, and it appears to resemble a primitive retrovirus [81]. A retrovirus is an RNA virus that, after being uncoated in the host cell, converts its RNA to a DNA copy by the enzyme reverse transcriptase. This enzyme is encoded by the retroviral polymerase gene. The DNA copy of the retrovirus is inserted into the eukaryotic genome, and it remains there as a provirus until it is excised and undergoes transcription to produce new viral particles [81]. While the expression of Ty4 LTR (YGLCTAU3) and Ty1 LTR (YHLWDELTA2) were up-regulated by a remarkable 15- and 24-fold, respectively, most transposition elements (a total of 7) were repressed 3- to 6-fold. LTR-retrotransposons have been

extensively studied in *Saccharomyces cerevisiae*, and five distinct families have been identified in this organism, designated Ty1, Ty2, Ty3, Ty4 and Ty5 [82]. The Ty elements transpose through an RNA intermediate by reverse transcription [83]. While differential expression of these genes could reflect a general cellular stress response, differential expression was not observed with other DNA damaging agents including the DNA alkylating agent methyl methanesulfonate and the DNA cleaving agent calicheamicin γ_1 I [78] (**Figure 36**). Moreover, recent studies have shown that when DNA replication is compromised in yeast, Ty elements constitute a preferred site for double-strand DNA breaks, analogous to fragile sites observed in mammalian chromosomes [84].

Additionally, classification and correlation of the majority of the gene changes revealed activation of genes in the MEC1 checkpoint or sensory pathway involved in DNA double-strand break repair (**Figure 37**). DUN1, a serine-threonine kinase required for DNA damage-induced transcription, plays a pivotal role in the MEC1 pathway and was enhanced in its expression by 4-fold. The cell cycle checkpoint protein induces G2/M arrest after DNA damage and controls post-replicative DNA repair [85]. In accordance with this, we observed down-regulation of TOM1 (YDR457W), a ubiquitin ligase required for the G2/M transition [86, 87]. Down-regulation implies that the transition from G2 to M was halted at this transition or during S phase. The yeast pheromones α -mating factor and a-mating factor were up-regulated 6- and 10-fold in expression. Both pheromones act by G1 phase synchronization of cell populations in preparation for mating [88]. The expression of MF(ALPHA)2 (YGL089C) was up-regulated 2-fold and 6-fold at 10 μ g/mL and 100 μ g/mL, and MFA1 (YDR461W) was up-regulated 10-fold. Cells respond to these pheromones during conjugation and cellular fusion, and they interact to induce cell cycle arrest [89, 90]. Tos4 (TLR183C), a transcription factor that binds promoter regions of genes involved in pheromone response and cell cycle, was up-regulated 22-fold at 100 μ g/mL. Expression of TOS4 is induced in G1 by bound SBF (Swi4-Swi6 cell cycle box binding factor) [91, 92]. The SBF factors bind the promoters of genes with roles in G1/S events including DNA replication, bud growth, and spindle pole complex formation, as well as the general activities of mitochondrial function, transcription, and protein synthesis [93]. DUN 1, up-regulated at 100 μ g/mL 3-fold, has also been shown to regulate the expression of HUG1 (YML058-A). HUG1 is a protein involved with the DNA damage checkpoint response, controlling replication arrest; it was up-regulated 16-fold and 73-fold at 10 μ g/mL and 100 μ g/mL, respectively [94].

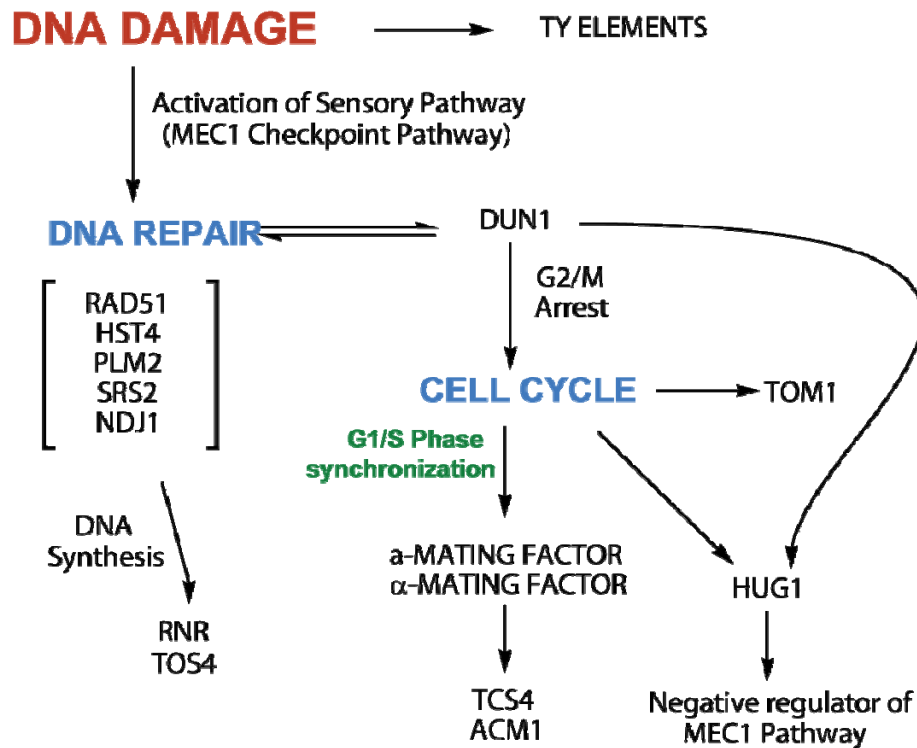
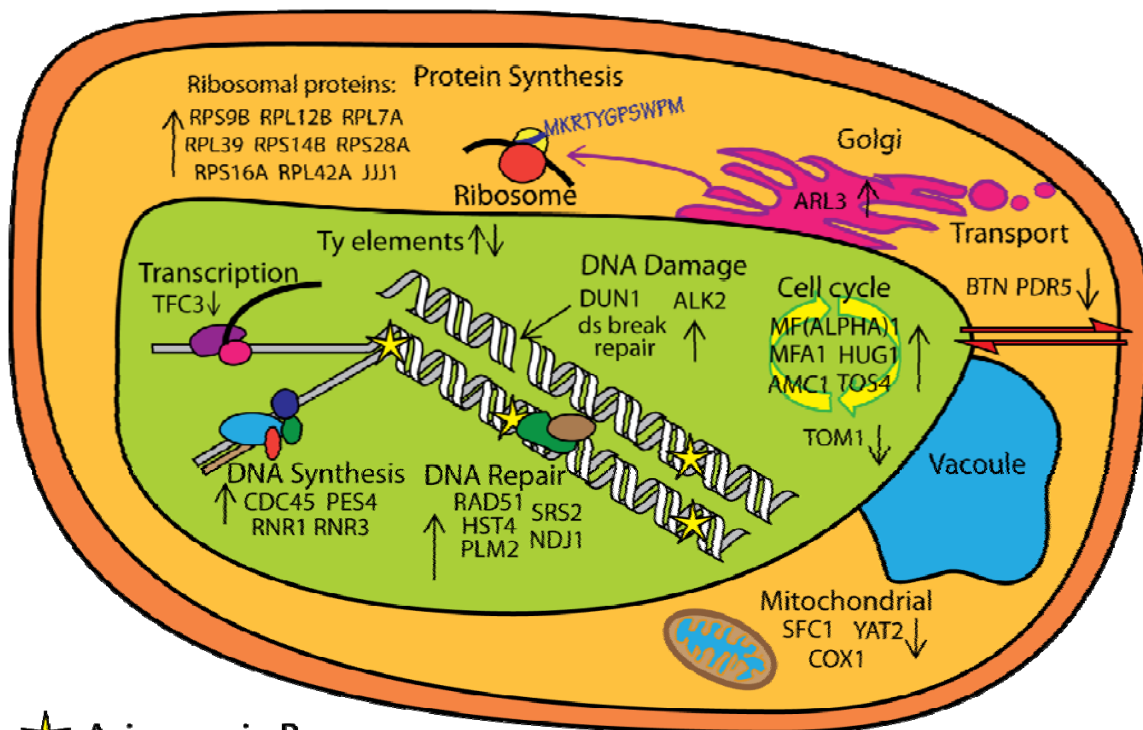


Figure 37. Diagram of Gene Changes Observed from Azinomycin B Treatment.

Similarly, DUN1 has been shown to regulate double strand break repair, resulting in activation of DNA damage repair genes, a major mechanism to providing genomic stability. Critical DNA repair genes were up-regulated in response to azinomycin B treatment. The DNA strand exchange protein RAD51 (YER095W), which is involved in recombinational repair of double-strand breaks [95], was enhanced in expression by 3-fold at 100 $\mu\text{g}/\text{mL}$. Deletion of this gene has been demonstrated to give rise to the accumulation of double-strand breaks, and the resulting lesions are both radiation-sensitive and defective in gene conversions [96]. PLM2 (YDR501W), a transcription factor involved with plasmid stability and maintenance, was up-regulated in its expression, exhibiting a dose dependent response [91]: mRNA expression of this gene product was enhanced almost 3-fold and 9-fold at 10 $\mu\text{g}/\text{mL}$ and 100 $\mu\text{g}/\text{mL}$, respectively. HST4 (YDR191W), a member of the SIR2 family of protein deacetylases [91], was increased in expression 9-fold at 100 $\mu\text{g}/\text{mL}$. This protein has a variety of biological roles, including double-strand break repair, silencing of telomeres, cell cycle progression, radiation resistance, genomic stability, and involvement in short-chain fatty acid metabolism [97]. Likewise, expression of MIP6 (YHR015W), a DNA helicase and DNA dependent ATPase involved in DNA/double

strand break repair by non-homologous end-joining [98, 99], was up-regulated more than 3-fold at 100 $\mu\text{g}/\text{mL}$. ALK2 (YBL009W), a protein with strong similarity to the DNA damage response element, was enhanced 4-fold at 100 $\mu\text{g}/\text{mL}$ azinomycin B.

Genes involved in DNA synthesis and replication were also affected by azinomycin exposure, consistent with the DNA damage and cross-linking effects demonstrated for the agent *in vitro*. For example, the expression of the chromosomal DNA replication protein CDC45 (YLR103C) [100, 101] was up-regulated more than 6-fold at 100 $\mu\text{g}/\text{mL}$. The expression of ribonucleotide reductase subunits RNR1 and RNR3 were up-regulated 3-fold at 100 $\mu\text{g}/\text{mL}$ and 2.5-fold at 10 $\mu\text{g}/\text{mL}$. These subunits comprise components of the ribonucleotide-diphosphate reductase (RNR) large subunit, which catalyzes the rate-limiting step in dNTP and DNA synthesis, and which is tightly regulated by DNA replication and DNA damage checkpoint pathways [102]. DUN1 null mutants, for example, have been shown not only to be defective in DNA damage repair, but also to be defective in DNA damage-responsive induction of RNR genes.



★ Azinomycin B

Figure 38. Illustration of the Damage and Induction of Observed Gene Expression in Response to Azinomycin B Exposure in an Example Yeast Cell in S Phase.

Figure 38 illustrates the gene changes observed by the transcriptional array profiling as they are related in a yeast cell. Much of the information about the genes was initially gathered from SGD, *Saccharomyces* Genome Database.

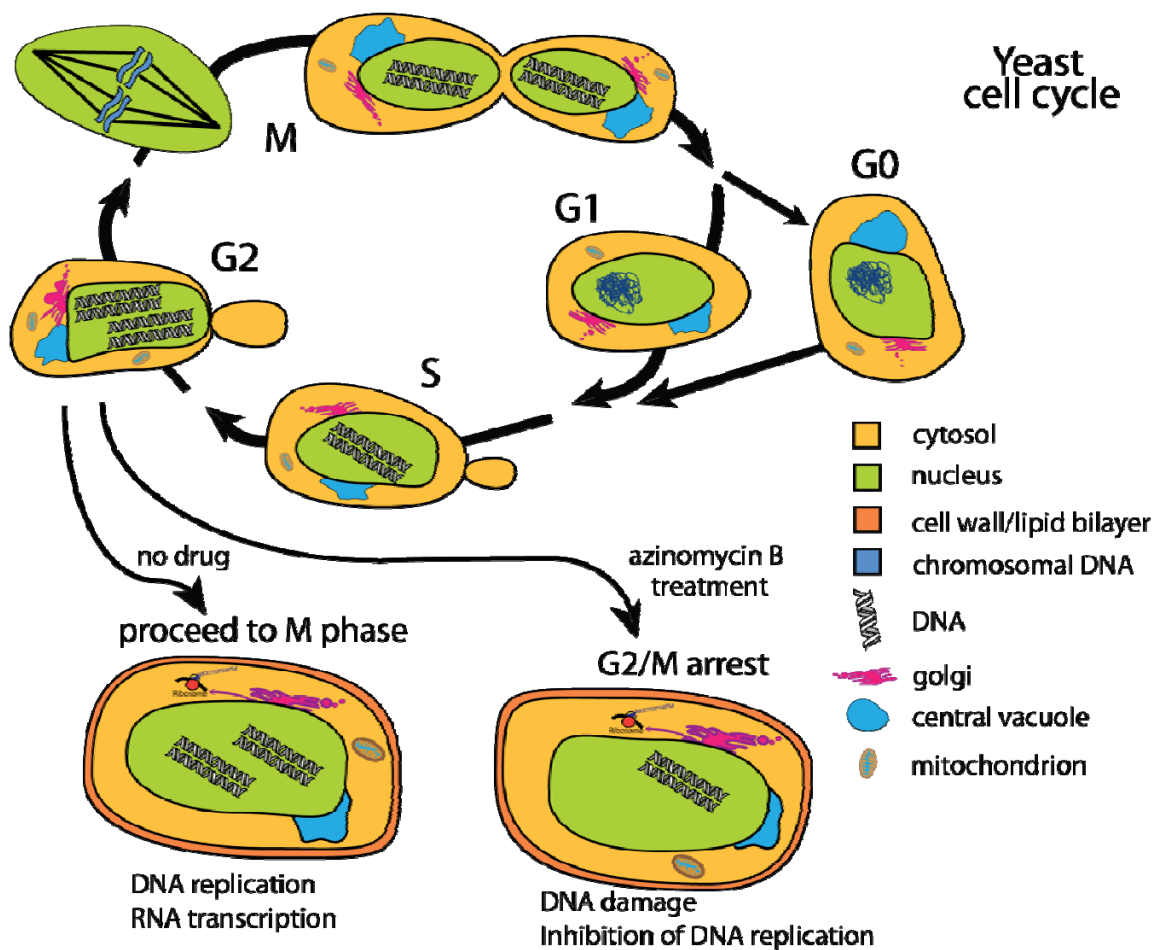


Figure 39. Diagram of the Yeast Cell Cycle and the Observed Impact of Azinomycin B Treatment.

Figure adapted from van der Kuyl *et al.* [103].

CELL CYCLE EFFECTS

(COLLABORATION BETWEEN DR. ROGER SMITH III AND THE AUTHOR)

When the gene-profiling results are interpreted, the transcriptional effects of azinomycin B treatment in yeast suggest a G1/S phase shift. The yeast cultures treated with azinomycin B were not synchronized with any particular drug before treatment in the 6 hour exposures used in the

transcriptional array profiles. As such, the populations were an asynchronous population distributed throughout the cell cycle seen in **Figure 39**. As such, any immediate impact upon the population would have an array of results, likely resulting in a large distribution of expressed mRNAs. Cells in different stages of the cell cycle would respond differently. The results from the transcriptional array profile that suggest a G1/S phase shift indicate that the yeast population was effectively halting replication responding to the assault by azinomycin B. In order to corroborate these findings, we examined the effects of azinomycin B on the yeast cell cycle by using flow cytometry.

Flow cytometry is a method used to examine, count, and sort microscopic particles in a suspended liquid. It allows for multi-parameter optical detection methods, flow rates, and real-time analysis on samples. This method allows for analysis of individual cells as they pass through the detector, resulting in a detection event. This allows for analysis of mixtures, exclusion of non-conforming particles, and accumulation of resulting data. One typical approach in analysis is to use a fluorescently tagged marker to differentiate cell populations. This can provide additional quantitative data. As such, for analysis we were interested in differentiating our cell population based upon the distribution in the cell cycle. One way to access this is to measure the quantity of DNA in each cell. In G1 or G0 the diploid yeast have half as much DNA as when the cells are in G2 or M (before separation of the daughter cell). In S phase, the amount of DNA is somewhere in between as the 13 mega base pair genome is twice copied. For an ideal detection, the agent used would need to target the DNA and be highly detectable.

Propidium iodide and SYTOX® Green dye (Molecular Probes) are healthy membrane-impermeable nuclear stains that mark cells with compromised cell membranes. Both dyes target DNA for intercalation. Unlike propidium iodide, which stains nuclear material red, the SYTOX® Green cyanine dye emits a bright green color, making it suitable for use with Cy3 and Cy5 labels. The SYTOX dye is completely excluded from live eukaryotic and prokaryotic live cells and apoptotic cells, but stains necrotic or ethanol killed (fixed) cells with intense green fluorescence [Excitation (max): 502nm; Emission (max): 523nm] [104, 105]. SYTOX® Green stain is readily excited by the 488-nm line of the argon ion laser. This type of laser was used in the detection method we employed. SYTOX® Green stain also enabled us to analyze the live/dead ratio of the yeast population of the treated samples.

Yeast was treated with azinomycin B at concentrations of 10 µg/mL and 100 µg/mL for 6 h and 12 h, respectively, and was examined by flow cytometry (**Figure 40**) [106]. **Figure 40A** shows wild-type yeast cells stained with SYTOX® Green. **Figure 40B** depicts the cell cycle

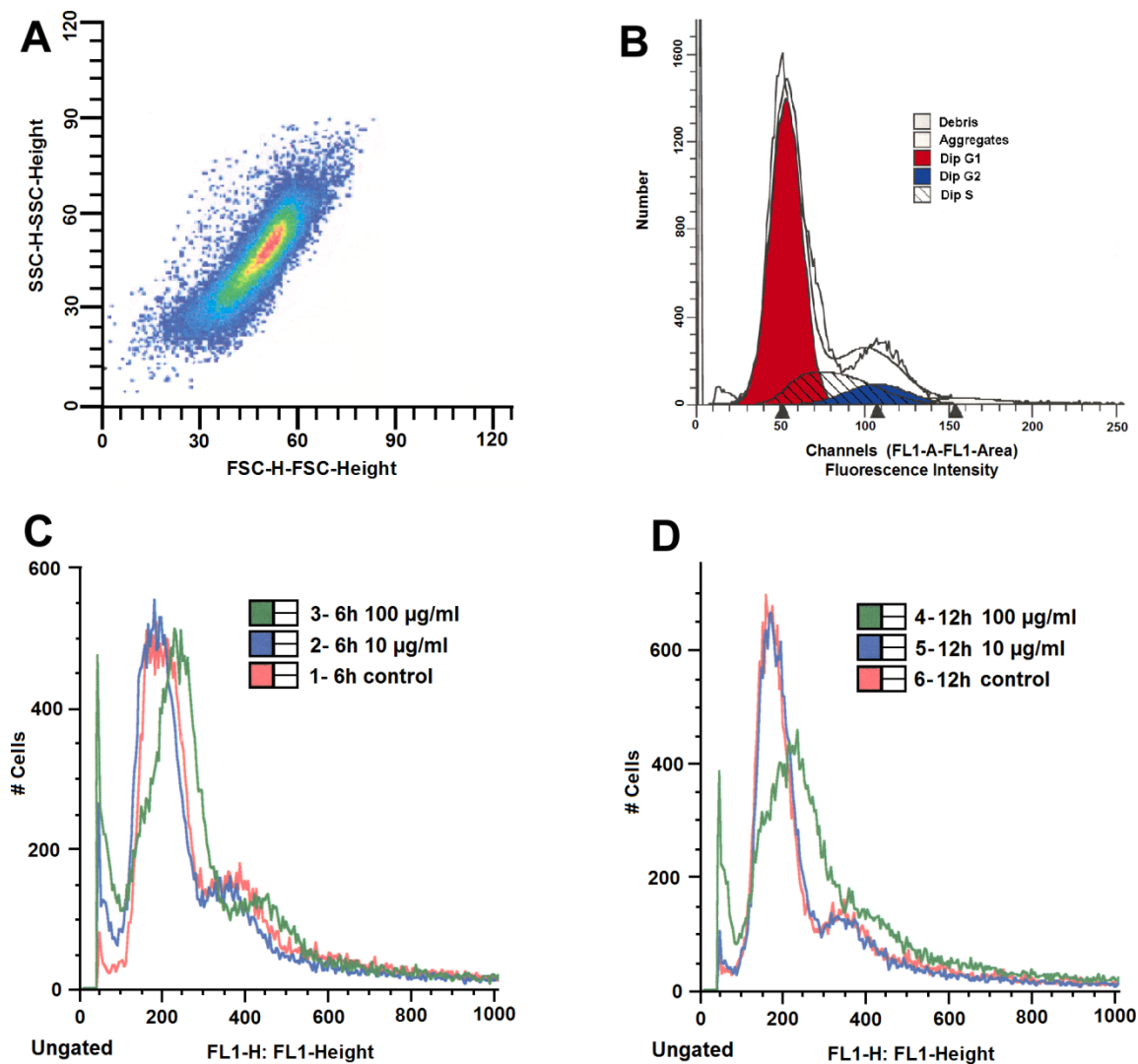


Figure 40. Flow Cytometry Analysis of Azinomycin B Treated Yeast Cultures.

(A) Wild-type yeast cells stained with SYTOX® Green (Molecular Probes) DNA binding dye measured by flow cytometry. (B) Cell cycle analysis [using ModFit LT® software (Verity Software House)] of wild-type yeast cells revealing normal asynchronous distribution in the cell cycle. (C) Cell cycle profile of yeast cultured for 6 h: control (pink), 10 µg/mL of azinomycin (blue), and 100 µg/mL of azinomycin (green). (D) Cell cycle profile of yeast cultured for 12 h: control (pink), 10 µg/mL of azinomycin B (blue), and 100 µg/mL of azinomycin B (green).

analysis of these cells. **Figure 40C** and **D** show the cell cycle profile of yeast cells at 6 h and 12 h, with and without azinomycin B treatment. When compared to the wild-type cells, azinomycin B treated cells exhibited a predominant S phase shift. A decrease in the G2/M population was apparent at 12 h at both concentrations of agent. An increase in the S phase population would

logically reflect pausing to repair damage from azinomycin B and an accumulation of individuals undergoing this repair process. DNA damage repair is required before the cell can enter G2 or M. It is also possible that not all of the cells in the population were affected enough to fully impact the procession of the cell cycle. Treated cultures continued to grow during the 6 or 12 hours of treatment, though at a slightly lower rate than those treated with an ethanol control treatment. It should be noted that the transcriptional array profiles were conducted with a 6 hour exposure to azinomycin B. To observe detectable differences by flow cytometry, we needed to extend the exposure to 12 hours.

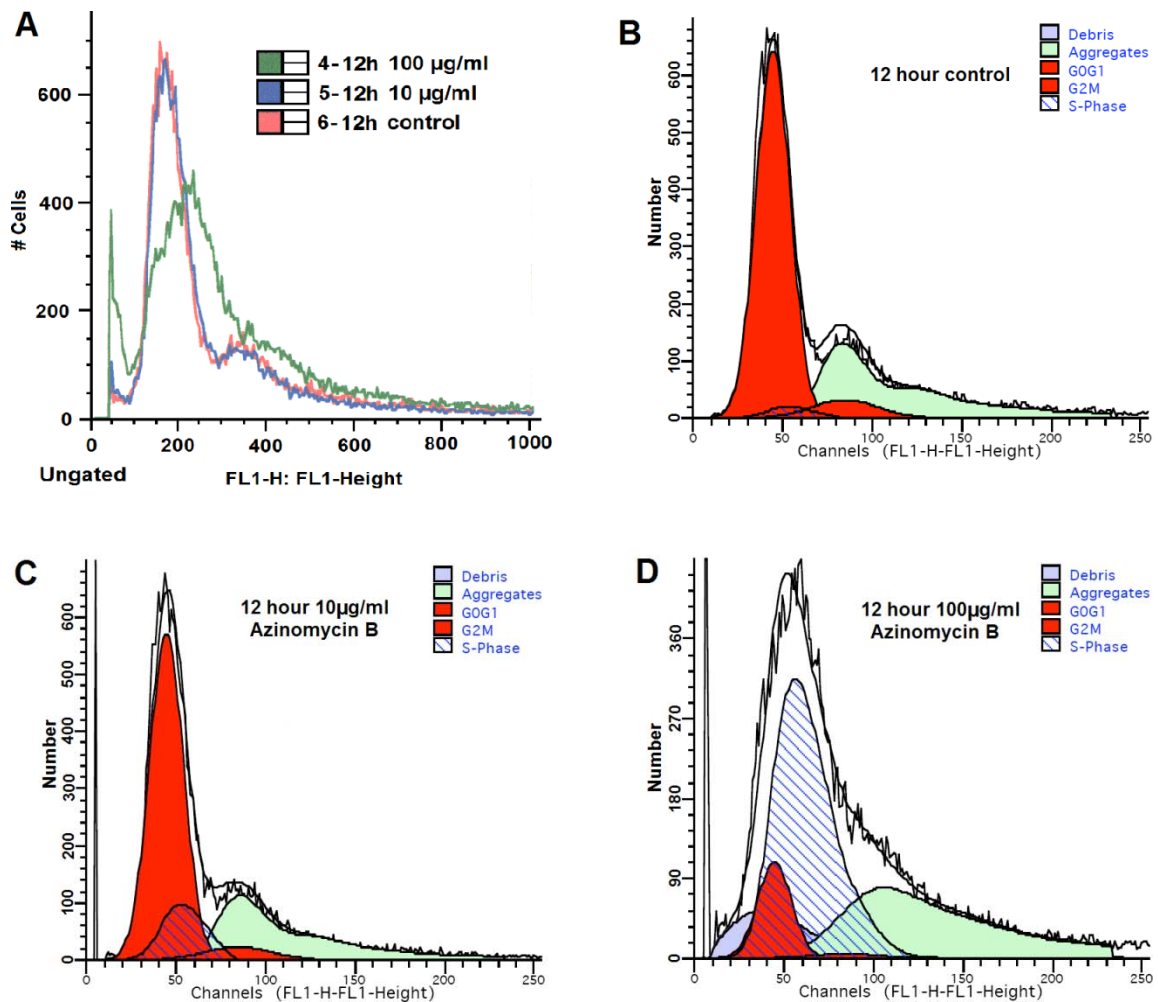


Figure 41. Closer Inspection of Flow Cytometry Data Analysis of 12hr Azinomycin B Treatment Set.

(A) Raw data sets overlaid. (B) Control treatment, show normal distribution. (C) 10µg/mL treatment. (D) 100µg/mL treatment.

A closer analysis with ModFit LT software of the 12 hour treatments, seen overlaid in **Figure 41A**, revealed the large extent to which the 100 $\mu\text{g}/\text{mL}$ azinomycin B treated population was distributed in S phase (**Figure 41D**). The Modfit LT analysis revealed a significant portion of defined “debris” in all three samples. Remarkably the control (**Figure 41B**) and the 10 $\mu\text{g}/\text{mL}$ treatment of azinomycin B (**Figure 41C**) have very similar profiles and population distributions. This result is similar to the observed effects and analysis of the 10 $\mu\text{g}/\text{mL}$ treatment level azinomycin B transcriptional array results, which displayed few gene changes. The 12 hour, 100 $\mu\text{g}/\text{mL}$ azinomycin B treated yeast population displayed significantly more “aggregates.” This may reflect a significant part of the population with cells connected to an extent that a pepsin digest failed to part them. These cells would also overlap with a population usually detected as G2/M. The large population of cells in the S phase at this highest treatment level indicates significant effect of azinomycin B to halt the population at this critical time of DNA replication. This evidence supports our 100 $\mu\text{g}/\text{mL}$ transcriptional array profile results.

CONFIRMATION OF SELECTED GENE CHANGES BY RT-PCR

(COLLABORATION BETWEEN DR. CORAN M. H.WATANABE AND THE AUTHOR)

Validation of the transcriptional effects induced by azinomycin B treatment was demonstrated by semi-quantitative reverse-transcriptase PCR (abbreviated (RT)-PCR) of an arbitrary subset of the gene changes, including HUG1, RAD51, TOM1, and PLM2. (RT)-PCR is a technique that uses RNA, not DNA, as the initial template and employs an initial reverse transcriptase to convert the RNA of interest to a DNA template. This is not to be confused with the technique real-time PCR, (abbreviated qPCR for quantitative PCR). Frequently, real-time polymerase chain reaction is combined with reverse transcription polymerase chain reaction to quantify low abundance messenger RNA (mRNA), enabling one to quantify relative gene expression at a particular time. (RT)-PCR, while less sensitive and quantitative than real-time PCR is capable of confirming a transcriptional response, the presence or absence of a transcriptional effect. Normalization of the RNA/cDNA was based upon glyceraldehyde-3-phosphate dehydrogenase (GAPDH) that was unaffected by drug exposure. Total RNA was extracted from control cells and cells treated with azinomycin B (10 $\mu\text{g}/\text{mL}$ and 100 $\mu\text{g}/\text{mL}$). First strand cDNA synthesis of the DNA was performed followed by PCR analysis. The PCR primers were specifically designed to avoid redundancy in other possible transcript sequences. The exponential phase of each PCR product was estimated by varying the number of PCR cycles for each template or gene of interest [107]. PCR products were stained with SYBR Green and fluorescence was measured with a micro plate

reader (Figure 42). The results reinforce the effects and levels of expression observed in the transcriptional microarray analysis.

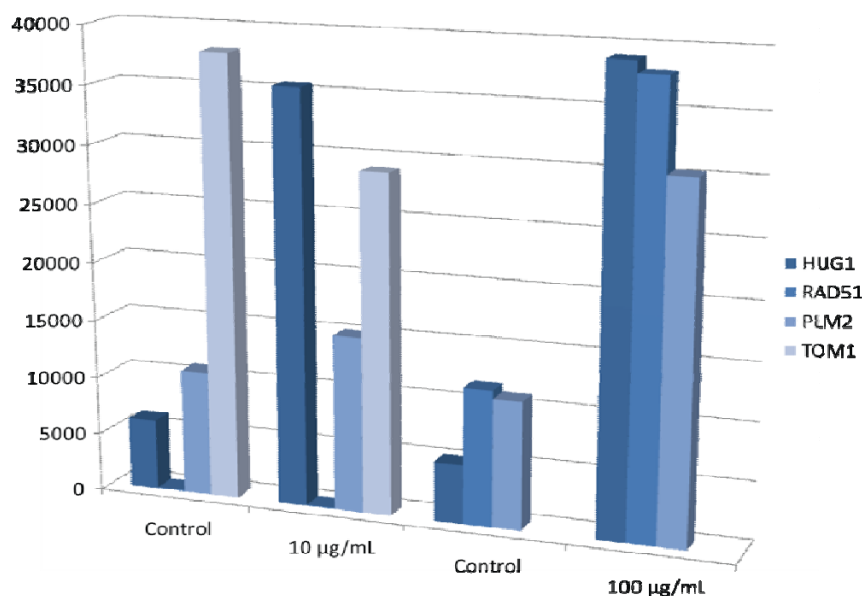


Figure 42. Semi-quantitative Reverse Transcriptase (RT)-PCR Analysis of the Selected Genes: HUG1, RAD51, PLM2, and TOM1.

SIGNIFICANCE

The azinomycins A and B are natural products that possess promising antitumor activity. Central to the biological action of these molecules is the presence of two electrophilic carbons present within the epoxide moiety and the structurally and functionally unique aziridino[1,2-*a*]pyrrolidine core substructure. Evaluation of the azinomycins *in vitro* has demonstrated that the molecules bind to DNA within the major groove and form covalent interstrand cross-links. The exquisite ability of these natural products to functionalize and append to DNA notwithstanding, the cellular target of these molecules *in vivo* had not previously established. In efforts to address this issue, we have examined the cellular localization pattern of azinomycin B in *Saccharomyces cerevisiae*, which paralleled that of the DNA intercalator propidium iodide.

Additionally, genomic DNA isolated from drug treated cells showed significant shearing of the DNA, and experiments with oligonucleotide microarrays revealed transcriptional effects that were closely associated with DNA damage and repair. Genes involved in DNA synthesis and the cell cycle were altered in their expression, reflecting an S phase shift. This effect was

further substantiated in flow cytometry experiments. Some genes differentially expressed in response to azinomycin B treatment were also induced by calicheamicin γ_1 I or methyl methanesulfonate exposure, although a significant number of the genes that were affected by azinomycin B were not common to these other agents. Transcriptional profiling could prove to be a definitive tool in the study of the mechanism of action of DNA damaging agents.

These results provide the first demonstration of the *in vivo* actions of azinomycin B. While the experiments presented here are consistent with the proposed role of the drug as a DNA cross-linking agent, definitive proof for this mechanism must come from experiments that can conclusively demonstrate drug•DNA adduct formation.

EXPERIMENTAL PROCEDURES

INSTRUMENTATION AND GENERAL METHODS

Yeast cell cycle experiments were performed with a Becton-Dickinson FACS Calibur flow cytometer. (RT)-PCR reactions were carried out with an MJ Research PT600 PCR machine and fluorescence measurements were made with a Biotek FL800 fluorescence microplate reader. Cellular localization studies were conducted with a Zeiss microscope, and the Affymetrix platform was used in all GeneChip experiments. Unless otherwise specified, biochemical reagents were obtained from Sigma Biochemicals (St. Louis, MO).

ORGANISMS

The yeast *Saccharomyces cerevisiae* wild-type strain [#404; BY4741; MATa his3 Δ 1 leu2 Δ 0 met15 Δ 0 ura3 Δ 0] was obtained from Dr. Michael Klade at the Department of Biochemistry, Texas A&M University. *Streptomyces sahachiroi* (NRRL 2485) was obtained from the American Type Culture Collection (ATCC; Manassas, VA).

CULTURE CONDITIONS

(THE AUTHOR)

Saccharomyces cerevisiae was maintained on YPD plates and subsequently cultured at 30 °C and 250 rpm in YPD medium [108]. *Streptomyces sahachiroi* was initially cultured on GYM plates until sporulation, typically 5-7 days at 28 °C. GYM agar plates contained the following components per liter: glucose monohydrate, 4 g; yeast extract, 4 g; malt extract, 10 g; CaCO₃, 2 g; agar, 12 g; and tap water adjusted to pH 6.8 with 1 M NaOH prior to sterilization [109]. A

starting culture of *Streptomyces sahachiroi* in PS5 medium (100 mL) was prepared by inoculation of a loop of spores from the GYM plates. PS5 medium was prepared from 5 g/L of Pharmamedia (yellow cotton seed flour, Traders Protein; Memphis, TN) and 5 g/L of soluble starch, adjusted to pH 7.0. Following 24 h growth at 30 °C and 250 rpm, 25 mL of the starting culture was used to inoculate 500 mL of PS5 in 2 L baffled Erlenmeyer flasks. The cultures were grown for 64 h at 30 °C and 250 rpm [109].

AZINOMYCIN B ISOLATION

(THE AUTHOR, INITIAL SAMPLE PROVIDED BY DR. ROBERT S. COLEMAN)

The natural product was isolated with slight modification of literature protocols [1, 17]. Following fermentation, culture broths of *Streptomyces sahachiroi* were harvested by centrifugation (8,000 rpm). The supernatant was extracted once with an equal volume of chloroform. The chloroform extract was concentrated to 5 mL and diluted with hexane (30 mL). The resulting suspension was centrifuged (3,000 rpm), giving a white azinomycin-containing precipitate that was further purified by washing with ether (10 mL) followed by dissolution in chloroform (50 mL). Hexane was added gradually, and with the initial addition of hexane, a precipitate was generated and discarded. Further addition of hexane resulted in the precipitation of azinomycin B as a white amorphous solid. The azinomycin was collected by centrifugation and stored under anhydrous diethyl ether at -80 °C.

NUCLEAR LOCALIZATION EXPERIMENTS

(THE AUTHOR)

Yeast was grown at 30 °C in liquid culture to an OD₆₀₀ of 1.0. Samples (1 mL) were centrifuged and the cell pellets re-suspended in 1 mL sterile Dulbecco's phosphate buffered saline. The cells were centrifuged, and treated as follows: azinomycin treated live cells (at 100 µg/mL and 4000 µg/mL), naphthoate treated cells (500 µg/mL) [18, 110] and propidium iodide (1 µg/mL). Propidium iodide stained cells were fixed by addition of 70% ethanol (final volume, 30 min incubation at room temperature) prior to re-suspension in Dulbecco's phosphate buffered saline and treatment with propidium iodide. After 4 h incubation at room temperature, the cells were centrifuged, the supernatant was removed, and the cells were re-suspended in Dulbecco's phosphate buffered saline. The cells were viewed on slides with a Zeiss fluorescence microscope and the images captured digitally at 1000X magnification. The exposure times were kept constant.

GENOMIC ANALYSIS

(COLLABORATION BETWEEN DR. CORAN M. H. WATANABE AND THE AUTHOR)

Saccharomyces cerevisiae was cultured in 10 mL aliquots at 30 °C to an OD₆₀₀ of 1.0 and subsequently treated with either 100 µL of azinomycin B (to give final concentrations of 10 µg/mL and 100 µg/mL, respectively) or ethanol. The cells were cultured for an additional 12 h with shaking, centrifuged, and the genomic DNA was isolated as follows. The cells were re-suspended in 500 µL of solution consisting of 1 M sorbitol and 0.2 M EDTA, pH 7.5 at which point 5 µL of zymolyase (0.5 mg/mL) was added, and the suspension was incubated at 37 °C for 60 min. The cells were centrifuged, re-suspended in 500 µL of 50 mM Tris pH 7.4, 20 mM EDTA, and 25 µL of 20% SDS added. Following incubation of the mixture at 50 °C for 30 min, to the solution was added 5 µL of proteinase K (10 mg/mL) and 200 µL of 5 M potassium acetate. The reaction was placed on ice for 60 min, and the cellular debris was removed by centrifugation. The supernatant was transferred to a new tube, and one volume of isopropanol was added. The mixture was allowed to stand at room temperature for 5 min. The DNA was isolated by centrifugation (5 min) and dissolved in 100 µL of TE buffer containing 1 µL of RNase. The suspension was incubated at 37 °C for 30 min; then the DNA was precipitated by addition of 400 µL 5 M NH₄OAc and 200 µL of isopropanol, centrifuged, washed with 1 mL of 80 % EtOH, dried and dissolved in 100 µL of TE buffer. The DNA, 5 µL of each sample, was analyzed by standard 1% agarose gel electrophoresis and stained with SYBR green dye following the manufacturer's protocol (Molecular Probes, Invitrogen; Carlsbad, CA).

YEAST SAMPLE PREPARATION AND GENECHIP EVALUATION

(COLLABORATION BETWEEN DR. CORAN M. H. WATANABE AND THE AUTHOR)

Yeast was cultured overnight in YPD broth [108] to an OD₆₀₀ of 1.0. Total RNA was extracted with an SDS/hot phenol extraction method. Yeast cell samples were centrifuged and the supernatant was decanted. Each cell sample was washed with 30 mL of de-ionized distilled water and subsequently centrifuged (repeated 3X). Yeast pellets were frozen in liquid nitrogen and lysed by the following protocol: Each cell pellet was treated with 10X high-salt solution (3 M NaCl, 200 mM Tris, pH 8.0, 100 mM EDTA) and de-ionized distilled water to a final volume of 700 µL. Each sample was brought to 1% SDS by the addition of 10% SDS (70 µL), at which time hot phenol (65 °C, 600 µL) was added. Samples were vortexed, incubated at 65 °C for 4 min, and then chilled on ice for 2–4 min. Samples were microcentrifuged for 2 min, and the

supernatant was transferred to new tubes. The phenol extraction procedure was repeated, and was followed by extraction with a 25:24:1 phenol: chloroform: isoamyl alcohol. After centrifugation, the supernatant of each sample was transferred to new tubes. The RNA was precipitated by the addition of ethanol to the top of each microfuge tube. Samples were mixed by vortexing, stored at 20 °C for 1 h, and then pelleted by centrifugation. The supernatant was decanted, and the pellet from each sample was washed twice with 70% ethanol. Residual ethanol was removed, and the cell pellet was re-suspended in 100 µL water. The resulting total RNA was then treated with DNase: total RNA (30 µL) was incubated at room temperature with 5 µL of first strand buffer (Gibco BRL cDNA Superscript Choice Kit) and 1 µL of DNase I (RNase-free, Ambion). Samples were heat-inactivated at 75 °C for 15 min and purified with an RNeasy kit (Qiagen). Samples (15 µg of total RNA per sample) were provided to the Texas A&M GeneChip facility, where they were amplified, biotinylated, and hybridized to GeneChips according to the protocol detailed by Affymetrix (Santa Clara, CA). Microarray data are available through the NCBI Geo Database (Accession number: GSE4311).

GENECHIP EVALUATION BY (RT)-PCR

(COLLABORATION BETWEEN DR. CORAN M. H. WATANABE AND THE AUTHOR)

(RT)-PCR analysis of a subset of the genes including HUG1, RAD51, TOM1, and PLM2, was carried out as follows. Total RNA (10 µg) was extracted and transcribed into single stranded cDNA using the Superscript Choice system (GIBCO/BRL). The cDNA was purified with a Qiagen nucleotide removal kit. Glyceraldehyde-3-phosphate dehydrogenase (GAPDH) was employed as an endogenous amplification standard (*i.e.*, used to normalize the amount of RNA in control and treatment samples). PCR conditions were optimized so that amplification of both GAPDH and the cDNA of interest were in the exponential phase. PCR cycles consisted of Step 1: 5 min denaturation at 95 °C; Step 2: 1 min of denaturation at 95 °C; Step 3: 1 min of primer annealing at 55 °C; Step 4: 1 min of extension at 72 °C. Steps 2–4 were repeated for the requisite number of cycles.

PRIMERS

HUG1 (YML058W-A)

Forward: 5'-ATGACCATGGACCAAGGCCTTAACC-3'

Reverse: 5'-TTAGTTGGAAGTATTCTTACCAATG-3'

RAD51 (YER095W)

Forward: 5'-CGGATGTGAAAAAACTAAGGGAGAG-3'

Reverse: 5'-TCTTAACTGATGATCGGCGTTATAG-3'

TOM1 (YDR457W)

Forward: 5'-AACAGCTCGGTTCCATGAATTTGAT-3'

Reverse: 5'-TAATTACGGAACGTGCTAGCATTCC-3'

PLM2 (YDR501W)

Forward: 5'-TTGGCTAAAGGTGAAACTGTTACTT-3'

Reverse: 5'-GCGAAAGATTCTTCTTCATTAATGC-3'

GAPDH (YJR009C)

Forward: 5'-ACATTGACATCGCCATTGACTCCAC-3'

Reverse: 5'-TTTCATCGTAGGTGGTTTCCTTGTT-3'

Following PCR, each reaction was visualized by agarose gel electrophoresis (15 μ L per lane) and stained with ethidium bromide. The resulting PCR products were sliced out of the gel and dialyzed against TAE buffer. The dialyzed gel pieces were stained with SYBR Green (Molecular Probes, Invitrogen; Carlsbad, CA), placed in a 96-well plate, and fluorescence was measured with a Biotek FL800 micro plate reader (filters: 485/30 for excitation and 528/20 for emission).

CELL CYCLE ANALYSIS BY FLOW CYTOMETRY

(COLLABORATION BETWEEN DR. ROGER SMITH III AND THE AUTHOR)

Yeast were grown at 30 °C in liquid culture to an OD₆₀₀ of 1.0 and exposed to azinomycin B (10 and 100 μ g/mL, in triplicate) for 6 and 12 h. The yeast population was asynchronous. Cells were centrifuged, the medium was removed, and the cells were washed with 10 mM Tris, pH 7.5. The cells were fixed by treatment with 70% ethanol for 1 h at room temperature. Cells were centrifuged, the supernatant was discarded, and the pellet was incubated with 0.5 mL of 50 mM Tris pH 7.5 supplemented with 2 mg/mL RNase A at 37 °C for 2-12 h. Following incubation, cells were centrifuged, and the supernatant was discarded. The cells were re-suspended in 0.2 mL proteinase solution (5 mg/mL pepsin, 4.5 μ l/mL concentrated HCl in H₂O) for 15-20 min at 37 °C. The cells were centrifuged, the supernatant was discarded, and the cells were re-suspended in 0.5 mL Tris pH 7.5, 1X SYTOX Green (100 nM; Molecular Probes, Invitrogen; Carlsbad, CA). The samples proceeding directly to the analysis step [111].

NAPHTHOATE SYNTHESIS

(DR. CHAOMIN LIU)

Details provided in Appendix.

CHAPTER III

IN VITRO BIOSYNTHESIS OF THE ANTITUMOR AGENT AZINOMYCIN B*

INTRODUCTION

Azinomycins A and B (**Figure 43**) are antitumor antibiotics isolated from two *Streptomyces* species, *S. sahachiroi* [1] and *S. griseofuscus*, [2, 17] respectively. Both compounds exhibit *in vitro* cytotoxic activity at submicromolar levels and demonstrate antitumor activities comparable to that of mitomycin C *in vivo* [77]. Unique to this class of natural products is the presence of an aziridino[1,2-*a*]pyrrolidine (1-azabicyclo[3.1.0]hexane) ring system, coupled with an epoxide moiety. These structural functionalities impart the ability to form interstrand cross-links with DNA via the electrophilic C10 and C21 carbons of azinomycin and the N7 positions of suitably disposed purine bases [14, 27, 69, 71-73, 112].

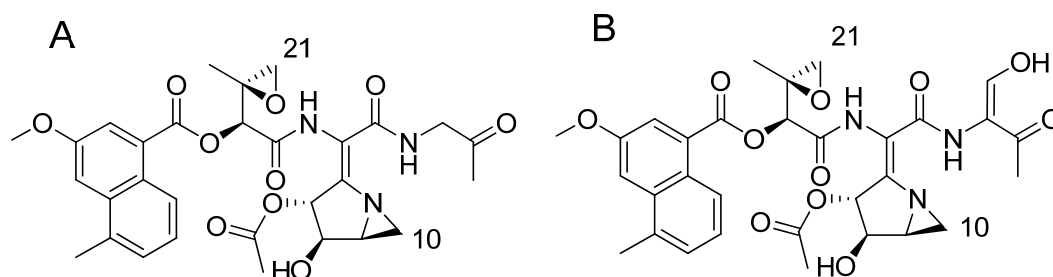


Figure 43. Structures of Azinomycin A and B.

The novel architecture, intricate functionalization, and mode of action of the azinomycins have made these agents attractive targets from both a synthetic and a biosynthetic perspective. Synthetic routes to the azabicyclic system have been reported including total

*Reprinted with permission from “*In Vitro* Biosynthesis of the Antitumor Agent Azinomycin B” by Liu, C. M., Kelly, G. T., and Watanabe, C. M. H., 2006. *Organic Letters*, 8, 1065-1068, Copyright [2006] by American Chemical Society.

synthesis of azinomycin A [18, 27, 68]. A variety of synthetic analogues have also been generated [26, 27, 113]. Considerably less is known about the biosynthetic origin of these compounds.

In this chapter, the details of the first cell-free system capable of supporting *in vitro* biosynthesis of azinomycin B are presented. Investigations of natural product biosynthesis have used the cell-free enzyme (CFE) preparation approach to study a number of natural products [114-117]. These investigations have yielded insight into both the substrates and types of enzymes and cofactors involved in the natural product's biosynthesis. Investigations of the biosynthetic steps from the initial construction of the naphthoate fragment of the molecule to the formation of the azabicyclic ring system have been achieved using a cell-free protein extract (CFE) of *Streptomyces sahachiroi*. We have used this method of CFE preparation to investigate inhibition of the pathway and the cofactor as well as substrate requirements of the pathway.

RESULTS AND DISCUSSION

DEVELOPMENT OF THE CELL FREE EXTRACT SYSTEM

(COLLABORATION BETWEEN DR. CHAOMIN LIU, DR. CORAN M. H. WATANABE AND THE AUTHOR)*

As the production of azinomycin B from live culture was erratic, our interests turned to making use of the productive cell cultures by producing a cell free extract to investigate the natural product's biosynthesis. Reconstruction of a functional biosynthetic pathway in an artificial environment provides numerous challenges. Ensuring a proper ratio of necessary substrates, cofactors, and maintaining the biosynthetic enzymes in a functional state are significant challenges. Rendering functional enzymes from whole cells is a process requiring great care. It poses the innate requirement that the isolated enzymes function in an artificial environment. If the enzymes are removed in the process, incomplete or no biosynthesis will result.

The fortified crude enzyme preparation was generated by culturing *S. sahachiroi* (**Figure 44A**) and flash freezing the cells from azinomycin B producing cultures in liquid nitrogen (**Figure 44B**). The frozen material was transferred to a bead beater containing cell-free extract buffer (pH 7.5) and glass beads. The cells were pulverized (utilizing 10 intermittent cycles) and centrifuged to generate the crude cell-free extract (**Figure 44C**).

* Denotes major contributor(s) to each section.

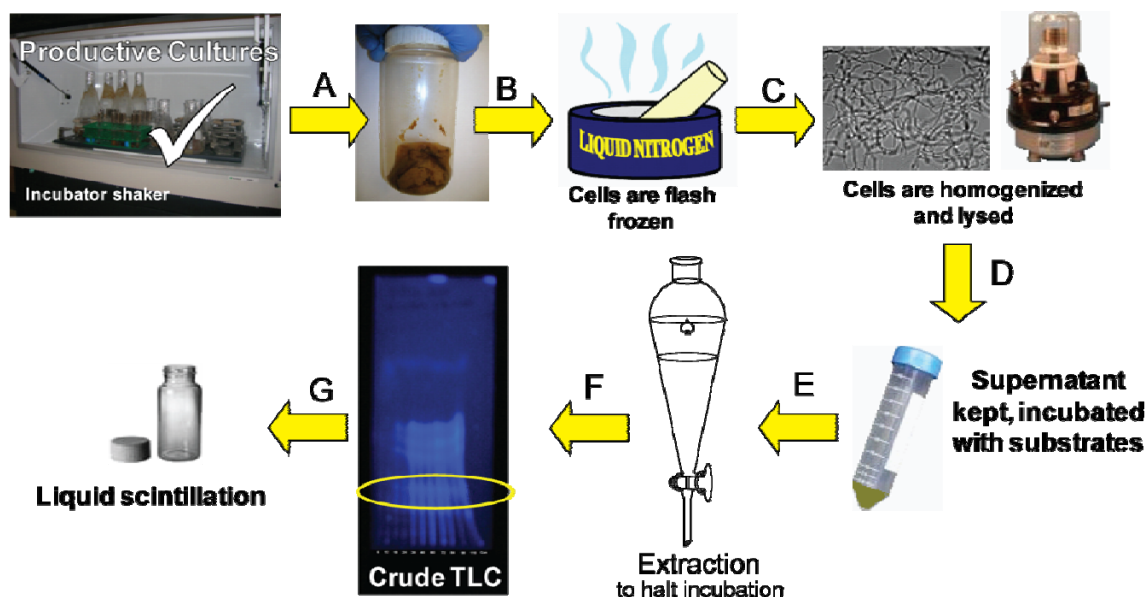


Figure 44. Preparation and Analysis of the Cell Free Extract (CFE).

(A) Azinomycin B producing cultures of *S. sahachiroi* are centrifuged and (B) Cell pellet collected and flash frozen in liquid nitrogen. (C) Frozen pellets are homogenized and lysed using a bead-beater and (D) Lysate is centrifuged and supernatant retained. (E) Supernatant was then incubated with radioactive substrates, with the control being a heat denatured supernatant. (F) The incubation is halted by extraction with CH_2Cl_2 and the organic extract separated by TLC and analyzed using liquid scintillation counting.

Initially, we examined the cell-free preparation for its ability to support synthesis of the naphthoate core of azinomycin A and azinomycin B. The enzyme assay was performed in duplicate by incubating the protein extract with acetyl-CoA, cofactors (nicotinamide adenine dinucleotide phosphate (NADPH), S-adenosylmethionine (SAM), and flavin adenine dinucleotide (FAD)), and radiolabeled $[1-^{14}\text{C}]$ malonyl-CoA for 24 h. NADPH was added to ensure reductive equivalents were available for the anabolic enzymes involved with azinomycin B's construction. Because S-adenosylmethionine was thought to be involved in the biosynthesis of azinomycin B's methoxy group of the naphthoate [31], additional S-adenosylmethionine was included. This involvement was confirmed; it prevents the concentration of SAM from being a limiting factor. FAD was added to provide additional redox equivalents. Although the production of azinomycin B is not produced in copious amounts, it is not considered a trace natural product, therefore no additional Mg^{2+} or NADH were included to inhibit acetate diversion in the citric acid cycle, as they are often added in CFE systems interested in trace natural

products [114]. Following incubation, the reactions were quenched by vortexing with dichloromethane and centrifuged (**Figure 44E**). The dichloromethane fraction was transferred to new tubes and evaporated to dryness. The organic residue was resolubilized in a minimal volume of dichloromethane containing standards of azinomycin B or naphthoate. Regions of the TLC plate corresponding to products with appropriate R_f values (as observed by UV analysis) (**Figure 44F**) were scraped from the plate and analyzed by scintillation counting (**Figure 44G**).

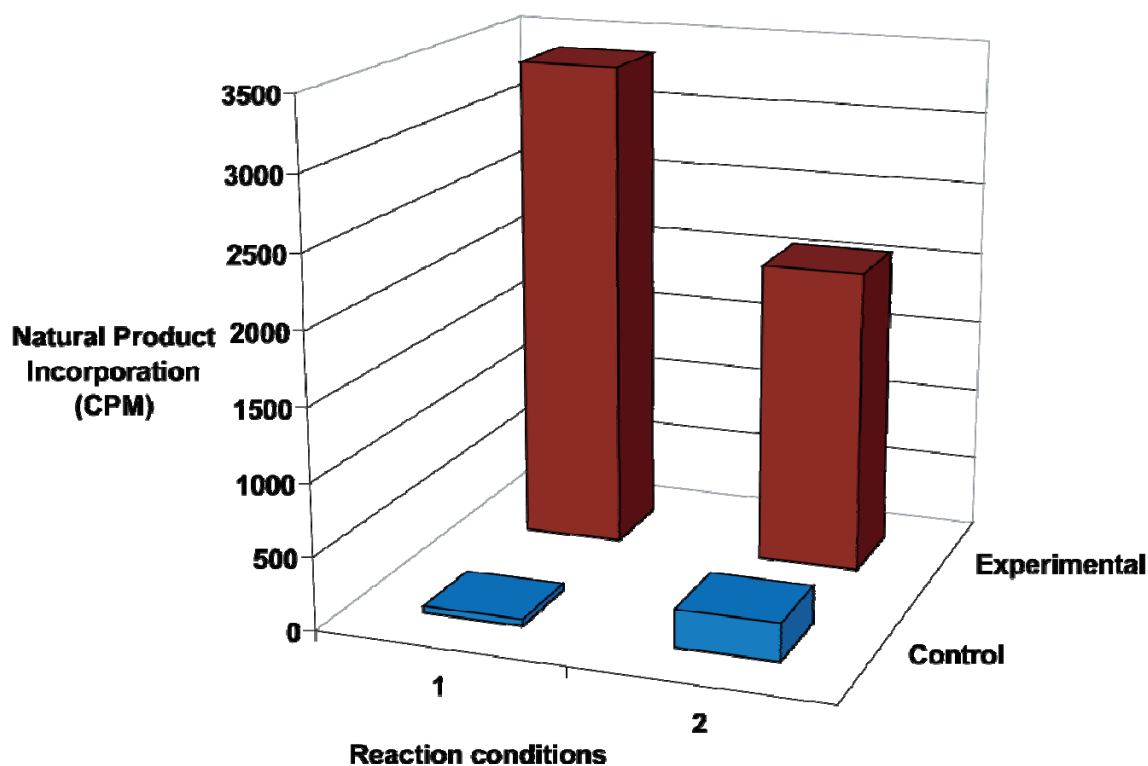


Figure 45. Demonstration of *In Vitro* Biosynthesis.

Controls: cpm \pm 10. Experimental: cpm \pm 50. (1) Conversion to the naphthoate. (2) Conversion to azinomycin B. Reaction conditions: CFE + [1- 14 C] malonyl-CoA, acetyl-CoA, SAM, FAD, NADPH.

The results of this initial experiment are depicted in **Figure 45** (reaction 1, conversion to the naphthoate; reaction 2, conversion to azinomycin B). The control experiment for these reactions consisted of boiled cell-free extract (5 mL) incubated with test substrates and cofactors as detailed above. The incorporation of [1- 14 C] malonyl-CoA into the naphthoate portion of the molecule (**Figure 45:1**) and azinomycin B (**Figure 45:2**) was observed by scintillation counting and confirmed by HPLC co-injection. The relative strength of incorporation which appeared to

be higher in the naphthoate was likely due to two factors: 1) biosynthesis of azinomycin B involves many more enzymatic steps, thus fewer molecules might have been produced in the incubation period, resulting in merely a product concentration issue; and 2) it is possible that naphthoate moiety of the isolated azinomycin B could have originated before the introduction of [1-¹⁴C] malonyl-CoA. These successful initial incorporation experiments provide a basis of comparison for the naphthoate and azinomycin B biosynthetic steps from which we may compare with additional results obtained from probing substrates, cofactors, biosynthesis inhibitors.

INHIBITORS

As an additional control for these experiments, we examined the effect of the FAS/PKS inhibitor cerulenin (**Figure 46A**) [118, 119] on these reactions as well as that of P-450 inhibitors chloramphenicol (**Figure 46B**) [120], miconazole (**Figure 46C**) [121, 122], and metyrapone (**Figure 46D**) [123]. Cerulenin is known to inhibit fatty acid biosynthesis by covalently binding to the β -keto-acyl-ACP synthase, blocking the addition of malonyl-CoA units [118, 124]. A covalent thioacylation of the enzyme's residue and the epoxide of cerulenin render the enzyme permanently inactivated. Cerulenin inactivates PKS enzymes in a similar fashion. Cerulenin has been shown to specifically inhibit the formation of several PKS natural products such as: leucomycin, a macrolide antibiotic [125, 126]; 6-methylsalicylic acid [127]; esperamicin A1 [128]; the mycotoxins alternariol (AOH) and alternariol monomethyl ether (AME) [129] and aflatoxin B1 [130]. If the production of the naphthoate portion of the molecule truly has polyketide origins, we would expect to see its formation inhibited by cerulenin.

Miconazole is notably used as an antifungal agent used to inhibit the biosynthesis of ergosterol, a component of fungal cell walls. Metyrapone blocks cortisol synthesis by inhibiting steroid 11 β -hydroxylase in people. Metyrapone was found to inhibit the action of P-450 enzymes in biosynthesis [131, 132]. Chloramphenicol is a bacteriostatic antimicrobial originally isolated from *Streptomyces venezuelae* [46]. Chloramphenicol was found to have an inhibitory effect on human cytochrome P-450 isoforms [120]. Inhibition of P-450 enzymes would potentially impact azinomycin B biosynthesis if the P-450 enzymes are involved in the oxidative modifications required to produce both the naphthoate moiety and azinomycin B. It is also possible that P-450 enzymes are involved in the formation of the epoxide moiety and the hydroxylations in the aziridinopyrrolidine moiety of the azinomycin molecule.

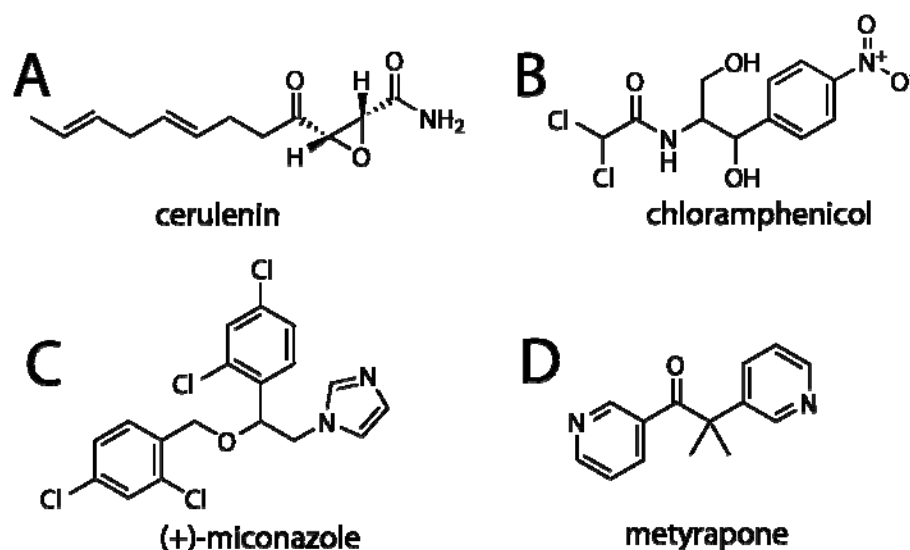


Figure 46. Structures of Biosynthesis Inhibitors Used in this Study.

Oxidative modifications in natural products involve ‘mixed-function oxidases,’ the most prevalent of which are cytochrome P-450-dependent mono-oxygenases. These are involved in hydroxylations and other oxidative modifications (**Figure 47**). The iron-porphyrin complex (heme) is bound to the enzyme which carries a redox charge involving the Fe atom allowing binding and cleavage of an oxygen atom. NADPH is usually the hydrogen donor.

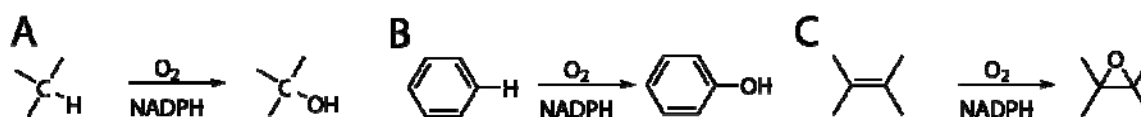


Figure 47. Mono-oxygenases.

Mono-oxygenases have been found to perform many types of oxygen additions: (A) Simple hydroxylation (B) hydroxylation of an aromatic group (C) epoxide formation from an alkene.

The aromatic naphthoate group is likely to have been modified by a mono-oxygenase. In 2004, Lowden and coworkers fed a series of naphthoate derivatives with various deuterated positions to whole cells of *S. sahachiroi* (**Figure 48A-E**) [31]. The result of their study indicated that the molecule with the highest rate of incorporation was the most advanced precursor. Additionally the movement of the deuterium in molecule **D**, indicated an ‘NIH shift’ type mechanism, implying the action of a P-450 oxygenase. The NIH shift, discovered by

research scientists at the National Institutes of Health, is illustrated in **Figure 49** with the naphthoate group.

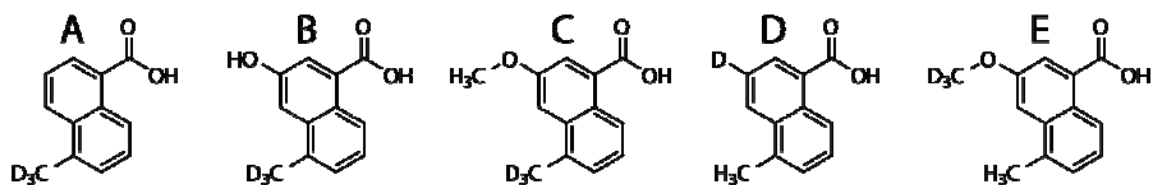


Figure 48. Naphthoate Compound Series Fed by Lowden, *et al.*

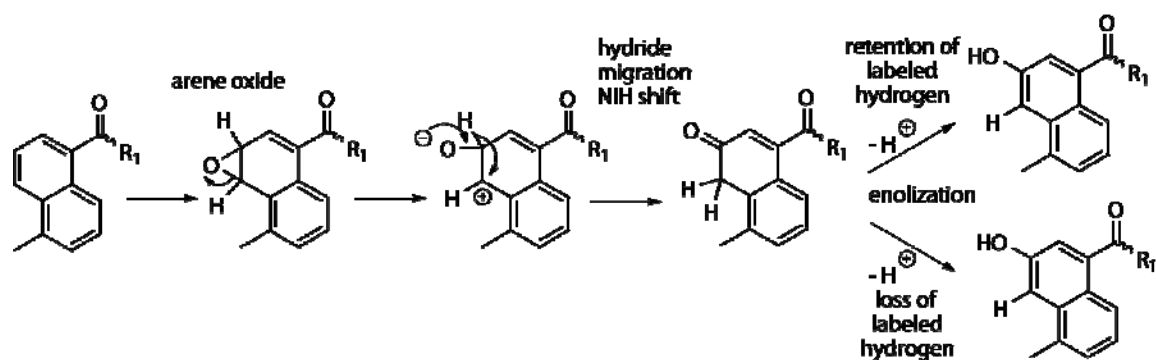


Figure 49. Hydroxylation of the Naphthoate Involving the NIH Shift Associated with Mono-oxygenases.

Table 3. Effect of Enzyme Inhibitors on Naphthoate Production.

Reaction condition	Inhibitor	CPM (10 μ M)	CPM (100 μ M)
1 (Cont.)	—	59	59
1 (Expt.)	—	945	945
2 (Cont.)	miconazole	37	37
2 (Expt.)	miconazole	38	43
3 (Cont.)	metyrapone	34	34
3 (Expt.)	metyrapone	41	91
4 (Cont.)	chloramphenicol	32	26
4 (Expt.)	chloramphenicol	73	93
5 (Cont.)	cerulenin	33	38
5 (Expt.)	cerulenin	55	47

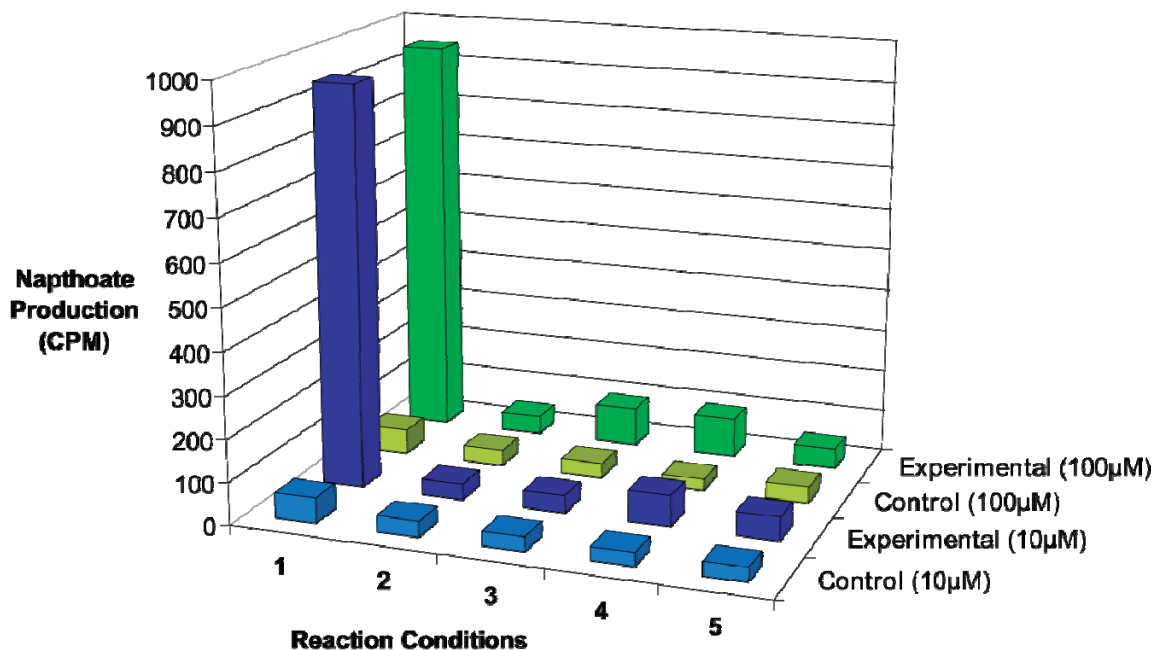


Figure 50. Effect of Enzyme Inhibitors on Naphthoate Production. Reaction 1 experimental: $\text{cpm} \pm 50$. Reactions 1-5: $\text{cpm} \pm 10$. Inhibitors used miconazole (2), metyrapone (3), chloramphenicol (4), and cerulenin (5).

Our reactions were incubated with 10 and 100 μM of each inhibitor, respectively, and assayed for both naphthoate and azinomycin B production (**Figure 50**, **Figure 51**, **Table 3** and **Table 4**). As expected, cerulenin exhibited inhibition against formation of the naphthoate (the putative PKS product) and azinomycin B. Likewise, all P-450 inhibitors had a marked effect on both naphthoate and azinomycin production. This suggests minimally the involvement of a P-450 oxygenase in the first step of the biosynthesis to generate what becomes the 3'-hydroxyl of the naphthoate fragment (**Figure 43**), which is subsequently methylated, via a SAM-dependent process likely involving a methyltransferase, to give the final product, supporting previous reports [30, 31]. Completion of the biosynthesis of azinomycin B requires a number of oxidative transformations and could also involve other P-450-dependent processes.

Table 4. Effect of Enzyme Inhibitors on Azinomycin B Production.

Reaction condition	Inhibitor	CPM (10 μ M)	CPM (100 μ M)
1 (Cont.)	—	40	40
1 (Expt.)	—	714	714
2 (Cont.)	miconazole	32	32
2 (Expt.)	miconazole	360	164
3 (Cont.)	metyrapone	36	30
3 (Expt.)	metyrapone	348	292
4 (Cont.)	chloramphenicol	36	30
4 (Expt.)	chloramphenicol	523	307
5 (Cont.)	Ceruleinin	38	95
5 (Expt.)	Ceruleinin	178	119

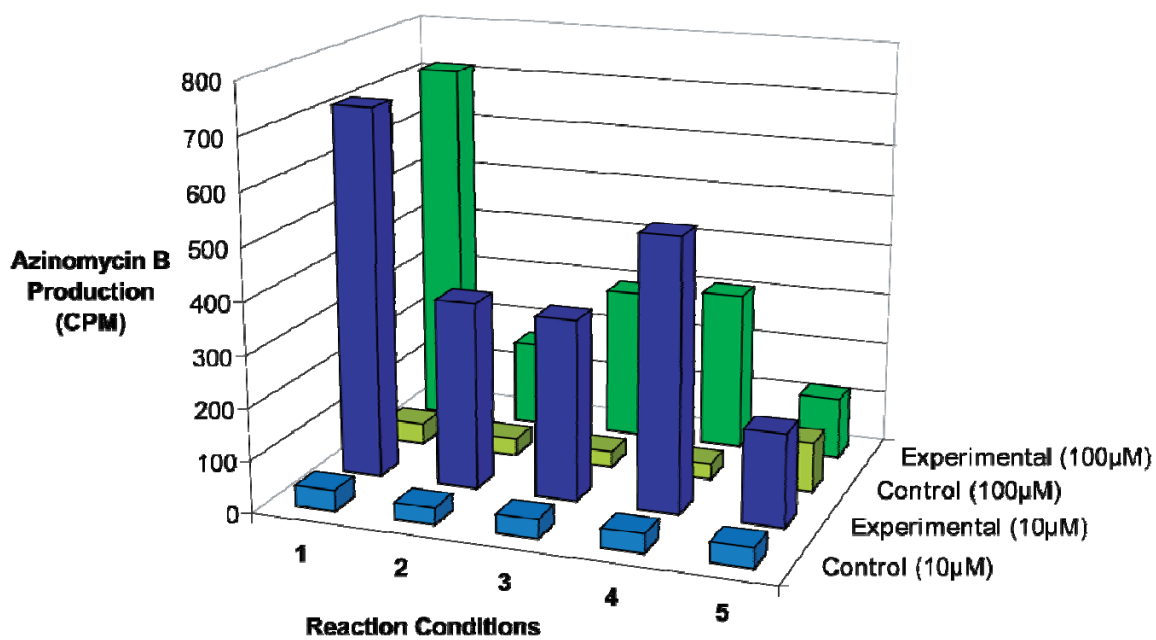


Figure 51. Effect of Enzyme Inhibitors on Azinomycin B Production.

Controls: cpm \pm 10. Experimental: cpm \pm 50. Inhibitors used miconazole (2), metyrapone (3), chloramphenicol (4), and cerulenin (5).

COFACTOR REQUIREMENTS

The cell-free system was used to probe the cofactor requirements of the azinomycin biosynthetic pathway. Enzyme assays were performed as previously described varying only the cofactor preparation. Cofactors are shown in **Figure 52**. The results are shown in **Figure 53**. Not surprisingly, elimination of NADPH from the reaction mixture abolished production of azinomycin B. NADPH is tied directly to both oxidative processes, such as the action of P-450 enzymes as their inhibition was shown to abolish azinomycin production. Neither the removal of THF or FAD appeared to have an effect. FAD could have been a cofactor to a dehydrogenase enzyme, but it is also possible that formation of any alkenes in the biosynthesis of azinomycin B follows a different route. Azinomycin production thus requires the involvement of two cofactors, NADPH and SAM. The participation of SAM in the biosynthesis has been demonstrated by Lowden and co-workers through feeding experiments and later confirmed in our laboratory [30, 31] [133]. Both NADPH and SAM can be projected to play critical roles in the construction of the naphthoate fragment of the molecule. ATP (a necessary cofactor in NRPS biosynthesis) had a marginal effect on azinomycin B production. Presumably, ATP levels in the cell extract were near saturation, negating a conclusive result.

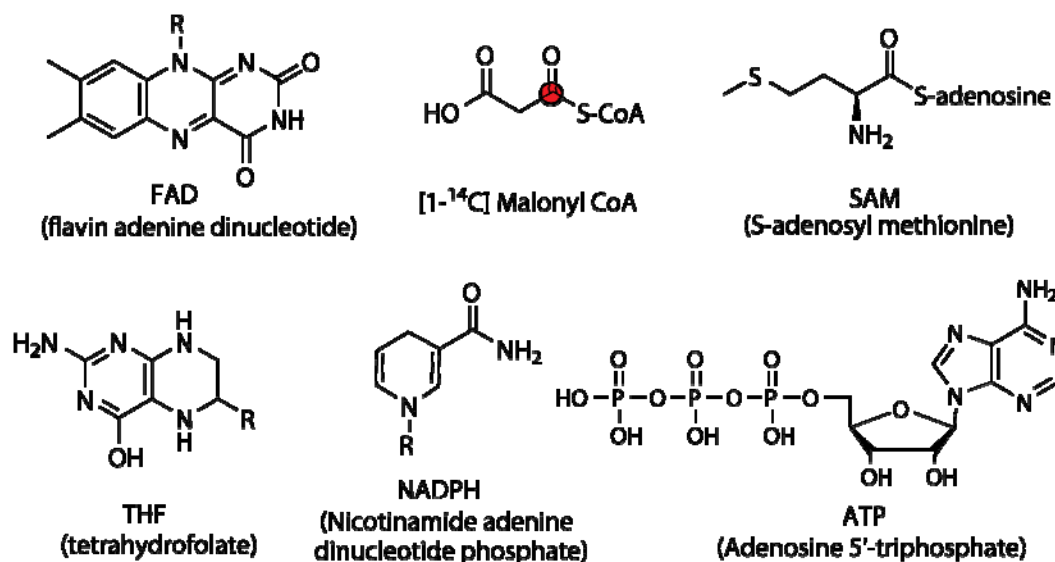


Figure 52. Cofactors Used in Probing Cofactor Requirements of Azinomycin B Biosynthetic Pathway (Conversion to Azinomycin B).

● = ^{14}C

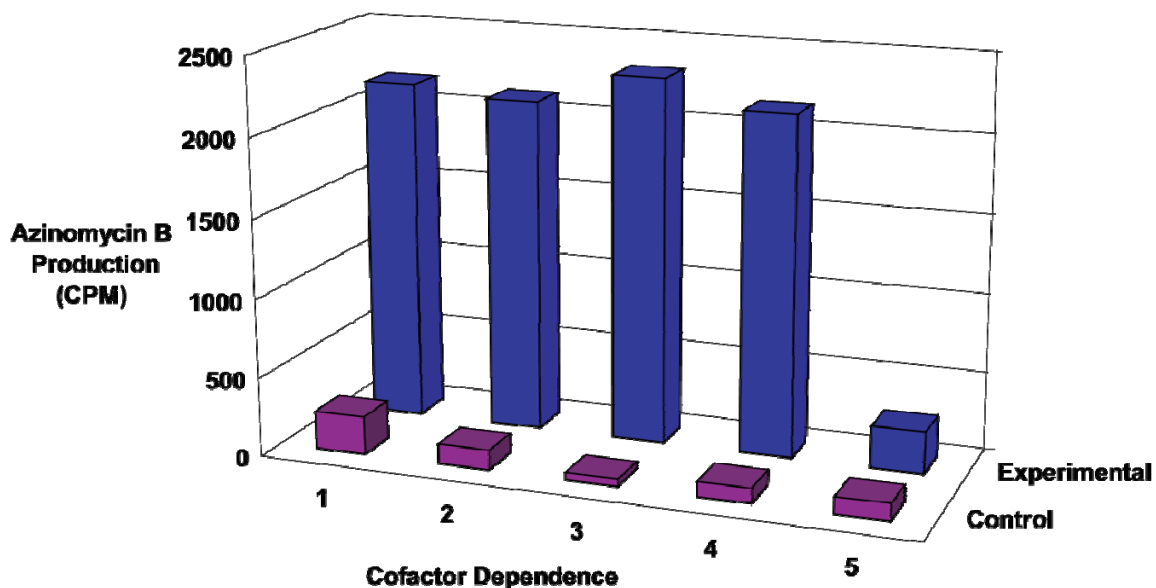


Figure 53. Cofactor Requirements of Azinomycin B Biosynthetic Pathway (Conversion to Azinomycin B).

Controls: cpm \pm 10. Experimental \pm 50. (1) Reaction conditions: CFE + [$1-^{14}\text{C}$] malonyl-CoA, acetyl-CoA, SAM, FAD, and NADPH. (2) Reaction conditions: CFE + [$1-^{14}\text{C}$] malonyl-CoA, acetyl-CoA, SAM, and NADPH. (3) Reaction conditions: CFE + [$1-^{14}\text{C}$] malonyl-CoA, acetyl-CoA, ATP, SAM, FAD, and NADPH. (4) Reaction conditions: CFE + [$1-^{14}\text{C}$] malonyl-CoA, acetyl-CoA, THF, SAM, FAD, and NADPH. (5) Reaction conditions: CFE + [$1-^{14}\text{C}$] malonyl-CoA, acetyl-CoA, THF, SAM, and FAD.

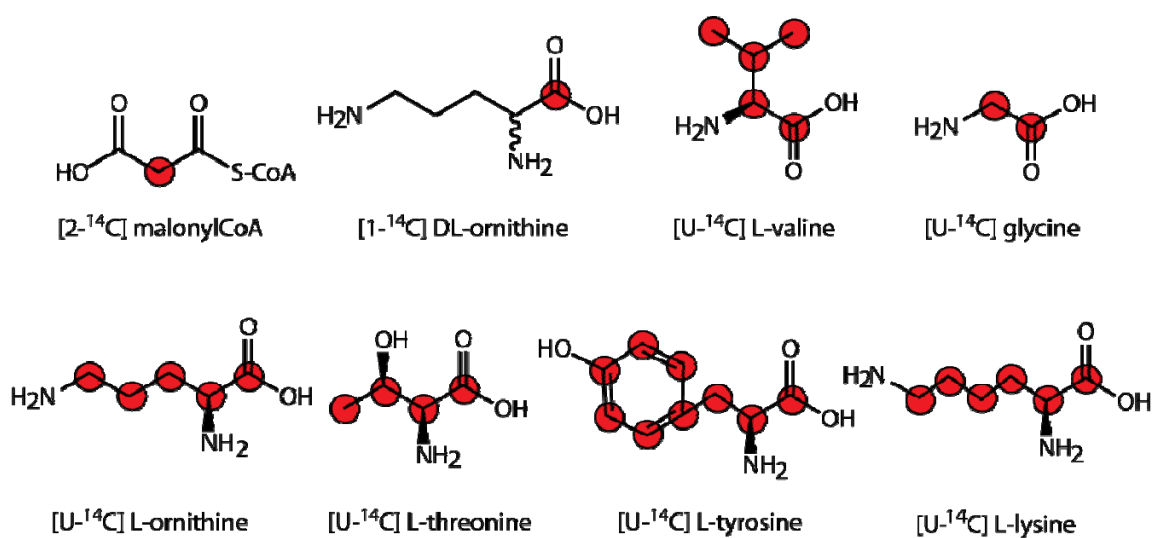


Figure 54. Substrates Used to Probe Azinomycin B Biosynthesis.

● = ^{14}C

SUBSTRATE REQUIREMENTS

The cell-free enzyme system was further exploited to investigate the substrate requirements of the azinomycin biosynthetic pathway. Proposed intermediate building blocks are represented in **Figure 54**. Enzyme assays were performed as previously described with the following modification: With the exception of the CFE enzyme control reaction (**reaction 1**), to each protein extract was added unlabeled malonyl-CoA, acetyl-CoA, and radiolabeled substrate. The results are depicted in **Figure 55** and **Table 5**.

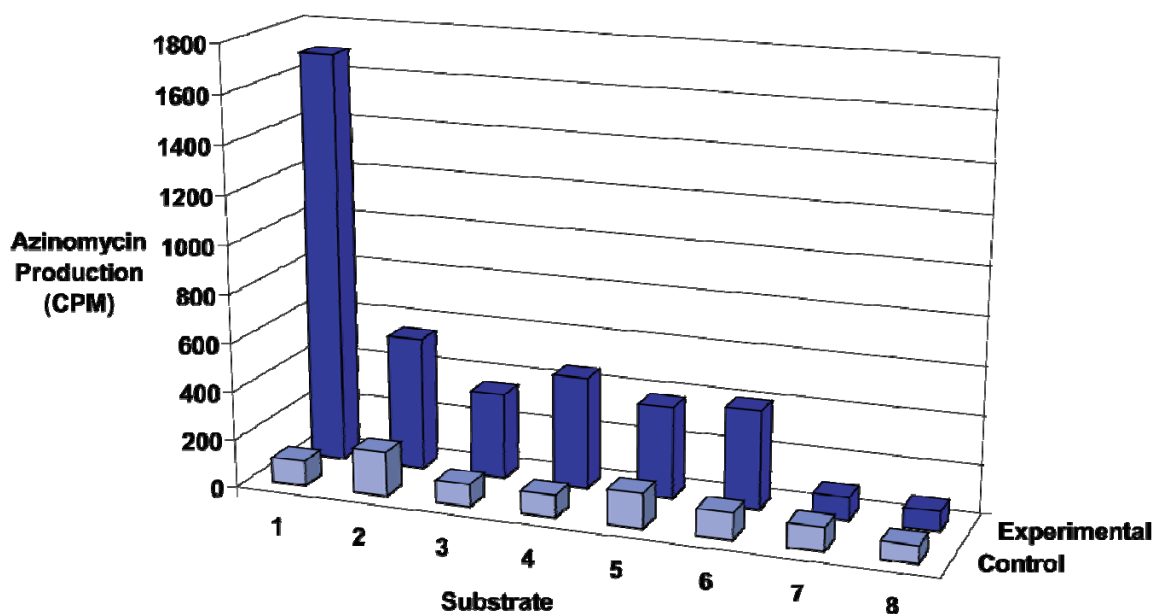


Figure 55. Investigation of the Principle Building Blocks of the Azinomycin B Pathway. Controls: cpm \pm 10. Experimental: cpm \pm 50. (1) [2-¹⁴C] malonyl-CoA, (2) [1-¹⁴C] DL-ornithine, (3) [U-¹⁴C] glycine, (4) [U-¹⁴C] L-valine, (5) [U-¹⁴C] L-ornithine, (6) [U-¹⁴C] L-threonine, (7) [U-¹⁴C] L-lysine, and (8) [U-¹⁴C] L-tyrosine.

All suspected intermediates (as shown in **Figure 55**) showed positive incorporation, except for tyrosine (an amino acid with no suspected involvement in the pathway) and lysine, which were included as negative controls. Although lysine could be projected to give rise to the azabicyclic ring system of azinomycin B (**Figure 56**), lack of incorporation of S-adenosylmethionine (by way of [¹³C-methyl]-methionine) [109] [134] and background level counts observed *in vitro* with radiolabeled lysine contradict such a mechanism. Moreover, THF, a cofactor that can also facilitate methyl transfer, did not exhibit an effect *in vitro*. The higher levels of incorporation observed with malonyl-CoA versus other amino acid substrates are a

reflection of the multiple malonyl units (five) incorporated into the naphthoate fragment of the molecule. All other substrates are represented only once. It should be noted that the results of this assay do not specifically imply location of incorporation into the molecule. The location is implied largely by deduction and implication of previously reported stable isotope feeding studies by Lowden and coworkers [30, 31]. Incorporation of stable isotopes for direct location information is explored in a subsequent chapter of this dissertation.

Table 5. Investigation of the Principle Building Blocks of the Azinomycin B Pathway.

Reaction condition	Substrate	Azinomycin B Production (CPM)
1 (Cont.)	[2- ¹⁴ C] malonyl CoA	103
1 (Expt.)	[2- ¹⁴ C] malonyl CoA	1694
2 (Cont.)	[1- ¹⁴ C] DL-ornithine	182
2 (Expt.)	[1- ¹⁴ C] DL-ornithine	548
3 (Cont.)	[U- ¹⁴ C] glycine	92
3 (Expt.)	[U- ¹⁴ C] glycine	352
4 (Cont.)	[U- ¹⁴ C] L-valine	92
4 (Expt.)	[U- ¹⁴ C] L-valine	460
5 (Cont.)	[U- ¹⁴ C] L-ornithine	144
5 (Expt.)	[U- ¹⁴ C] L-ornithine	378
6 (Cont.)	[U- ¹⁴ C] L-threonine	109
6 (Expt.)	[U- ¹⁴ C] L-threonine	403
7 (Cont.)	[U- ¹⁴ C] L-lysine	97
7 (Expt.)	[U- ¹⁴ C] L-lysine	94
8 (Cont.)	[U- ¹⁴ C] L-tyrosine	72
8 (Expt.)	[U- ¹⁴ C] L-tyrosine	81

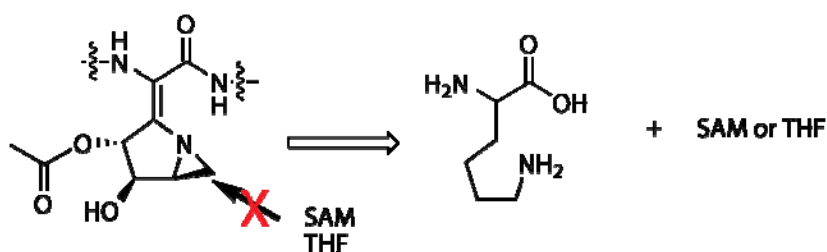


Figure 56. Possible Formation of the Azabicyclic Ring from Lysine.
 [U-¹⁴C] L-lysine showed no incorporation into azinomycin B.

SIGNIFICANCE

These experiments taken together indicate the origins of azinomycin B as conveyed in **Figure 57**, with color coded substrates. These results support previously reported origins for the naphthoate group, a putative PKS product, but indicate more specifically the origin of the right hand part of the molecule, a putative NRPS product. These insights played a large role in shaping the series of stable isotope feeding experiments we subsequently pursued.

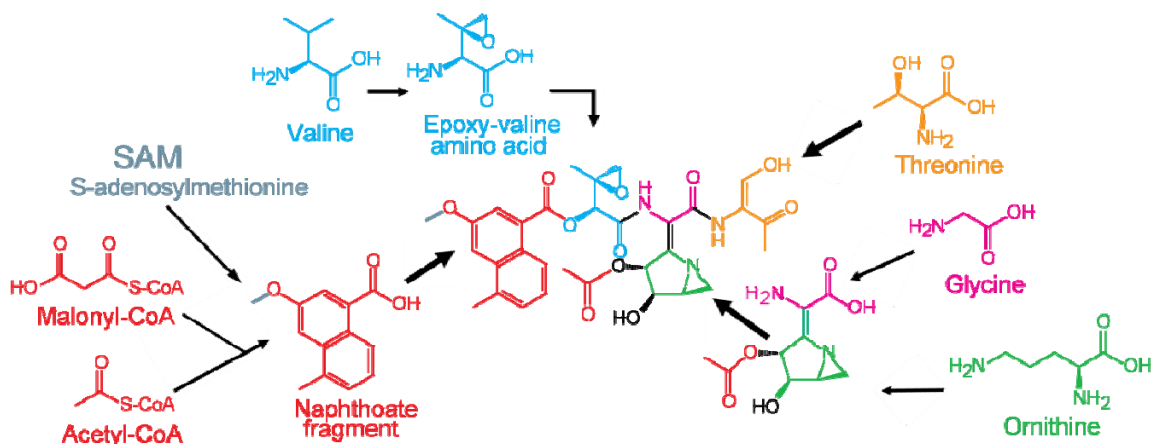


Figure 57. Diagram Depicting Possible Substrate Requirements of Azinomycin B Biosynthetic Pathway.

The results provide the first demonstration of a cell-free enzyme system that supports biosynthesis of the interstrand DNA cross-linker azinomycin B. Investigations with this enzyme preparation rendered important information regarding the inhibition of and the substrate and

cofactor requirements of the pathway, corroborating our hypothesis of the PKS-NRPS hybrid origin of azinomycin B biosynthesis.

EXPERIMENTAL PROCEDURES

GENERAL

Radiolabeled substrates including: [2-¹⁴C] malonyl-CoA, [U-¹⁴C] L-lysine, and [U-¹⁴C] L-proline were obtained from Moravек Biochemicals (Brea, CA). All radiolabeled substrates including: [1-¹⁴C] DL-ornithine, [U-¹⁴C] glycine, [U-¹⁴C] L-valine, [1-¹⁴C] DL-glutamic acid, [U-¹⁴C] L-tyrosine, [U-¹⁴C] L-threonine, and [U-¹⁴C] L-ornithine were acquired from American Radiolabeled Chemicals (St. Louis, MO).

TLC plates were purchased from Analtech (Newark, DE). Co-factors (SAM, FAD, and NADPH) and all cell media and buffer components were obtained from Sigma Biochemicals (St. Louis, MO) unless otherwise specified. OPTI-Fluor O was purchased from Perkin Elmer (Wellesley, MA). The FAS/PKS inhibitor cerulenin was purchased from Sigma Biochemicals (St. Louis, MO). All cytochrome P-450 enzyme inhibitors (metyrapone, chloramphenicol., and miconazole) were obtained from Aldrich (Milwaukee, WI).

INSTRUMENTATION

¹H and ¹³C NMR spectra were recorded on either a Varian Inova 500 or Varian Inova 300. ¹H NMR chemical shifts are reported as δ values in ppm relative to CDCl₃ (7.26 ppm) and coupling constants (*J*) are reported in Hertz (Hz). Infrared spectra were recorded on a Bruker Tensor 27 spectrometer. Unless otherwise indicated, deuteriochloroform (CDCl₃) served as an internal standard (77.0 ppm) for all ¹³C spectra. Mass spectra (ESI) were obtained at the Laboratory for Biological Mass Spectrometry at the Department of Chemistry, Texas A&M University using an API QStar Pulsar, MDS Sciex (Toronto, ON, Canada), or Quadrupole-TOF hybrid spectrometer. Gas chromatography/low resolution mass spectra were recorded on a Trace DSQ GCMS spectrometer from ThermoElectron Corporation (Austin, TX, USA). APCI was recorded on a Thermofinnigan LC-Q DECA mass spectrometer. Radioactive products were measured on a Beckman LS5810 scintillation counter. The Bead Beater used in the preparation of cell-free extracts was purchased from Biospec (Bartlesville, OK).

ORGANISM

Streptomyces sahachiroi (NRRL 2485) was obtained from the American Type Culture Collection (ATCC; Manassas, VA).

CULTURE CONDITIONS

(THE AUTHOR)

Streptomyces sahachiroi was initially cultured on GYM plates until sporulation, typically 5-7 days at 28 °C. GYM agar plates contained per liter: glucose monohydrate, 4 g; yeast extract (Difco), 4 g; malt extract (Difco), 10 g; CaCO₃, 2 g; Bacto-agar (Difco), 12 g; and tap water adjusted to pH 6.8 with 1 M NaOH prior to sterilization. A starting culture of *Streptomyces sahachiroi* in PS5 medium (100 mL) was prepared by inoculation of a loop full of spores from the GYM plates. PS5 medium was prepared from 5 g/L of Pharmamedia (yellow cotton seed flour; Traders Protein; Memphis, TN) and 5 g/L of soluble starch, adjusted to a pH of 7.0. Following 24 h of growth at 30 °C, 250 rpm, 25 mL of the starting culture was used to inoculate 500 mL of PS5 in 2 L baffled Erlenmeyer flasks. The cultures were grown for 64 h (30 °C, 250 rpm). The cells were harvested by centrifugation, and the cell pellet was frozen in liquid nitrogen (in aliquots) and stored at -80 °C.

CELL-FREE EXTRACT PREPARATION

(DR. CHAOMIN LIU)

The cell-free extract was prepared by combining frozen cells (13-15 g), glass beads (28 g; 0.1 mm), and cell-free extract buffer (100 mM potassium phosphate, pH 7.5; 50% glycerol, 2 mM dithiothreitol, and 1 mM EDTA; 80 mL; 4 °C) in a bead beater equipped with an ice water jacket. The cells were pulverized employing ten 1 min. cycles separated by 1 min. intervals to prevent warming of the protein extract. The lysate was centrifuged (7,660 G, 15 min) to give the crude cell-free extract.

ENZYME ACTIVITY ASSAYS

(DR. CHAOMIN LIU)

To each aliquot of the protein extract (5 mL) was added 1 µL of acetyl-CoA (1 mg/1 mL), 80 µL of co-factor solution (FAD, 1 mg; SAM, 1 mg; NADPH, 1 mg in 1 mL of deionized distilled water), and 0.25 µCi of ¹⁴C-radiolabeled material. The resulting reaction mixture was incubated at 37 °C for 24 h. The reactions were vortexed with dichloromethane (3 mL); organics were

transferred to fresh tubes and evaporated to dryness. The organic residue was resolubilized in a minimal volume of dichloromethane (60 μ L) and applied to TLC (5:0.3; dichloromethane:methanol; R_f = 0.25, naphthoate; R_f = 0.37, azinomycin B) to which was added unlabeled naphthoate or azinomycin B (isolated from *Streptomyces sahachiroi* cultures). Samples (TLC spots) with appropriate R_f values were scraped from the TLC plate, transferred to vials containing OPTI-Fluor O, and analyzed by scintillation counting.

HPLC COINJECTION ASSAYS

(COLLABORATION BETWEEN DR. CHAOMIN LIU AND THE AUTHOR)

Enzyme activity assays were performed as detailed above. Following extraction and evaporation of the samples to dryness, the organic residue was solubilized in methanol (100 μ L), to which was added unlabeled naphthoate or azinomycin B, and analyzed by Reverse Phase HPLC with a Phenomenex C8 column (250 x 4.6 mm), employing a gradient of acetonitrile/water. Conditions are listed in **Table 6**.

Table 6. HPLC Conditions for the Separation of Naphthoate and Azinomycin B.

HPLC conditions		
Minutes	% acetonitrile	% water
0	10	90
1	10	90
5	35	65
14	95	5
15	95	5
20	10	90
25	10	90

Retention times were 14.9 min. (naphthoate) and 16.2 min. (azinomycin B), respectively. The corresponding peaks were collected, and the samples were evaporated, transferred to vials containing OPTI-Fluor O, and analyzed by scintillation counting.

PROTEIN INHIBITION ASSAYS

(DR. CHAOMIN LIU)

To each aliquot of the protein extract (3 mL) was added 1 μ L of acetyl-CoA (1 mg/1 mL), 0.25 μ Ci of [2-¹⁴C] malonyl-CoA, 80 μ L of cofactor solution (FAD, 1 mg; SAM, 1 mg; NADPH, 1 mg in 1 mL of deionized distilled water) in addition to 10 μ M or 100 μ M inhibitor.

NAPHTHOATE SYNTHESIS

(DR. CHAOMIN LIU)

Details provided in Appendix.

CHAPTER IV

**AN IMPROVED METHOD FOR CULTURING *STREPTOMYCES SAHACHIROI*
FOR THE PRODUCTION OF AZINOMYCIN B ***

INTRODUCTION

The azinomycins (**Figure 58 A and B**) comprise a family of aziridine-containing natural products produced by *Streptomyces sp.* that possess potent anti-tumor activity [2, 17, 77]. *In vitro* experiments reveal the inherent ability of azinomycin B to bind within the major groove of DNA. The electrophilic C-10 and C-21 carbons contained within the aziridino[1,2a]pyrrolidine (1-azabicyclo[3.1.0]hexane) and epoxide fragments impart the ability of the natural product to form interstrand crosslinks with the N7 positions of suitably disposed purine bases of DNA [14, 69-73]. Recent studies with DNA microarrays and fluorescence imaging with the natural product provide the first demonstration of DNA damage caused by azinomycin B in whole cells, correlating *in vitro* DNA cross-linking observed with the metabolite with an *in vivo* cellular response [135].

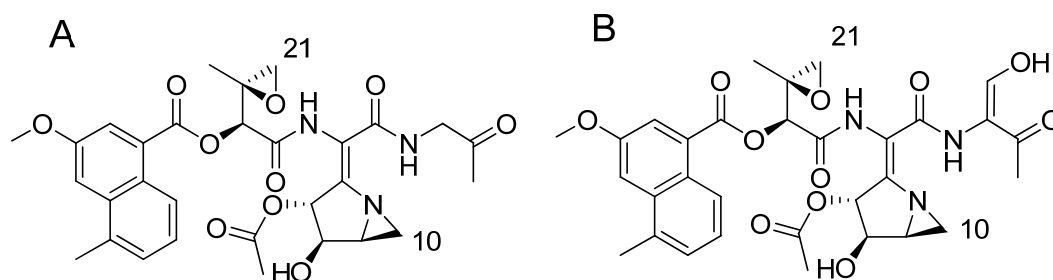


Figure 58. Structures of Azinomycin A and B.

*Reprinted with permission from “An Improved Method for Culturing *Streptomyces sahachiroi*: Biosynthetic Origin of the Enol Fragment of Azinomycin B” by Kelly, G. T., Sharma, V., and Watanabe, C. M. H., 2008. *Bioorganic Chemistry*, 36, 4-15, Copyright [2008] by Cell Press and Elsevier.

The unusual architecture of the azinomycins, coupled with their potent anti-tumor activity, has captured the attention of both the biosynthetic and synthetic communities. The total synthesis of azinomycin A was achieved in 2001 by Coleman and co-workers and a number of synthetic analogues have also been reported [18]. Notwithstanding these gains, even after 50 years beyond its initial isolation [1] and more than two decades of structure correction[2] [17, 77], there is no total synthesis yet reported for azinomycin B. This is a major barrier to in-depth studies involving biological activity of the natural product. In addition, biosynthetic investigations on the compound have lagged considerably. While some gains have been made to establish the polyketide origin of the naphthoate moiety [30, 31], and while a cell-free system has been developed to support synthesis of azinomycin B *in vitro* [110], progress in this area has been impeded primarily by difficulties with the culture method and by the lack of a consistent source of the natural product. Following literature protocols [2], we found production of the natural product by *Streptomyces sahachiroi* to be inconsistent. As a great majority of biosynthetic studies, including isotopic labeling studies and gene disruption experiments, hinge upon having reliable production of the natural product, a new culture method has been needed. Here we present details of experiments performed to achieve optimized growth conditions for the production of azinomycin B.

RESULTS AND DISCUSSION

DEVELOPMENT OF THE CULTURE SYSTEM

(THE AUTHOR)*

In the course of evaluating solid and liquid media types, the production of azinomycin was erratic when literature protocols were followed [1, 2, 30]. A collaborator, Dr. Robert Coleman of The Ohio State University Department of Chemistry, had similar problems when he attempted to get azinomycin A and B for mode of action studies and spectroscopic comparison in his efforts towards total synthesis of both azinomycin A and B. Dr. Coleman had been using The Ohio State University's fermentation facility to have the culture grown to produce the azinomycins. They observed production from the *Streptomyces sahachiroi* strain once, but could not reproduce this result. We obtained both *Streptomyces sahachiroi* (NRRL 2485) and *Streptomyces griseofuscus* (NRRL B-5429) strains reported to produce azinomycins from American Type Culture Collection (ATCC) [2, 136]. From these two strains we followed literature protocols and

* Denotes major contributor(s) to each section.

found *Streptomyces sahachiroi* to be a better producer of the natural product. Therefore we set out to improve the cell culture conditions of this strain.

SOLID MEDIA EVALUATION

(THE AUTHOR)

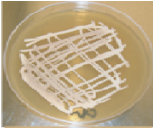

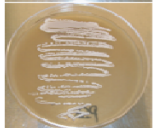
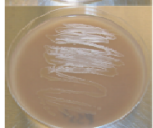

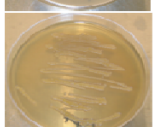
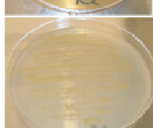

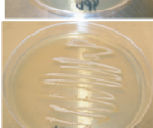

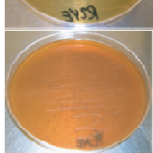
As the production of secondary metabolites from *Streptomyces* frequently coincides with or precedes the formation of aerial hyphae on solid media [137], we initially examined a variety of media conditions including LB, ISP+ [138], NB+, YPD [108], TO [139], GYM [69], PS5 [69], MS [140], YEME [140], and R2YE [140]. Several solid media conditions were evaluated by streaking a loop full of *S. sahachiroi* spore stock upon prepared plates. The growth was evaluated at regular intervals. All plates showed growth of *Streptomyces*; however, only cultures grown on GYM, MS, PS5, PS5+, TO, and YPD plates exhibited sporulation (see **Table 7**). As azinomycin B production was undetectable in organic extracts of the spores, the plates were inoculated into Erlenmeyer flasks containing 100 mL of PS5 medium. After a 72 h post-inoculation period at 30°C, the cultures were extracted with dichloromethane, concentrated, and analyzed by TLC and mass spectrometry. Results revealed that while the MS plates showed traces of azinomycin B production, the GYM plates produced the most robust and productive spores at 5-7 days growth, especially when inoculated from spores stocks generated from spores stored on dehydrated GYM plates.

DEHYDRATED PLATES

(THE AUTHOR)

After evaluating several media types and selecting GYM as the best solid medium for inoculation of liquid culture for production of the azinomycins, some erratic behavior with production was observed, where production would have been seen then lost for several weeks to months. Several experimental avenues were explored to account for these losses of production: plate to plate spore transfer, spore stock analysis, and use of dehydrated culture plates. Continual transfer of productive spores from one plate to another seemed to maintain a productive line. This method of preparation of plates was pursued for a period of time. However, this approach suffered from the problem of genetic drift, wherein particular traits in the spore population may become more rare or common. Chromosomal instability and end deletion of the linear chromosome have been reported in *Streptomyces* species [141, 142]. Since production of azinomycin is not a trait which is maintained by selection in continuing growth on the GYM plate, there is no barrier to the loss

Table 7. Evaluation of Solid Media for Growth and Production of Azinomycin B.

Media Type	Growth Description	Production of azinomycin B	Actual Plate
GYM	Robust, with mature grey spores by the second day	Yes	
MS	Robust, with mature grey spores by the third day	Traces	
PS5	Slow sporulation, flat colonies	No	
PS5+	Slow sporulation, flat colonies	No	
TO	Slow sporulation, flat colonies	No	
ISP+	<i>S. sahachiroi</i> grew rapidly but no sporulation seen	No	
LB	<i>S. sahachiroi</i> grew rapidly but no sporulation seen	No	
YPD	<i>S. sahachiroi</i> grew slowly, slow sporulation seen	No	
NB+	<i>S. sahachiroi</i> grew slowly but no sporulation seen	No	
R2YE	<i>S. sahachiroi</i> grew slowly but no sporulation seen	No	
YEME	<i>S. sahachiroi</i> grew slowly but no sporulation seen	No	

Plates shown at 60 hours' growth after streaking plate with a loop full of *Streptomyces sahachiroi* spore stock made from spores originally isolated from a desiccated solid GYM media plate.

of this trait to genetic drift. When erratic production occurred after several generations of successive plate-to-plate transfer, the original spore stocks we purchased from ATCC were evaluated. The purchased spore stocks were dehydrated, and stored in a sealed glass vial. Glycerol stocks were made from these dehydrated spores and stored at $-80\text{ }^{\circ}\text{C}$. Cultures grown on GYM media from this stock were not consistently productive.

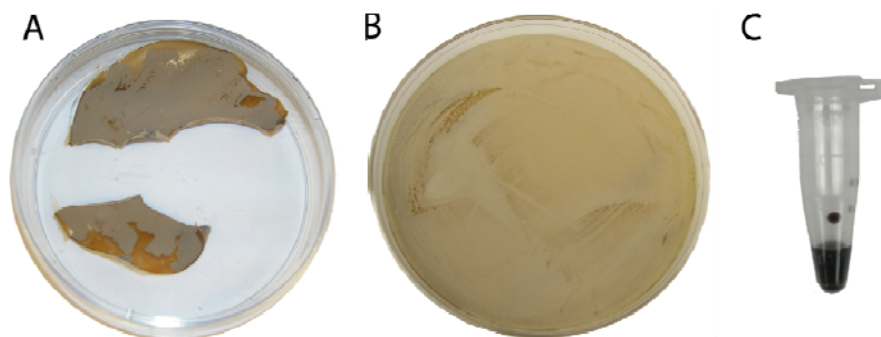


Figure 59. Making Effective Spore Stocks.

(A) Parts of a dehydrated GYM agar plate with *S. sahachiroi* culture. (B) *S. sahachiroi* culture spread upon a GYM plate (3 days growth). (C) Concentrated spore stock originating from dehydrated plates.

In an effort to reproduce previous levels of production, portions of dehydrated *S. sahachiroi* cultures grown on GYM plates which had been productive months earlier were used to inoculate a culture and to transfer spores to a fresh GYM plate for subsequent cultures. While the cultures produced azinomycin consistently, the source of dehydrated plates was limited. Thus a set of spore stocks was made from these spores using an MS plate. The resulting spore stocks were successfully used thereafter (see **Figure 59**).

LIQUID MEDIA EVALUATION

(THE AUTHOR)

A variety of media formulations (YPD, R2YE, PS5, PS5+, LB, TO, GYM, MS, YEME, NB+, and ISP+) [108, 138-140] were examined for their ability to support azinomycin production by *S. sahachiroi* in shake flasks and by fermentation, as summarized in **Table 8**. Since secondary metabolite production is generally confined to the stationary phase of the growth curve, in shake culture (Erlenmeyer flasks or baffled flasks) we evaluated each medium composition by

generating a first stage culture (from GYM plates), which was used to inoculate and produce the culture in modest to large scale (in 0.5, 1, 2 or 4 Liter Erlenmeyer flasks or 2 Liter baffled flasks). The cells were harvested at a fixed time of 72 h. The cultures were centrifuged and extracted with dichloromethane, then concentrated. Under these growth conditions, azinomycin B production was observed in YPD, R2YE, PS5, and PS5+, but not in LB, TO, GYM, MS, YEME, NB+, and ISP+ as determined by TLC, mass spectrometry, ¹H-NMR and ¹³C-NMR spectroscopy.

WATER SOURCE

(THE AUTHOR)

Another variable explored was the source of water used in the media. Tap water, distilled, and distilled/de-ionized/sterile filtered water were used. The main difference between these waters was the presence or absence of trace metals and additives, in particular extra calcium in tap water. There was also a difference in the pH of these waters. After some initially more encouraging results from the use of tap water, the best, most consistent production results in shake flasks, and later in the fermenter system, was from the distilled/de-ionized/sterile filtered water.

BIO-AVAILABILITY

(THE AUTHOR)

The nutritional content of the medium is a significant factor in deciding what medium might be optimal for the production of a natural product. *Streptomyces* are very sensitive to their environment, resulting in culture wide adjustment in response. The availability of key nutrient groups is important. Although wild type *Streptomyces* are often fully capable of biosynthesizing their own primary metabolites if they are not present in the environment, nutrient shortage has often been shown to prompt production of secondary metabolites. Secondary metabolites often are present in higher production when the growth of the mycelia is in a stationary phase of growth. The production of these metabolites is thought to be a measure of defense against growth of nearby organisms [4]. Competition over limited resources in the soil is thought to have pressured these microorganisms to develop such a diverse and potent range of secondary metabolites. Nutrient limitation and varying the culture period from 1-6 days were investigated. In all cases, azinomycin production was low and/or inconsistent.

Table 8. Liquid Culture and Fermentation Conditions.

Entry	Conditions	Result ^b
Media Screen		
1	100 mL Erlenmeyer PS5 culture, 24 h, 250 rpm, 30°C	Traces
2	250 mL Erlenmeyer various medias ^c , 72 h, 250 rpm, 30°C	PS5 media showed maximum production
Increased culture size of secondary cultures^d		
3	500 mL Erlenmeyer PS5 2 nd culture, 72 h, 250 rpm, 30°C	Inconsistent
4	400 mL-1000 mL Erlenmeyer PS5 2 nd culture, 24-144 h, 250 rpm, 30°C	Inconsistent
5	2500 mL Erlenmeyer PS5 2 nd culture, 72 h, 250 rpm, 30°C	Low yields
Fernbach (baffled flask for greater aeration)		
6	400 mL Fernbach PS5, 2 nd culture, 72 h, 200-250 rpm, 28-30°C	Higher than 1-5, but inconsistent
7	500 mL Fernbach PS5, 2 nd culture, 72 h, 200-250 rpm, 28-30°C	Higher than 1-6, but inconsistent
8	600 mL Fernbach PS5, 2 nd culture, 72 h, 200-250 rpm, 28-30°C	Higher than 1-7, but inconsistent
pH adjustment		
9	Adjust 450-600 mL Fernbach PS5 media to pH 6.0-8.0 with HCl/NaOH pre-sterilization, 72 h, 250 rpm, 30°C	Inconsistent
10	Adjust 450, 600 mL Fernbach PS5 media with phosphate buffer to pH 8.0, 10.0, 72 h, 250 rpm, 30°C	No production
11	Adjust 450, 600 mL Fernbach PS5 media to pH 8.0 with NaOH at regular intervals during growth, 72 h, 250 rpm, 30°C	No production, pH reset
Increase size of culture using fermenter		
12	1 st stage culture 3X100mL PS5, 24 h, 30°C; 2 nd stage culture 15L PS5 in fermenter, 72 h, 10L/min aeration, 250 rpm, 28°C	Over bubbling, uncontrolled foaming, no production
13	1 st stage culture 1X100mL PS5, 24 h, 30°C; 2 nd stage culture 2X600mL PS5 Fernbach, 24 h, 30°C; 3 rd stage culture 10L PS5 in fermenter, 72 h, 10L/min aeration, 250 rpm, 28°C	Over bubbling, uncontrolled foaming, no production
14	1 st stage culture 3X100mL PS5, 24 h, 30°C; 2 nd stage culture 6X600mL PS5 Fernbach, 24 h, 30°C; 3 rd stage culture 8L PS5 in fermenter, 72 h, 10L/min aeration, 250 rpm, 28°C	foaming issues, ~25 mg azinomycin B
Nutrient deprivation		
15	2nd stage 600 mL Fernbach 50-100% PS5 reduction, 72 h, 30°C	No production
16	2 nd stage 600 mL Fernbach PS5, 24 h, 30°C; Pellet transfer (2 nd stage to 3 rd stage); 3 rd stage 600 mL Fernbach PS5, 72 h, 250 rpm, 30°C	No production
17	2nd stage culture 2X600mL Fernbach PS5, 24h; 3rd stage culture 10L 50% PS5 reduction in fermenter, 48h, 8L/min aeration, 250 rpm, 28°C	~15mg azinomycin B
18	2nd stage culture 2X600mL Fernbach PS5, 24h; 3rd stage culture 10L 50% PS5 reduction in fermenter, 72h, 8L/min aeration, 250 rpm, 28°C	~12mg azinomycin B
19	2nd stage culture 2X600mL Fernbach PS5, 24h; 3rd stage culture 10L 75% PS5 reduction in fermenter, 72h, 8L/min aeration, 250 rpm, 28°C	~40mg azinomycin B
20	2nd stage culture 2X600mL Fernbach PS5, 24h; 3rd stage culture 10L 75% PS5 reduction in fermenter, 72h, 8L/min aeration, 250 rpm, 28°C	~30mg azinomycin B
21	2nd stage culture 2X600mL Fernbach PS5, 24h; 3rd stage culture 10L 90% PS5 reduction in fermenter, 72h, 8L/min aeration, 250 rpm, 28°C	~17 mg azinomycin B

(a) Inoculation using ¼ GYM plate spread with *S. sahachiroi* spores, 5 days growth, 37°C; (b) extracted with dichloromethane, dried over MgSO₄ or NaSO₄, concentrated, then analyzed by TLC, APCI-MS, 1H NMR; c: Liquid media: GYM, ISP+, LB, MS, NB+, PS5, PS5+, TO, R2YE, YEME, and YPD; d: Inoculation using 25mL of 1st stage culture shaken at 250 rpm, 30 °C, 24 h.

LARGE SCALE FERMENTATION SYSTEM

(THE AUTHOR)

As modifying liquid shake culture protocols did not give much improvement, a large scale fermentation system was explored (**Figure 60A**). Such an approach affords more control over several factors not easily controlled with shake flasks, such as degree of aeration and foaming. Initially the fermenter (15 L capacity) was inoculated with two 24 h first stage cultures (100 mL, generated from GYM plates), agitated at 250 rpm, and aerated at 6 L/min with sterile filtered air for 72 H. The experiment resulted in considerable foaming, leading to loss of culture and low production of the azinomycins. The volume of medium was therefore decreased to 10 L and the experiment was repeated, inoculating with two 24 h second stage cultures (600 mL each) that were generated by inoculating 2 L baffled flasks with 25 mL of a 24 h first stage culture. As azinomycin production was minimal, nutrient starvation was explored (see **Table 8, entries 15-21**). The component composition of the PS5 medium (10 L) was reduced by 50% and inoculated with two 600 mL second stage cultures. After 72 h, the cells were harvested and approximately 30 mg of azinomycin B was obtained from 10 L. To further investigate the stress imposed by medium deprivation, the medium composition was reduced by 75%, inoculated with two second stage cultures (600 mL), and harvested after 72 H. This sequence yielded approximately 40 mg of azinomycin B from 10 L of culture. By increasing nutrient deprivation to 90%, we isolated only 17mg of pure azinomycin B out of 65mg of crude material extracted. Further reduction of the PS5 medium composition resulted in lower levels of azinomycin production (**Figure 60C**). By increasing the volume of the two second stage cultures to 1 L and the aeration rate to 8 L/min, we can now obtain reliably about 60 mg of azinomycin from 10 L. Interestingly, the pH of the cell culture steadily increased to ~8.0 over a period of 4 days. **Figure 60B** and **D** show the pH profile and the amount of azinomycin B produced as functions of time. Optimal production of the natural product was observed between 64-72 h (**Figure 60D**) corresponding to pH 7.4-7.8 (**Figure 60B**), probably due to instability of the molecule under strongly acidic or alkaline conditions. Manual adjustment of the pH throughout the culture period with bicarbonate did not have a dramatic effect on production levels, and 40-60 mg of azinomycin was obtained by this method.

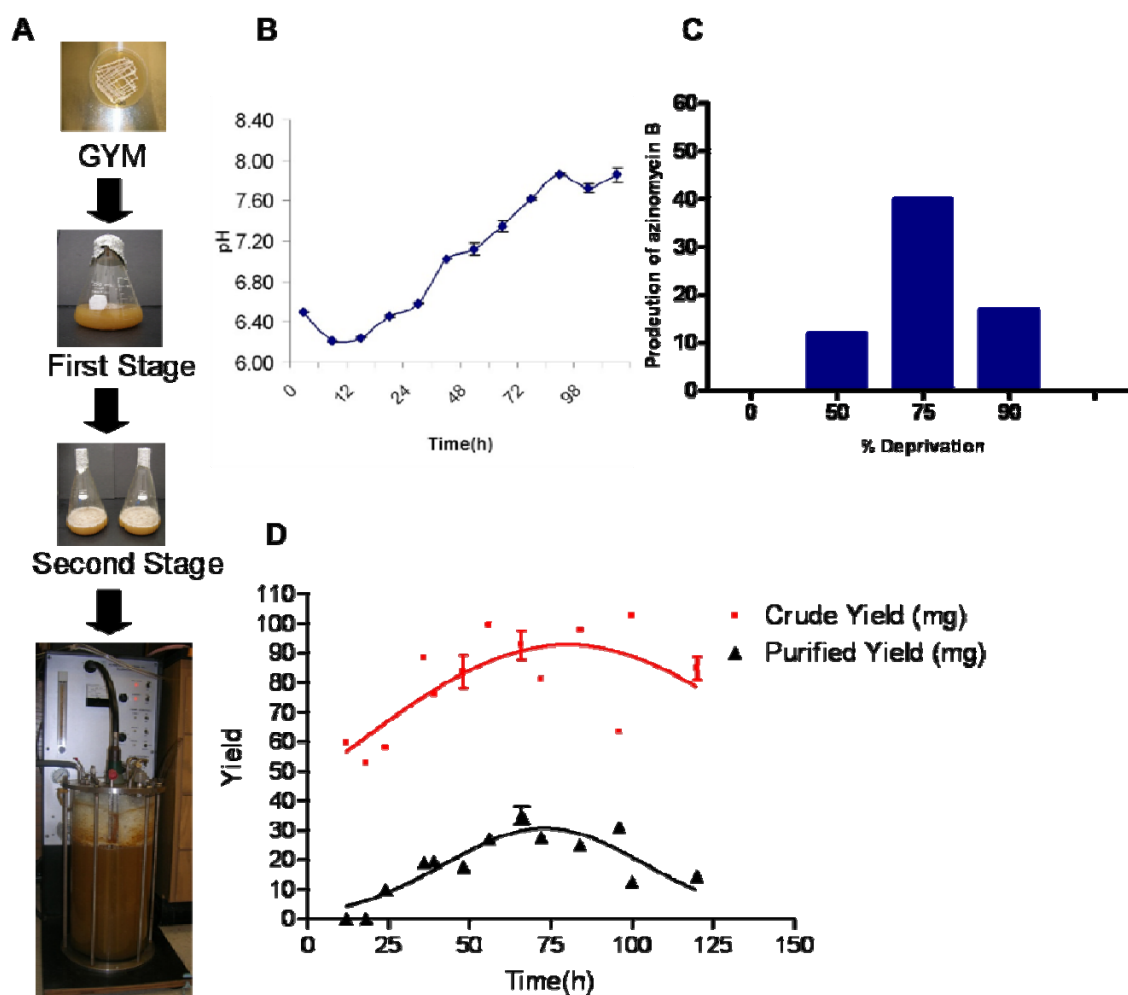


Figure 60. Evaluation of Fermentation System.

(A) Sequence of fermentation system: Culture of *S. sahachiroi*. (B) pH profile as a time course. (C) Effect of nutrient deprivation on production of azinomycin B. (D) Time course production of azinomycin B with 75% nutrient deprivation (second stage culture, 600 mL baffled flask). Crude yield of azinomycins and purified azinomycin B are shown as a function of time.

SIGNIFICANCE

While *in vivo* applications and experiments with azinomycin B show significant promise, the clinical potential of the agent remains largely unexplored due to a dearth of synthetic procedures for the molecule as well as unreliable culture methods for the producing organism. Our reliable fermentation procedure for *S. sahachiroi*, the azinomycin producer, yields up to 60 mg of purified compound can be obtained from 10 L of culture. This system has been employed

successfully to investigate the biosynthetic origin of azinomycin B using stable isotope studies described in subsequent chapters in this dissertation.

EXPERIMENTAL PROCEDURES

INSTRUMENTATION AND GENERAL METHODS

^1H & ^{13}C NMR spectra were recorded on either a Varian Inova 500 or Varian Inova 300. ^1H NMR chemical shifts are reported as δ values in ppm relative to CDCl_3 (7.26 ppm) and coupling constants (J) are reported in Hertz (Hz). Infrared spectra were recorded on a Bruker Tensor 27 spectrometer. Unless otherwise indicated, deuteriochloroform (CDCl_3) served as an internal standard (77.0 ppm) for all ^{13}C spectra. Mass spectra (ESI) were obtained at the Laboratory for Biological Mass Spectrometry at the Department of Chemistry, Texas A&M University, with an API QStar Pulsar, MDS Sciex (Toronto, ON, Canada), or Quadrupole-TOF hybrid spectrometer. Gas chromatography/low resolution mass spectra were recorded on a Trace DSQ GCMS spectrometer from ThermoElectron Corporation (Austin, TX, USA). APCI was recorded on a Thermofinnigan LC-Q DECA mass spectrometer. Fermentations were run on Fermentation Design Inc. Model # MS21 (Allentown, PA, USA). The total capacity of the fermentation system is 15 L.

ORGANISM

Streptomyces sahachiroi (NRRL 2485) and *Streptomyces griseofuscus* (NRRL B-5429) were obtained from the American Type Culture Collection (ATCC).

SPORE STOCKS

Streptomyces sahachiroi spores from dehydrated GYM (Glucose, Yeast Extract, and Maltose Extract) plates (per liter of medium: glucose monohydrate, 4 g; yeast extract, 4 g; malt extract, 10 g; CaCO_3 , 2 g; and tap water adjusted to pH 6.8 with 1 M NaOH prior to sterilization) were streaked onto large MS (Mannitol Soya flour, per liter medium: Mannitol, 20 g; Soya flour, 20 g; and deionized water) plates and allowed to incubate at 30 °C for 15 days. At this time the grey spores were removed with sterile water and agitation. The spores were filtered through sterile cotton, washed three times with sterile water, centrifuged at 3000 rpm, re-suspended in a minimal amount of 10% glycerol solution, flash frozen, and stored at -80 °C.

MEDIA CONDITIONS

GYM (Glucose, Yeast Extract, and Maltose Extract) agar plates contained the following components per liter: glucose monohydrate, 4 g; yeast extract, 4 g; malt extract, 10 g; CaCO₃, 2 g; and tap water; adjusted to pH 6.8 with 1 M NaOH prior to sterilization [69].

PS5 (Pharmamedia/Starch) medium contained the following components per liter: 5 g/L of Pharmamedia (yellow cotton seed flour) 5 g/L of soluble starch, and deionized water adjusted to pH 7.0 prior to sterilization [69].

PS5+ (Pharmamedia/Starch plus additives) medium contained the following components per liter: Pharmamedia (yellow cotton seed flour), 5 g; soluble starch, 5 g; Glucose, 2 g; Casein hydrolysate, 2 g; NH₄SO₄, 0.5 g; lysine, .5 g; ornithine, .5 g; glycine, .5 g; and deionized water adjusted to pH 7.0 prior to sterilization.

NB+ (Nutrient Broth plus additives) medium contained the following components per liter: Beef Extract, 3 g; Bacto-peptone, 5 g; NH₄SO₄, 2 g; Glucose, 2 g; 1 mM All 20 amino acids; 1 mM ornithine; and deionized water.

ISP+ (International Streptomyces Protocol Broth plus additives) medium contained the following components per liter: Yeast Extract, 4 g; Oxoid malt extract, 10 g; Glucose, 4 g; NH₄SO₄, 2 g; 1 mM All 20 amino acids; 1 mM ornithine; and deionized water [138].

LB (Luria-Bertani) medium contained the following components per liter: Bacto-peptone, 10 g; Yeast extract, 5 g; Sodium chloride, 5 g; and deionized water.

TO (Tomato Paste/Oatmeal) medium contained the following components per liter: Tomato Paste, 10 g; Ground Oatmeal, 10 g; and deionized water [139].

YPD (Yeast Peptone Dextrose)medium contained the following components per liter: Yeast extract, 5 g; Bacto-peptone, 5 g; Glucose, 20 g; and deionized water [108].

MS (Mannitol Soya Flour) medium contained the following components per liter: Mannitol, 20 g; Soya flour, 20 g; and deionized water [140].

YEME (Yeast Extract/Maltose Extract)medium contained the following components per liter: Yeast extract, 3 g; Bacto-peptone, 5 g; Oxoid malt extract, 3 g; Glucose, 10 g; Sucrose, 340 g; After autoclaving, add: 2 ml MgCl₂•6H₂O (2.5M) and deionized water [140].

R2YE (Required Growth factors added/Yeast Extract)medium contained the following components per liter: Yeast extract, 4 g; Bacto-peptone, 4 g; Bacto-tryptone, 2 g; Glucose, 10 g; Sucrose, 103 g; K₂SO₄, 0.25 g; MgCl₂.6H₂O, 10.12 g; Casaminoacids, 1 g; 10 mL KH₂PO₄ (0.5%); 80 mL CaCl₂.2H₂O (3.68 %); 15 mL L-proline (20%); 2 mL *Trace element solution; 5 mL NaOH (1N); 25 mL Tris-HCl (1M, pH 7.5); Adjust to pH 6.8 with HCl or NaOH. *Trace

element solution contained the following components per liter: ZnCl_2 , 40 mg; $\text{FeCl}_3 \cdot 6\text{H}_2\text{O}$, 200 mg; $\text{CuCl}_2 \cdot 2\text{H}_2\text{O}$, 10 mg; $\text{MnCl}_2 \cdot 4\text{H}_2\text{O}$, 10 mg; $\text{Na}_2\text{B}_4\text{O}_7 \cdot 10\text{H}_2\text{O}$, 10 mg; $(\text{NH}_4)_6\text{Mo}_7\text{O}_{24} \cdot 4\text{H}_2\text{O}$, 10 mg; and deionized water [140].

Agar plates of the above media were prepared by adding 20 g/L bacto-agar. All media were autoclaved at 121 °C for 20 minutes.

SOLID PLATES

Solid media formulations were evaluated by streaking a loop full of *S. sahachiroi* spore stock onto prepared plates. The plates were grown at 30 °C in a Fisher Scientific Isotemp incubator for 5-7 days. Once grown, ¼ of the plate was inoculated into Erlenmeyer flasks containing 100 mL PS5 medium and shaken at 250 rpm at 30 °C. First and second stage cultures were prepared by streaking a 5 µL aliquot of the *S. sahachiroi* spore stock suspension onto the surface of the GYM plates.

DEHYDRATED PLATES

Dehydrated plates were prepared by streaking a loop full of *S. sahachiroi* spore stock onto the surface of the GYM plate, incubating at 37 °C, and storing them at room temperature to dryness (either over a period of weeks at 37 °C or several months at RT).

FIRST STAGE CULTURE

Streptomyces sahachiroi (inoculated from spore stock derived from dehydrated plates) was grown on GYM plates for 5-7 days at 37 °C. A 1 cm² piece of the GYM plate was used to inoculate 100 mL of PS5 media (Pharmamedia (yellow cotton seed flour), 5 g; soluble starch, 5 g) in a 250 mL Erlenmeyer flask. The culture was incubated at 30 °C for 24 h at 250 rpm.

SECOND STAGE CULTURE

The second stage culture was prepared by inoculating 2 L Erlenmeyer baffled flasks (Fernbach; containing 600 mL of PS5 medium) with 25 mL of the first stage culture. The culture was incubated at 30 °C for 24 h at 250 rpm.

FERMENTATION

The fermenter containing 10 L of the 75% reduced concentration PS5, per liter of medium: Pharmamedia (yellow cotton seed flour), 1.25 g; corn starch, 1.25 g;) medium was autoclaved at

121 °C for 20 min, then quick cooled to room temperature. Following inoculation (with two 600 mL second stage cultures), the fermenter was agitated at ~300 rpm and aerated with sterile filtered air (8 L/min) for 72 h.

ISOLATION AND PURIFICATION OF AZINOMYCIN B

Following fermentation, the cultures were centrifuged at 7,000 rpm at 4 °C. The cell pellets were discarded, and the medium was extracted with an equal volume of methylene chloride (CH₂Cl₂). The organic layer was collected, dried over anhydrous magnesium sulfate, and concentrated *in vacuo*. The resulting crude extract was stored under diethyl ether at -80 °C. The solid was dissolved in a minimal amount of dichloromethane and precipitated with the addition of hexane to give a ratio of 1:29 CH₂Cl₂/hexane. The resulting suspension was centrifuged at 1,500 rpm, and the supernatant was discarded. Diethyl ether (2 mL) was added to the pellet, which was subsequently agitated, centrifuged at 3000 rpm, and the supernatant was discarded. The resulting residue was dissolved in dichloromethane (600 µL) to which hexanes (2 mL) was added. The heterogeneous mixture was centrifuged at 3,000 rpm, and the supernatant was retained. To the solution was added hexanes (4 mL), and the suspension was centrifuged at 3,000 rpm to give azinomycin B as a solid.

When full purification was not achieved, azinomycin B was further purified by flash column chromatography (95: 5 CH₂Cl₂: methanol). Azinomycin exhibits an R_f of 0.23. A short column was used to minimize overall contact with the silica gel and degradation by hydrolysis. The process can be repeated if necessary. The compound was stored at -80 °C under anhydrous diethyl ether when necessary. The azinomycin B we isolated in this manner matched the NMR spectrum provided by Yokoi *et al.* [17].

AZINOMYCIN B

Pale-white amorphous powder (1:9 CH₂Cl₂:hexane); IR (neat) ν_{\max} 3338.4(br), 2957.1, 2925.3, 2872.8, 1725.92(br), 1619.3, 1601.7, 1511.2, 1417.6 cm⁻¹; ¹H NMR (300MHz, CDCl₃) δ 12.40(1H, br), 12.32(1H, s), 8.54 (1H, dd, *J*=3.6, 7.0Hz), 8.20 (1H, br), 7.94 (1H, d, *J*=2.9Hz), 7.46 (1H, d, *J*=2.9Hz), 7.32 (1H, s), 7.32 (1H, s), 7.32 (1H, s), 5.50 (1H, d, *J*= 4.0Hz), 5.12 (1H, s), 4.64 (1H, dd, *J*= 4.0, 4.8Hz), 3.96 (3H, s), 3.96 (1H, br), 3.36 (1H, m), 2.98 (1H, d, *J*=4.3Hz), 2.80 (1H, d, *J*= 4.3Hz), 2.70 (1H, s), 2.66 (3H, s), 2.30 (1H,s), 2.24 (1H, s), 2.18 (1H, s), 1.52 (1H, s); ¹³C NMR (75MHz, CDCl₃) δ 191.5, 173.0, 165.7, 164.0, 162.0, 156.0, 153.0, 150.8, 134.5, 133.3, 128.1, 127.9, 127.0, 125.4, 123.9, 122.3, 119.3, 118.6, 108.5, 84.4, 77.4*, 77.1*,

56.2, 55.7, 53.9, 46.4, 36.7, 24.5, 21.0, 20.3, 17.2. APCI-MS (LRMS) 624.2, found 624.2 (* obscured by CDCl₃ solvent peak).

CHAPTER V

STABLE ISOTOPE FEEDING STUDIES*

INTRODUCTION

The unusual architecture of the azinomycins (**Figure 61A and B**), coupled with its potent anti-tumor activity, has captured the attention of both the biosynthetic and synthetic communities. The total synthesis of azinomycin A was achieved in 2001 by Coleman and co-workers, and a number of synthetic analogues have also been reported [18]. The overall structure of azinomycin B suggests a mixed biosynthetic origin based upon a polyketide synthase (PKS)/Non-ribosomal peptide synthetase (NRPS) skeleton (**Figure 61**). Formation of the naphthoate ring system can be rationalized by the successive condensation of acetate and malonate units by a PKS. Further functionalization of the natural product by the action of an NRPS and various tailoring enzymes would give the epoxide, enol, and azabicyclo. Biosynthetic investigations on the compound have

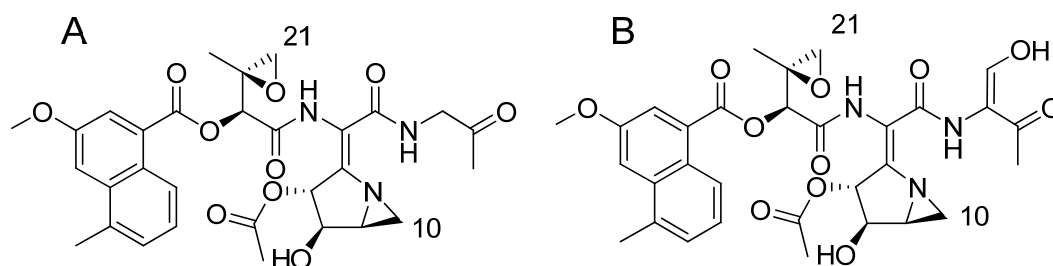


Figure 61. Azinomycin A and B.

*Reprinted with permission from “An Improved Method for Culturing *Streptomyces sahachiroi*: Biosynthetic Origin of the Enol Fragment of Azinomycin B” by Kelly, G. T., Sharma, V., and Watanabe, C. M. H., 2008. *Bioorganic Chemistry*, 36, 4-15, Copyright [2008] by Elsevier.

*Reprinted with permission from “Exploration of the molecular origin of the azinomycin epoxide: Timing of the biosynthesis revealed” by Sharma, V., Kelly, G. T., and Watanabe, C. M. H., 2008. *Organic Letters*, 10, 4815-4818, Copyright [2008] by American Chemical Society.

lagged considerably. While some gains have been made to establish the polyketide origin of the naphthoate moiety [30, 31], and while a cell-free system has been developed to support synthesis of azinomycin B *in vitro* [110], progress in this area has been impeded largely by difficulties with the culture method and difficulties in securing a consistent source of the natural product.

As discussed in the previous chapter of this dissertation, following literature protocols [2], we found production of the natural product by *Streptomyces sahachiroi* to be highly erratic (production would be observed once then not seen for three weeks or more). As a great majority of biosynthetic studies hinge upon having reliable production of the natural product, including isotopic labeling studies and gene disruption experiments, the development of a new culture method discussed in chapter III was necessary. Using stable isotopes and our refined culture conditions, we aimed to confirm and further explore the results of our *in vitro* cell free extract system to reconfirm the building blocks of azinomycin B.

As is the standard course of action in studying biosynthesis, several previously suspected metabolic building blocks were investigated. Incorporation of a labeled compound often produces a yes or no result. Carbon 14 radioactively labeled compounds were used for the *in vitro* biosynthesis studies. The benefit of using the radioactively labeled compounds was that it was a very sensitive method which was required for our cell free extract system. However, this approach has its limitations, as the radioactivity may only indicate incorporation of labeled carbons, not necessarily intact incorporation of the substrate. Metabolic processing, even in the cell free extract, is a concern. To truly match a position to a labeled compound, one requires spectroscopically observable labels. Singly labeled carbon-13 compounds are particularly attractive for this application, because there is a relatively large increase in the carbon signal compared with neighboring carbon signals; the other carbons have a relatively low natural abundance of carbon-13, specifically 1.109%. This low abundance of carbon 13 in the molecule has several consequences of interest: ^{13}C -NMR spectra require much longer than ^1H -NMR spectra to obtain, and have a lower signal to noise ratio. ^{13}C -NMR spectra are decoupled to avoid multiple splitting of the signals by ^1H signals. Signal splitting is a consequence one encounters when there are two or more carbon 13 atoms next to each other in a molecule. The split patterns can be difficult to decipher and may overlap other signals of natural abundance. On the other hand, incorporation of multiple position labeled compounds can provide an extra level of detail of the fate of the entire molecular building block. In the case of ^{15}N -labeled compounds, detection is rarely performed with ^{15}N -NMR, but rather indirectly using ^1H -NMR (where the ^1H signal is split) or ^{13}C -NMR. Often, because of the low signal in natural abundance, ^{15}N -labeled

compounds are double labeled in adjacent carbons with ^{13}C to ensure detection. In the case of some substrates the $^{15}\text{N}/^{13}\text{C}$ double label is a way to measure retention of the particular carbon or nitrogen in the molecule. Other labels that are commonly used include ^{18}O and ^{17}O . ^{17}O is NMR active with a spin of $5/2$ and is found at 0.037% of natural abundance. ^{18}O is not NMR active and is found at 0.2% of natural abundance. ^{18}O produces an upfield shift in NMR signals relative of the atoms next to it.

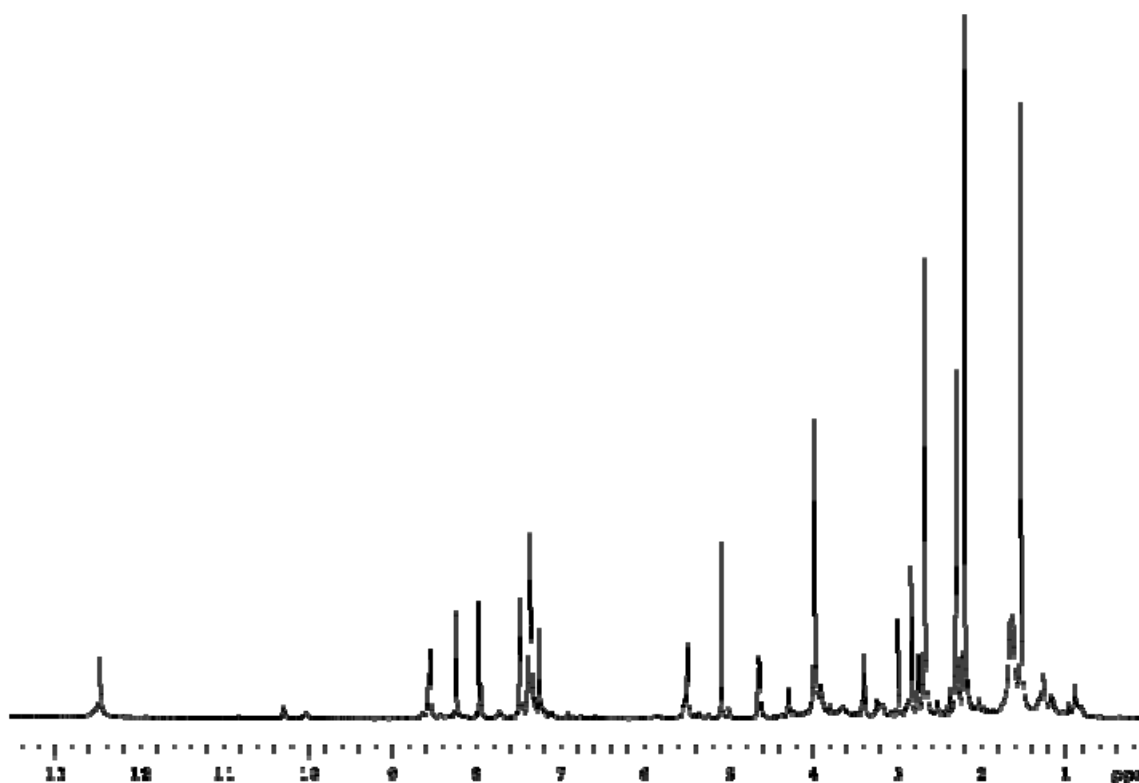


Figure 62. Azinomycin B Proton Spectrum.
 ^1H NMR for azinomycin B isolated from fermentation of *S. sahachiroi*.

Analysis of ^{13}C -NMR signals may be interpreted through integration or peak height. While integration of carbon spectra for abundance analysis is not directly comparative within a spectrum, the integrals of carbon spectra can be compared against the same signals in a different spectra provided the compound concentration and spectra development time were the same. This yields difficult results when issues of sample concentration and carbon types vary. Making sure that there is an extended relaxation time between pulses is critical for observing some carbons to

get a true reading that could be comparable to unlabeled samples without signal interference from protons. Early on, this was our approach. This approach is less reliable and difficult if significant incorporation interferes with proper phasing of the resulting spectrum. However, a more commonly used approach is to consider the peak height of the carbon signal when comparing the incorporation of the carbon labels. By checking the peak height for a particular carbon in the molecule we were able to generate a set of peak heights for “unlabeled” azinomycin B in comparison to spectra resulting from azinomycin B produced from a “labeled compound feeding” using a particular carbon as a control. Depending on the calculation, one can determine fold incorporation or percent incorporation. Using this approach we were able to determine relative amounts of incorporation of labeled compounds into the natural product. To determine the relative amount of incorporation of carbons into azinomycin B, we first obtained spectra of natural-abundance or “unlabeled” azinomycin B. Examples of these spectra, ^1H and ^{13}C -NMR, are seen in **Figure 62** and **Figure 63**, respectively.

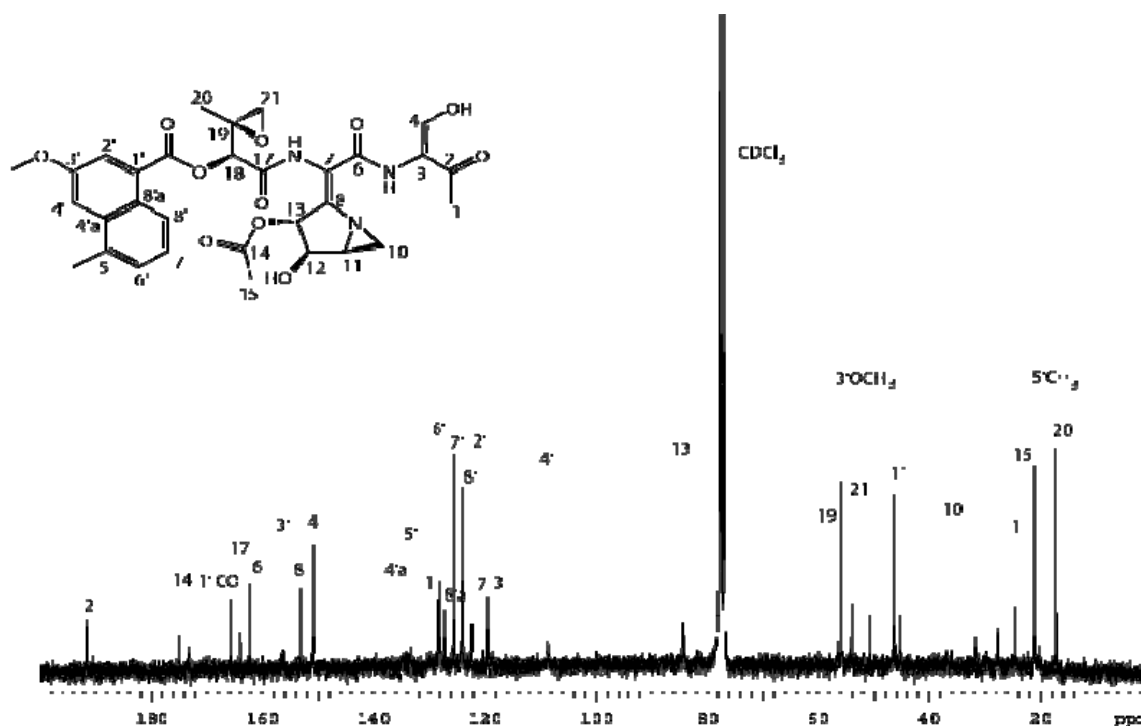


Figure 63. Azinomycin B Carbon Spectrum and Assignment.

^{13}C NMR spectrum for azinomycin B isolated from fermentation of *S. sahachiroi*.

METABOLISM IN STREPTOMYCES

Metabolism in *Streptomyces* is slowly becoming more understood and appreciated [143, 144]. With the analysis of several *Streptomyces* species genomes, the broad capabilities of the organisms have been revealed. *Streptomyces* share metabolic pathways common in most microorganisms. A comparison of known and reported metabolic pathways and identification of corresponding *Streptomyces* known genes can be found in the Kyoto Encyclopedia of Genes and Genomes (KEGG) and the web interface (<http://www.genome.jp/kegg/>). Metabolic pathway maps and genes from the relevant microorganisms are available. Until the genome of *Streptomyces sahachiroi* is fully sequenced and available, this method provides the means to check for possible for the pathways in *sahachiroi*.

Understanding pathways is crucial to evaluate the fate of labeled metabolic precursor molecules in the organism and to determine incorporation into the natural product. Major metabolic considerations in feeding experiments include competition from unlabeled molecules made by the microorganism or available from the environment (media) and metabolic “scrambling” of the labeled portion of the molecule. Consider pyruvate and its relationship to gluconeogenesis and the citric acid cycle (**Figure 64**). In a single pass through the citric acid cycle, carbons originating from pyruvate, oxaloacetate, and bicarbonate ion are potentially scrambled. Given the centrality of the citric acid cycle in both anabolism and catabolism, the potential for ambiguous results is high. The natural flux of molecular resources in bacteria is sensitive to their environment and reacts dynamically in response to changing conditions. *Streptomyces* are equipped to adapt. As soil dwelling organisms, they have the ability to break down and consume a wide variety of nutrient sources ranging from complex plant matter to simple sugars. Additionally, they are able to biosynthesize basic metabolites, amino acids, lipids, nucleic acids, and sugars from the simplest organic compounds. However, the bacteria do not often employ biosynthetic pathways if they are not necessary. In the case of the media conditions we have employed to induce the production of azinomycin B, there are many dynamics involved which have consequences for our “feeding studies.” The reduced medium in the fermenter/3rd stage of the culture relative to the 1st and 2nd stage cultures resulted in a slightly altered environment for the bacterial culture. As the bacteria grew and the culture matured beyond the exponential growth or log phase into the stationary phase, the concentration of available nutrients was reduced. It was at this point, as is often observed with *Streptomyces*, that the production of the secondary metabolites, azinomycins, was produced in greater quantities.

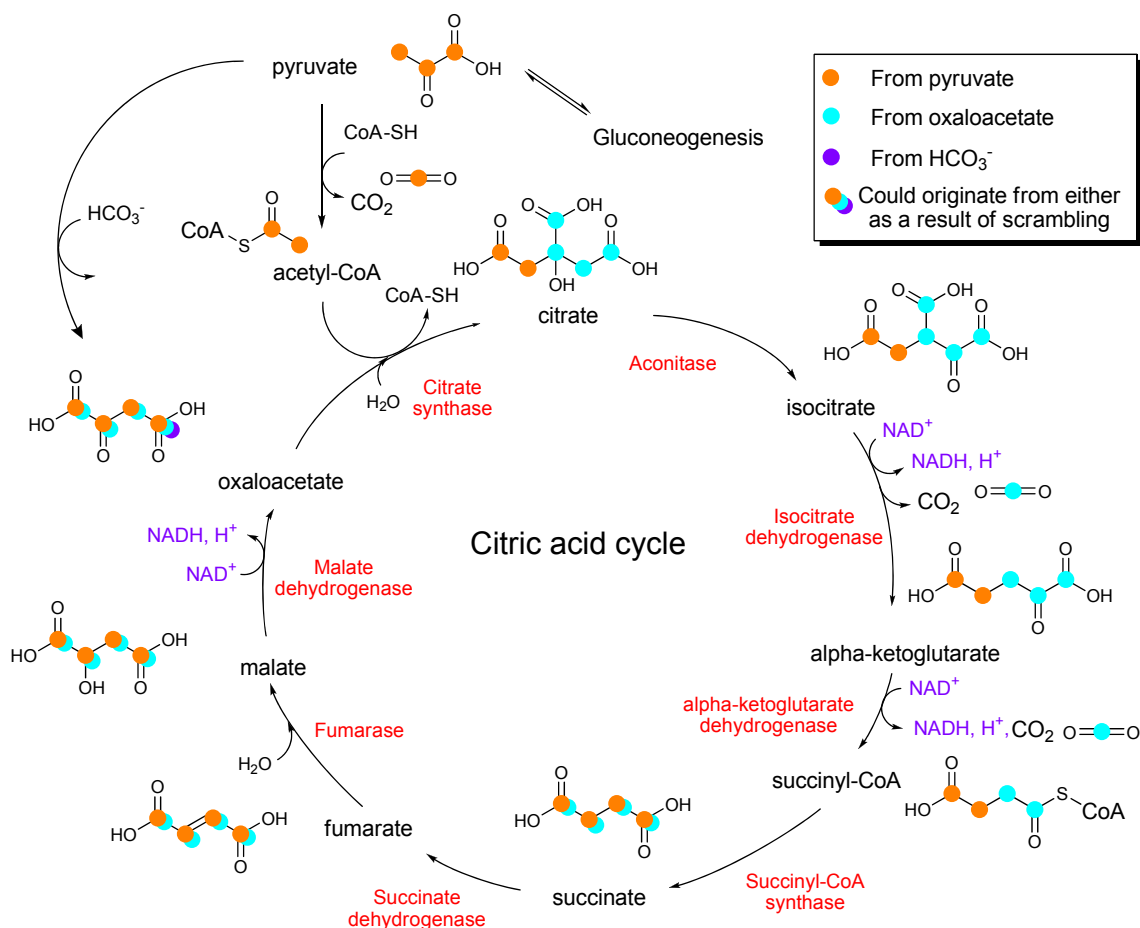


Figure 64. Scrambling of Carbons in Metabolism. Metabolic scrambling of carbons from pyruvate, oxaloacetate, and bicarbonate ion occurs in the citric acid cycle.

RESULTS AND DISCUSSION

SYSTEM FOR STUDIES

(THE AUTHOR)*

The amount of isotopically labeled compound administered to the *Streptomyces sahachiroi* culture in the fermenter was determined from a combination of a number of factors principally the small material costs and the amount of available compound in the medium (from

* Denotes major contributor(s) to each section.

manufacturer analysis mitigating dilution issues). Labeled compounds were supplied to the fermenter in two lots at 24 and 48 h post-inoculation. The culture was harvested 72 h post-induction (inoculation of the second stage culture into the fermenter). This procedure was the standard procedure in all compound feedings.

INCORPORATION OF METHIONINE

(THE AUTHOR)

For our first feeding experiment we turned to what seemed to be one of the easiest targets, the C3'-O-methoxy carbon. As we suspected the naphthoate group to have PKS origins, typical O-methoxy groups have been found to originate from the co-factor SAM (*S*-adenosylmethionine). This is typically a post PKS assembly modification of the PKS backbone [35].

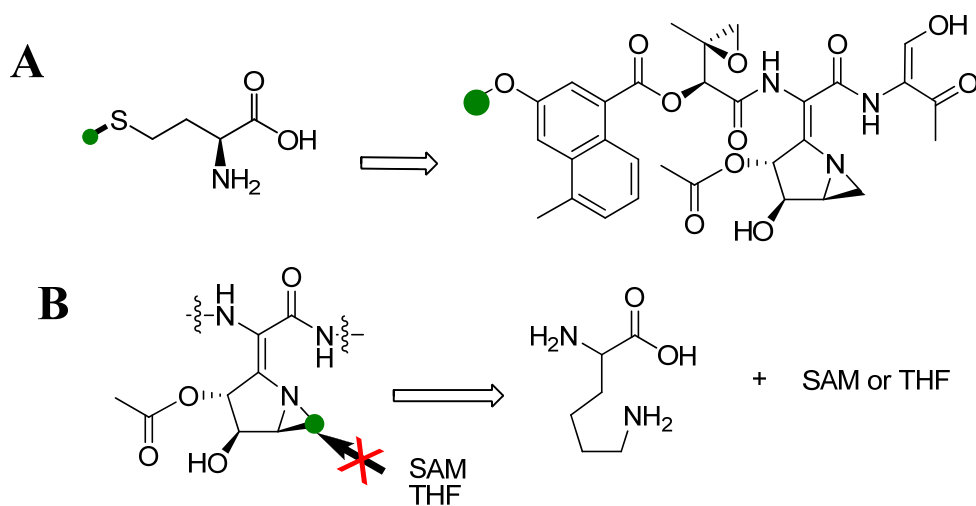


Figure 65. Incorporation of [^{13}C -methyl] L-methionine.

(A) Incorporation of the [^{13}C -methyl] L-methionine into only the C3' methoxy position precludes (B) the origin of the aziridine carbon, C10, from originating from a biosynthesis involving SAM and ornithine.

We fed [^{13}C -methyl] methionine to cell suspensions of *S. sahachiroi*. The feedings of 500 and 50 mg [^{13}C -methyl] methionine to cultures of *S. sahachiroi* gave an unambiguous clear enhancement of signal (nearly 100% and 57% incorporation respectively, **Figure 65A**) at the methoxy carbon of the molecule. The finding not only supports the involvement of the co-factor SAM (*S*-adenosylmethionine) in the biosynthesis of the methoxy group of the naphthoate, but

also excludes the involvement of SAM in the formation of the aziridinopyrrolidine ring system (specifically, the electrophilic C-10 carbon does not arise from SAM) (**Figure 65B**). These results support a previously reported incorporation of [¹³C-methyl] methionine into azinomycin B [30].

INCORPORATION OF ACETATE

(THE AUTHOR)

The next natural substrate we explored was acetate by way of sodium acetate. Acetate is a central player in metabolism as a byproduct and building block in the activated form of acetyl-CoA. Acetate is derived from many pathways including glycolysis/gluconeogenesis, the citric acid cycle, pyruvate metabolism, and multiple amino acid metabolisms. The activated acetate, acetyl-CoA, plays a significant role in nearly every type of metabolism including fatty acid biosynthesis/metabolism. Due to the centrality of this metabolism and its close association with polyketide biosynthesis, we were interested in tracking acetate incorporation into azinomycin B.

Table 9. Percent Incorporation of [1-¹³C] acetate (1g) into azinomycin B. Due to signal overlap with CDCl₃, C12 and C18's percent incorporation could not be calculated. Incorporation at C12 was observed.

Carbon Position	Carbon shift ppm	Carbon Reference	
		3'OCH ₃	C20
C1	24.5	4.9	4.8
C2	191.5	2.3	2.3
C4	150.8	5.0	4.9
C6	162	5.0	4.9
C12	77.4	seen	seen
C14	173	5.7	5.7
C1' CO	165.7	3.7	3.6
C2'	122.3	5.1	5.0
C4'	108.5	6.0	5.9
C5'	133.3	5.2	5.1
C7'	125.4	6.4	6.3
C8'a	127	4.1	4.0

We fed [1-¹³C] acetate to cell suspensions of *Streptomyces sahachiroi*. The isotopically-labeled compound was provided to the cultures in two separate aliquots (in equal 500 mg portions), the first after 24 h of incubation and the second 24 h later. As expected, whole cell feeding of [1-¹³C] acetate (**Table 9**) gave rise to an alternate labeling pattern within the

naphthoate fragment owing to its PKS origin and confirming the results reported by Lowden [30] (**Figure 66** and **Figure 67**, blue; C2'-C8a', 3.7.9-6.4% incorporation). Furthermore, both carbons C1 and C4 revealed moderate incorporation (**Figure 66** and **Figure 67**, blue, C1, 4.9%; C2, 2.3%; and C4, 5.0%), supporting the hypothesis that scrambling of label could occur to give threonine via oxaloacetate in the citric acid cycle [145] or that threonine via glycine and acetate. The results further suggest that C-14 (**Figure 66** and **Figure 67**, blue, 8.2%) of the molecule is derived from acetate and does not arise from rearrangement of a more advanced precursor or Baeyer-Villiger oxidation.

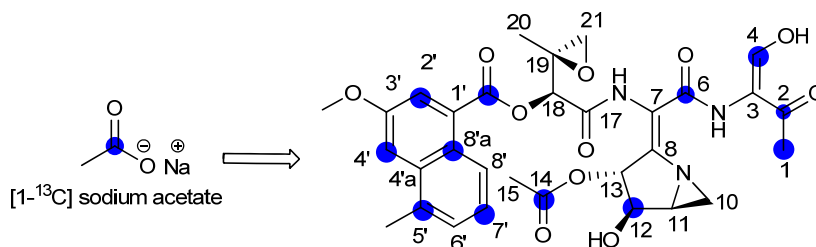


Figure 66. Incorporation of [1-¹³C] Sodium Acetate into Azinomycin B. [1-¹³C] sodium acetate incorporates at C1, C2, C4, C6, C12 (obscured by CDCl₃ solvent signal), C14, C1'CO-, C2', C4', C5', C7', and C8a' as reported by Kelly, et al. [133].

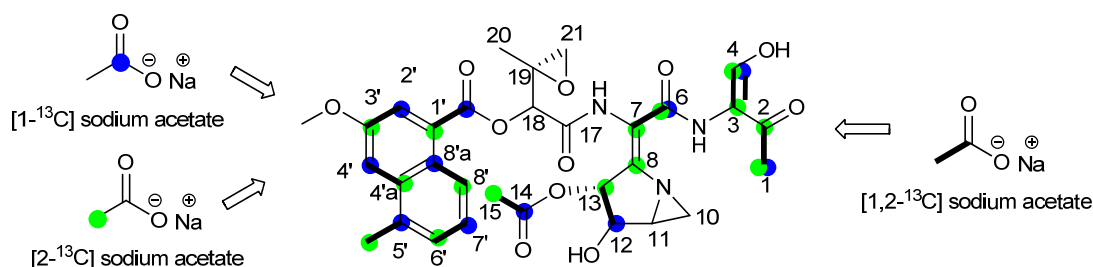


Figure 67. Incorporation of [1-¹³C], [2-¹³C], and [1, 2-¹³C] Sodium Acetate into Azinomycin B. As reported by Lowden, *et al.* [30].

Our data mirrored Lowden's work, giving us confidence in our fermentation and feeding regimen, and led us to speculate further upon the metabolic origins of the whole molecule. As one evaluates the incorporation patterns observed in the feeding of labeled acetates, a picture of direct and secondary incorporation appears. As acetate units are a common denominator in catabolism and anabolism, their incorporation may only be secondary to the primary route of

incorporation. As suggested by Lowden [30], acetate units could easily be scrambled in subsequent rounds of incorporation into the citric acid cycle seen in **Figure 68**. It is suggested that the enol fragment is likely derived from oxaloacetate and subsequently through the amino acid threonine as the right hand portion of the molecule appears to display NRPS morphology. In addition the acetate incorporation pattern seen in the aziridine fragment appears to display the pattern one would see in an α -ketoglutarate derivative.

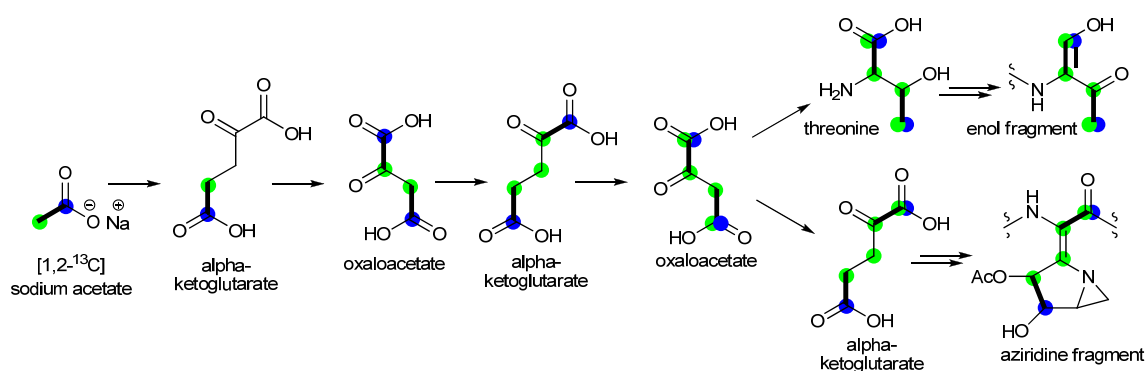


Figure 68. Incorporation of Labeled Acetate into the Citric Acid Cycle Byproducts. Oxaloacetate (and subsequently threonine and the enol) and α -ketoglutarate (and subsequently into the aziridine fragment) as suggested by Lowden, *et al.* [30].

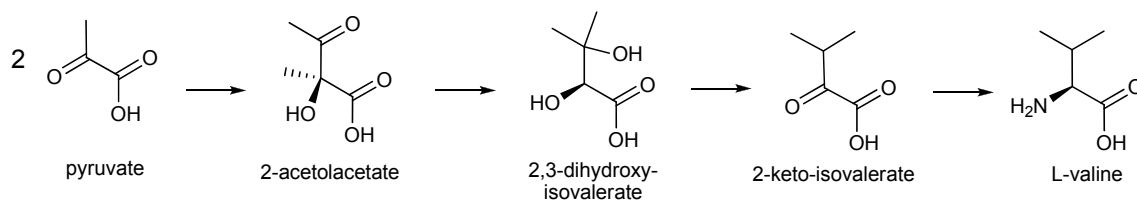


Figure 69. Biosynthesis of the Amino Acid L-valine as Determined from Analyzed *Streptomyces* Species Sequence Information.

Biosynthesis of basic molecules, such as L-valine, is common in *Streptomyces* once scavenging resources are depleted.

BIOSYNTHETIC ROUTE TO THE EPOXIDE MOIETY

(COLLABORATION BETWEEN DR. VASUDHA SHARMA, DR. CHAOMIN LIU, AND THE AUTHOR)

We explored the biosynthetic route to the azinomycin epoxide, where exact timing of individual enzymatic transformations and intermediacy of metabolites were substantiated by whole cell

feeding studies with isotopically labeled substrates. Structural evaluation and results from the recent cell-free study [146] would suggest that L-valine serves as a logical precursor. After the incorporation of labeled acetate did not yield incorporation into the epoxide moiety of azinomycin B, metabolically related units were eliminated from consideration for the origin of the epoxide. Valine is biosynthesized from pyruvate starting units and is therefore fairly removed from the typical flow of acetate metabolism (**Figure 69**).

We decided to initially feed 100 mg of [1-¹³C] L-valine to the *Streptomyces sahachiroi* culture, using the culture and feeding conditions we had previously employed to replicate the [1-¹³C] sodium acetate and [1³C-methyl] methionine isotope incorporation studies. Incorporation of [1-¹³C] L-valine into the azinomycin B molecule was apparent and specific in the ¹³C NMR. The singular enrichment of signal at C-17, 164.0 ppm was nearly 8.71 % (**Figure 70**). This incorporation confirmed our cell free work [146].

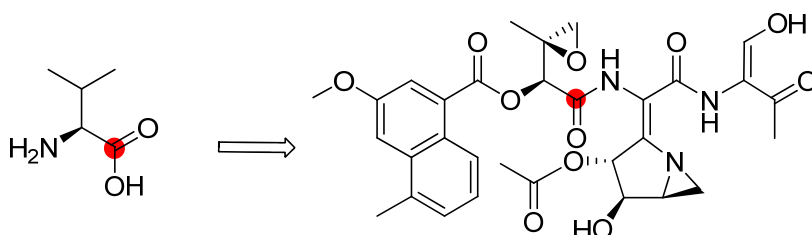


Figure 70. Incorporation of [1-¹³C] L-valine into Azinomycin B.

However, our curiosity was piqued by the promiscuity of the pathway with respect to the timing of the pathway's incorporation of L-valine and the modifications towards the epoxide moiety. These modifications include: transamination (removal of the native amine and replacement with a ketone), reductions, oxidation, dehydration, activation, addition to the naphthoate group, and addition to the rest of the azinomycin molecule. To evaluate these stages a series of related, [1-¹³C] molecules were synthesized initially by Dr. Chaomin Liu, but primarily by Dr. Vasudha Sharma.

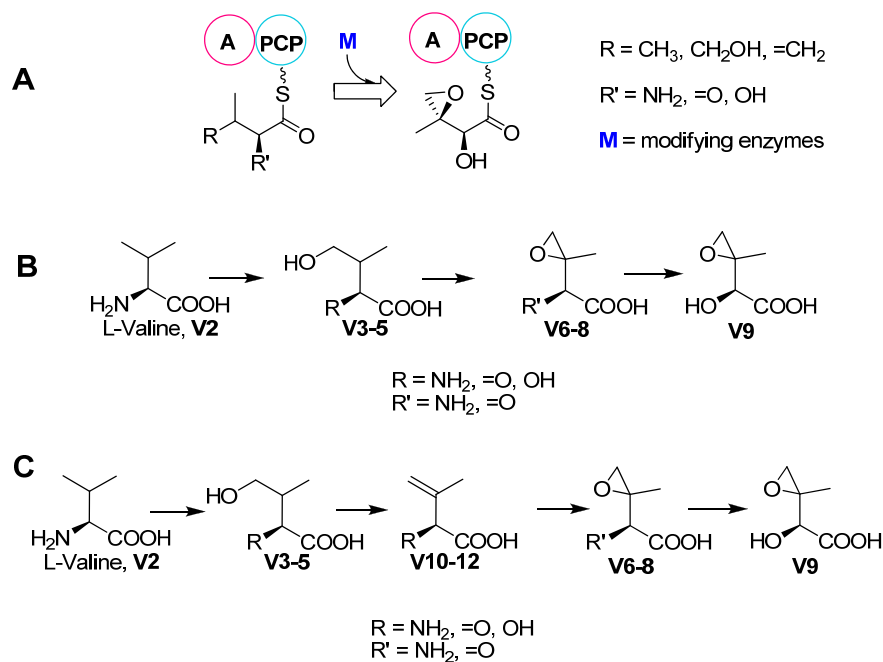


Figure 71. Possible Paths of Valine Modifications to Produce the Azinomycin Epoxide. In this version, valine remains tethered to the NRPS domain as it is modified before incorporation into the natural product.

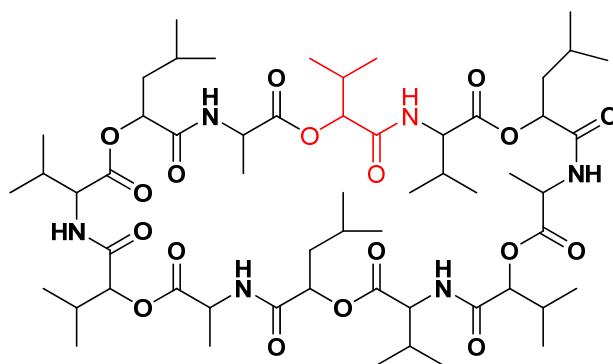


Figure 72. Incorporation of a Modified Valine Substrate into Cereulide.

There are a variety of scenarios in which the L-valine is transformed and incorporated into the epoxide moiety of the azinomycins. One possibility is that valine or respective advanced precursors are converted to the epoxide while tethered to the NRPS (**Figure 71, path A**), and catalysis is achieved by modifying enzymes either contained within NRPS domains or elsewhere within the gene cluster. In cereulide biosynthesis (**Figure 72**), for example, a reductase module found within NRPS adenylation domains, reduces tethered α -keto acids (α -ketoisocaproic acid

and α -ketoisovaleric acid) to α -hydroxy acids, while still bound to their respective PCP domains [147].

Alternatively, it is conceivable that the epoxide moiety is fully constructed by other biosynthetic pathway enzymes prior to activation by its respective adenylation module. For instance, the epoxide might be derived from radical cyclization of a terminal alcohol (**Figure 71**, path B) [148, 149]. In contrast, the epoxide might originate from reaction with molecular oxygen via oxygen insertion into an olefin [150]. This olefin might in turn be derived from a terminal alcohol (**Figure 71**, path C) [151]. In either case (**Figure 71**, path B or C), the amino group of valine also requires biochemical conversion to give the α -hydroxy group of the epoxide fragment **V9**, presumably arising by transamination and subsequent reduction of the resulting ketone to give the alcohol. The exact timing of these biosynthetic transformations and feasibility of the overall route can only be resolved through experimentation. Therefore, to test our hypotheses, we exogenously fed valine and a variety of synthesized advanced precursors in isotopically labeled form to whole cells (**Table 10**).

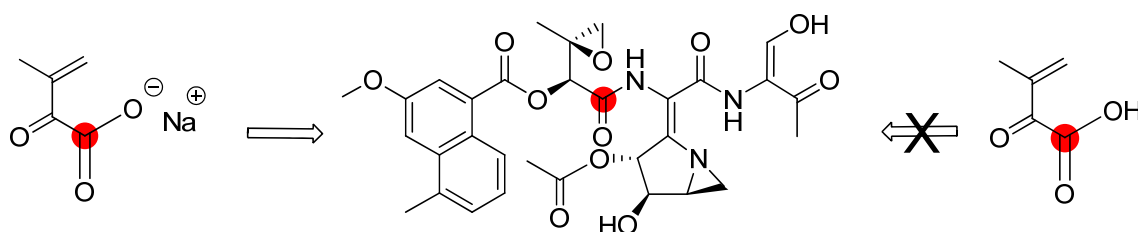


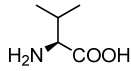
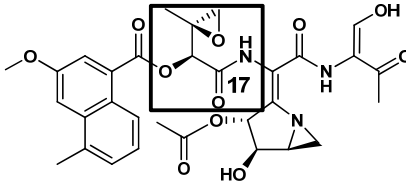
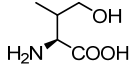
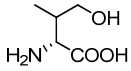
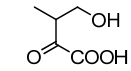
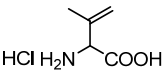
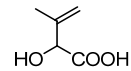
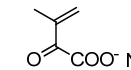
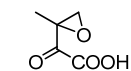
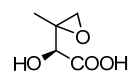
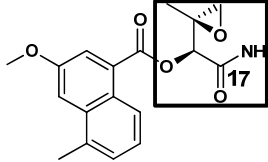
Figure 73. Incorporation of [1- ^{13}C] Sodium Allylketocarboxylate into Azinomycin B.

One of the first derivatives that we fed to the culture was the sodium salt of [1- ^{13}C] allylketocarboxylate (3-methyl-2-oxobutenoic acid). Incorporation of this molecule could indicate the ability of the pathway to take up an intermediate that has already been de-aminated in the process of epoxide formation. This was clearly the case as we saw an incorporation of ~ 4.5 fold at the C-17 position. This was repeated a second time with the same result. It should be noted that the acid version did not incorporate (**Error! Reference source not found.**). This might be due to the stability of the sodium salt versus the acid form or better transport across the bacterial membranes of the charged salt species. Salts are able to traverse this barrier easier than

neutral species. To test this hypothesis we prepared and fed [1-¹³C] valine trifluoroacetic acid salt. We saw an incorporation rate of the same magnitude as the [1-¹³C] valine.

Table 10. Percent Incorporation at C-17 of Azinomycin B and the Epoxyamide.

Samples were prepared as detailed in Kelly *et al.* [133] and chapter IV of this dissertation. L-Valine TFA salt showed an overall incorporation of 6.97%. The R-keto carboxylic acid (V11) degraded rapidly. The percent incorporation is $[(A - B)/B] \times 1.10$ where A) intensity of labeled carbon normalized to the intensity of the 3'OCH₃ of azinomycin B and the C18 of the epoxyamide; B) intensity of normalized unlabeled carbon; 1.10) natural abundance of ¹³C. The table entry reads n.d. if incorporation was not detected by ¹³C NMR.

Compound	#	%Incorporation at C17			
		Azinomycin B	Epoxyamide		
	V2	8.71	n.d.	 Azinomycin B	
	V3	4.18	3.2		
	V3*	n.d.	n.d.		
	V5	8.10	0.32		
	V10	n.d.	n.d.		
	V11	n.d.	n.d.		
	V8	n.d.	n.d.		
	V9	n.d.	n.d.		
	V12	6.03	2.95		 Epoxyamide

We continued to investigate the valine series by examining incorporation of [1-¹³C] isodehydrovaline (V10), [1-¹³C] allylhydroxy carboxylate valine (V11), [1-¹³C] hydroxy epoxy valine (V9), and [1-¹³C] keto epoxy valine (V8). None of these substrates incorporated into azinomycin at the C-17 position or any other position and were each supplied as salts. There are several implications from these results. No incorporation of the [1-¹³C] isodehydrovaline indicates that the molecule is not incorporated at that point in modification into the epoxide

moiety. It is possible that the pathway has such an intermediate type sequestered, although the incorporation of the [1-¹³C] allylketocarboxylate implies that entry to the pathway is not restricted to valine exclusively. Additionally, it does not appear that [1-¹³C] allylhydroxy carboxylate valine plays a role in the production of the epoxide.

[1-¹³C] γ -hydroxy- α -keto-carboxylate valine, [1-¹³C] γ -hydroxy L-valine and [1-¹³C] γ -hydroxy D-valine were fed on different occasions to the *Streptomyces sahachiroi* culture with mixed results. The feeding of the [1-¹³C] γ -hydroxy- α -keto-carboxylate valine synthesized by Dr. Chaomin Liu resulted in non-incorporation into the whole azinomycin, but rather resulted in incorporation into a related truncated metabolite, epoxyamide (**Table 10**). This truncated metabolite was first reported by Nakashima, *et al.* in 1986 [17]. Additionally, it was observed in two separate feeding experiments that [1-¹³C] γ -hydroxy L-valine incorporated into this metabolite as well as in the first feeding case, whole azinomycin. On the other hand, feeding of [1-¹³C] γ -hydroxy D-valine resulted in no incorporation into either whole azinomycin or the related truncated metabolite.

Each of the modified valine derivatives was synthesized in ¹³C-labeled form (at C-1) and fed separately to whole cell suspension cultures as detailed previously. **Table 10** provides the feeding results for all of the amino acid precursors. In addition to valine **V2**, only substrates **V3**, **V5**, and **V12** resulted in site-specific incorporation above background at 164.0 ppm. Interestingly, incorporation was also observed at 168.7 ppm corresponding to the epoxyamide (**Table 10**), a metabolite that frequently accompanies production of the azinomycins. We were gratified to find that L- γ -hydroxyvaline **V3** was unambiguously incorporated, substantiating its involvement in either forming the epoxide directly (**Figure 71, path B**) or generating an olefin where subsequent oxygen insertion would give the epoxide (**Figure 71, path C**). As expected, only the L-isomer **V3** served as a substrate over its corresponding D-isomer **V3***, confirming the stereospecific nature of these reactions. The site-specific incorporation of R-keto hydroxy acid **V5** was also observed and suggests that hydroxylation of valine (to **V3**) precedes transamination. Reconstitution of the enzymes involved in these transformations will, however, be required to rigorously establish this notion. The most advanced putative precursor shown to be processed by the azinomycin biosynthetic machinery was 3-methyl-2-oxobutenoic acid **V12**, negating direct formation of the epoxide from the alcohol (**Figure 71, path B**). In contrast, isodehydrovaline **V10** failed to incorporate, further substantiating the order of biosynthetic steps (favoring **Figure 71, path C**), where dehydration of the γ -alcohol to the double bond is suggested to follow transamination.

Interestingly, neither of the epoxide derivatives showed incorporation into the natural product. This is likely attributed to their instability in aqueous medium, which increased dramatically over time (**Figure 74**), with ring opened products and considerable lactonization occurring over a 24 h period at room temperature (data not shown). Notwithstanding the instability of epoxide **V8** and **V9**, the lifetimes of the other amino acid derivatives in aqueous media were sufficient, under the conditions of our feeding regimen (two separate and equal aliquots fed 24 h apart pH 7.1-7.5, 30 °C), to yield reliable incorporation data [133].

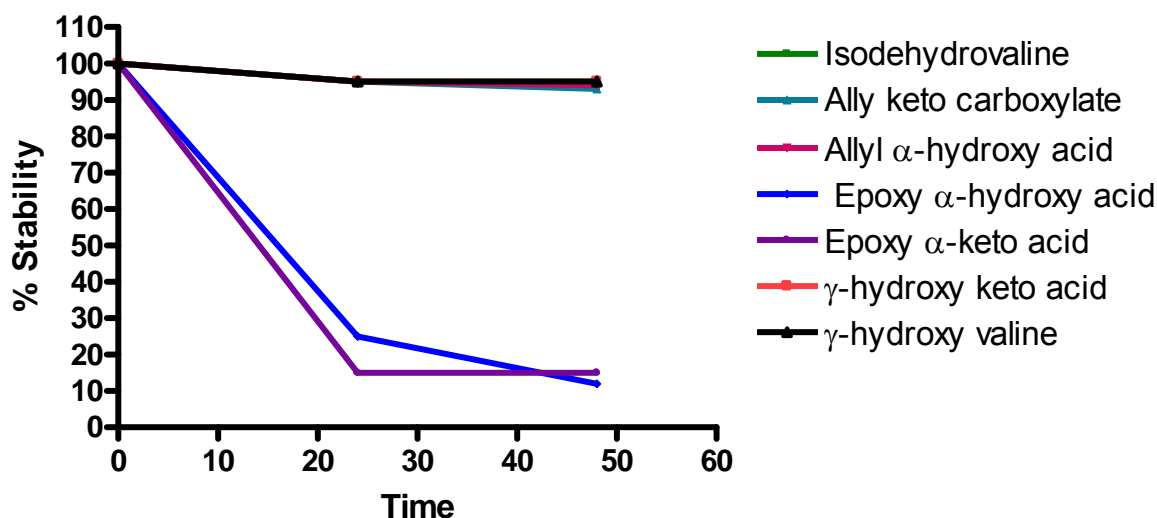


Figure 74. Stability Profile of V3-V12.

Stability tests were performed by shaking samples for 48 h in aqueous medium at pH 7-7.5 at 30 °C.

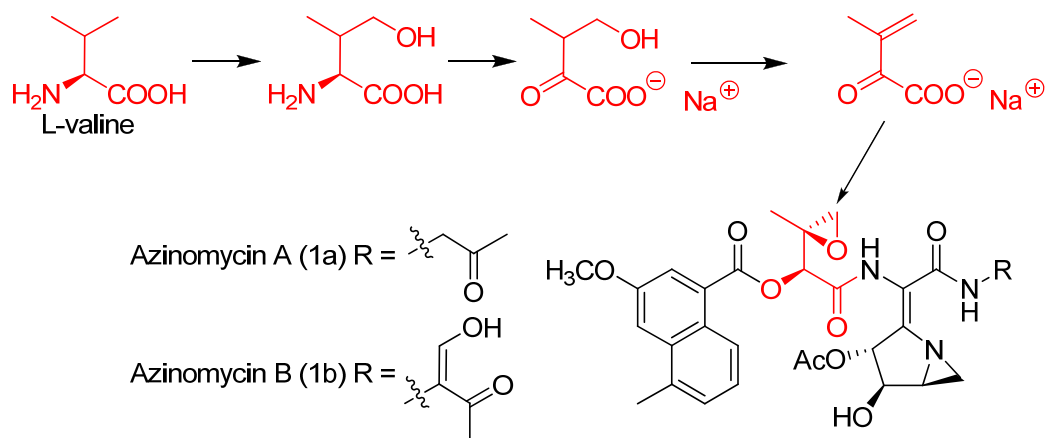


Figure 75. Biosynthetic Route to the Epoxide Moiety in the Azinomycins.

The failure to incorporate **V11** suggests that 3-methyl-2-oxobutenoic acid **V12** is epoxidized to **V8** which is then reduced to **V9**.

In this investigation, we demonstrated timing and intermediacy of several metabolites along the biosynthetic route to the epoxide moiety (**Figure 75**). We were intrigued to find that the majority, if not all, of the enzymatic steps required to generate the epoxide fragment occur prior to loading onto the NRPS machinery (invalidating **Figure 71, path A**).

BIOSYNTHETIC ROUTE TO THE ENOL FRAGMENT

(COLLABORATION BETWEEN DR. VASUDHA SHARMA AND THE AUTHOR)

Considering what we had already learned through previous feeding studies, we decided to probe the biosynthesis of the late stages of the pathway in the construction of the enol fragment of azinomycin B. Previous studies had indicated a secondary acetate incorporation into the keto enol moiety such that it appeared to be derived from oxaloacetate [30]. The structure of the enol fragment suggests that it might originate from (L)-threonine (**Figure 76**); the β -alcohol of the amino acid would require oxidation and the terminal carboxylate reduction (**Figure 77A**). Our earlier results from cell-free extract studies [110] and acetate labeling experiments support such an argument. Neither approach has shown, however, that the amino acid is site-specifically incorporated into the enol fragment of the natural product.

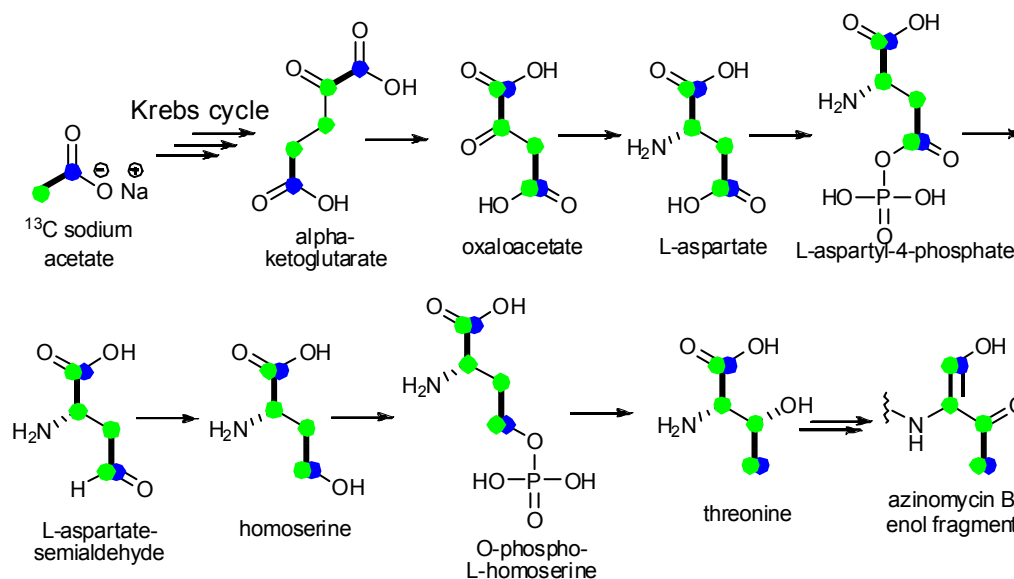


Figure 76. Incorporation of Labeled Acetate into the Krebs Cycle Byproducts Oxaloacetate (and Subsequently Threonine then the Enol Moiety).

Therefore we examined uptake of [U-¹³C] L-threonine (**T2**, **Figure 77A**). The experiment resulted in labeling of all four carbons (C1-C4) of the enol fragment (**Figure 77A**, **red**). This ‘tail-to-tail’ incorporation clearly suggested that threonine was site-specifically incorporated. Close inspection of the ¹³C NMR indicated intact incorporation (C1-C4, 7.9-11.7% incorporation calculated by extended carbon relaxation signal integration) of the [U-¹³C] labeled threonine. Isotopic labeling was evident at C1 as a doublet of a doublet ($J_1=55.8$, $J_2=180.0$ Hz) flanking the natural abundance peak at 24.1 Hz (see **Figure 77** and **Figure 134**). Similarly, C4 gave a doublet of doublet ($J_1=38.7$, $J_2=324.6$ Hz) flanking the natural abundance peak (see **Figure 137**). C2 and C3 showed multiple splitting patterns, indicating intact incorporation (see **Figure 135** and **Figure 136**).

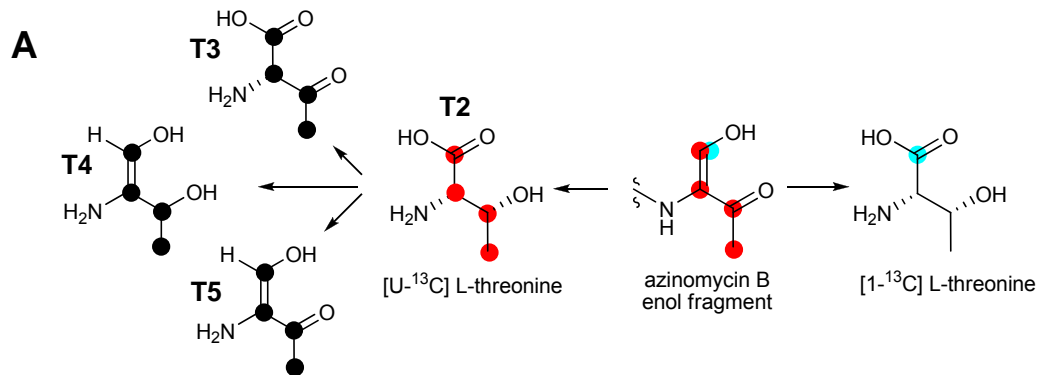


Figure 77. Summary of Feeding Studies Targeting Enol Fragment.

(A) [U-¹³C] threonine, T2, incorporates C1-C4 (B) % incorporation = $[(A-B)/B] \times 1.07$; where A= intensity of labeled Carbon, B=intensity of unlabeled Carbon, 1.07 is the natural abundance of ¹³C; n.d.: not detectable by ¹³C NMR (C) Representative comparison of C1 of azinomycin B via feeding of [U-¹³C] -labeled threonine, T3, T4 and T5 to that of the negative control peak at 149.5 Hz. Multiplets were observed for carbons C2 and C3 probably owing to extensive ¹³C-¹³C coupling.

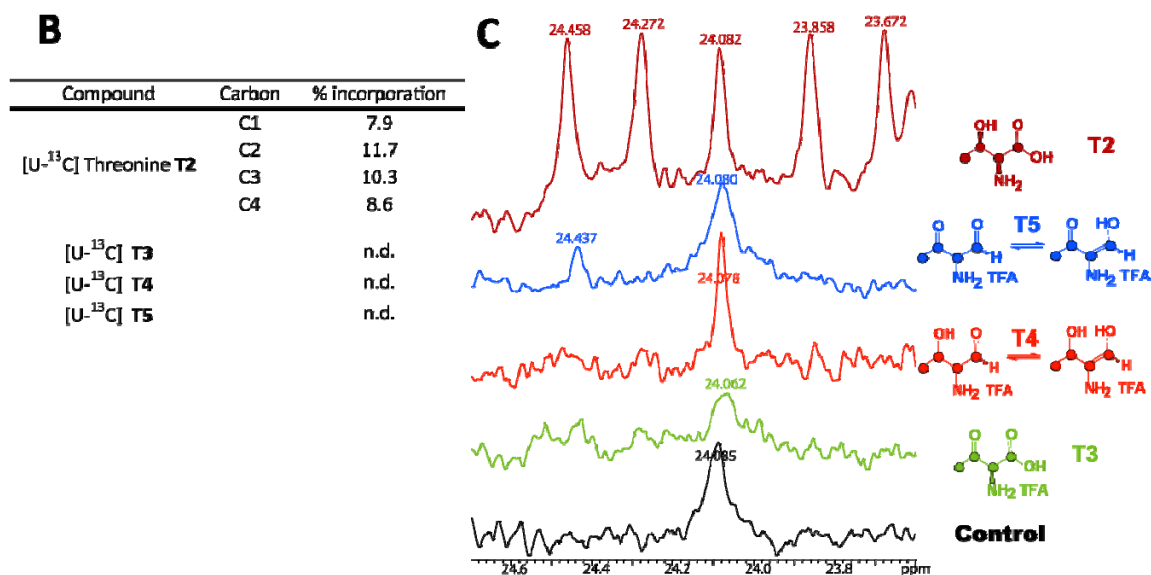


Figure 77. Continued.

To address the order of events in the timing of the biosynthesis in the oxidation of the alcohol and reduction of the carboxylate of **T2**, we synthesized β -ketoamino acid **T3**, β -hydroxyamino aldehyde **T4**, and β -ketoaminoaldehyde **T5** in labeled form (**Figure 78**). Synthesis of such precursors is important to establish whether the enol fragment or its respective intermediates are pre-formed prior to loading onto the NRPS or generated at a later stage in the biosynthesis.

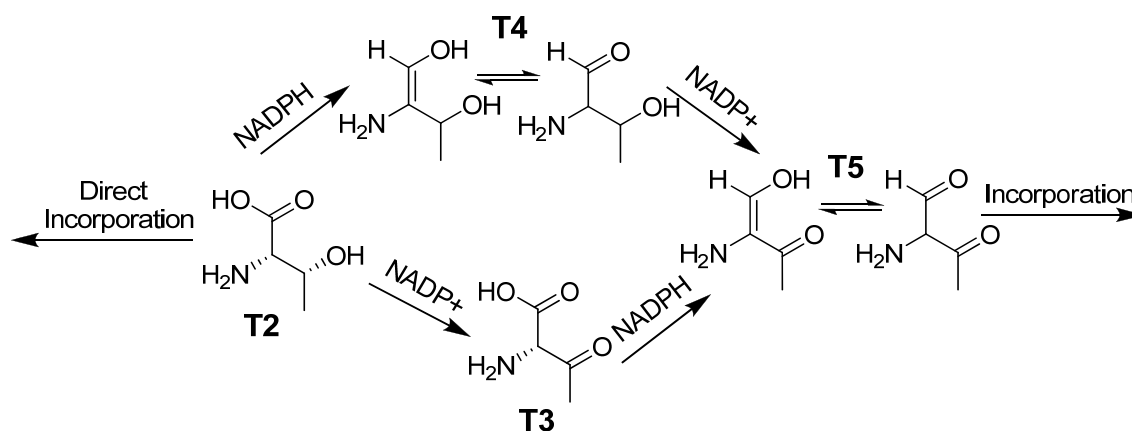


Figure 78. Proposed Biosynthetic Routes to the Enol Fragment of Azinomycin B.

The results (**Figure 77 B** and **C**) clearly indicate that only L-threonine (**T5**) is incorporated rather than any advanced precursors. This indicates the redox modifications that produce the keto enol moiety of azinomycin B are performed either while L-threonine is attached to the NRPS domain or after the natural product is released by the NRPS.

BIOSYNTHETIC ROUTE TO THE END FRAGMENT OF AZINOMYCIN A

(COLLABORATION BETWEEN DR. VASUDHA SHARMA, JENNIFER FOULKE-ABEL AND THE AUTHOR)

Several different biosynthetic scenarios can be envisioned to give the aminoacetone fragment of azinomycin A. One possibility is that threonine undergoes modification while tethered to the NRPS and azinomycin B gets modified to provide azinomycin A (**Figure 79, path A**). Alternatively, azinomycin A could arise by hydrolysis from PCP, followed by oxidation, and decarboxylation (**Figure 79, path B**). Another possibility is that the terminal aminoacetone moiety is fully constructed prior to being incorporated in the natural product. For instance, aminoacetone might be derived from threonine where threonine dehydrogenase (**Figure 79, path C**) catalyzes the formation of a β -keto amino acid followed by subsequent decarboxylation to give aminoacetone [152-154]. In contrast, aminoacetone might also originate from glycine through action of 2-amino 3-ketobutyrate CoA ligase, facilitating a condensation reaction with acetyl CoA and loss of CO₂ (**Figure 79, path D**) [155-157].

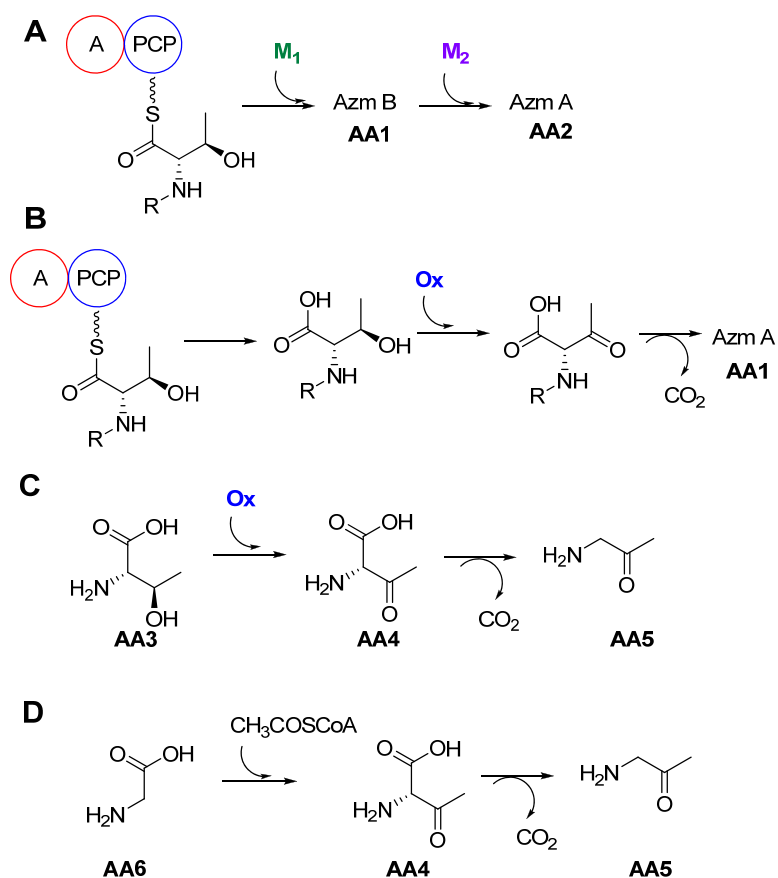


Figure 79. Proposed Biosynthetic Routes for Production of the Aminoacetone Moiety of Azinomycin A.

M_1 , M_2 = modifying enzymes; Ox = Oxidase/Dehydrogenase.

In either case (**Figure 79**, path **C** or **D**), the β -keto amino acid **AA4** must be formed *in situ* to give aminoacetone **AA5** by decarboxylation. Metabolic enzymes mediating the biosynthesis of L-2-amino-3-ketobutyrate **AA4** from both threonine **AA3** and glycine **AA6** have been reported in other *Streptomyces* species, *S. coelicolor*, *S. griseus*, and *S. avermitilis* (**Figure 80**), where the aminoacetone generated is utilized in porphyrin biosynthesis and pyruvate metabolism [32, 34, 158-160]. We have identified the genes for L-threonine 3-dehydrogenase and 2-amino-3-ketobutyrate CoA ligase via genomic sequencing of *S. sahachiroi* (**Figure 110** and **Figure 111**), supporting the possibility of aminoacetone formation from either threonine or glycine.

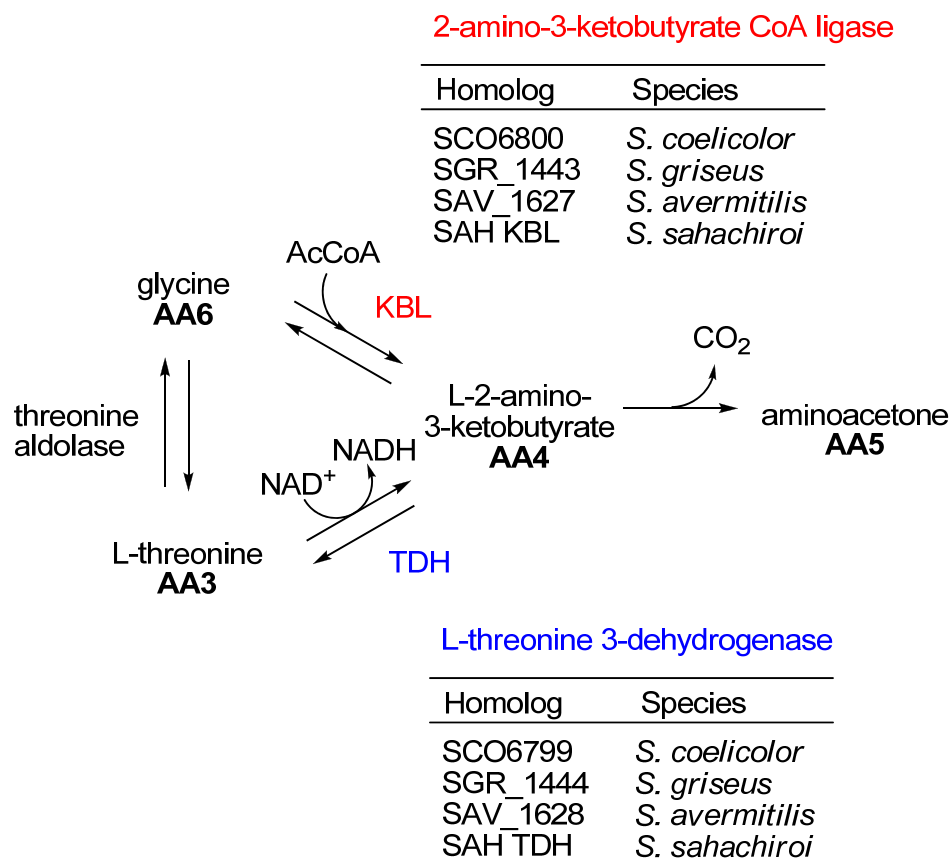


Figure 80. Biosynthetic Pathways Linking Conversion of Glycine and Threonine to L-2-amino-3-ketobutyrate, Which Decarboxylates to Form Aminoacetone.

To distinguish between these mechanistic hypotheses, we fed isotopically labeled (^{15}N , and ^{13}C) threonine, glycine and aminoacetone (**Table 11** and **Table 12**) exogenously to whole cells. When $[\text{U-}^{13}\text{C}]$ threonine was administered to cultures of *S. sahachiroi*, “end-to-end” enrichment was observed at C-1 through C-4 of azinomycin B, corroborating our earlier cell-free experiments with $[1\text{-}^{14}\text{C}]$ threonine [133, 146]. Interestingly, incorporation of $[\text{U-}^{13}\text{C}]$ threonine was observed at C-1 through C-3 of azinomycin A, as detected by ^{13}C NMR (**Figure 138**).

This suggests direct involvement of threonine in the biosynthesis of the terminal end of azinomycin A, either by modification of azinomycin B (**Figure 79, path A**) or via generation of a β -keto aminoacid, (**Figure 79, path B** or **C**). In order to test the possible role of glycine (**Figure 79, path D**) we also evaluated a series of precursors as shown in **Table 11** and **Table 12**.

Table 11. Percent Incorporation at C-2 of Azinomycin A and B.

¹ incorporation at C-3 of azinomycin A, label scattered through the molecule (see Figure 143 and Figure 144). ² incorporation at C-4 of azinomycin B. % incorporation = [(A-B)/B] X 1.10 where A, intensity of labeled carbon; B, intensity of unlabeled carbon; 1.10, natural abundance of ¹³C; n.d. = not detected by APCI Mass Spec or ¹³CNMR.

Entry	Compound	% incorporation in azinomycin A (AA1)	% incorporation in azinomycin B (AA2)
1	[U- ¹³ C] L-threonine(AA3)	1.9	12
2	[2- ¹³ C] aminoacetone(AA5)	26.3	n.d.
3	[2- ¹³ C] glycine(AA6) ¹	<1	1.8
4	[1- ¹³ C] glycine(AA6) ²	n.d.	n.d.

Table 12. Feeding Results for [¹⁵N] –threonine and [¹⁵N]- glycine.

% incorporation = [(A-B)/B] X 1.10 where A, intensity of peak for labeled material; B, intensity of peak for unlabeled material; 1.10, natural abundance of ¹³C; n.d. not detected by APCI Mass Spec. *Detected by ¹H NMR seen in Figure 81.

Entry	Compound	% incorporation in azinomycin A	% incorporation in azinomycin B
1	[¹⁵ N] Threonine	n.d.	5.5*
2	[¹⁵ N]-Glycine	1.49	1.41

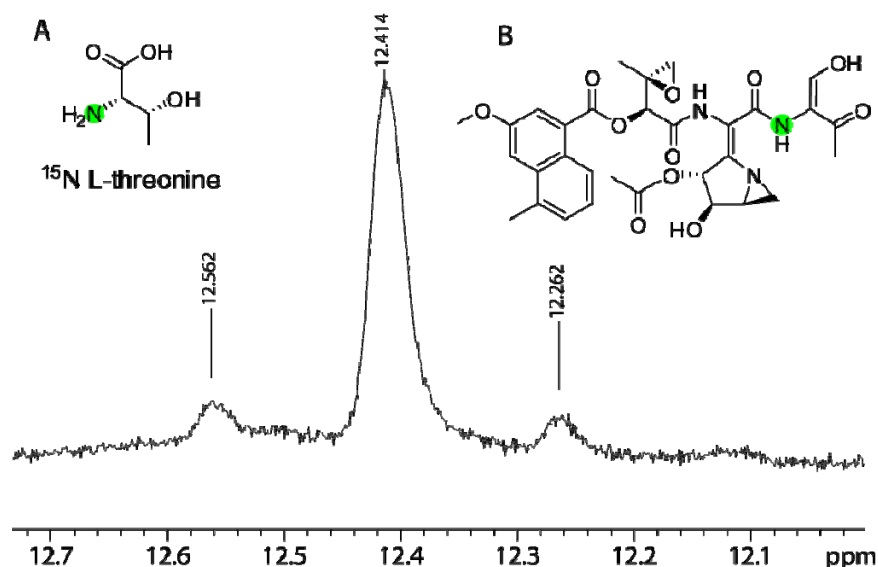
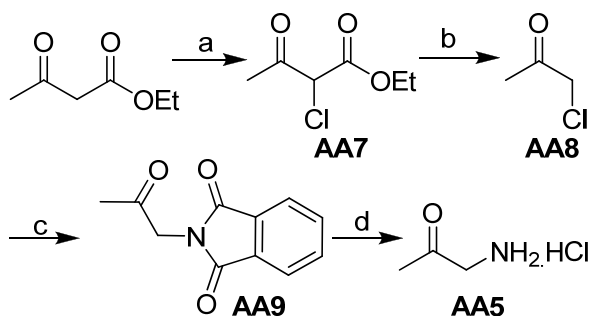


Figure 81. ^{15}N -L-threonine Incorporation into the Azinomycin B Detected by ^1H NMR. The nearby ^{15}N atom results in splitting of the proton signal normally seen at 12.414 ppm (1H, d, $J=90\text{Hz}$).



Scheme 1. Synthesis of Aminoacetone Hydrogen Chloride.

(a) SO_2Cl_2 , 0°C , 36h; (b) 2 equiv. conc. H_2SO_4 , aq. THF, reflux; (c) Potassium phthalimide, DMF, 16h; (d) conc. HCl, reflux, 7h.

Isotopically labeled $[2-^{13}\text{C}]$ aminoacetone was synthesized as its hydrochloride salt from $[3-^{13}\text{C}]$ ethylacetoacetate as depicted in **Scheme 1**. Briefly, ethyl acetoacetate was treated with SO_2Cl_2 giving ethyl 2-chloroacetoacetate (**AA7**), [161] which when hydrolyzed with conc. H_2SO_4 gave chloroacetone (**AA8**) upon decarboxylation. Chloroacetone was treated with potassium phthalimide to give N-acetyl phthalimide (**AA9**), which upon acidic hydrolysis afforded $[2-^{13}\text{C}]$ aminoacetone hydrochloride (**AA5**) in four steps with an overall $\sim 75\%$ yield.

When $[2-^{13}\text{C}]$ aminoacetone (entry 2, **Table 13** and **Figure 149**) was supplied to whole cells, unambiguous incorporation (26%) was observed in azinomycin A but not in azinomycin B.

Direct incorporation of [2-¹³C]aminoacetone (**AA5**) discounts the modification of intact azinomycin B (**AA2**) to produce azinomycin A (**1**) (**Figure 79, paths A and B**). When [2-¹³C]glycine was provided in cell culture, enrichment of signal was observed at C-3 of azinomycin A, albeit low (<1%) suggesting a possible role for glycine in the formation of aminoacetone via α -C-acylation followed by decarboxylation (**Figure 79, path D**). Azinomycin B was also labeled at C-3 (1.8%) as threonine can be biosynthesized from glycine [32, 34, 133, 158-160]. As expected, metabolic scattering was observed as exhibited by the incorporation of label at other sites within the molecule and contributing to the low levels of incorporation at C-3 (<1%). These results were further substantiated by the lack of any measurable incorporation seen in azinomycin A when [1-¹³C]glycine was supplied to whole cells. This is presumably due to the loss of labeled carbon as CO₂. Moreover, feeding of 2, 2-D, D-glycine to *S. sahachiroi* led to an observed decrease in the production of azinomycin A by 66% as compared to the unlabeled control. This suggests that deprotonation at α -C of glycine is kinetically significant in the production of **AA4**. The crystal structure of *E. coli* 2-amino-3-ketobutyrate CoA ligase complexed with the L-2-amino-3-ketobutyrate and pyridoxal 5'-phosphate (PLP) in the active site suggests a reaction mechanism in which PLP-activated glycine is deprotonated by a lysine residue [162]. Conceivably, the rate of deprotonation could be kinetically controlled, but such studies in the enzyme have not been undertaken. Since 2-amino-3-ketobutyrate CoA ligase is evolutionarily conserved, a similar mechanism would likely be at work in *S. sahachiroi* aminoacetone biosynthesis.

Upon feeding [U-¹³C]-**AA4**, we did not observe any enhancement of signal either in azinomycin A or B [133]. Kinetic data on 2-amino-3-ketobutyrate CoA ligase, the enzyme catalyzing the transition between glycine and L-2-amino-3-ketobutyrate reveals that it has a 50-fold preference for L-2-amino-3-ketobutyrate cleavage over formation, and favors the reaction equilibrium towards glycine production [163]. The enzyme binds coenzyme A (CoA), the acetyl acceptor in the L-2-amino-3-ketobutyrate cleavage reaction, more tightly than acetyl-CoA; this competitive inhibition promotes turnover with respect to glycine formation [163, 164]. In *E. coli*, the presence of glycine and absence of threonine slows growth, whereas cells grown in the presence of threonine and absence of glycine thrive at a normal rate, indicating a primarily catabolic role for this enzyme in threonine metabolism [163]. Thus, feeding *S. sahachiroi* with L-2-amino-3-ketobutyrate, **AA4** would most likely form glycine before decarboxylation occurs, and hence, could be scrambled into a number of primary metabolic pathways. These studies suggest that the most advanced putative precursor in the biosynthesis of azinomycin A is

aminoacetone (5), as derived from glycine (AA6) (Figure 79, path D) and threonine(AA3) (Figure 79, path C) through the intermediate L-2-amino-3-ketobutyrate(AA4).

Table 13. Feeding Details and Conditions of All Compounds Fed for Biosynthetic Route to the End Fragment of Azinomycin A Section.

Note: Entries 1-9 were administered as described previously in Kelly, *et al.* [133] and chapter IV. Briefly, the labeled material was weighed in equal portions and solubilized in autoclaved distilled water. The first aliquot was administered after 24 h, followed by addition of the second provided 24 h later. The culture was harvested 72 h post-induction (inoculation of the second stage culture into the fermenter)

*Entry 10: fed in 72 lots of 3 mg/mL starting 24 h after fermenter inoculation, the lot administration time accelerated to peak at 48 hours post inoculation.

**Entry 11-13: The compound was dissolved in autoclaved distilled water and aliquoted in eight equal portions at 3 mg.mL⁻¹. The first aliquot was administered after 24 h, followed by addition of the subsequent lots every 5 hours. The culture was harvested 72 h post-induction (inoculation of the second stage culture into the fermenter).

Entry	Compound fed	Total amount fed
1	[U- ¹³ C] L-threonine (AA3)	100 mg @ 0.8 mmol per 10L culture
2	[¹⁵ N] L-threonine (AA3)	230 mg@ 1.9 mmol per 10L culture
3	[U- ¹³ C] 2-amino-3ketobutyrate (AA4)	114 mg @ 0.9 mmol per 10L culture
4	[2- ¹³ C] glycine (AA6)	1g @13.1 mmol per 10L culture
5	[1- ¹³ C] glycine (AA6)	1g @13.1 mmol per 10L culture
6	[1- ¹³ C] glycine (AA6)	1g @13.1 mmol per 10L culture
7	[¹⁵ N] glycine (AA6)	1g @13.1 mmol per 10L culture
8	[2,2-D2] glycine (AA6)	1g @13.1 mmol per 10L culture
9	aminoacetone•HCl (AA5)	1.25 g @ 14.3 mmol per 10L culture
10*	[2- ¹³ C] aminoacetone•HCl (AA5)	0.3 g@ 2.7 mmol per 10L culture
11**	aminoacetone•HCl (AA5)	0.3 g@ 2.7 mmol per 10L culture
12**	aminoacetone•HCl (AA5)	0.7 g@ 6.4 mmol per 10L culture
13**	aminoacetone•HCl (AA5)	1.0 g @ 11.4 mmol per 10L culture

Representative dosage profile for aminoacetone (300 mg)

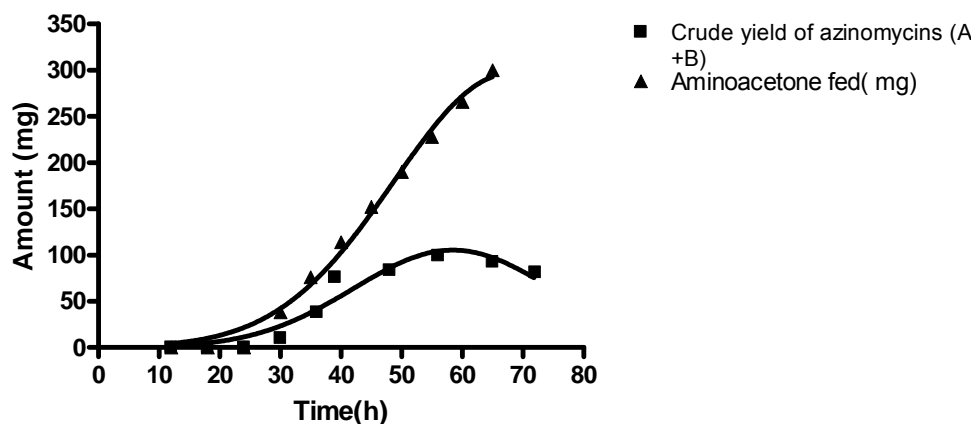


Figure 82. Dosage Profile for Aminoacetone (AA5) within the Optimized Range for Production of Azinomycins.

Intrigued by these results, we reasoned that the availability of aminoacetone in the cell might compete with threonine impacting the ratio of azinomycin A to B produced in *S. sahachiroi*. Aminoacetone is implied to produce oxy radicals and cytotoxic oxidative stress via production of methyl glyoxal in various species of bacteria [165-169]. *S. sahachiroi* was no exception. Production of natural product was not observed when aminoacetone was supplied at high concentrations (Table 14, entry 5). Hence, in order to prevent toxicity in bacterial culture, we decided to control the amount of aminoacetone that would be available at any given time. Consequently, unlabeled aminoacetone was provided to suspension cells in eight aliquots, which was supplied over a period of 2 days (Table 14 and Figure 82). The percentage of azinomycin A produced relative to B was calculated for each amount of aminoacetone fed (Table 14, Figure 83).

Table 14. Production of Azinomycin A as a Function of Amount of Aminoacetone Fed Per 10 Liters of Culture.

* feeding done in two lots of 0.25 g/mL each, all other amount feedings lots were at 0.003g/mL and fed in eight lots over 40 hours. ∇ % azn A = [azn A/(azn A + azn B)].

Entry	Amount of aminoacetone (AA5) fed (mg)	% azn A (AA1) produced ∇
1	0	28
2	300	52
3	700	80
4	1000	79
5	1250*	No production

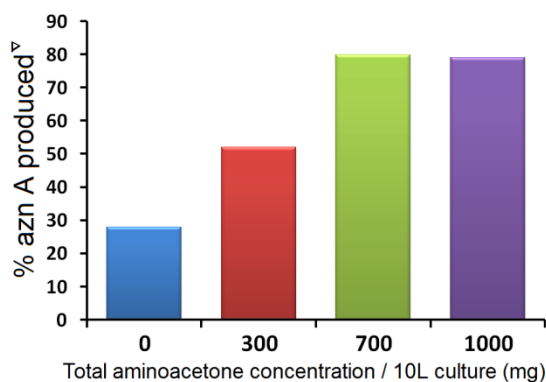


Figure 83. Production of Azinomycin A as a Function of the Amount of Aminoacetone, AA5 Fed Per 10 Liter Culture.

$$^{\nabla} \% \text{ azn A (1)} = [\text{azn A}/(\text{azn A} + \text{azn B})]$$

Under native conditions, azinomycin A comprises about 28% of the total mixture (A and B) isolated from the organism. The amount of azinomycin A produced was found to be directly proportional to the amount of aminoacetone fed. Increasing amounts of supplied aminoacetone resulted in enhanced production of azinomycin A, which is suggestive of a competitive role between aminoacetone and threonine for the NRPS module. Saturation occurs at higher concentrations (**Figure 83**) and could be attributed to the low levels of threonine contained within the Pharmamedia, a major component in our culture medium, or that produced by the organism to maintain primary metabolic processes.

In this investigation, we have demonstrated the dependency of azinomycin A production on availability of aminoacetone, a metabolite whose production has been confirmed in several microorganisms but can cause oxidative stress and cytotoxicity at high concentrations. A proposed biosynthetic route for the formation of aminoacetone and its subsequent incorporation into azinomycin A is provided in **Figure 84**. We were intrigued to find that aminoacetone can compete directly with threonine to favor the production of azinomycin A over azinomycin B. It is likely that the adenylation domain of the threonine NRPS module for azinomycin would be able to accept both threonine and aminoacetone. We attribute the observed production preference for azinomycin B to the limited native concentration of aminoacetone.

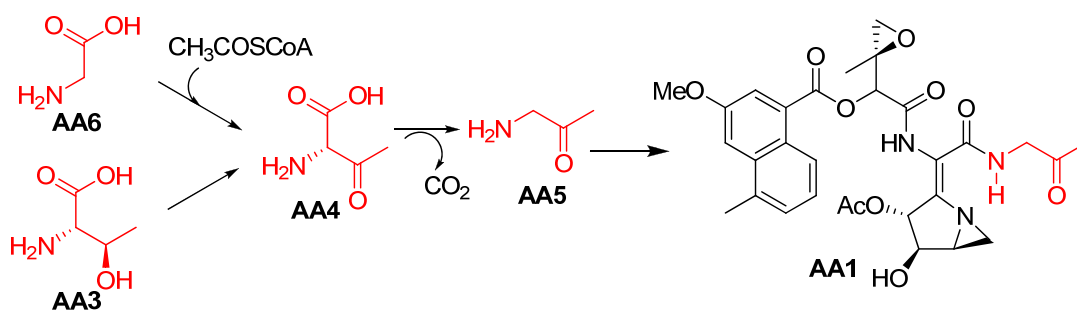


Figure 84. Proposed Biosynthetic Route for the Formation of Aminoacetone and Its Subsequent Direct Incorporation into Azinomycin A.

Positional incorporation of threonine, glycine in azinomycin A suggests convergent synthesis of aminoacetone via L-2-amino-3-ketobutyrate.

INCORPORATION OF MOLECULAR OXYGEN INTO AZINOMYCIN B

(THE AUTHOR)

The origin of the oxygen atoms in the azinomycins informs the biosynthetic origin of the molecule. Some of these atoms, such as the carbonyl oxygen atoms, are considered to be derived from the original metabolic building blocks, acetate units and amino acids. Our previous experiments with the cell free extract *S. sahachiroi* system indicated that known P450 inhibitors metyrapone, chloramphenicol, and (+)-miconazole inhibited azinomycin biosynthesis [146]. The oxygen atoms in the keto enol moiety next to C2 and C4 are derived from L-threonine which itself is derived from oxaloacetate (**Figure 85**). The acetate feeding studies revealed the origin of carbons C6, C14, and the C1' carbonyl carbon; therefore the oxygen atoms also originate from these acetate units. Feeding of [1-¹³C] L-valine revealed that the origin of the C17 oxygen atom is derived from valine. The additional derivative studies suggest a possible transamination where the oxygen atom next to C18 might be derived from, H₂O. The oxygen atom next to C3' appears to originate from an oxidative modification of the naphthoate by the action of a mixed function oxidase. This would suggest that the oxygen atom would originate from molecular oxygen (O₂). The epoxide moiety's oxygen atom also appears to be from a mixed function oxidase. The origin of the oxygen atoms next to C12 and C13 is unclear. The acetate incorporation pattern observed [30] would indicate that the original metabolite was a α -ketoglutarate derivative, which would indicate that the oxygen atoms might result from oxidative modifications, perhaps from a mixed function oxidase such as a cytochrome P450 oxidase. However, these oxygen atoms may originate from hydroxyl oxygen atoms on a sugar that is modified to produce the aziridinopyrrolidino moiety.

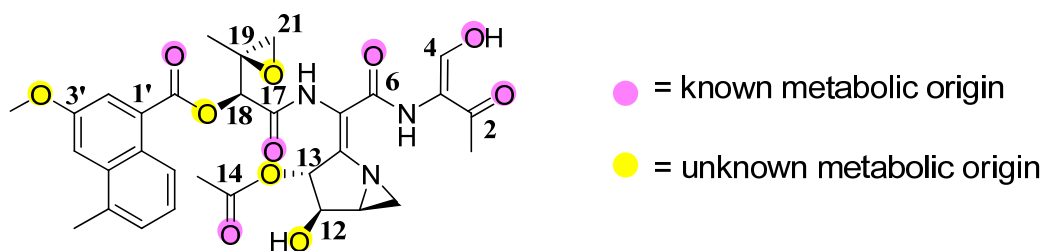


Figure 85. Origin of Oxygen Atoms in Azinomycin B.

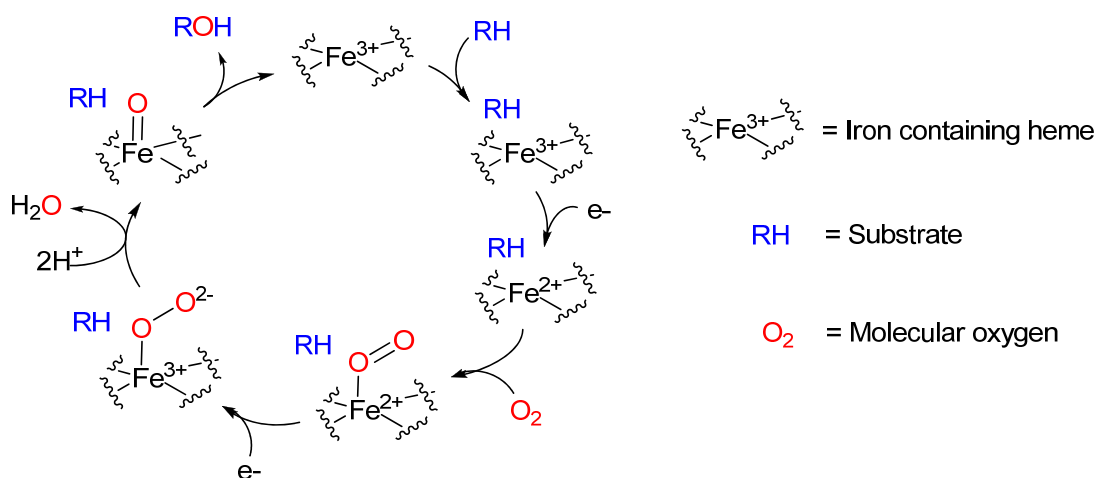


Figure 86. Active Site of a Cytochrome P450 Monooxygenase During Oxygen Insertion. Cytochrome P450 mechanism. These enzymes bind O_2 and use one oxygen atom to hydroxylate or epoxidate their substrates [170].

CYTOCHROME P450 MONOOXYGENASE

Cytochrome P450 enzymes are a family of enzymes well known for their role in detoxification and modification of substrates through redox reactions. These enzymes are from an expansive and diverse superfamily of hemoproteins found in nearly every form of life [170, 171]. Usually they form part of multicomponent electron transfer chains, called P450-containing systems. The active site of cytochrome P450 contains a heme iron center. The iron is tethered to the P450 protein via a thiolate ligand derived from a cysteine residue. This cysteine and several flanking residues are highly conserved in known cytochrome P450 enzymes [170]. Bacterial cytochrome P450s are often soluble enzymes and are involved in critical metabolic processes and secondary metabolism. These enzymes are also well characterized in an actinomycetes such as

Streptomyces [172]. The cytochrome P450 iron and heme-containing active site facilitates the use of molecular oxygen to introduce an oxygen atom into a molecule (**Figure 86**). The ability of the iron atom to exist in several oxidative states allows the transfer of electrons that enables the separation and activation of the oxygen atoms.

Incorporation of molecular oxygen into azinomycin B may be traced using the heavy isotope from $^{18}\text{O}_2$ ($^*\text{O}$) and observed via a shift in the ^{13}C NMR signal of the neighboring carbon atoms. It has been proposed that a cytochrome P450-like monooxygenase is responsible for the insertion of an oxygen atom into **O1** to form the epoxide, **O2**, (**Figure 87**) and the subsequent hydroxyl naphthoate, **O5**, resulting in the 3' methoxy oxygen atom via an “NIH shift” passing from **O3** to **O4** then to **O5** and subsequently to the 3' methoxy naphthoate **O6**. Evidence of the NIH shift mechanism in the formation of the azinomycin naphthoate **O6** was reported by Lowden *et al.* [30] in experiments with naphthoate groups decorated with deuterated C3' position. The *in vitro* study also indicated that known cytochrome P450-like monooxygenase enzyme inhibitors successfully diminished azinomycin B or naphthoate production [146].

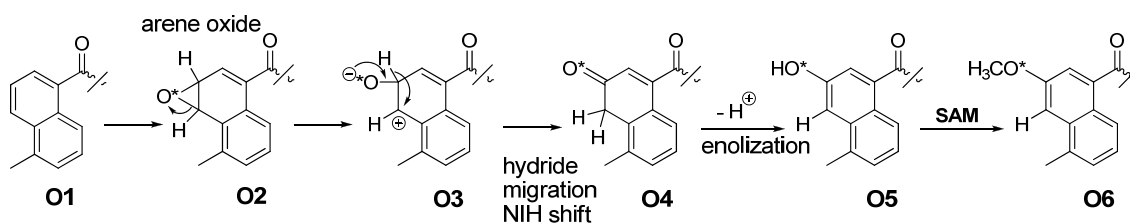


Figure 87. Oxygen Insertion by a Monooxygenase to Produce the C3' Methoxy Oxygen.

HEAVY OXYGEN INTRODUCTION

$^{18}\text{O}_2$ is quite expensive, currently selling for approximately \$500 per liter at 98% purity. This expense imposed a financial limitation on the experimental design for oxygen incorporation experiments. As the typical rate of air flow through the fermenter is 8 liters per minute, it is obvious that a sealed oxygen gas atmosphere recirculation system is required to make the experiment economically feasible. Retention of the expensive $^{18}\text{O}_2$ and avoiding diffusion exchange with air require a completely sealed system. These types of systems have been used before for examination of heavy oxygen uptake [151, 173]. Typically, a recirculation system involves a looped system with a point of introduction for oxygen and heavy oxygen. A basic design of a recirculation system (**Figure 88**) shows the flow of the atmosphere which is bubbled

through 5M KOH, as a scrubber for carbon dioxide, and water to moisten the atmosphere and catch any aerosol spill over from the the 5M KOH.

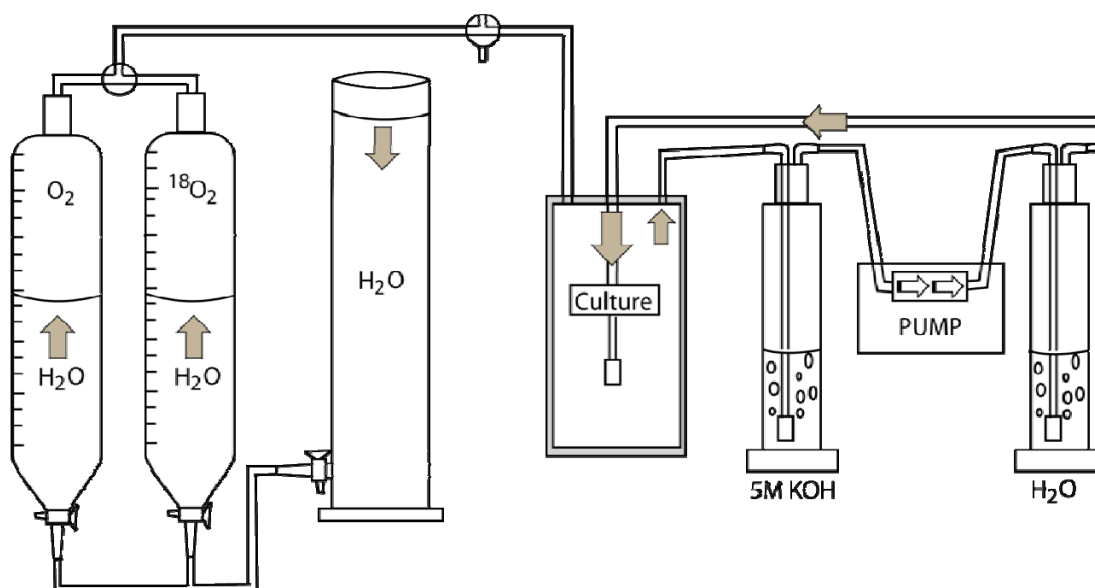


Figure 88. A Standard Oxygen Recirculation System.

Our case was a bit more complicated as it was not simply a problem of recirculating an atmosphere through a single shaking flask. The basic set-up for our fermenter based recirculation system is shown in **Figure 89**. The volume of the fermenter and associated atmosphere introduction required a large volume of atmosphere increasing the basic cost and heightening concerns over leak points. The fermenter design includes several designed exit points, seals, and a central rotating rod upon which the paddles are attached. As our standard practice of sterilizing the fermenter includes a cycle through the autoclave while containing medium, the fermenter seals and bearings are degraded over time. These were initially replaced in October 2006, but after about 160 runs, these were replaced in early September 2008 (**Figure 90D & E**). Additionally, the welding seals were re-welded, and silicone sealant was applied. Additionally the main seal at the interface of the glass container and the lid was replaced and greased. These adjustments resulted in negligible leaking. Leaking was measured by applying pressure on each component and measuring the volume lost. This was essential as quantifying the amount of oxygen consumed by the system during the production of a batch of azinomycin is critical for deciding the volume of $^{18}\text{O}_2$ to acquire.

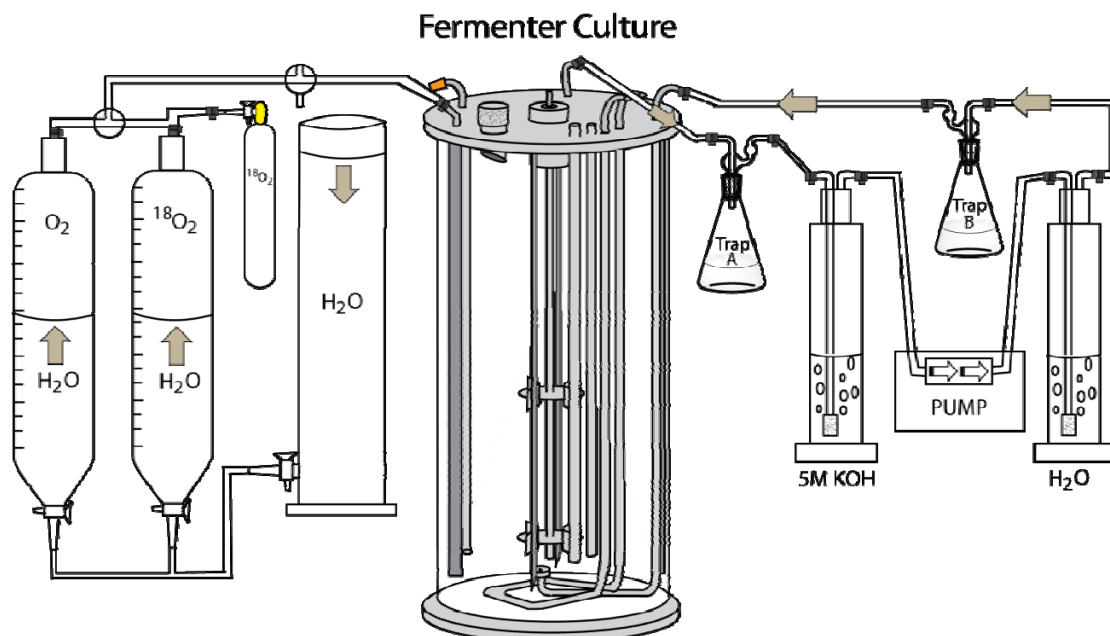


Figure 89. Our Fermenter Culture Based Oxygen Recirculation System.

A strong pump is needed to continue to push the atmosphere through the ten plus liters of culture, maintain an equal flow balance so the system has an equal flow of atmosphere and no build-up or pressure drop resulting in undo atmosphere pull from the atmosphere reservoirs. Additionally, foaming of the culture and over-bubbling of the 5M KOH and water bubblers can be an issue. Therefore traps A and B were added to the system although it does increase the amount of atmospheric space that must be balanced with added $^{18}O_2$. The traps protect the culture and pump from KOH spill over complications.

The ideal experiment would involve incorporating heavy oxygen into a molecule and using ^{13}C NMR to analyze the result would use an equal mixture of $^{18}O_2/^{16}O_2$. This allows one to have an internal standard carbon 13 signal next to the shifted signal of the carbon next to a heavy oxygen atom. To ensure this volume, several trial runs were conducted monitoring the oxygen consumed and replacing it with additional oxygen. The optimal time of exposure to the heavy oxygen and the recirculation system was also a priority. Initially, an exposure time of approximately 48 hours was considered as it mirrors the feeding types typically employed with the administration of the previous isotopically labeled substrates. By avoiding the first 24 hours in the fermenter, one avoids the substrates being consumed for growth purposes rather than for production of the natural products. Consumption of oxygen is a requirement for living, as is

avoiding built-up levels of carbon dioxide or exposure of the culture to high pressures or high levels of oxygen.

The initial trials indicated a total oxygen consumption of approximately 5.5-6 liters for 44-48 hours. In the initial attempt of an incorporation experiment we used 3 liters of $^{18}\text{O}_2$ and 3 liters of regular oxygen. The material isolated in this experiment was of poor quality; the pH of the culture had dropped. Even our analysis attempts by mass spectrometry were not useful. This was a failed run.

After this disappointment, we turned to evaluating ways to ensure a better productive run to ensure that the system itself was not causing the poor yield and material. New trials revealed that the system had developed some leak points; these were addressed with the replacement of bearings, oil seals, main lid seal, and sealing the edges of the features of the lid with silicone caulk. Additionally, rubber gaskets were added to the rotating rod buffering the oil seals. The equipment was also carefully cleaned with soap and bleach.

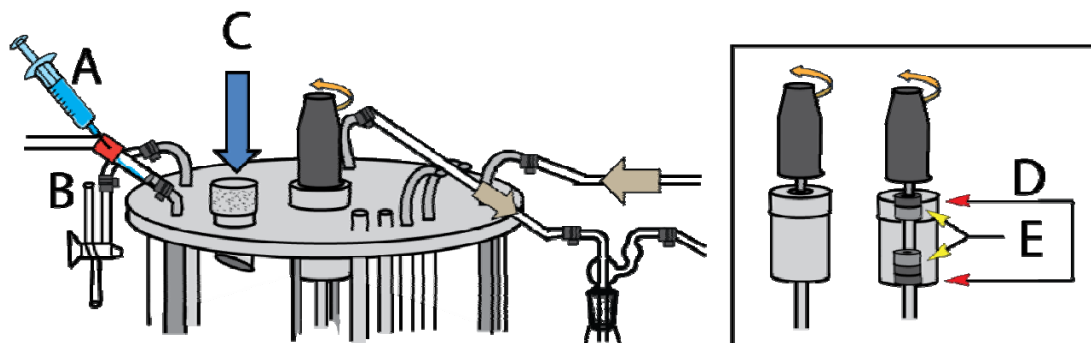


Figure 90. Improvements to the Fermenter Culture Based Oxygen Recirculation System. Modifications included: (A) the ability to introduce liquid materials without causing a leak in the sealed system using a syringe and rubber sealing material, (B) a stopcock enabling sterile culture sampling, (C) replacement of the rubber gasket underneath the screw cap used for 2nd stage culture introduction, (D) replacement of the oil seals and (E) bearings about the central rod.

Modification to the experimental design for the second attempt included improvements to pH monitoring and adjustment and production of the natural product. Modifications (**Figure 90**) included an option to introduce material such as alkaline buffer (1M sodium bicarbonate) or supplemental substrate (**Figure 90A**), a stopcock for sterile sampling of the culture (**Figure 90B**), replacement of the gasket material underneath the screw cap used for inoculation of the

fermenter culture (**Figure 90C**), and replacement of seals, bearings, (**Figure 90D & E**) and the central rod.

The system, now completely sealed, was ready for trials. The amount of oxygen consumed and added to the system was monitored to ensure proper amounts, duration, and production before the expensive heavy oxygen was used. Trials from the final 48 hours to 68 hours of growth under the system were evaluated. Additionally, supplements of unlabeled 66 mg L-methionine and 120 mg L-valine were used to increase the single yield of azinomycin B. This boost in production had been noted with previous supplemental experiments with the production system.

Table 15. Oxygen Consumption Trials with the Recirculation System.

* $^{18}\text{O}_2/\text{O}_2$ (50:50) was used in this trial. V = L-valine, M = L-methionine.

Trial Entry	Oxygen consumed (mL)	Total Oxygen Added (mL)	Hours	Rate of consumption (mL/Hour)	Final pH	Added Supplement	Production Result
1	4800	5440	48.75	98.4	7.87	none	normal
2	7220	7680	63.00	114.6	8.54	none	marginal
3	8220	9120	64.75	126.9	8.43	none	marginal
4	5740	6780	47.75	120.2	7.79	100mg V, 60mg M	better
5	10300	10300	68.00	151.5	9.00	100mg V, 60mg M	poor
6	9680	10080	69.50	139.3	8.66	120mg V, 66mg M	marginal
7*	6540	6900	57.00	114.7	8.00	120mg V, 66mg M	better

The trials revealed that oxygen consumption is greater early in the 72 hour period. Following 2nd stage inoculation into the fermenter; there is a phase of growth and increased oxygen consumption. It was also observed that under the recirculation system, the pH of the culture rose beyond that of the normal pH profile with longer duration under the atmosphere recirculation system (**Table 15, entries 2, 3, 5, and 6**). The addition of supplemental amino acids

(L-valine and L-methionine) improved the production of azinomycin B. The supplemental runs best coupled with shorter exposure time to the system (**Table 15, entry 4**). Theoretically, increasing the time of exposure time of the *Streptomyces sahachiroi* culture to the mixed isotope atmosphere increases the probability to incorporate the ^{18}O isotope into azinomycin. We had 5 liters of compressed $^{18}\text{O}_2$ available for the experiment and wanted to be conservative on the use of the $^{18}\text{O}_2$ gas we chose an optimal route: exposure for 57 hours with the $^{18}\text{O}_2/\text{O}_2$ (50:50) and adding supplemental L-valine and L-methionine (in three lots) (**Table 15, entry 7**). These conditions yielded a very healthy, azinomycin B producing culture. The final culture's pH was 8.00, and the yield was good (crude: 107.6 mg, purified for azinomycin B: 35.9 mg).

ANALYSIS OF $^{18}\text{O}_2/\text{O}_2$ EXPOSED AZINOMYCIN B

Extraction and purification of azinomycin B from the media afforded approximately 35.9 mg of purified natural product. The sample was analyzed by proton decoupled ^{13}C -NMR spectroscopy as isotopic substitution with ^{18}O gives rise to an upfield shift in the position of resonances of directly bound carbon atoms [174]. The ^{13}C - $\{^1\text{H}\}$ -NMR spectrum of ^{18}O : ^{16}O -labeled azinomycin B revealed that four of the eleven oxygen atoms were derived from molecular oxygen corresponding to those at carbon centers C3', C3'OCH₃, C21, C19, C13, C14, and C12.

The sample was analyzed initially by 300 MHz NMR, but this did not fully resolve the signals. 500 MHz NMR provided resolution. **Table 16** reports the shifts seen in the carbons next to heavy oxygen atoms affected, and

Figure 91 displays the ^{13}C NMR signals observed. The analysis reveals incorporation of 4 heavy oxygen atoms into azinomycin B from molecular oxygen (**Figure 92**). The shifts reported are in line with previously reported carbon shifts for single ^{13}C - ^{18}O bonds [174]. Incorporation of the heavy atoms into azinomycin B was also confirmed through APCI mass spectrometry.

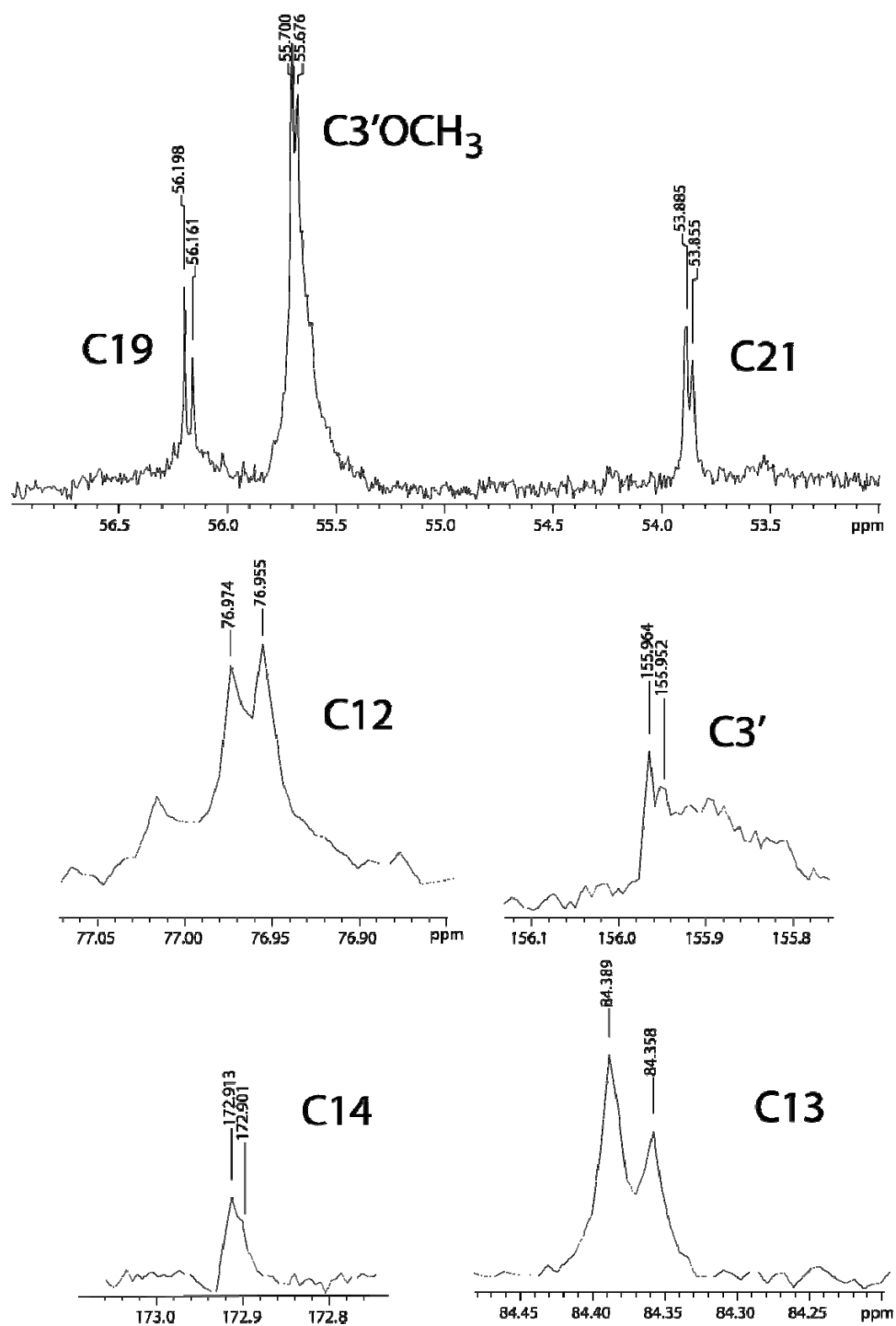
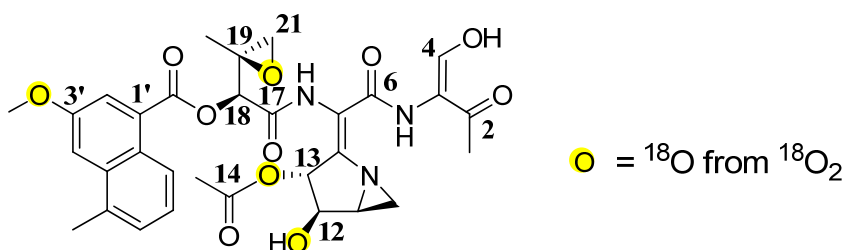


Figure 91. ^{13}C Signals Displaying a Shift from $^{18}\text{O}_2$ Incorporation. Shifts were observed in carbons 12, 13, 14, 19, 21, 3' and the 3' methoxy.

Table 16. ^{13}C Shifts Observed in Carbons Next to Oxygen in Azinomycin B.

CDCl_3 was used to obtain all spectra except for $^*\text{C}12$ observed in CD_2Cl_2 . Azinomycin B carbon shifts in CD_2Cl_2 have been previously reported by Lowden, *et al.* [30, 109].

Carbon position	δ/ppm ^{16}O	δ/ppm ^{18}O	δ difference (ppm)
3'	155.964	155.952	0.012
3'OCH ₃	55.700	55.676	0.024
21	53.885	53.855	0.030
19	56.198	56.161	0.037
13	84.389	84.358	0.030
14	172.913	172.901	0.012
12	76.974	76.955	0.019

Figure 92. Positional Incorporation of Heavy Oxygen Atoms from $^{18}\text{O}_2$.

The pattern of incorporation suggests the operation of a cytochrome P450-like monooxygenase for the incorporation of the oxygen atoms in the methoxy and the epoxide. Given the previous evidence of allylketocarboxylate (V12) as the most advanced precursor for incorporation into the azinomycin backbone [175], it is reasonable to envision a monooxygenase inserting an oxygen atom from molecular oxygen into the double bond to produce the epoxide moiety (**Figure 93**).

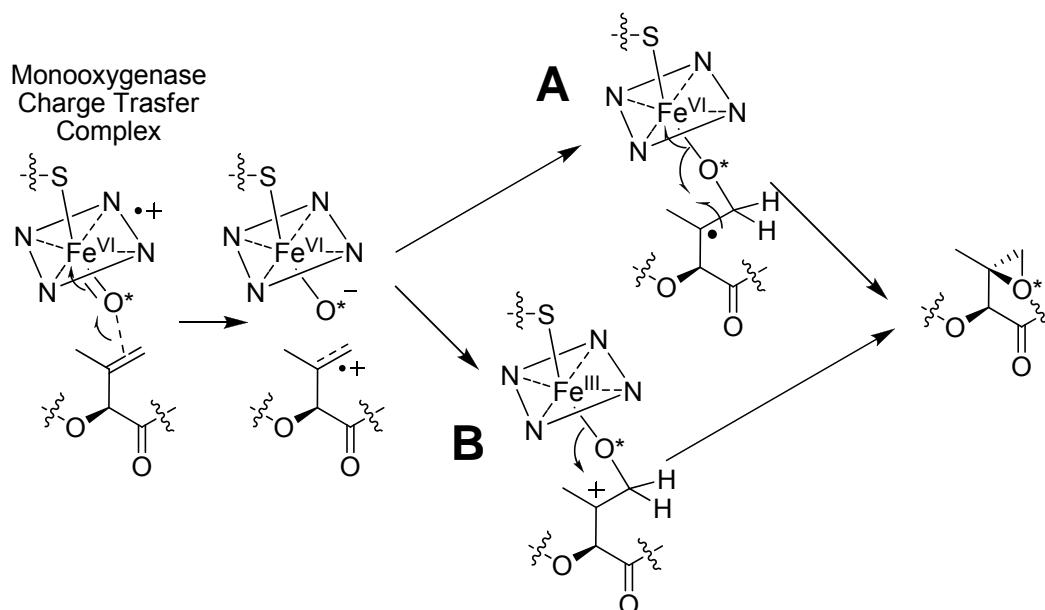


Figure 93. A Proposed Mechanism for the Insertion of a Heavy Oxygen Atom Via a Monoxygenase for the Formation of the Epoxide Moiety.

The mechanism could take one of two paths to generate the epoxide. (A) Radical mechanism where the charge resulting charge transfer complex has a Fe^{VI} or (B) an electron pair transfer with the charge transfer complex with a Fe^{III}. Adapted from Gruschow *et al.* [150].

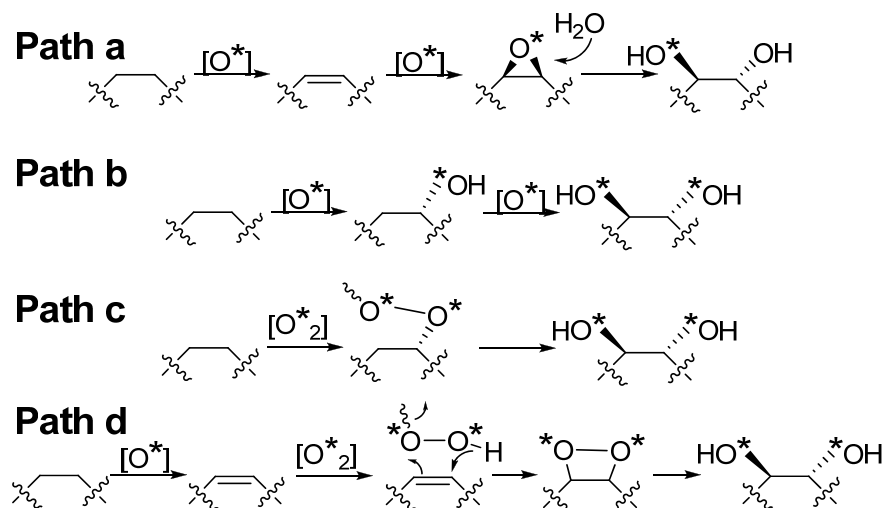


Figure 94. Proposed Mechanisms for the Hydroxylation of the Pyrrolide Ring at C12 and C13.

The most revealing result was the incorporation of molecular oxygen at both positions on the aziridinopyrrolidine ring. The equal incorporation of oxygen 18 relative to oxygen 16

eliminates a route that would involve formation of an epoxide and subsequent formation of a diol via hydrolysis by water (**Figure 94, path a**). If this is the case, one oxygen atom would originate from molecular oxygen ($^{18}\text{O}_2/^{16}\text{O}_2$) and the other from natural abundance water, predominantly H_2^{16}O . The anti-stereochemistry of the oxygen atoms suggests the either the oxygen atoms are inserted sequentially by two cytochrome P450-like monooxygenases before or after ring closure (**Figure 94, path b**) or a dioxygenase acts before ring formation allowing bond rotation and the alternating stereochemistry (**Figure 94, path c** or **path d**). Given the dearth of examples dioxygenases acting in this manner, it suggest that the route sequential cytochrome P450-like monooxygenases would be more likely, though a determination from these results is not definite.

BIOSYNTHETIC ROUTE TO THE AZIRIDINO[1,2A]PYRROLIDINE MOIETY

(THE AUTHOR)

The results of the cell free system suggested incorporation of sodium acetate, L-ornithine, and glycine (**Figure 95**). The cell free system did not, however, provide information regarding molecular location. This ambiguity led to a series of stable isotope feedings with decidedly mixed results. The origin of the acetate in this portion of the molecule was determined with the $[1-^{13}\text{C}]$ sodium acetate feeding experiment. Our feeding of the $[1-^{13}\text{C}]$ sodium acetate did not, however, have a significant incorporation in the aziridino [1,2a] pyrrolidine fragment. We did see some incorporation at C6 and C12 (though it was obscured by solvent). This incorporation pattern is consistent with incorporation of glycine as the amino acid is closely related metabolically to acetate. Considering the results of Lowden, *et al.* [30] with their $[1-^{13}\text{C}]$, $[2-^{13}\text{C}]$, and $[1, 2-^{13}\text{C}]$ sodium acetate incorporation studies, the incorporation pattern seen suggests that the major part of the aziridino fragment's backbone was derived from α -ketoglutarate (**Figure 68**). Interestingly, the acetate incorporation reflected here does not suggest significant incorporation into C10 or C11. This incorporation pattern is consistent with the incorporation pattern observed with acetate that occurs in a number of metabolites in their respective biosynthesis.

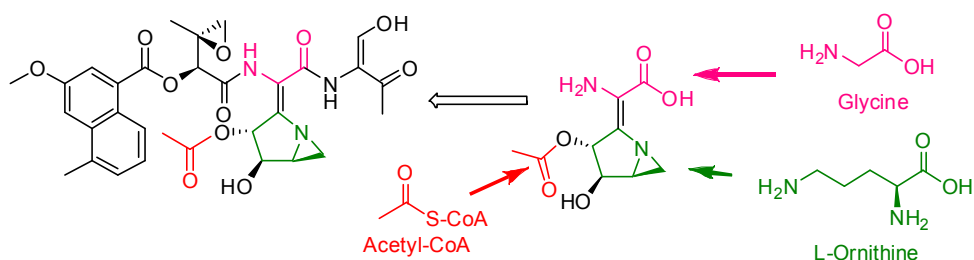


Figure 95. Biosynthetic Routes to the Aziridino[1,2a]pyrrolidine Fragment of Azinomycin B Indicated by Results from the Cell Free Extract Experiments.

The incorporation of [1- ^{14}C] L-ornithine, [U- ^{14}C] L-ornithine, [2- ^{14}C] malonyl-CoA, and [U- ^{14}C] glycine, as described in Table 5 and Figure 55, indicate the incorporation of these metabolites leading to a possible incorporation scenario seen above.

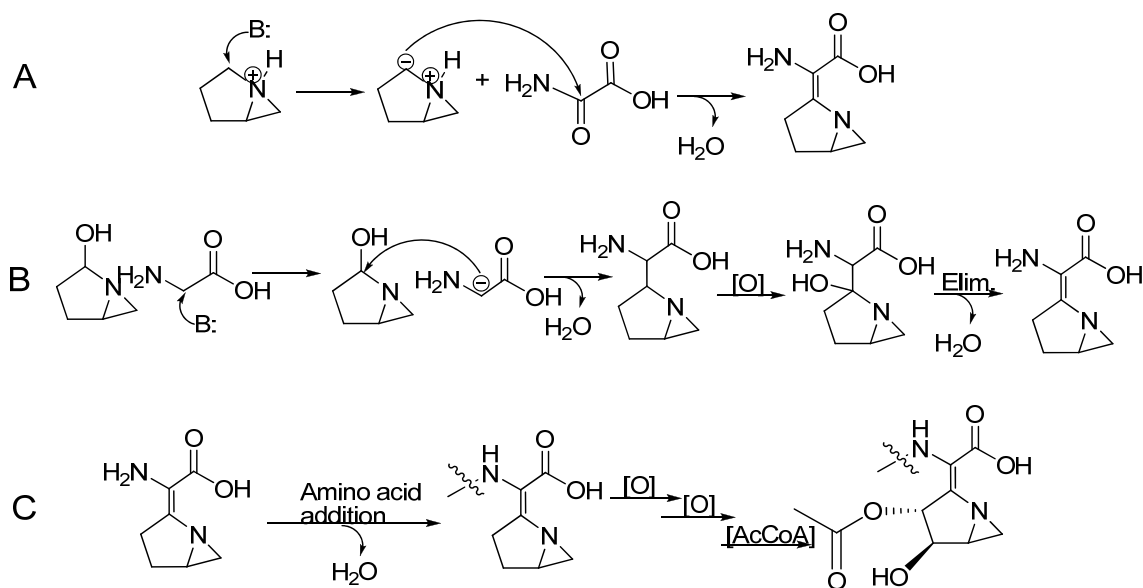


Figure 96. Possible Mechanism for the Formation of Aziridino-pyrrolidine Containing Amino Acid.

Construction possibilities based on the results of the cell free extract experiments could proceed down several different avenues. One possibility is that the 1-azabicyclo[3.1.0]hexane ring is pre-assembled and then coupled to oxamic acid by nucleophilic addition (**Figure 96A**). However, the 1-azabicyclo[3.1.0]hexane alcohol unit could also be coupled to glycine by $\text{S}_{\text{N}}2$ attack (**Figure 96B**) to generate a unique amino acid containing the aziridino-pyrrolidine ring which can be incorporated by the NRPS biosynthetic machinery. The molecule is subsequently modified by oxidation and acetylation (**Figure 96C**).

There are several possible routes to the 1-azabicyclo[3.1.0]hexane ring. As shown in **Figure 97**, biosynthesis can originate from ornithine whereby the aziridine ring is formed through loss of water, followed by transamination and formation of the hemiaminal to give the alcohol (blue pathway in **Figure 97A**). Alternatively, formation of the 1-azabicyclo[3.1.0]hexane ring could originate from proline forming the aziridine ring after reduction (green pathway **Figure 97B**). Or the reaction could initiate from ornithine or glutamate to give glutamate γ -semialdehyde, proceeding through proline (**Figure 97C**). This approach is limited as the formation of the aziridine carbon, C10, would have to originate from a single carbon source. As SAM was eliminated as a possibility (**Figure 65**), this would require a more exotic origin for this single carbon not derived from acetate or methionine.

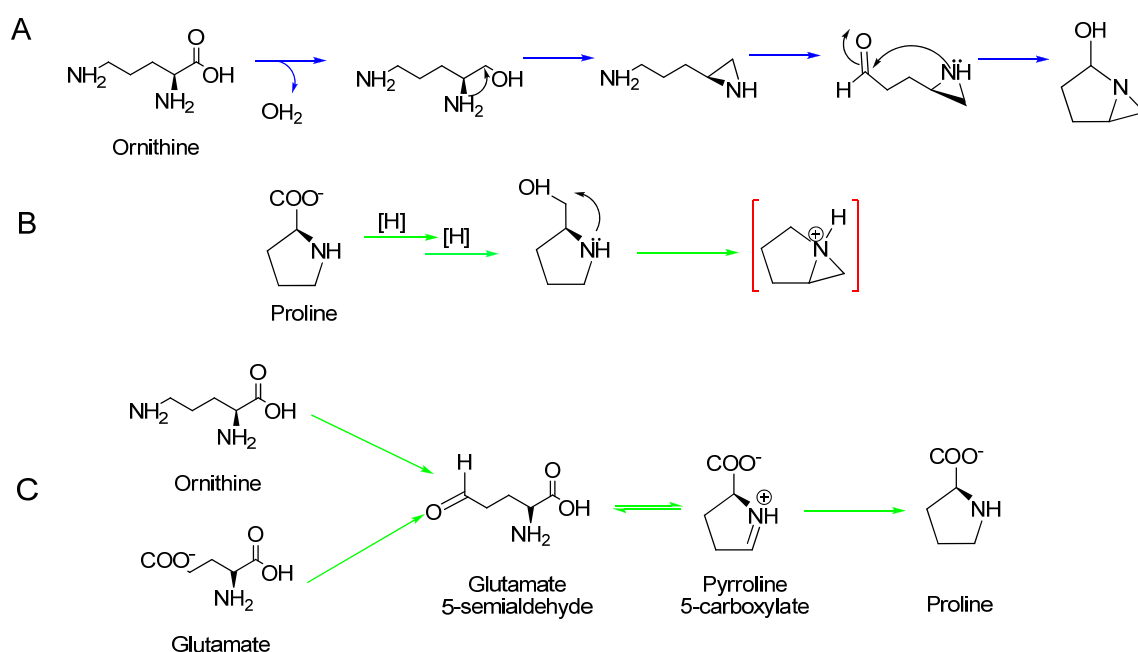


Figure 97. Potential Routes for the Formation of the 1-azabicyclo[3.1.0]hexane Ring Involving Formation of the Pyrrolidine Ring Before Attachment to the Natural Product Backbone.

An alternative biosynthesis could originate from ornithine whereby the ornithine comprises the backbone (C6-C8, C12, and C13) of the aziridinopyrrolidine modified amino acid (**Figure 98**). This arrangement would be most in line with the acetate incorporation pattern for an amino acid derived from α -ketoglutarate (**Figure 68**) and postulated by Lowden [30]. The aziridine ring is formed through an addition of a 2 carbon phospho-diol unit (**Figure 98A**) with

subsequent transamination at C11, followed by oxidative modifications to yield the oxygen atoms on C12 and C13 (**Figure 98B**) permitting the appropriate stereochemistry to be set before ring closure. The pyrrolidine ring is formed via the amine attack upon the double bond between C7 and C8 (**Figure 98B**). The aziridine ring is subsequently formed after a sulfotransferase transfers a sulfate to the C10 alcohol, resulting in the formation of the aziridine ring (**Figure 98C**). This modified amino acid would then be added upon the growing molecule via a NRPS mechanism (**Figure 98C**). The acetylation would occur as a post assembly modification (**Figure 98C**).

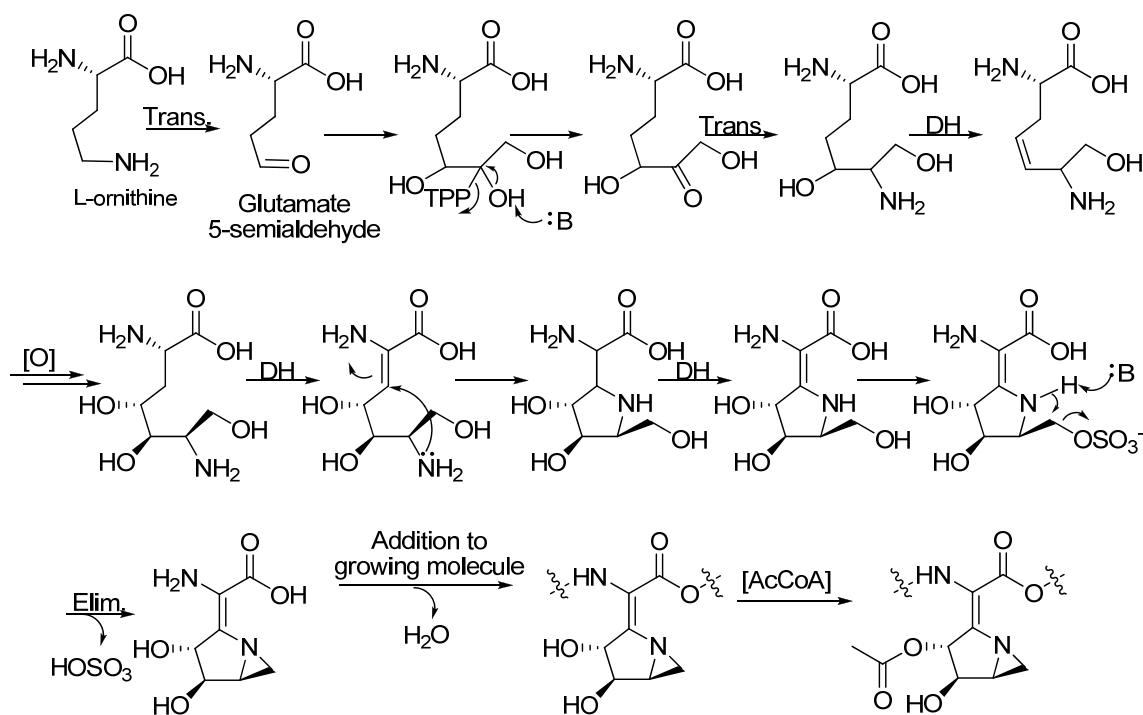


Figure 98. Potential Routes for the Formation of the 1-azabicyclo[3.1.0]hexane Ring from a Glutamate Derivative, Two Carbon Sugar Derivative, Sulfotransferase, and Formation of the Diol from Molecular Oxygen.

While these possibilities seem to be logical extensions from previous experimental evidence, it is still possible that the ring has decidedly different origins. The alternate stereochemical arrangement of the oxygen atoms on the ring suggests that a modified sugar might be a possibility. Additionally, other amino acids such as aspartate, serine, lysine, and

arginine should not be ignored, even though initial investigations do not indicate their involvement.

THE SUBSTRATES

A series of isotopically labeled substrates were administered to cultures of *Streptomyces sahachiroi* and the resulting azinomycin B produced analyzed by NMR or mass spectrometry for isotopic incorporation. These substrates (**Figure 99**) included: proteogenic amino acids, non-

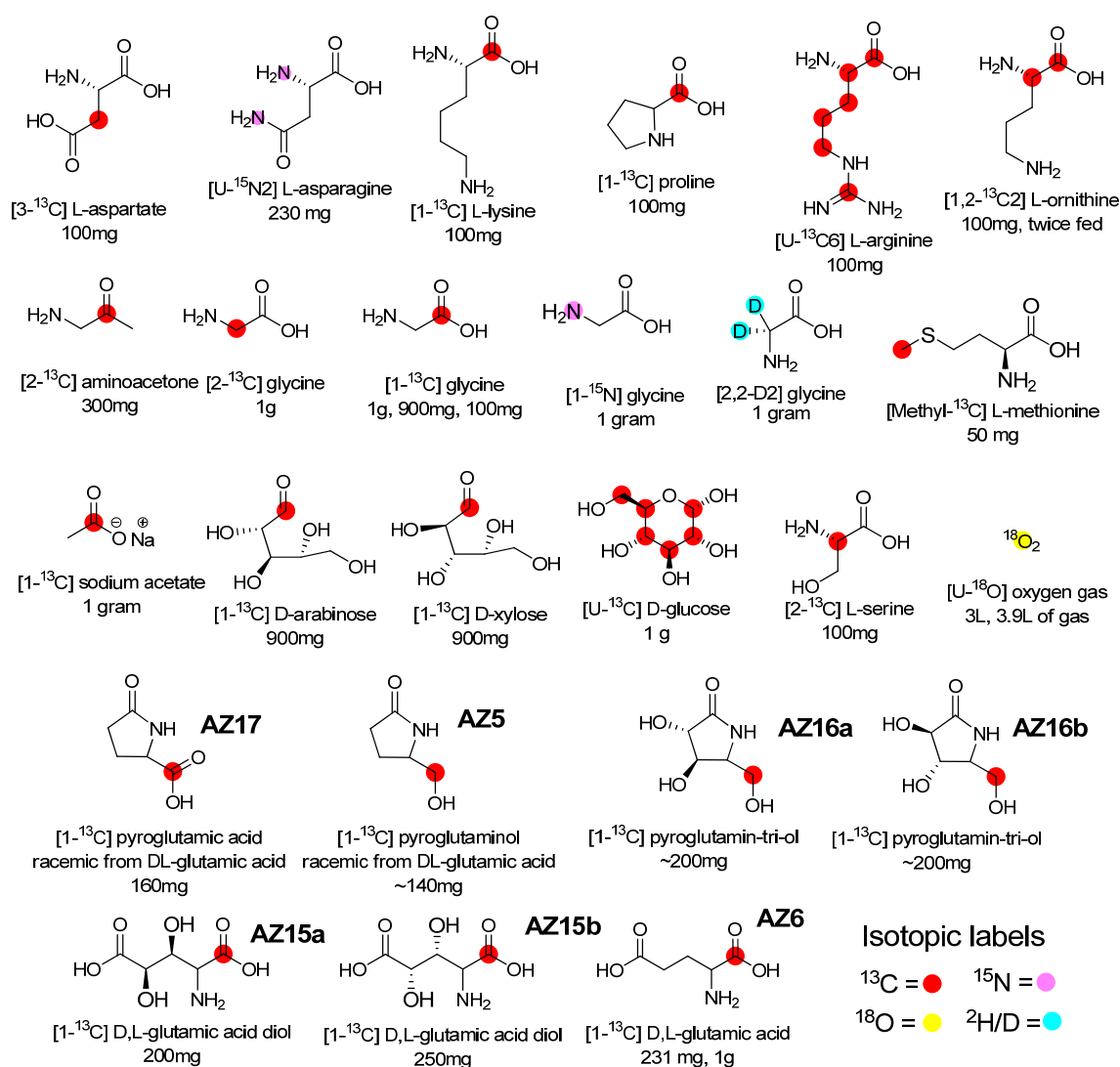


Figure 99. Stable Isotope Substrates Employed in Exploring the Biosynthesis of the Azirdinopyrrolidine Moiety.

proteogenic amino acids, a range of synthetic derivatives (**AZ1-5**), natural sugars, and the previously discussed heavy oxygen gas. The amount used for these feedings was initially based upon feedings and incorporations seen in other parts of the molecule.

ORNITHINE

(THE AUTHOR)

In an effort to confirm the incorporation of L-ornithine observed in the *in vitro* biosynthesis (experiments discussed in chapter III) and to identify the specific position of incorporation of L-ornithine into azinomycin B, we fed ^{13}C enriched L-ornithine. We administered 100 mg of [1,2- ^{13}C] L-ornithine•HCl, but did not observe incorporation of the labeled carbons specifically into the carbon skeleton such as C6-C7 as in **Figure 98** or C8-C13 as in **Figure 97A** and subsequently in **Figure 96B**. The non-significant incorporation indicates one of two possibilities: that ornithine is not a true precursor or the amount used was not significant enough to be incorporated. Ornithine is a closely related derivative of glutamic acid which is highly involved in metabolic processes. Due to the prohibitively high costs of feeding larger amounts of L-ornithine, we proceeded to examine other substrates.

GLYCINE

(THE AUTHOR)

Another substrate observed to be involved in construction of the azinomycins in the cell free extracts experiments was glycine. We fed 100 mg [1- ^{13}C] glycine, but did not see any specific incorporation. We then we fed 900 mg [1- ^{13}C] glycine with 100 mg [1- ^{13}C] L-valine control. Evaluation of this double feeding revealed no specific incorporation at C6 as speculated from the cell free extract experiments. We later fed 1 gram [1- ^{13}C] glycine by itself, but again, did not observe specific incorporation. We then fed 1 gram [2- ^{13}C] glycine and observed significant scattering effects and high incorporation into the 3'OCH₃ indicating that the glycine C1 underwent decarboxylation and the C2 was reconstituted into [1,2- ^{13}C] acetate units (**Figure 100**, **Figure 143**, and **Figure 144**). Overall incorporation of the ^{13}C labeled glycines is seen in **Table 17**.

We also evaluated [^{15}N] glycine. We were able to observe incorporation of this labeled nitrogen into not only azinomycins A and B, but also into the epoxyamide, indicating that glycine may easily serve as a source of nitrogen perhaps by transamination for the construction of these

molecules. Multiple incorporation of label was observed by mass spectrometry, evidenced by $M+H+1$ and $M+H+2$ (see **Figure 148**).

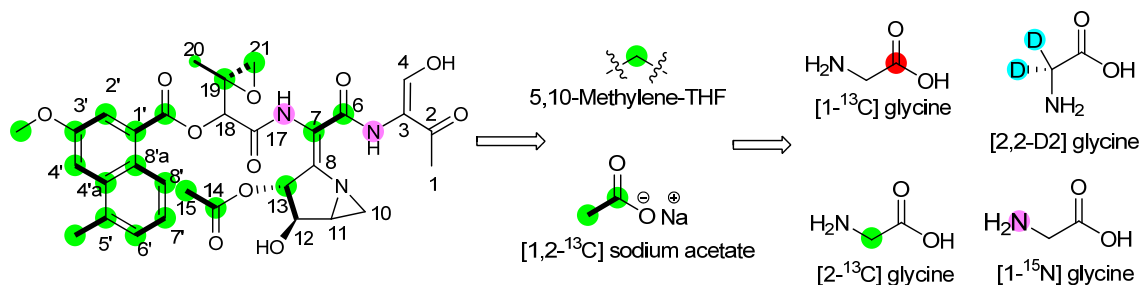


Figure 100. Observed Incorporation of Various Isotopically Labeled Glycines into Azinomycin B.

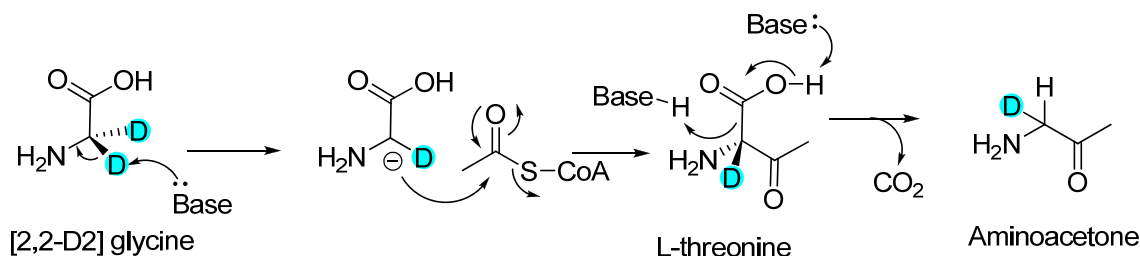


Figure 101. Formation of Aminoacetone from [2,2-D₂] Glycine.

[2,2-D] glycine was also evaluated. Interestingly, this resulted in a reduced overall yield of azinomycins, particularly azinomycin A. This indicates the construction of the molecule requires a rate limiting step involving one of the deuterium atoms from glycine. In the case of azinomycin A, the construction of the aminoacetone unit could be envisioned to have a rate limiting step involving the removal of a deuterium (**Figure 101**). It could be envisioned that the construction of acetate units from glycine could also involve such a step as suggested by the [2-¹³C] glycine patterning and incorporation pattern observed in **Figure 100**. Incorporation of [¹⁵N] glycine into azinomycin A and B observed by mass spectrometry indicated incorporation higher than unlabeled for single incorporation (1.4%, .96%) and double incorporation (4.24% and 5.51%) respectively (**Figure 147** and **Figure 148**). This indicates that it is possible that any of the 3 nitrogen atoms in the molecule could originate from glycine, but more likely that the aziridine and end fragment nitrogen atoms may originate from glycine, perhaps by a simple

transamination or specific incorporation as in the construction of L-threonine or aminoacetone (**Figure 101**).

Table 17. Percent Incorporation into Azinomycin B for ^{13}C Labeled L-proline and Glycine.
*Incorporation based upon stated reference carbon and calculated as previously mentioned.

Substrate	Reference carbon	% Incorporation*						
		C6	C7	C8	C10	C11	C12	C13
[1- ^{13}C] Proline	C3'OCH ₃	0.24	0.08	-0.24	-0.32	-0.24	n/a	-0.31
100mg	C20	0.73	0.51	0.09	-0.03	0.08	n/a	-0.02
[1- ^{13}C] glycine	C3'OCH ₃	-0.16	-0.18	-0.14	-0.28	-0.22	n/a	-0.23
100 mg	C20	0.16	0.15	0.19	0.01	0.09	n/a	0.08
[1- ^{13}C] glycine	C3'OCH ₃	-0.51	-0.75	-1.00	-0.74	-0.91	n/a	-0.88
1000 mg	C20	1.08	0.21	-0.70	0.25	-0.38	n/a	-0.27
[2- ^{13}C] glycine	C3'OCH ₃	-1.00	-1.01	-1.11	-1.10	-1.09	n/a	-1.07
1000 mg	C20	0.45	0.25	-1.18	-1.00	-0.79	n/a	-0.57

PROLINE

(THE AUTHOR)

We also examined L-proline. It could be envisioned (**Figure 97B and C**) for proline to be involved in the formation of the ring system. It could also be suggested that proline would be converted into another α -ketoglutarate derivative. This could also be considered (along with other α -ketoglutarate derivatives) to extend into the backbone of azinomycin. We fed 100 mg L-proline, but we did not observe any significant incorporation (**Table 17**).

CARBOHYDRATES

(THE AUTHOR)

To ensure that the aziridine was not derived from a modified sugar, we investigated a few sugars. Initially we examined D-arabinose and D-xylose as it could be envisioned that the ring system could be derived from the five carbon sugar D-arabinose and attached to a glycine unit for the

modified amino acid (**Figure 102**). This would explain the origin of the oxygen atoms and the specific stereochemistry of the diol. A transamination and subsequent ring closure by a sulfotransferase would produce the aziridine ring. To balance the results we also fed D-xylose as a control, as the stereochemistry is different at the carbons. Feeding 900mg each, we did not observe any specific incorporation, only lower level increases in the naphthoate carbons signals indicating metabolic scrambling of the label into acetate. We also examined [U-¹³C] D-glucose's incorporation into azinomycin. The curious origin of the carbons 10 and 11 with no incorporation of acetate could indicate an origin from a sugar derivative. We fed 1 gram of [U-¹³C] D-glucose and did not observe specific incorporation by signal increase at any particular position by carbon or by mass spectrometry. ¹³C labeled sugar incorporation results for the azabicyclic fragment are summarized in **Table 18**. It is possible that the addition of sugar substrates to the nutrient deprived medium resulted in the sugars being completely consumed for mere nutrition without any diversion to azinomycin biosynthesis. While no incorporation was observed (either single incorporation or multiple labels (which results in signal splitting)) it does not eliminate completely the possibility of a sugar related metabolite being involved in azinomycin biosynthesis.

Table 18. Percent Incorporation into Azinomycin B for ¹³C Labeled D-arabinose, D-xylose, and D-glucose.

*Incorporation based upon stated reference carbon and calculated as previously mentioned.

Substrate	Reference carbon	% Incorporation*						
		C6	C7	C8	C10	C11	C12	C13
[1- ¹³ C] D-arabinose	C3'OCH ₃	0.66	0.57	0.64	1.00	1.09	n/a	1.37
900mg	C20	0.84	0.72	0.81	1.28	1.40	n/a	1.75
[1- ¹³ C] D-xylose	C3'OCH ₃	0.53	1.88	1.94	0.67	0.53	n/a	0.00
900mg	C20	-0.62	-0.21	-0.19	-0.58	-0.62	n/a	-0.78
[U- ¹³ C6] D-glucose	C3'OCH ₃	-0.54	-0.19	-0.34	-1.00	-0.96	n/a	-0.58
1000 mg	C20	-0.17	0.43	0.17	-0.94	-0.86	n/a	-0.23

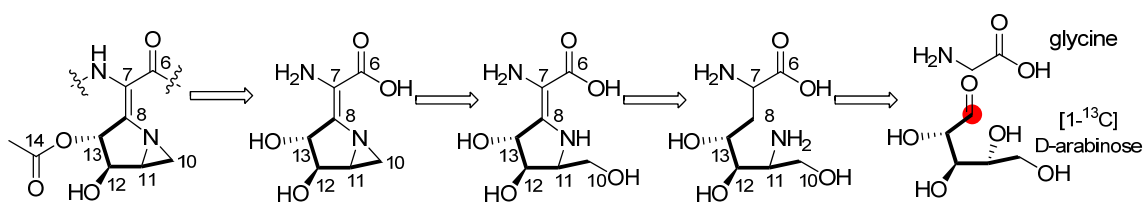


Figure 102. Possible Formation of the 1-azabicyclo[3.1.0]hexane Ring from D-arabinose and Glycine.

No specific incorporation was observed.

ASPARTATE, ASPARAGINE, LYSINE, ARGININE, AND SERINE

(THE AUTHOR)

After failing to see incorporation of the previous substrates we examined possible incorporation of seemingly less likely substrates, given the carbon length. We examined the incorporation of [3-¹³C] L-aspartate. As we had become concerned with the possibility of decarboxylation of the amino acids and loss of the labeled carbon, we decided, given the positional isotope price, that 100 mg [3-¹³C] L-aspartate was a reasonable option. One could envision incorporation of L-aspartate into different positions in the 1-azabicyclo[3.1.0]hexane ring (**Figure 103**). No specific incorporation was observed. [U-¹⁵N₂] L-asparagine (230mg) was also fed to observe possible incorporation of the nitrogen atoms into the aziridinopyrrolidine unit or the whole molecule. Interestingly, by mass spectrometry, only a slightly higher than normal shift in M+1 and M+2 was observed, indicating generic or secondary incorporation into azinomycin A or azinomycin B.

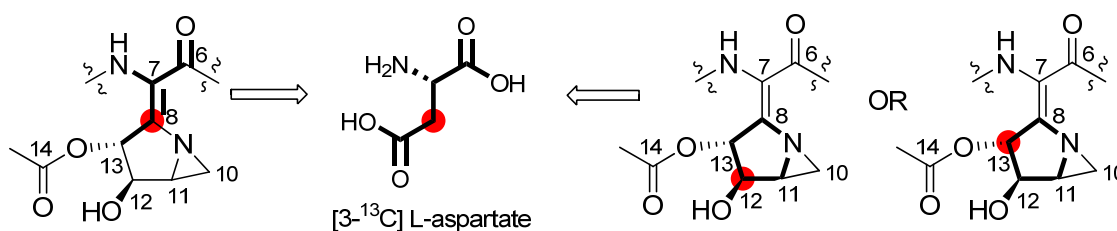


Figure 103. Possible Formation of the 1-azabicyclo[3.1.0]hexane Ring from [3-¹³C] L-aspartate. No specific incorporation was observed.

[1-¹³C] L-lysine (100 mg) was also examined for incorporation into the azinomycins. As the cell free extract experiments indicated, there was no observed incorporation into the azinomycins. Although it could be envisioned to incorporate (**Figure 65B**), this is even more doubtful given non-incorporation of the labeled [¹³C methyl] L-methionine into the C10 position.

[U-¹³C₆] L-arginine (100mg) was also examined for incorporation into the aziridinopyrrolidine unit. No major incorporation was observed by mass spectrometry or by ¹³C NMR except for C11 as referenced to C20. We also examined [2-¹³C] L-serine (100 mg) as a possible precursor. It could be envisioned that the [2-¹³C] L-serine labeled carbon would incorporate at C8, C13, or C11 (**Figure 104**). We did not observe these increases. The only result we observed was a signal increase at C8'a, C5', C12 and C18. Scattering could explain these results, but it is also possible that L-serine could participate in the ring construction. ¹³C labeled aspartate, lysine, arginine, and serine incorporation results for the azabicyclic fragment are summarized in **Table 19**. It is possible that the amounts fed were not sufficient to observe significant incorporation.

Table 19. Percent Incorporation into Azinomycin B for ¹³C Labeled Aspartate, Lysine, Arginine, and Serine.

*Incorporation based upon stated reference carbon and calculated as previously mentioned. Scattering into the naphthoate region or contaminating naphthamide signal overlap also observed.

Substrate	Reference carbon	% Incorporation*						
		C6	C7	C8	C10	C11	C12	C13
[3- ¹³ C] L-aspartate 100mg	C3'OCH ₃	-0.25	-0.18	-0.75	-0.72	-0.61	n/a	-0.66
	C20	0.94	1.12	-0.24	-0.17	0.09	n/a	-0.03
[1- ¹³ C] L-lysine 100 mg	C3'OCH ₃	-0.39	-0.65	-0.62	-0.79	-0.70	n/a	-0.75
	C20	2.04	0.89	1.06	0.30	0.70	n/a	0.45
[U- ¹³ C ₆] L-arginine 100 mg	C3'OCH ₃	-0.69	-0.69	-0.86	-0.87	-0.11	n/a	-0.86
	C20	0.86	0.84	0.05	0.02	3.59	n/a	0.06
[2- ¹³ C] L-serine 100 mg	C3'OCH ₃	0.00	-0.15	-0.30	-0.57	-0.55	n/a	-0.52
	C20	-0.24	-0.36	-0.48	-0.69	-0.67	n/a	-0.65

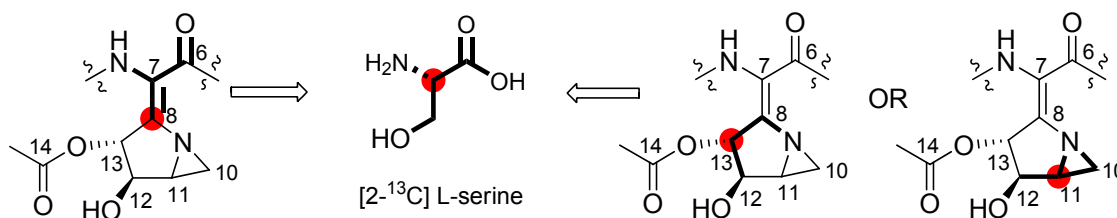


Figure 104. Possible Formation of the 1-azabicyclo[3.1.0]hexane Ring from [2-¹³C] L-serine. No incorporation at the indicated positions was observed.

SYNTHETIC PRECURSOR SERIES FOR THE DISCRETE FORMATION OF THE 1-AZABICYCLO[3.1.0]HEXANE RING

(COLLABORATION BETWEEN DR. VASUDHA SHARMA AND THE AUTHOR)

In view of the non incorporation of simple amino acid and sugar incorporation into the azabicyclic scaffold, we evaluated a series of more advanced precursors. The azabicyclic can be envisioned to form from an aldol-type condensation between glycine and pyroglutamate derived azabicyclic, **AZ4**, in **Figure 105**.

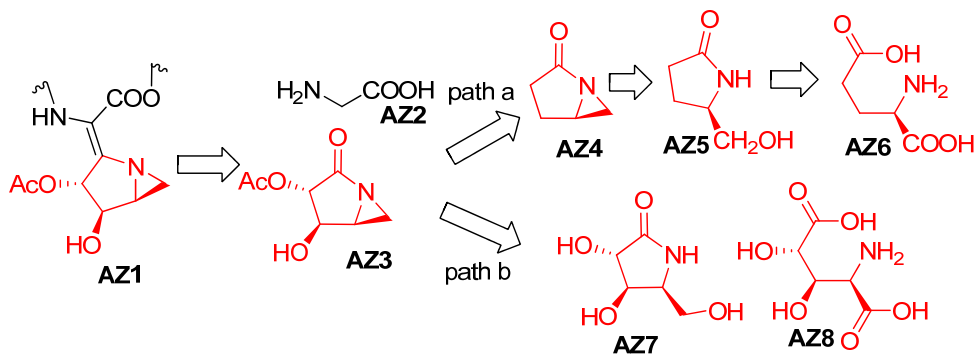
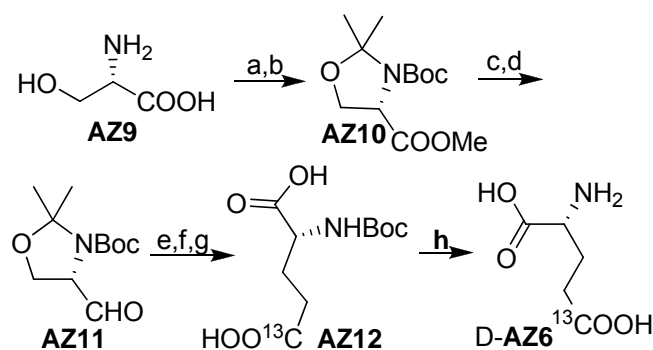


Figure 105. Possible Scaffolds Contributing towards Origin of Azabicyclic, AZ3.

The azabicyclic itself can be seen to originate from either path A, wherein D-glutamic acid, **AZ6** can undergo cyclization to afford pyroglutamic acid which after series of reduction could generate the nascent bicyclic **AZ4**. The nascent bicyclic could undergo functionalization to generate **AZ3**. Alternatively, **AZ3** could be generated by path b, wherein a functionalized structure such as **AZ8**, could undergo cyclization followed by reduction to provide an azasugar, **AZ7**. During the preparation of this manuscript, Liu *et al.* have proposed the possible role of

glutamic acid in the NRPS segment of the molecule [176]. Our *in vitro* studies however, have shown a role of glycine in the fragment [146].

The relatively inexpensive DL-glutamic acid (1g for \$485 from Cambridge Isotopes) became available in mid 2007. Our previous interest in glutamic acid and synthetic derivatives had been tempered by the prohibitive cost of materials and synthesis. All synthetic aziridine derivatives described below were synthesized by Dr. Vasudha Sharma and were administered and analyzed by the author in the same manner as previously described in Kelly *et al.* [133].



Scheme 2. Synthesis of D-glutamic acid, AZ6.

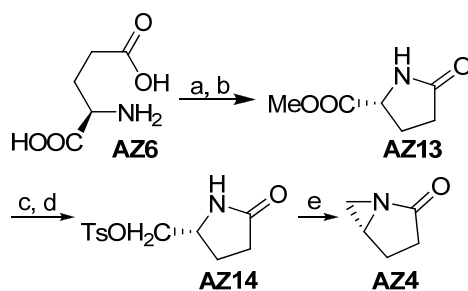
(a) (i) SOCl_2 , MeOH, reflux, 2h.(ii) Boc_2O , NaHCO_3 , 36h. (b) 2-methoxy propene, CSA, 3h. (c) LiAlH_4 , THF:MeOH (3:2) (d) IBX, EtOAc, reflux, 3.5 h.(e) $(\text{OEt})_2\text{P}(\text{O})\text{CH}_2^{13}\text{COOEt}$, NaH, THF.(f) H_2 (1 atm), 10% Pd/C, MeOH. (g) Jones' reagent, acetone, 12h then iPrOH, 15'. (h) $\text{NaOH}(\text{aq.})$, EtOH (6:1) then acidify.

(SYNTHESIS BY DR. VASUDHA SHARMA)

Garner aldehyde, **AZ11** was prepared using a modification of procedure by Dondoni *et al.* [177]. We have previously utilized this strategy for the synthesis of threonine analog of Garner's aldehyde [133]. Briefly, serine, **AZ9** was methylated to afford the methyl ester hydrochloride which was N-protected with Boc_2O . N-Boc protected methyl ester of serine was then treated with 2-methoxypropene under mildly acidic conditions to afford the acetonide methyl ester, **AZ10**. Upon reduction of the ester group to provide the alcohol, followed by mild oxidation with IBX, the Garner's aldehyde, **AZ11** was achieved. This set the stage for a HWE reaction with triethylphosphite[178] using NaH as the base to provide the alkene unit as a mixture of cis-trans isomers as well as rotamers. The product was subjected to hydrogenation using 10%Pd/C as the catalyst. This C-4 substituted acetonide unit was then treated with Jones' reagent [179] to

facilitate hydrolysis of acetonide followed by oxidation of the primary alcohol and provide the N-Boc protected 5-ethyl ester of D-glutamic acid, **AZ12** (**Scheme 2**).

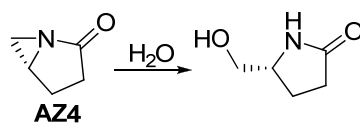
Retrosynthetic analysis of **AZ4** (**Figure 105**) suggests its formation from chiral glutamic acid after cyclization to provide pyroglutamate, followed by reduction and intra-molecular nucleophilic substitution. D-glutamic acid, **AZ6** was converted into chiral pyroglutamic acid by dehydration, which after methylation afforded the methyl pyroglutamate **AZ13**. Subsequently, reduction of the ester group using NaBH_4 generated the primary alcohol (**Scheme 3**). The primary alcohol was protected by TsCl to afford the tosylate **AZ14** which upon treatment of a strong base such as KH afforded facilitated the nucleophilic attack of the N on the methylene leading to loss of the tosyl group and generation of the azabicyclic scaffold **AZ4** [180]. Similar attempts with Ms group as the leaving group did not provide the desired azabicyclic and lead to decomposition of starting material. The formation of the aziridine ring was detected on TLC by disappearance of starting material. Infrared analysis of the crude reaction mixture revealed a carbonyl absorption at 1743 cm^{-1} by IR indicating the presence of N-acylaziridine [180].



Scheme 3. Synthesis of the Azabicyclic AZ4.

(a) H_2O , sealed tube, 15h, $130\text{ }^\circ\text{C}$ (b) AcCl , MeOH , $0^\circ\text{C} \rightarrow \text{r. t.}$ (c) NaBH_4 (3 eq.), $\text{THF}:\text{MeOH}$ (3:2) (d) TsCl , Et_3N , CH_2Cl_2 (e) KH , THF (anhyd.).

However, as anticipated, the azabicyclic **AZ4**, proved to be very unstable to aqueous conditions even at room temperature and readily suffered a nucleophilic attack by water at the methylene carbon to give pyroglutaminol (**Scheme 4**).



Scheme 4. Ring Opening of Azabicyclic AZ4.

Since the azabicyclic did not prove to be stable, we pursued (**Figure 105, path b**) in synthesizing the 3,4-dihydroxy-5-(hydroxymethyl)pyrrolidin-2-one and 2-amino-3,4-dihydroxypentanedioic acid as potential biosynthetic precursors for the azabicyclic pendant in the azinomycin scaffold. The trihydroxylated pyrrolidin-2-ones **AZ16a** and **AZ16b** as well as the dihydroxylated glutamic acids **AZ15a** and **AZ15b**, could be useful intermediates in the synthesis of various interesting compounds. **AZ16a** and **AZ16b** can be envisioned to lead to the corresponding pyrrolidines which are known as azasugars and have shown promising activities as glycosidase inhibitors [181-183]. Further, they constitute a chiral template in the synthesis of more complex pyrrolizidine alkaloids such as alexine, australine, and 3-epi-analogues [184, 185]. Finally, the specificity of the enzyme could be probed by feeding labeled diastereomeric forms **AZ15a**, **AZ15b** and **AZ16a**, **AZ16b** (**Figure 106**).

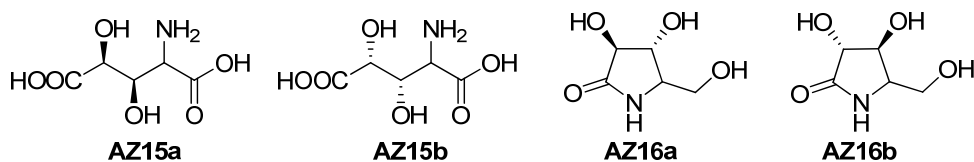
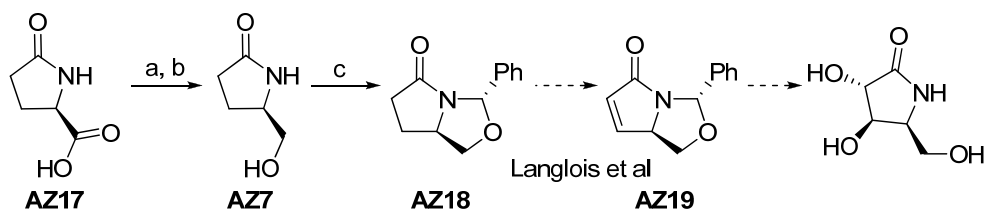


Figure 106. Proposed Aza-sugars **AZ15a**, **AZ15b** and Dihydroxy Glutamic Acids **AZ16a** and **AZ16b**.

AZ16a and **AZ16b** can be envisioned to be synthesized starting from pyroglutamic acid, **AZ17** and converting it into ester, **AZ13** and subsequently reducing to a primary alcohol, pyroglutaminol, **AZ7**. The nucleophilic groups could be suitably protected as an *N, O*-acetal, **AZ18** [186] which could be converted into the versatile α,β -unsaturated lactam, **AZ19**, **Scheme 5**. This unsaturated lactam upon epoxidation followed by subsequent region- and stereo-selective ring opening could provide entry to access the pyrrolidinone units as described earlier by Langlois *et al.* [187].

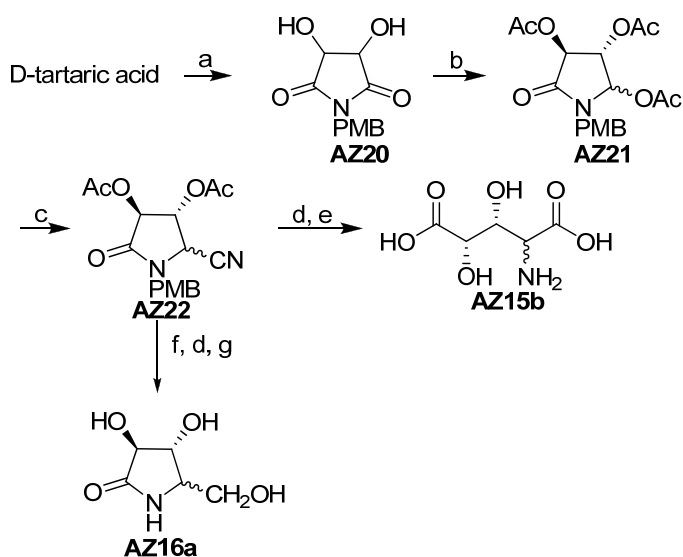


Scheme 5. Synthesis of 2-(hydroxymethyl) 3, 4- dihydroxy Pyrrolidinone Unit.

(a) AcCl, MeOH, 0°C → r. t. (b) NaBH₄ (3 eq.), THF: MeOH (3:2) (c) PhCHO, p-TsOH, benzene, reflux.

However, in our hands, yields for the conversion of **AZ18** to **AZ19** were low, a result not desirable for reactions involving isotopically labeled compounds. Further, purification of labeled *N,O*-acetal **AZ19** via distillation became challenging at a small scale and effected further steps.

Hence, the failure of the strategy described above prompted us to use tartaric acid to access the dihydroxy glutamic acid units **AZ15a** and **AZ15b** as well as the trihydroxy pyrrolidinones **AZ16a** and **AZ16b** using a modified strategy of Nishiyama *et al.* [188, 189]. Starting with L or D tartaric acid which provides the desired stereochemistry of the hydroxy groups for either **AZ15a** or **AZ15b** and **AZ16a** or **AZ16b**, the optically active cyclic imides **AZ20** were derived as shown in **Scheme 6**. The cyclic imides were then reduced with NaBH₄ and converted into acetoxylactams, **AZ21**. Treatment with *in situ* generated Me₃SiCN afforded the cyano diacetoxylactams, **AZ22** which upon deprotection of PMB group followed by hydrolysis afforded the dihydroxy glutamic acids **AZ15a** or **AZ15b**. Methanolysis of cyano group in **AZ22** after deprotection of PMB followed by reduction afforded the desired trihydroxy pyrrolidinones **AZ16a** or **AZ16b**.



Scheme 6. Synthesis of AZ15a, AZ15b, AZ16a, AZ16b.

(a) PMB-NH₂, xylenes, 36h, reflux. (b) (i) NaBH₄, THF. (ii) Ac₂O, Pyridine. (c)(i) BF₃-OEt₂ (ii) K¹³CN/TMSCl, KI. (d) Ce(NH₄)₂(NO₃)₆, 4h. (e) 6N HCl, reflux. (f) (i) SOCl₂, MeOH, reflux. (g) NaBH₄, THF. Use of L-tartaric acid generated the opposite isomers required.

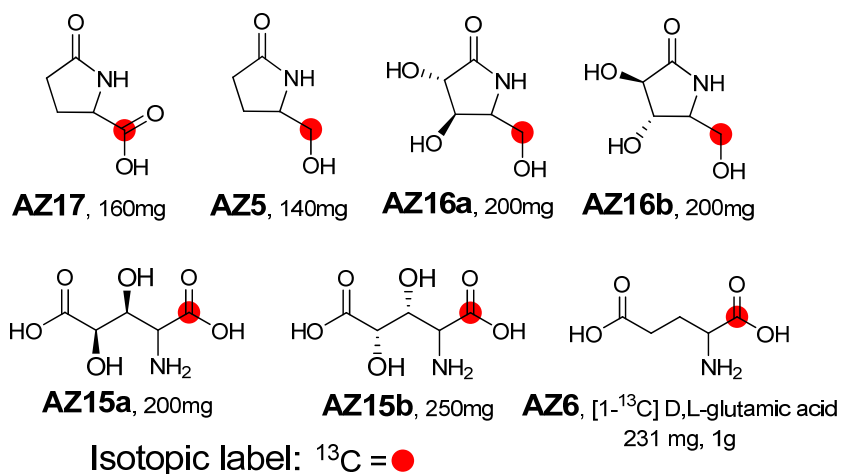


Figure 107. ¹³C labeled Substrates Synthesized for Feeding to *S. sahachiroi* Cultures for Potential Incorporation into Azinomycin B.

The precursors synthesized (**Figure 107**) were administered in the same manner as previously described in Kelly *et al.* [133]. The substrates **AZ5**, **AZ17**, **AZ16a**, **AZ16b**, **AZ15a**, and **AZ15b** were fed, but no incorporation was observed by mass spectrometry or ¹³C NMR into the azabicyclic moiety carbons C6-C13 (**Table 20**). Only a scattering incorporation into the

naphthoate portion of the molecule was observed. The lack of incorporation of these precursors cast doubt on the discrete formation of the 1-azabicyclo[3.1.0]hexane ring and attachment to a glycine unit as in **Figure 105 path a** or **b**.

Table 20. Positional Percent Incorporation of Labeled Precursors into Azinomycin B.

*Positional incorporation of the labeled substrate into azinomycin B. % incorporation = $[(A-B)/B] \times 1.10$ where A, intensity of labeled carbon; B, intensity of unlabeled carbon; 1.10, natural abundance of ^{13}C ; n/a = not detected due to solvent overlap in ^{13}C NMR.

**small C20 signal threw off percent incorporation calculations.

Substrate	Reference carbon	% Incorporation*						
		C6	C7	C8	C10	C11	C12	C13
[1- ^{13}C] AZ17	C3'OCH ₃	-0.73	-0.80	-0.99	-0.91	-0.91	n/a	-0.93
160 mg	C20	0.94	0.59	-0.44	-0.04	-0.03	n/a	-0.13
[1- ^{13}C] AZ5	C3'OCH ₃	-0.02	-0.19	-0.78	-0.54	-0.80	n/a	-0.63
140 mg	C20	0.72	0.43	-0.55	-0.16	-0.58	n/a	-0.31
[1- ^{13}C] AZ16a	C3'OCH ₃	-0.83	-0.76	-1.09	-0.78	-0.86	n/a	-0.96
200 mg	C20	0.73	1.15	-0.98	1.01	0.54	n/a	-0.16
[1- ^{13}C] AZ16b	C3'OCH ₃	-0.26	-0.21	-1.11	-0.60	-0.97	n/a	-0.64
200 mg	C20	0.57	0.65	-1.11	-0.11	-0.84	n/a	-0.19
[1- ^{13}C] AZ15a**	C3'OCH ₃	-1.11	-0.79	-0.93	-0.64	0.74	n/a	-1.01
200 mg	C20	-1.11	11.41	5.82	17.46	72.09	n/a	2.82
[1- ^{13}C] AZ15b	C3'OCH ₃	-1.11	-1.02	-1.03	-0.95	-0.72	n/a	-1.07
250 mg	C20	-1.11	-0.52	-0.60	-0.01	1.55	n/a	-0.84
[1- ^{13}C] AZ6	C3'OCH ₃	-0.10	-0.91	-0.82	-0.96	-0.91	n/a	-0.96
231 mg	C20	3.50	-0.21	0.21	-0.45	-0.20	n/a	-0.44
[1- ^{13}C] AZ6	C3'OCH ₃	1.09	-0.71	-0.90	-0.72	-0.81	n/a	-0.85
1000 mg	C20	5.20	0.04	0.02	0.02	-0.26	n/a	-0.35

GLUTAMIC ACID

With the lack of incorporation of the synthesized azabicyclo derivatives, we considered that such advanced precursors may not be readily incorporated into the azinomycin natural product. We

also considered the alternative scenario presented in **Figure 98** and in the following **Figure 108 path a** whereby the origin of the aziridinopyrrolidine amino acid moiety's attachment to the molecule is through a glutamic acid derivative rather than by glycine or other unit as originally suggested in **Figure 96** and subsequently in **Figure 105 path a** or **path b**. No incorporation into C10 was detected by mass spectrometry or ^{13}C NMR. $[1-^{13}\text{C}]$ DL-glutamic acid was examined in an initial dosage of 230 mg, discounting **Figure 108 path b**. Incorporation into C6 was detected at 5.2%, **Table 20**. Subsequent feeding of 1 gram $[1-^{13}\text{C}]$ DL-glutamic acid resulted in a detected incorporation at C6 of 5.2% with reference to C20 carbon, **Table 20**. The specific % incorporation of the label indicates that there is metabolic interference (glutamic acid is readily used in many metabolic processes) or we are observing the effect of a secondary incorporation. Glutamic acid and glutamine are readily used in many metabolic processes and are found in highest concentration of amino acids (22.4%) in the fermentation media. Such key metabolites are particularly susceptible to metabolic scattering and lower rates of incorporation [174]. This could mean that the previous feedings of ornithine were unsuccessful because of scattering and the smaller amount.

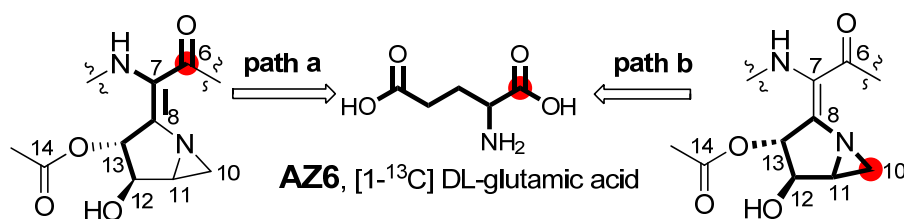


Figure 108. Possible Formation of the 1-azabicyclo[3.1.0]hexane Ring from $[1-^{13}\text{C}]$ DL-glutamic Acid.

This does, however, indicate that the construction of the 1-azabicyclo[3.1.0]hexane ring and subsequent attachment to a glycine unit appears to be unlikely (**Figure 96** & **Figure 97**). Given the incorporation of $[1-^{13}\text{C}]$ DL-glutamic acid and the previously mentioned oxygen incorporation results, the proposed construction appears to be closer to what was suggested in **Figure 98**.

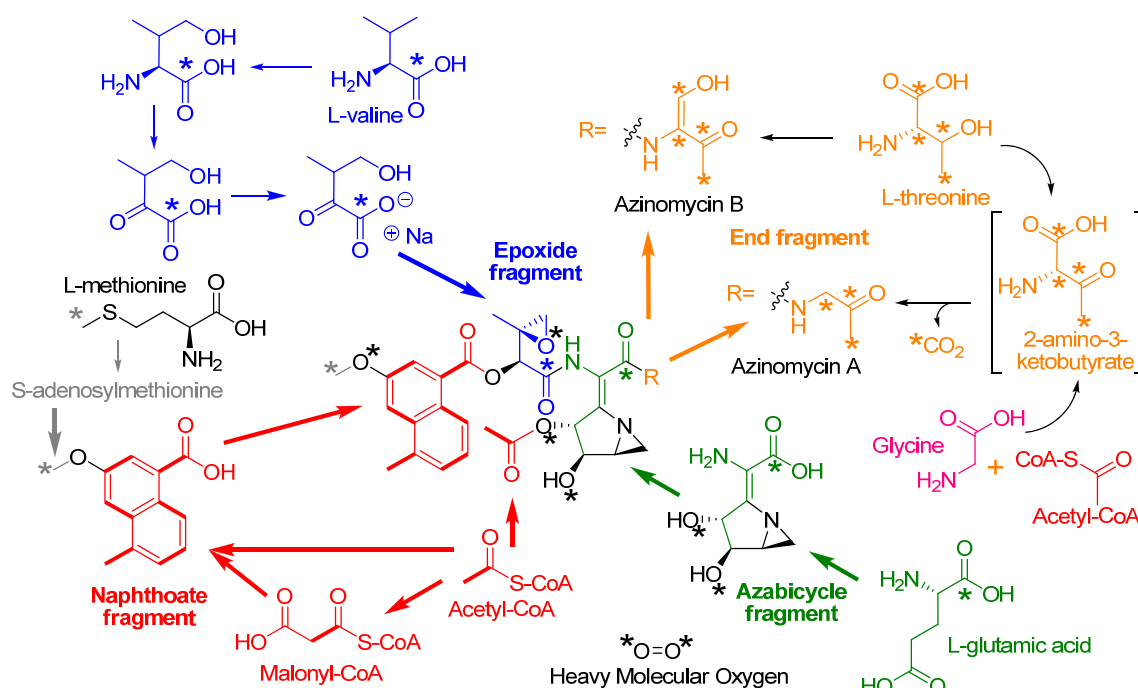


Figure 109. Biosynthesis of the Azinomycins as Indicated by Stable Isotope Feeding Studies.

SIGNIFICANCE

The azinomycins represent a structurally unusual class of DNA cross-linking agents produced by nature. Investigation of the biosynthesis of the azinomycins was affected by use of stable isotope enriched substrates. This series of stable isotope feeding experiments has revealed a more detailed biosynthetic origin for the azinomycins. The current view of azinomycin biosynthetic precursors is displayed in **Figure 109**. Nearly all portions of the molecule were attributed to one or more precursor sources. The remaining C10 and C11 stand out as their origin was not revealed. It is possible that their source may not be easily uncovered using stable isotope feeding studies. It is likely that analysis of the sequence of the genes encoding enzymes used in azinomycin biosynthesis will shed light upon their origin. The numerous molecules fed and subsequently incorporated or rejected have revealed much about the construction units and have shed light on the probable mechanisms for construction. This knowledge provides insight to the complex biosynthesis of unique molecules, and combined with future full characterization of the biosynthetic enzymes, may lead to custom design of natural products and pharmaceuticals.

EXPERIMENTAL PROCEDURES

INSTRUMENTATION AND GENERAL METHODS

^1H & ^{13}C NMR spectra were recorded on either a Varian Inova 500 or Varian Inova 300. ^1H NMR chemical shifts are reported as δ values in ppm relative to CDCl_3 (7.26 ppm) and coupling constants (J) are reported in Hertz (Hz). Infrared spectra were recorded on a Bruker Tensor 27 spectrometer. Unless otherwise indicated, deuteriochloroform (CDCl_3) served as an internal standard (77.0 ppm) for all ^{13}C spectra. Mass spectra (ESI) were obtained at the Laboratory for Biological Mass Spectrometry at the Department of Chemistry, Texas A&M University, with API QStar Pulsar, MDS Sciex (Toronto, ON, Canada) Quadrupole-TOF hybrid spectrometer. Gas chromatography/low resolution mass spectra were recorded on a Trace DSQ GCMS spectrometer, ThermoElectron Corporation (Austin, TX, USA). APCI was recorded on a Thermofinnigan LC-Q DECA mass spectrometer. Fermentations were run on Fermentation Design Inc. Model # MS21 (Allentown, PA, USA). The total capacity of the fermentation system is 15 L.

MATERIALS

All ^2H (D), ^{13}C , and ^{15}N materials were obtained from Cambridge Isotope Laboratories, Inc. Andover, MA 01810-5413. The $^{18}\text{O}_2$ was obtained from ICON Services Summit, NJ 07901. Dr. Vasudha Sharma and Dr. Chaomin Liu synthesized the ^{13}C derivatives.

ORGANISM

Streptomyces sahachiroi (NRRL 2485) was obtained from the American Type Culture Collection (ATCC).

CULTURE CONDITIONS

(THE AUTHOR)

Spore stocks: *Streptomyces sahachiroi* spores prepared from dehydrated GYM (glucose, yeast extract, and maltose extract) plates (per liter of medium: glucose monohydrate, 4 g; yeast extract, 4 g; malt extract, 10 g; CaCO_3 , 2 g; and tap water; adjusted to pH 6.8 with 1 M NaOH prior to sterilization) were streaked onto large MS (mannitol Soya flour, per liter medium: mannitol, 20 g; Soya flour, 20 g; and deionized water) plates and allowed to incubate at 30 °C for 15 days. At this time the grey spores were removed with sterile water and agitation. The spores were then

filtered through sterile cotton, washed three times with sterile water, centrifuged at 3000 rpm, re-suspended in a minimal amount of 10% glycerol solution, flash frozen, and stored at -80 °C.

i) *Solid medium*. Solid medium cultures were inoculated by streaking a loop full of *S. sahachiroi* spore stock onto prepared GYM plates. The plates were grown at 30 °C in a Fisher Scientific Isotemp incubator for 5-7 days before use in the first stage culture.

ii) *First Stage Culture*. *Streptomyces sahachiroi* (inoculated from dehydrated plates) was grown on GYM plates for 5-7 days. A 1 cm² piece of the GYM plate was used to inoculate 100 mL of PS5 media in a 250 mL Erlenmeyer flask. The culture was incubated at 30 °C for 24 h at 250 rpm.

ii) *Second Stage Culture*. The second stage culture was prepared by inoculating 2 L Erlenmeyer baffled flasks (Fernbach; containing 600 mL of PS5 medium) with 25 mL of the first stage culture. The culture was incubated at 30 °C for 24 h at 250 rpm.

iv) *Fermentation*. The fermenter containing 10 L of the reduced PS5 medium (Pharmamedia/Starch plus additives, per liter of medium: Pharmamedia (yellow cotton seed flour), 12.5 g; soluble starch, 12.5 and deionized water adjusted to pH 6.5 naturally prior to sterilization) reduced by 75% compared the concentration of the first and second stage cultures was autoclaved at 121 °C for 20 min. Following inoculation (with two 600 mL second stage cultures) the fermenter was agitated at ~300 rpm and aerated with sterile filtered air (8 L/min) for 72 h.

GENERAL FEEDING CONDITIONS

(THE AUTHOR)

The labeled material was weighed in equal portions and solubilized in autoclaved distilled water. The first aliquot was administered after 24 h, followed by addition of the second provided 24 h later. The culture was harvested 72 h post-induction (inoculation of the second stage culture into the fermenter). Note: Compound T4 and T5 were administered in D₂O immediately after synthesis. Supporting information in chapter V appendix provides details on the amounts of each compound fed.

ISOLATION AND PURIFICATION OF AZINOMYCIN B

(THE AUTHOR)

Following fermentation, the cultures were centrifuged at 7,000 rpm at 4 °C. The cell pellets were discarded and the medium extracted with an equal volume of methylene chloride (1X).

The organic layer was collected, dried over anhydrous magnesium sulfate, and concentrated *in vacuo*. The resulting crude extract was stored under diethyl ether at -80 °C. The solid was dissolved in a minimal amount of dichloromethane and precipitated with the addition of hexane to give a ratio of 1:29 CH₂Cl₂/hexane. The resulting suspension was centrifuged at 1,500 rpm and the supernatant discarded. Diethyl ether (2 mL) was added to the pellet, which was subsequently agitated, centrifuged at 3000 rpm and the supernatant discarded. The resulting residue was dissolved in dichloromethane (600 µL) to which hexanes (2 mL) was added. The heterogeneous mixture was centrifuged at 3,000 rpm and the supernatant retained. To the solution was added hexanes (4 mL) and the suspension centrifuged at 3,000 rpm to give azinomycin B as a solid.

If full purification is not achieved, azinomycin B can be further purified by flash column chromatography (95: 5 CH₂Cl₂: methanol). By TLC azinomycin exhibits an R_f of 0.23. A short column should be utilized to minimize overall contact with the silica gel and degradation by hydrolysis. The process can be repeated if necessary. The compound can be safely stored at -80 °C under anhydrous diethyl ether. For shorter periods of time it may be stored as a precipitant from a solution of 20:1 hexanes:chloroform/dichloromethane. The azinomycin B isolated matched the NMR spectrum provided by Yokoi *et al.* [17].

AZINOMYCIN A

Pale-white amorphous powder (1:9 CH₂Cl₂:hexane); IR (neat) ν_{\max} 3450.1, 3323.2, 3025.3, 2972.8, 1735.4(br), 1660.4, 1618.6, 1601.1, 1531.4, 1417.6 1242.3, 1090.7, 1043.6 cm⁻¹; ¹H NMR (300MHz, CDCl₃) δ 10.09(1H, dd, *J*=5.1, 5.1), 8.56 (1H, dd, *J*=5.9, 3.3Hz), 8.54 (1H, s), 7.93 (1H, d, *J*=2.6Hz), 7.48 (1H, d, *J*=2.6Hz), 7.35 (1H, dd, *J*=5.9, 5.9), 7.34 (1H, dd, *J*=5.9, 3.3), 5.53 (1H, d, *J*= 3.8Hz), 5.01 (1H, s), 4.62 (1H, dd, *J*= 5.4, 3.8Hz), 4.28 (1H, dd, *J*= 19.8, 5.1Hz), 3.98 (3H, s), 3.98 (1H, s), 3.23 (1H, m), 3.00 (1H, d, *J*=4.4Hz), 2.84 (1H, d, *J*= 4.4Hz), 2.67 (3H, s), 2.53 (1H, d, *J*= 5.1Hz), 2.21 (1H, d, *J*= 4.5Hz), 2.20 (1H, s), 2.19 (1H, s), 1.52 (1H, s); ¹³C NMR (75MHz, CDCl₃) δ 202.6, 172.7, 165.7, 163.8, 163.2, 156.0, 149.6, 134.4, 133.1, 128.4, 127.7, 126.9, 125.1, 123.9, 121.8, 120.1, 108.6, 84.0, 76.9*, 76.7*, 56.0, 55.6, 53.7, 50.6, 45.4, 35.8, 27.2, 20.7, 20.0, 17.0. (* obscured by CDCl₃ solvent peak). TOF-MS (APCI), *m/z* 596.22 (calcd for C₃₀H₃₃N₃O₁₀⁺ H: 596.22).

AZINOMYCIN B

Pale-white amorphous powder (1:9 CH₂Cl₂:hexane); IR (neat) ν_{\max} 3338.4(br), 2957.1, 2925.3, 2872.8, 1725.92(br), 1619.3, 1601.7, 1511.2, 1417.6 cm⁻¹; ¹H NMR (300MHz, CDCl₃) δ 12.40(1H, br), 12.32(1H, s), 8.54 (1H, dd, $J=3.6, 7.0$ Hz), 8.20 (1H, br), 7.94 (1H, d, $J=2.9$ Hz), 7.46 (1H, d, $J=2.9$ Hz), 7.32 (1H, s), 7.32 (1H, s), 7.32 (1H, s), 5.50 (1H, d, $J=4.0$ Hz), 5.12 (1H, s), 4.64 (1H, dd, $J=4.0, 4.8$ Hz), 3.96 (3H, s), 3.96 (1H, br), 3.36 (1H, m), 2.98 (1H, d, $J=4.3$ Hz), 2.80 (1H, d, $J=4.3$ Hz), 2.70 (1H, s), 2.66 (3H, s), 2.30 (1H,s), 2.24 (1H, s), 2.18 (1H, s), 1.52 (1H, s); ¹³C NMR (75MHz, 125MHz, CDCl₃) δ 191.5, 173.0, 165.7, 164.0, 162.0, 156.0, 153.0, 150.8, 134.5, 133.3, 128.1, 127.9, 127.0, 125.4, 123.9, 122.3, 119.3, 118.6, 108.5, 84.4, 77.4*, 77.1*, 56.2, 55.7, 53.9, 46.4, 36.7, 24.5, 21.0, 20.3, 17.2. (* obscured by CDCl₃ solvent peak). ¹³C NMR (125MHz, CD₂Cl₂) δ 191.3, 172.8, 165.8, 164.3, 162.2, 156.2, 154.1, 150.6, 134.6, 133.7, 128.4, 127.9, 126.9, 125.3, 123.8, 122.3, 191.3, 118.6, 108.4, 84.5, 76.9, 77.0, 56.1, 55.8, 53.8, 46.9, 36.9, 24.4, 20.9, 20.1, 17.1. APCI-MS (LRMS) 624.2, found 624.2.

CHAPTER VI

CONCLUSION

Tremendous advances have occurred in the field of natural products in the last century. It has developed from rare medicines to industrially produced pharmaceuticals. The study of metabolism and biosynthesis has led to the discovery of exotic pathways that produce amazingly bioactive compounds. Currently the power of genomic sequencing, cell-based screens, and gene overexpression have enabled discovery of rare or silent natural product pathways from even uncultivable natural sources. It is in this realm that the azinomycins live.

The unique aziridinopyrrolidine ring and the DNA cross-linking activity of the azinomycins have long been of synthetic, medicinal, and biosynthetic interest. Given the advances in gene sequencing and gene manipulation, it is only a matter of time before systems amenable to modular swaps for mixed PKS/NRPS and other biosynthetic systems are developed and used industrially to produce custom pharmaceuticals or other byproducts. The development of such systems has resulted in a keen interest in the biosynthesis of natural products with unique spatial or chemical structures.

The path towards understanding the azinomycins has been a long one reflecting the trends of the times. The isolation of the azinomycins and the producing bacteria were a product of an expansive concerted effort of microorganism screening and natural product isolation. Additionally the first clinical uses of azinomycins reflected the needs of the times in Japan. The anti-tumor property of the azinomycins was investigated on real patients with real cancers. Although the toxic effects of the natural product were revealed, interest in its potential has remained, inspiring many to move forward again by focusing on structural characterization of the molecule and then efforts towards total synthesis and exploration of the structure-activity relationships of derivatives of azinomycin. Although this work culminated with the total synthesis of azinomycin A [190], the efforts in this have been significantly explored [20-25, 27, 28, 68, 70, 113, 191-213]. Synthetic efforts yielded many variations upon the azinomycin structure. The mode of action of the azinomycins was explored *in vitro* using many of these derivatives [28, 29, 69, 70, 112, 193, 214-219]. The mode of action of the azinomycins has been explored increasingly *in silico* (performed on computer or via computer simulation) [74, 76]. Our *in vivo* mode of action studies with yeast supported the suspected DNA damaging and cross-

linking action of the azinomycins [135] using transcriptional array profiling, flow cytometry, microscopy, and nucleic acid isolation. The use of state of the art methods has provided a greater understanding of this unique set of natural products.

As the interest in this natural product has moved into the genetic and molecular origins of azinomycin biosynthesis, both traditional and state of the art methods were implemented. The first studies on the biosynthesis of the azinomycins used a traditional method of feeding isotopically enriched isotopes [109, 220]. Our cell free extract system revealed specific cofactors and substrates involved in the biosynthesis as well as inhibitors capable of disrupting the biosynthesis [146]. Using traditional methods of culture and production improvement, a consistent system for the production of azinomycin B was established [133]. This system was subsequently used to explore multiple possible stable isotope substrates for azinomycin biosynthesis. The origin of the naphthoate portion, the epoxide fragment, the enol fragment, and the origins of the oxygen atoms in azinomycin B were revealed. Additionally the origin of the end fragment of azinomycin A and a means to modulate the ratio of azinomycin A: azinomycin B was revealed. Significant work has been done to examine the origin of the aziridinopyrrolidine fragment; results indicate this highly modified alkaloid-type amino acid was derived from a glutamate-related molecule and additional two carbon subunits, possibly sugar derived. The results of heavy oxygen incorporation in the aziridinopyrrolidine ring indicate that modifications are made before the incorporation of an intact pyrrolidine amino acid subunit into the azinomycin molecule.

While we have pursued biosynthetic studies of the azinomycins, we and others have also pursued the genetic basis for azinomycin biosynthesis. The identification and sequencing of the azinomycin biosynthetic gene cluster was a challenging goal. Our approach initially was based upon state of the art approach at the time: production of a genomic library and screening with degenerate probes. This approach was problematic as production of *Streptomyces sahachiroi* genomic libraries in a bacterial artificial chromosome (BAC, 100-250 kilo bases), cosmid (COS, 30-50 kilo bases), or fosmid (FOS, 30-50 kilo bases) all have size restrictions and construction biases. The potential size of the azinomycin biosynthetic gene cluster could be near the maximum capacity of cloning vectors. The result is a series of statistical problems involving an array of potential clones that must be overcome to obtain the full sequence. My involvement in this portion of the project was limited and ultimately ended as the entire project scope grew. As efforts towards isolating the cluster and important genes within proceeded, advances in state of the art cluster isolation, cluster analysis, and DNA sequencing evolved the approach to these

problems. Significant improvement in DNA probe specificity for a particular biosynthetic gene type was possible after analysis and integration of increasingly available sequence information from the analysis of other natural products. Additionally, the analysis of the genomic DNA of more *Streptomyces* species has improved the field of gene analysis. As analysis of the in-house genomic libraries from *Streptomyces sahachiroi* went forward, we also prepared to explore genomic sequencing for this microorganism. The advances in genomic sequences, particularly for sequencing organisms with high GC content genomic DNA, have enabled whole organism sequencing to be an economically viable and scientifically desirable goal. With complex biosynthetic construction, determining the outer limits of the gene cluster is difficult. Having the organism's entire sequence eliminates problems associated with loss of genes on the periphery of gene clusters.

During the process of our sequencing efforts (and the preparation of this dissertation), an article by Zhao, *et al.* appeared revealing the putative azinomycin biosynthetic cluster [176]. The authors report the sequence and a cursory analysis of the genes with a proposed biosynthesis based on the analyzed sequence similarity to publicly available genes. The authors identified the cluster by designing targeted PCR primers for a type I iterative PKS, much like the previously identified type I iterative PKS discussed in the introduction of this work (**Figure 18 & Figure 20A**). Zhao, *et al.* primarily examined a knock-out and heterologous expression of the PKS gene to prove its role in azinomycin production and as a proof for the identification of the correct biosynthetic cluster. While initial inspection of the gene cluster reveals a number of genes whose role could be linked to azinomycin biosynthesis, their experiments warrant some concern related to their transformations or conjugation procedure. Putative genetic knockouts were compared to the wild-type strain and not to the wild-type strain housing an empty vector. In the Watanabe lab's hands, including the author's own hands, protoplasting procedures that have enabled transformation with empty vectors have also abolished production of azinomycin B. Moreover, a postdoctoral fellow in our lab who is well-versed with *Streptomyces* conjugation procedures has not yet been able to successfully repeat their conjugation procedure, while has been able to successfully transform other *Streptomyces* strains including another azabicyclic producing microorganism, *Streptomyces ficellus*. To ensure the proper localization of the pathway and/or that the pathway does not act in trans, the Watanabe lab is in the process of sequencing the genome of *S. sahachiroi*.

Zhao, *et al.*'s proposed biosynthesis falls short of truly revealing the exact biosynthetic construction of the azinomycins. The reported gene cluster misses key elements and is

incongruent with our empirical feeding experiment results. Zhao, *et al.* contends that α -ketoisovaleric acid is the substrate incorporated for the formation of the epoxide moiety. Zhao's findings partially corroborate our discovery of the modification of valine, but our results show the most advanced putative precursor shown to be processed by the azinomycin biosynthetic machinery was 3-methyl-2-oxobutenoic acid. Additionally, Zhao's characterization of the origin of the hydroxyl groups of the aziridinopyrrolidine ring is inconsistent with our molecular oxygen feeding results as they propose the C12 hydroxyl arises from the reduced end portion of a glutamate derivative. The enol moiety which we showed was derived from whole incorporation of L-threonine is theorized by Zhao, *et al.* to be modified, as our results indicated, post incorporation by an "acyl-CoA dehydrogenase." Interestingly Zhao, *et al.* also attribute to a similar "acyl-CoA dehydrogenase" the modification of the epoxide unit to a double bond before introduction of the oxygen of the epoxide. Zhao, *et al.* then suggest that decarboxylation at the C3 position by an unidentified enzyme could lead to azinomycin A, whereas our results suggest a direct competition between aminoacetone and L-threonine for incorporation into the end unit of the azinomycins yielding azinomycin A and B, respectively. While our results cannot completely eliminate modifications of azinomycin B to yield azinomycin A (with the incorporation of [U-¹³C] L-threonine into azinomycin A) the direct incorporation of aminoacetone clearly supports an incorporation competition model.

As discussed earlier, there are definite limitations to whole cell feeding studies. One is limited in determination of the exact mechanism for biosynthesis. Analysis, combined with knowledge of previously reported systems, may yield a strong case for the biosynthetic construction and the employed mechanisms. The complete characterization of the construction of the unique moieties of the azinomycins will require full and thorough sequence analysis in combination with enzymatic reconstitution. This work is an ongoing endeavor in the laboratory of Dr. Coran M. H. Watanabe. While we have no doubt made some inroads to understanding the mode of action and biosynthesis of the azinomycins, much remains to be done and discovered.

The potential knowledge and insight gained from understanding the mode of action and biosynthetic construction of the azinomycins could be of great significance. This unique natural product with PKS, NRPS, and alkaloid construction may serve as a model hybrid system. Future analysis of the construction of each moiety of the azinomycins could yield understanding of the nature of modular construction and its amenability toward modification for use in novel hybrid natural product biosynthesis. The promise of modular construction of natural products is that one would be able to specifically construct custom and novel natural products. Such hybrid natural

products, produced by rational or combinatorial methods, may help address the growing problem of antibiotic resistant microorganisms or the need for other pharmaceuticals. The greater understanding of natural product construction, the closer we are to advancing the ancient tradition of beneficial use of natural products. The research and results discussed in this dissertation aim to enhance our understanding and to help achieve this goal.

REFERENCES

1. Hata, T., Koga, F., Sano, Y., Kanamori, K., Matsumae, A., Sugawara, R., Hoshi, T., Shima, T., Ito, S., and Tomizawa, S. (1954). Carzinophilin, a new tumor inhibitory substance produced by *Streptomyces*. I. J. Antibiot. 7, 107-112.
2. Nagaoka, K., Matsumoto, M., Oono, J., Yokoi, K., Ishizeki, S., and Nakashima, T. (1986). Azinomycins A and B, new antitumor antibiotics. I. Producing organism, fermentation, isolation, and characterization. J. Antibiot. 39, 1527-1532.
3. Shimada, N., Uekusa, M., Denda, T., Ishii, Y., Iizuka, T., Sato, Y., Hatori, T., Fukui, M., and Sudo, M. (1955). Clinical studies of carzinophilin, an antitumor substance. J. Antibiot. 8, 67-76.
4. Hopwood, D.A. (2007). *Streptomyces* in Nature and Medicine: The Antibiotic Makers (New York: Oxford University Press).
5. Newman, D.J., and Cragg, G.M. (2007). Natural products as sources of new drugs over the last 25 years. J. Nat. Prod. 70, 461-477.
6. Kristiansen, J.E., Hendricks, O., Delvin, T., Butterworth, T.S., Aagaard, L., Christensen, J.B., Flores, V.C., and Keyzer, H. (2007). Reversal of resistance in microorganisms by help of non-antibiotics. J. Antimicrob. Chemother. 59, 1271-1279.
7. Kamada, H., Wakaki, S., Fujimoto, Y., Tomioka, K., Ueyama, S., Marumo, H., and Uzu, K. (1955). Studies on carzinophilin. I. The properties of carzinophilin A. J. Antibiot. 8, 187-188.
8. Kuroyanagi, S., Miyajima, S., Hirota, M., and Yamana, T. (1956). Effect of carzinophilin on malignant tumors. Gan 47, 359-360.
9. Ishii, T., Sato, Y., Hatori, T., Fukui, T., Kubouchi, K., Noguchi, T., Sukigara, K., and Takeishi, T. (1956). The clinical and histological studies on the cases treated by carzinophilin. Gan 47, 360-363.
10. Tanaka, M., Kishi, T., and Maruta, Y. (1959). Carzinophilin. I. The structure of methanolysis product. J. Antibiot. 13, 361-364.
11. Tanaka, M., Kishi, T., and Maruta, Y. (1960). Carzinophilin. II. The structure of methanolysis product. II. J. Antibiot. 13, 177-181.
12. Onda, M., Konda, Y., Noguchi, A., Omura, S., and Hata, T. (1969). Revised structure for the naphthalencarboxylic acid from carzinophilin. J. Antibiot. 22, 42-44.

13. Lown, J.W., and Hanstock, C.C. (1982). Structure and function of the antitumor antibiotic carzinophilin A: The first natural intercalative bisalkylator. *J. Am. Chem. Soc.* *104*, 3213-3214.
14. Lown, J.W., and Majumdar, K.C. (1977). Studies related to antitumor antibiotics. Part IX. Reactions of carzinophilin with DNA assayed by ethidium fluorescence. *Can. J. Biochem.* *55*, 630-635.
15. Onda, M., Konda, Y., Hatano, A., Hata, T., and Omura, S. (1983). Structure of carzinophilin. 3. Structure elucidation by nuclear magnetic-resonance spectroscopy .1. *J. Am. Chem. Soc.* *105*, 6311-6312.
16. Onda, M., Konda, Y., Hatano, A., Hata, T., and Omura, S. (1984). Structure of carzinophilin. IV. Structure elucidation by nuclear magnetic resonance spectroscopy. (2). *Chem. Pharm. Bull.* *32*, 2995-3002.
17. Yokoi, K., Nagaoka, K., and Nakashima, T. (1986). Azinomycins A and B, new antitumor antibiotics. II. Chemical structures. *Chem. Pharm. Bull.* *34*, 4554-4561.
18. Coleman, R.S., Li, J., and Navarro, A. (2001). Total Synthesis of Azinomycin A. *Angew. Chem. Int. Ed. Engl.* *40*, 1736-1739.
19. Ando, K., Yamada, T., and Shibuya, M. (1989). Synthetic approach toward azinomycins. *Heterocycles* *29*, 2209-2218.
20. Coleman, R.S., and Carpenter, A.J. (1992). Synthesis of the aziridino[1,2-a]pyrrolidine substructure of the antitumor agents azinomycin A and azinomycin B. *J. Org. Chem.* *57*, 5813-5815.
21. Armstrong, R.W., Tellew, J.E., and Moran, E.J. (1992). Stereoselective synthesis of (E) and (Z)-1-azabicyclo[3.1.0]hex-2-ylidene dehydroamino acid-derivatives. *J. Org. Chem.* *57*, 2208-2211.
22. Moran, E.J., Tellew, J.E., Zhao, Z.C., and Armstrong, R.W. (1993). Dehydroamino acid-derivatives from D-arabinose and L-serine - synthesis of models for the azinomycin antitumor antibiotics. *J. Org. Chem.* *58*, 7848-7859.
23. Coleman, R.S., Sarko, C.R., and Gittinger, J.P. (1997). Efficient stereoselective synthesis of the epoxyacid fragment of the azinomycins. *Tetrahedron Lett.* *38*, 5917-5920.
24. Coleman, R.S., Richardson, T.E., and Carpenter, A.J. (1998). Synthesis of the azabicyclic core of the azinomycins: Introduction of differentiated trans-diol by crotylstannane addition to serinal. *J. Org. Chem.* *63*, 5738-5739.

25. Coleman, R.S., Kong, J.S., and Richardson, T.E. (1999). Synthesis of naturally occurring antitumor agents: Stereocontrolled synthesis of the azabicyclic ring system of the azinomycins. *J. Am. Chem. Soc.* *121*, 9088-9095.
26. Hartley, J.A., Hazrati, A., Kelland, L.R., Khanim, R., Shipman, M., Suzenet, F., and Walker, L.F. (2000). A synthetic azinomycin analogue with demonstrated DNA cross-linking activity: Insights into the mechanism of action of this class of antitumor agent. *Angew. Chem. Int. Ed. Engl.* *39*, 3467-3470.
27. Hodgkinson, T.J., Kelland, L.R., Shipman, M., and Suzenet, F. (2000). Chemical synthesis and cytotoxicity of some azinomycin analogues devoid of the 1-azabicyclo[3.1.0]hexane subunit. *Bioorg. Med. Chem. Lett.* *10*, 239-241.
28. Hartley, J.A., Hazrati, A., Hodgkinson, T.J., Kelland, L.R., Khanim, R., Shipman, M., and Suzenet, F. (2000). Synthesis, cytotoxicity and DNA cross-linking activity of symmetrical dimers based upon the epoxide domain of the azinomycins. *Phys. Chem. Chem. Phys.* *2*, 2325-2326.
29. Hodgkinson, T.J., and Shipman, M. (2001). Chemical synthesis and mode of action of the azinomycins. *Tetrahedron* *57*, 4467-4488.
30. Corre, C., and Lowden, P.A. (2004). The first biosynthetic studies of the azinomycins: Acetate incorporation into azinomycin B. *Chem. Commun.*, 990-991.
31. Corre, C., Landreau, C.A., Shipman, M., and Lowden, P.A. (2004). Biosynthetic studies on the azinomycins: The pathway to the naphthoate fragment. *Chem. Commun.*, 2600-2601.
32. Bentley, S.D., Chater, K.F., Cerdeno-Tarraga, A.M., Challis, G.L., Thomson, N.R., James, K.D., Harris, D.E., Quail, M.A., Kieser, H., Harper, D., *et al.* (2002). Complete genome sequence of the model actinomycete *Streptomyces coelicolor* A3(2). *Nature* *417*, 141-147.
33. Ikeda, H., Ishikawa, J., Hanamoto, A., Shinose, M., Kikuchi, H., Shiba, T., Sakaki, Y., Hattori, M., and Omura, S. (2003). Complete genome sequence and comparative analysis of the industrial microorganism *Streptomyces avermitilis*. *Nat. Biotechnol.* *21*, 526-531.
34. Ohnishi, Y., Ishikawa, J., Hara, H., Suzuki, H., Ikenoya, M., Ikeda, H., Yamashita, A., Hattori, M., and Horinouchi, S. (2008). Genome sequence of the streptomycin-producing microorganism *Streptomyces griseus* IFO 13350. *J. Bacteriol.* *190*, 4050-4060.
35. Dewick, P.M. (2002). *Medicinal Natural Products: A Biosynthetic Approach*, 2nd Edition (New York: Wiley).

36. Brobst, S.W., and Townsend, C.A. (1994). The potential role of fatty-acid initiation in the biosynthesis of the fungal aromatic polyketide aflatoxin B-1. *Can. J. Chem.* *72*, 200-207.
37. Silva, J.C., Minto, R.E., Barry, C.E., Holland, K.A., and Townsend, C.A. (1996). Isolation and characterization of the versicolorin B synthase gene from *Aspergillus parasiticus* - Expansion of the aflatoxin B-1 biosynthetic gene cluster. *J. Biol. Chem.* *271*, 13600-13608.
38. Watanabe, C.M.H., Wilson, D., Linz, J.E., and Townsend, C.A. (1996). Demonstration of the catalytic roles and evidence for the physical association of type I fatty acid synthases and a polyketide synthase in the biosynthesis of aflatoxin B-1. *Chem. Biol.* *3*, 463-469.
39. Minto, R.E., and Townsend, C.A. (1997). Enzymology and molecular biology of aflatoxin biosynthesis. *Chem. Rev.* *97*, 2537-2555.
40. Yu, J.J., Chang, P.K., Ehrlich, K.C., Cary, J.W., Bhatnagar, D., Cleveland, T.E., Payne, G.A., Linz, J.E., Woloshuk, C.P., and Bennett, J.W. (2004). Clustered pathway genes in aflatoxin biosynthesis. *Appl. Environ. Microbiol.* *70*, 1253-1262.
41. Crawford, J.M., Dancy, B.C.R., Hill, E.A., Udworthy, D.W., and Townsend, C.A. (2006). Identification of a starter unit acyl-carrier protein transacylase domain in an iterative type I polyketide synthase. *Proc. Natl. Acad. Sci. U S A* *103*, 16728-16733.
42. Gay, G.R., Inaba, D.S., Sheppard, C.W., and Newmeyer, J.A. (1975). Cocaine: History, epidemiology, human pharmacology and treatment. A perspective on a new debut for an old girl. *Clinical Toxicology* *8*, 149-178.
43. Williams, D.H., and Bardsley, B. (1999). The vancomycin group of antibiotics and the fight against resistant bacteria. *Angew. Chem. Int. Ed.* *38*, 1173-1193.
44. Levine, D.P. (2006). Vancomycin: A history. *Clin. Infect. Dis.* *42 Suppl 1*, S5-12.
45. Wani, M.C., Taylor, H.L., Wall, M.E., Coggon, P., and McPhail, A.T. (1971). Plant antitumor agents. VI. The isolation and structure of taxol, a novel antileukemic and antitumor agent from *Taxus brevifolia*. *J. Am. Chem. Soc.* *93*, 2325-2327.
46. He, J., Magarvey, N., Pirae, M., and Vining, L.C. (2001). The gene cluster for chloramphenicol biosynthesis in *Streptomyces venezuelae* ISP5230 includes novel shikimate pathway homologues and a monomodular non-ribosomal peptide synthetase gene. *Microbiology* *147*, 2817-2829.

47. Kuzuyama, T. (2002). Mevalonate and nonmevalonate pathways for the biosynthesis of isoprene units. *Biosci., Biotechnol., Biochem.* *66*, 1619-1627.
48. Durr, C., Schnell, H.J., Luzhetskyy, A., Murillo, R., Weber, M., Welzel, K., Vente, A., and Bechthold, A. (2006). Biosynthesis of the terpene phenalinolactone in *Streptomyces* sp. Tu6071: Analysis of the gene cluster and generation of derivatives. *Chem. Biol.* *13*, 365-377.
49. Humphrey, A.J., and O'Hagan, D. (2001). Tropane alkaloid biosynthesis. A century old problem unresolved. *Nat. Prod. Rep.* *18*, 494-502.
50. Hu, Y., Phelan, V., Ntai, I., Farnet, C.M., Zazopoulos, E., and Bachmann, B.O. (2007). Benzodiazepine biosynthesis in *Streptomyces refuineus*. *Chem. Biol.* *14*, 691-701.
51. Fischbach, M.A., and Walsh, C.T. (2006). Assembly-line enzymology for polyketide and nonribosomal peptide antibiotics: Logic, machinery, and mechanisms. *Chem. Rev.* *106*, 3468-3496.
52. Bruheim, P., Borgos, S.E.F., Tsan, P., Sletta, H., Ellingsen, T.E., Lancelin, J.M., and Zotchev, S.B. (2004). Chemical diversity of polyene macrolides produced by *Streptomyces noursei* ATCC 11455 and recombinant strain ERD44 with genetically altered polyketide synthase NysC. *Antimicrob. Agents Chemother.* *48*, 4120-4129.
53. Khosla, C., Tang, Y., Chen, A.Y., Schnarr, N.A., and Cane, D.E. (2007). Structure and mechanism of the 6-deoxyerythronolide B synthase. *Annu. Rev. Biochem.* *76*, 195-221.
54. Hopwood, D.A. (1999). Forty years of genetics with *Streptomyces*: From *in vivo* through *in vitro* to *in silico*. *Microbiology* *145*, 2183-2202.
55. Watanabe, K., Praseuth, A.P., and Wang, C.C.C. (2007). A comprehensive and engaging overview of the type III family of polyketide synthases. *Curr. Opin. Chem. Biol.* *11*, 279-286.
56. Bedford, D.J., Schweizer, E., Hopwood, D.A., and Khosla, C. (1995). Expression of a functional fungal polyketide synthase in the bacterium *Streptomyces coelicolor* A3(2). *J. Bacteriol.* *177*, 4544-4548.
57. Sthapit, B., Oh, T.J., Lamichhane, R., Liou, K., Lee, H.C., Kim, C.G., and Sohng, J.K. (2004). Neocarzinostatin naphthoate synthase: An unique iterative type I PKS from neocarzinostatin producer *Streptomyces carzinostaticus*. *FEBS Lett.* *566*, 201-206.
58. Liu, W., Nonaka, K., Nie, L.P., Zhang, J., Christenson, S.D., Bae, J., Van Lanen, S.G., Zazopoulos, E., Farnet, C.M., Yang, C.F., *et al.* (2005). The neocarzinostatin

- biosynthetic gene cluster from *Streptomyces carzinostaticus* ATCC 15944 involving two iterative type I polyketide synthases. *Chem. Biol.* *12*, 293-302.
59. Shao, L., Qu, X.D., Jia, X.Y., Zhao, Q.F., Tian, Z.H., Wang, M., Tang, G.L., and Liu, W. (2006). Cloning and characterization of a bacterial iterative type I polyketide synthase gene encoding the 6-methylsalicylic acid synthase. *Biochem. Biophys. Res. Commun.* *345*, 133-139.
 60. Beck, J., Ripka, S., Siegner, A., Schiltz, E., and Schweizer, E. (1990). The multifunctional 6-methylsalicylic acid synthase gene of *Penicillium patulum*: Its gene structure relative to that of other polyketide synthases. *Eur. J. Biochem.* *192*, 487-498.
 61. Dimroth, P., Walter, H., and Lynen, F. (1970). Biosynthesis of 6-methylsalicylic acid. *Eur. J. Biochem.* *13*, 98.
 62. Shen, Q.T., Chen, X.L., Sun, C.Y., and Zhang, Y.Z. (2004). Dissecting and exploiting nonribosomal peptide synthetases. *Acta. Biochim. Biophys. Sin.* *36*, 243-249.
 63. Kim, H.B., Smith, C.P., Micklefield, J., and Mavituna, F. (2004). Metabolic flux analysis for calcium dependent antibiotic (CDA) production in *Streptomyces coelicolor*. *Metab. Eng.* *6*, 313-325.
 64. Hojati, Z., Milne, C., Harvey, B., Gordon, L., Borg, M., Flett, F., Wilkinson, B., Sidebottom, P.J., Rudd, B.A.M., Hayes, M.A., *et al.* (2002). Structure, biosynthetic origin, and engineered biosynthesis of calcium-dependent antibiotics from *Streptomyces coelicolor*. *Chem. Biol.* *9*, 1175-1187.
 65. Shen, B., Chen, M., Cheng, Y., Du, L., Edwards, D.J., George, N.P., Huang, Y., Oh, T., Sanchez, C., Tang, G., *et al.* (2005). Prerequisites for combinatorial biosynthesis: Evolution of hybrid NRPS/PKS gene clusters. *Biocombinatorial Approaches for Drug Finding*, B. Shen, ed. (Springer, Berlin), pp. 107-126.
 66. Pritchard, D.I. (2005). Sourcing a chemical succession for cyclosporin from parasites and human pathogens. *Drug Discov. Today* *10*, 688-691.
 67. Gates, K.S. (1999). Covalent modification of DNA by natural products. *Comprehensive Natural Products Chemistry*, Volume 7, Barton, D. Nakanishi, K., Meth-Cohn, O. Eds. (Oxford: Pergamon Press), pp. 491-552.
 68. Coleman, R.S. (2004). Total Synthesis of the Azinomycin Family of Antitumor Agents. *Strategies and Tactics in Organic Synthesis*, Volume 5, M. Harmata, ed. (London:Elsevier Science), pp. 55-81.

69. Coleman, R.S., Perez, R.J., Burk, C.H., and Navarro, A. (2002). Studies on the mechanism of action of azinomycin B: definition of regioselectivity and sequence selectivity of DNA cross-link formation and clarification of the role of the naphthoate. *J. Am. Chem. Soc.* *124*, 13008-13017.
70. LePla, R.C., Landreau, C.A.S., Shipman, M., Hartley, J.A., and Jones, G.D.D. (2005). Azinomycin inspired bisepoxides: Influence of linker structure on in vitro cytotoxicity and DNA interstrand cross-linking. *Bioorg. Med. Chem. Lett.* *15*, 2861-2864.
71. Armstrong, R.W., Salvati, M.E., and Nguyen, M. (1992). Novel interstrand cross-links induced by the antitumor antibiotic carzinophilin azinomycin B. *J. Am. Chem. Soc.* *114*, 3144-3145.
72. Zang, H., and Gates, K.S. (2000). DNA binding and alkylation by the "left half" of azinomycin B. *Biochemistry* *39*, 14968-14975.
73. Fujiwara, T., Saito, I., and Sugiyama, H. (1999). Highly efficient DNA interstrand crosslinking induced by an antitumor antibiotic, carzinophilin. *Tetrahedron Lett.* *40*, 315-318.
74. Alcaro, S., Ortuso, F., and Coleman, R.S. (2002). DNA cross-linking by azinomycin B: Monte Carlo simulations in the evaluation of sequence selectivity. *J. Med. Chem.* *45*, 861-870.
75. Kwon, Y., Xi, Z., Kappen, L.S., Goldberg, I.H., and Gao, X. (2003). New complex of post-activated neocarzinostatin chromophore with DNA: Bulge DNA binding from the minor groove. *Biochemistry* *42*, 1186-1198.
76. Alcaro, S., and Coleman, R.S. (2000). A molecular model for DNA cross-linking by the antitumor agent azinomycin B. *J. Med. Chem.* *43*, 2783-2788.
77. Ishizeki, S., Ohtsuka, M., Irinoda, K., Kukita, K., Nagaoka, K., and Nakashima, T. (1987). Azinomycins A and B, new antitumor antibiotics. III. Antitumor activity. *J. Antibiot.* *40*, 60-65.
78. Watanabe, C.M.H., Supekova, L., and Schultz, P.G. (2002). Transcriptional effects of the potent enediyne anti-cancer agent calicheamicin γ_1^1 . *Chem. Biol.* *9*, 245-251.
79. Wilson, R.M., and Danishefsky, S.J. (2007). Applications of total synthesis toward the discovery of clinically useful anticancer agents. *Chem. Soc. Rev.* *36*, 1207-1226.
80. Lundin, C., North, M., Erixon, K., Walters, K., Jenssen, D., Goldman, A.S.H., and Helleday, T. (2005). Methyl methanesulfonate (MMS) produces heat-labile DNA

- damage but no detectable in vivo DNA double-strand breaks. *Nucleic Acids Res.* *33*, 3799-3811.
81. Roeder, G.S., and Fink, G.R. (1982). Movement of yeast transposable elements by gene conversion. *Proc. Natl. Acad. Sci. U S A* *79*, 5621-5625.
 82. Jordan, I.K., and McDonald, J.F. (1999). Comparative genomics and evolutionary dynamics of *Saccharomyces cerevisiae* Ty elements. *Genetica* *107*, 3-13.
 83. Scholes, D.T., Kenny, A.E., Gamache, E.R., Mou, Z.M., and Curcio, M.J. (2003). Activation of a LTR-retrotransposon by telomere erosion. *Proc. Natl. Acad. Sci. U S A* *100*, 15736-15741.
 84. Lemoine, F.J., Degtyareva, N.P., Lobachev, K., and Petes, T.D. (2005). Chromosomal translocations in yeast induced by low levels of DNA polymerase: A model for chromosome fragile sites. *Cell* *120*, 587-598.
 85. Zhao, X.L., and Rothstein, R. (2002). The Dun1 checkpoint kinase phosphorylates and regulates the ribonucleotide reductase inhibitor SmI1. *Proc. Natl. Acad. Sci. U S A* *99*, 3746-3751.
 86. Utsugi, T., Hirata, A., Sekiguchi, Y., Sasaki, T., Toh-e, A., and Kikuchi, Y. (1999). Yeast *tom1* mutant exhibits pleiotropic defects in nuclear division, maintenance of nuclear structure and nucleocytoplasmic transport at high temperatures. *Gene* *234*, 285-295.
 87. Laney, J.D., and Hochstrasser, M. (2004). Ubiquitin-dependent control of development in *Saccharomyces cerevisiae*. *Current Opin. Microbiol.* *7*, 647-654.
 88. Wang, Y.Q., and Dohlman, H.G. (2004). Pheromone signaling mechanisms in yeast: A prototypical sex machine. *Science* *306*, 1508-1509.
 89. Singh, A., Chen, E.Y., Lugovoy, J.M., Chang, C.N., Hitzeman, R.A., and Seeburg, P.H. (1983). *Saccharomyces cerevisiae* contains 2 discrete genes-coding for the alpha-factor pheromone. *Nucleic Acids Res.* *11*, 4049-4063.
 90. Kurjan, J., and Herskowitz, I. (1982). Structure of a yeast pheromone gene (Mf-Alpha) - a putative alpha-factor precursor contains 4 tandem copies of mature alpha-factor. *Cell* *30*, 933-943.
 91. Horak, C.E., Luscombe, N.M., Qian, J.A., Bertone, P., Piccirillo, S., Gerstein, M., and Snyder, M. (2002). Complex transcriptional circuitry at the G1/S transition in *Saccharomyces cerevisiae*. *Genes Dev.* *16*, 3017-3033.

92. Sundin, B.A., Chiu, C.H., Riffle, M., Davis, T.N., and Muller, E.G.D. (2004). Localization of proteins that are coordinately expressed with Cln2 during the cell cycle. *Yeast* 21, 793-800.
93. Koch, C., Schleiffer, A., Ammerer, G., and Nasmyth, K. (1996). Switching transcription on and off during the yeast cell cycle: Cln/Cdc28 kinases activate bound transcription factor SBF (Swi4/Swi6) at Start, whereas Clb/Cdc28 kinases displace it from the promoter in G(2). *Genes Dev.* 10, 129-141.
94. Basrai, M.A., Velculescu, V.E., Kinzler, K.W., and Hieter, P. (1999). NORF5/HUG1 is a component of the MEC1-mediated checkpoint response to DNA damage and replication arrest in *Saccharomyces cerevisiae*. *Mol. Cell. Biol.* 19, 7041-7049.
95. Aylon, Y., and Kupiec, M. (2004). New insights into the mechanism of homologous recombination in yeast. *Mutat. Res. Rev. Mutat. Res.* 566, 231-248.
96. Saffran, W.A., Ahmed, S., Bellevue, S., Pereira, G., Patrick, T., Sanchez, W., Thomas, S., Alberti, M., and Hearst, J.E. (2004). DNA repair defects channel interstrand DNA cross-links into alternate recombinational and error-prone repair pathways. *J. Biol. Chem.* 279, 36462-36469.
97. Tong, A.H.Y., Lesage, G., Bader, G.D., Ding, H.M., Xu, H., Xin, X.F., Young, J., Berriz, G.F., Brost, R.L., Chang, M., *et al.* (2004). Global mapping of the yeast genetic interaction network. *Science* 303, 808-813.
98. Bhattacharyya, S., and Lahue, R.S. (2004). *Saccharomyces cerevisiae* Srs2 DNA helicase selectively blocks expansions of trinucleotide repeats. *Mol. Cell. Biol.* 24, 7324-7330.
99. Van Komen, S., Reddy, M.S., Krejci, L., Klein, H., and Sung, P. (2003). ATPase and DNA helicase activities of the *Saccharomyces cerevisiae* anti-recombinase Srs2. *J. Biol. Chem.* 278, 44331-44337.
100. Qin, J., and Li, L. (2003). Molecular anatomy of the DNA damage and replication checkpoints. *Radiat. Res.* 159, 139-148.
101. Tye, B.K. (1999). MCM proteins in DNA replication. *Annu. Rev. Biochem.* 68, 649-686.
102. Domkin, V., Thelander, L., and Chabes, A. (2002). Yeast DNA damage-inducible Rnr3 has a very low catalytic activity strongly stimulated after the formation of a cross-talking Rnr1/Rnr3 complex. *J. Biol. Chem.* 277, 18574-18578.

103. van der Kuyl, A.C., van den Burg, R., Zorgdrager, F., Dekker, J.T., Maas, J., van Noesel, C.J., Goudsmit, J., and Cornelissen, M. (2002). Primary effect of chemotherapy on the transcription profile of AIDS-related Kaposi's sarcoma. *BMC Can.* 2, 21.
104. Roth, B.L., Poot, M., Yue, S.T., and Millard, P.J. (1997). Bacterial viability and antibiotic susceptibility testing with SYTOX Green nucleic acid stain. *Appl. Environ. Microbiol.* 63, 2421-2431.
105. Gaforio, J.J., Serrano, M.J., Ortega, E., Algarra, I., and de Cienfuegos, G.A. (2002). Use of SYTOX green dye in the flow cytometric analysis of bacterial phagocytosis. *Cytometry* 48, 93-96.
106. Yellman, C.M., and Burke, D.J. (2004). Assaying the spindle checkpoint in the budding yeast *Saccharomyces cerevisiae*. *Methods Mol. Biol.* 280, 275-290.
107. Watanabe, C.M.H., Wolfram, S., Ader, P., Rimbach, G., Packer, L., Maguire, J.J., Schultz, P.G., and Gohil, K. (2001). The in vivo neuromodulatory effects of the herbal medicine ginkgo biloba. *Proc. Natl. Acad. Sci. U S A* 98, 6577-6580.
108. Sambrook, J., and Russell, D.W. (2001). *Molecular Cloning a Laboratory Manual Third Edition, 3rd Edition* (Cold Spring Harbor, NY: Cold Spring Harbor Laboratory Press).
109. Corre, C., and Lowden, P.A.S. (2004). The first biosynthetic studies of the azinomycins: Acetate incorporation into azinomycin B. *Chem. Commun.*, 990-991.
110. Liu, C., Kelly, G.T., and Watanabe, C.M. (2006). *In vitro* biosynthesis of the antitumor agent azinomycin B. *Org. Lett.* 8, 1065-1068.
111. Darzynkiewicz, Z.a.J., G (1997). DNA content measurement for DNA ploidy and cell cycle analysis. *Current Prot. Cytom.*, 7.5.1-7.5.24.
112. Coleman, R.S., Burk, C.H., Navarro, A., Brueggemeier, R.W., and Diaz-Cruz, E.S. (2002). Role of the azinomycin naphthoate and central amide in sequence-dependent DNA alkylation and cytotoxicity of epoxide-bearing substructures. *Org. Lett.* 4, 3545-3548.
113. Casely-Hayford, M.A., Pors, K., Patterson, L.H., Gerner, C., Neidle, S., and Searcey, M. (2005). Truncated azinomycin analogues intercalate into DNA. *Bioorg. Med. Chem. Lett.* 15, 653-656.
114. Kerr, R.G., Lawry, J., and Gush, K.A. (1996). *In vitro* biosynthetic studies of the bryostatins, anti-cancer agents from the marine bryozoan *Bugula neritina*. *Tetrahedron Lett.* 37, 8305-8308.

115. Coleman, A.C., Mydlarz, L.D., and Kerr, R.G. (1999). *In vivo* and *in vitro* investigations into the biosynthetic relatedness of the pseudopterosins. *Org. Lett.* *1*, 2173-2175.
116. Tazaki, H. (2000). Biosynthetic studies on secondary metabolites of *in vitro* cultured liverworts. *J. Jap. Soc. Biosci. Biotech. Agrochem.* *74*, 137-143.
117. Wu, N., and Khosla, C. (2000). Investigating the combinatorial biosynthetic potential of a modular polyketide synthase system: *In vitro* substrate specificity studies on individual modules of 6-deoxyerythronolide B synthase. *Abstr. Pap. Amer. Chem. Soc.* *219*, U212-U212.
118. Omura, S. (1976). Antibiotic cerulenin, a novel tool for biochemistry as an inhibitor of fatty-acid synthesis. *Bacteriol. Rev.* *40*, 681-697.
119. Hiltunen, M., and Soderhall, K. (1992). Inhibition of polyketide synthesis in *Alternaria alternata* by the fatty-acid synthesis inhibitor cerulenin. *Appl. Environ. Microbiol.* *58*, 1043-1045.
120. Park, J.Y., Kim, K.A., and Kim, S.L. (2003). Chloramphenicol is a potent inhibitor of cytochrome P450 isoforms CYP2C19 and CYP3A4 in human liver microsomes. *Antimicrob. Agents Chemother.* *47*, 3464-3469.
121. Rodrigues, A.D., Gibson, G.G., Ioannides, C., and Parke, D.V. (1987). Interactions of imidazole antifungal agents with purified cytochrome P-450 proteins. *Biochem. Pharmacol.* *36*, 4277-4281.
122. Rodrigues, A.D., Lewis, D.F.V., Ioannides, C., and Parke, D.V. (1987). Spectral and kinetic-studies of the interaction of imidazole antifungal agents with microsomal cytochromes-P-450. *Xenobiotica* *17*, 1315-1327.
123. Williams, P.A., Cosme, J., Vinkovic, D.M., Ward, A., Angove, H.C., Day, P.J., Vonrhein, C., Tickle, I.J., and Jhoti, H. (2004). Crystal structures of human cytochrome P450 3A4 bound to metyrapone and progesterone. *Science* *305*, 683-686.
124. Omura, S. (1981). Cerulenin. *Methods Enzymol.* *72*, 520-532.
125. Omura, S., and Takeshim.H (1974). Inhibition of the biosynthesis of leucomycin, a macrolide antibiotic, by cerulenin. *J. Biochem.* *75*, 193-195.
126. Takeshima, H., Kitao, C., and Omura, S. (1977). Inhibition of the biosynthesis of leucomycin, a macrolide antibiotic, by cerulenin. *J. Biochem.* *81*, 1127-1132.
127. Child, C.J., and Shoolingin-Jordan, P.M. (1998). Inactivation of the polyketide synthase, 6-methylsalicylic acid synthase, by the specific modification of Cys-204 of the beta-ketoacyl synthase by the fungal mycotoxin cerulenin. *Biochem. J.* *330*, 933-937.

128. Lam, K.S., Gustavson, D.R., Veitch, J.A., and Forenza, S. (1993). The effect of cerulenin on the production of esperamicin A1 by *Actinomadura verrucosospora*. *Journal of Industrial Microbiology* 12, 99-102.
129. Hiltunen, M., and Soderhall, K. (1992). Inhibition of polyketide synthesis in *Alternaria alternata* by the fatty acid synthesis inhibitor cerulenin. *Appl. Environ. Microbiol.* 58, 1043-1045.
130. Watanabe, C.M.H., and Townsend, C.A. (2002). Initial characterization of a type I fatty acid synthase and polyketide synthase multienzyme complex NorS in the biosynthesis of aflatoxin B1. *Chem. Biol.* 9, 981-988.
131. Wright, M.C., Paine, A.J., Skett, P., and Auld, R. (1994). Induction of rat hepatic glucocorticoid-inducible cytochrome-P450 3a by metyrapone. *Journal of Steroid Biochemistry and Molecular Biology* 48, 271-276.
132. de Kraker, J.W., Franssen, M.C.R., Dalm, M.C.F., de Groot, A., and Bouwmeester, H.J. (2001). Biosynthesis of germacrene A carboxylic acid in chicory roots. Demonstration of a cytochrome P450 (+)-germacrene A hydroxylase and NADP(+)-dependent sesquiterpenoid dehydrogenase(s) involved in sesquiterpene lactone biosynthesis. *Plant Physiol.* 125, 1930-1940.
133. Kelly, G.T., Sharma, V., and Watanabe, C.M.H. (2008). An improved method for culturing *Streptomyces sahachiroi*: Biosynthetic origin of the enol fragment of azinomycin B. *Bioorg. Chem.* 36, 4-15.
134. Kelly, G.T., Sharma, V., and Watanabe, C.M. (2007). An Improved Method for Culturing *Streptomyces sahachiroi*: Biosynthetic Origin of the Enol Fragment of Azinomycin B *Bioorganic*.
135. Kelly, G.T., Liu, C., Smith, R., 3rd, Coleman, R.S., and Watanabe, C.M.H. (2006). Cellular effects induced by the antitumor agent azinomycin B. *Chem. Biol.* 13, 485-492.
136. Sakamoto, J.J., Kondo, S., Arishima, M., and Yumoto, H. (1962). Bundlins a and B, 2 antibiotics produced by *Streptomyces griseofuscus* Nov. Sp. *J. Antibiot.* 15, 98-102.
137. Bibb, M.J. (2005). Regulation of secondary metabolism in streptomycetes. *Current Opin. Microbiol.* 8, 208-215.
138. Shirling, E.B., and D. Gottlieb. (1966). Methods for characterization of *Streptomyces* species. *Int. J. Syst. Bacteriol.* 16, 313-340.

139. Malmberg, L.H., Hu, W.S., and Sherman, D.H. (1993). Precursor flux control through targeted chromosomal insertion of the lysine epsilon-aminotransferase (*lat*) gene in cephamycin C biosynthesis. *J. Bacteriol.* *175*, 6916-6924.
140. Kieser, T., Bibb, M.J., Buttner, M.J., Chater, K.F., and Hopwood, D.A. (2000). Media, Buffers and Suppliers. In *Practical Streptomyces Genetics*. (Norwich, United Kingdom: The John Innes Foundation), pp. 408-418.
141. Birch, A.H., A.; Hütter, R. (1990). Genome rearrangement and genetic instability in *Streptomyces spp.* *J. Bacteriol.* *172*, 4138-4142.
142. Volff, J.N.A., J. (1998). Genetic instability of the *Streptomyces* chromosome. *Mol. Microbiol.* *27*, 239-246.
143. Hodgson, D.A. (2000). Primary metabolism and its control in *Streptomyces*: A most unusual group of bacteria. *Advances in Microbial Physiology*, Vol 42 *42*, 47-238.
144. Hodgson, D.R.W., and Sanderson, J.M. (2004). The synthesis of peptides and proteins containing non-natural amino acids. *Chem. Soc. Rev.* *33*, 422-430.
145. Mathews, C.K.v.H., K.E.; Ahern, K.G. *Biochemistry*, 3rd Edition (San Francisco: Addison Wesley Longman).
146. Liu, C.M., Kelly, G.T., and Watanabe, C.M.H. (2006). *In vitro* biosynthesis of the antitumor agent azinomycin B. *Org. Lett.* *8*, 1065-1068.
147. Magarvey, N.A., Ehling-Schulz, M., and Walsh, C.T. (2006). Characterization of the cereulide NRPS alpha-hydroxy acid specifying modules: Activation of alpha-keto acids and chiral reduction on the assembly line. *J. Am. Chem. Soc.* *128*, 10698-10699.
148. Yan, F., Munos, J.W., Liu, P., and Liu, H.W. (2006). Biosynthesis of fosfomycin, re-examination and re-confirmation of a unique Fe(II)- and NAD(P)H-dependent epoxidation reaction. *Biochemistry* *45*, 11473-11481.
149. Munos, J.W., Moon, S.J., Mansoorabadi, S.O., Chang, W., Hong, L., Yan, F., Liu, A., and Liu, H.W. (2008). Purification and characterization of the epoxidase catalyzing the formation of fosfomycin from *Pseudomonas syringae*. *Biochemistry* *47*, 8726-8735.
150. Gruschow, S., and Sherman, D.H. (2006). The Biosynthesis of Epoxides. In *Aziridines and Epoxides in Organic Synthesis*, A.K. Yudin, ed. (Weinheim, Germany: WILEY-VCH), pp. 349-398.
151. Watanabe, C.M.H., and Townsend, C.A. (1996). Incorporation of molecular oxygen in aflatoxin B-1 biosynthesis. *J. Org. Chem.* *61*, 1990-1993.

152. Green, M.L., and Elliott, W.H. (1964). Enzymic formation of aminoacetone from threonine and its further metabolism. *Biochem. J.* *92*, 537- 549.
153. Bell, S.C., and Turner, J.M. (1976). L-Threonine catabolism via aminoacetone: A search for a pathway in bacteria. *Biochem Soc Trans* *4*, 497-500.
154. Bell, S.C., and Turner, J.M. (1976). Bacterial catabolism of threonine: Threonine degradation initiated by L-threonine-NAD⁺ oxidoreductase. *Biochem. J.* *156*, 449-458.
155. Haralambie, G., and Mossinger, M. (1980). Metabolites of the aminoacetone pathway in blood after exercise. *Metabolism* *29*, 1258-1261.
156. Dale, R.A. (1978). Catabolism of threonine in mammals by coupling of L-threonine 3-dehydrogenase with 2-amino-3-oxobutyrate-CoA ligase. *Biochim Biophys Acta* *544*, 496-503.
157. Bird, M.I., Nunn, P.B., and Lord, L.A. (1984). Formation of glycine and aminoacetone from L-threonine by rat liver mitochondria. *Biochim Biophys Acta* *802*, 229-236.
158. Kanehisa, M., Araki, M., Goto, S., Hattori, M., Hirakawa, M., Itoh, M., Katayama, T., Kawashima, S., Okuda, S., Tokimatsu, T., *et al.* (2008). KEGG for linking genomes to life and the environment. *Nucleic Acids Res.* *36*, D480-484.
159. Kanehisa, M., Goto, S., Hattori, M., Aoki-Kinoshita, K.F., Itoh, M., Kawashima, S., Katayama, T., Araki, M., and Hirakawa, M. (2006). From genomics to chemical genomics: New developments in KEGG. *Nucleic Acids Res.* *34*, D354-357.
160. Kanehisa, M., and Goto, S. (2000). KEGG: Kyoto encyclopedia of genes and genomes. *Nucleic Acids Res.* *28*, 27-30.
161. Dekimpe, N., Decock, W., and Schamp, N. (1987). A convenient synthesis of 1-chloro-2-alkanones. *Synthesis-Stuttgart*, 188-190.
162. Schmidt, A., Sivaraman, J., Li, Y., Larocque, R., Barbosa, J.A.R.G., Smith, C., Matte, A., Schrag, J.D., and Cygler, M. (2001). Three-Dimensional Structure of 2-Amino-3-ketobutyrate CoA Ligase from *Escherichia coli* Complexed with a PLP-Substrate Intermediate: Inferred Reaction Mechanism. *Biochemistry* *40*, 5151-5160.
163. Marcus, J.P., and Dekker, E.E. (1993). Threonine formation via the coupled activity of 2-amino-3-ketobutyrate coenzyme A lyase and threonine dehydrogenase. *J. Bacteriol.* *175*, 6505-6511.
164. Zang, H., and Gates, K.S. (2000). DNA binding and alkylation by the "left half" of azinomycin B. *Biochemistry* *39*, 14968-14975.

165. Urata, G., and Granick, S. (1963). Biosynthesis of alpha-aminoketones and the metabolism of aminoacetone. *J. Biol. Chem.* *238*, 811-820.
166. Rahhal, D.A., Turner, J.M., and Willetts, A.J. (1967). The role of aminoacetone in L-threonine metabolism by *Bacillus subtilis*. *Biochem. J.* *103*, 73P.
167. Bechara, E.J., Dutra, F., Cardoso, V.E., Sartori, A., Olympio, K.P., Penatti, C.A., Adhikari, A., and Assuncao, N.A. (2007). The dual face of endogenous alpha-aminoketones: Pro-oxidizing metabolic weapons. *Comp. Biochem. Physiol. C Toxicol. Pharmacol.* *146*, 88-110.
168. Szent-Györgyi, A. (1968). Bioelectronics. Intermolecular electron transfer may play a major role in biological regulation, defense, and cancer. *Science* *161*, 988-990.
169. Bechara, E.J.H. (1995). *The Oxygen Paradox*, K.J.A. Davies and F. Ursini, eds. (Padova, Italy CLEUP University Press), pp. 503–513.
170. Meunier, B., de Visser, S.P., and Shaik, S. (2004). Mechanism of oxidation reactions catalyzed by cytochrome P450 enzymes. *Chem. Rev.* *104*, 3947-3980.
171. Harayama, S., Kok, M., and Neidle, E.L. (1992). Functional and evolutionary relationships among diverse oxygenases. *Annu. Rev. Microbiol.* *46*, 565-601.
172. O'Keefe, D.P., and Harder, P.A. (1991). Occurrence and biological function of cytochrome P450 monooxygenases in the actinomycetes. *Mol. Microbiol.* *5*, 2099-2105.
173. Moore, R.N., Bigam, G., Chan, J.K., Hogg, A.M., Nakashima, T.T., and Vederas, J.C. (1985). Biosynthesis of the hypocholesterolemic agent mevinolin by *Aspergillus terreus*: Determination of the origin of carbon, hydrogen, and oxygen atoms by C-13-NMR and Mass Spectrometry. *J. Am. Chem. Soc.* *107*, 3694-3701.
174. Vederas, J.C. (1987). The use of stable isotopes in biosynthetic studies. *Nat. Prod. Rep.* *4*, 277-337.
175. Sharma, V., Kelly, G.T., and Watanabe, C.M. (2008). Exploration of the molecular origin of the azinomycin epoxide: Timing of the biosynthesis revealed. *Org. Lett.* *10*, 4815-4818.
176. Zhao, Q., He, Q., Ding, W., Tang, M., Kang, Q., Yu, Y., Deng, W., Zhang, Q., Fang, J., Tang, G., *et al.* (2008). Characterization of the azinomycin B biosynthetic gene cluster revealing a different iterative type I polyketide synthase for naphthoate biosynthesis. *Chem. Biol.* *15*, 693-705.
177. Dondoni, A., and Perrone, D. (1999). Synthesis of 1,1-dimethylethyl (S)-4-formyl-2,2-dimethyl-3-oxazolidinecarboxylate by oxidation of the alcohol. *Organic Synth.* *77*, 64.

178. Rathke, M.W., and Nowak, M. (1985). The Horner-Wadsworth-Emmons modification of the Wittig reaction using triethylamine and lithium or magnesium salts. *The Journal of Organic Chemistry* *50*, 2624-2626.
179. Foss Jr, F.W., Snyder, A.H., Davis, M.D., Rouse, M., Okusa, M.D., Lynch, K.R., and Macdonald, T.L. (2007). Synthesis and biological evaluation of [gamma]-aminophosphonates as potent, subtype-selective sphingosine 1-phosphate receptor agonists and antagonists. *Bioorgan Med Chem* *15*, 663-677.
180. Brown, I., Edwards, O.E., McIntosh, J.M., and Vocelle, D. (1969). Internal addition of acyl nitrenes to olefins. *Can. J. Chem.* *47*, 2751-2762.
181. Griffart-Brunet, D., and Langlois, N. (1994). A short diastereoselective synthesis of the natural (2R, 3R, 4R)-2-hydroxymethyl-3,4-dihydroxypyrrolidine. *Tetrahedron Lett.* *35*, 2889-2890.
182. Ryu, Y., and Kim, G. (1995). A practical and divergent way to trihydroxylated pyrrolidine derivatives as potential glycosidase inhibitors via stereoselective intermolecular cis-amidoalkylations. *The Journal of Organic Chemistry* *60*, 103-108.
183. Huang, Y., Dalton, D.R., and Carroll, P.J. (1997). The efficient, enantioselective synthesis of aza sugars from amino acids. 1. The polyhydroxylated pyrrolidines. *The Journal of Organic Chemistry* *62*, 372-376.
184. Nash, R.J., Fellows, L.E., Dring, J.V., Fleet, G.W.J., Derome, A.E., Hamor, T.A., Scofield, A.M., and Watkin, D.J. (1988). Isolation from and x-ray crystal structure of alexine, (1r,2r,3r,7s,8s)-3-hydroxymethyl-1,2,7-trihydroxypyrrolizidine [(2r,3r,4r,5s,6s)-2-hydroxymethyl-1-azabicyclo[3.3.0]octan-3,4,6-triol], a unique pyrrolizidine alkaloid. *Tetrahedron Lett.* *29*, 2487-2490.
185. Nash, R.J., Fellows, L.E., Plant, A.C., Fleet, G.W.J., Derome, A.E., Baird, P.D., Hegarty, M.P., and Scofield, A.M. (1988). Isolation from and x-ray crystal structure of 3,8-diepilexine, (1r,2r,3s,7s,8r)-3-hydroxymethyl-1,2,7-trihydroxypyrrolizidine [(2s,3r,4r,5s,6r)-2-hydroxymethyl-1-azabicyclo[3.3.0]octan-3,4,6-triol]. *Tetrahedron* *44*, 5959-5964.
186. Thottathil, J.K., Moniot, J.L., Mueller, R.H., Wong, M.K.Y., and Kissick, T.P. (1986). Conversion of L-pyroglutamic acid to 4-alkyl-substituted L-prolines. The synthesis of trans-4-cyclohexyl-L-proline. *The Journal of Organic Chemistry* *51*, 3140-3143.

187. Langlois, N., and Moro, A. (1999). Regio- and stereoselective opening of oxiranes through neighbouring group participation: Stereocontrolled synthesis of enantiopure hydroxylated oxazolidin-2-ones. *Eur. J. Org. Chem.* 1999, 3483-3488.
188. Oba, M., Koguchi, S., and Nishiyama, K. (2002). A concise approach to homochiral 3,4-dihydroxyglutamic acids. *Tetrahedron* 58, 9359-9363.
189. Oba, M., Koguchi, S., and Nishiyama, K. (2001). A concise diastereoselective synthesis of (2S,3S,4R)-3,4-dihydroxyglutamic acid. *Tetrahedron Lett.* 42, 5901-5902.
190. Coleman, R.S., Li, J., and Navarro, A. (2001). Total synthesis of azinomycin A. *Angew. Chem. Int. Ed.* 40, 1736-1739.
191. Coleman, R.S., Tierney, M.T., Cortright, S.B., and Carper, D.J. (2007). Synthesis of functional "top-half" partial structures of azinomycin A and B. *J. Org. Chem.* 72, 7726-7735.
192. LePla, R.C., Landreau, C.A., Shipman, M., Hartley, J.A., and Jones, G.D. (2005). Azinomycin inspired bisepoxides: Influence of linker structure on in vitro cytotoxicity and DNA interstrand cross-linking. *Bioorg. Med. Chem. Lett.* 15, 2861-2864.
193. Casely-Hayford, M.A., Pors, K., James, C.H., Patterson, L.H., Hartley, J.A., and Searcey, M. (2005). Design and synthesis of a DNA-crosslinking azinomycin analogue. *Org. Biomol. Chem.* 3, 3585-3589.
194. Kunda-Yamada, Y., Asano, K., Satou, T., Monma, S., Sakayanagi, M., Satou, N., Takeda, K., and Harigaya, Y. (2005). Application of intramolecular 1,3-dipolar cyclic addition of azide and olefin; Construction of (pyrrolidine-2-ylidene)glycinate and glycinamides. *Chem. Pharm. Bull.* 53, 529-536.
195. Watson, I.D.G., and Yudin, A.K. (2003). Ring-opening reactions of nonactivated aziridines catalyzed by tris(pentafluorophenyl)borane. *J. Org. Chem.* 68, 5160-5167.
196. Hashimoto, M., Matsumoto, M., and Terashima, S. (2003). Synthetic studies of carzinophilin. Part 1: Synthesis of 2-methylidene-1-azabicyclo[3.1.0]hexane systems related to carzinophilin. *Tetrahedron* 59, 3019-3040.
197. Hashimoto, M., Matsumoto, M., and Terashima, S. (2003). Synthetic studies of carzinophilin. Part 2: Synthesis of 3,4-dibenzyloxy-2-methylidene-1-azabicyclo[3.1.0]hexane systems corresponding to the C1-C17 fragment of carzinophilin. *Tetrahedron* 59, 3041-3062.
198. Hashimoto, M., Sugiura, M., and Terashima, S. (2003). Synthetic studies of carzinophilin. Part 3: Synthetic approach toward carzinophilin and successful synthesis

- of 13-O-desacetyl-12,13-di-O-benzyl-4-O-methylcarzinophilin. *Tetrahedron* *59*, 3063-3087.
199. Hashimoto, M., Matsumoto, M., Yamada, K., and Terashima, S. (2003). Synthetic studies of carzinophilin. Part 4: Chemical and biological properties of carzinophilin analogues. *Tetrahedron* *59*, 3089-3097.
200. Goujon, J.Y., and Shipman, M. (2002). Concise route to alpha-acylamino-beta-keto amides: Application to the synthesis of a simplified azinomycin A analogue. *Tetrahedron Lett.* *43*, 9573-9576.
201. Miyashita, K., Park, M., Adachi, S., Seki, S., Obika, S., and Imanishi, T. (2002). A 3,4-epoxypiperidine structure as a novel and simple DNA-cleavage unit. *Bioorg. Med. Chem. Lett.* *12*, 1075-1077.
202. Bryant, H.J., Dardonville, C.Y., Hodgkinson, T.J., Hursthouse, M.B., Malik, K.M.A., and Shipman, M. (1998). Asymmetric synthesis of the left hand portion of the azinomycins. *J. Chem. Soc. Perkin Trans. 1*, 1249-1255.
203. Hashimoto, M., and Terashima, S. (1998). A stereoselective synthesis of 4-O-methyl-13-desacetyl-12,13-di-O-benzylcarzinophilin. *Heterocycles* *47*, 59-64.
204. Coleman, R.S., and Carpenter, A.J. (1997). The development of strategies for construction of the aziridine core of the antitumor agents azinomycins A and B. *Tetrahedron* *53*, 16313-16326.
205. Bryant, H.J., Dardonville, C.Y., Hodgkinson, T.J., Shipman, M., and Slawin, A.M.Z. (1996). Asymmetric synthesis of the epoxide portion of the azinomycins. *Synlett*, 973-974.
206. Konda, Y., Machida, T., Akaiwa, M., Takeda, K., and Harigaya, Y. (1996). A convenient synthesis of the five-membered lactams from D-ARABINOSE. *Heterocycles* *43*, 555-565.
207. Hashimoto, M., Matsumoto, M., Yamada, K., and Terashima, S. (1994). Synthesis, chemical-property, and cytotoxicity of the carzinophilin congeners carrying a 2-(1-acylamino-1-alkoxycarbonyl)methylidene-1-azabicyclo[3.1.0]hexane system. *Tetrahedron Lett.* *35*, 2207-2210.
208. Konda, Y., Machida, T., Sasaki, T., Takeda, K., Takayanagi, H., and Harigaya, Y. (1994). Convenient synthesis of the epoxy fragment of azinomycin B. *Chem. Pharm. Bull.* *42*, 285-288.

209. Hashimoto, M., and Terashima, S. (1994). A novel synthesis of the C1-C17 fragment of carzinophilin. *Tetrahedron Lett.* 35, 9409-9412.
210. Hashimoto, M., and Terashima, S. (1994). A stereoselective synthesis of a novel model compound of carzinophilin carrying the C6-C-13 unit with correct stereochemistry. *Chem Lett*, 1001-1002.
211. Coleman, R.S., and Carpenter, A.J. (1993). Stereoselective bromination of dehydroamino acids with controllable retention or inversion of olefin configuration. *J. Org. Chem.* 58, 4452-4461.
212. Shishido, K., Omodani, T., and Shibuya, M. (1992). Simple and efficient access to the left-hand segment of azinomycins. *J. Chem. Soc. Perkin Trans. 1*, 2053-2054.
213. Hashimoto, M., Yamada, K., and Terashima, S. (1992). Synthesis, chemical reactivity, and cytotoxicity of 2-bis(alkoxycarbonyl)methyliden-1-azabicyclo[3.1.0]hexane systems related to antitumor antibiotic carzinophilin A. *Chem Lett*, 975-978.
214. Coleman, R.S., Woodward, R.L., Hayes, A.M., Crane, E.A., Artese, A., Ortuso, F., and Alcaro, S. (2007). Dependence of DNA sequence selectivity and cell cytotoxicity on azinomycin A and B epoxyamide stereochemistry. *Org. Lett.* 9, 1891-1894.
215. Coleman, R.S. (2006). Mechanistic studies on the DNA cross-linking agent azinomycin B. *Chem Res Toxicol* 19, 1677-1677.
216. David-Cordonnier, M.H., Casely-Hayford, M., Kouach, M., Briand, G., Patterson, L.H., Bailly, C., and Searcey, M. (2006). Stereoselectivity, sequence specificity and mechanism of action of the azinomycin epoxide. *ChemBioChem* 7, 1658-1661.
217. LePla, R.C., Landreau, C.A., Shipman, M., and Jones, G.D. (2005). On the origin of the DNA sequence selectivity of the azinomycins. *Org. Biomol. Chem.* 3, 1174-1175.
218. Le Pla, R.C., Landreau, C.A.S., Shipman, M., Slawin, A.M.Z., and Hartley, J.A. (2004). The role of the naphthoate moiety and its substituents upon the efficiency of DNA interstrand cross-linking by the azinomycins. *Mutagenesis* 19, 516-516.
219. Landreau, C.A.S., LePla, R.C., Shipman, M., Slawin, A.M.Z., and Hartley, J.A. (2004). Delineating noncovalent interactions between the azinomycins and double-stranded DNA: Importance of the naphthalene substitution pattern on interstrand cross-linking efficiency. *Org. Lett.* 6, 3505-3507.
220. Corre, C., Landreau, C.A.S., Shipman, M., and Lowden, P.A.S. (2004). Biosynthetic studies on the azinomycins: The pathway to the naphthoate fragment. *Chem. Commun.*, 2600-2601.

221. Dess, D.B., and Martin, J.C. (1991). A useful 12-I-5 triacetoxypersulfonamide (the Dess-Martin persulfonamide) for the selective oxidation of primary or secondary alcohols and a variety of related 12-I-5 species. *J. Am. Chem. Soc.* *113*, 7277-7287.
222. More, J.D., and Finney, N.S. (2002). A simple and advantageous protocol for the oxidation of alcohols with, *o*-iodoxybenzoic acid (IBX). *Org. Lett.* *4*, 3001-3003.
223. Chenna, R., Sugawara, H., Koike, T., Lopez, R., Gibson, T.J., Higgins, D.G., and Thompson, J.D. (2003). Multiple sequence alignment with the Clustal series of programs. *Nucleic Acids Res.* *31*, 3497-3500.
224. Sharma, V., Kelly, G.T., and Watanabe, C.M.H. (2008). Exploration of the molecular origin of the azinomycin epoxide: Timing of the biosynthesis revealed. *Org. Lett.* *10*, 4815-4818.
225. Ho, W., Tutwiler, G.F., Cottrell, S.C., Morgans, D.J., Tarhan, O., and Mohrbacher, R.J. (1986). Alkylglycidic acids: Potential new hypoglycemic agents. *J. Med. Chem.* *29*, 2184-2190.
226. Brown, H.C., and Chen, J.C. (1981). Hydroboration. *57*. Hydroboration with 9-borabicyclo[3.3.1]nonane of alkenes containing representative functional groups. *J. Org. Chem.* *46*, 3978-3988.
227. Otsubo, K., Inanaga, J., and Yamaguchi, M. (1987). A highly stereoselective conversion of α,β -epoxy esters to α -hydroxy esters - an efficient route to optically-active α -hydroxyesters. *Tetrahedron Lett.* *28*, 4435-4436.
228. Bonini, C., Difabio, R., Sotgiu, G., and Cavagnero, S. (1989). Oxirane rings: Studies and applications of a new chemo and regio selective reductive opening of epoxides. *Tetrahedron* *45*, 2895-2904.
229. Stork, G., and Rychnovsky, S.D. (1987). Iterative butenolide construction of polypropionate chains. *J. Am. Chem. Soc.* *109*, 1564-1565.
230. Hanessian, S., and Murray, P.J. (1987). Stereochemical control of nature's biosynthetic pathways - a general strategy for the synthesis of polypropionate-derived structural units from a single chiral progenitor. *Tetrahedron* *43*, 5055-5072.
231. Sharma, V., Lansdell, T.A., Jin, G.Y., and Tepe, J.J. (2004). Inhibition of cytokine production by hymenialdisine derivatives. *J. Med. Chem.* *47*, 3700-3703.
232. Englisch-Peters, S. (1989). Synthesis of omega-hydroxy analogs of valine, leucine and isoleucine. *Tetrahedron* *45*, 6127-6134.

233. Galantay, E., Szabo, A., and Fried, J. (1963). Synthesis of alpha-amino-gamma-hydroxy acids - gamma,gamma'-dihydroxyvaline. *J. Org. Chem.* *28*, 98-102.
234. Coleman, R.S., and Carpenter, A.J. (1992). Diastereoselective addition of vinyl organometallic reagents to L-serinal. *Tetrahedron Lett.* *33*, 1697-1700.
235. Fujisawa, T., Nagai, M., Koike, Y., and Shimizu, M. (1994). Diastereoface discrimination in the addition of acetylide to a chiral aldehyde, leading to a synthesis of (+)-deoxybiotin in enantiomerically pure form starting from L-cysteine. *J. Org. Chem.* *59*, 5865-5867.
236. D'Aniello, F., Mann, A., Taddei, M., and Wermuth, C.G. (1994). 1,3-diastereocontrol with bromoallenes - synthesis of enantiomerically pure beta-branched alpha-amino-acids. *Tetrahedron Lett.* *35*, 7775-7778.
237. Kahne, D., Yang, D., and Lee, M.D. (1990). Preparation of the 4-ethylamino sugar of calicheamicin - assignment of absolute-configuration. *Tetrahedron Lett.* *31*, 21-22.
238. Roush, W.R., and Hunt, J.A. (1995). Asymmetric allylboration of 2-N,3-O-isopropylidene-N-Boc-L-serinal - diastereoselective synthesis of the calicheamicin gamma(1)(I) amino sugar. *J. Org. Chem.* *60*, 798-806.
239. Dondoni, A., Merino, P., and Perrone, D. (1993). Totally chemical synthesis of azasugars via thiazole intermediates - stereodivergent routes to (-)-nojirimycin, (-)-mannojirimycin and their 3-deoxy derivatives from serine. *Tetrahedron* *49*, 2939-2956.
240. Nimkar, S., Menaldino, D., Merrill, A.H., and Liotta, D. (1988). A stereoselective synthesis of sphingosine, a protein kinase-C inhibitor. *Tetrahedron Lett.* *29*, 3037-3040.
241. Garner, P., Park, J.M., and Malecki, E. (1988). A stereodivergent synthesis of D-erythro-sphingosine and D-threo-sphingosine from L-serine. *J. Org. Chem.* *53*, 4395-4398.
242. Dondoni, A., Fantin, G., Fogagnolo, M., and Pedrini, P. (1990). Stereochemistry associated with the addition of 2-(trimethylsilyl)thiazole to differentially protected alpha-amino aldehydes - applications toward the synthesis of amino-sugars and sphingosines. *J. Org. Chem.* *55*, 1439-1446.
243. Soai, K., and Takahashi, K. (1994). Asymmetric alkenylation of chiral and prochiral aldehydes catalyzed by chiral or achiral amino-alcohols - catalytic diastereoselective synthesis of protected erythro-sphingosine and enantioselective synthesis of chiral diallyl alcohols. *J. Chem. Soc. Perkin Trans. 1*, 1257-1258.

244. Ruan, F.Q., Yamamura, S., Hakomori, S., and Igarashi, Y. (1995). Synthesis of sphingosine conjugate with controlled-pore glass-beads. *Tetrahedron Lett.* *36*, 6615-6618.
245. Garner, P., and Park, J.M. (1988). An asymmetric-synthesis of 5-O-carbamoylpolyoxamic acid from D-serine. *J. Org. Chem.* *53*, 2979-2984.
246. Sakai, N., and Ohfuné, Y. (1990). Efficient synthesis of the revised structure of (-)-galantinic acid. *Tetrahedron Lett.* *31*, 4151-4154.
247. Jako, I., Uiber, P., Mann, A., Wermuth, C.G., Boulanger, T., Norberg, B., Evrard, G., and Durant, F. (1991). Stereoselective synthesis of 3-alkylated glutamic acids - application to the synthesis of secokainic acid. *J. Org. Chem.* *56*, 5729-5733.
248. Golebiowski, A., Kozak, J., and Jurczak, J. (1991). Syntheses of destomic acid and anhydrogalantinic acid from L-serinal. *J. Org. Chem.* *56*, 7344-7347.
249. Griffith, W.P., Ley, S.V., Whitcombe, G.P., and White, A.D. (1987). Preparation and use of tetra-normal-butylammonium per-ruthenate (Tbap reagent) and tetra-normal-propylammonium per-ruthenate (Tpap reagent) as new catalytic oxidants for alcohols. *J. Chem. Soc., Chem. Commun.*, 1625-1627.
250. Corey, E.J., and Suggs, J.W. (1975). Pyridinium chlorochromate - efficient reagent for oxidation of primary and secondary alcohols to carbonyl compounds. *Tetrahedron Lett.*, 2647-2650.
251. Corey, E.J., and Schmidt, G. (1979). Useful procedures for the oxidation of alcohols involving pyridinium dichromate in aprotic media. *Tetrahedron Lett.*, 399-402.
252. Dess, D.B., and Martin, J.C. (1983). Readily accessible 12-I-5 oxidant for the conversion of primary and secondary alcohols to aldehydes and ketones. *J. Org. Chem.* *48*, 4155-4156.
253. Nahm, S., and Weinreb, S.M. (1981). N-methoxy-N-methylamides as effective acylating agents. *Tetrahedron Lett.* *22*, 3815-3818.
254. Dondoni, A., Marra, A., and Massi, A. (1999). Design and use of an oxazolidine silyl enol ether as a new homoalanine carbanion equivalent for the synthesis of carbon-linked isosteres of O-glycosyl serine and N-glycosyl asparagine. *J. Org. Chem.* *64*, 933-944.
255. So, R.C., Ndonye, R., Izmirian, D.P., Richardson, S.K., Guerrero, R.L., and Howell, A.R. (2004). Straightforward synthesis of sphingamines via a serine-derived Weinreb amide. *J. Org. Chem.* *69*, 3233-3235.

256. Ageno, G., Banfi, L., Cascio, G., Guanti, G., Manghisi, E., Riva, R., and Rocca, V. (1995). Enantiospecific and diastereoselective synthesis of 4,4-disubstituted-3-amino-2-azetidinones, starting from D-serine. *Tetrahedron* *51*, 8121-8134.
257. Reetz, M.T. (1991). New approaches to the use of amino-acids as chiral building-blocks in organic-synthesis. *Angew. Chem. Int. Ed. Engl.* *30*, 1531-1546.
258. Myers, A.G., Kung, D.W., and Zhong, B.Y. (2000). Observations concerning the existence and reactivity of free alpha-amino aldehydes as chemical intermediates: Evidence for epimerization-free adduct formation with various nucleophiles. *J. Am. Chem. Soc.* *122*, 3236-3237.

APPENDIX
LIST OF FIGURES

	Page
Figure 110. FramePlot analysis of a contig from genomic sequencing of <i>S. sahachiroi</i>	191
Figure 111. CLUSTALW alignment of threonine-3-dehydrogenases and 2-amino-3-ketobutyrate CoA ligases in <i>Streptomyces sp.</i>	192
Figure 112. Major species identified in the purification of the azinomycins with carbon positional number assignment.....	195
Figure 113. ¹ H Spectra standard for azinomycin B	197
Figure 114. Standard azinomycin B carbon spectrum with numbers assigned	198
Figure 115. Representative APCI Mass Spectrometry Spectrum detecting azinomycin B and related structures.....	199
Figure 116. Azinomycin B, fed [Methyl- ¹³ C] L-methionine 50mg.....	200
Figure 117. Azinomycin B, fed [1- ¹³ C] sodium acetate 1000mg	200
Figure 118. Azinomycin B, fed [1- ¹³ C] L-valine (V2) 100mg	201
Figure 119. Azinomycin B, fed [1- ¹³ C] L-γ-hydroxyvaline ((2S)-2-amino-4-hydroxy-3-methylbutanoic acid) (V3) 140mg	201
Figure 120. Azinomycin B, fed [1- ¹³ C] D-γ-hydroxyvaline ((2R)-2-amino-4-hydroxy-3-methylbutanoic acid) (V3) 100mg	202
Figure 121. Azinomycin B, fed [1- ¹³ C] R-keto hydroxy acid (4-hydroxy-3-methyl-2-oxobutanoic acid) (V5) 150mg.....	202
Figure 122. Azinomycin B, fed [1- ¹³ C] epoxy-keto acid (2-(2-methyloxiran-2-yl)-2-oxoacetic acid) (V8) 90mg.....	203
Figure 123. Azinomycin B, fed [1- ¹³ C] epoxy-hydroxy acid ((2S)-2-hydroxy-2-(2-methyloxiran-2-yl)acetic acid) (V9) 75mg.....	203
Figure 124. Azinomycin B, fed [1- ¹³ C] Isodehydrovaline (2-amino-3-methylbut-3-enoic acid hydrochloride) (V10) 90mg.....	204
Figure 125. Azinomycin B, fed [1- ¹³ C] allyl-hydroxy acid (2-hydroxy-3-methylbut-3-enoic acid) (V11) 100mg	204
Figure 126. Azinomycin B, fed [1- ¹³ C] sodium allylketocarboxylate (sodium 3-methyl-2-oxobut-3-enoate) (V12) 127mg.....	205

	Page
Figure 127. Epoxyamide ((S)-2-amino-1-((S)-2-methyloxiran-2-yl)-2-oxoethyl 3-methoxy-5-methyl-1-naphthoate) (Supplied pure courtesy of Dr. Robert Coleman).....	205
Figure 128. Overlay of Azinomycin B ¹³ C-NMR Spectra at 164.0 ppm and 168.9 ppm for all the fed valine derivative series and the epoxyamide	206
Figure 129. Azinomycin B, fed [1- ¹³ C] L-threonine (T2) 100mg with [1- ¹³ C] L-Valine (V2) 100mg	207
Figure 130. Azinomycin B, fed [U- ¹³ C] L-threonine (T2) 97mg	207
Figure 131. Azinomycin B, fed [U- ¹³ C] ketocarboxylate threonine TFA ((S)-2-amino-3-oxobutanoic acid) (T3) 124mg	208
Figure 132. Azinomycin B, fed [U- ¹³ C] hydroxy aldehyde threonine TFA ((2S)-2-amino-3-hydroxybutanal) (T4) 163mg	208
Figure 133. Azinomycin B, fed [U- ¹³ C] keto aldehyde threonine TFA ((R)-2-amino-3-oxobutanal) (T5) 169mg.....	209
Figure 134. Overlay of Azinomycin B ¹³ C-NMR Spectra for [U- ¹³ C] L-threonine derivative series (T2-T5), incorporation into azinomycin C1 of azinomycin B ...	210
Figure 135. Overlay of Azinomycin B ¹³ C-NMR Spectra for [U- ¹³ C] L-threonine derivative series (T2-T5), incorporation into azinomycin C2 of azinomycin B ...	211
Figure 136. Overlay of Azinomycin B ¹³ C-NMR Spectra for [U- ¹³ C] L-threonine derivative series (T2-T5), incorporation into azinomycin C3 of azinomycin B ...	212
Figure 137. Overlay of Azinomycin B ¹³ C-NMR Spectra for [U- ¹³ C] L-threonine derivative series (T2-T5), incorporation into azinomycin C4 of azinomycin B ...	213
Figure 138. Azinomycin A ¹³ C-NMR Spectra for [U- ¹³ C] L-threonine (T2/AA3), incorporation into C1-3 of azinomycin A	214
Figure 139. Azinomycin B, fed [¹⁵ N] L-threonine (AA3) 230mg	215
Figure 140. Azinomycin B, fed [¹⁵ C] threonine (AA3) 230mg	215
Figure 141. Azinomycin B, fed [1- ¹³ C] glycine (AA6) 100mg	216
Figure 142. Azinomycin B, fed [1- ¹³ C] glycine (AA6) 1000mg	216
Figure 143. Azinomycin B, fed [2- ¹³ C] glycine (AA6) 1000mg	217
Figure 144. Azinomycin B, fed [2- ¹³ C] glycine (AA6) 1000mg spectral blow ups	217

	Page
Figure 145. Azinomycin B, fed [2,2-D2] glycine (AA6) 1000mg	220
Figure 146. Azinomycin B, fed [¹⁵ N] glycine (AA6) 1000mg	220
Figure 147. APCI-Mass Spectrometry for ¹⁵ N-glycine (AA6) incorporation into the epoxyamide	221
Figure 148. APCI-Mass Spectrometry for ¹⁵ N-glycine (AA6) incorporation into the azinomycin A & B.....	222
Figure 149. Spectral overlay of feeding 300mg aminoacetone (AA5): [2- ¹³ C] aminoacetone purified for azinomycin A, [2- ¹³ C] aminoacetone purified for azinomycin B, and unlabeled aminoacetone purified both azinomycins	223
Figure 150. Azinomycin B, fed aminoacetone HCl (AA5) 1250mg	224
Figure 151. Azinomycin B, fed aminoacetone HCl (AA5) 700mg	224
Figure 152. Azinomycin B, fed aminoacetone HCl (AA5) 1000mg	225
Figure 153. APCI-Mass Spectrometry for ¹⁸ O ₂ incorporation into azinomycins A and B from crude extract	226
Figure 154. ¹⁸ O Incorporation into truncated Naphthoate moiety detected by APCI-MS	226
Figure 155. ¹ H Spectra of ¹⁸ O ₂ incorporated azinomycin B	227
Figure 156. ¹³ C Spectra of ¹⁸ O ₂ incorporated azinomycin B	227
Figure 157. Azinomycin B, fed [3- ¹³ C] L-aspartate 100mg	228
Figure 158. Azinomycin B, fed [U- ¹⁵ N ₂] L-asparagine 220mg	228
Figure 159. Azinomycin B, fed [U- ¹⁵ N ₂] L-asparagine 220mg	229
Figure 160. Azinomycin B, fed [1,2- ¹³ C ₂] L-ornithine•2HCl 100mg.....	230
Figure 161. Azinomycin B, fed [1,2- ¹³ C ₂] L-ornithine•2HCl 100mg.....	230
Figure 162. Azinomycin B, fed [1- ¹³ C] L-proline 100mg	231
Figure 163. Azinomycin B, fed [1- ¹³ C] L-lysine•HCl 100mg co-fed with [1- ¹³ C] L-valine 100mg.....	231
Figure 164. Azinomycin B, fed [2- ¹³ C] L-serine 100mg.....	232

	Page
Figure 165. Azinomycin B, fed [U- ¹³ C] L-arginine 100mg	232
Figure 166. Azinomycin B, fed [1- ¹³ C] D-arabinose 900mg.....	233
Figure 167. Azinomycin B, fed [1- ¹³ C] D-Xylose 900mg.....	233
Figure 168. Azinomycin B, fed [U- ¹³ C] D-Glucose 1000mg	234
Figure 169. Azinomycin B, fed [1- ¹³ C] Pyroglutaminol (5-(hydroxymethyl)pyrrolidin-2-one), (AZ5) 140mg.....	235
Figure 170. Azinomycin B, fed [1- ¹³ C] Pyroglutamic acid (5-oxopyrrolidine-2-carboxylic acid), (AZ17) 160mg.....	235
Figure 171. Azinomycin B, fed [1- ¹³ C] (3S,4R)-3,4-dihydroxy-5-(hydroxymethyl)pyrrolidin-2-one, (AZ16a) 200mg.....	236
Figure 172. Azinomycin B, fed [1- ¹³ C] (3R,4S)-3,4-dihydroxy-5-(hydroxymethyl)pyrrolidin-2-one, (AZ16b) 200mg	236
Figure 173. Azinomycin B, fed [1- ¹³ C] 3, 4 dihydroxy glutamic acid ((3S,4R)-2-amino-3,4-dihydroxypentanedioic acid) (AZ15a) 200mg.....	237
Figure 174. Azinomycin B, fed [1- ¹³ C] 3, 4 dihydroxy glutamic acid (3R,4S)-2-amino-3,4-dihydroxypentanedioic acid) (AZ15b) 200mg	237
Figure 175. Azinomycin B, fed [1- ¹³ C] DL-glutamic acid (AZ6) 231mg.....	238
Figure 176. Azinomycin B, fed [1- ¹³ C] DL-glutamic acid (AZ6) 1000mg.....	238
Figure 177. Stability profile of V3-12.	278
Figure 178. Stability curve as a function of time for T3, T4, T5.....	283

LIST OF SCHEMES

	Page
Scheme 7. Synthesis of 1-o-Tolyl-propan-2-ol.....	187
Scheme 8. Synthesis of 1-o-Tolylpropan-2-one.....	188
Scheme 9. Synthesis of 2-Hydroxy-4-oxo-5-o-tolyl-pent-2-enoic acid ethyl ester	188
Scheme 10. Synthesis of 3-Hydroxy-5-methyl-naphthalene-1-carboxylic acid ethyl ester.	189
Scheme 11. Synthesis of 3-Methoxy-5-methyl-naphthalene-1-carboxylic acid (naphthoate)..	189
Scheme 12. Synthesis towards V10.....	269
Scheme 13. Synthesis towards V3	276
Scheme 14. Proposed biosynthetic routes to the enol fragment of azinomycin B	279
Scheme 15. Synthesis of threonine derivatives.....	280
Scheme 16. Synthesis of threonine derivatives.....	281
Scheme 17. Synthesis of Aminoacetone Hydrogen Chloride	291

LIST OF TABLES

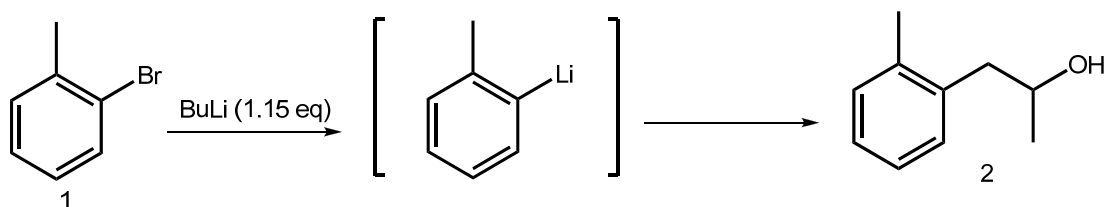
	Page
Table 21. Stable isotope compounds and amounts administered	193
Table 22. Stable isotope compounds and amounts administered (continued).....	194
Table 23. Carbon shifts (ppm) for azinomycin B and related compounds.....	196
Table 24. Stable isotope compounds and the calculated % Incorporation as calculated in standardized reference to C3'OCH ₃ or C20.....	239
Table 25. Stable isotope compounds and the calculated % Incorporation as calculated in standardized reference to C3'OCH ₃ or C20.....	240
Table 26. Stable isotope compounds and the calculated % Incorporation as calculated in standardized reference to C3'OCH ₃ or C20.....	241
Table 27. Stable isotope compounds and the calculated % Incorporation as calculated in standardized reference to C3'OCH ₃ or C20.....	242
Table 28. Stable isotope compounds and the calculated % Incorporation as calculated in standardized reference to C3'OCH ₃ or C20.....	243
Table 29. Stable isotope compounds and the calculated % Incorporation as calculated in standardized reference to C3'OCH ₃ or C20.....	244
Table 30. Stable isotope compounds and the calculated % Incorporation as calculated in standardized reference to C3'OCH ₃ or C20.....	245
Table 31. Stability of compounds T3, T4, T5 after 48 h under aqueous conditions as judged by NMR spectroscopy	283

SUPPLEMENTARY DATA FOR CHAPTER II AND CHAPTER III

NAPHTHOIC ACID SYNTHESIS

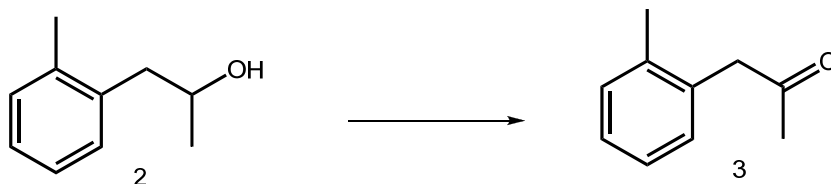
COMPOUND USED IN CHAPTER II AND CHAPTER III

(SYNTHESIZED BY DR. CHAOMIN LIU)



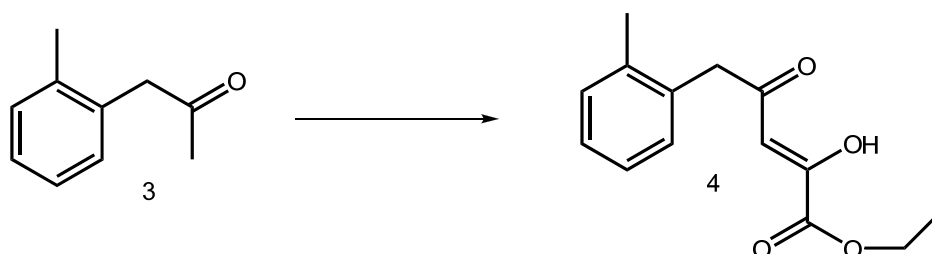
Scheme 7. Synthesis of 1-o-Tolyl-propan-2-ol.

To a solution of 2-Bromotoluene, **1**, (171 mg, 1.0 mmol) in dry ethyl ether (5 mL) at -78 °C was added butyllithium (0.46 mL, 2.5 M in hexane) drop wise. Following addition, the cold bath was removed, and the reaction mixture was allowed to warm to room temperature (RT). After an additional 3 h of stirring, the reaction mixture was cooled to -78 °C, and a solution of propylene oxide (0.14 mL in 0.14 mL of ethyl ether) was added drop wise. Stirring was continued at -78 °C for an additional hour, and then the reaction was allowed to warm to RT. The reaction was allowed to stir overnight and subsequently was quenched by the addition of water. The resulting mixture was extracted with ethyl acetate (10 mL x 3), and the organic phase was dried over MgSO₄ and concentrated. The crude product was purified by flash silica chromatography (230-400 mesh), eluting with EtOAc/hexanes (1:6), to afford **2** as a colorless oil (514 mg, yield 63%) (**Scheme 7**). 1-o-Tolyl-propan-2-ol ¹H NMR (300 MHz, CDCl₃, 25 °C) δ: 7.15 (m, 4H), 4.00 (m, 1H), 2.77 (dd, *J* = 5.4, 13.8 Hz, 1H), 2.73 (dd, *J* = 7.8, 1H, 13.8 Hz), 2.33 (s, 3H), 1.25 (d, *J* = 6.3 Hz, 3H) ¹³C NMR (75 MHz, CDCl₃, 25 °C) δ: 137.0 (C), 136.8 (C), 130.7 (CH), 130.3 (CH), 126.8 (CH), 126.2 (CH), 68.1 (CH), 43.1 (CH₂), 23.2 (CH₃), 19.8 (CH₃).



Scheme 8. Synthesis of 1-o-Tolylpropan-2-one.

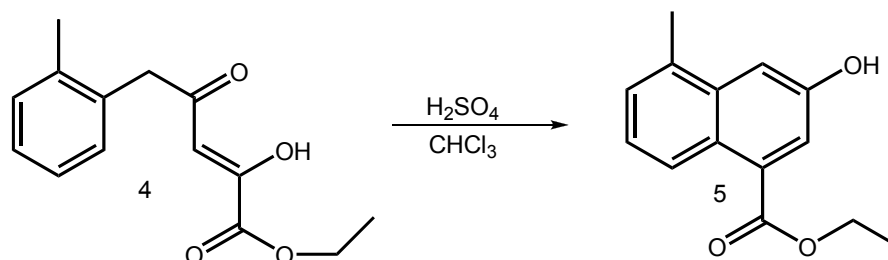
To a solution of 1-o-Tolylpropan-2-ol, **2**, (50 mg, 0.33 mmol) in ethyl acetate (2.5 mL) was added 1-hydroxy-1,2-benziodoxol-3(1H)-one-1-oxide (IBX), (280 mg, 1.0 mmol), and the reaction was stirred vigorously at 80 °C for ca. 5 h. [222] [223]. The resulting suspension was filtered, and the filter cake was rinsed three times with ethyl acetate. The combined filtrate was concentrated to afford the crude product, which was then purified by flash silica chromatography [ethyl acetate and hexane (1:6)] to afford **3** as a colorless oil (44.5 mg, yield 91%) (**Scheme 8**). 1-o-Tolylpropan-2-one ^1H NMR (300 MHz, CDCl_3 , 25 °C) δ : 7.20 (m, 4H), 3.72 (s, 2H), 2.25 (s, 3H), 2.15 (s, 3H) ^{13}C NMR (75 MHz, CDCl_3 , 25 °C) δ : 206.6 (C), 137.0 (C), 133.3 (C), 130.7 (CH), 130.5 (CH), 127.6 (CH), 126.4 (CH), 49.3 (CH_2), 29.4 (CH_3), 19.8 (CH_3).



Scheme 9. Synthesis of 2-Hydroxy-4-oxo-5-o-tolyl-pent-2-enoic acid ethyl ester.

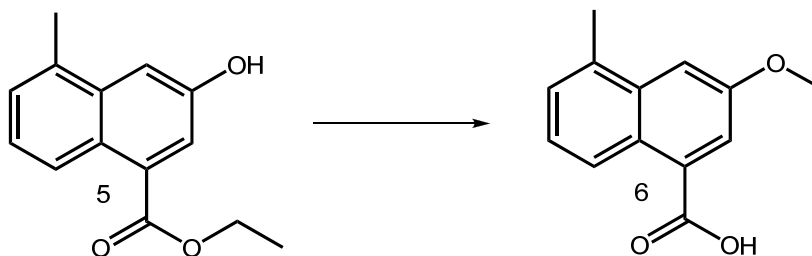
A solution of 1-o-Tolylpropan-2-one, **3**, (1.9 g, 12.8 mmol) in diethyl ether (60 mL) was cooled to 0 °C to which a solution of sodium ethoxide, NaOEt, (294 mg sodium metal, 12.8 mmol in 5 mL of ethanol) was added dropwise. The reaction was allowed to stir for about 30 min. at 0 °C, followed by the dropwise addition of diethyl oxalate (1.87 g, 12.8 mmol). The reaction mixture was subsequently stirred at RT for 24 h. The resulting pale yellow solid product was collected by filtration and washed with cold ethyl ether, giving the desired product **4** as its sodium enolate in 85% yield (2.9 g) (**Scheme 9**). The enolate was directly used in the next step without further

purification. Sodium enolate salt ^1H NMR (300 MHz, CDCl_3 , 25 °C) δ : 6.97-7.01 (m, 4H), 5.76 (s, 1H), 3.97 (q, 2H, $J = 7.2$ Hz), 3.38 (s, 2H), 2.11 (s, 3H), 1.15 (t, $J = 7.2$ Hz, 3H).



Scheme 10. Synthesis of 3-Hydroxy-5-methyl-naphthalene-1-carboxylic acid ethyl ester.

Concentrated sulfuric acid (0.5 mL) was added slowly to a chilled solution of the sodium enolate of **4** (65.7 mg, 0.24 mmol) in chloroform (9 mL), with vigorous stirring. Following addition, the reaction mixture was stirred continuously at 0 °C for about 20 min. The reaction was then warmed to RT and stirred for an additional 30 min. The reaction mixture was poured into ground ice (25 mL), extracted with methylene chloride (25 mL x 4), dried over MgSO_4 , and concentrated in vacuo. The organic residue was subsequently purified by flash silica chromatography (1:5 EtOAc/Hexanes) to generate the desired product 3-hydroxy-5-methyl-naphthalene-1-carboxylic acid ethyl ester **5** (38.7 mg, 71% yield) (**Scheme 11**). 3-hydroxy-5-methyl-naphthalene-1-carboxylic acid ethyl ester ^1H NMR (300 MHz, CDCl_3 , 25 °C) δ : 8.61 (m, 1H), 7.81 (d, $J = 2.7$ Hz, 1H), 7.54 (dd, $J = 0.75, 2.7$ Hz, 1H), 7.34-7.38 (m, 2H), 5.81 (bs, 1H, OH), 4.50 (q, $J = 7.2$ Hz, 2H), 2.63 (s, 3H), 1.48 (t, $J = 7.2$ Hz, 3H) ^{13}C NMR (75 MHz, CDCl_3 , 25 °C) δ : 168.0 (C), 152.2 (C), 134.8 (C), 133.2 (C), 130.2 (C), 127.8 (CH), 127.1 (C), 125.1 (CH), 124.1 (CH), 121.1 (CH), 111.7 (CH), 61.7 (CH_2), 20.2 (CH_3), 14.6 (CH_3).



Scheme 11. Synthesis of 3-Methoxy-5-methyl-naphthalene-1-carboxylic acid (naphthoate).

To a solution of 3-Hydroxy-5-methyl-naphthalene-1-carboxylic acid ethyl ester **5** (101 mg, 1.0 mmol) and dimethyl sulfate (142.3 mg, 1.1 mmol) in 0.5 mL of dioxane was added a 25% solution of aqueous sodium hydroxide (1.5 mL). After stirring at RT for 30 min, the mixture was heated to ~100 °C for 6 h and cooled to RT.

The resulting basic mixture was extracted with dichloromethane (3 mL x 2). The aqueous phase was acidified to pH 5 by addition of concentrated hydrochloride and extracted with ethyl acetate (5 mL x 3). The organics were dried over MgSO₄ and concentrated *in vacuo* to afford the final product **6** as a pale white solid in quantitative yield (**Scheme 11**). 3-Methoxy-5-methyl-naphthalene-1-carboxylic acid (naphthoate) ¹H NMR (300 MHz, CDCl₃, 25 °C) δ: 8.30 (m, 1H), 8.05 (d, *J* = 2.4 Hz, 1H), 7.54 (d, *J* = 2.4 Hz, 1H), 7.38-7.43 (m, 2H), 3.99 (s, 3H), 2.69 (s, 3H) ¹³C NMR (75 MHz, CDCl₃, 25 °C) δ: 172.9 (C), 155.8 (C), 134.4 (C), 133.2 (C), 127.8 (C), 127.6 (CH), 127.1 (C), 125.2 (CH), 123.9 (CH), 122.8 (CH), 109.3 (CH), 55.5 (CH₃), 20.2 (CH₃).

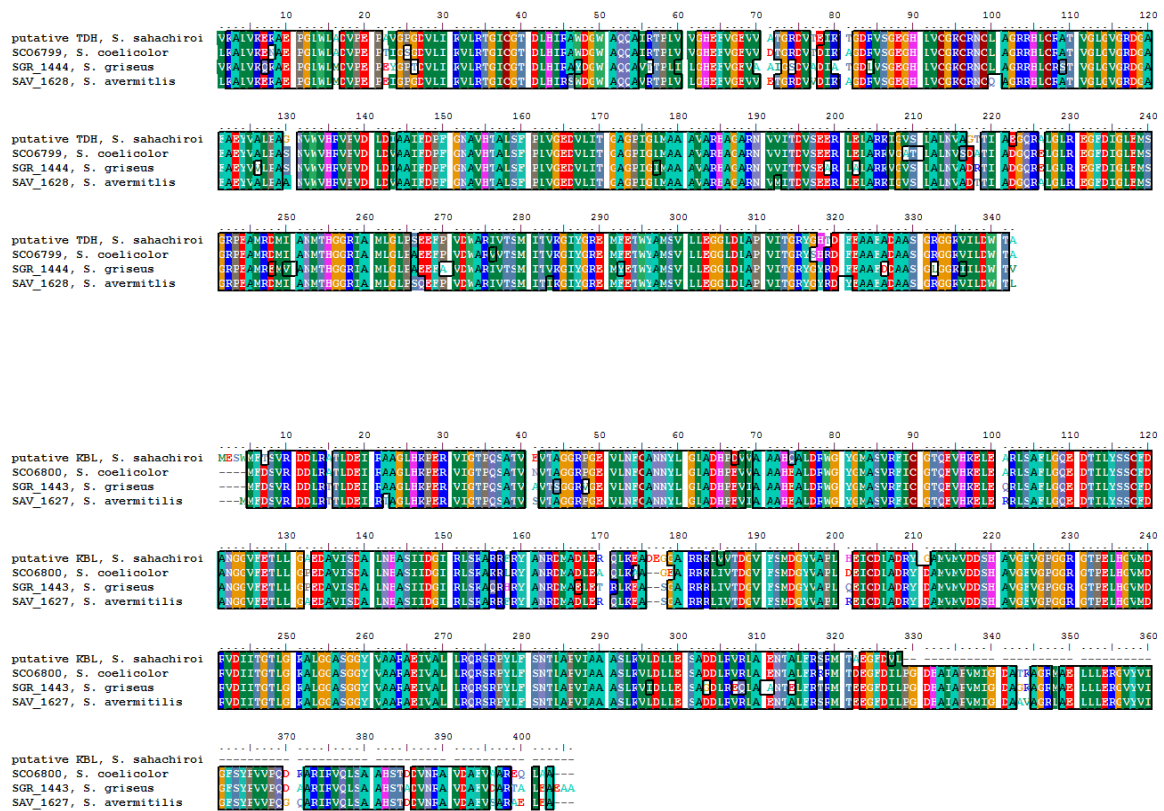


Figure 111. CLUSTALW alignment of threonine-3-dehydrogenases and 2-amino-3-ketobutyrate CoA ligases in *Streptomyces sp.*

Table 21. Stable isotope compounds and amounts administered.

Substrate	ID	Amount administered	
		mg	mmoles
[Methyl- ¹³ C] L-methionine		50	0.333
[1- ¹³ C] sodium acetate		1000	12.044
Epoxide Moiety Series			
[1- ¹³ C] L-valine	V2	100	0.847
[1- ¹³ C] L-valine TFA	V2	100	0.847
[1- ¹⁵ N] L-valine	V2	250	2.119
[1- ¹³ C] L-γ-hydroxyvaline ((2S)-2-amino-4-hydroxy-3-methylbutanoic acid)	V3	140	1.045
[1- ¹³ C] D-γ-hydroxyvaline ((2R)-2-amino-4-hydroxy-3-methylbutanoic acid)	V3*	140	1.045
[1- ¹³ C] R-keto hydroxy acid (4-hydroxy-3-methyl-2-oxobutanoic acid)	V5	166	1.239
[1- ¹³ C] epoxy-keto acid (2-(2-methyloxiran-2-yl)-2-oxoacetic acid)	V8	90	0.687
[1- ¹³ C] epoxy-hydroxy acid ((2S)-2-hydroxy-2-(2-methyloxiran-2-yl)acetic acid)	V9	75	0.564
[1- ¹³ C] isodehydrovaline HCl (2-amino-3-methylbut-3-enoic acid hydrochloride)	V10	90	0.596
[1- ¹³ C] allyl-hydroxy acid (2-hydroxy-3-methylbut-3-enoic acid)	V11	100	0.855
[1- ¹³ C] sodium allylketocarboxylate (sodium 3-methyl-2-oxobut-3-enoate)	V12	127	0.927
[1- ¹³ C] allylketocarboxylate (3-methyl-2-oxobut-3-enoate)	V12	127	0.927
Enol and azinomycin A end fragment Series			
[U- ¹³ C4] L-threonine	T2/AA3	97	0.708
[U- ¹³ C4] Ketocarboxylate threonine TFA ((S)-2-amino-3-oxobutanoic acid)	T3/AA4	124	0.569
[U- ¹³ C4] Hydroxy aldehyde threonine TFA ((2S)-2-amino-3-hydroxybutanal)	T4	163	0.799
[U- ¹³ C4] Keto aldehyde threonine TFA ((R)-2-amino-3-oxobutanal)	T5	169	0.837
[1- ¹³ C] L-Threonine	T2/AA3	100	0.746
[¹⁵ N] L-Threonine	T2/AA3	230	1.716
[2- ¹³ C] glycine	AA6	1000	13.146
[1- ¹³ C] glycine	AA6	100	1.315
[1- ¹³ C] glycine	AA6	1000	13.146
[¹⁵ N] glycine	AA6	1000	13.146
[2,2-D2] glycine	AA6	1000	12.975
[2- ¹³ C] aminoacetone (1-aminopropan-2-one)	AA5	300	4.049

Table 22. Stable isotope compounds and amounts administered (continued).

Substrate	ID	Amount administered	
		mg	mmoles
Oxygen Origin Series			
[U- ¹⁸ O ₂] oxygen gas		3 Liters	133.929
[U- ¹⁸ O ₂] oxygen gas		3.7 Liters	165.179
Azabicyclic Moiety Series			
[3- ¹³ C] L-aspartate		100	0.746
[U- ¹⁵ N ₂] L-asparagine		220	1.641
[1,2- ¹³ C ₂] L-ornithine		100	0.745
[1- ¹³ C] L-proline		100	0.862
[1- ¹³ C] L-lysine		100	0.680
[2- ¹³ C] L-serine		100	0.943
[U- ¹³ C ₆] L-arginine		100	0.555
[1- ¹³ C] D-arabinose		900	5.955
[1- ¹³ C] D-xylose		900	5.955
[U- ¹³ C ₆] D-glucose		1000	5.372
[1- ¹³ C] pyroglutamic acid, 17	AZ17	160	1.230
[1- ¹³ C] pyroglutaminol, 5	AZ5	140	1.206
[1- ¹³ C] (3S,4R)-3,4-dihydroxy-5-(hydroxymethyl)pyrrolidin-2-one, 16a	AZ16a	200	1.350
[1- ¹³ C] (3R,4S)-3,4-dihydroxy-5-(hydroxymethyl)pyrrolidin-2-one, 16b	AZ16b	200	1.350
[1- ¹³ C] 3, 4 dihydroxy glutamic acid ((3S,4R)-2-amino-3,4-dihydroxypentanedioic acid), 15a	AZ15a	200	1.110
[1- ¹³ C] 3, 4 dihydroxy glutamic acid ((3R,4S)-2-amino-3,4-dihydroxypentanedioic acid), 15b 250mg	AZ15b	250	1.388
[1- ¹³ C] DL-glutamic acid	AZ6	231	1.559
[1- ¹³ C] DL-glutamic acid	AZ6	1000	6.751

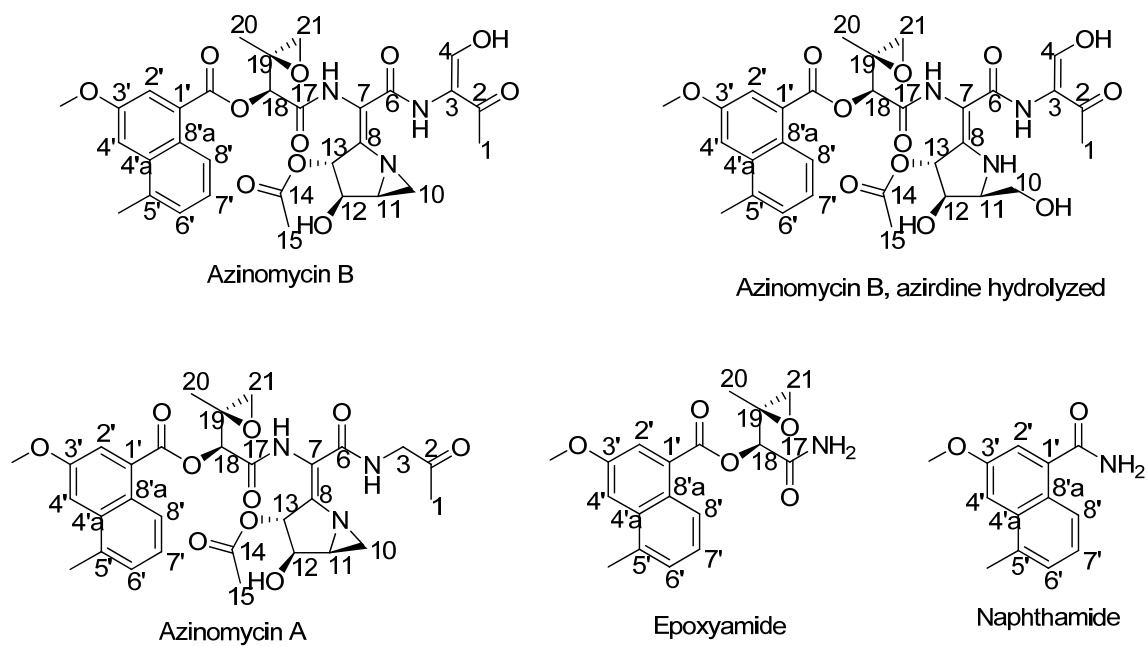


Figure 112. Major species identified in the purification of the azinomycins with carbon positional number assignment.

Many of these species were found in crude extract spectra from *S. sahachiroi*. ^{13}C shifts are reported in Table 23.

Table 23. Carbon shifts (ppm) for azinomycin B and related compounds.
Carbon positions as numbered in Figure 112.

Carbon Position	Azinomycin B	Azinomycin B, azirdine hydrolyzed	Azinomycin A	Epoxyamide	Naphthamide
	ppm	ppm	ppm	ppm	ppm
C1	24.5	24.3	27.2		
C2	191.5	191.3	202.6		
C3	118.6	118.1	50.6		
C4	150.8	149.7			
C6	162.0	166.2	163.2		
C7	119.3	93.0	120.1		
C8	153.0	157.2	149.6		
C10	36.7	63.3	35.8		
C11	46.4	43.7	45.4		
C12	77.4	73.9	76.9		
C13	84.4	81.2	84.0		
C14	173.0	171.6	172.7		
C15	21.0	21.2	20.7		
C17	164.0	168.6	163.8	168.7	
C18	77.1	77.6	76.7	75.9	
C19	56.2	56.4	56.0	55.8	
C20	17.2	18.0	17.0	17.6	
C21	53.9	54.1	53.7	53.3	
C1'	128.1	128.4	128.4	128.3	133.6
C1' CO	165.7	166.9	165.7	165.6	173.3
C2'	122.3	122.5	121.8	122.0	117.5
C3'	156.0	156.1	156.0	155.9	156.6
C3' OCH ₃	55.7	55.9	55.6	55.6	55.6
C4'	108.5	108.9	108.6	108.5	105.7
C4'a	134.5	134.7	134.4	134.4	134.6
C5'	133.3	133.5	133.1	133.2	133.6
C5' CH ₃	20.3	20.5	20.0	20.0	20.0
C6'	127.9	128.1	127.7	127.8	128.0
C7'	125.4	125.6	125.1	125.2	124.6
C8'	123.9	124.2	123.9	123.8	123.7
C8'a	127.0	127.2	126.9	126.9	125.9

Spectral Data for Isotopically Labeled Compound Feeding Experiments.

***X denotes impurity.**

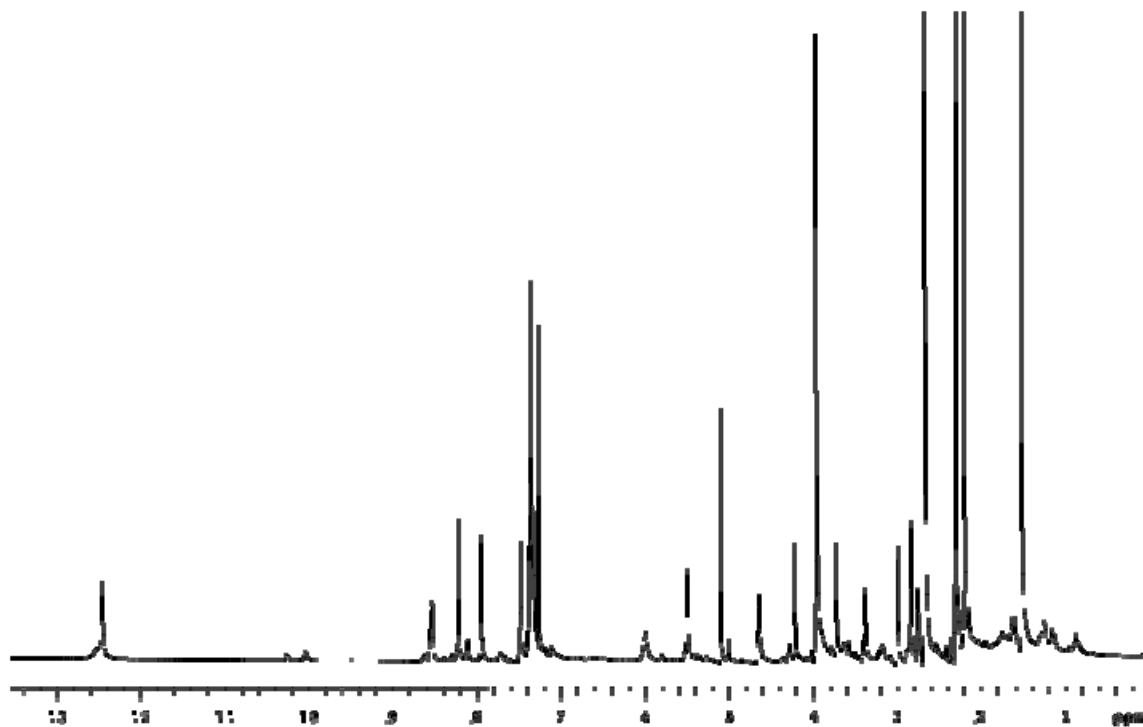


Figure 113. ^1H Spectra standard for azinomycin B.

D:\Coran\GA02

8/14/2008 4:37:16 PM

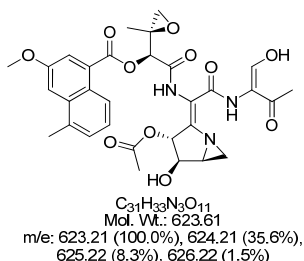
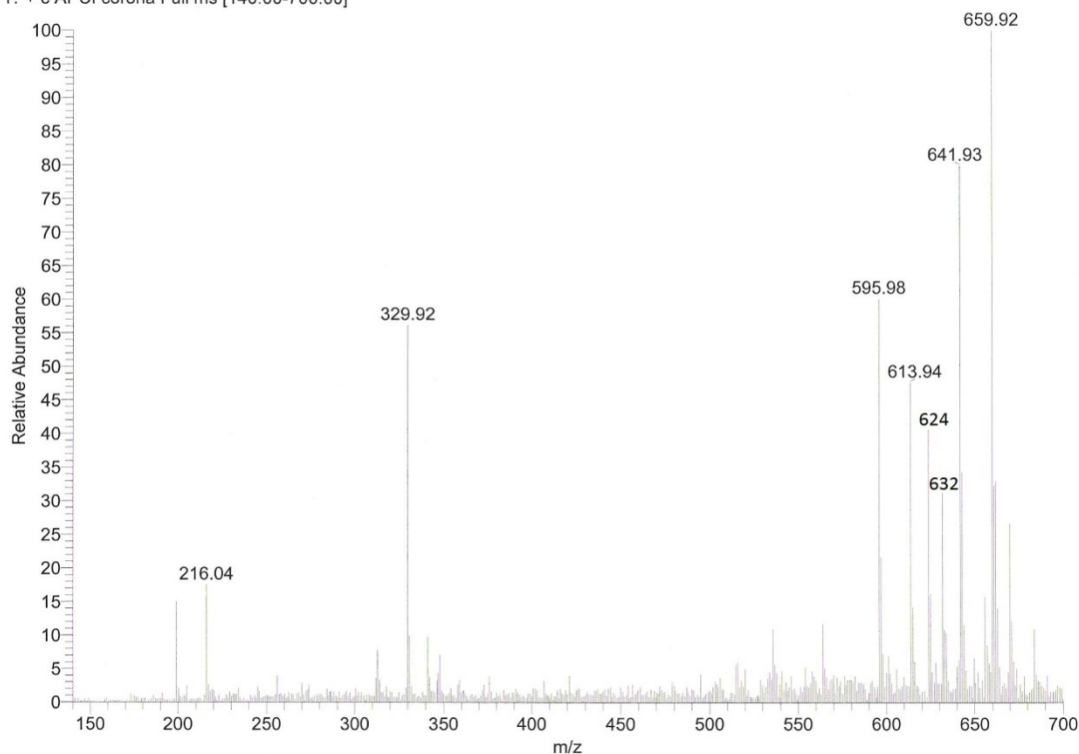
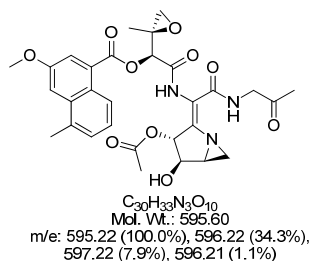
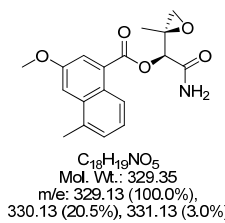
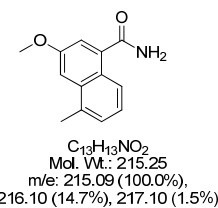
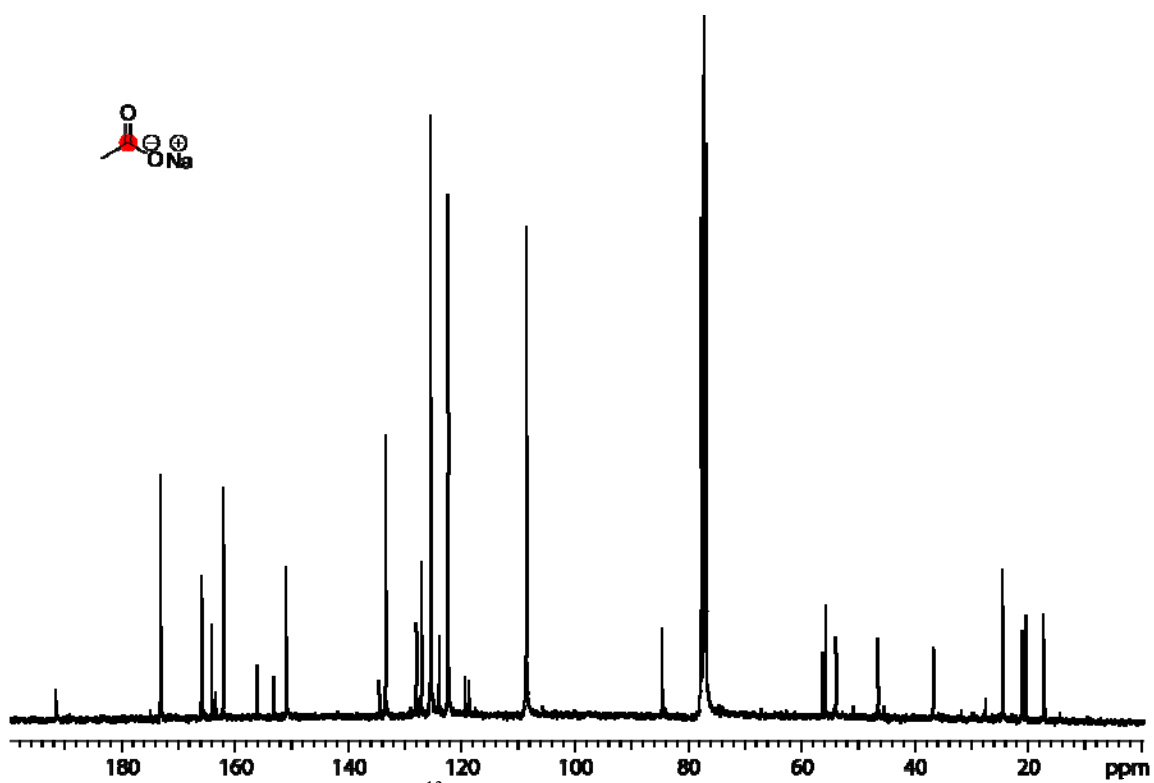
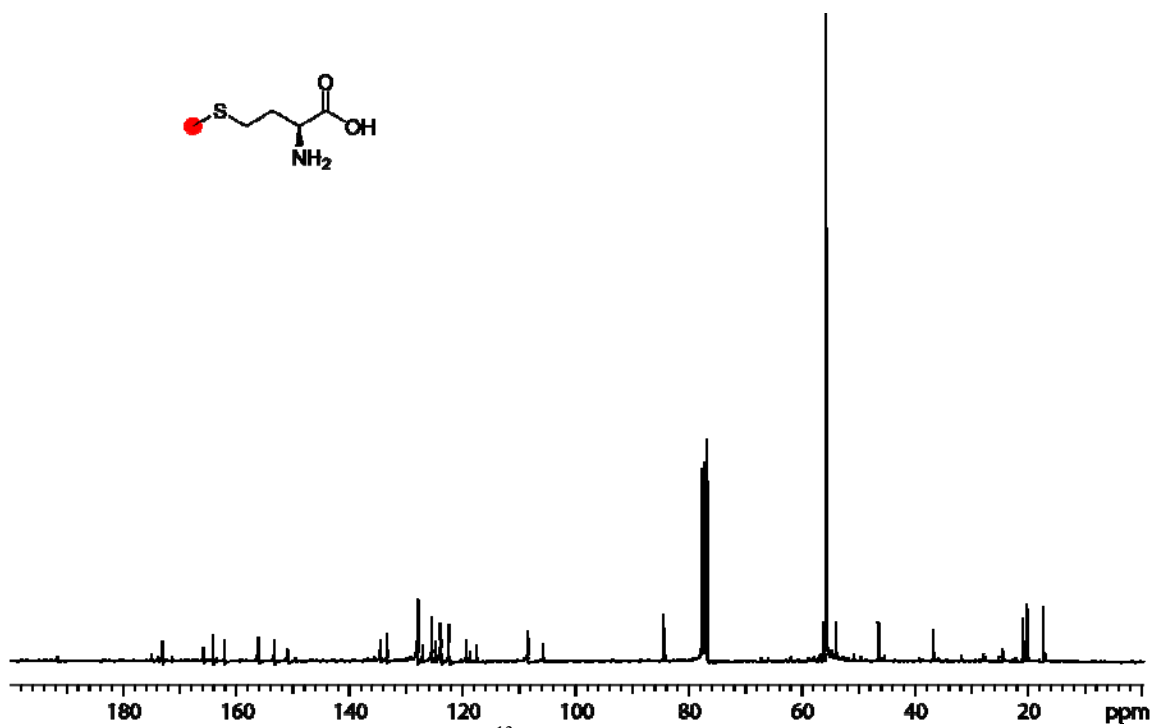
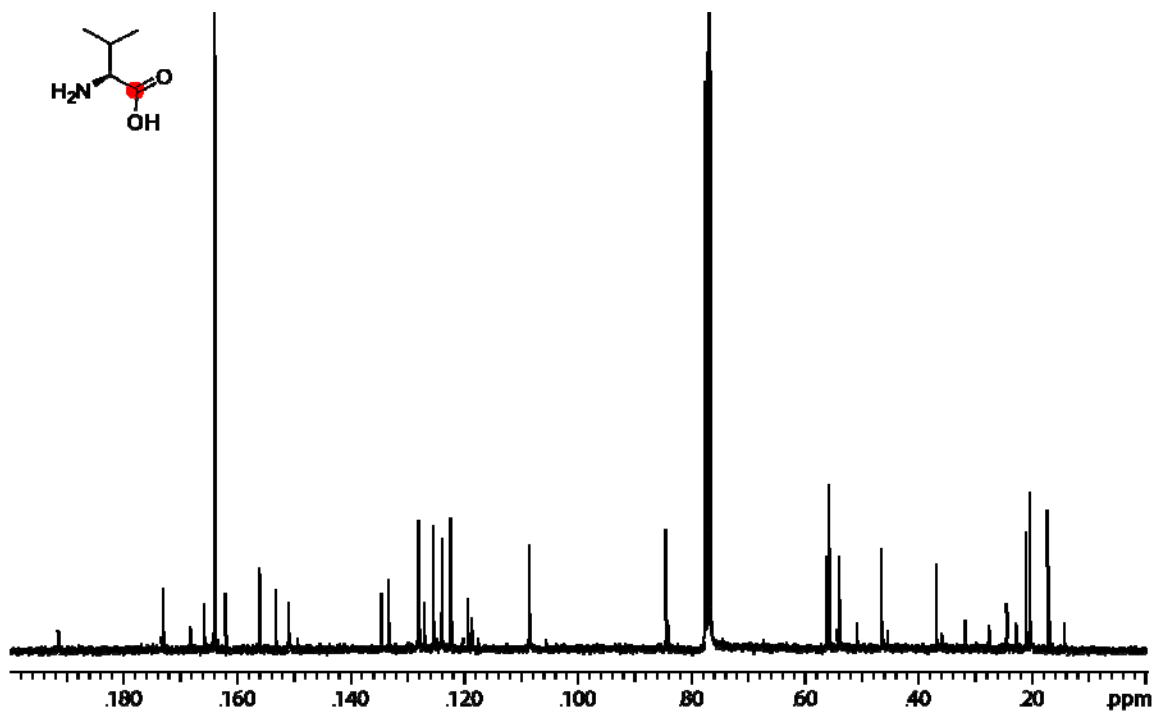
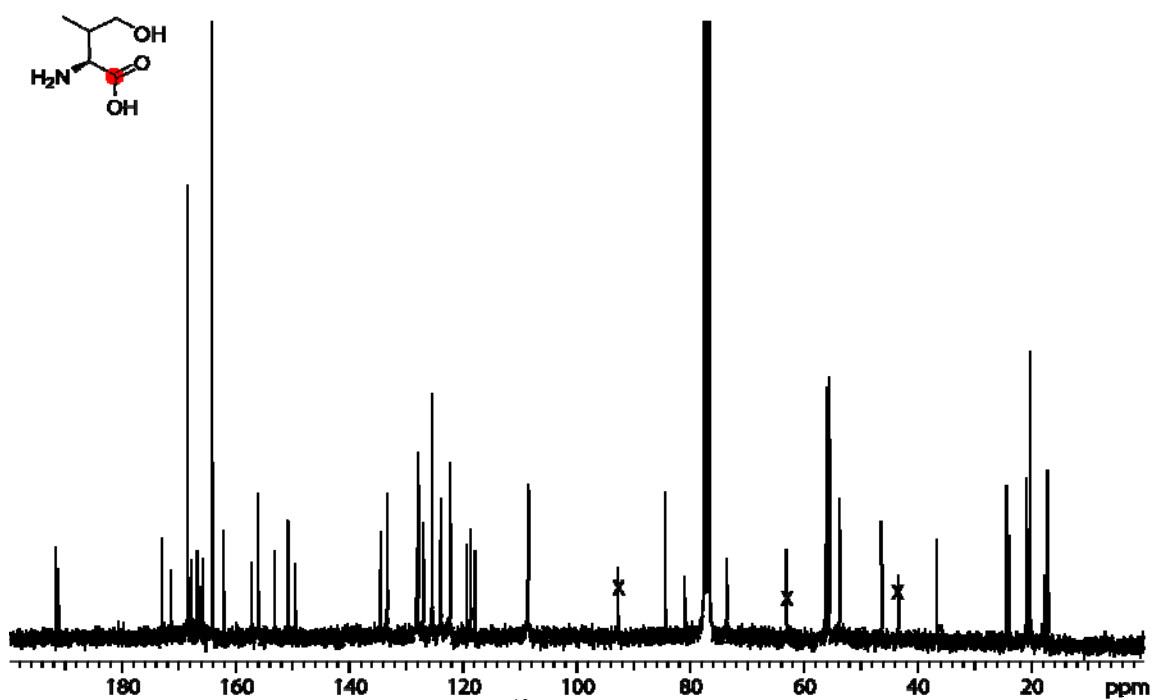
GA02 #71-280 RT: 0.78-2.95 AV: 210 NL: 1.89E7
T: + c APCI corona Full ms [140.00-700.00]**Azinomycin B****Azinomycin A****Epoxyamide****Naphthamide**

Figure 115. Representative APCI Mass Spectrometry Spectrum detecting azinomycin B and related structures.

A typical analysis of an azinomycin sample using atmospheric pressure chemical ionization mass spectrometry (APCI-MS). Key species observed (structures shown below) include: 216 (naphthamide + H⁺); 330 (epoxyamide + H⁺); 556 (azinomycin A + H⁺); 614 (azinomycin A (with 1 ring hydrolyzed) + H⁺); 632 (azinomycin A (with 2 rings hydrolyzed) + H⁺); 624 (azinomycin B + H⁺); 642 (azinomycin B (with 1 ring hydrolyzed) + H⁺); 660 (azinomycin B (with 2 rings hydrolyzed) + H⁺).



BIOSYNTHETIC ROUTE TO THE EPOXIDE MOIETY INCORPORATION SERIES

Figure 118. Azinomycin B, fed [1-¹³C] L-valine (V2) 100mg.Figure 119. Azinomycin B, fed [1-¹³C] L-γ-hydroxyvaline ((2S)-2-amino-4-hydroxy-3-methylbutanoic acid) (V3) 140mg.

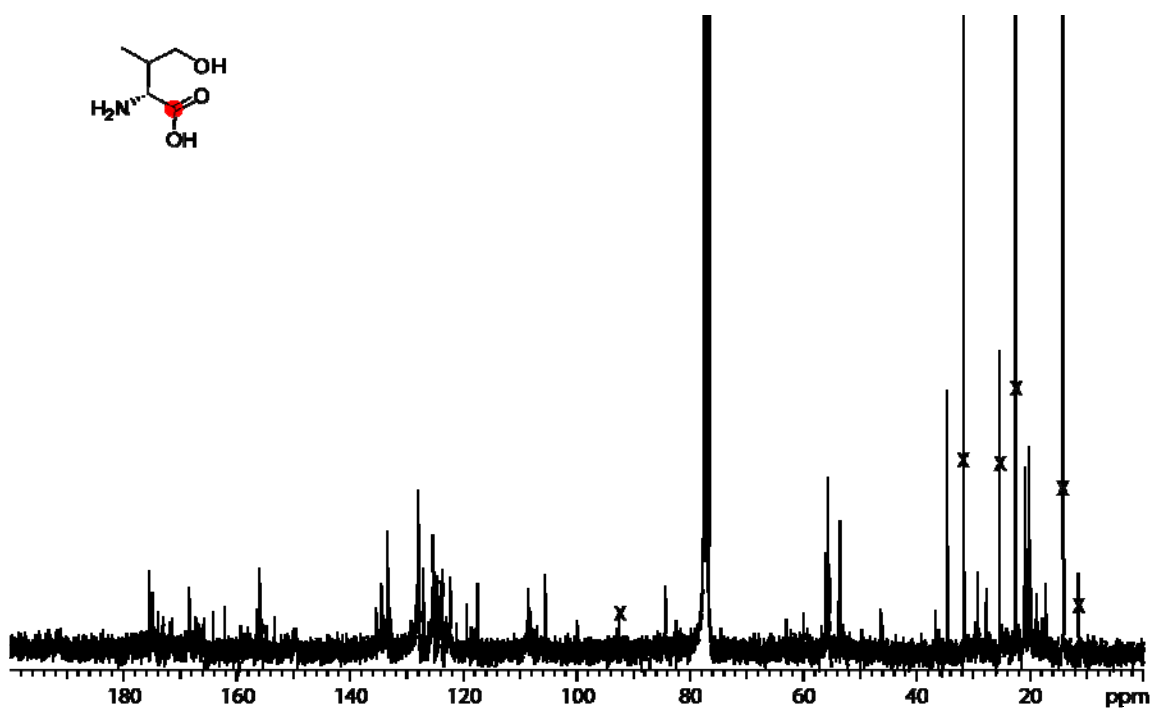


Figure 120. Azinomycin B, fed [^{13}C] D- γ -hydroxyvaline ((2R)-2-amino-4-hydroxy-3-methylbutanoic acid) (V3) 100mg.

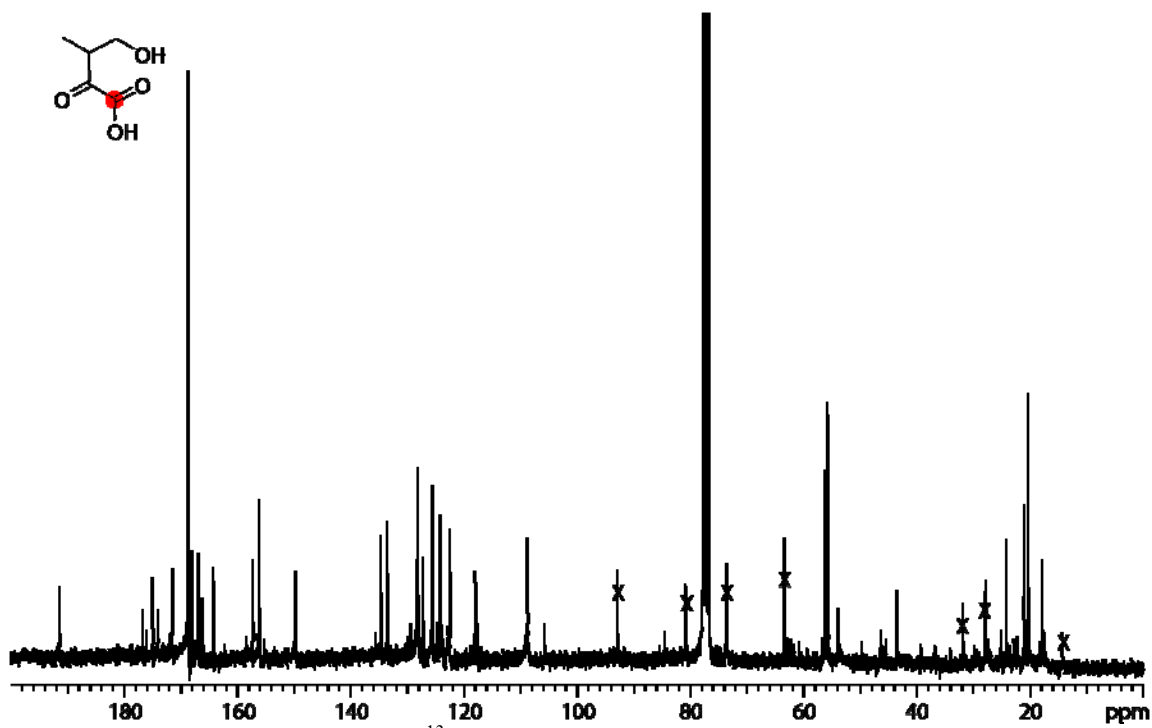
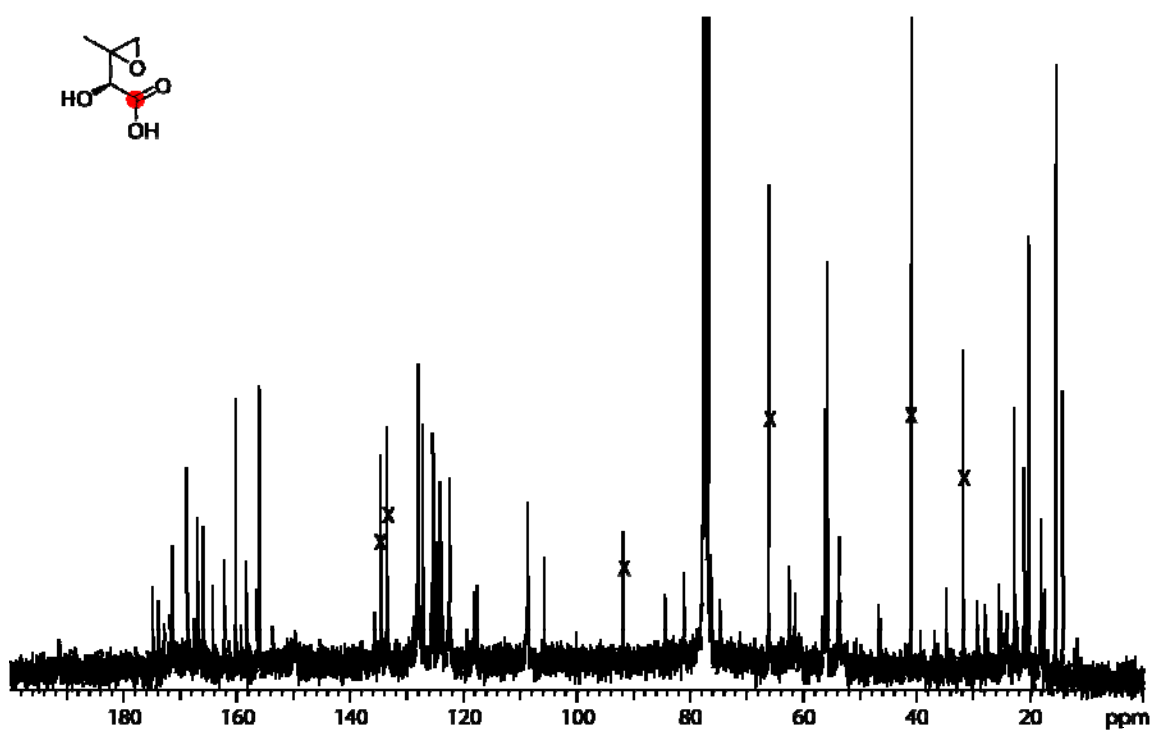
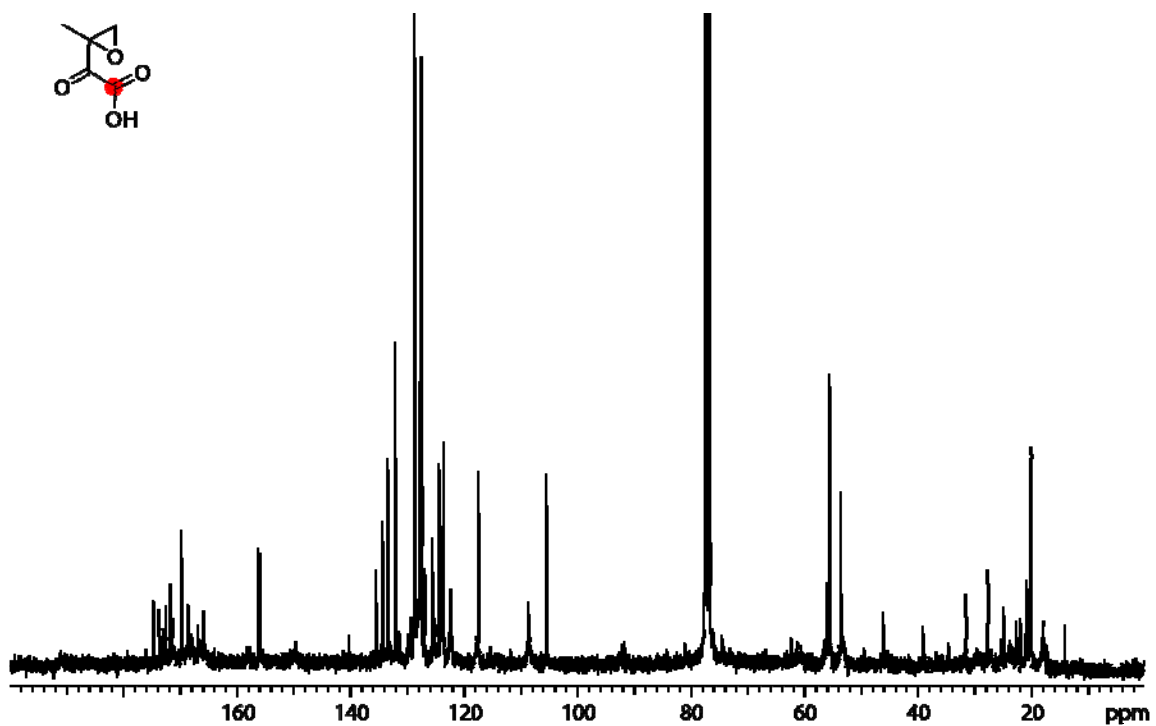


Figure 121. Azinomycin B, fed [^{13}C] R-keto hydroxy acid (4-hydroxy-3-methyl-2-oxobutanoic acid) (V5) 150mg.



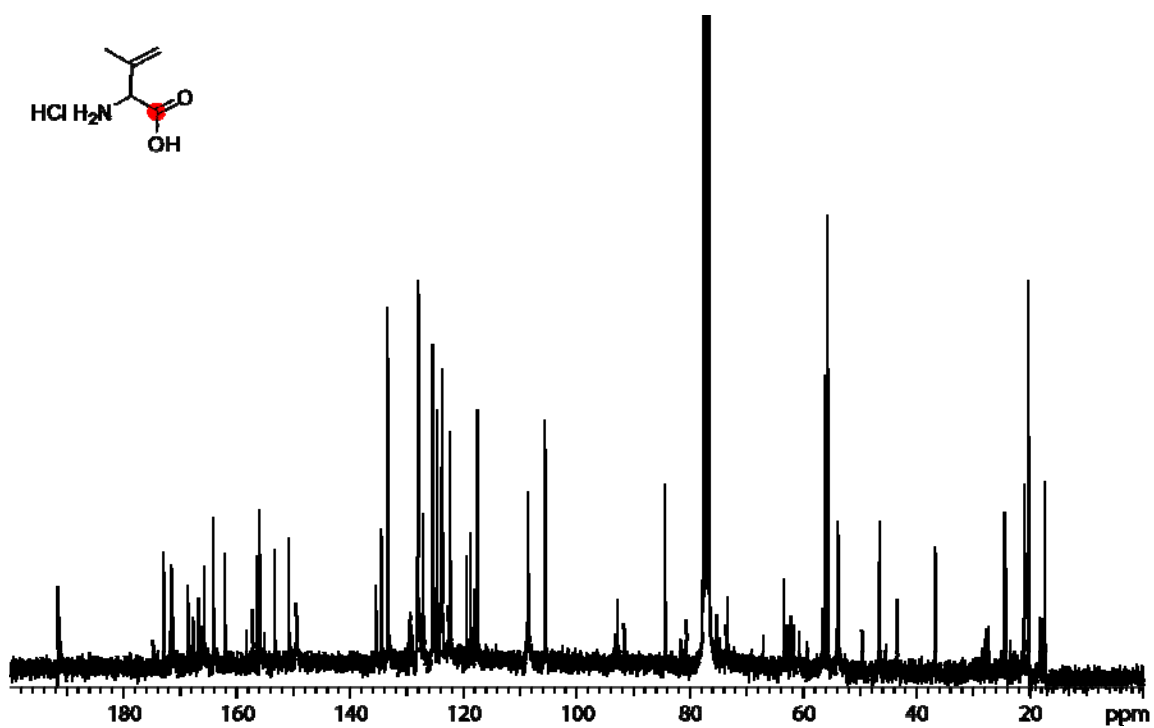


Figure 124. Azinomycin B, fed [¹³C] Isodehydrovaline (2-amino-3-methylbut-3-enoic acid hydrochloride) (V10) 90mg.

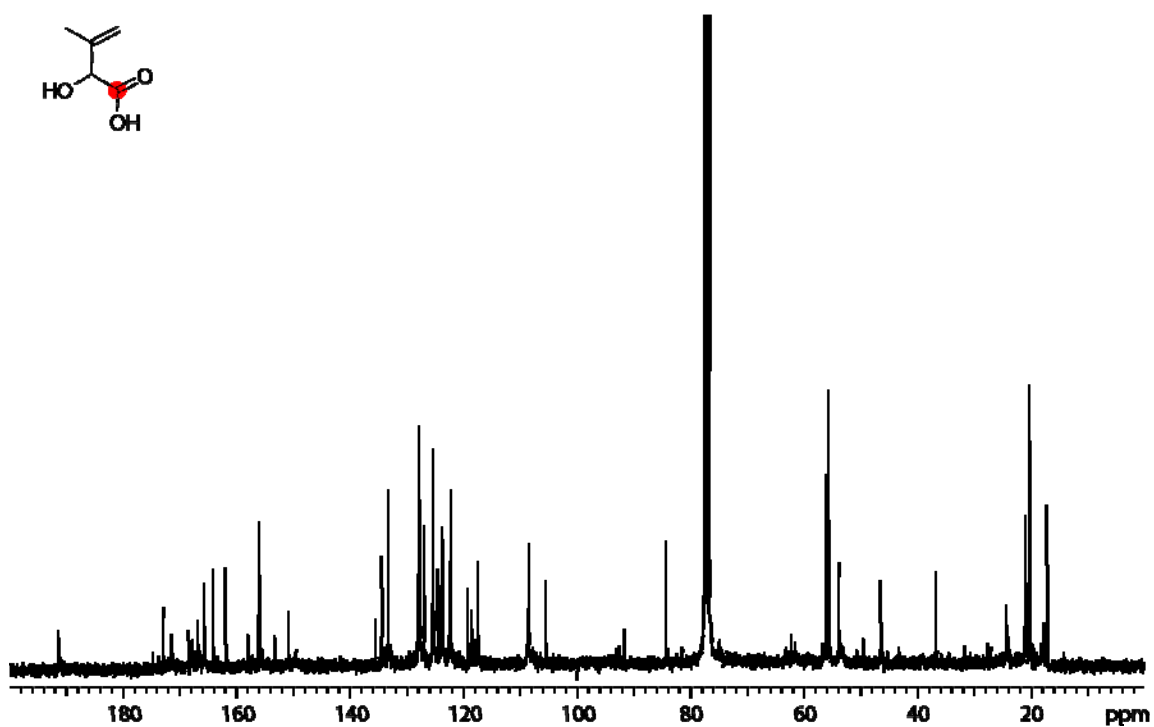


Figure 125. Azinomycin B, fed [¹³C] allyl-hydroxy acid (2-hydroxy-3-methylbut-3-enoic acid) (V11) 100mg.

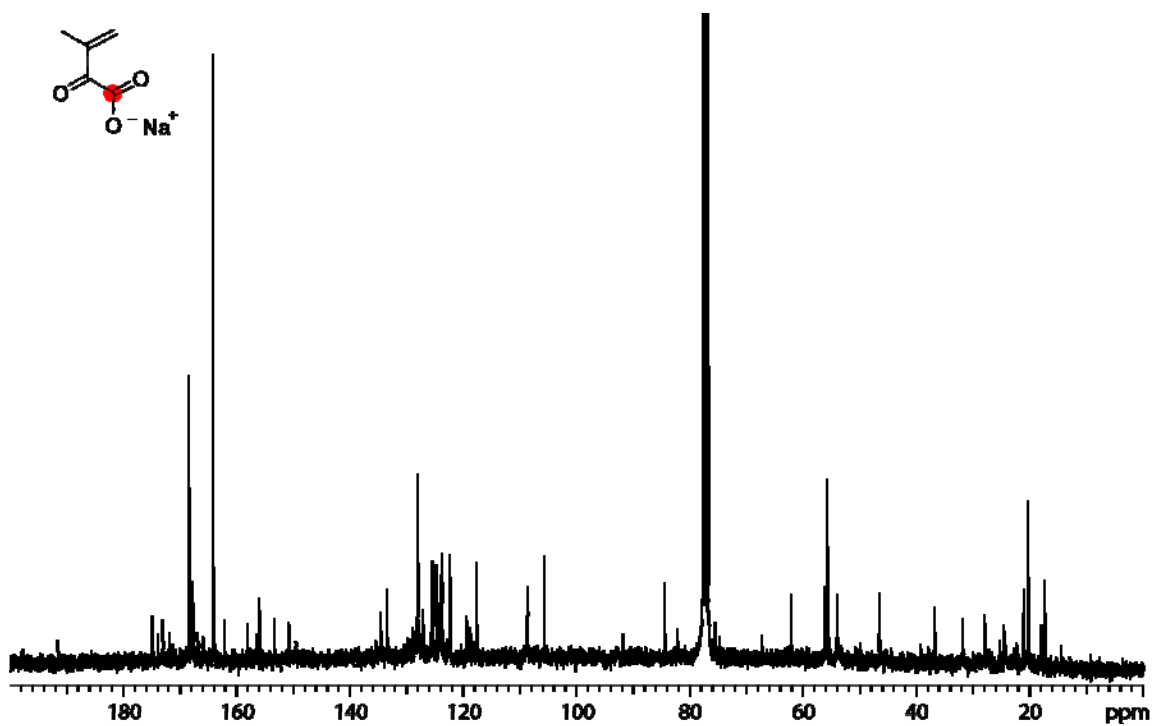


Figure 126. Azinomycin B, fed [^{13}C] sodium allylketocarboxylate (sodium 3-methyl-2-oxobut-3-enoate) (V12) 127mg.

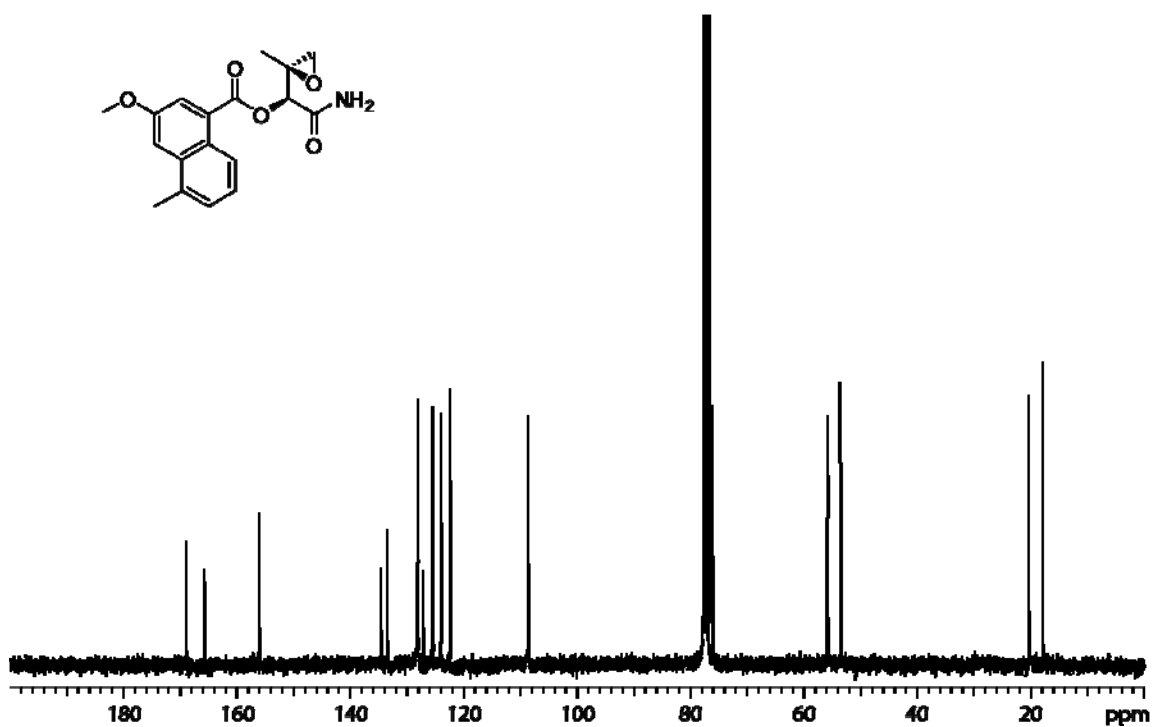


Figure 127. Epoxyamide ((S)-2-amino-1-((S)-2-methyloxiran-2-yl)-2-oxoethyl 3-methoxy-5-methyl-1-naphthoate) (Supplied pure courtesy of Dr. Robert Coleman).

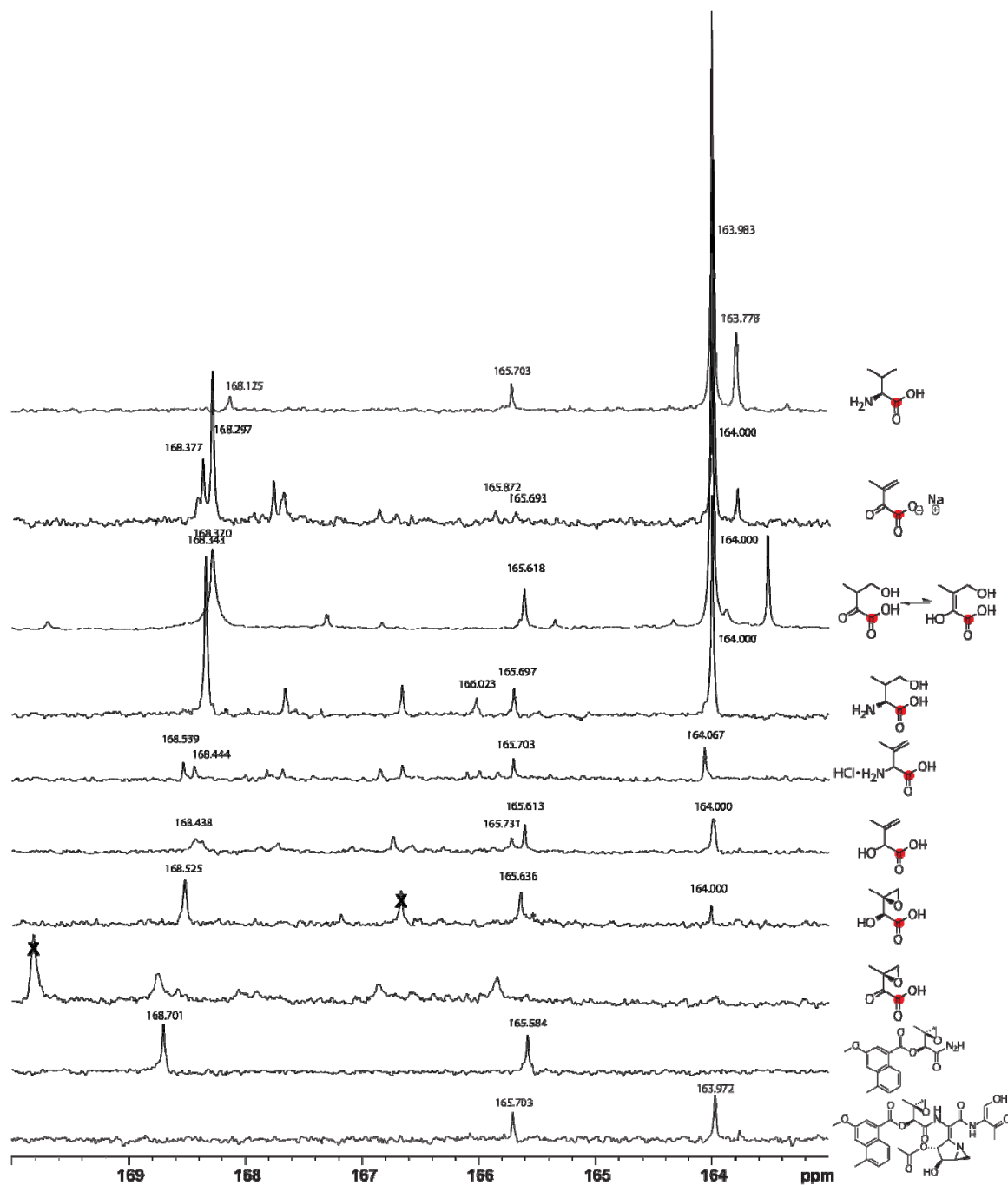


Figure 128. Overlay of Azinomycin B ^{13}C -NMR Spectra at 164.0 ppm and 168.9 ppm for all the fed valine derivative series and the epoxyamide.

BIOSYNTHETIC ROUTE TO THE ENOL MOIETY INCORPORATION SERIES.

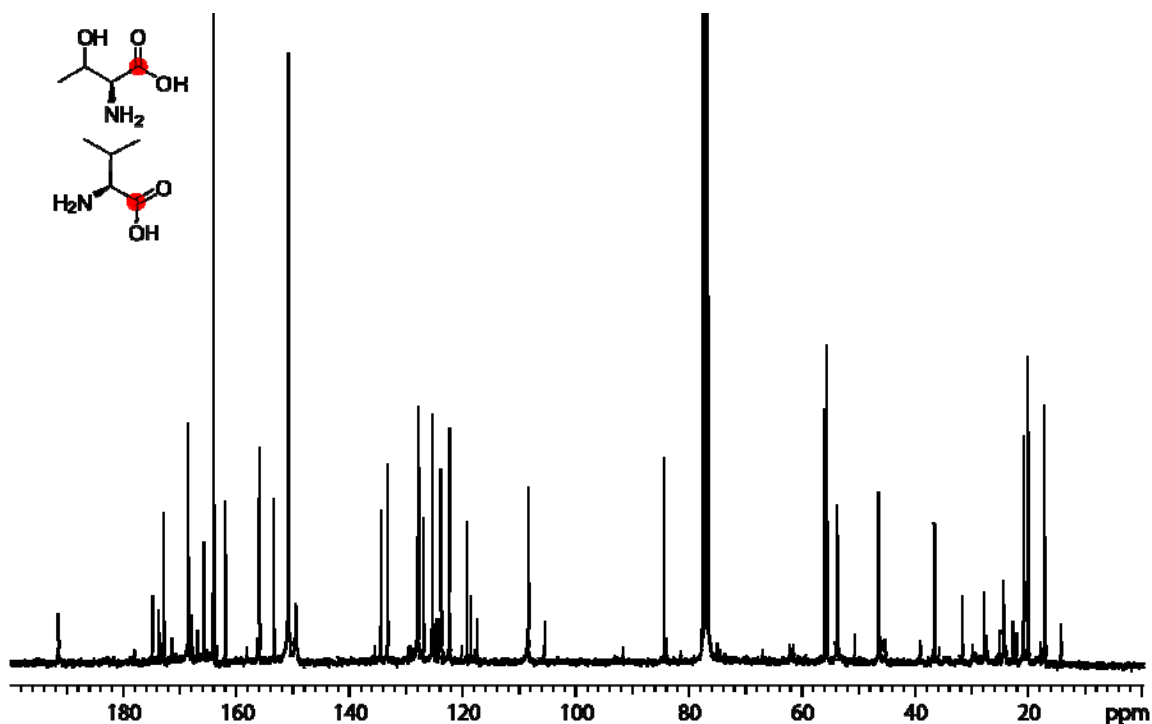


Figure 129. Azinomycin B, fed $[1-^{13}\text{C}]$ L-threonine (T2) 100mg with $[1-^{13}\text{C}]$ L-Valine (V2) 100mg.

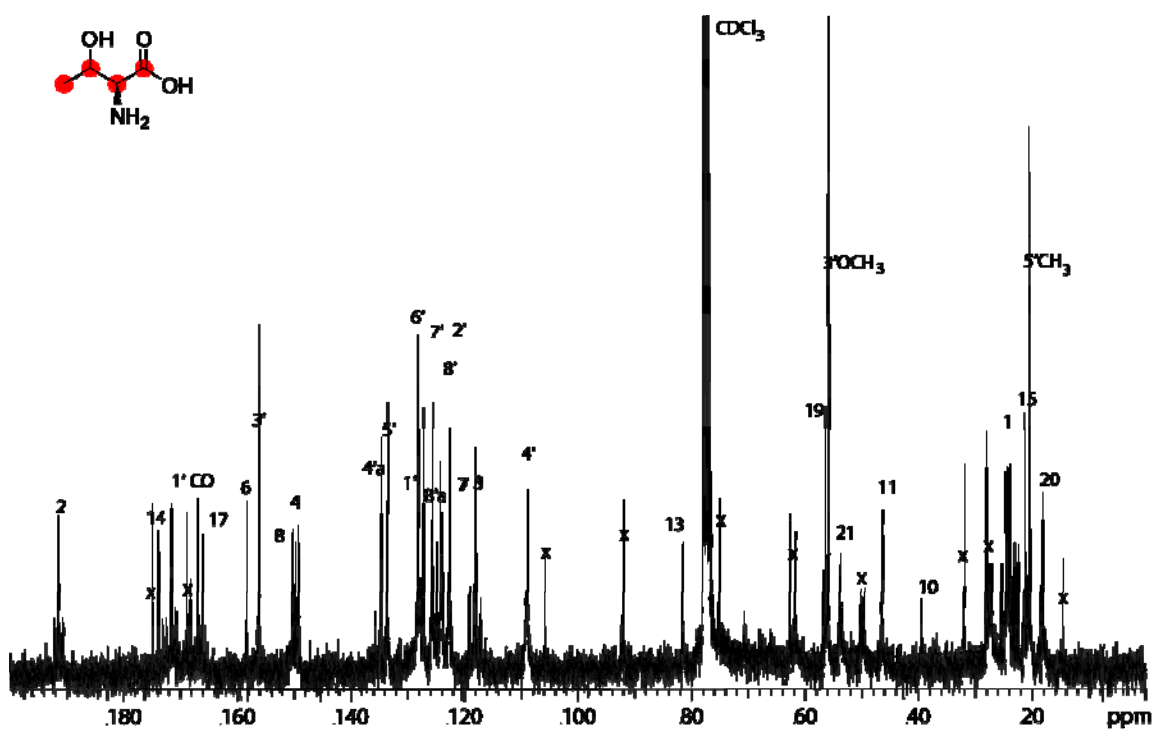


Figure 130. Azinomycin B, fed $[U-^{13}\text{C}]$ L-threonine (T2) 97mg.

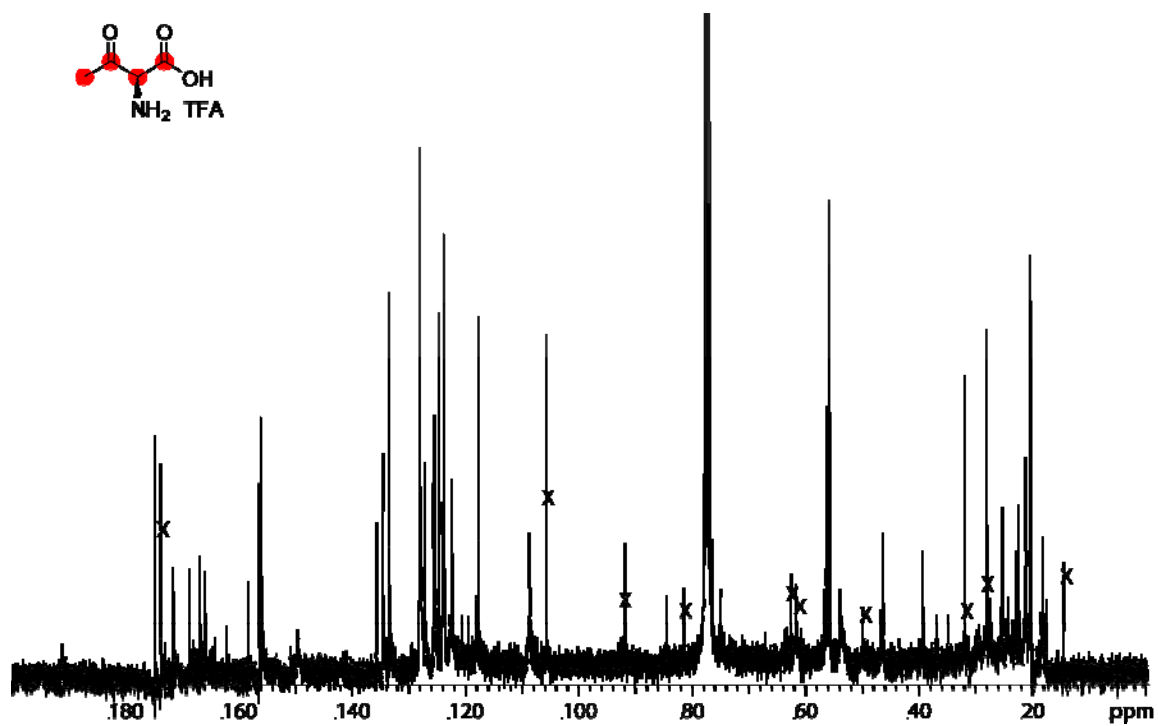


Figure 131. Azinomycin B, fed [U-¹³C] ketocarboxylate threonine TFA ((S)-2-amino-3-oxobutanoic acid) (T3) 124mg.

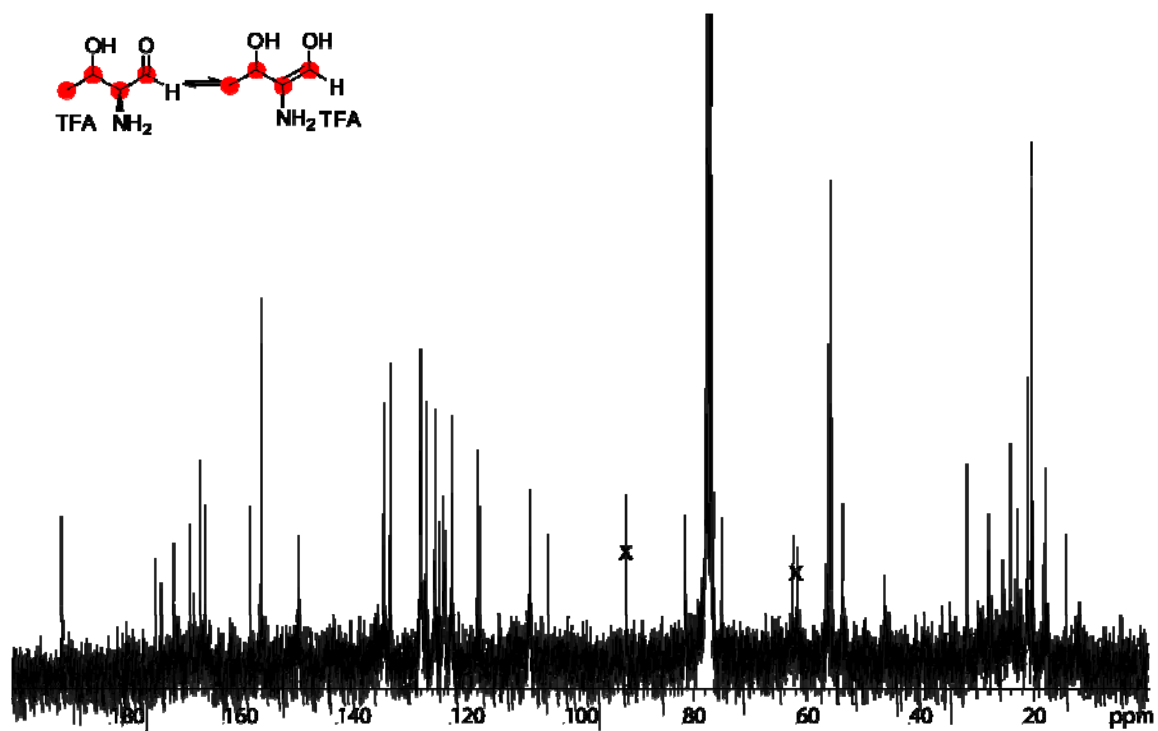


Figure 132. Azinomycin B, fed [U-¹³C] hydroxy aldehyde threonine TFA ((2S)-2-amino-3-hydroxybutanal) (T4) 163mg.

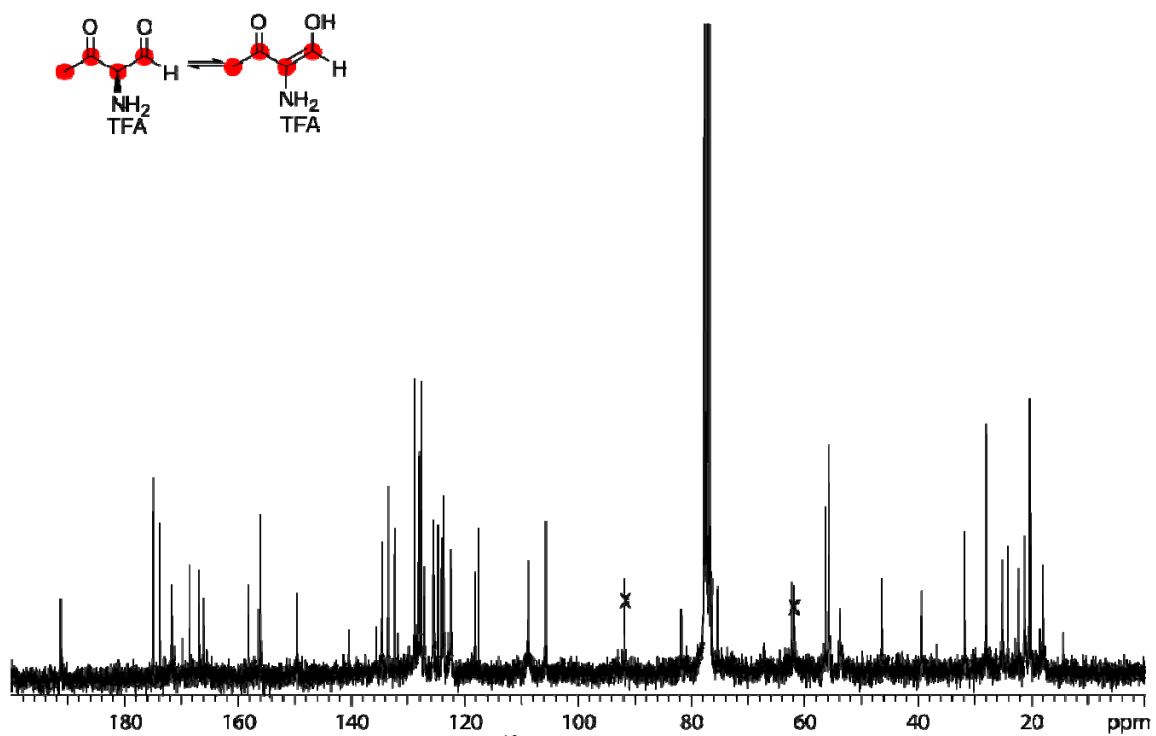


Figure 133. Azinomycin B, fed [U-¹³C] keto aldehyde threonine TFA ((R)-2-amino-3-oxobutanal) (T5) 169mg.

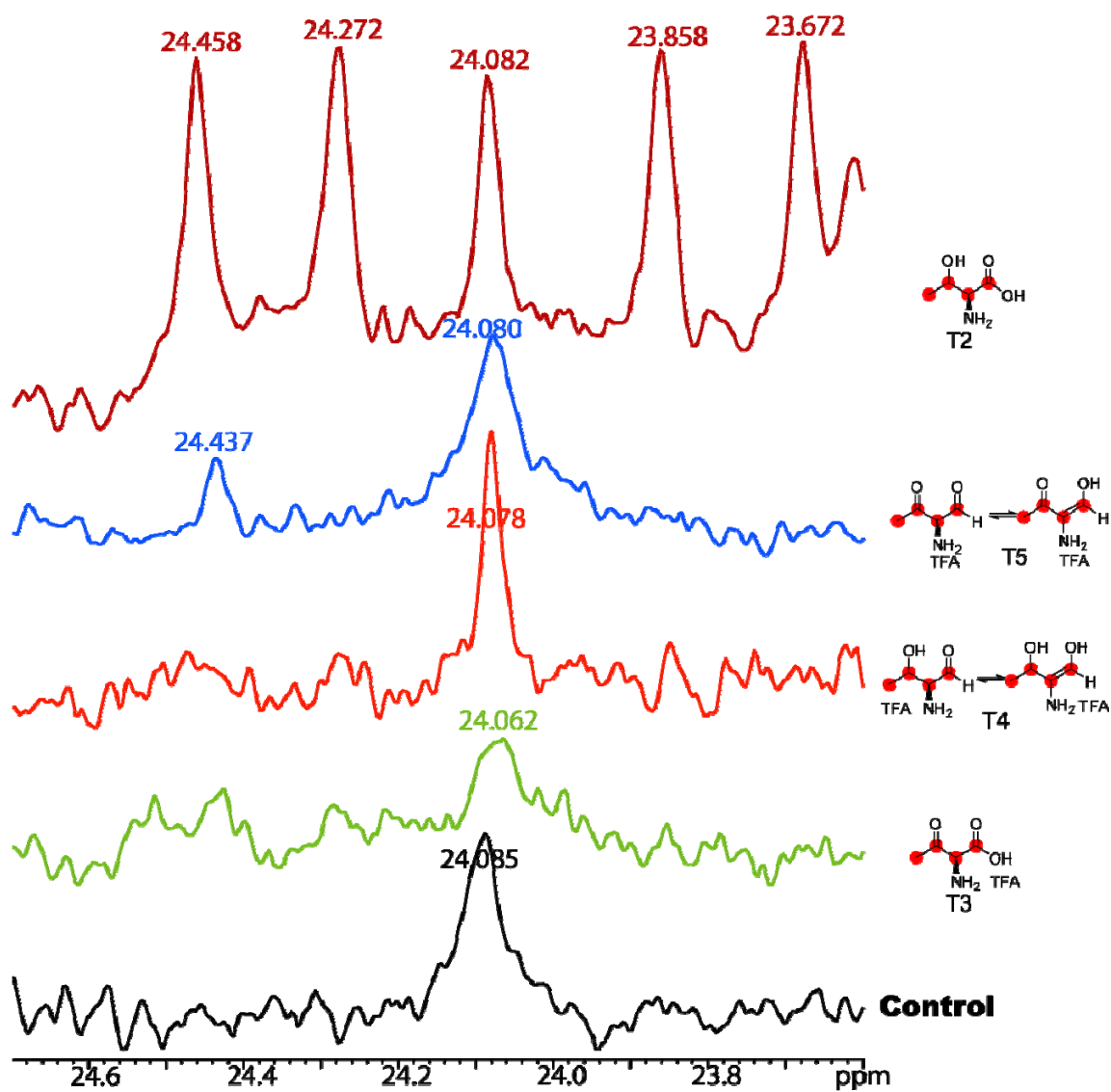


Figure 134. Overlay of Azinomycin B ^{13}C -NMR Spectra for $[\text{U-}^{13}\text{C}]$ L-threonine derivative series (T2-T5), incorporation into azinomycin C1 of azinomycin B. Splitting of the C1 signal seen in the feeding of $[\text{U-}^{13}\text{C}]$ L-Threonine (T2) only.

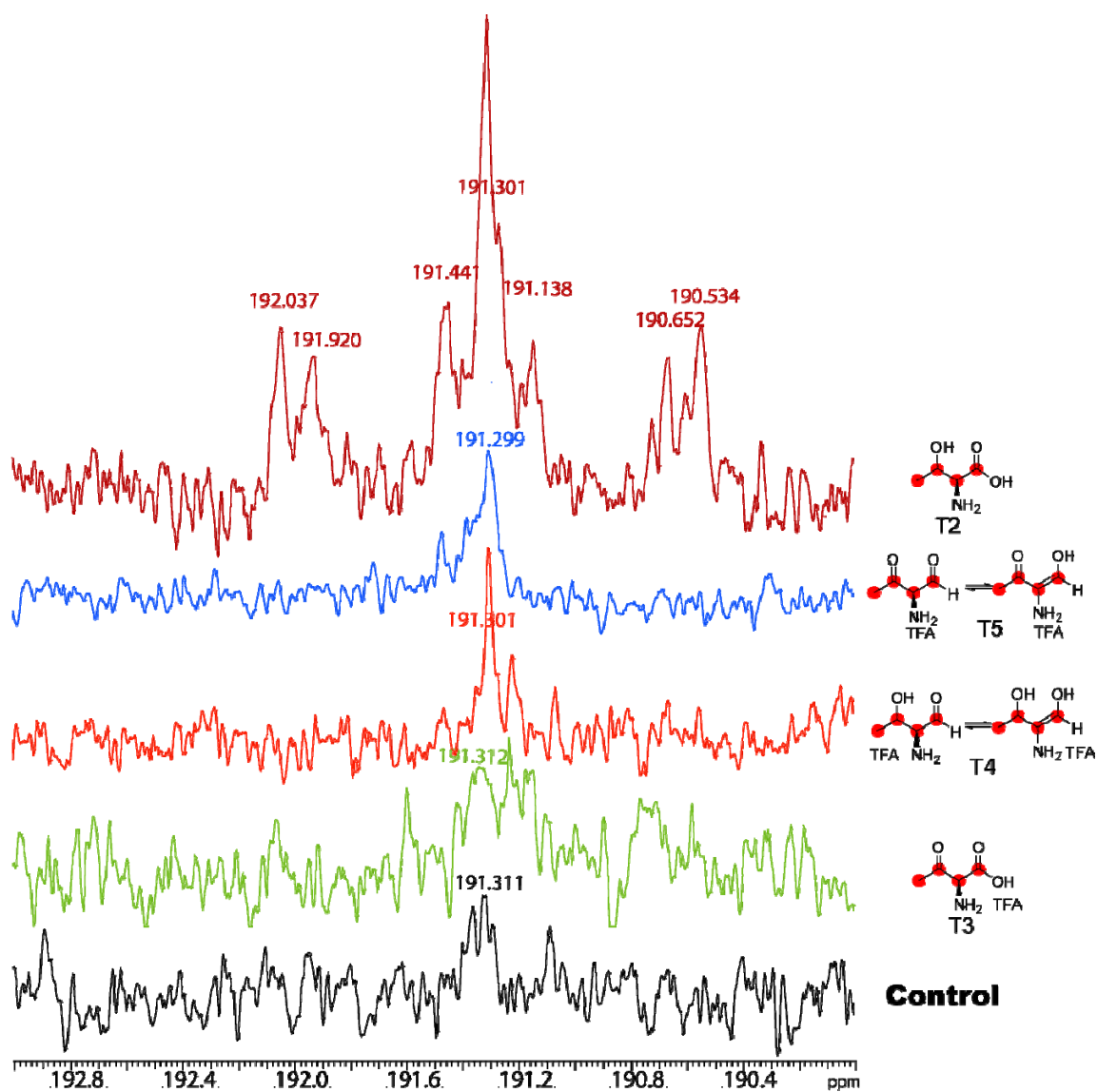


Figure 135. Overlay of Azinomycin B ^{13}C -NMR Spectra for $[\text{U-}^{13}\text{C}]$ L-threonine derivative series (T2-T5), incorporation into azinomycin C2 of azinomycin B. Splitting of the C2 signal seen in the feeding of $[\text{U-}^{13}\text{C}]$ L-Threonine (T2) only.

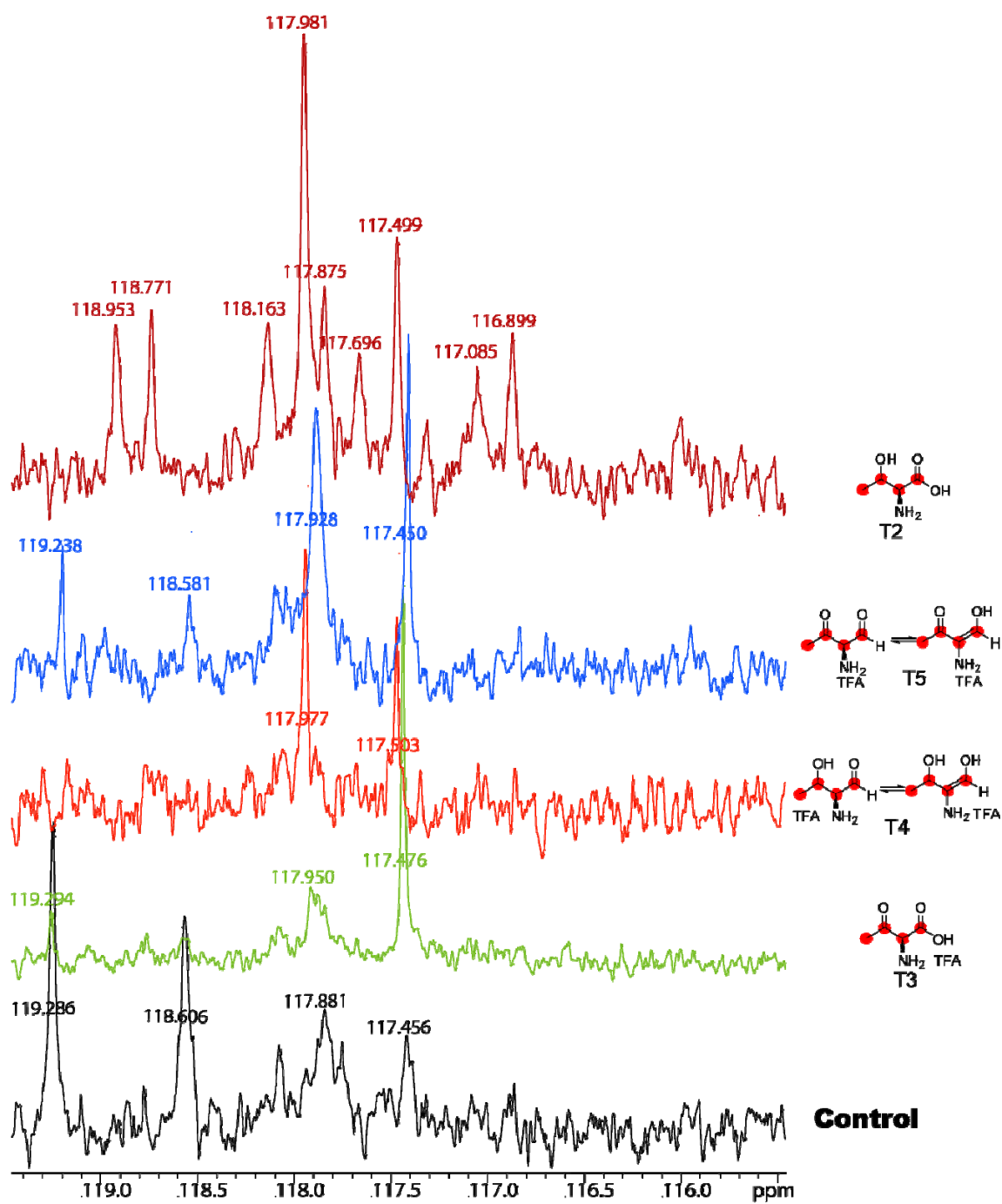


Figure 136. Overlay of Azinomycin B ^{13}C -NMR Spectra for $[\text{U}-^{13}\text{C}]$ L-threonine derivative series (T2-T5), incorporation into azinomycin C3 of azinomycin B. Splitting of the C3 signal seen in the feeding of $[\text{U}-^{13}\text{C}]$ L-Threonine (T2) only.

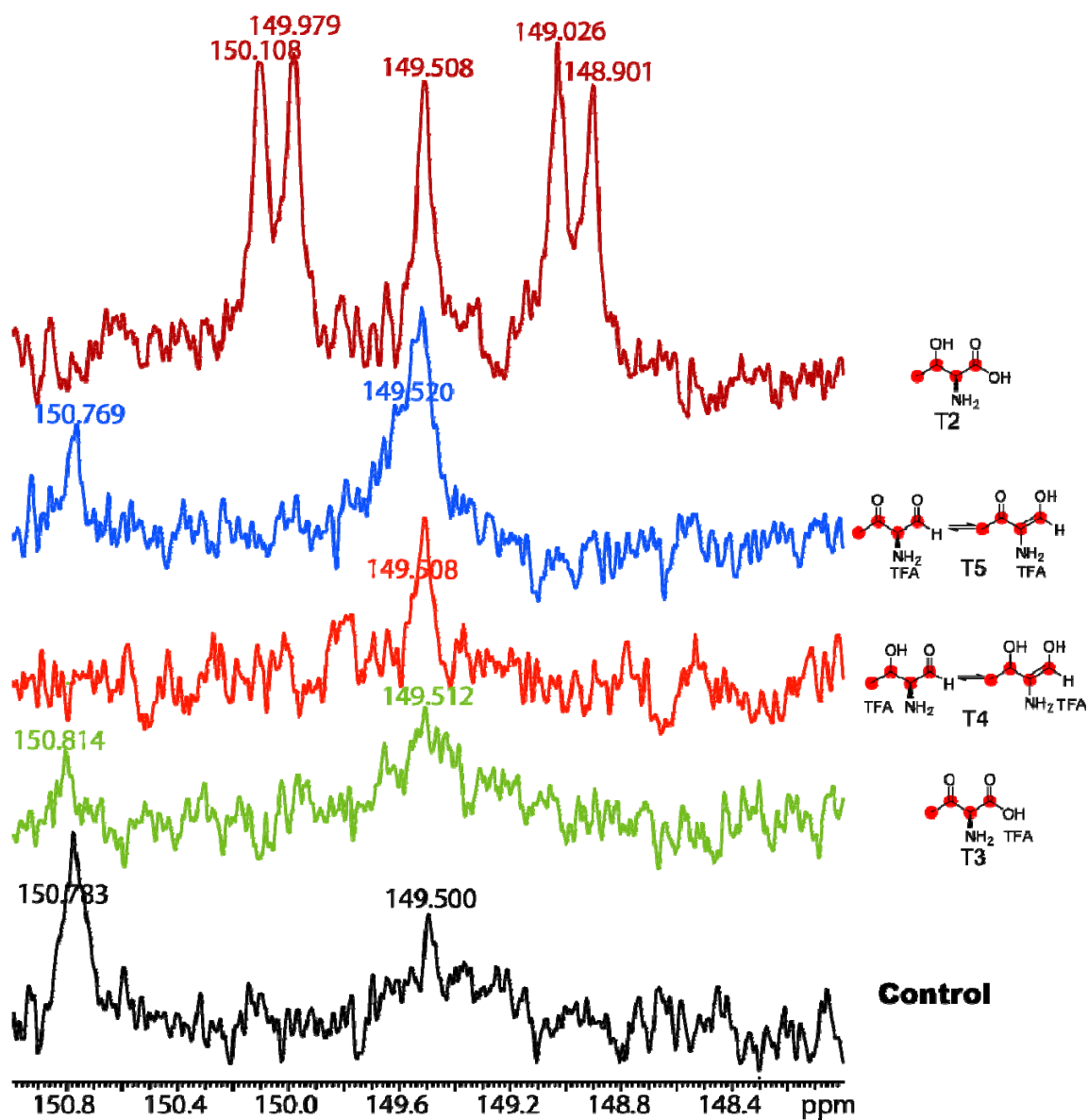


Figure 137. Overlay of Azinomycin B ^{13}C -NMR Spectra for $[\text{U-}^{13}\text{C}]$ L-threonine derivative series (T2-T5), incorporation into azinomycin C4 of azinomycin B. Splitting of the C4 signal seen in the feeding of $[\text{U-}^{13}\text{C}]$ L-Threonine (T2) only.

BIOSYNTHETIC ROUTE TO THE END FRAGMENT OF AZINOMYCIN A.
INCORPORATION SERIES

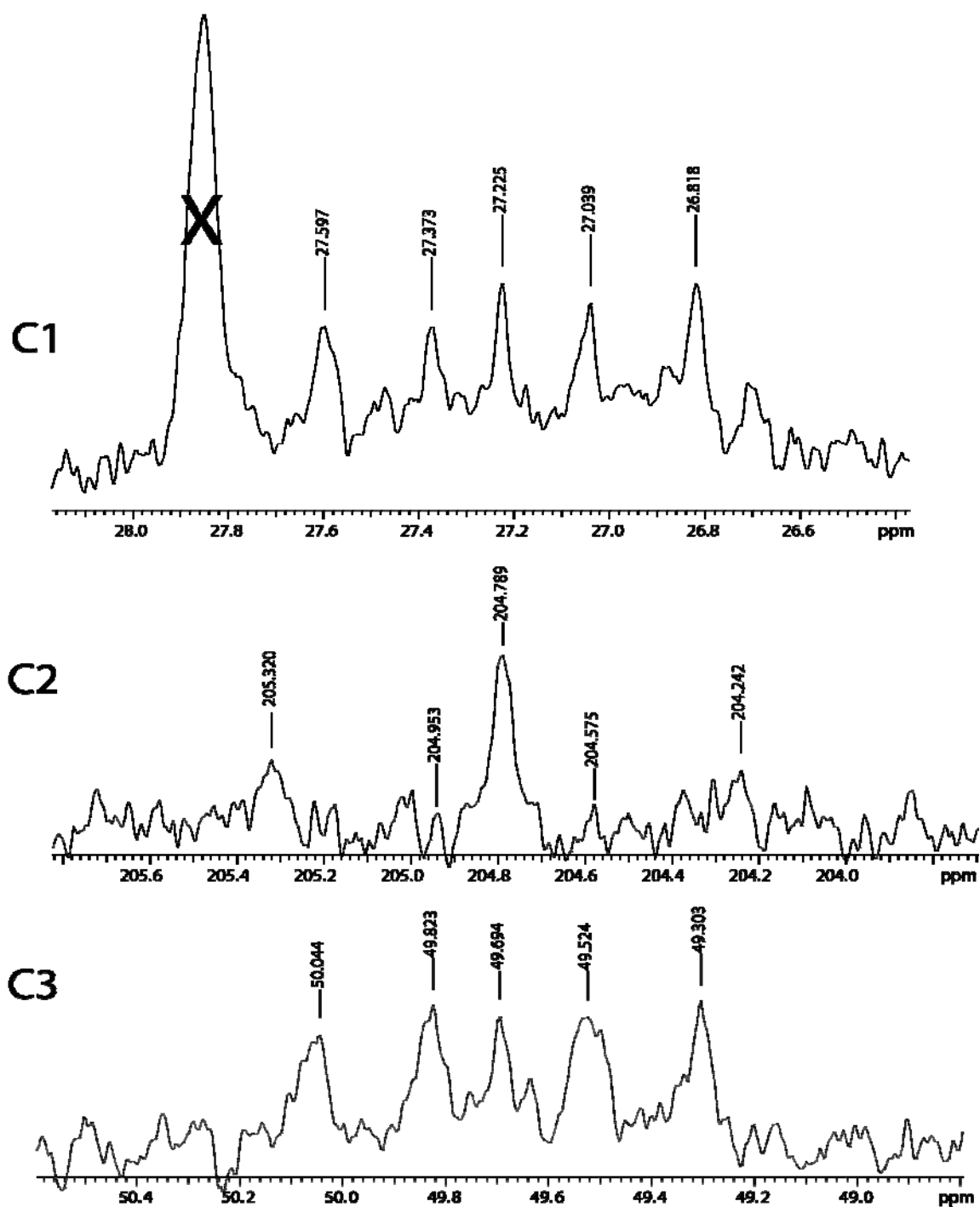


Figure 138. Azinomycin A ^{13}C -NMR Spectra for $[\text{U}-^{13}\text{C}]$ L-threonine (T2/AA3), incorporation into C1-3 of azinomycin A.

Splitting of the carbon signals seen in the feeding of $[\text{U}-^{13}\text{C}]$ L-Threonine (T2-5) from the threonine series into azinomycin A. No splitting signals were seen with the feeding of 2-amino-3-ketobutyrate (T3/AA4).

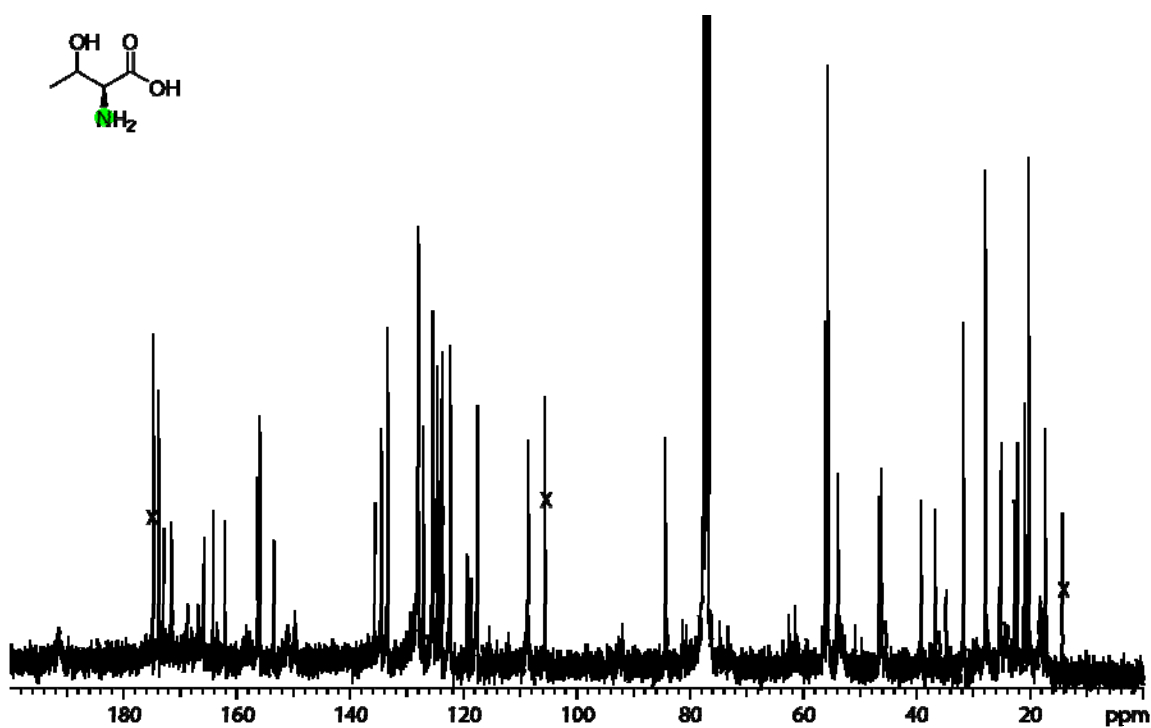


Figure 139. Azinomycin B, fed [^{15}N] L-threonine (AA3) 230mg.

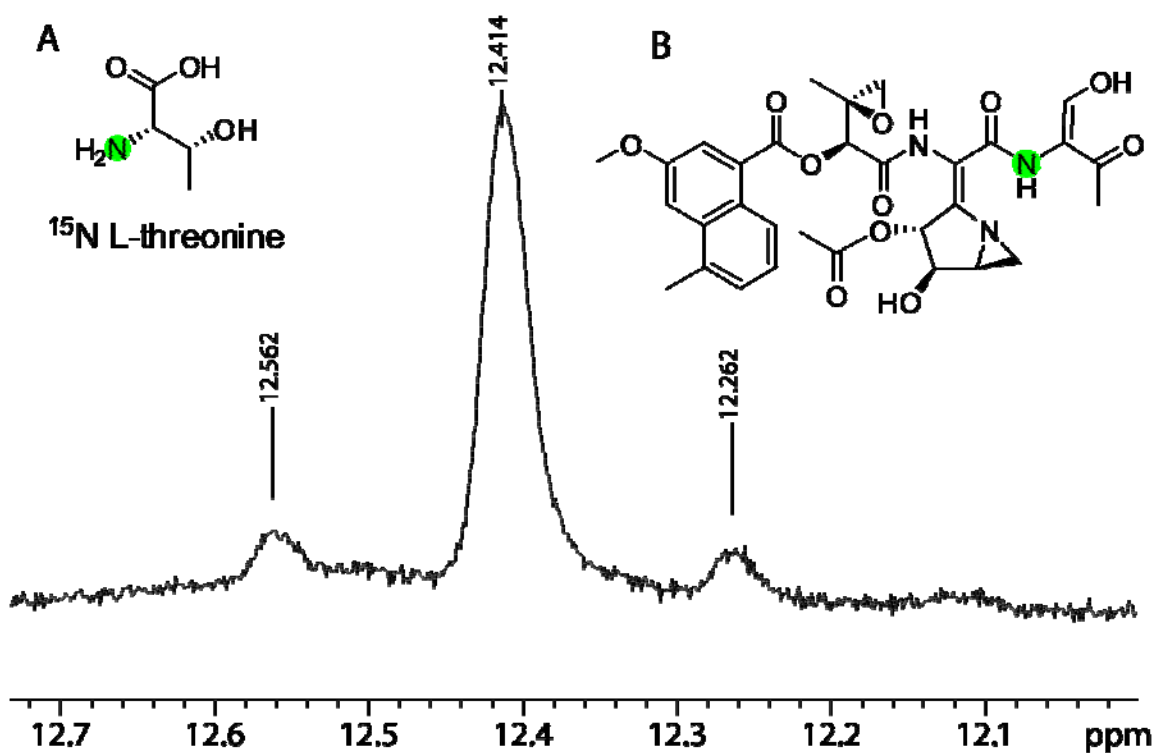


Figure 140. Azinomycin B, fed [^{15}N] threonine (AA3) 230mg ^1H -NMR.

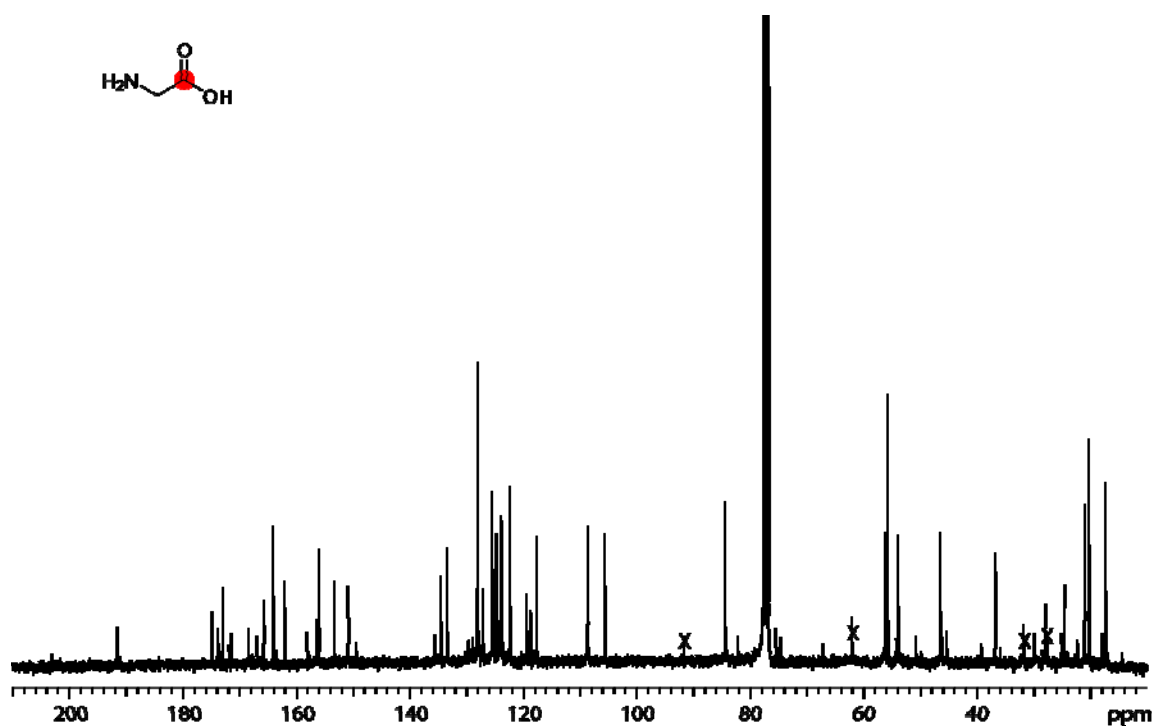


Figure 141. Azinomycin B, fed [1-¹³C] glycine (AA6) 100mg.

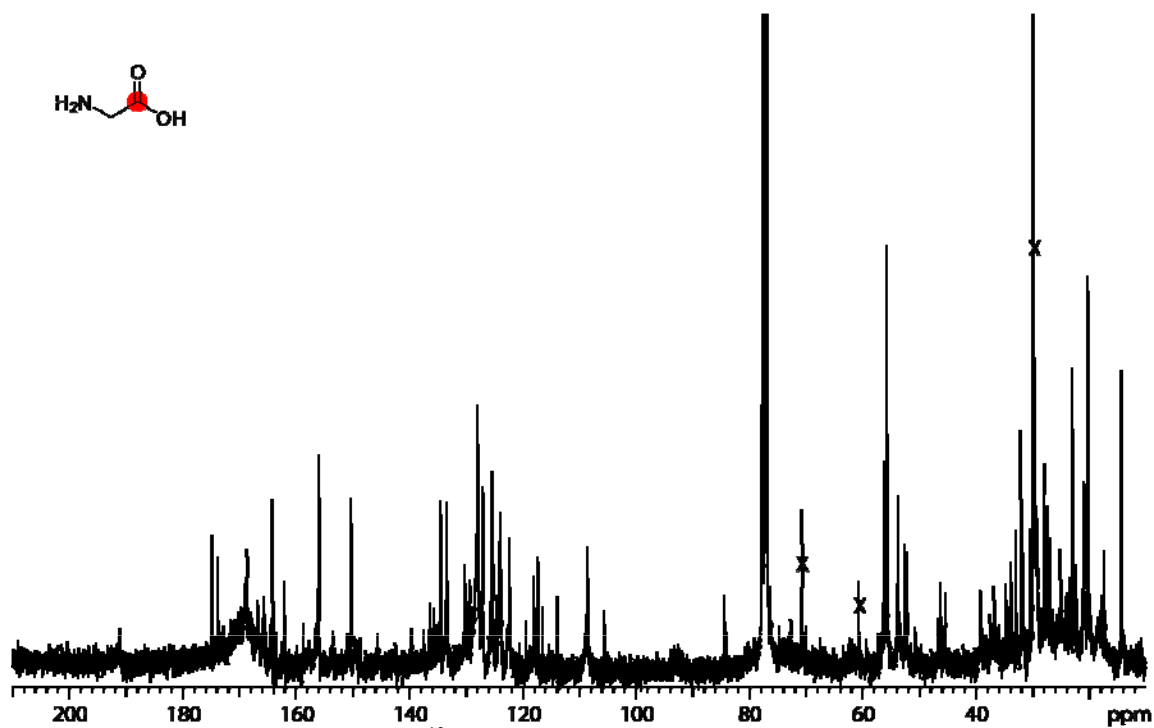


Figure 142. Azinomycin B, fed [1-¹³C] glycine (AA6) 1000mg.

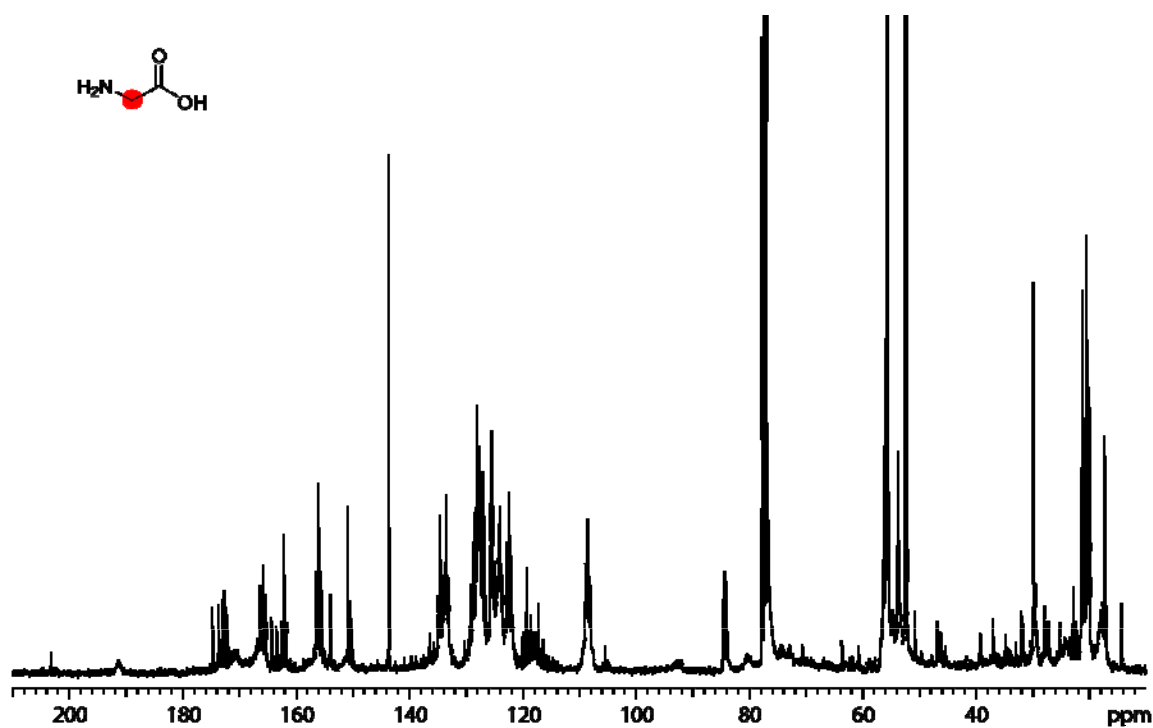


Figure 143. Azinomycin B, fed [2-¹³C] glycine (AA6) 1000mg.

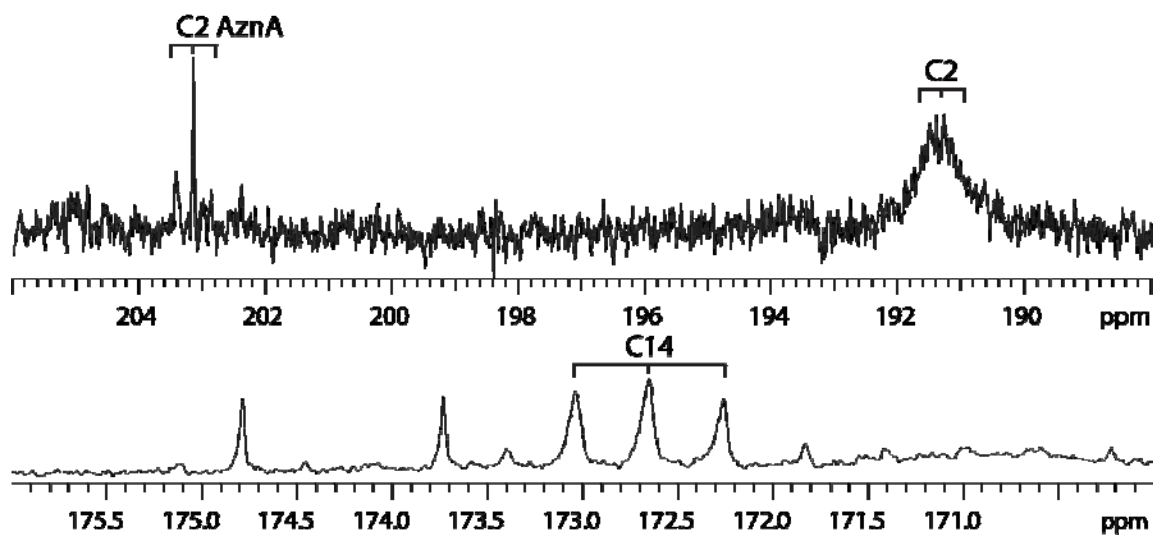


Figure 144. Azinomycin B, fed [2-¹³C] glycine (AA6) 1000mg spectral blow ups

The following are blow ups of the above 1g [2-¹³C] glycine incorporation into azinomycin B spectra showing the observed splitting pattern indicative of neighboring labeled units, such as being converted to [1,2-¹³C2] Acetyl-CoA units, or simply into ¹³C labeled methyl groups to for the C3'OCH₃.

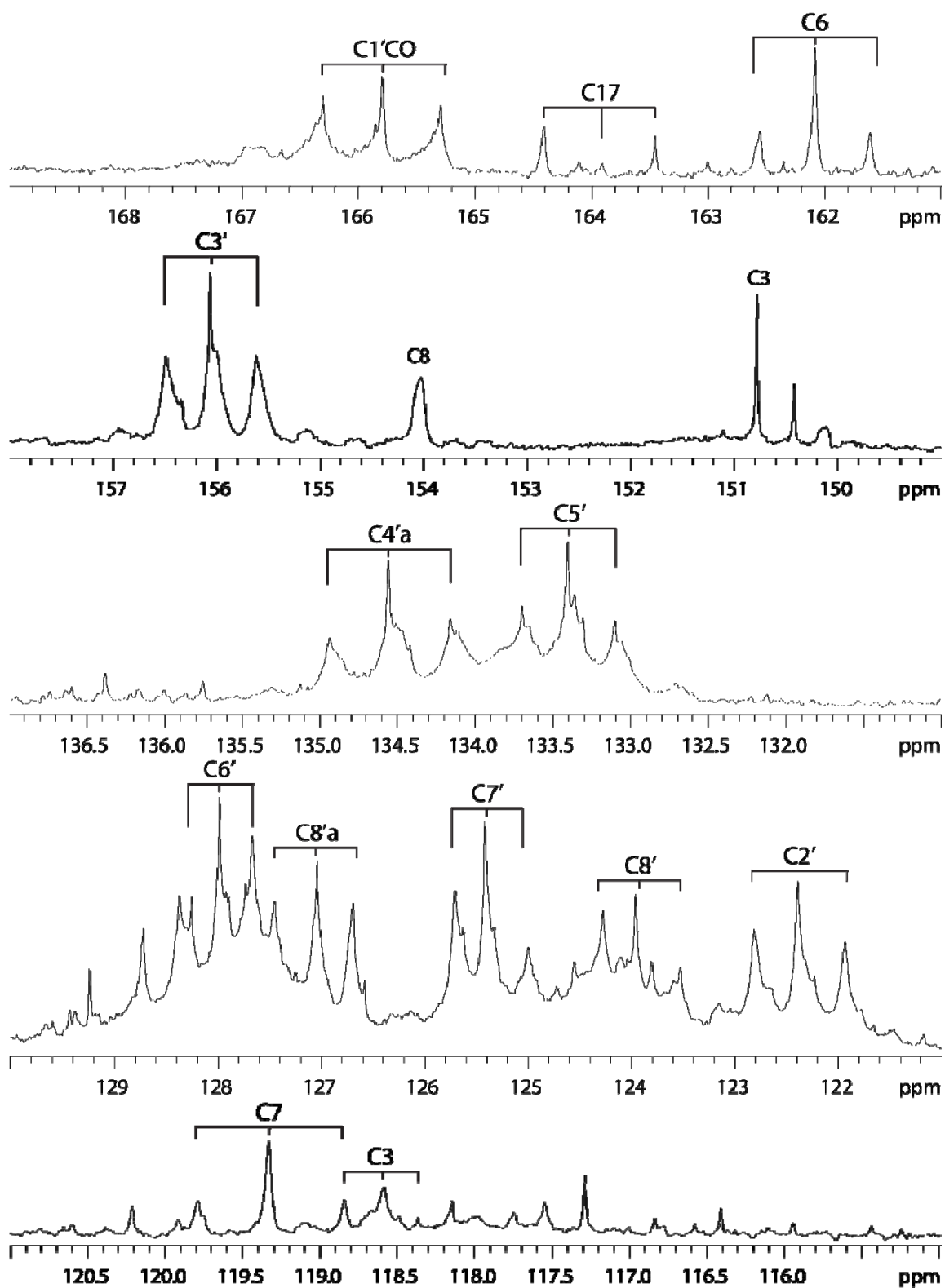


Figure 144. Splitting patterns observed in Azinomycin B fed $[2-^{13}\text{C}]$ glycine (AA6) 1000mg. Continued.

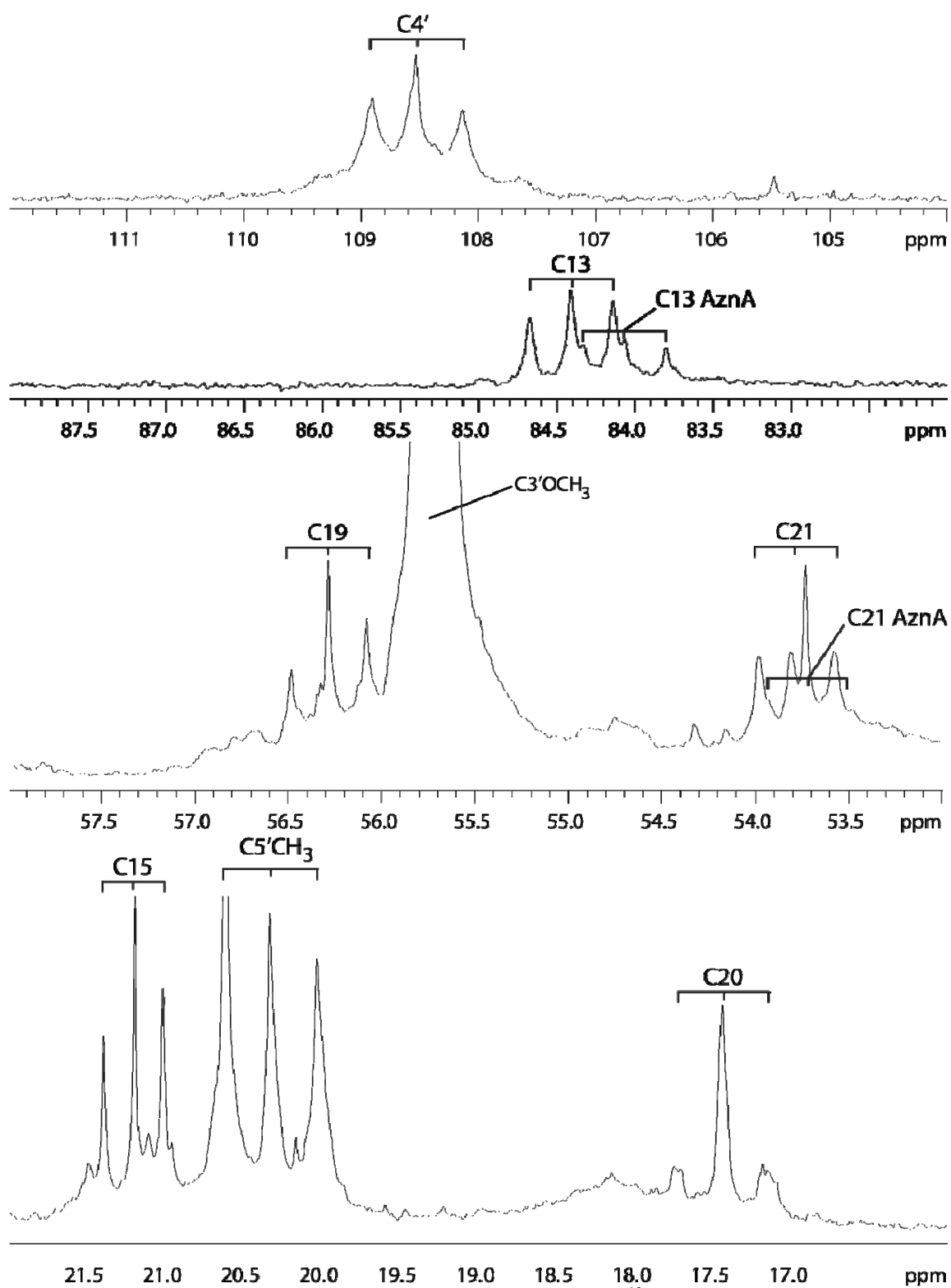
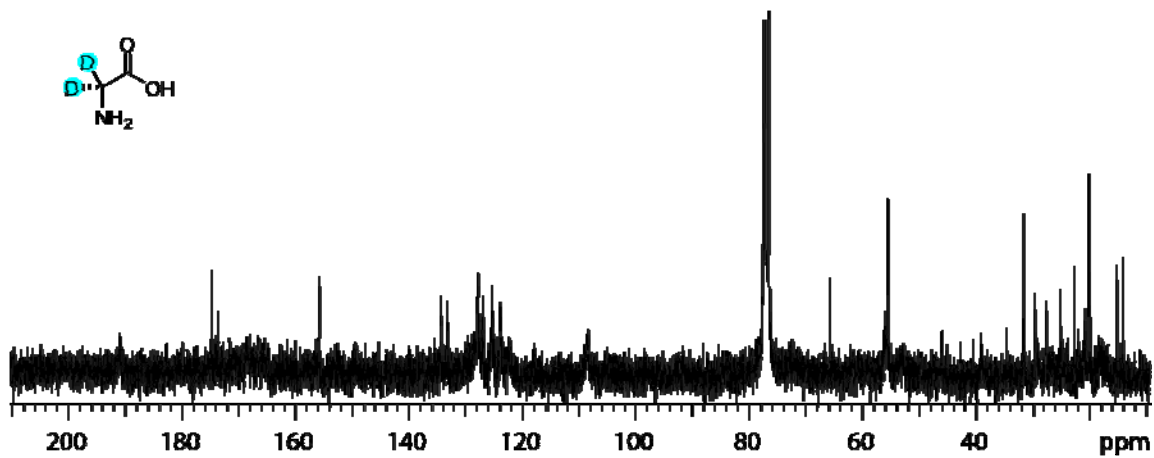
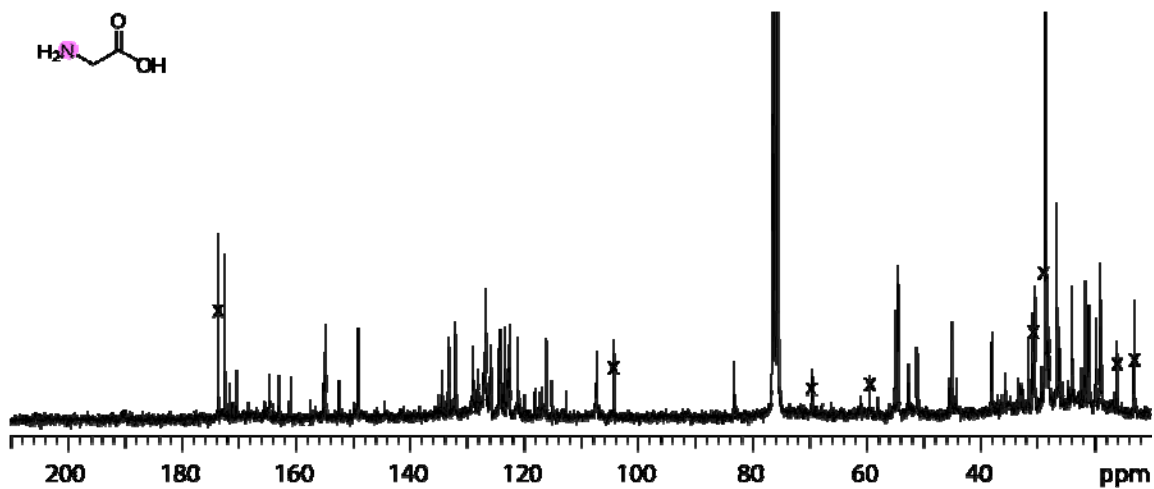


Figure 144. Splitting patterns observed in Azinomycin B fed $[2-^{13}\text{C}]$ glycine (AA6) 1000mg, Continued.

Figure 145. Azinomycin B, fed [2,2-D₂] glycine (AA6) 1000mg.Figure 146. Azinomycin B, fed [¹⁵N] glycine (AA6) 1000mg.

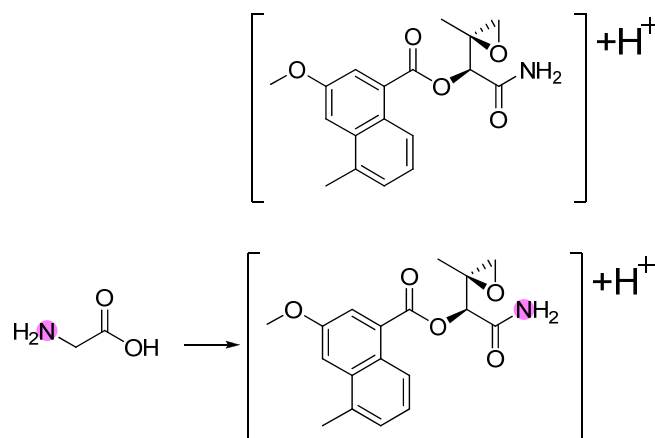
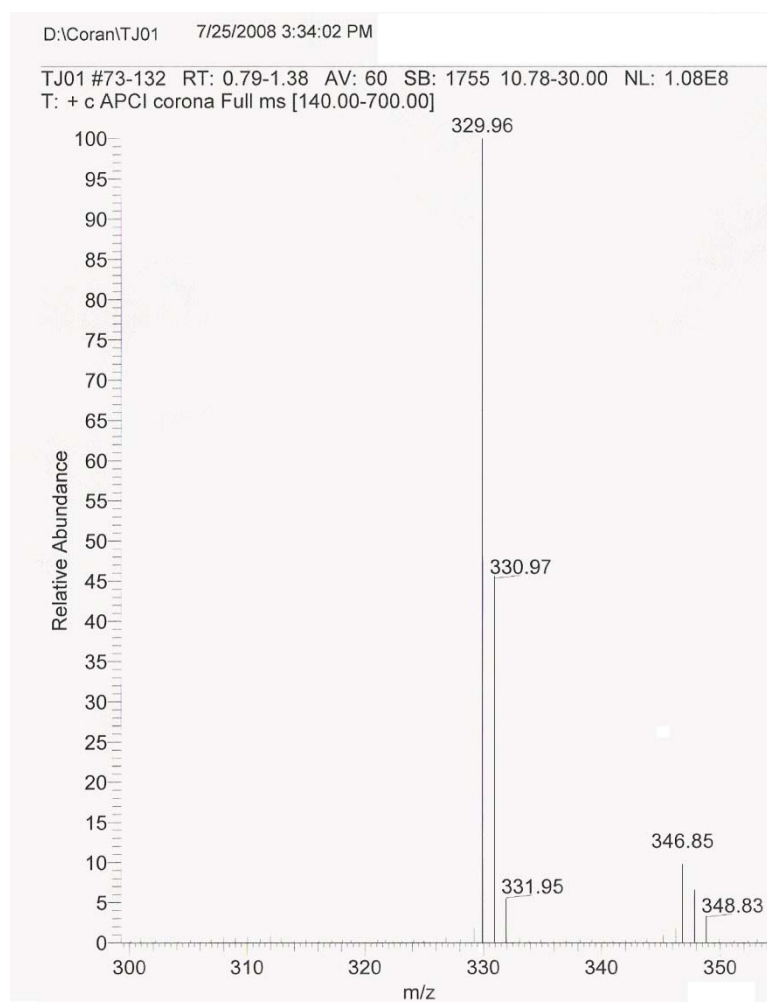


Figure 147. APCI-Mass Spectrometry for ^{15}N -glycine (AA6) incorporation into the epoxyamide. Epoxyamide ($M+H = 330$, $M+H+1 = 331$). This may indicate that the 1gram introduction of nitrogen labeled glycine served as a general source of extra nitrogen for transamination reactions.

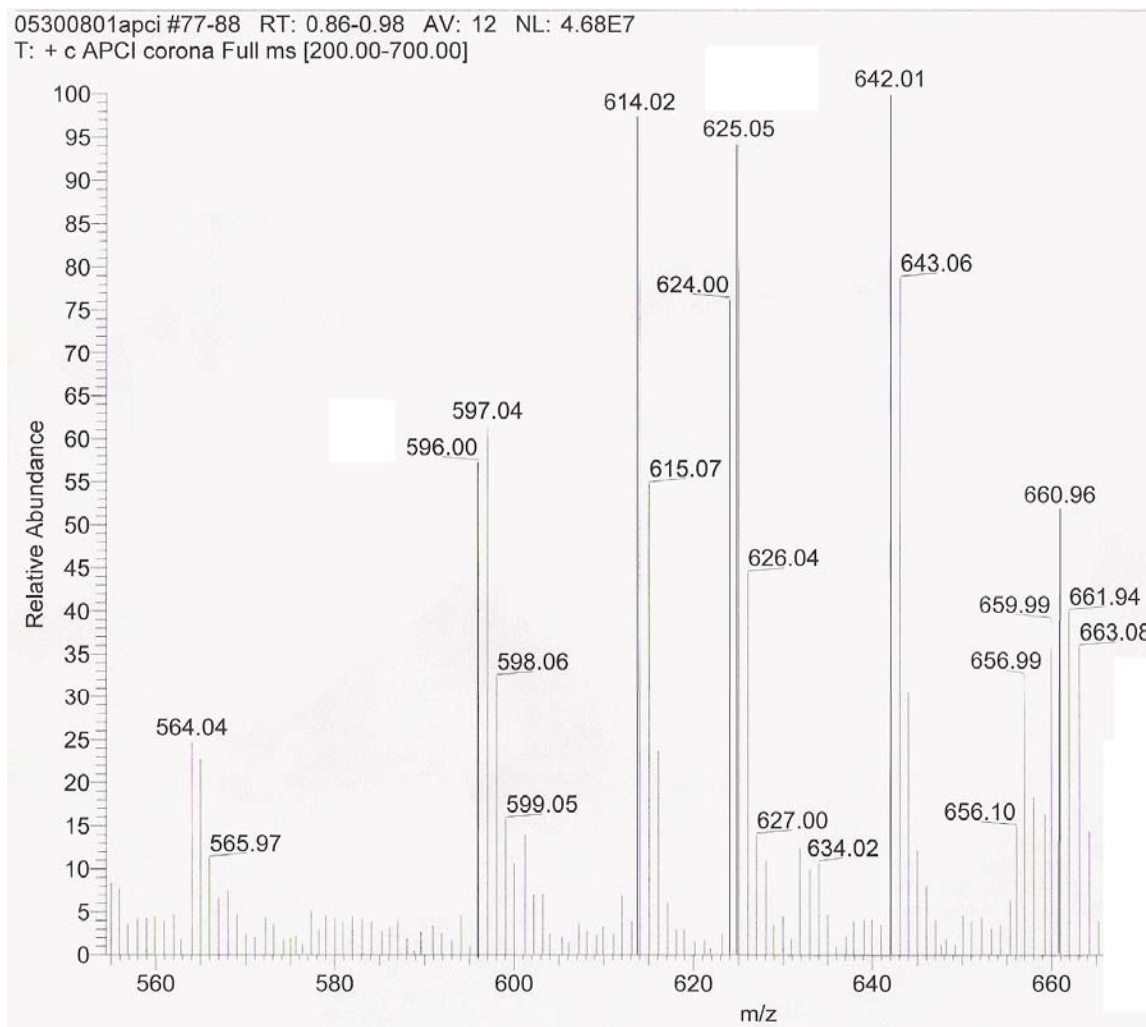


Figure 148. APCI-Mass Spectrometry for ^{15}N -glycine (AA6) incorporation into the azinomycin A & B.

Azinomycin A ($M+H = 596$, $M+H+H_2O = 614$) & azinomycin B ($M+H = 624$, $M+H+H_2O = 642$, $M+H+2H_2O = 660$). Incorporation seen at: 597 & 598, (Azinomycin A $[M+H+1]$ and $[M+H+2]$); 615, (Azinomycin A $[M+H_2O+H+1]$); 625 & 626, (Azinomycin B $[M+H+1]$ and $[M+H+2]$); 643 & 644, (Azinomycin B $[M+H_2O+H+1]$ and $[M+H_2O+H+2]$); and 661 & 662, (Azinomycin B $[M+2H_2O+H+1]$ and $[M+2H_2O+H+2]$).

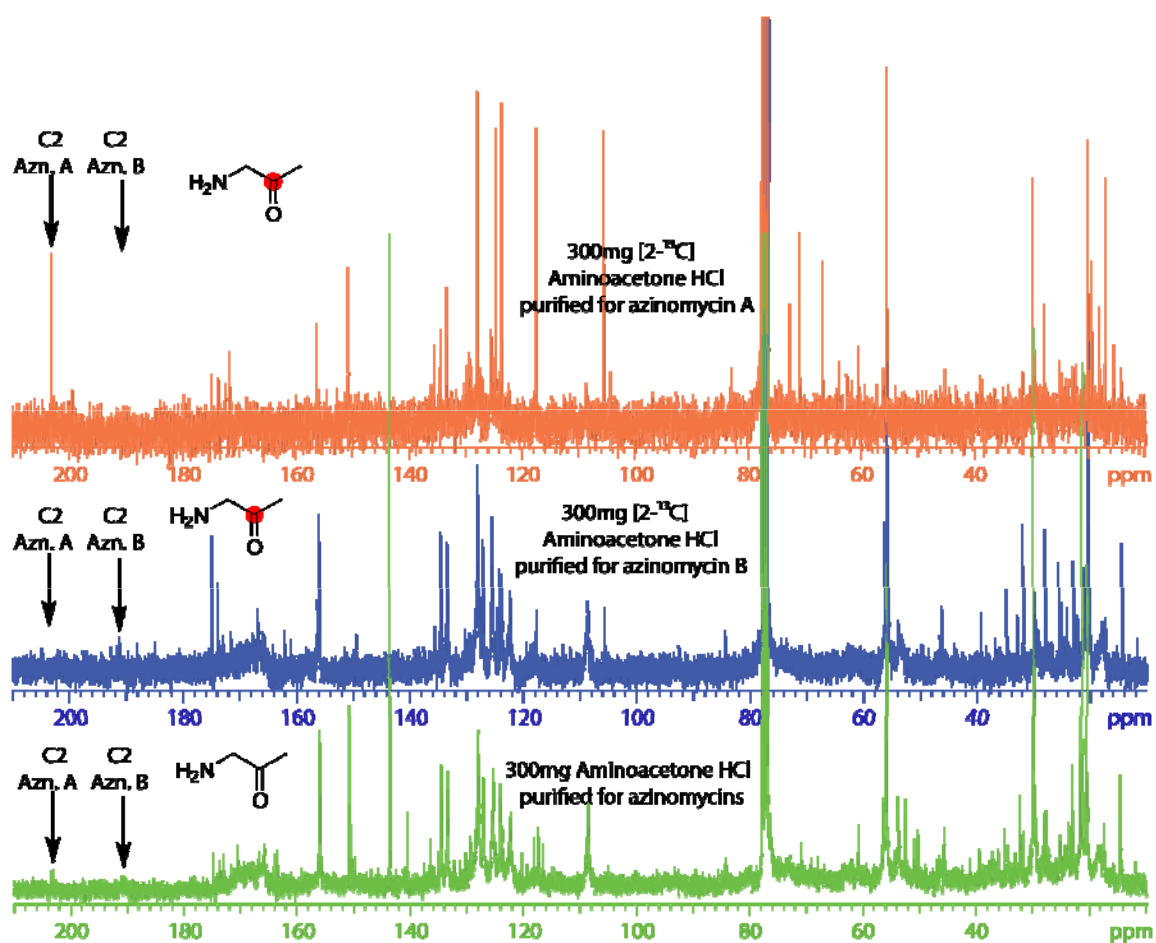


Figure 149. Spectral overlay of feeding 300mg aminoacetone (AA5): $[2-^{13}\text{C}]$ aminoacetone purified for azinomycin A, $[2-^{13}\text{C}]$ aminoacetone purified for azinomycin B, and unlabeled aminoacetone purified both azinomycins.

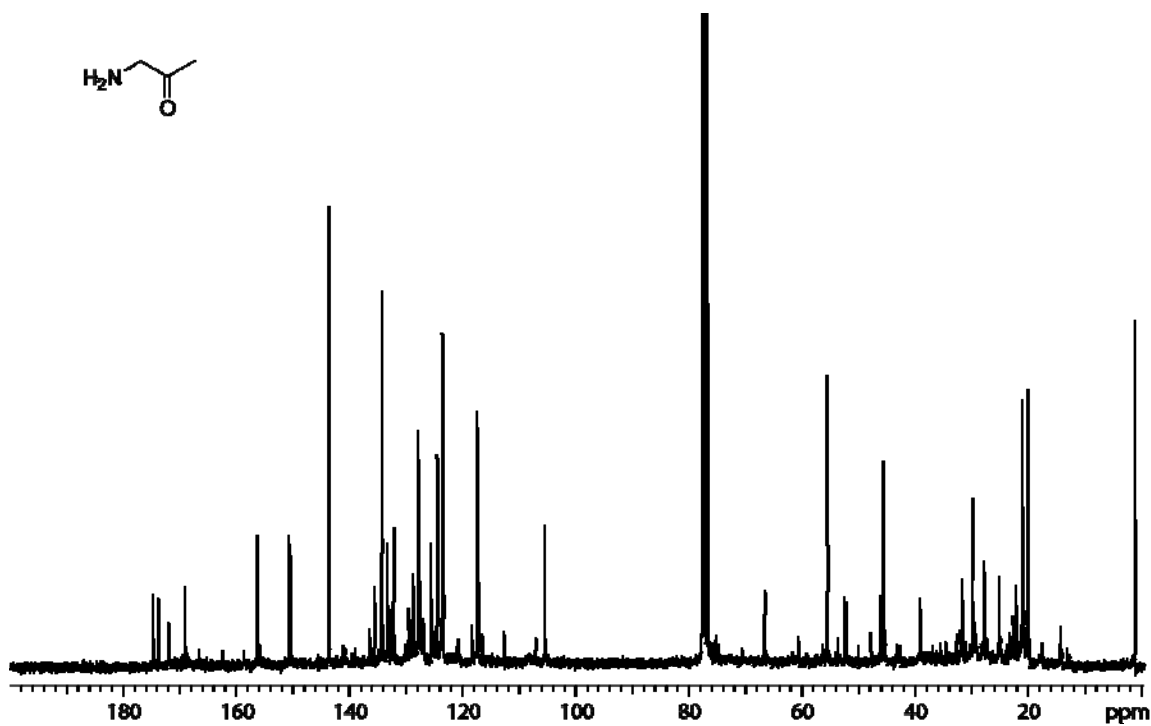


Figure 150. Azinomycin B, fed aminoacetone HCl (AA5) 1250mg.
Fed in two 625mg parts, essentially only naphthamide (3-methoxy-5-methyl-1-naphthamide) and silicone grease present.

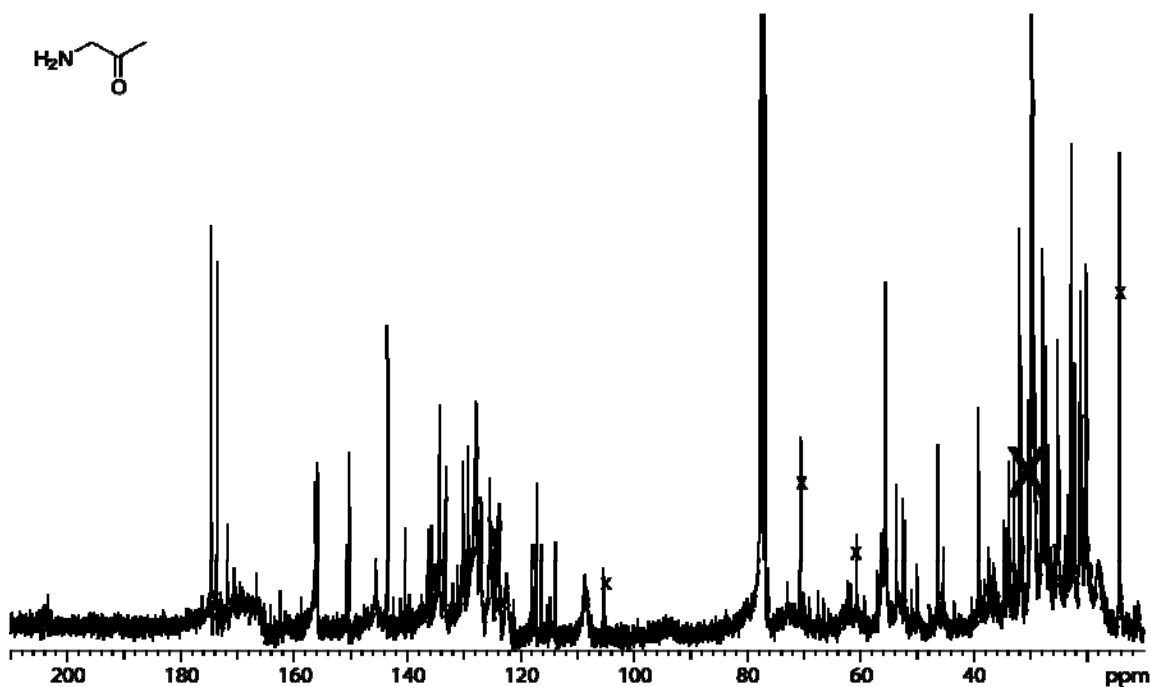


Figure 151. Azinomycin B, fed aminoacetone HCl (AA5) 700mg.
Fed in eight 87.5 mg parts from a 3mg/ml solution of aminoacetone HCl. Contaminating solvent, naphthamide (3-methoxy-5-methyl-1-naphthamide), and silicone grease are present. Culture was reasonably healthy.

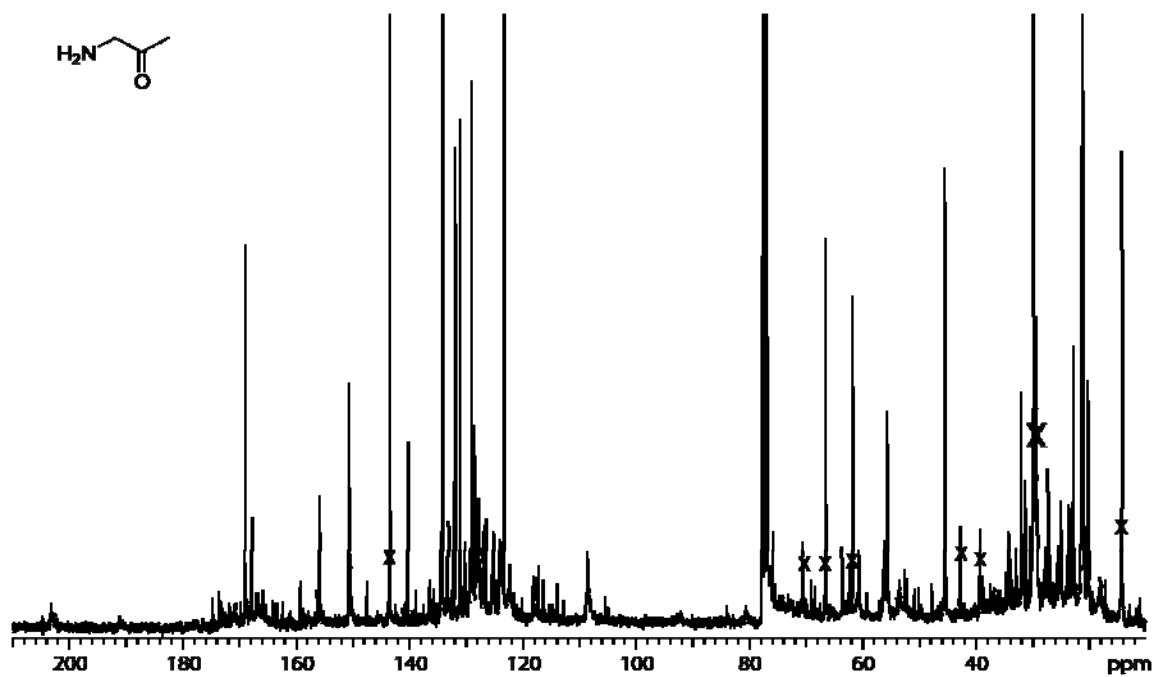


Figure 152. Azinomycin B, fed aminoacetone HCl (AA5) 1000mg.
Fed in eight 125 mg parts from a 3mg/ml solution of aminoacetone HCl. Contaminating solvent, naphthamide (3-methoxy-5-methyl-1-naphthamide), and silicone grease are present. Culture was reasonably healthy.

INCORPORATION OF MOLECULAR OXYGEN INTO AZINOMYCIN B.
COMPOUND FEEDING SPECTRA SERIES

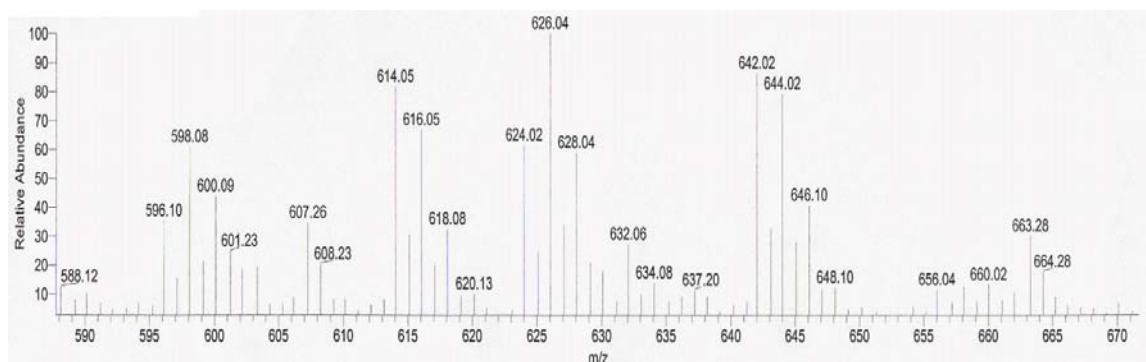


Figure 153. APCI-Mass Spectrometry for $^{18}\text{O}_2$ incorporation into azinomycins A and B from crude extract.

Azinomycin A ($M+H = 596$, $M+H+H_2O = 614$) & azinomycin B ($M+H = 624$, $M+H+H_2O = 642$, $M+H+2H_2O = 660$). Incorporation seen at: 598 & 600, (Azinomycin A $[M+H+2]$ and $[M+H+4]$); 616 & 618, (Azinomycin A $[M+H_2O+H+2]$ and $[M+H_2O+H+4]$); 626 & 628, (Azinomycin B $[M+H+2]$ and $[M+H+4]$); 644 & 646 & 648, (Azinomycin B $[M+H_2O+H+2]$, $[M+H_2O+H+4]$, and $[M+H_2O+H+6]$).

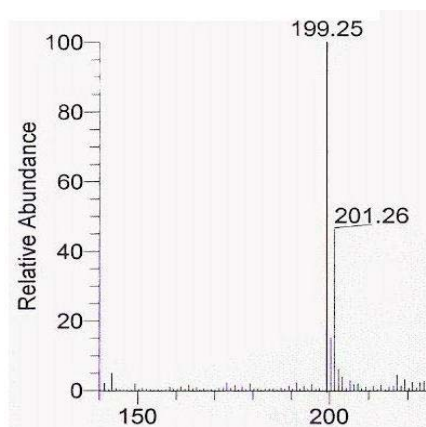


Figure 154. ^{18}O Incorporation into truncated Naphthoate moiety detected by APCI-MS. Truncated naphthoate = $[M+H] = 199$, $[M+H+2] = 201$ indicating incorporation of an oxygen atom at the $C3'OCH_3$.

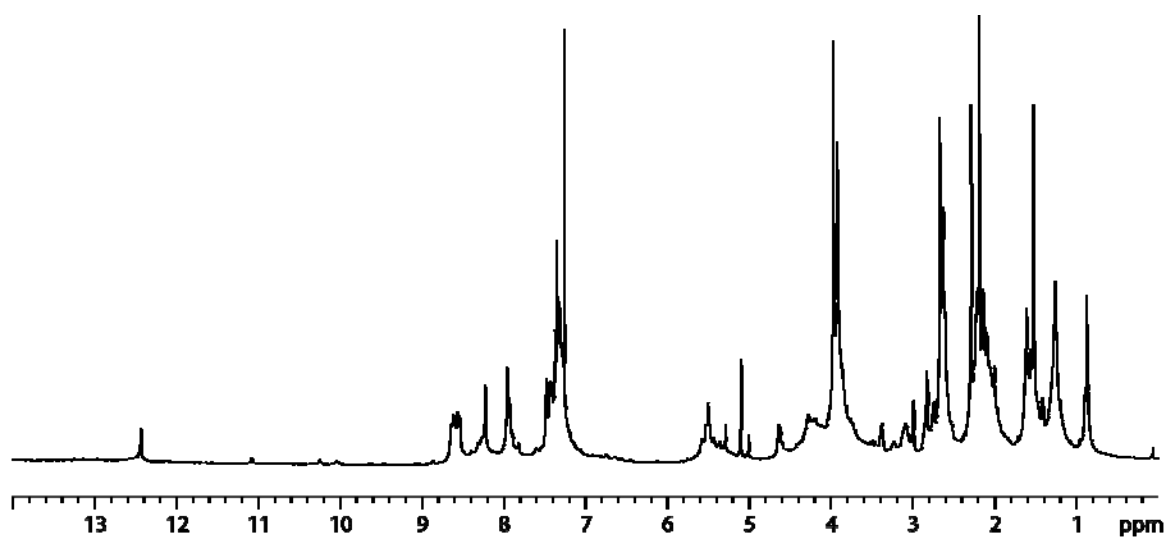


Figure 155. ^1H Spectra of $^{18}\text{O}_2$ incorporated azinomycin B.

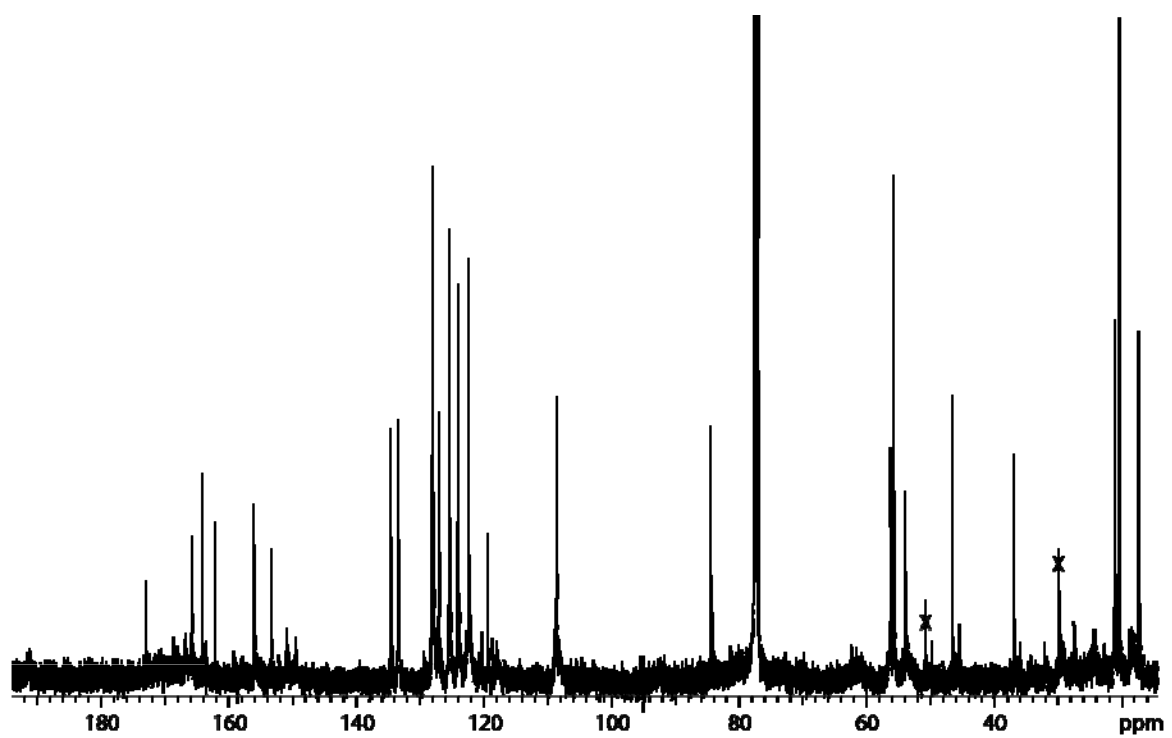


Figure 156. ^{13}C Spectra of $^{18}\text{O}_2$ incorporated azinomycin B.

BIOSYNTHETIC ROUTE TO *THE AZIRIDINO[1,2A]PYRROLIDINE (1-AZABICYCLO[3.1.0]HEXANE) MOIETY OF AZINOMYCIN B.*

COMPOUND FEEDING SPECTRA SERIES

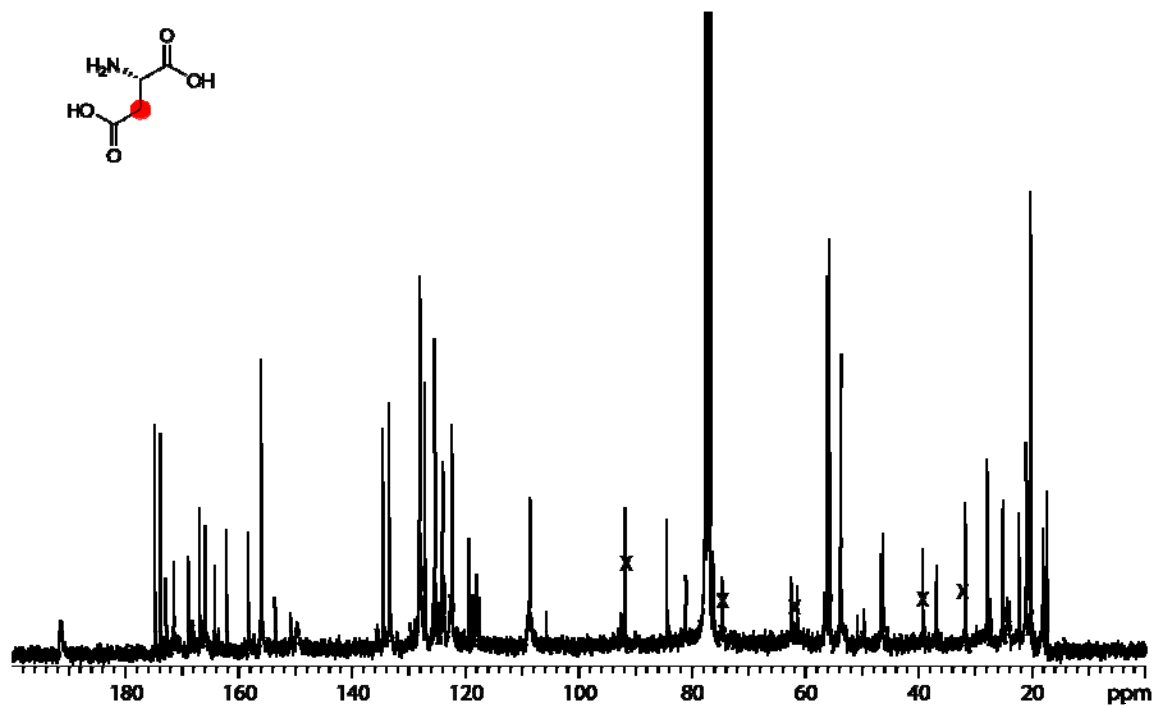


Figure 157. Azinomycin B, fed [3-¹³C] L-aspartate 100mg.

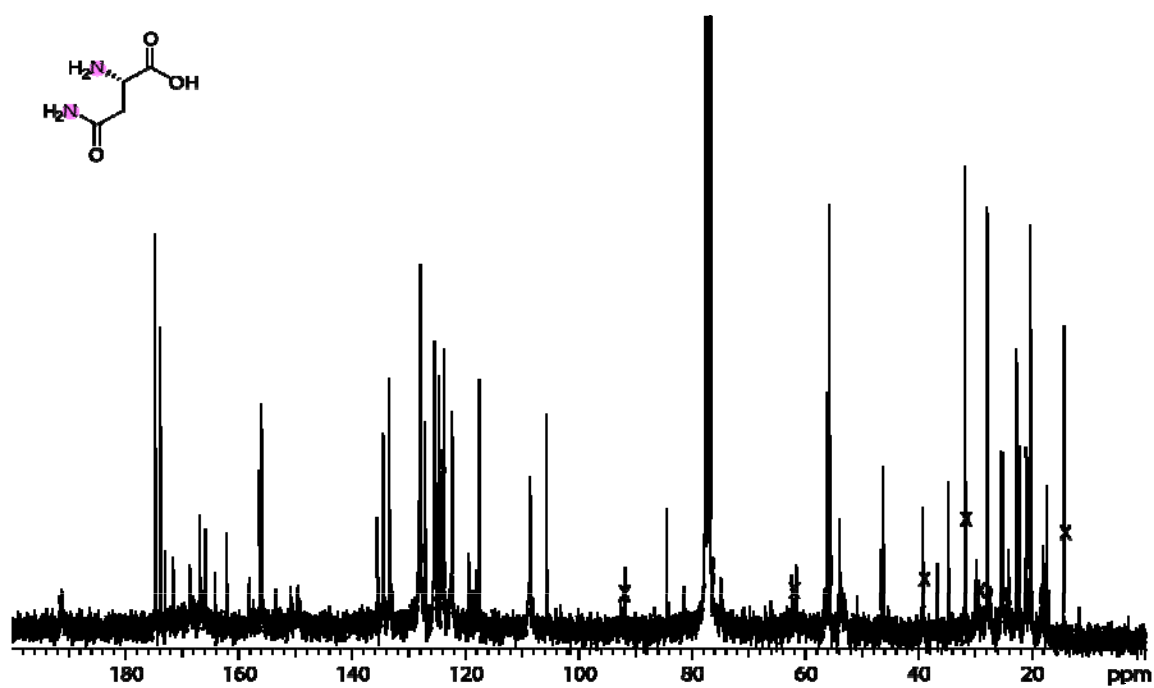


Figure 158. Azinomycin B, fed [U-¹⁵N₂] L-asparagine 220mg.

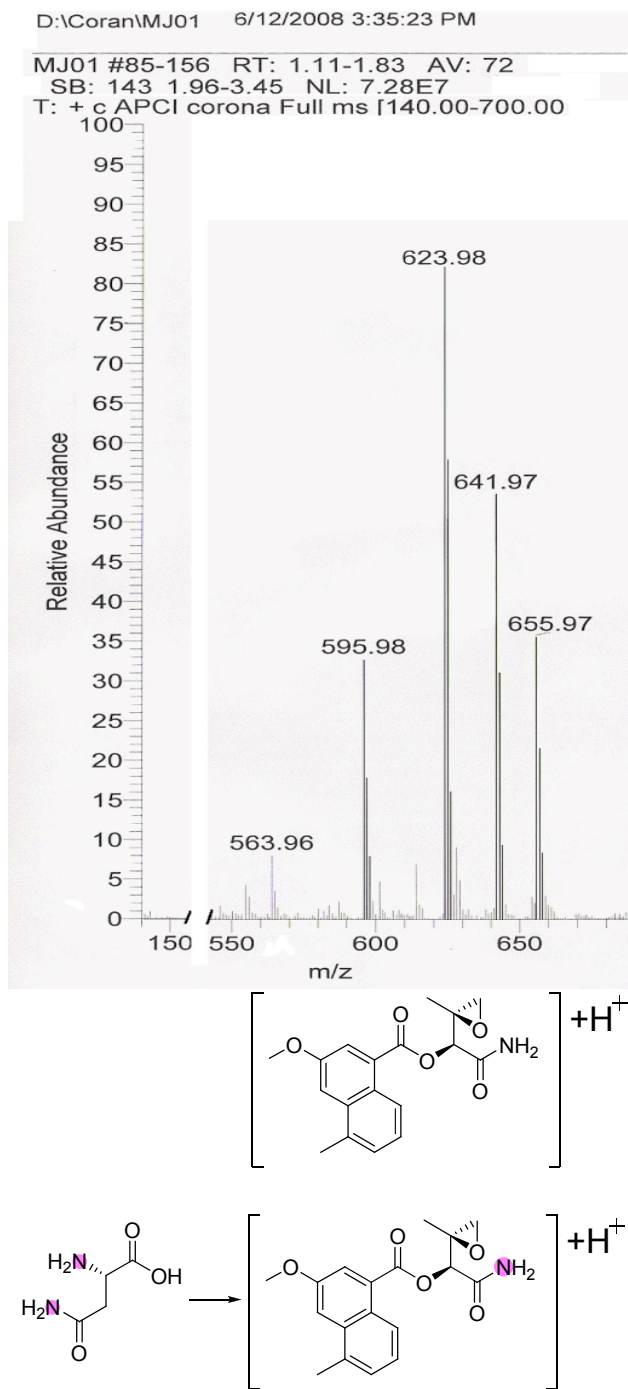


Figure 159. Azinomycin B, fed $[\text{U-}^{15}\text{N}_2]$ L-asparagine 220mg. Incorporation into azinomycin A & B observed, lower than that of $1\text{g }^{15}\text{N}$ glycine. Azinomycin A ($\text{M}+\text{H} = 596$, $\text{M}+\text{H}+\text{H}_2\text{O} = 614$) & azinomycin B ($\text{M}+\text{H} = 624$, $\text{M}+\text{H}+\text{H}_2\text{O} = 642$, $\text{M}+\text{H}+2\text{H}_2\text{O} = 660$). Incorporation seen at: 597 & 598, (Azinomycin A $[\text{M}+\text{H}+1]$ and $[\text{M}+\text{H}+2]$); 625 & 626, (Azinomycin B $[\text{M}+\text{H}+1]$ and $[\text{M}+\text{H}+2]$); and 643 & 644, (Azinomycin B $[\text{M}+\text{H}_2\text{O}+\text{H}+1]$ and $[\text{M}+\text{H}_2\text{O}+\text{H}+2]$).

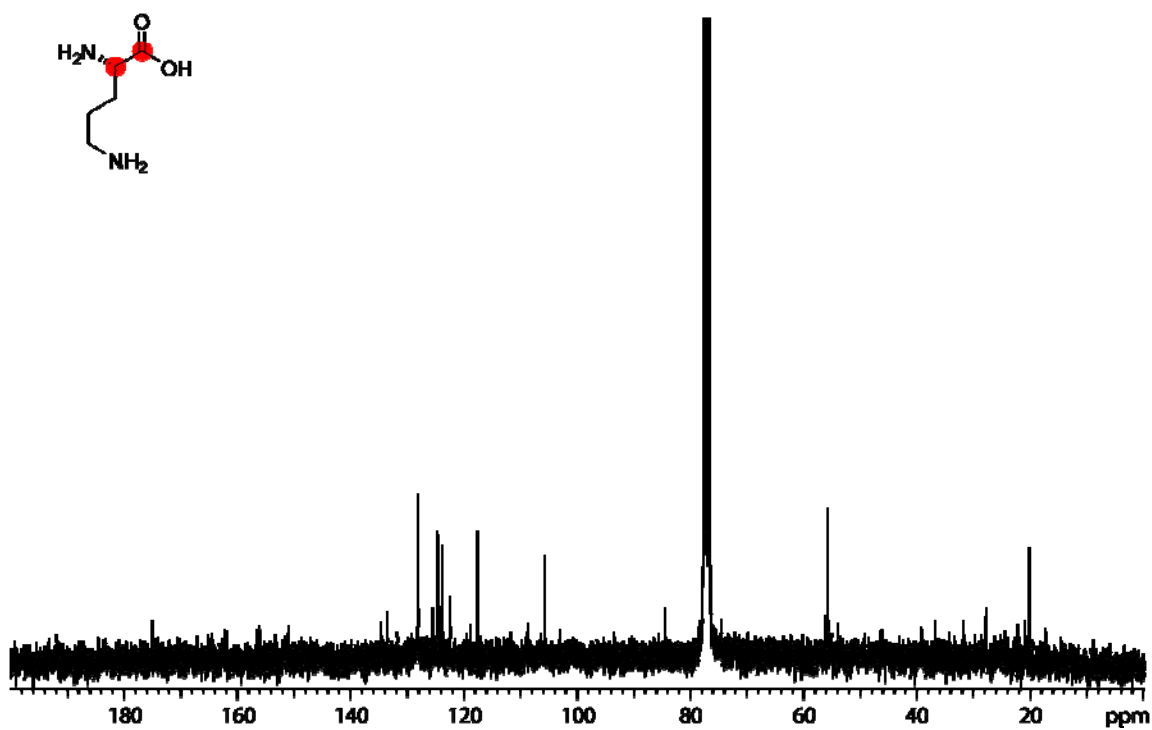


Figure 160. Azinomycin B, fed $[1,2-^{13}\text{C}_2]$ L-ornithine•2HCl 100mg.
Poor yielding culture, no intelligible incorporation, 12/12/2005.

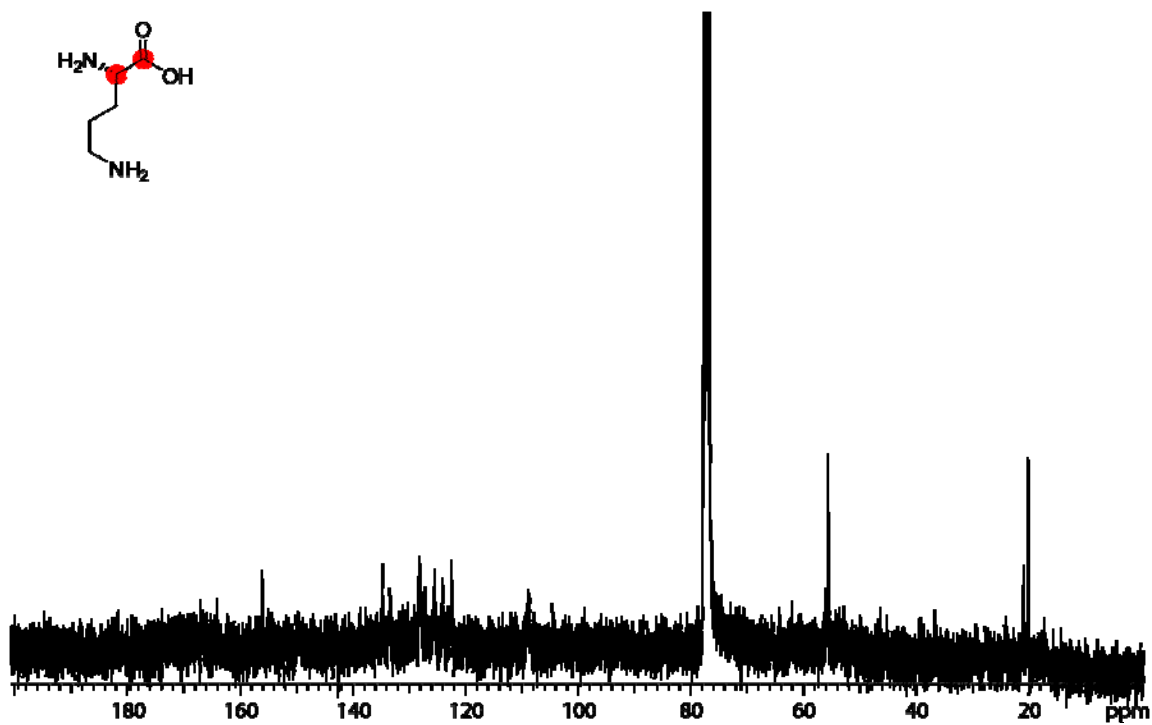


Figure 161. Azinomycin B, fed $[1,2-^{13}\text{C}_2]$ L-ornithine•2HCl 100mg.
Poor yielding culture, no intelligible incorporation, 2/8/2006.

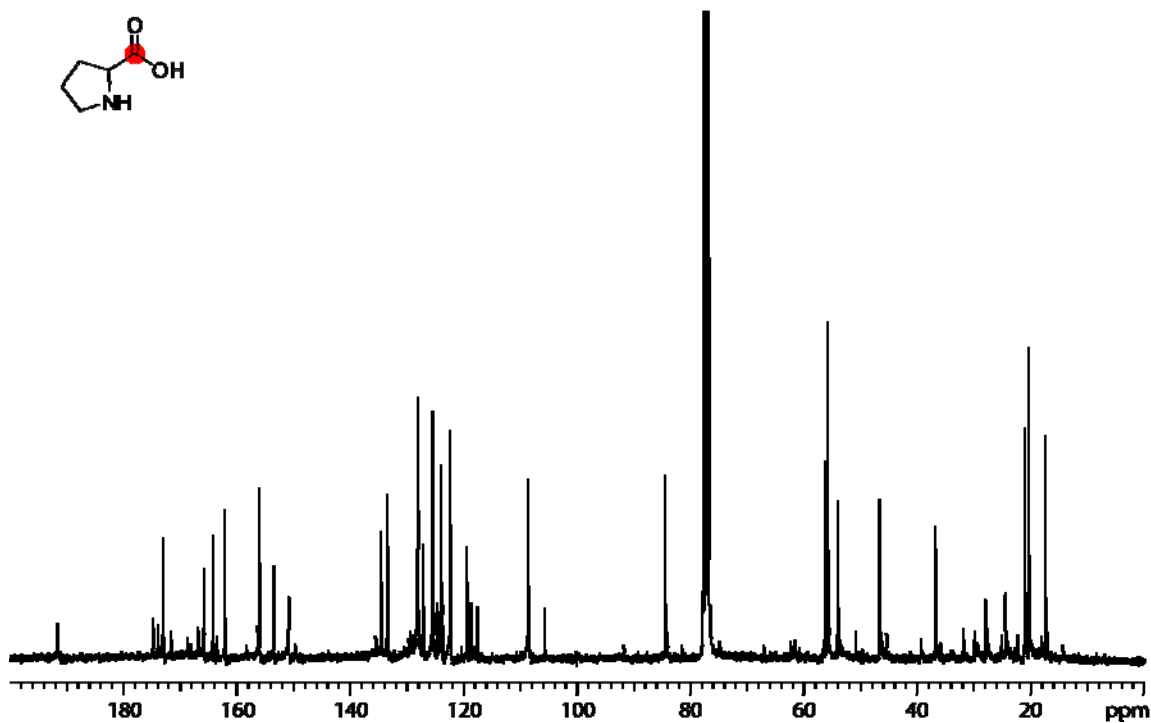


Figure 162. Azinomycin B, fed [1-¹³C] L-proline 100mg.

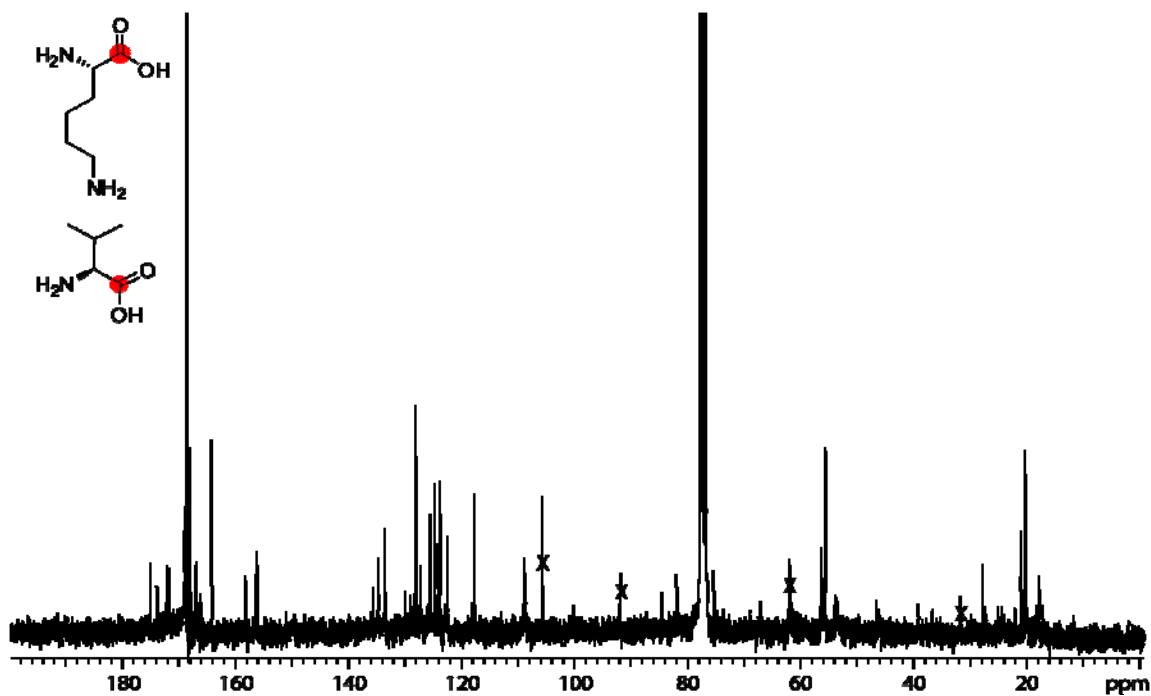


Figure 163. Azinomycin B, fed [1-¹³C] L-lysine•HCl 100mg co-fed with [1-¹³C] L-valine 100mg.

[1-¹³C] L-valine appears to have been incorporated in to the epoxyamide derivative with C17 at 168.7ppm, with some incorporation C17 of azinomycin B at 164.0 ppm. No obvious incorporation of [1-¹³C]lysine.

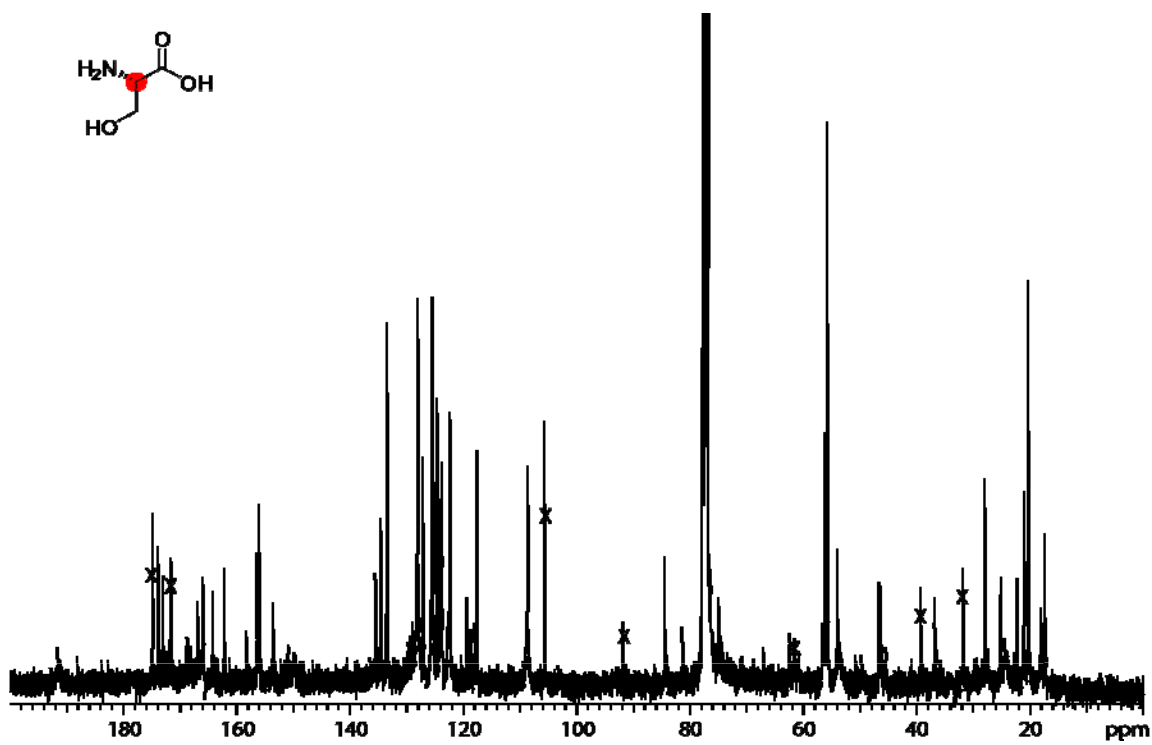


Figure 164. Azinomycin B, fed $[2\text{-}^{13}\text{C}]$ L-serine 100mg.

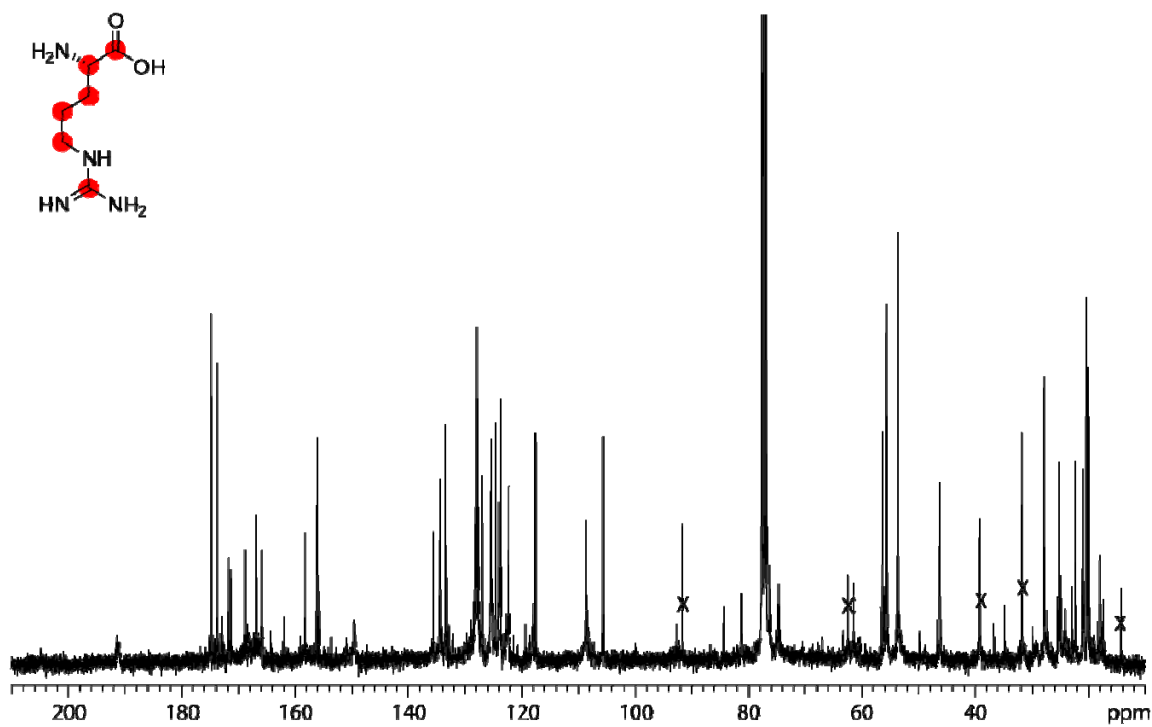


Figure 165. Azinomycin B, fed $[U\text{-}^{13}\text{C}_6]$ L-arginine 100mg.
No splitting patterns observed to indicate incorporation of the universally labeled substrate.

Sugars

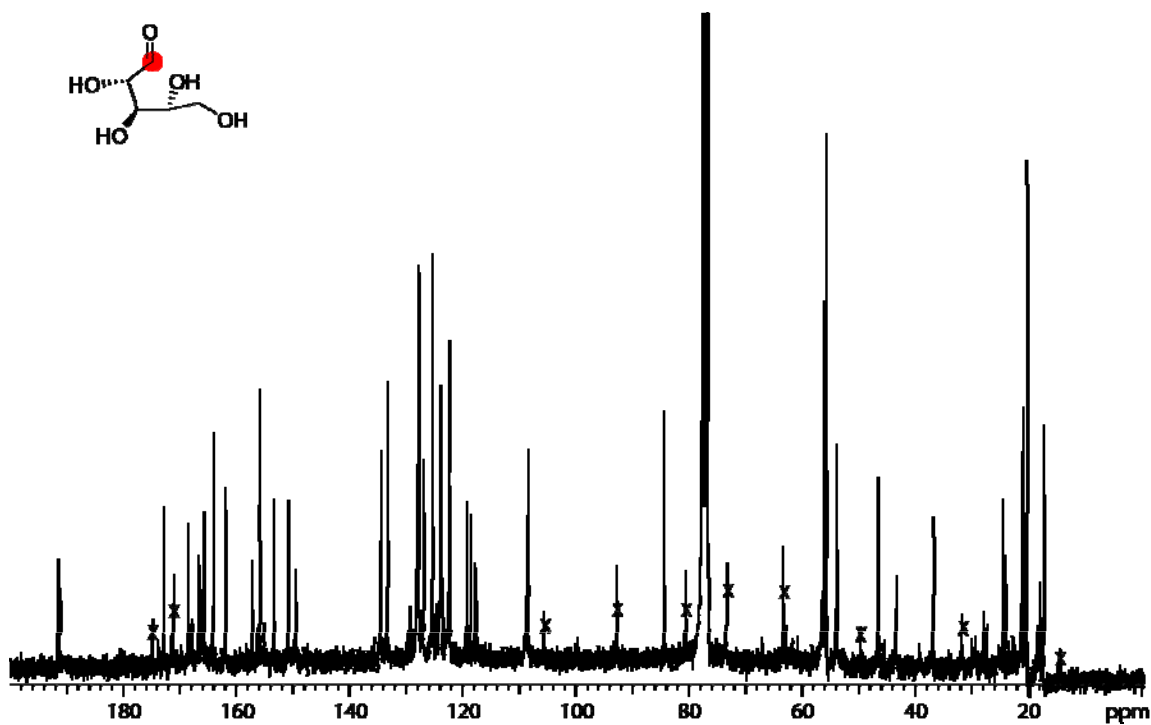


Figure 166. Azinomycin B, fed [1-¹³C] D-arabinose 900mg.
No Incorporation observed.

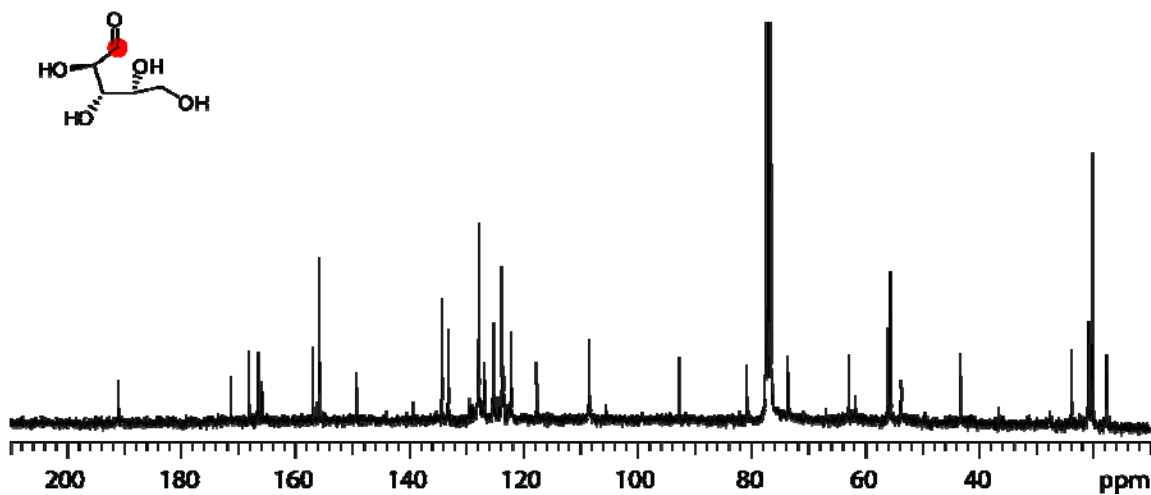


Figure 167. Azinomycin B, fed [1-¹³C] D-Xylose 900mg.
No significant incorporation seen. Azinomycin B aziridine ring hydrolyzed product isolated and seen in above spectrum.

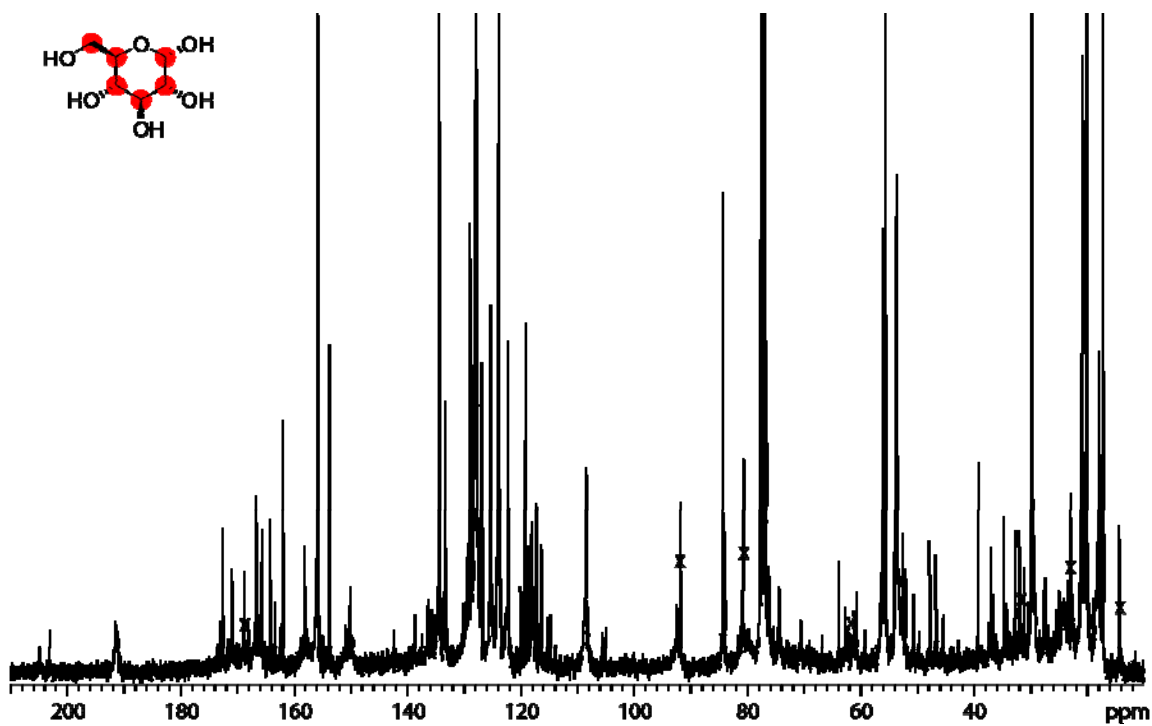


Figure 168. Azinomycin B, fed $[\text{U-}^{13}\text{C}_6]$ D-Glucose 1000mg.

No splitting patterns are observed in the carbons, azinomycin B, azinomycin A, naphthamide are present in the sample.

Synthesized azabicyclic compounds

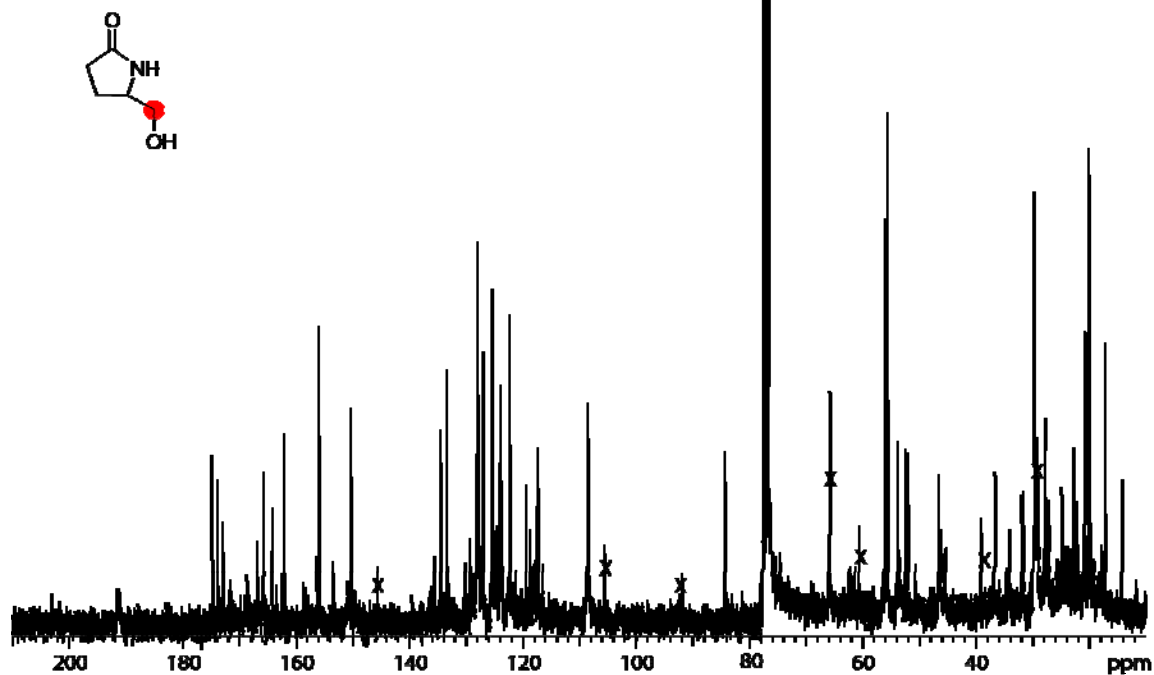


Figure 169. Azinomycin B, fed [^{13}C] Pyroglutaminol (5-(hydroxymethyl)pyrrolidin-2-one), (AZ5) 140mg.

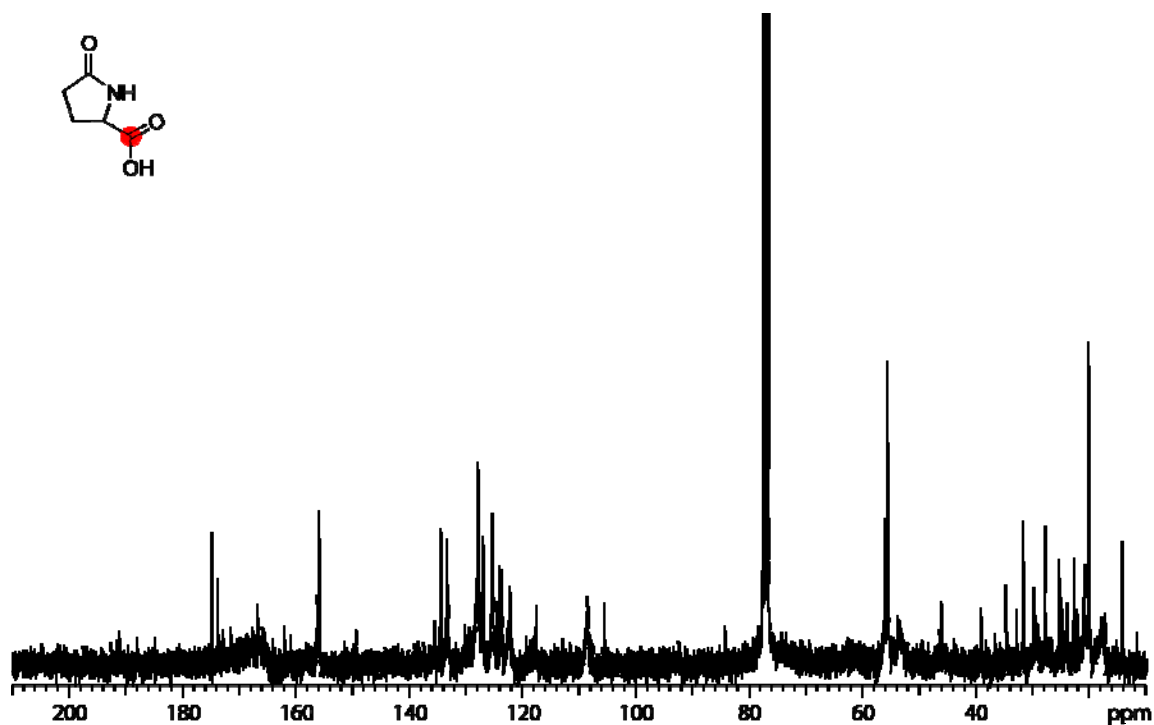


Figure 170. Azinomycin B, fed [^{13}C] Pyroglutamic acid (5-oxopyrrolidine-2-carboxylic acid), (AZ17) 160mg.

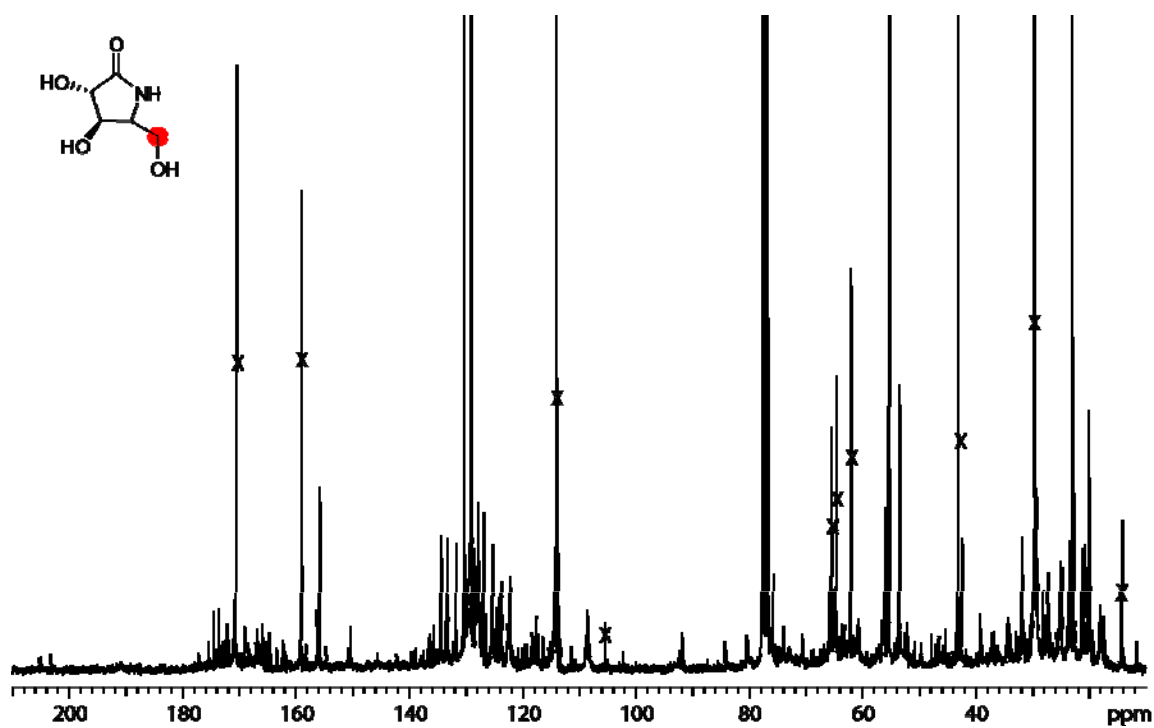


Figure 171. Azinomycin B, fed $[1-^{13}\text{C}]$ (3S,4R)-3,4-dihydroxy-5-(hydroxymethyl)pyrrolidin-2-one, (AZ16a) 200mg.

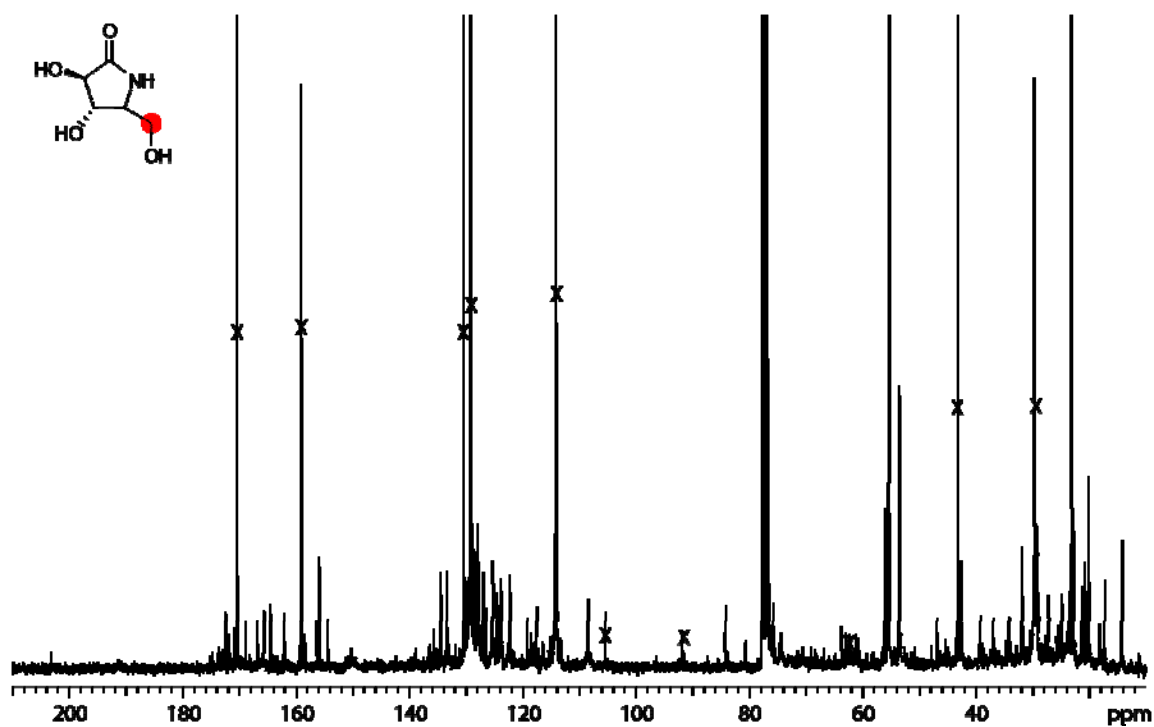


Figure 172. Azinomycin B, fed $[1-^{13}\text{C}]$ (3R,4S)-3,4-dihydroxy-5-(hydroxymethyl)pyrrolidin-2-one, (AZ16b) 200mg.

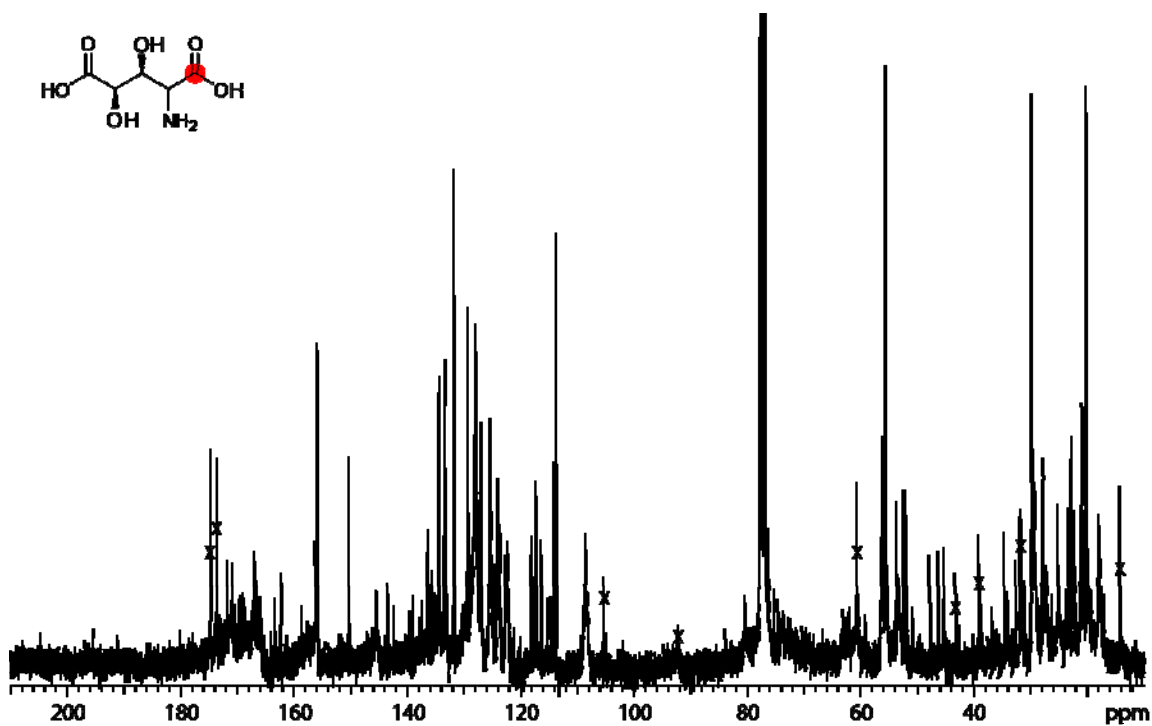


Figure 173. Azinomycin B, fed [¹³C] 3, 4 dihydroxy glutamic acid ((3S,4R)-2-amino-3,4-dihydroxypentanedioic acid) (AZ15a) 200mg.

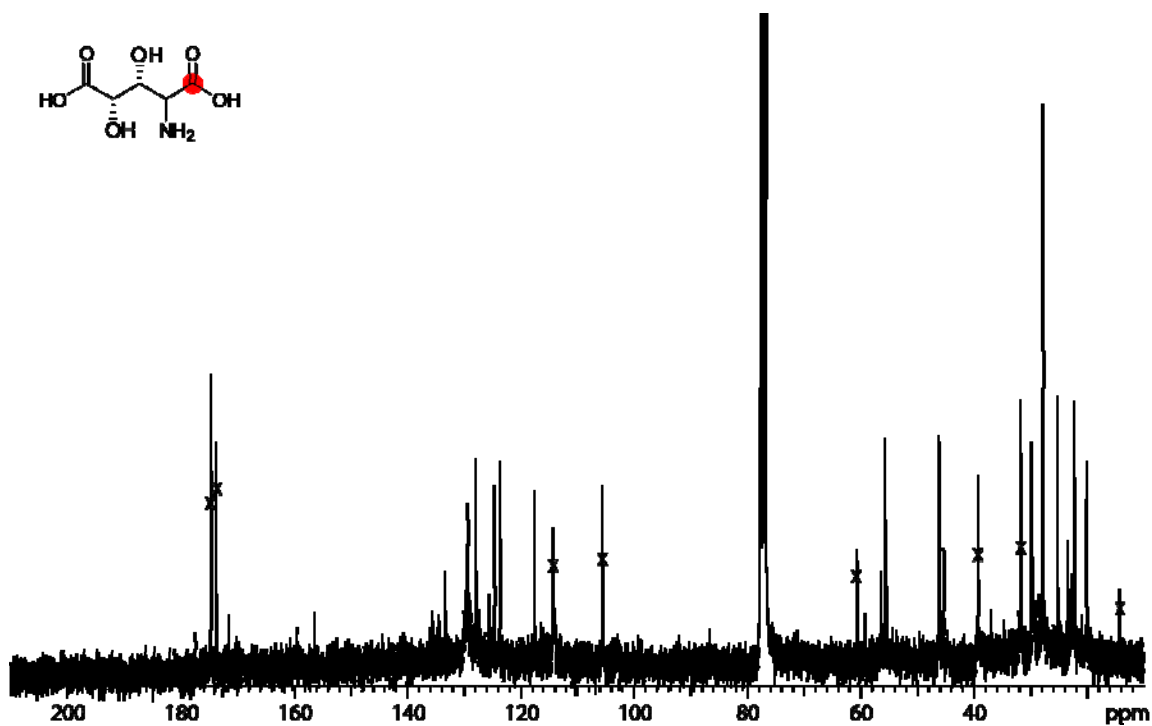
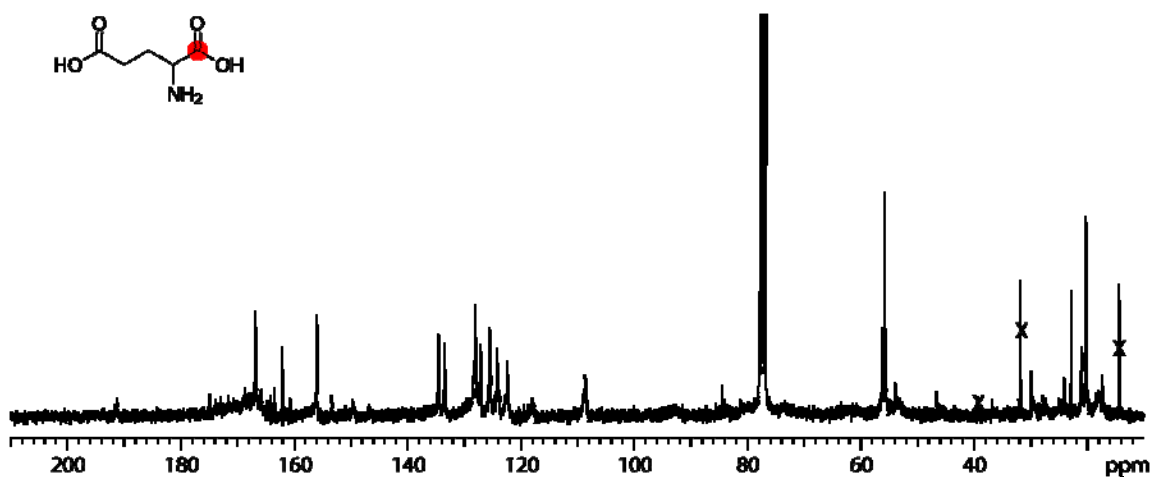
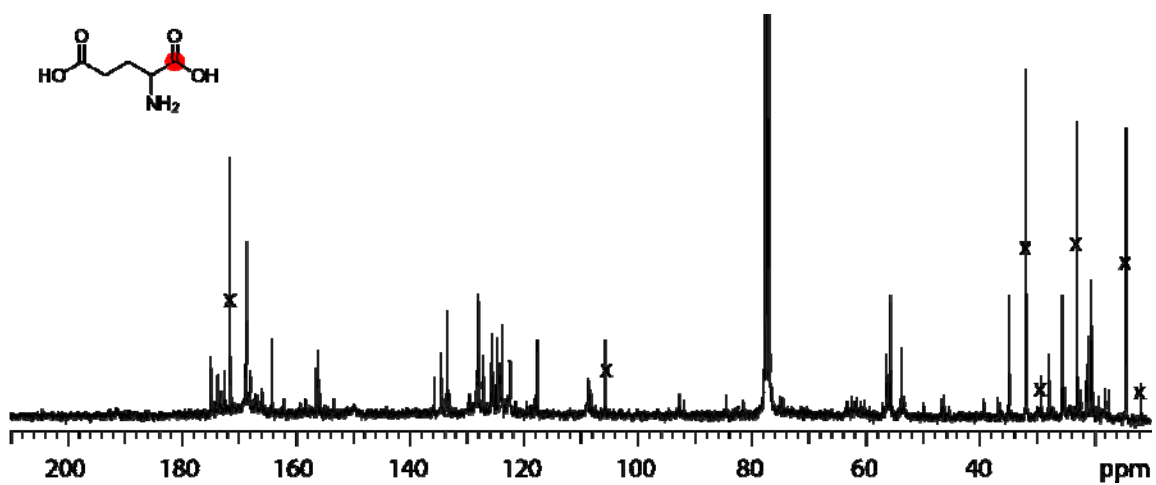


Figure 174. Azinomycin B, fed [¹³C] 3, 4 dihydroxy glutamic acid (3R,4S)-2-amino-3,4-dihydroxypentanedioic acid) (AZ15b) 200mg.



PERCENT INCORPORATION NUMERICAL DATA FOR ISOTOPICALLY LABELED
COMPOUND FEEDING EXPERIMENTS.

Table 24. Stable isotope compounds and the calculated % Incorporation as calculated in standardized reference to C3'OCH₃ or C20.

% Incorporation is defined as $[A_{C\#N} - B_{C\#N}]/[B_{C\#N}] \times 1.10$ for ¹³C carbons where A_{C#N} is the given # carbon's signal peak height normalized to the stated reference carbon (in this case C3'OCH₃ or C20) for the labeled compound feeding treatment and B_{C#N} is the given # carbon's signal peak height normalized to the stated reference carbon (in this case C3'OCH₃ or C20) for unlabeled (natural abundance) azinomycin B. 1.10 is the % of ¹³C standardly found. In most cases when the molar amount of compound series was not exactly on standard, the culture volume was adjusted to make up for a lower amount of labeled compound. In the few cases when a larger than normal amount was administered, a numerical normalization factor (N) is added to the calculation, to adjust downwards the impact of administered compound. As this is only used in comparative series, the normalization factor (N) is not usually employed.

Basic Units

Substrates Carbon Position	shift ppm	[1- ¹³ C] sodium acetate 1g Carbon Reference		Methyl ¹³ C Methionine 50mg Carbon Reference		1- ¹³ C threonine100mg, 1- ¹³ C valine 100mg Carbon Reference	
		3'OCH ₃	C20	3'OCH ₃	C20	3'OCH ₃	C20
C1	24.5	4.89	4.82	-1.10	-0.43	0.09	0.23
C2	191.5	2.32	2.28	-1.09	0.05	0.87	1.11
C3	118.6	0.55	0.53	-1.09	0.33	-0.11	0.01
C4	150.8	4.97	4.89	-1.09	0.18	7.64	8.69
C6	162	5.02	4.94	-1.09	0.37	0.44	0.62
C7	119.3	0.26	0.24	-1.08	0.49	0.46	0.65
C8	153	0.08	0.07	-1.09	0.15	0.51	0.70
C10	36.7	0.17	0.15	-1.09	0.02	-0.23	-0.13
C11	46.4	0.21	0.19	-1.09	0.41	-0.13	-0.01
C12	77.4	n/a	n/a	n/a	n/a	n/a	n/a
C13	84.4	0.07	0.06	-1.09	0.25	-0.16	-0.05
C14	173	5.75	5.66	-1.09	0.22	0.41	0.59
C15	21	0.00	-0.02	-1.09	0.10	-0.09	0.03
C17	164	0.85	0.82	-1.09	0.08	8.43	9.57
C18	77.1	n/a	n/a	n/a	n/a	n/a	n/a
C19	56.2	0.01	0.00	-1.09	0.40	0.39	0.57
C20	17.2	0.01	0.00	-1.09	0.00	-0.12	0.00
C21	53.9	0.00	-0.02	-1.09	0.10	-0.09	0.03
C1'	128.1	0.11	0.10	-1.08	0.64	0.46	0.64
C1' CO	165.7	3.68	3.62	-1.09	0.26	0.34	0.51
C2'	122.3	5.11	5.03	-1.09	-0.04	-0.10	0.02
C3'	156	0.10	0.08	-1.09	0.10	0.57	0.77
C3' OCH ₃	55.7	0.00	-0.01	0.00	70.64	0.00	0.13
C4'	108.5	5.98	5.89	-1.09	0.07	-0.19	-0.08
C4'a	134.5	0.04	0.02	-1.09	0.26	0.46	0.65
C5'	133.3	5.21	5.13	-1.09	0.44	0.49	0.68
C5' CH ₃	20.3	-0.11	-0.12	-1.09	0.33	-0.82	-0.78
C6'	127.9	0.11	0.09	-1.08	0.62	0.05	0.18
C7'	125.4	6.44	6.34	-1.08	0.50	0.02	0.15
C8'	123.9	0.08	0.07	-1.08	0.54	-0.12	0.00
C8'a	127	4.09	4.03	-1.08	0.67	0.63	0.84

Table 25. Stable isotope compounds and the calculated % Incorporation as calculated in standardized reference to C3'OCH₃ or C20.

% Incorporation is defined as $[A_{C\#N} - B_{C\#N}]/[B_{C\#N}] \times 1.10$ for ¹³C carbons where A_{C#N} is the given # carbon's signal peak height normalized to the stated reference carbon (in this case C3'OCH₃ or C20) for the labeled compound feeding treatment and B_{C#N} is the given # carbon's signal peak height normalized to the stated reference carbon (in this case C3'OCH₃ or C20) for unlabeled (natural abundance) azinomycin B. 1.10 is the % of ¹³C standardly found. In most cases when the molar amount of compound series was not exactly on standard, the culture volume was adjusted to make up for a lower amount of labeled compound. In the few cases when a larger than normal amount was administered, a numerical normalization factor (N) is added to the calculation, to adjust downwards the impact of administered compound. As this is only used in comparative series, the normalization factor (N) is not usually employed.

Epoxide Moiety Series

Substrates Carbon Position	shift ppm	[1-13C] V2 TFA									
		[1-13C] V2 100mg		100mg		[1-13C] V3 120mg		[1-13C] V3 140mg		[1-13C] V5 166mg	
		Carbon Reference 3'OCH3	C20	Carbon Reference 3'OCH3	C20	Carbon Reference 3'OCH3	C20	Carbon Reference 3'OCH3	C20	Carbon Reference 3'OCH3	C20
C1	24.5	0.17	0.26	0.56	0.91	-0.87	0.17	1.46	2.50	-0.54	1.10
C2	191.5	0.43	0.55	1.88	2.51	-0.32	2.39	3.24	5.02	-0.65	0.08
C3	118.6	-0.22	-0.15	0.36	0.67	-0.70	0.86	0.82	1.58	-0.04	5.42
C4	150.8	0.20	0.29	0.41	0.74	-0.77	0.60	0.90	1.70	-0.49	1.49
C6	162	-0.07	0.01	0.31	0.61	-0.72	0.79	0.14	0.63	-0.21	3.93
C7	119.3	-0.02	0.06	0.23	0.51	-0.70	0.88	0.15	0.64	-0.11	4.87
C8	153	0.03	0.11	-0.62	-0.51	-1.02	-0.41	-0.06	0.35	-0.72	-0.47
C10	36.7	-0.07	0.00	-0.32	-0.15	-0.86	0.21	-0.33	-0.04	-0.43	2.07
C11	46.4	0.01	0.10	-0.31	-0.13	-0.86	0.23	-0.28	0.04	-0.65	0.11
C12	77.4	n/a	n/a	n/a	n/a	n/a	n/a	n/a	n/a	n/a	n/a
C13	84.4	-0.05	0.03	-0.24	-0.06	-0.92	-0.01	-0.47	-0.23	-0.41	2.24
C14	173	0.09	0.18	-0.19	0.00	-0.47	1.81	0.12	0.61	-0.53	1.12
C15	21	-0.10	-0.02	-0.06	0.16	-0.50	1.66	-0.45	-0.20	-0.08	5.13
C17	164	8.71	9.44	6.63	8.27	0.54	5.90	4.18	6.34	8.10	76.90
C18	77.1	n/a	n/a	n/a	n/a	n/a	n/a	n/a	n/a	n/a	n/a
C19	56.2	-0.04	0.04	0.35	0.66	-0.08	3.37	0.66	1.36	0.27	8.20
C20	17.2	-0.08	0.00	-0.19	0.00	-0.91	0.00	-0.30	0.00	-0.66	0.00
C21	53.9	-0.10	-0.02	-0.08	0.16	-0.50	1.66	-0.45	-0.20	-0.08	5.13
C1'	128.1	-0.09	-0.01	0.49	0.83	0.49	5.66	0.25	0.79	0.41	9.44
C1' CO	165.7	-0.06	0.02	0.34	0.64	-0.20	2.91	0.16	0.66	0.37	9.09
C2'	122.3	-0.02	0.06	-0.12	0.09	-0.47	1.79	-0.18	0.18	-0.22	3.89
C3'	156	0.11	0.20	0.47	0.80	0.38	5.25	0.26	0.80	0.58	10.95
C3' OCH3	55.7	0.00	0.08	0.00	0.24	0.00	3.70	0.00	0.43	0.00	5.81
C4'	108.5	-0.06	0.01	-0.19	0.00	-0.62	1.19	-0.17	0.19	-0.24	3.66
C4'a	134.5	0.00	0.08	0.39	0.70	0.79	6.92	0.22	0.74	0.40	9.32
C5'	133.3	-0.03	0.05	0.49	0.83	1.38	9.30	0.30	0.85	0.18	7.40
C5' CH3	20.3	-0.06	0.02	-0.08	0.16	0.22	4.59	0.09	0.56	-0.03	5.58
C6'	127.9	0.01	0.10	-0.02	0.21	0.12	4.20	-0.08	0.31	-0.11	4.84
C7'	125.4	-0.03	0.05	0.07	0.32	-0.07	3.42	0.23	0.75	-0.15	4.47
C8'	123.9	-0.01	0.07	-0.14	0.07	-0.38	2.17	-0.22	0.12	-0.22	3.89
C8'a	127	-0.03	0.04	0.54	0.89	1.05	7.95	0.54	1.19	0.41	9.37

Table 26. Stable isotope compounds and the calculated % Incorporation as calculated in standardized reference to C3'OCH₃ or C20.

% Incorporation is defined as $[A_{C\#N} - B_{C\#N}]/[B_{C\#N}] \times 1.10$ for ¹³C carbons where A_{C#N} is the given # carbon's signal peak height normalized to the stated reference carbon (in this case C3'OCH₃ or C20) for the labeled compound feeding treatment and B_{C#N} is the given # carbon's signal peak height normalized to the stated reference carbon (in this case C3'OCH₃ or C20) for unlabeled (natural abundance) azinomycin B. 1.10 is the % of ¹³C standardly found. In most cases when the molar amount of compound series was not exactly on standard, the culture volume was adjusted to make up for a lower amount of labeled compound. In the few cases when a larger than normal amount was administered, a numerical normalization factor (N) is added to the calculation, to adjust downwards the impact of administered compound. As this is only used in comparative series, the normalization factor (N) is not usually employed.

Epoxide Moiety Series

Substrates Carbon Position	[1-13C] V8 100mg Carbon Reference shift ppm	[1-13C] V9 TFA 100mg				[1-13C] V10 HCl 90mg		[1-13C] V12 127mg	
		Carbon Reference		Carbon Reference		Carbon Reference		Carbon Reference	
		3'OCH ₃	C20	3'OCH ₃	C20	3'OCH ₃	C20	3'OCH ₃	C20
C1	24.5	-0.95	2.05	-0.72	0.73	1.25	2.35	-0.14	0.74
C2	191.5	-0.48	11.11	-0.20	3.17	2.31	3.91	0.39	1.81
C3	118.6	-1.01	0.88	-0.80	0.37	1.01	2.00	-0.19	0.65
C4	150.8	-0.88	3.35	-0.79	0.42	0.85	1.76	-0.11	0.80
C6	162	-1.02	0.55	-0.31	2.68	0.04	0.57	-0.37	0.29
C7	119.3	-0.99	1.24	-0.78	0.44	0.20	0.81	-0.19	0.64
C8	153	-1.01	0.85	-0.79	0.39	0.12	0.70	-0.32	0.38
C10	36.7	-1.05	0.02	-0.93	-0.24	-0.31	0.06	-0.46	0.09
C11	46.4	-0.78	5.23	-0.89	-0.08	-0.22	0.20	-0.38	0.27
C12	77.4	n/a	n/a	n/a	n/a	n/a	n/a	n/a	n/a
C13	84.4	-1.04	0.27	-0.85	0.13	-0.22	0.20	-0.43	0.17
C14	173	-0.70	6.98	-0.77	0.50	0.12	0.69	-0.34	0.35
C15	21	-0.91	2.85	-0.41	2.19	-0.24	0.16	-0.66	-0.30
C17	164	-0.99	1.22	-0.64	1.12	0.06	0.61	6.03	13.22
C18	77.1	n/a	n/a	n/a	n/a	n/a	n/a	n/a	n/a
C19	56.2	-0.99	1.26	0.09	4.54	0.73	1.59	-0.29	0.44
C20	17.2	-1.05	0.00	-0.87	0.00	-0.35	0.00	-0.51	0.00
C21	53.9	-0.91	2.85	-0.41	2.19	-0.24	0.16	-0.66	-0.30
C1'	128.1	-0.31	14.52	0.61	6.98	0.33	1.00	-0.12	0.79
C1' CO	165.7	-0.89	3.20	0.21	5.12	0.17	0.77	-0.52	-0.02
C2'	122.3	-0.77	5.44	-0.48	1.83	-0.03	0.48	-0.28	0.47
C3'	156	-0.17	17.27	0.61	7.01	0.20	0.81	-0.22	0.58
C3' OCH ₃	55.7	0.00	20.57	0.00	4.12	0.00	0.52	0.00	1.03
C4'	108.5	-1.02	0.82	-0.80	0.37	-0.14	0.32	-0.39	0.25
C4'a	134.5	0.47	29.75	0.31	5.59	0.38	1.08	-0.19	0.84
C5'	133.3	0.57	31.88	0.40	6.02	1.97	3.41	-0.08	0.86
C5' CH ₃	20.3	-0.29	14.88	0.08	4.41	0.32	0.99	-0.13	0.77
C6'	127.9	0.27	25.79	-0.04	3.94	0.75	1.62	0.33	1.70
C7'	125.4	-0.83	4.37	-0.49	1.83	0.45	1.18	-0.28	0.47
C8'	123.9	-0.71	6.89	-0.68	0.91	-0.02	0.49	-0.31	0.41
C8'a	127	0.06	21.78	1.16	9.58	0.83	1.73	-0.02	0.98

Table 27. Stable isotope compounds and the calculated % Incorporation as calculated in standardized reference to C3'OCH₃ or C20.

% Incorporation is defined as $[A_{C\#N} - B_{C\#N}]/[B_{C\#N}] \times 1.10$ for ¹³C carbons where A_{C#N} is the given # carbon's signal peak height normalized to the stated reference carbon (in this case C3'OCH₃ or C20) for the labeled compound feeding treatment and B_{C#N} is the given # carbon's signal peak height normalized to the stated reference carbon (in this case C3'OCH₃ or C20) for unlabeled (natural abundance) azinomycin B. 1.10 is the % of ¹³C standardly found. In most cases when the molar amount of compound series was not exactly on standard, the culture volume was adjusted to make up for a lower amount of labeled compound. In the few cases when a larger than normal amount was administered, a numerical normalization factor (N) is added to the calculation, to adjust downwards the impact of administered compound. As this is only used in comparative series, the normalization factor (N) is not usually employed.

Basic Units

Substrates Carbon Position	shift ppm	[1-13C] glycine 1g		[1-13C] glycine 100mg		[1-13C] glycine 900mg, 1-13C valine 100mg		[2-13C] glycine 1g	
		Carbon Reference		Carbon Reference		Carbon Reference		Carbon Reference	
		3'OCH3	C20	3'OCH3	C20	3'OCH3	C20	3'OCH3	C20
C1	24.5	-0.67	0.50	0.25	0.73	0.44	0.50	-1.07	-0.58
C2	191.5	-0.20	2.24	0.72	1.36	0.86	0.93	-1.08	-0.77
C3	118.6	-0.89	-0.31	-0.17	0.16	-0.06	-0.02	-1.04	-0.19
C4	150.8	-0.81	0.00	0.22	0.69	0.45	0.51	-0.90	1.75
C6	162	-0.51	1.08	-0.16	0.16	0.78	0.86	-1.00	0.45
C7	119.3	-0.75	0.21	-0.18	0.15	0.20	0.25	-1.01	0.25
C8	153	-1.00	-0.70	-0.14	0.19	0.24	0.29	-1.11	-1.18
C10	36.7	-0.74	0.25	-0.28	0.01	-0.17	-0.14	-1.10	-1.00
C11	46.4	-0.91	-0.38	-0.22	0.09	-0.02	0.02	-1.09	-0.79
C12	77.4	n/a	n/a	n/a	n/a	n/a	n/a	n/a	n/a
C13	84.4	-0.88	-0.27	-0.23	0.08	-0.06	-0.02	-1.07	-0.57
C14	173	-0.91	-0.39	-0.19	0.13	0.29	0.34	-1.05	-0.29
C15	21	-0.51	1.10	-0.26	0.03	-0.02	0.03	-0.96	1.00
C17	164	-0.72	0.30	0.10	0.51	18.43	19.20	-1.10	-1.00
C18	77.1	n/a	n/a	n/a	n/a	n/a	n/a	n/a	n/a
C19	56.2	-0.20	2.24	-0.19	0.13	0.08	0.12	-0.99	0.52
C20	17.2	-0.81	0.00	-0.29	0.00	-0.04	0.00	-1.03	0.00
C21	53.9	-0.51	1.10	-0.26	0.03	-0.02	0.03	-0.96	1.00
C1'	128.1	0.03	3.06	0.00	0.38	0.10	0.15	-0.93	1.33
C1' CO	165.7	-0.43	1.37	-0.20	0.12	0.05	0.09	-1.00	0.39
C2'	122.3	-0.70	0.39	-0.21	0.10	0.01	0.05	-1.04	-0.18
C3'	156	0.05	3.14	-0.04	0.33	0.18	0.23	-0.98	0.68
C3' OCH3	55.7	0.00	2.97	0.00	0.39	0.00	0.04	0.00	14.35
C4'	108.5	-0.64	0.61	-0.26	0.04	-0.35	-0.32	-1.05	-0.22
C4'a	134.5	0.05	3.15	-0.03	0.34	0.24	0.29	-0.97	0.82
C5'	133.3	0.16	2.36	0.00	0.38	0.24	0.29	0.99	0.61
C5' CH3	20.3	-0.08	2.69	-0.19	0.13	-0.09	-0.05	-1.01	0.31
C6'	127.9	-0.25	2.06	0.50	1.06	0.01	0.05	-1.00	0.36
C7'	125.4	-0.46	1.26	-0.18	0.14	0.01	0.05	-1.01	0.23
C8'	123.9	-0.50	1.12	-0.21	0.10	-0.04	0.00	-1.04	-0.08
C8'a	127	0.54	4.94	-0.04	0.32	0.15	0.20	-0.90	1.78

Table 28. Stable isotope compounds and the calculated % Incorporation as calculated in standardized reference to C3'OCH₃ or C20.

% Incorporation is defined as $[A_{C\#N} - B_{C\#N}]/[B_{C\#N}] \times 1.10$ for ¹³C carbons where A_{C#N} is the given # carbon's signal peak height normalized to the stated reference carbon (in this case C3'OCH₃ or C20) for the labeled compound feeding treatment and B_{C#N} is the given # carbon's signal peak height normalized to the stated reference carbon (in this case C3'OCH₃ or C20) for unlabeled (natural abundance) azinomycin B. 1.10 is the % of ¹³C standardly found. In most cases when the molar amount of compound series was not exactly on standard, the culture volume was adjusted to make up for a lower amount of labeled compound. In the few cases when a larger than normal amount was administered, a numerical normalization factor (N) is added to the calculation, to adjust downwards the impact of administered compound. As this is only used in comparative series, the normalization factor (N) is not usually employed.

Substrates:		[1-13C] Proline 100mg		2-13C L-serine 100mg		[3-13C] Apartic Acid 100mg		[U-13C] L-Arginine 100mg		[1-13C] lysine 100mg, [1-13C] valine 100mg	
Carbon	Position	Carbon Reference		Carbon Reference		Carbon Reference		Carbon Reference		Carbon Reference	
	shift ppm	3'OCH ₃	C20	3'OCH ₃	C20	3'OCH ₃	C20	3'OCH ₃	C20	3'OCH ₃	C20
C1	24.5	-0.19	0.14	-0.48	-0.62	-0.58	0.17	-0.67	0.95	-0.41	1.98
C2	191.5	0.28	0.79	0.33	0.01	-0.33	0.76	-0.03	3.97	-0.42	1.92
C3	118.6	-0.31	-0.01	-0.31	-0.48	-0.52	0.30	-0.70	0.79	-0.57	1.25
C4	150.8	-0.25	0.06	-0.57	-0.69	-0.75	-0.26	-0.76	0.55	-0.61	1.09
C6	162	0.24	0.73	0.00	-0.24	-0.25	0.94	-0.69	0.86	-0.39	2.04
C7	119.3	0.08	0.51	-0.15	-0.36	-0.18	1.12	-0.69	0.84	-0.65	0.89
C8	153	-0.24	0.09	-0.30	-0.48	-0.75	-0.24	-0.86	0.05	-0.62	1.06
C10	36.7	-0.32	-0.03	-0.57	-0.69	-0.72	-0.17	-0.87	0.02	-0.79	0.30
C11	46.4	-0.24	0.08	-0.55	-0.67	-0.61	0.09	-0.11	3.59	-0.70	0.70
C12	77.4	n/a	n/a	n/a	n/a	n/a	n/a	n/a	n/a	n/a	n/a
C13	84.4	-0.31	-0.02	-0.52	-0.65	-0.66	-0.03	-0.86	0.06	-0.75	0.45
C14	173	0.06	0.48	-0.02	-0.26	-0.58	0.15	-0.66	1.02	-0.74	0.52
C15	21	-0.14	0.22	-0.56	-0.68	-0.40	0.59	-0.28	2.80	-0.41	1.94
C17	164	-0.24	0.07	-0.42	-0.57	-0.65	-0.01	-0.86	-0.04	3.37	18.55
C18	77.1	n/a	n/a	n/a	n/a	n/a	n/a	n/a	n/a	n/a	n/a
C19	56.2	0.00	0.41	0.40	0.07	0.60	2.99	0.21	5.08	0.05	4.00
C20	17.2	-0.30	0.00	-0.53	-0.65	-0.65	0.00	-0.87	0.00	-0.86	0.00
C21	53.9	-0.14	0.22	-0.56	-0.68	-0.40	0.59	-0.28	2.80	-0.41	1.94
C1'	128.1	0.18	0.66	0.52	0.17	0.49	2.73	0.76	7.66	0.89	7.68
C1' CO	165.7	-0.08	0.30	-0.34	-0.51	0.01	1.57	0.19	5.01	-0.53	1.42
C2'	122.3	-0.18	0.16	0.05	-0.21	-0.37	0.67	-0.37	2.34	-0.39	2.06
C3'	156	0.15	0.62	0.31	0.00	0.64	3.08	0.59	6.85	0.31	5.10
C3' OCH ₃	55.7	0.00	0.41	0.90	0.46	0.00	1.55	0.00	4.10	0.00	3.76
C4'	108.5	-0.22	0.11	0.05	-0.21	-0.55	0.22	-0.39	2.26	-0.69	0.71
C4'a	134.5	0.13	0.58	0.60	0.23	0.19	2.02	0.08	4.47	0.16	4.44
C5'	133.3	0.14	0.60	1.85	1.20	0.41	2.54	0.73	7.54	1.43	10.05
C5' CH ₃	20.3	-0.09	0.28	0.32	0.00	0.12	1.83	0.11	4.60	-0.04	3.57
C6'	127.9	0.01	0.42	0.66	0.27	0.19	2.02	0.20	5.02	1.57	10.64
C7'	125.4	-0.05	0.34	0.68	0.29	0.40	2.52	-0.13	3.48	-0.01	3.70
C8'	123.9	-0.16	0.18	-0.12	-0.34	-0.38	0.65	-0.70	0.81	-0.52	1.50
C8'a	127	0.20	0.68	1.63	1.03	1.34	4.77	1.05	9.02	0.95	7.95

Table 29. Stable isotope compounds and the calculated % Incorporation as calculated in standardized reference to C3'OCH₃ or C20.

% Incorporation is defined as $[A_{C\#N} - B_{C\#N}]/[B_{C\#N}] \times 1.10$ for ¹³C carbons where A_{C#N} is the given # carbon's signal peak height normalized to the stated reference carbon (in this case C3'OCH₃ or C20) for the labeled compound feeding treatment and B_{C#N} is the given # carbon's signal peak height normalized to the stated reference carbon (in this case C3'OCH₃ or C20) for unlabeled (natural abundance) azinomycin B. 1.10 is the % of ¹³C standardly found. In most cases when the molar amount of compound series was not exactly on standard, the culture volume was adjusted to make up for a lower amount of labeled compound. In the few cases when a larger than normal amount was administered, a numerical normalization factor (N) is added to the calculation, to adjust downwards the impact of administered compound. As this is only used in comparative series, the normalization factor (N) is not usually employed.

Substrates:		[1- ¹³ C] AZ6 1g		[1- ¹³ C] AZ6 231mg		[1- ¹³ C] Xylose 900mg		[1- ¹³ C] Arabinose 900mg		[U- ¹³ C6] DGlucose 1000mg	
Carbon	Position	Carbon Reference		Carbon Reference		Carbon Reference		Carbon Reference		Carbon Reference	
	shift ppm	3'OCH ₃	C20	3'OCH ₃	C20	3'OCH ₃	C20	3'OCH ₃	C20	3'OCH ₃	C20
C1	24.5	-0.63	0.27	-0.81	0.26	-1.11	-1.11	0.44	0.56	-0.73	-0.84
C2	191.5	-0.50	0.63	-0.07	3.66	-0.76	6.52	0.15	0.20	-0.52	-0.69
C3	118.6	-0.71	0.04	-0.87	-0.01	-0.90	3.46	0.42	0.54	-0.39	-0.60
C4	150.8	-0.90	-0.51	-0.92	-0.23	-0.87	4.21	0.44	0.56	-0.89	-0.95
C6	162	1.09	5.20	-0.10	3.50	-0.95	2.42	0.66	0.84	-0.16	-0.43
C7	119.3	-0.71	0.04	-0.91	-0.21	-0.93	2.81	0.57	0.72	0.43	0.00
C8	153	-0.90	-0.49	-0.82	0.21	-1.00	1.21	0.64	0.81	0.17	-0.19
C10	36.7	-0.72	0.02	-0.96	-0.45	0.12	25.73	1.00	1.28	-0.93	-0.96
C11	46.4	-0.81	-0.28	-0.91	-0.20	-1.04	0.37	1.09	1.40	-0.85	-0.93
C12	77.4	n/a	n/a	n/a	n/a	n/a	n/a	n/a	n/a	n/a	n/a
C13	84.4	-0.85	-0.35	-0.96	-0.44	-1.05	0.28	1.37	1.75	-0.23	-0.47
C14	173	-0.85	-0.36	-0.84	0.12	-0.94	2.54	0.62	0.79	-0.55	-0.71
C15	21	-0.47	0.73	-0.75	0.53	-0.16	19.63	1.41	1.80	0.00	-0.31
C17	164	-0.80	-0.23	-0.89	-0.11	-1.07	-0.19	0.85	1.09	-0.68	-0.80
C18	77.1	n/a	n/a	n/a	n/a	n/a	n/a	n/a	n/a	n/a	n/a
C19	56.2	-0.11	1.76	-0.46	1.88	0.08	24.83	1.06	1.36	-0.06	-0.35
C20	17.2	-0.72	0.00	-0.87	0.00	-1.06	0.00	1.64	2.09	0.00	-0.31
C21	53.9	-0.47	0.73	-0.75	0.53	-0.16	19.63	1.41	1.80	0.00	-0.31
C1'	128.1	-0.02	2.03	-0.34	2.42	1.09	46.87	0.50	0.65	1.75	0.95
C1' CO	165.7	-0.42	0.86	-0.65	1.00	-1.01	1.12	0.52	0.67	-0.45	-0.64
C2'	122.3	-0.62	0.30	-0.77	0.43	-0.28	17.03	1.46	1.87	-0.54	-0.70
C3'	156	0.13	2.45	-0.07	3.63	1.80	57.97	0.80	1.03	1.65	0.87
C3' OCH ₃	55.7	0.00	2.08	0.00	3.97	0.00	23.09	1.80	2.30	0.75	0.22
C4'	108.5	-0.61	0.32	-0.81	0.28	-0.89	3.69	1.20	1.54	-0.69	-0.81
C4'a	134.5	-0.12	1.72	0.00	3.99	1.58	57.46	0.61	0.78	1.75	0.94
C5'	133.3	-0.16	1.61	-0.32	2.52	0.47	33.41	0.78	1.00	-0.25	-0.49
C5' CH ₃	20.3	-0.21	1.46	-0.18	3.26	0.85	41.62	1.82	2.32	1.18	0.54
C6'	127.9	-0.35	1.08	-0.43	1.99	0.78	40.20	1.39	1.78	1.07	0.46
C7'	125.4	-0.47	0.73	-0.56	1.40	-0.15	19.84	1.39	1.77	-0.45	-0.63
C8'	123.9	-0.63	0.28	-0.69	0.83	0.57	35.61	1.23	1.57	0.43	0.00
C8'a	127	0.13	2.44	0.17	4.73	0.40	31.80	0.53	0.67	0.35	-0.06

Table 30. Stable isotope compounds and the calculated % Incorporation as calculated in standardized reference to C3'OCH₃ or C20.

% Incorporation is defined as $[A_{C\#N} - B_{C\#N}]/[B_{C\#N}] \times 1.10$ for ¹³C carbons where A_{C#N} is the given # carbon's signal peak height normalized to the stated reference carbon (in this case C3'OCH₃ or C20) for the labeled compound feeding treatment and B_{C#N} is the given # carbon's signal peak height normalized to the stated reference carbon (in this case C3'OCH₃ or C20) for unlabeled (natural abundance) azinomycin B. 1.10 is the % of ¹³C standardly found. In most cases when the molar amount of compound series was not exactly on standard, the culture volume was adjusted to make up for a lower amount of labeled compound. In the few cases when a larger than normal amount was administered, a numerical normalization factor (N) is added to the calculation, to adjust downwards the impact of administered compound. As this is only used in comparative series, the normalization factor (N) is not usually employed.

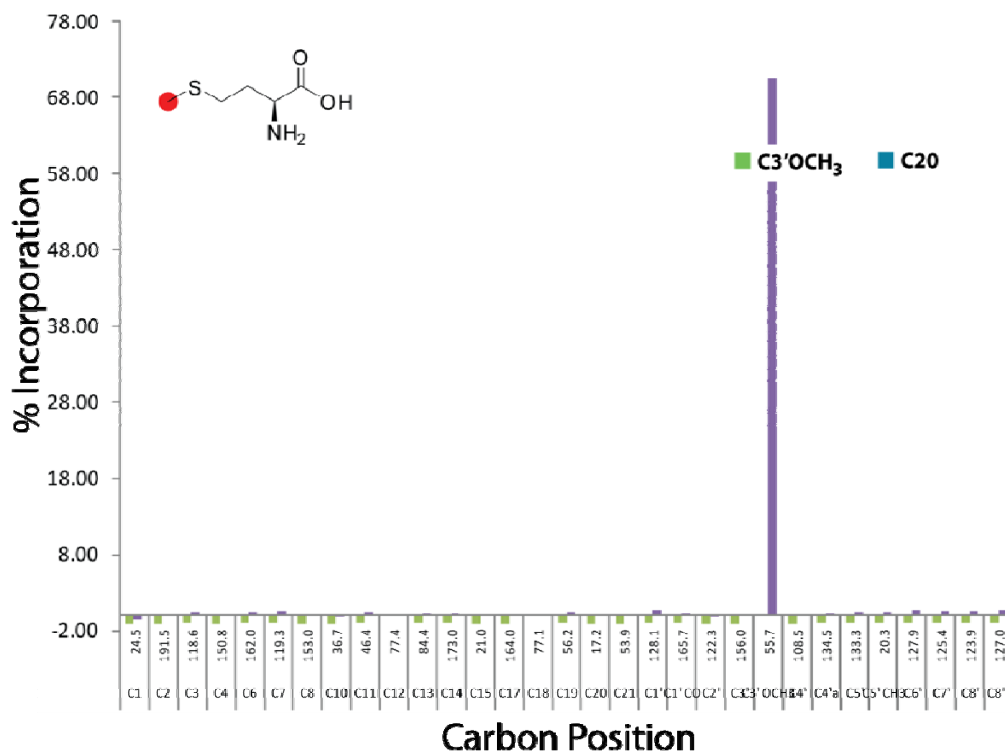
Synthesized derivatives

Substrates:	[1- ¹³ C] AZ17 100mg	[1- ¹³ C] AZ5 140mg	[1- ¹³ C] AZ16b	[1- ¹³ C] AZ16a	[1- ¹³ C] AZ15a	[1- ¹³ C] AZ15b	
Carbon Position	shift: ppm	Carbon Reference 3'OCH3 C20	Carbon Reference 3'OCH3 C20	Carbon Reference 3'OCH3 C20	Carbon Reference 3'OCH3 C20	Carbon Reference 3'OCH3 C20	
C1	24.6	-0.63 1.49	-0.49 -0.07	-0.67 -0.04	-0.69 1.61	-0.92 0.36	-0.60 22.01
C2	191.6	0.24 6.25	-0.44 0.02	-0.66 -0.60	-1.01 -0.47	-0.61 3.67	-1.11 -1.11
C3	118.0	-0.74 0.90	-0.31 0.23	-0.30 0.48	-0.71 1.48	-1.05 -0.63	-0.70 15.05
C4	150.8	-0.87 0.19	-0.80 -0.59	-0.90 -0.69	-0.74 1.30	-0.99 -0.20	-1.00 3.05
C6	162	-0.73 0.94	-0.62 0.72	-0.26 0.57	-0.83 0.73	-1.05 -0.64	-1.11 -1.11
C7	119.3	-0.80 0.59	-0.19 0.43	-0.21 0.65	-0.76 1.15	-1.03 -0.52	-0.79 11.41
C8	183	-0.99 -0.44	-0.78 -0.55	-1.11 -1.11	-1.09 -0.96	-0.61 1.27	-0.93 5.92
C10	39.7	-0.91 -0.04	-0.64 -0.16	-0.60 -0.11	-0.76 1.01	-1.09 -0.76	-0.64 17.49
C11	49.4	-0.91 -0.03	-0.80 -0.59	-0.97 -0.84	-0.98 0.64	-1.08 -0.75	0.74 72.09
C12	77.4	n/a n/a	n/a n/a	n/a n/a	n/a n/a	n/a n/a	n/a n/a
C13	64.4	-0.93 -0.13	-0.63 -0.31	-0.64 -0.19	-0.98 -0.16	-0.95 0.18	-1.01 2.82
C14	173	-0.76 0.80	-0.51 -0.11	-0.88 -0.61	-0.77 1.10	-0.95 0.93	-1.11 -1.11
C15	21	-0.67 1.29	-0.31 0.24	-0.31 0.45	-0.29 4.25	-0.49 3.72	-0.81 10.92
C17	184	-0.93 -0.16	-0.61 -0.27	-0.34 0.40	-0.99 -0.35	-0.88 -0.13	-1.11 -1.11
C18	77.1	n/a n/a	n/a n/a	n/a n/a	n/a n/a	n/a n/a	n/a n/a
C19	99.2	-0.21 3.62	0.37 1.39	0.61 2.09	0.26 7.76	-0.40 4.46	-0.34 29.39
C20	17.2	-0.91 0.09	-0.46 0.00	-0.64 0.00	-0.94 0.00	-0.67 0.00	-1.09 0.00
C21	53.9	-0.67 1.29	-0.31 0.24	-0.31 0.45	-0.29 4.25	-0.49 3.72	-0.81 10.92
C1'	129.1	0.25 6.34	0.15 1.01	-0.28 0.52	0.99 9.78	0.39 10.61	-0.42 28.29
C1' CO	165.7	-0.69 1.29	-0.03 0.70	0.00 1.07	-0.59 2.25	-0.82 1.12	-1.11 -1.11
C2'	122.3	-0.76 0.78	-0.29 0.26	-0.44 0.20	-0.54 2.59	-0.63 1.07	-0.96 3.49
C3'	196	-0.12 4.29	0.32 1.26	0.35 1.78	1.00 12.62	0.22 9.29	-0.93 5.97
C3' OCH3	65.7	0.00 4.98	0.00 0.78	0.00 1.07	0.00 6.12	0.00 7.99	0.00 42.84
C4'	109.6	-0.74 0.90	-0.41 0.06	-0.62 0.04	-0.67 1.75	-0.76 1.68	-0.96 4.63
C4'a	134.6	0.05 5.23	0.09 0.90	0.62 2.10	0.99 11.74	0.46 11.11	-0.42 28.16
C5'	133.3	-0.18 3.97	0.14 0.98	0.20 1.47	0.42 8.95	0.18 9.04	-0.07 39.99
C5' CH3	20.3	-0.91 4.91	-0.69 0.90	0.03 1.13	0.26 7.90	-0.05 7.21	-0.92 6.35
C6'	127.9	-0.15 4.11	-0.05 0.68	-0.01 1.06	0.00 6.15	-0.29 5.32	0.19 50.19
C7'	125.4	-0.40 2.79	-0.18 0.46	-0.29 0.50	-0.29 4.22	-0.52 3.51	-0.98 3.93
C8'	123.9	-0.61 1.61	-0.36 0.14	-0.34 0.40	-0.46 3.10	-0.68 2.23	-0.90 7.04
C8'a	127	0.47 7.63	0.87 2.21	0.79 2.62	1.98 17.09	0.41 10.89	-0.72 14.21

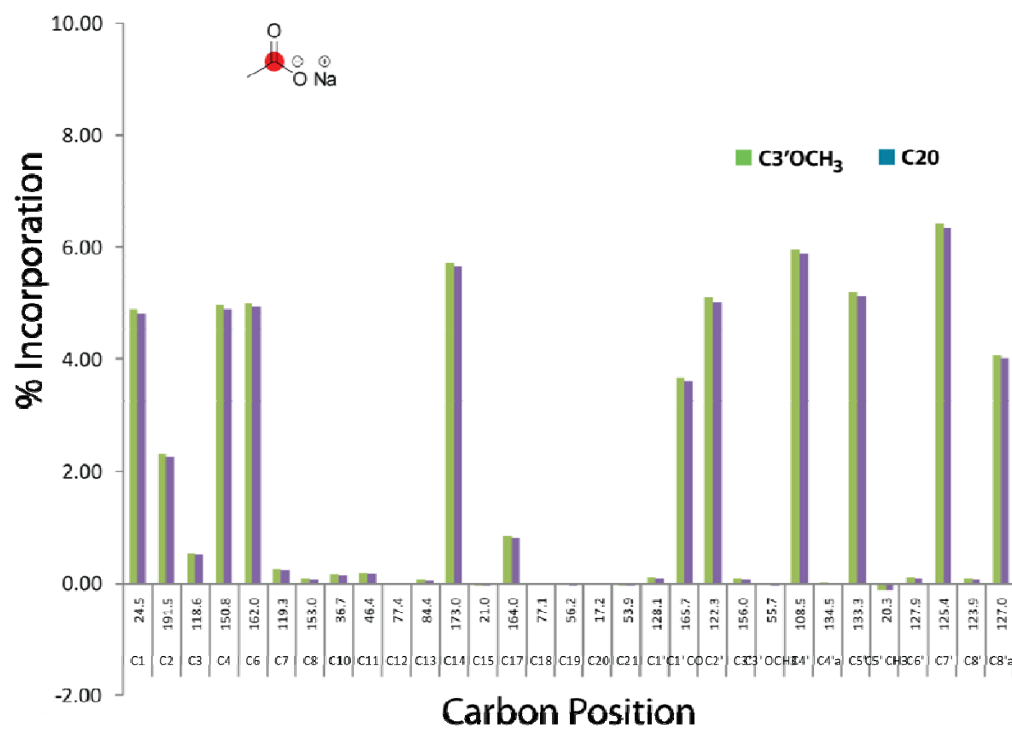
PERCENT INCORPORATION GRAPHICAL DATA FOR ISOTOPICALLY LABELED COMPOUND FEEDING EXPERIMENTS.

Positional Percent Incorporation Graphs.

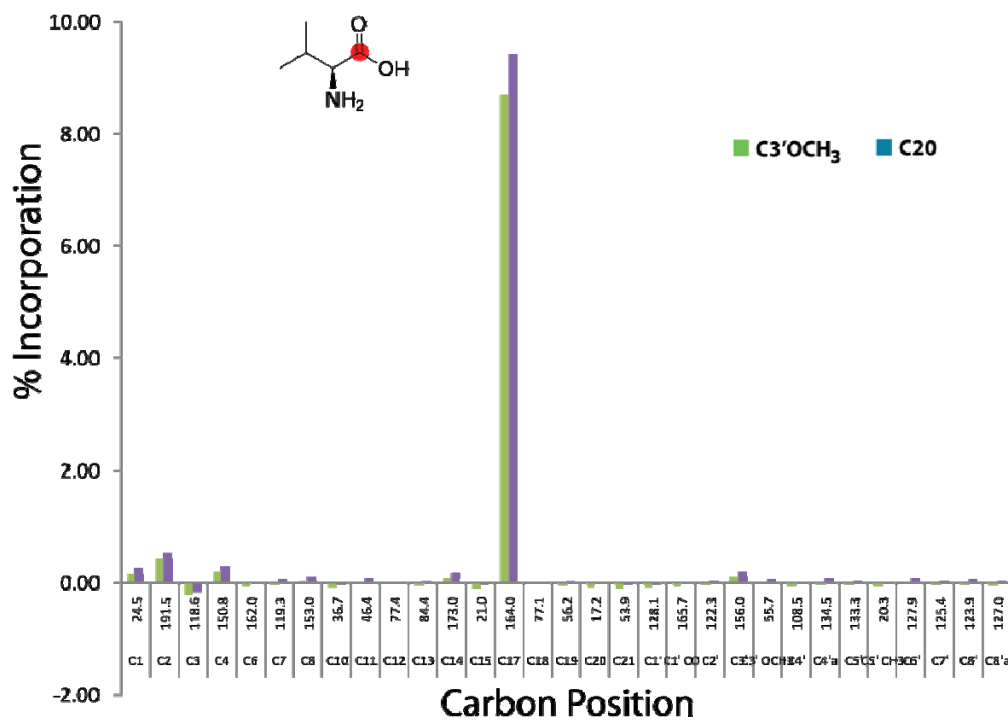
As a standard reference carbon, the C3'OCH3 and C20 were considered. Incorporation into C1-C8'a was considered significant. Some scattering in the naphthoate region was observed and may in part be attributed with possible naphthamide contamination. % Incorporation is defined as $[A-B]/[B] \times 1.10$ for ^{13}C carbons where A and B the carbon signal peak height normalized to the stated reference carbon for the labeled compound feeding treatment and unlabeled, respectively. Incorporation for MS is calculated by comparing observed M+H, M+1+H, etc. to the expected value. If these values are low or negative values, they are considered as n.d. or not detected.



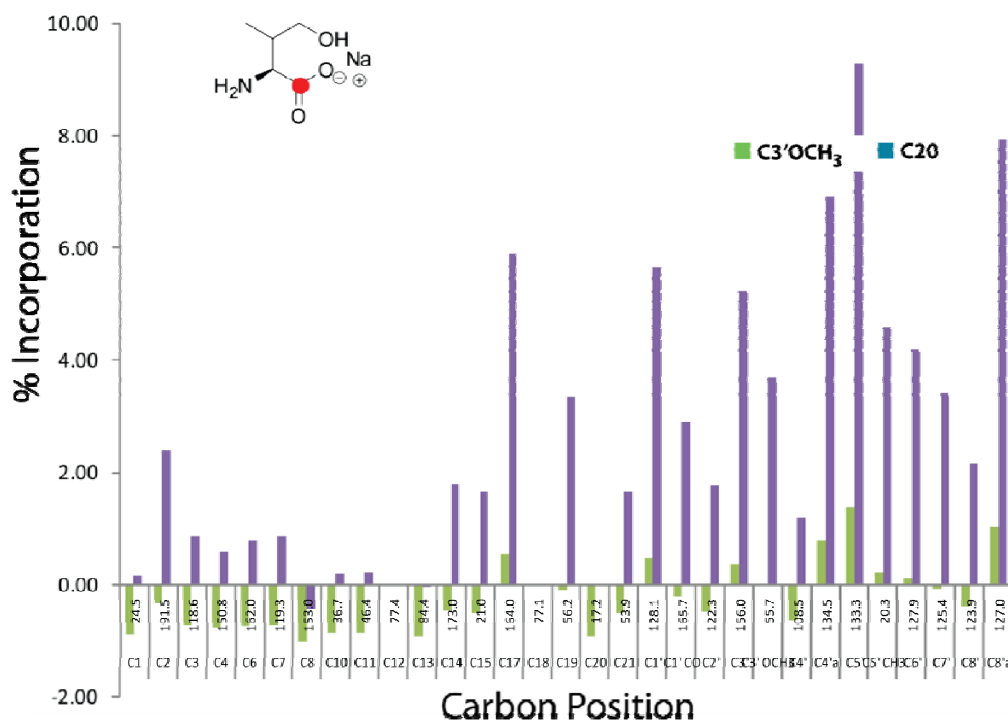
[Methyl- ^{13}C] L-methionine 50 mg (incorporation seen).



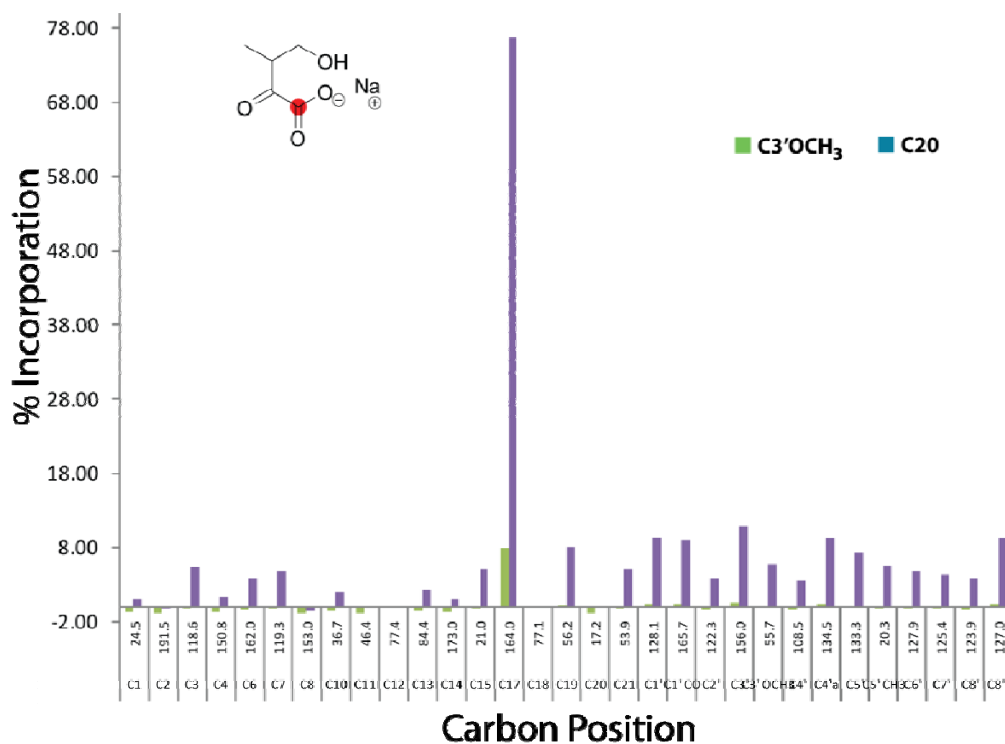
[1-¹³C] sodium acetate 1 gram (incorporation seen).



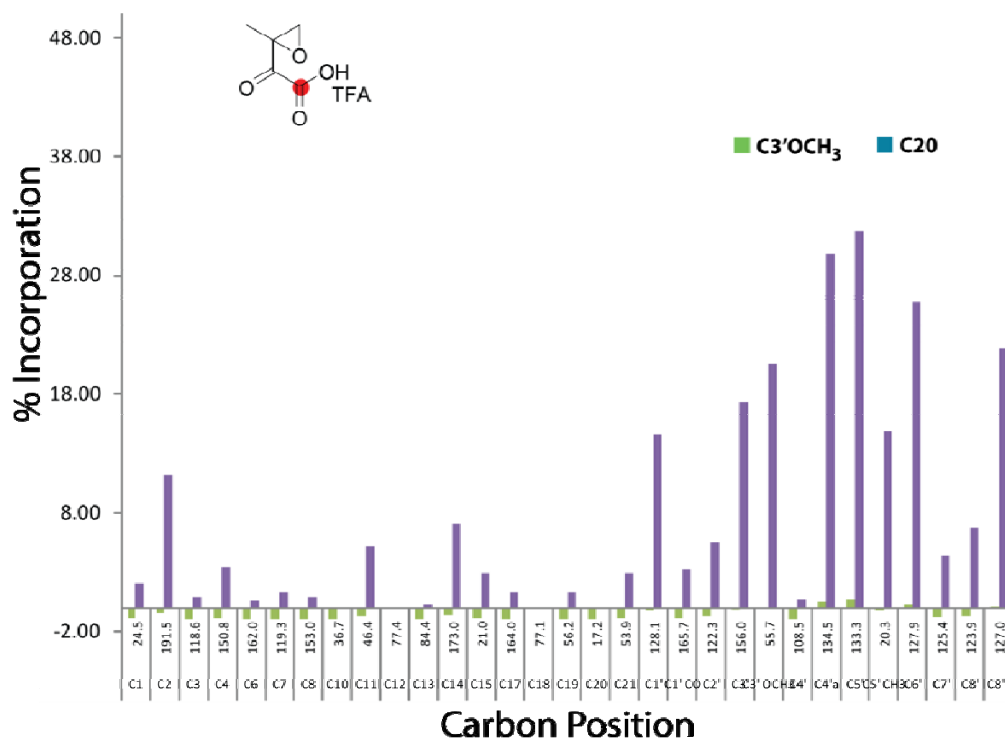
[1-¹³C] L-valine (V2) 100mg.



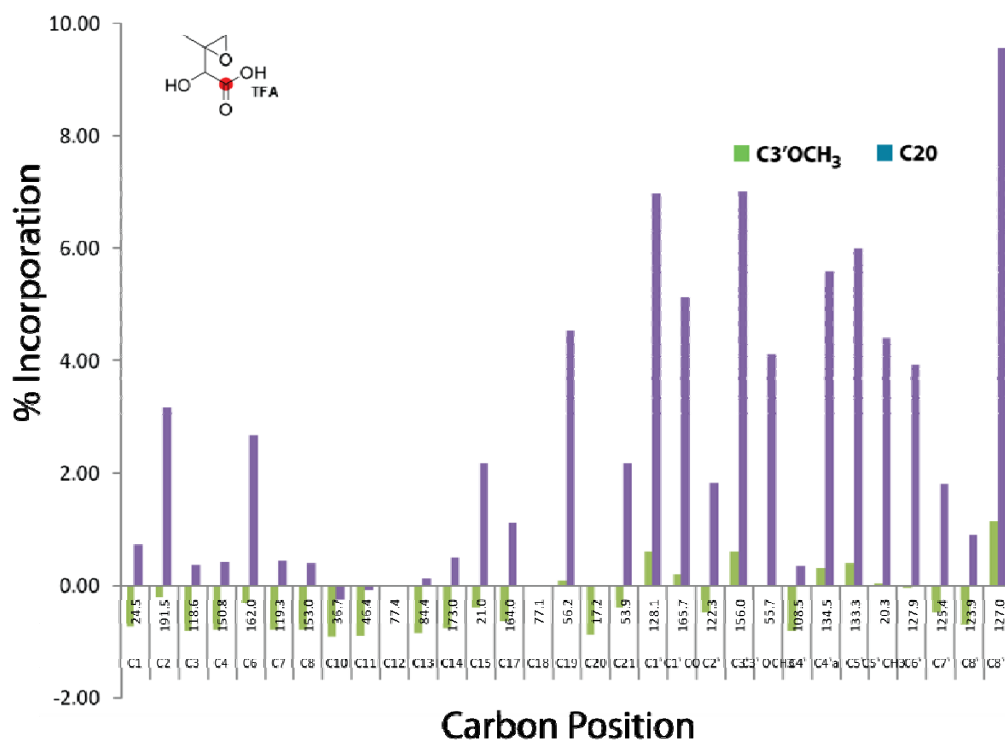
[1-¹³C] L-γ-hydroxyvaline ((2S)-2-amino-4-hydroxy-3-methylbutanoic acid) (V3) 140mg.



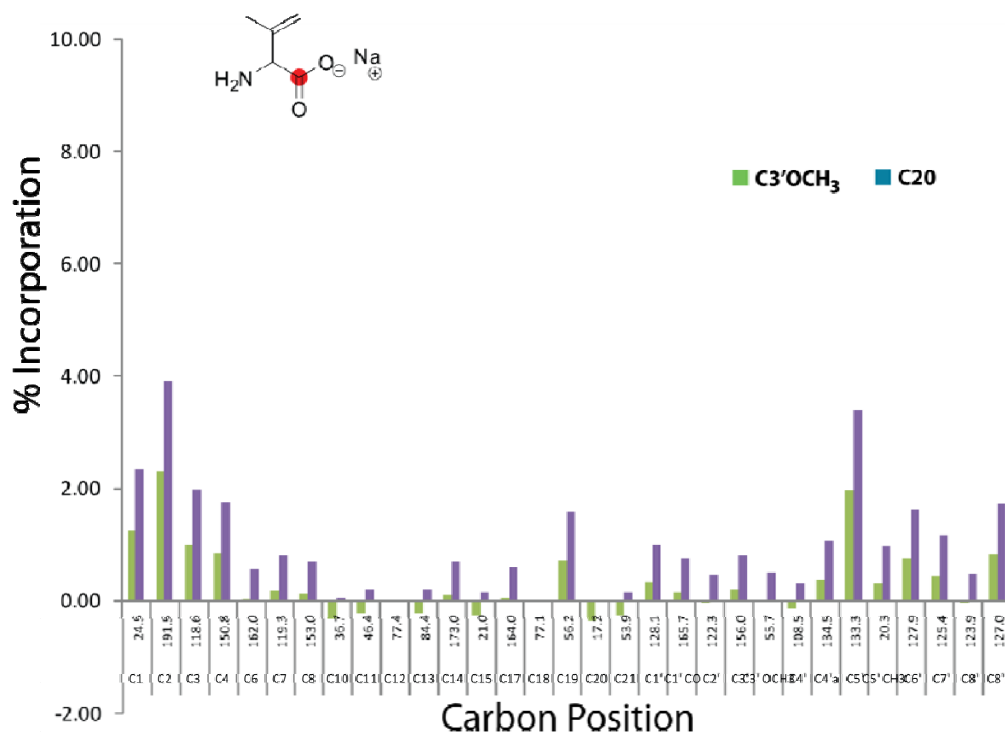
[1-¹³C] R-keto hydroxy acid (4-hydroxy-3-methyl-2-oxobutanoic acid) (V5) 166mg.



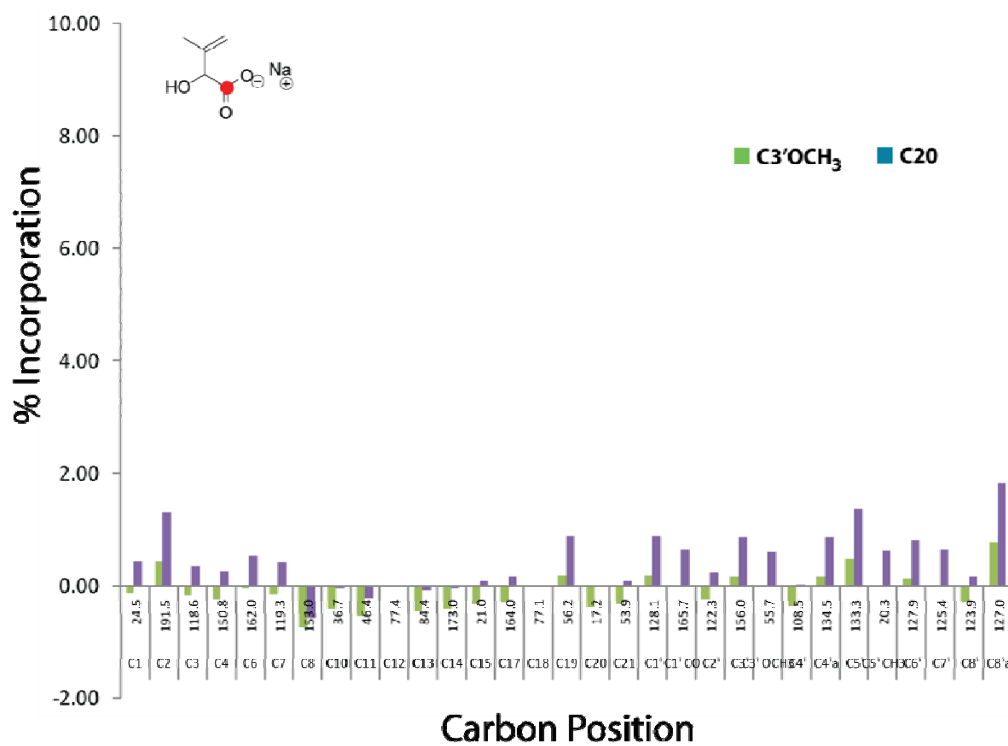
[1-¹³C] epoxy-keto acid (2-(2-methyloxiran-2-yl)-2-oxoacetic acid) (V8) 90mg, culture adjusted.



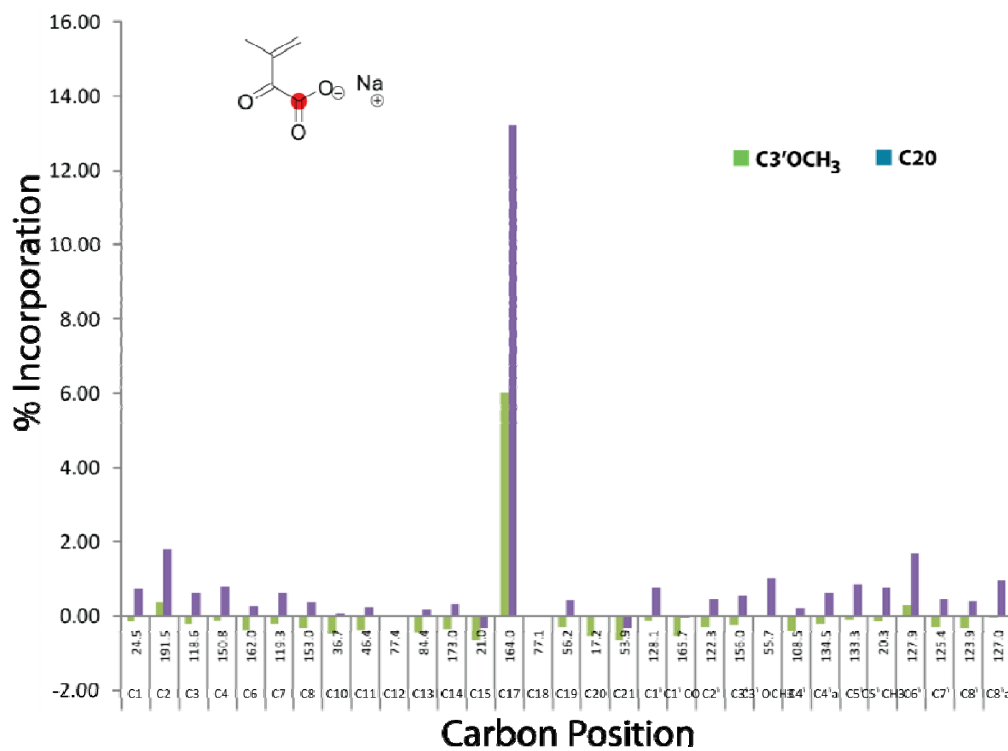
[1-¹³C] epoxy-hydroxy acid ((2S)-2-hydroxy-2-(2-methyloxiran-2-yl)acetic acid) (V9) 75mg, culture adjusted.



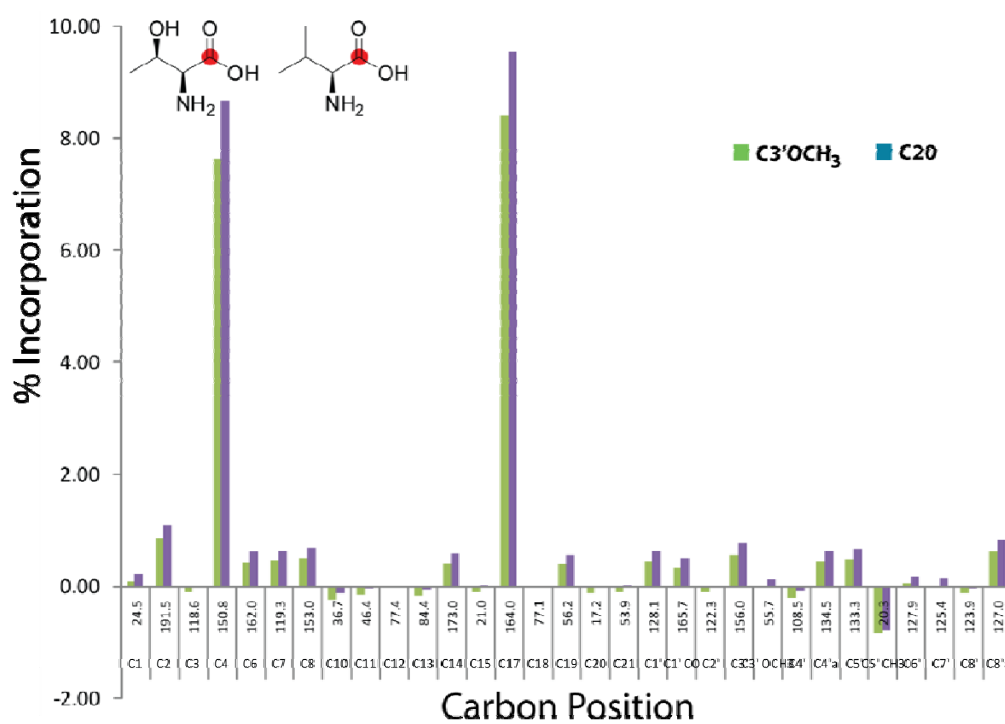
[1-¹³C] isodehydrovaline HCl (2-amino-3-methylbut-3-enoic acid hydrochloride) (V10) 90mg, culture adjusted.



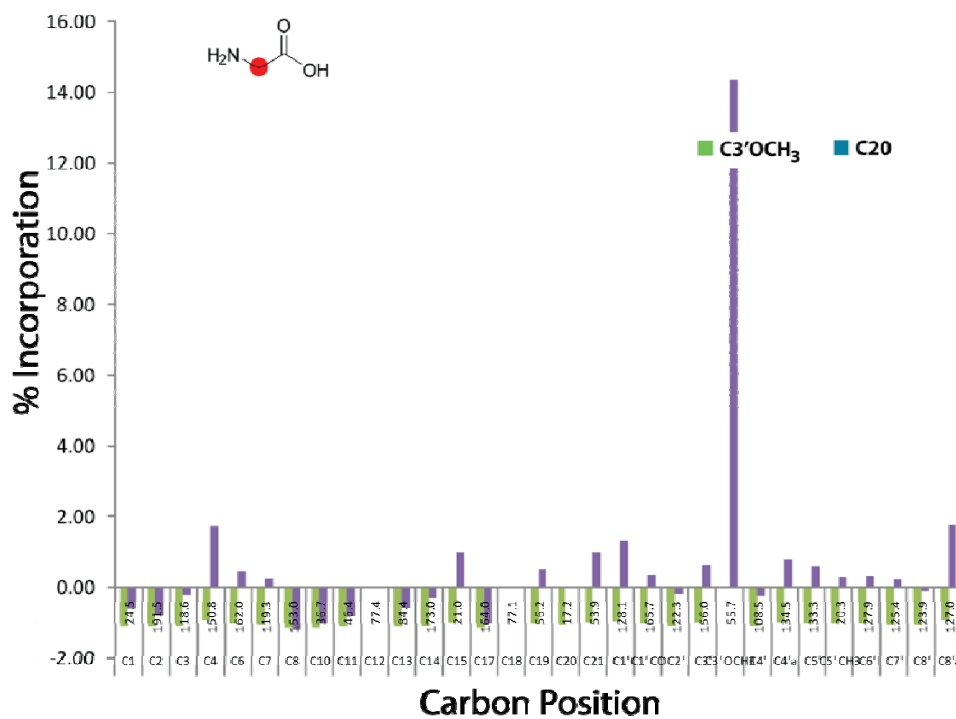
[1-¹³C] allyl-hydroxy acid (2-hydroxy-3-methylbut-3-enoic acid) (V11) 100mg.



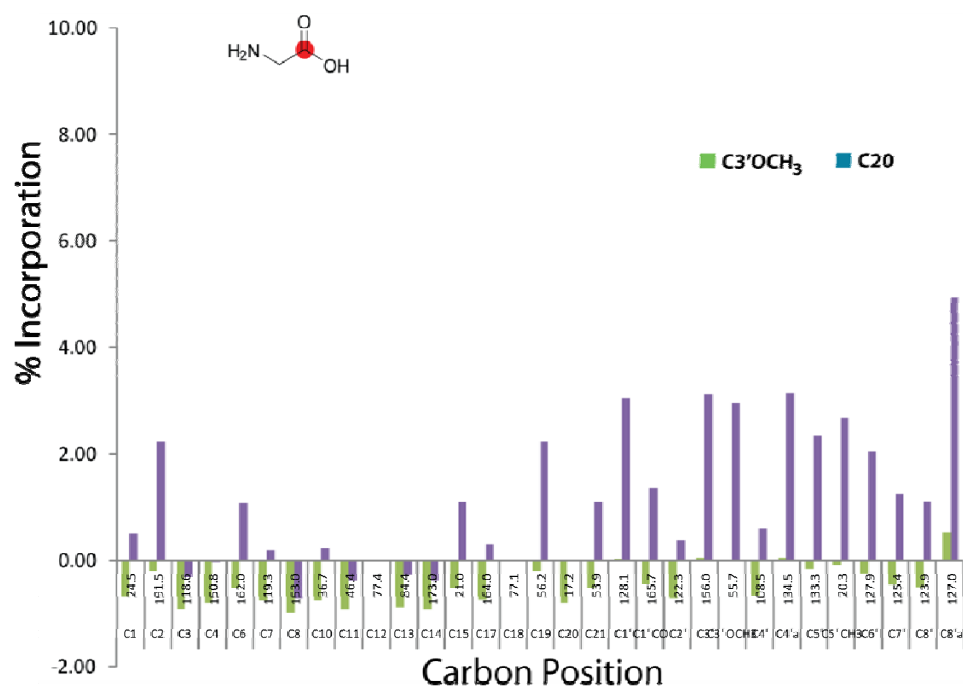
[1-¹³C] sodium allylketocarboxylate (sodium 3-methyl-2-oxobut-3-enoate) (V12) 165mg.



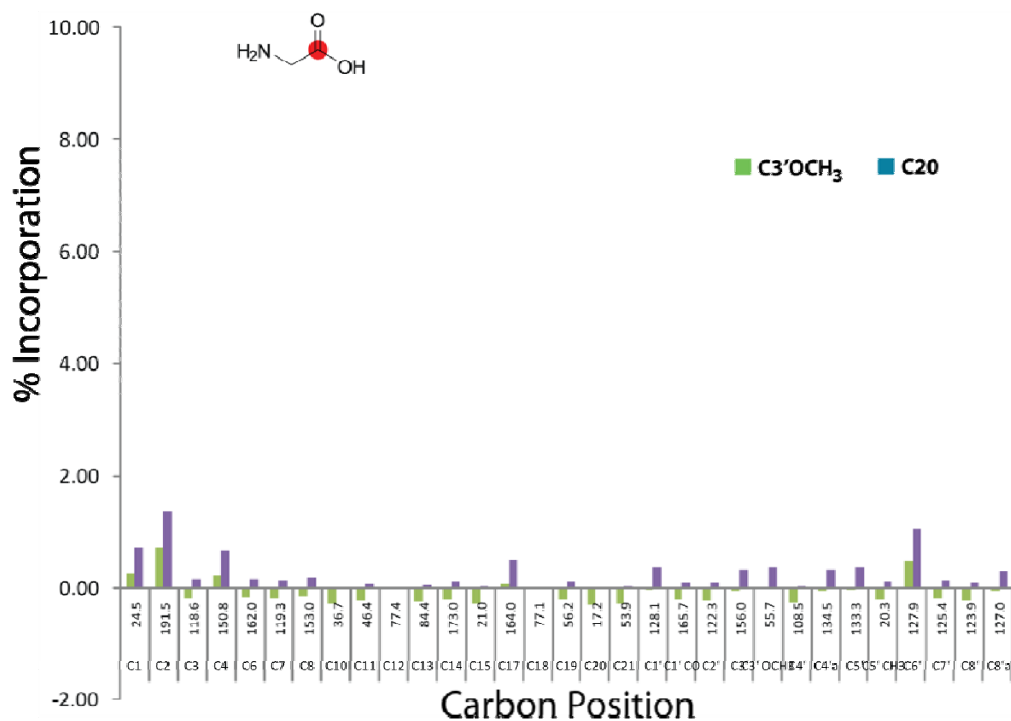
[1-¹³C] L-threonine (T2/AA3) 100mg with L-valine (V2) 100mg.



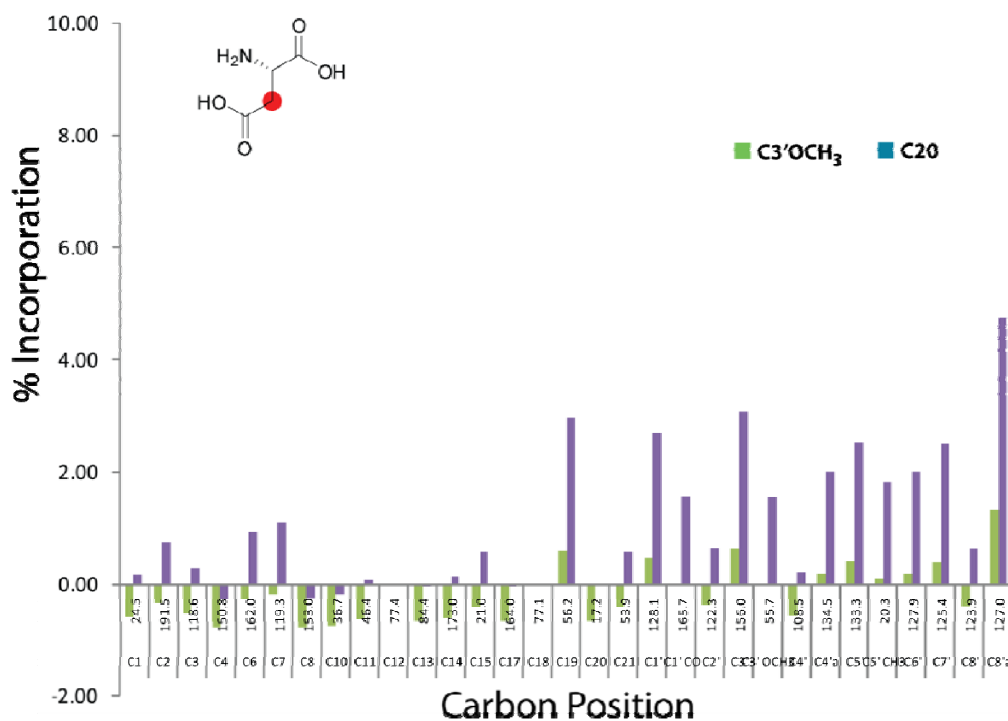
[2-¹³C] glycine 1g, Incorporation into the C3'OCH₃. Splitting pattern seen multiple carbons see Figure 143 and Figure 144.



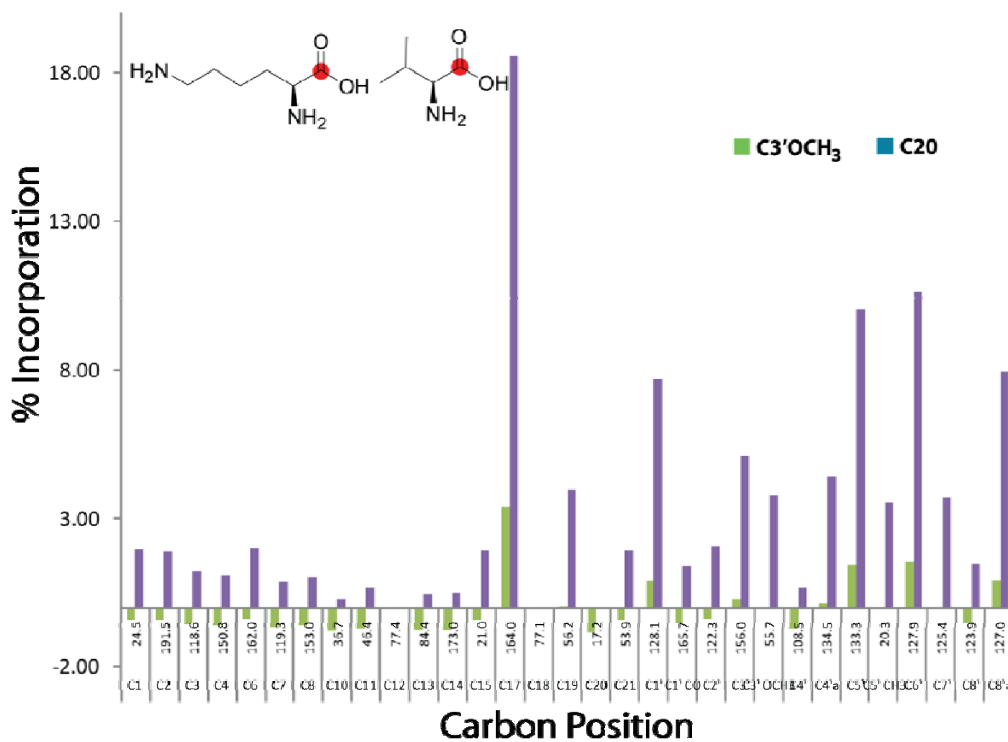
[1-¹³C] glycine 1g, low incorporation (with C20 reference carbon) into C2, C6, C15 and into the naphthoate carbons indicating acetate unit type scattering or naphthamide contaminant signal overlap.



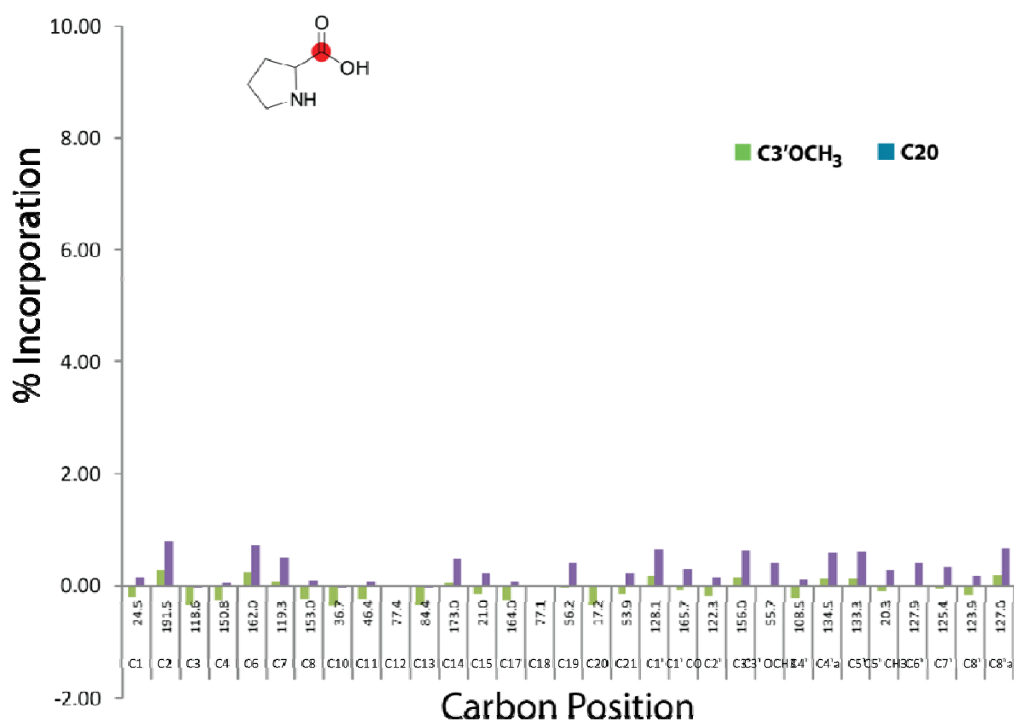
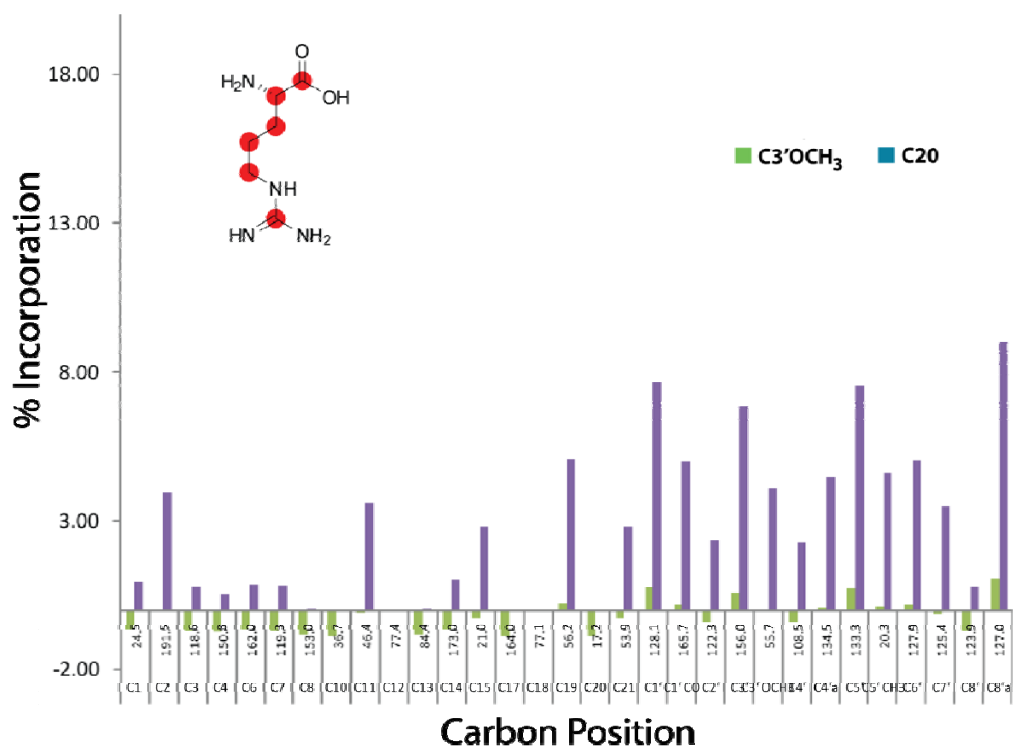
[1-¹³C] glycine 100mg, low incorporation into C2 and C6'.

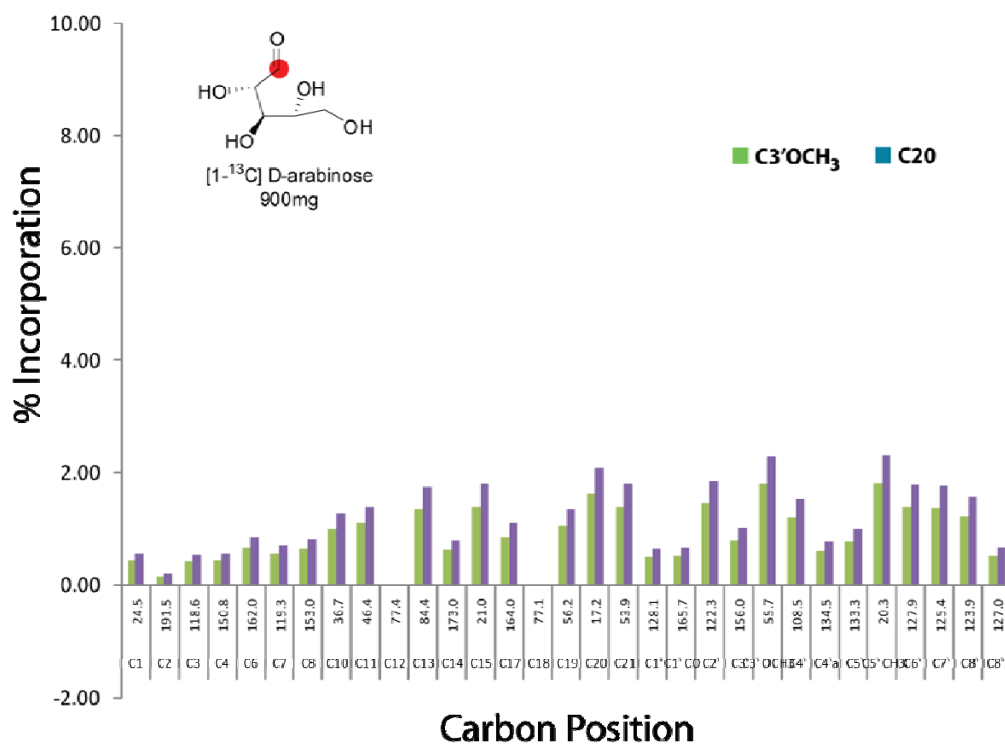


[3-¹³C] L-aspartate, 100mg. Incorporation observed relative to C20 found C19 and multiple incorporation into the naphthoate carbons.

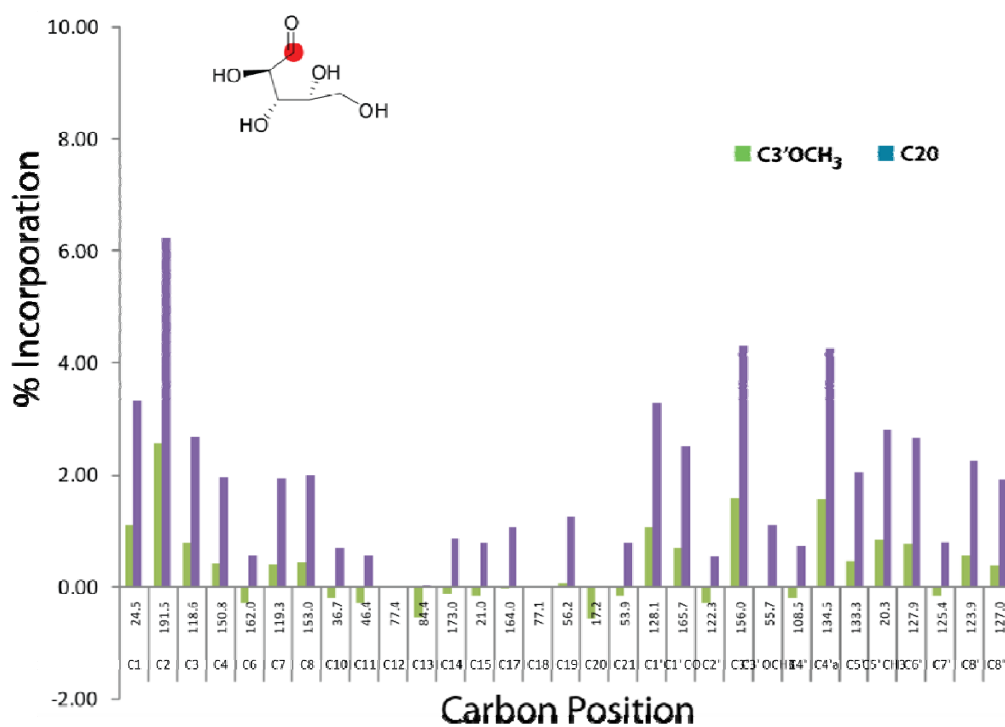


[1-¹³C] L-lysine 100mg with [1-¹³C] L-valine 100mg. Major incorporation into C17 from L-valine.

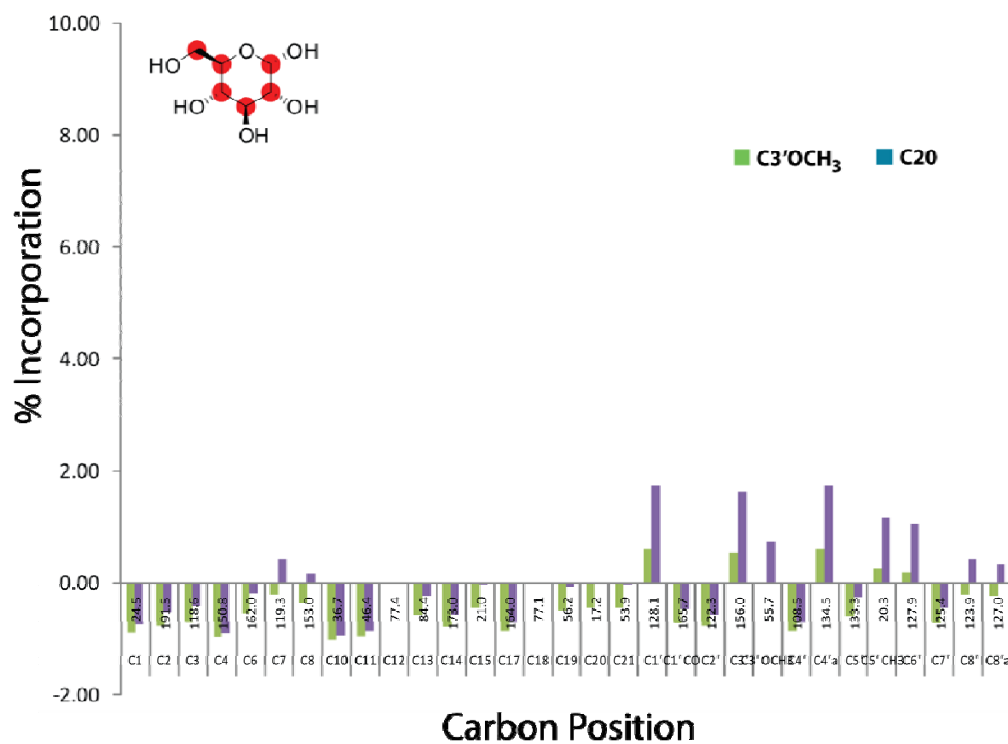
[1-¹³C] proline 100mg[U-¹³C₆] L-arginine 100mg, metabolic scattering and or naphthamide signal overlap.



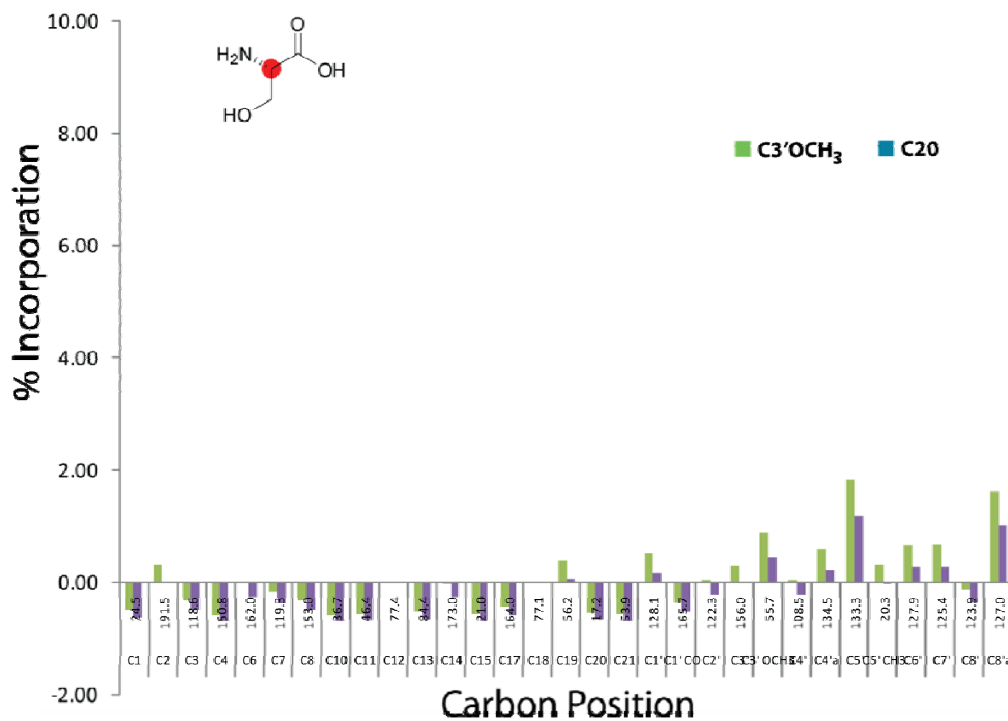
[1-¹³C] D-arabinose 900mg, low, non specific incorporation into most carbons.



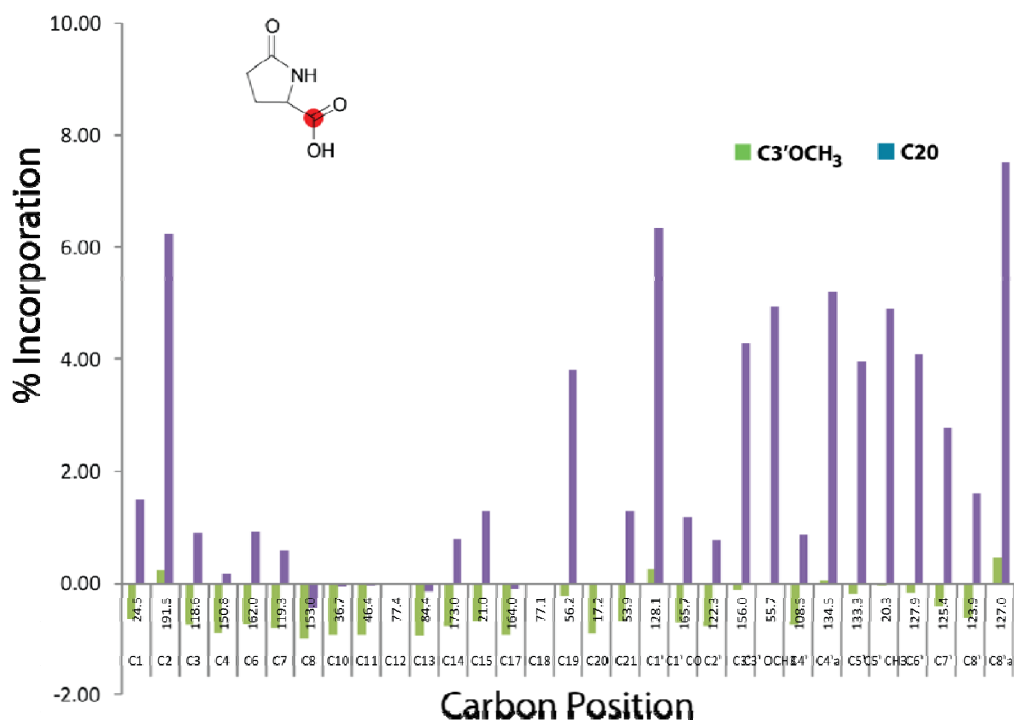
[1-¹³C] D-xylose 900mg, azinomycin B with aziridine ring opened.



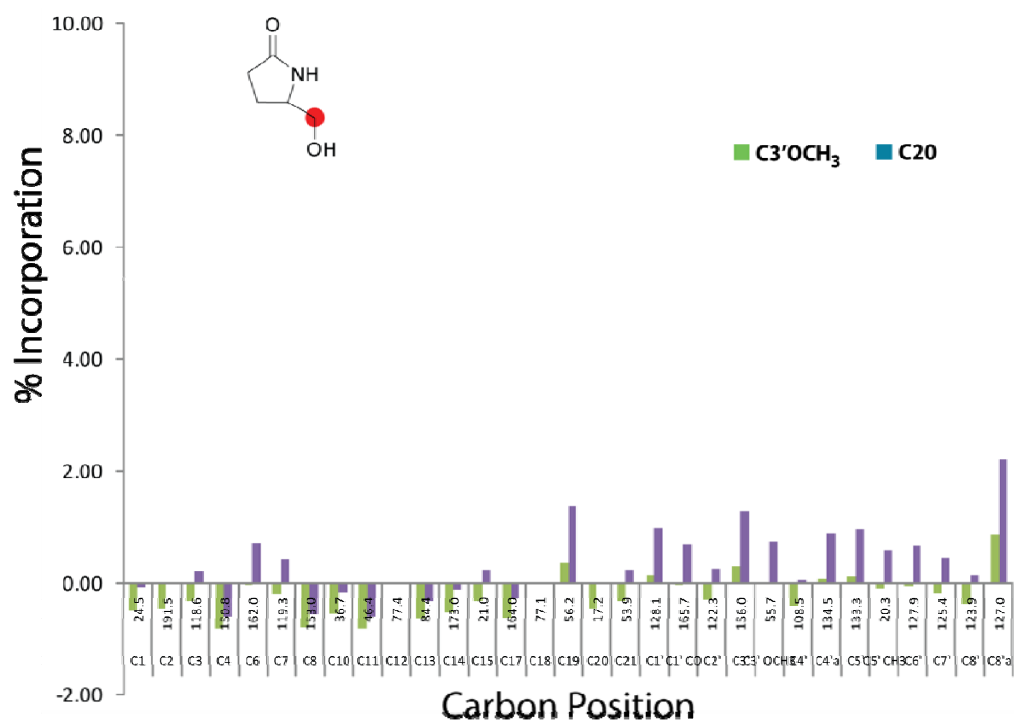
[1-¹³C] D-glucose 1000mg, Minimal scattering in naphthoate region.



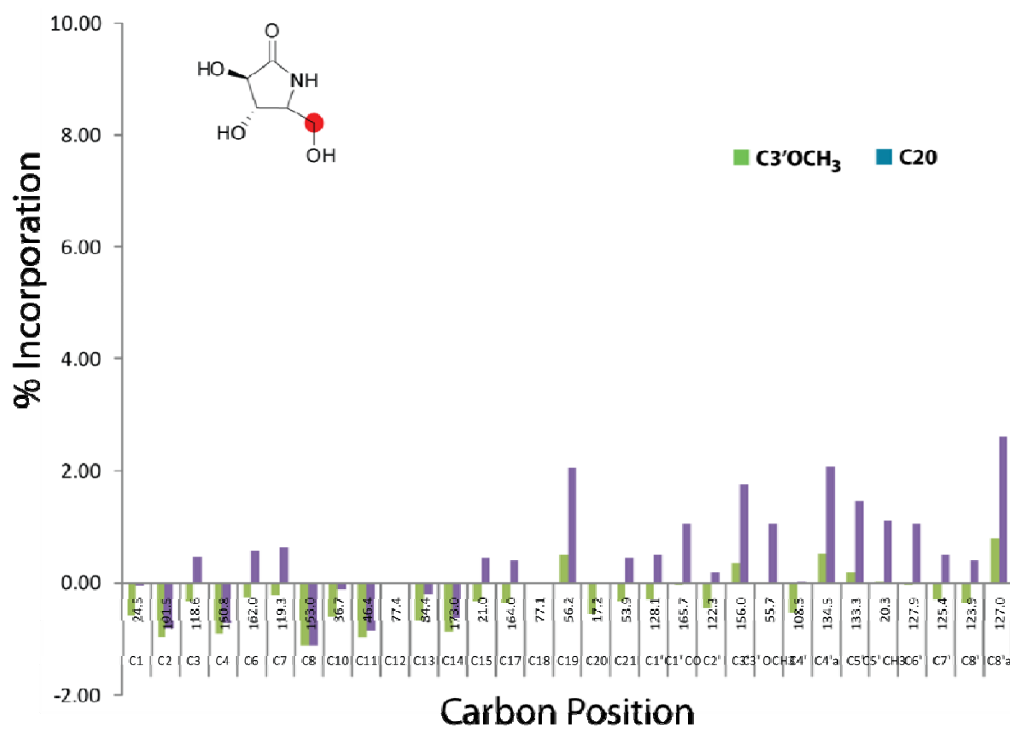
[2-¹³C] L-serine 100mg.



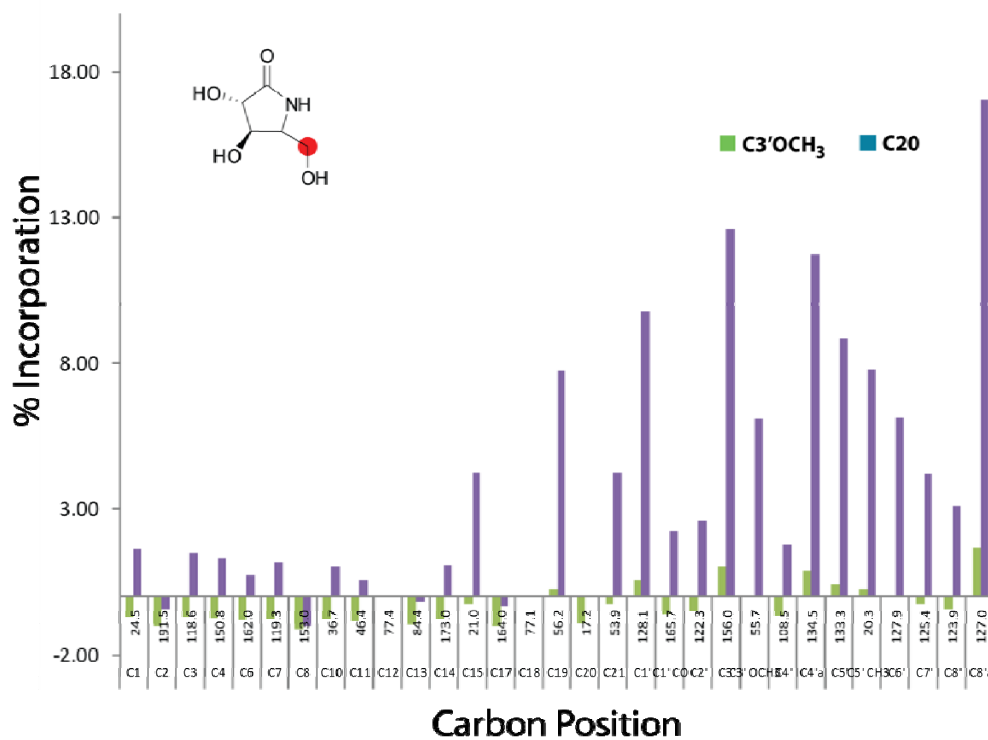
[1-¹³C] Pyroglutamic acid, AZ17 160mg, metabolic scattering and or naphthamide signal overlap.



[1-¹³C] pyroglutaminol, AZ5 140mg.



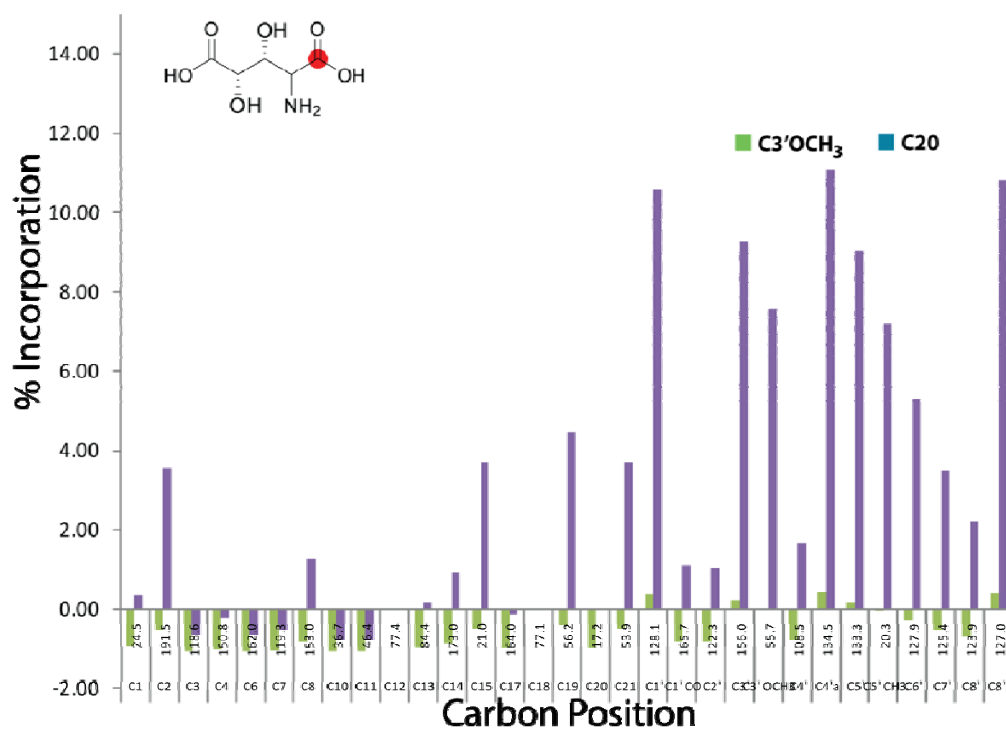
[1-¹³C] (3R,4S)-3,4-dihydroxy-5-(hydroxymethyl)pyrrolidin-2-one, 16a ~200mg.



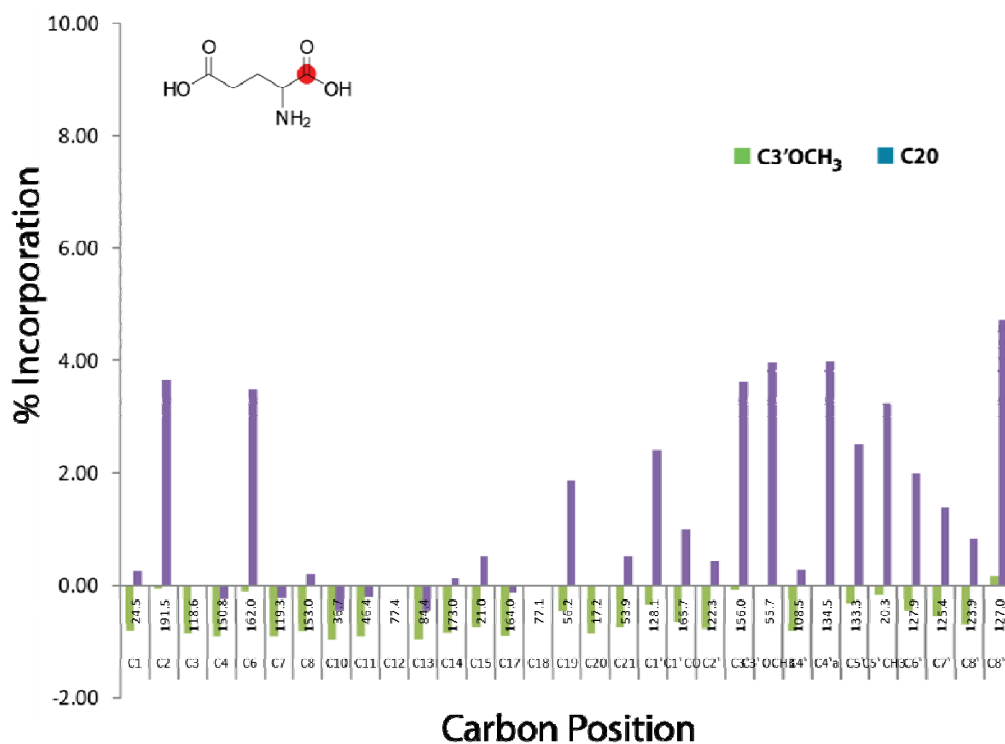
[1-¹³C] (3R,4S)-3,4-dihydroxy-5-(hydroxymethyl)pyrrolidin-2-one, 16b ~200mg, Low C20 signal, metabolic scattering and or naphthamide signal overlap.

Azinomycin B not produced!

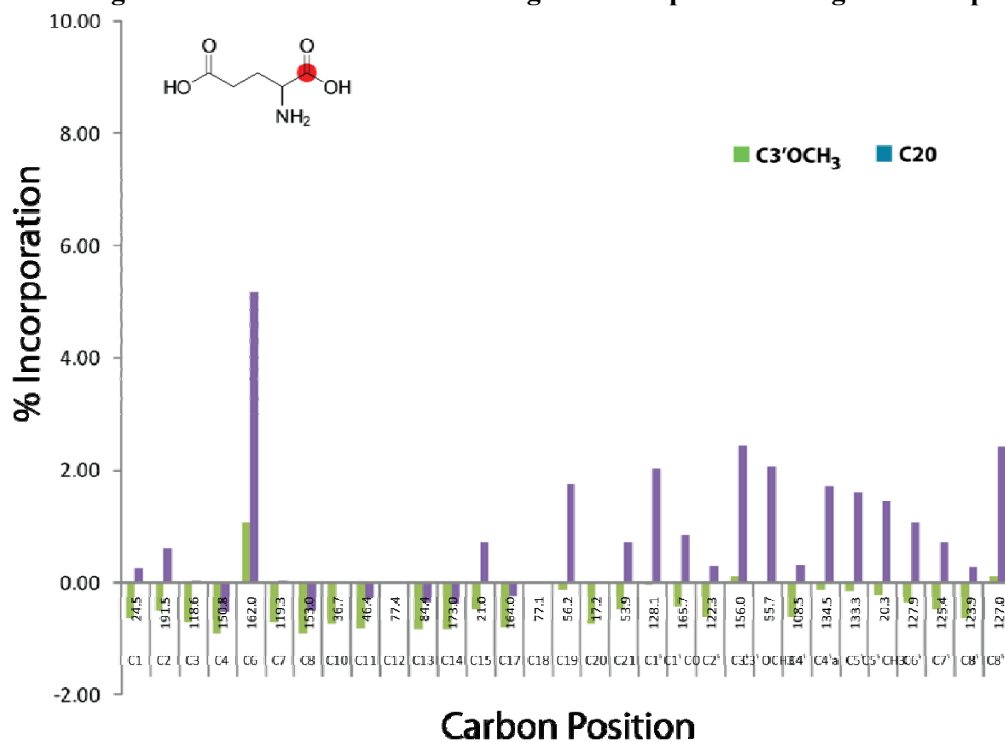
[1-¹³C] 3, 4 dihydroxy glutamic acid, 15a 200mg, Low C20 signal, metabolic scattering and or naphthamide signal overlap.



[1-¹³C] 3, 4 dihydroxy glutamic acid, 15b 250mg. Mostly not azinomycin B produced. (C20 peak was very small, throwing off calculations), metabolic scattering and or naphthamide signal overlap.



[1-¹³C] DL-glutamic acid 231 mg, with apparent incorporation into C2, C6, C19 and naphthoate region. Possible metabolic scattering and or naphthamide signal overlap.



[1-¹³C] DL-glutamic acid 1g, with apparent incorporation into C6 and naphthoate region. Possible metabolic scattering and or naphthamide signal overlap.

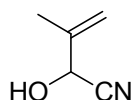
Synthesis of fed compounds (as reported by Dr. Vasudha Sharma)

Epoxide Moiety related compounds. As reported in supporting information of Sharma, *et al.* [225]*

*Reprinted with permission from “Exploration of the molecular origin of the azinomycin epoxide: Timing of the biosynthesis revealed” by Sharma, V., Kelly, G. T., and Watanabe, C. M. H., 2008. *Organic Letters*, 10, 4815-4818, Copyright [2008] by American Chemical Society.

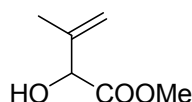
**Note: Spectral data of compounds V10, V16, V18-22, V24, V25, V31-33 were compared and found identical to those previously reported by others.

2-hydroxy-3-methylbut-3-enenitrile, V14



A suspension of NaCN (0.6g, 12.5mmol) in dry ethyl ether (10ml) was maintained at 0 °C in an ice bath. Glacial acetic acid (0.7ml, 12.9mmol) was added drop-wise and the mixture was stirred at 0°C for 30 min. Methacrolein (Aldrich)(0.5g, 7.1mmol), was added drop-wise and the temperature was allowed to rise to room temperature overnight. A thick white precipitate was formed which was filtered under vacuum, and washed with dry ethyl ether. The filtrate was evaporated on a rotary evaporator to yield the crude cyanohydrin as a colorless oil in ~82% yield. ¹H NMR & COSY (CDCl₃, 300MHz) 1.82 (s, 3H), 4.20 (bs, 1H), 4.82 (s, 1H), 5.05 (s, 1H), 5.24 (s, 1H). ¹³C NMR & HMQC (CDCl₃, 300MHz): δ17.8, 64.6, 115.3, 118.2, 139.7. IR (NaCl, thin film) cm⁻¹: 3415.8(br), 2922.4, 2854.3, 2250.3, 1661.2, 1448.0, 1054.3. MS (EI+)C₅H₇NO (M), 97.0, found, 70.9 (M-CN).

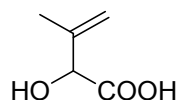
Methyl 2-hydroxy-3-methylbut-3-enoate, V15



Anhydrous methanol (9 ml) was cooled to -5 °C. SOCl₂ was added drop-wise and allowed to stir for 10 minutes. Cyanohydrin, **V14** (100mg, 1.03mmol) in 1ml methanol was added drop-wise and refluxed for 12h. The solvent was evaporated *in vacuo* and replenished and refluxed for another 10h. A white precipitate separated which was filtered. The filtrate was evaporated on a rotary evaporator to yield a thick buff colored oil. ¹H NMR & COSY (CDCl₃, 300MHz) 1.73 (s, 3H), 2.57 (br, 1H), 3.79 (s, 3H), 4.54 (s, 1H), 5.01 (s, 1H), 5.11 (s, 1H). ¹³C NMR (CDCl₃,

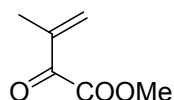
300MHz) 17.7, 52.9, 74.8, 115.3, 141.7, 174.0. IR (NaCl, thin film) cm^{-1} : 3141.4, 2922.4, 2854.3, 1741.1, 1403.6. HRMS (ESI+): m/z calcd for $\text{C}_6\text{H}_{10}\text{O}_3$ (M+Li), 137.0790 found, 137.0793.

2-hydroxy-3-methylbut-3-enoic acid, V11

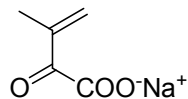


A solution of α -hydroxy ester, **V15** (350 mg, 2.67 mmol) in methanol (1ml) was stirred with 2N LiOH in water (8 ml) for 12 h. The solution was then washed with ether. The aqueous layer was collected and acidified with 1M KHSO_4 to pH \sim 3. The aqueous layer was then extracted with ethyl acetate (3X, 30 ml). The organic layer was dried over sodium sulfate and concentrated in vacuo to give a thick brown oil in 90% yield. ^1H NMR & COSY (CDCl_3 , 300MHz) 1.77 (s, 3H), 4.64 (s, 1H), 5.04 (s, 1H), 5.15 (s, 1H), 9.52 (s, br, 1H). ^{13}C NMR (CDCl_3 , 300MHz) 17.7, 74.5, 115.6, 141.3, 177.8. IR (NaCl, thin film) cm^{-1} : 3425.6(br), 3301.3(br), 2922.4, 2857.2, 1723.3, 1652.3, 1208.2. HRMS (ESI-): m/z calcd for $\text{C}_5\text{H}_8\text{O}_3$ (M-H), 115.0395 found, 115.0399.

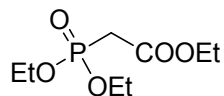
Methyl 3-methyl 2-oxo- but-3-enoate, V16



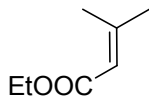
In a flame-dried flask, a solution of hydroxyl ester, **V15** (100 mg, 0.763 mmol) in anhydrous ether (0.8 ml) was stirred at room temperature away from light. Activated MnO_2 (0.39 g, 4.58 mmol) was added and the suspension stirred at room temperature for 1.5h. Another lot of MnO_2 was added and the reaction stirred for 0.5 h. The reaction was then filtered using glass wool and solvent evaporated under a gentle stream of N_2 to afford the pure product in 91% yield. *Note: the mild alkaline nature of Celite caused extensive decomposition of the product upon filtration. The product was used within 12-15 h.* ^1H NMR & COSY (CDCl_3 , 300MHz) 1.89 (s, 3H), 3.84 (s, 1H), 6.06 (m, 1H), 6.14 (m, 1H). ^{13}C NMR (CDCl_3 , 300MHz) 16.1, 52.5, 132.9, 140.9, 164.2, 188.6. IR (NaCl, thin film) cm^{-1} : 2925.3, 2848.4, 1729.3, 1681.9, 1264.5. HRMS (ESI+): m/z calcd for $\text{C}_6\text{H}_8\text{O}_3$ (M+ Li), 135.0633 found, 135.0631.

3-methyl 2-oxo-but-3-enoic acid, V12

A solution of keto ester, **V16** (100 mg, 0.763 mmol) in acetone (0.5 ml) and 3 ml Phosphate Buffer (1X, pH=8.0) was stirred at 28 °C. Esterase (120 mg, 2X 900 U) was added in two lots every 8 hours and the reaction stirred for 16 h. The precipitating salts were centrifuged and the supernatant lyophilized to afford the product in ~85% yield. ¹H NMR(CDCl₃, 300MHz) 1.72 (s, 3H), 5.93 (m, 1H), 6.11 (m, 1H). ¹³C NMR (CDCl₃, 300MHz) 15.0, 133.5, 140.3, 173.7, 199.8. IR (NaCl, thin film) cm⁻¹: 3425.6(br), 2925.3, 2845.4, 1700.7-1637.5 (br), 1596.0, 1415.5. HRMS (ESI+): *m/z* calcd for C₅H₅O₃Na (M+H), 137.0215, found, 137.0211; (M-CO₂-Na), 69.0340 found, 69.0341.

Ethyl 2-(Diethyl phosphoryl)acetate

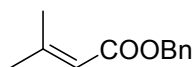
A mixture of ethyl bromoacetate (2.2g, 13.2 mmol) and triethylphosphite (2.19g, 13.2 mmol) was heated in a flame-dried flask to 130 °C for 10h. The mixture was allowed to cool down to room temperature to afford the desired product in 98% yield (2.83g) as a mixture of rotamers. ¹H NMR (CDCl₃, 300 MHz): δ 0.94 (m, 9H), 2.57(d, 2H, *J*=21.3 Hz), 3.81(m, 6H) ¹³C NMR (CDCl₃, 300 MHz): δ 13.24, 15.51, 32.6, 34.3, 60.6, 61.69, 164.8, 164.9. IR (NaCl, thin film) cm⁻¹: 29371.9, 1745.3, 1468.1 HRMS (ESI+): *m/z* calcd for C₈H₁₇O₅P (M+Li), 231.0974, found, 231.0977.

Ethyl 3-methyl 2-butenoate, V18

In a sealed tube, under a steady stream of N₂, NaH (0.14 g, 3.59 mmol) was washed with dry hexanes. Ethyl 2-(diethylphosphoryl)acetate **V10**(0.87 g, 3.87 mmol), dissolved in dry tetrahydrofuran (10 ml) was added at 0 °C. The mixture was stirred for 15 minutes. Acetone (0.15 g, 2.58 mmol) was added to the reaction mixture and stirred at 0 °C for 30 min, then at room temperature for 6h. The reaction was quenched by addition of a saturated NH₄Cl solution (5 ml). The aqueous layer was extracted with diethyl ether (3 X40 ml) and the organic fractions were collected, dried with MgSO₄, and filtered. Evaporation of the solvent *in vacuo* yielded the

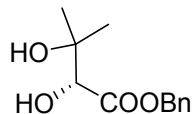
desired product **11** as a light-yellow oil (0.29 g, 90%). ^1H NMR (300 MHz, CDCl_3): δ 1.21 (t, 3H, $J=7.2$ Hz) 1.89(d, 3H, $J=1.2$ Hz) , 2.11 (d, 3H, $J=1.2$ Hz), 4.08 (q, 2H, $J= 7.2$ Hz), 5.61 (m, 1 H). ^{13}C NMR (75 MHz, CDCl_3): δ 14.2, 20.0, 27.3, 59.3,116.0,156.3,166.6. IR (NaCl, thin film) cm^{-1} : 2929.2, 2849.0, 2250.7, 1730.3, 1377.9, 1255.9. LRMS (GC-MS): m/z calcd for $\text{C}_7\text{H}_{12}\text{O}_2$ (M+H), 129.0, found, 129.0.

Benzyl 3-methylbut-2-enoate

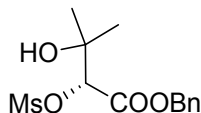


A solution of ethyl 3,3 dimethyl acrylate **V18** (300 mg, 2.34 mmol) in ethanol (0.5 ml) was stirred with an aqueous solution of LiOH (2N, 4ml) for 10h at room temperature. The solution was acidified with 1M KHSO_4 to pH=4.0 and extracted with ethyl acetate (4X, 50 ml). The organic extracts were combined, dried over Na_2SO_4 and concentrated *in vacuo*. ^1H NMR (300 MHz, CDCl_3) δ 1.90(s, 3H), 2.15 (s, 3H), 5.67-5.68 (m, 1H). ^{13}C NMR (75 MHz, CDCl_3) δ 20.7, 27.9, 115.9, 160.1, 172.6. IR (NaCl, thin film) cm^{-1} : 3239.1(br), 2928.3, 2857.2, 1702.6, 1643.4. HRMS (ESI+): m/z calcd for $\text{C}_5\text{H}_8\text{O}_2$ (M+Li), 107.0684, found, 107.0689; LRMS (ESI-) calcd for $\text{C}_5\text{H}_8\text{O}_2$ (M-H), 99.0, found 99.0.

A stirred solution of 3,3-dimethylacrylic acid (0.22 g, 2.22 mmol) and $\text{Bu}_4\text{N}^+\text{Br}^-$ (0.06 g, 0.19 mmol) in CHCl_3 (4 ml) at room temperature was mixed with an aqueous solution of KOH (0.13 g, 2.39 mmol in 1 ml water). Benzyl bromide (0.32 g, 0.19 m mol) was added drop-wise and the reaction refluxed for 18h. On cooling, water (15 ml) was added and the reaction mixture extracted with CH_2Cl_2 (3 X 40 ml). The organic extracts were combined and dried with anhydrous Na_2SO_4 , filtered and concentrated *in vacuo* to yield the desired product as a pale yellow liquid which upon column chromatography (5% EtOAc/hexane) gave the product in nearly quantitative yield (417 mg). ^1H NMR (500 MHz, CDCl_3) δ 1.91(s, 3H), 2.21 (s, 3H), 5.16 (s, 2H), 5.75-5.77 (m, 1H), 7.32-7.39(m, 5H). ^{13}C NMR (75 MHz, CDCl_3) δ 20.4, 27.7, 65.7, 116.1, 128.3, 128.7, 128.8, 136.9, 157.7, 166.7. IR (NaCl, thin film) cm^{-1} : 3034.9, 2966.8, 2877.9, 1720.4, 1649.3, 1453.9. HRMS (ESI): m/z calcd for $\text{C}_{12}\text{H}_{14}\text{O}_2$ (M+Li), 197.1154, found, 197.1151.

(R)-benzyl 2,3-dihydroxy-3-methylbutanoate, V19

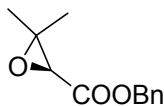
A solution of AD-mix- α (2.21 g), methanesulfonamide (0.15 g, 1.58 mmol) and NaHCO_3 (0.39 g, 4.73 mmol) in *tert*-butyl alcohol (6 ml) and water (6 ml) was maintained at room temperature. The reaction mixture was then cooled to 0 °C. Benzyl 3-methylbut-2-enoate (0.3g, 1.58 mmol) was added in one portion and the orange heterogeneous slurry stirred at 0 °C for 60 h. Anhydrous Na_2SO_3 (2.36 g, 18.8 mmol) was added at 0 °C and the reaction mixture was allowed to warm to room temperature and stirred further for 1 h. During this period the reaction mixture developed a pale-greenish brown color. The reaction mixture was extracted with ethyl acetate (3 \times 40 ml). The combined organic extracts were washed with 2 M aqueous KOH (15 ml, 1X), dried over Na_2SO_4 and concentrated *in vacuo* to give a colorless oil in 88% yield (312 mg). ^1H NMR (500 MHz, CDCl_3) δ 1.17(s, 3H), 1.26 (s, 3H), 2.81(br, 1H), 3.46(br, 1H), 4.01(s, 1H), 5.24 (2H, q, $J=12.5$ Hz), 7.36-7.38(m, 5H). ^{13}C NMR (75 MHz, CDCl_3) δ 25.0, 25.9, 67.8, 72.3, 77.4, 128.7, 128.8, 128.8, 134.9, 173.1. IR (NaCl, thin film) cm^{-1} : 3446.4, 3416.8, 2975.7, 2928.3, 2851.3, 1729.3, 1462.8. HRMS (ESI): m/z calcd for $\text{C}_{12}\text{H}_{16}\text{O}_4$ (M+Li), 231.1209, found, 231.1206.

(R)-1-((benzyloxy)carbonyl)-2-hydroxy-2-methylpropyl methanesulfonate

A stirred solution of the diol **V19** (0.16 g, 0.74 mmol) and triethylamine (0.11 g, 1.12 mmol) in dry CH_2Cl_2 (2 ml) was maintained at 0 °C under a nitrogen atmosphere. Methanesulfonyl chloride (0.09 g, 0.78 mmol) was added dropwise to the reaction mixture. The reaction mixture was stirred at 0 °C for 3 h and then quenched with saturated NaHCO_3 (aq.) (20 ml). The organic layer was separated and the aqueous layer extracted with CH_2Cl_2 (3 \times 40 ml). The combined organic extracts were then dried over Na_2SO_4 and concentrated *in vacuo* to give yellow oil. The product was purified by column chromatography (10% EtOAc/ CH_2Cl_2), which initially provided the bis-protected ester(2.5%); further elution provided the mono mesylate in 80% yield (180 mg). ^1H NMR (300 MHz, CDCl_3) δ 1.32(s, 3H), 1.33 (s, 3H), 2.81(br, 1H), 3.08(s, 3H), 4.88(s, 3H), 5.29 (2H, q, $J=12.5$ Hz), 7.30-7.41(m, 5H). ^{13}C NMR (75 MHz, CDCl_3) δ 25.6, 25.7, 38.9, 67.9, 71.5, 82.5, 128.6, 128.7, 128.8, 134.5,

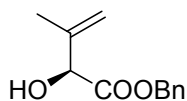
167.4. IR (NaCl, thin film) cm^{-1} : 3523.4, 2922.4, 2851.3, 1750.0, 1462.8, 1356.3, 1172.7. HRMS (ESI): m/z calcd for $\text{C}_{13}\text{H}_{18}\text{O}_6\text{S}$ (M+Li), 309.0984, found, 309.0987.

(S)-benzyl 3,3-dimethyloxirane-2-carboxylate, V20

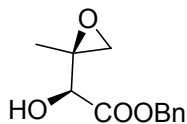


A stirred suspension of mesylate (75 mg, 0.25 mmol) and anhydrous potassium (264.2 mg, 2.5 mmol) in dry CH_3CN (4 ml) was heated at reflux under a nitrogen atmosphere for 48 h. The resulting pale yellow heterogeneous mixture was quenched with water (10 ml) and extracted with CH_2Cl_2 (3X, 20 ml). The combined organic extracts were dried (Na_2SO_4) and concentrated *in vacuo* to give a yellow liquid. The crude material was purified via a flash plug (10% EtOAc–hexanes) to give epoxide **V20** (46 mg, 90%) as a colorless liquid; $[\alpha]_D^{20}$ 7.34 (*c* 2.0, EtOH); ^1H NMR (500 MHz, CDCl_3) δ 1.36 (s, 3H), 1.42 (s, 3H), 3.38 (s, 1H), 5.18–5.24 (2H, m), 7.38–7.40 (5H, m); ^{13}C NMR (125 MHz, CDCl_3) δ 18.4, 24.4, 59.5, 60.7, 67.3, 128.8, 128.8, 128.9, 135.4, 168.7; IR (NaCl, thin film) cm^{-1} : 2922.4, 2854.3, 1732.2, 1575; HRMS (ESI): m/z calcd for $\text{C}_{12}\text{H}_{14}\text{O}_3$ (M+Li), 213.1103, found, 213.1104.

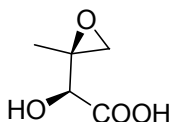
(S)-benzyl 2-hydroxy-3-methylbut-3-enoate, V21



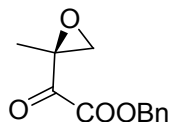
A stirred mixture of epoxide, **V20** (0.13 g, 0.66 mmol) and pTsOH (anhydrous) (0.018 g, 0.11 mmol) in dry benzene (70 ml) was heated at reflux under a nitrogen atmosphere for 10 h. On cooling, the heterogeneous mixture was filtered and concentrated *in vacuo* to give a pale yellow oil. Column chromatography (5% ethyl acetate–light petroleum) gave allylic alcohol (0.10 g, 77%) as a colourless oil, **V21**; ^1H NMR (500 MHz, CDCl_3) & gCOSY: δ 1.72 (s, 3H), 3.18 (br, 1H), 4.64 (s, 1H), 5.04 (1H, m), 5.15 (1H, m), 5.24–5.30 (2H, m), 7.33–7.42 (5H, m); ^{13}C NMR (125 MHz, CDCl_3) δ 17.9, 67.7, 75.0, 115.4, 128.3, 128.6, 128.7, 134.5, 141.9, 173.6; IR (NaCl, thin film) cm^{-1} : 3490.8, 2925.3, 2860.2, 1735.2, 1459.9; HRMS (ESI): m/z calcd for $\text{C}_{12}\text{H}_{14}\text{O}_3$ (M+Li), 213.1103, found, 213.1105.

(S)-benzyl 2-hydroxy-2-((S)-2-methyloxiran-2-yl)acetate, V22

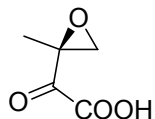
A stirred solution of (2S)-allylic alcohol, **V21** (59 mg, 0.28 mmol) and vanadyl acetylacetonate (7.6 mg, 0.028 mmol) in dry CH_2Cl_2 (3.5 ml) at -20°C under a nitrogen atmosphere was added a solution of anhydrous *tert*-butyl hydroperoxide (5–6 M in *n*-decane, 0.114 ml, *ca.* 0.578 mmol) drop-wise causing a color change from dark green to dark brown. The reaction mixture was allowed to warm to 0°C and stirred for 18 h during which time the color turned to orange. After quenching with water (2 ml), the organic layer was separated and the aqueous layer extracted with dichloromethane (3×50 ml). The combined organic extracts were dried with Na_2SO_4 and concentrated *in vacuo*. Column chromatography (20% ethyl acetate–hexanes) provided (2S,3S)epoxy alcohol as a white foamy solid (41.3 mg, 65%) and as a single diastereomer, **22**; $[\alpha]_{\text{D}}^{20}$ (Lit) 11.1 (*c* 1.9, EtOH), 16.5 (*c* 2.0, EtOH); ^1H NMR (500 MHz, CDCl_3) δ 1.32 (s, 3H), 2.65 (d, $J=5.0$ Hz, 1H), 2.86 (d, $J=5.0$, 1H), 2.90 (br, 1H), 4.00 (s, 1H), 5.28 (dd, $J=12, 33$ Hz), 7.38 (m, 5H); ^{13}C NMR (125 MHz, CDCl_3) δ 17.4, 51.8, 57.0, 67.9, 74.1, 128.3, 128.5, 128.6, 135.1, 172.2; IR (NaCl, thin film) cm^{-1} : 3367.1, 2919.3, 2854.1, 1711.8, 1453.9, 1113.7.

(S)-2-hydroxy-2-((S)-2-methyloxiran-2-yl) acetic acid, V9

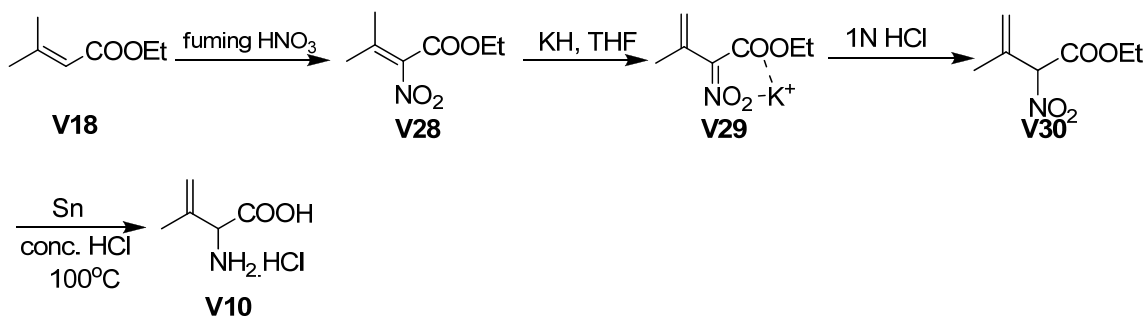
A stirred slurry of benzyl ester, **V22** (30 mg, 0.134 mmol) and 10% Pd-C (10% w/w) was added in methanol was maintained at room temperature. H_2 (1 atm, r.t.) was passed and the reaction was continued to stir at room temperature for 2h. The reaction was filtered through glass wool and dried under a gentle stream of nitrogen enough to concentrate the sample but not dry out completely. $[\alpha]_{\text{D}}^{20}$ 5.3 (*c* 0.05, CH_3OH); ^1H NMR & gCOSY (500 MHz, CD_3OD) δ 1.35 (s, 3H), 2.62 (d, $J=4.5$ Hz, 1H), 2.84 (d, $J=4.5$, 1H), 3.88 (s, 1H); ^{13}C NMR (125 MHz, CD_3OD) δ 17.4, 52.5, 58.3, 75.1, 170.0; IR (NaCl, thin film) cm^{-1} : 3419.8, 2925.3, 2851.3, 1729.3; HRMS (ESI): *m/z* calcd for $\text{C}_5\text{H}_8\text{O}_4$ (M+Li), 139.0583, found, 139.0586. ESI(-): *m/z* calcd for $\text{C}_5\text{H}_8\text{O}_4$ (M+Li), 131.0344, found, 131.0342.

Benzyl 2-((S)-2-methyloxiran-2-yl)-2-oxoacetate

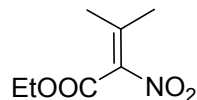
A stirred mixture of α -hydroxy benzyl ester, **V22** (35mg, 0.156 mmol) and IBX (297.6 mg (45% by weight), 0.48 mmol) in EtOAc (4 ml) was heated at reflux under a nitrogen atmosphere for 5 h. On cooling, the heterogeneous mixture was filtered and concentrated *in vacuo* to give a pale yellow oil in 95% yield **V18** (33 mg); $^1\text{H NMR}$ (300 MHz, CDCl_3) δ 1.56 (s, 3H), 2.96(d, $J=4.5$ Hz, 1H), 3.46(d, $J=4.5$, 1H), 5.26(s, 2H), 7.34-7.40(m, 5H); $^{13}\text{C NMR}$ (75 MHz, CDCl_3) δ 15.8, 53.3, 57.7, 67.7, 128.4, 128.8, 129.4, 141.9, 166.0, 194.6; IR (NaCl, thin film) cm^{-1} : 2925.3, 2842.2, 1702.6-1684.9 (br); HRMS (ESI): m/z calcd for $\text{C}_{12}\text{H}_{12}\text{O}_4$ (M+Li), 227.0896, found, 227.0903.

2-((S)-2-methyloxiran-2-yl)-2-oxoacetic acid, V8

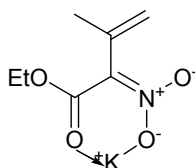
A stirred slurry of benzyl ester (33 mg, 0.149 mmol) and 10% Pd-C(10% w/w) was added in ethyl acetate (2 mL) was maintained at room temperature. H_2 (1 atm, r.t.) was passed and the reaction was continued to stir at room temperature for 2h. The reaction was then filtered through glass wool and ultracentrifuged. The supernatant was collected and dried under a gentle stream of nitrogen to provide the product in 98% yield, **V8** (19 mg). $^1\text{H NMR}$ (500 MHz, CD_3OD) δ 1.27(s, 3H), 2.91(d, $J=6.0$ Hz, 1H), 3.08(d, $J=5.5$, 1H); IR (NaCl, thin film) cm^{-1} : 3446.4, 2925.3, 2833.6, 1729.3-1684.9(br); LRMS (ESI+): m/z calcd for $\text{C}_5\text{H}_6\text{O}_4$ (M+(MeOH- H_2O)+H), 145.03, found, 145.05.



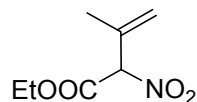
Scheme 12. Synthesis towards V10

Ethyl 3-methyl-2-nitrobut-2-enoate, V28

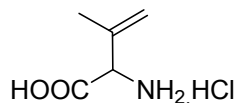
A solution of 2.94 ml of 90% fuming nitric acid and 0.4 ml of water was cooled to 0 °C. Ethyl 3,3-dimethylacrylate **V18** (1g, 7.8 mmol) was added over 1.25 h with vigorous stirring. The solution was stirred for 1.25 h at 0°C and 1 h at room temperature, then poured onto 400 ml of crushed ice and extracted CHCl₃ (100 ml, 4X). The chloroform extracts were combined and washed with water (100 ml, 4X), saturated NaHCO₃ (70 ml, 7X), and brine (100ml, 2X), dried over MgSO₄, and concentrated to provide 89% **V28** (1.2g) of the desired product (**Scheme 12**). ¹H NMR (300 MHz, CDCl₃): δ 1.07(t, 3H, *J*=7.2 Hz), 1.76(s, 3H), 2.038(s, 3H), 4.22(q, 2H, *J*=7.2 Hz) ¹³C NMR (75 MHz, CDCl₃): δ 13.8, 20.6, 22.4, 62.0, 141.5, 148.4, 158.9. IR (NaCl, thin film) cm⁻¹: 2991.2, 2851.0, 1741.1, 1369.2, 1234.7. LRMS (ESI): *m/z* calcd for C₇H₁₁O₂N(M+Li), 180.0848, found, 180.0851.

Potassium Salt of Ethyl 2-*aci*-Nitro-3-methylbut-3-enoate, V29

In a dry, N₂-flushed, 250-ml flask, ether-washed potassium hydride (1.99g, 15 mmol, 30% by wt.) was suspended in dry THF (50 ml) with vigorous stirring. The suspension was cooled to 0°C and a solution of 2.59 g (15 mmol) of the nitro ester **V28** in 5 ml of THF added over 1 h followed by an additional 2 ml of THF. After stirring at 0°C for 2 h the paste was filtered, washed three times with ether, and dried *in vacuo* to give 18.6 g (91.2 %) of **V29** as yellow crystals. m.p. 224-226 °C decompose (**Scheme 12**). ¹H NMR (300 MHz, D₂O) δ 1.11 (t, *J* = 7.2 Hz, 3 H), 1.77 (s, 3H), 4.08(q, *J*=7.2 Hz, 2H), 4.99 (s, 1H), 5.09 (m, 1H). ¹³C NMR (75 MHz, D₂O): δ 13.5, 20.1, 62.1, 117.1, 118.1, 136.7, 165.5. IR (NaCl, thin film) cm⁻¹: 2922.4, 2851.0, 1661.2, 1409.5. HRMS (ESI+): *m/z* calcd for C₇H₁₀O₄NK(M+H), 212.0325, found, 212.0330. LRMS (ESI-): *m/z* calcd for C₇H₁₀O₄NK (M-K), 172.0 found, 172.0.

Ethyl 2-Nitro-3-methylbut-3-enoate, V30

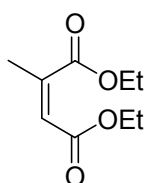
A solution of the potassium salt of the nitro-ester **V29** (0.073 g, 3.4 mmol) in 1ml of water was stirred while 1N HCl (0.5 ml) was added drop-wise at room temperature. The reaction was stirred for 10 minutes and the resulting oil was extracted with 10 ml of ice- cold ether (3X), and the extracts were combined, dried over Na₂SO₄, and concentrated to give 0.058 g (97%) of colorless oil **V30**, used directly without purification (**Scheme 12**). ¹HNMR (300 MHz, CDCl₃) δ 1.28(t, *J*=6.9 Hz, 3H), 1.89 (d, *J* = 2 Hz, 3H), 4.47 (q, *J* = 6.9 Hz, 2H), 5.23(s, 1H), 5.35(m, 1H), 5.60 (s, 1H). ¹³C NMR (75 MHz, CDCl₃) δ 13.8, 19.0, 63.0, 92.2, 123.1, 134.3, 163.5. IR (NaCl, thin film) cm⁻¹: 2950, 2853.0, 1741.1, 1680.0, 1444.4. LRMS (GC-MS): *m/z* calcd for C₇H₁₁NO₄ (M+H), 174.1, found, 174.1.

(±)-Isodehydrovaline Hydrochloride, V10

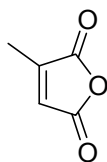
In a round-bottom flask, concentrated HCl (2.5 ml) was maintained at 50-65 °C. Nitro-ester **V30**(0.25g, 1.45 mmol) was added in one portion, and 20 mesh Sn metal (0.6g, 5.3 mmol) was added in small portions, with constant stirring to keep the temperature at 50-65 °C. After the addition was complete, the mixture was heated to 100°C for about 50 min until all the tin had dissolved, then cooled and concentrated to dryness. The residue was dissolved in the minimum amount of water, saturated with H₂S (to precipitate Sn) and filtered. The precipitated tin sulfides washed three times with water, and the filtrate concentrated to dryness. The residue was dried *in vacuo*, washed with dry acetone, and then with dry ether to give 0.2 g (77%) of amino acid hydrochloride, **V10** as a buff-white solid m.p. 206-207°C dec (**Scheme 12**). ¹HNMR (500 MHz, D₂O) δ 1.67(s, 3H), 4.35 (s, 1H), 5.11(s, 1H), 5.15(m, 1H). ¹³C NMR (75 MHz, D₂O) δ 18.0, 58.7, 120.3, 136.1, 169.3. IR (NaCl, thin film) cm⁻¹: 3242.1, 2919.4, 2853.0, 1723.4, 1650.0, 1406.6. LRMS (ESI): *m/z* calcd for C₅H₁₀NO₂Cl (M+H), 116.1, found, 116.1. ESI-, 35, 37 for Cl-

Note 1.

Various methods such as treatment with 9BBN [226, 227], MgI_2 /ether [228, 229] followed by reductive ring opening with Bu_3SnH etc. were employed to regioselectively open the epoxide ring in **V8** and generate **V5**. However, all of the pursued conditions either gave a mixture of products with undesired regiochemistry, degraded products or extremely low yields, making the routes cost-ineffective with respect to labeled material.

Diethyl 2-methylmaleate, V24

In a sealed tube, under a steady stream of N_2 , NaH (0.07 g, 1.76 mmol) was taken and washed with dry THF. Ethyl 2-(diethylphosphoryl)acetate (0.4 g, 1.78 mmol), dissolved in dry THF (8 mL) was added at 0 °C. The mixture was stirred for 30 minutes. Ethyl pyruvate (0.2 g, 1.76 mmol) was added to the anion of the phosphonate and stirred at 0 °C for 5 min, then warmed to 50 °C for 1h. The reaction was quenched by addition of a saturated NH_4Cl solution (5 mL). The aqueous layer was extracted with diethyl ether (3 X40 mL) and the organic fractions were collected, dried with $MgSO_4$, and filtered. Evaporation of the solvent *in vacuo* yielded the desired product as pale yellow oil. The crude product was subjected to column chromatography (EtOAc: hexane, 1:10) to afford **V24** (82%, 0.27g) of the product. 1H NMR (300 MHz, $CDCl_3$): δ 1.24 (t, 3H, $J=7.2$ Hz) 1.33(t, 3H, $J=7.2$ Hz), 2.06 (s, 3H), 4.18 (q, 2H, $J= 7.2$ Hz), 4.26(q, 2H, $J= 7.2$ Hz), 5.85 (m, 1 H). ^{13}C NMR (75 MHz, $CDCl_3$): δ 14.1, 14.2, 20.6, 60.7, 61.4, 121.1, 145.5, 163.0,169.1. IR (NaCl, thin film) 2962.9, 2851.3, 1739.5, 1729.3, 1652.3, 1445.1 cm^{-1} . HRMS (ESI): m/z calcd for $C_9H_{14}O_4(M+Li)$, 193.1052 found, 193.1057.

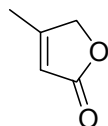
2-methylmaleic acid anhydride (citraconic anhydride), V25

A solution of diethyl 2-methyl maleate, **V24** in THF was maintained at 0 °C. 2N LiOH was added and the ice bath removed. The reaction mixture was allowed to stir for 8h at room

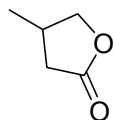
temperature. The solvent was removed and reaction mixture acidified with 1N HCl at 0 °C. The mixture was extracted with EtOAc to provide 1:2 mixture of anhydride and diacid which upon prolong standing and concentration yielded the cis-diacid in 84% yield. ¹H NMR (CDCl₃, 500 MHz) δ 2.16 (s, 3H), 6.05 (m, 1H), 9.05(br,1H); NOESY 1D, 1.4% between H and CH₃. ¹³CNMR (CDCl₃, 500MHz) δ 21.7, 122.7, 147.1, 169.6,171.8; IR (NaCl, thin film) 3458.2, 2928.3, 2857.2, 1737.5,1735.2, 1465.8 cm⁻¹. HRMS (ESI-): *m/z* calcd for C₅H₆O₄(M-H), 129.0188 found, 129.0191.

Diacid (1.21g, 9.3 mmol) was stirred with trifluoroacetic anhydride (93.04 mmol) overnight at room temperature. The resulting solution was evaporated *in vacuo* to provide the product, **V25** in 99% yield. ¹H NMR (CDCl₃, 500 MHz) δ 2.21 (d, *J*=1.5 Hz, 3H), 6.65 (q, *J*=1.5 Hz, 1H); ¹³CNMR (CDCl₃, 500MHz) δ 11.5, 129.9, 149.7, 164.4, 166.6; IR (NaCl, thin film) 3105.1, 2924.1, 1843.1, 1772.8, 1648.4 cm⁻¹. HRMS (ESI): *m/z* calcd for C₅H₄O₃(M+H), 113.0239 found, 113.0239.

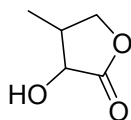
4-methylfuran-2(5H)-one, **V25**



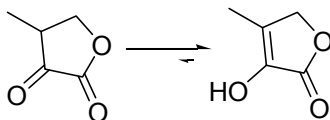
A stirred solution of anhydride, **V25** (100 mg, 0.89 mmol) in THF (2 mL), was maintained at 0 °C. NaBH₄ (84.5 mg, 2.22 mmol) was added in one lot and the reaction allowed to stir at 0 °C for 2 h. The reaction was quenched with water, acidified with dilute HCl and extracted with ethyl acetate (3X50 mL). The organic layer was washed with water, brine and dried over Na₂SO₄. Concentration of the organic layer *in vacuo* followed by silica gel column chromatographic purification of the residue using a mixture of ethyl acetate and petroleum ether (3:7) furnished pure product as a thick oil in 87% yield. ¹H NMR (CDCl₃, 500 MHz) δ 1.99 (s, 3H), 4.60 (s, 2H), 5.69 (m, 1H); ¹³CNMR (CDCl₃, 500MHz) d 13.8, 73.9, 115.8, 166.9, 174.6; IR (NaCl, thin film) 1780, 1750, 1647, 1246 cm⁻¹. LRMS (CI): *m/z* calcd for C₅H₆O₂(M+ Li), 105.05 found, 105.05.

Dihydro-4-methylfuran-2(3H)-one, V26

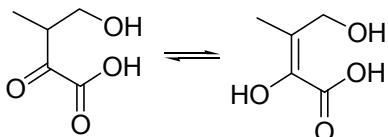
A stirred solution of lactone, (100 mg, 1.08 mmol) and 10%Pd/C (10% wt/wt) in EtOAc (2 mL) was subjected to H₂ (1atm, 24 °C) for 12h. The reaction was passed through celite and washed with hot EtOAc (2X, 10mL), The solvent was evaporated off to afford a pale yellow oil as the product **V26** in 97% yield. ¹H NMR& gCOSY (CDCl₃, 300 MHz) δ (0.98)1.17 (d, J=6.6 Hz, 3H), 2.16 (m, 1H), 2.66 (m, 2H), 3.88(m, 1H), 4.44(m, 1H); ¹³CNMR (CDCl₃, 500MHz) δ18.1(18.2), 30.5(30.9),36.3(36.4) 74.9,177.7; IR (NaCl, thin film) 2925.3, 2809.9, 1729.3 cm⁻¹. LRMS (CI): *m/z* calcd for C₅H₈O₂(M+H), 101.0 found, 101.0.

Dihydro-3-hydroxy-4-methylfuran-2(3H)-one, V27

A solution of the saturated lactone **V26** (83mg, 0.83 mmol) in THF was maintained at -78 °C. LiHMDS (2.5 eq.) was added and the reaction mixture allowed to stir for 30 minutes. Solid freshly prepared Vedej's reagent [230, 231], MoOPH (0.43g, 0.996 mmol) was added in a single batch and the oxidation allowed to proceed at -60 °C for 50 minutes. The reaction was then poured in to ether (50 mL) and freshly prepared saturated Na₂SO₃. The organic layer was collected, washed with NaCl(1X). The organic layer was washed dried over Na₂SO₄ and the solvent evaporated *in vacuo*. The product **V27** was obtained after purification from flash chromatography as a pale yellow oil in 64% yield. ¹H NMR & gCOSY (CDCl₃, 300 MHz) δ (1.04)1.11 (d, J=7.2 Hz, 3H), (2.2)2.75 (m, 1H), 4.02-4.5(m, 3H); ¹³CNMR (CDCl₃, 300MHz) δ11.8(11.8), 29.8(29.9), 70.3(70.9), 72.1(72.1), 177.9(178.8); IR (NaCl, thin film) 3449.3, 2928.3, 2845.4, 1767.8(br), 1456.9 cm⁻¹. HRMS (ESI+): *m/z* calcd for C₅H₈O₃(M+Li), 123.0633 found, 123.0632.

Dihydro-4-methylfuran-2,3-dione

A solution of the α -hydroxylactone (0.1g, 0.86 mmol) in EtOAc (10 mL) was refluxed gently with IBX (3 eq, 1.6 g of 45 % by wt) for 4.5 hours. The reaction was allowed to cool down. The white precipitate was removed by filtration. The reaction mixture was washed with NaHCO_3 (3X) and 1% cold HCl (1X, 10 mL). The organic layer was collected, and dried to yield the product. ^1H NMR (DMSO-*d*₆, 500 MHz) δ 1.82 (m, 3H), 4.59 (m, 2H); ^{13}C NMR (DMSO-*d*₆, 500 MHz) δ 9.7, 70.2, 129.2, 137.3, 170.7; IR (NaCl, thin film) 3404.9, 2928.3, 2851.3, 1785.5, 1758.9, 1225 cm^{-1} . LRMS (ESI): m/z calcd for $\text{C}_5\text{H}_6\text{O}_3(\text{M}+\text{Li})$, 121.0 found, 121.0.

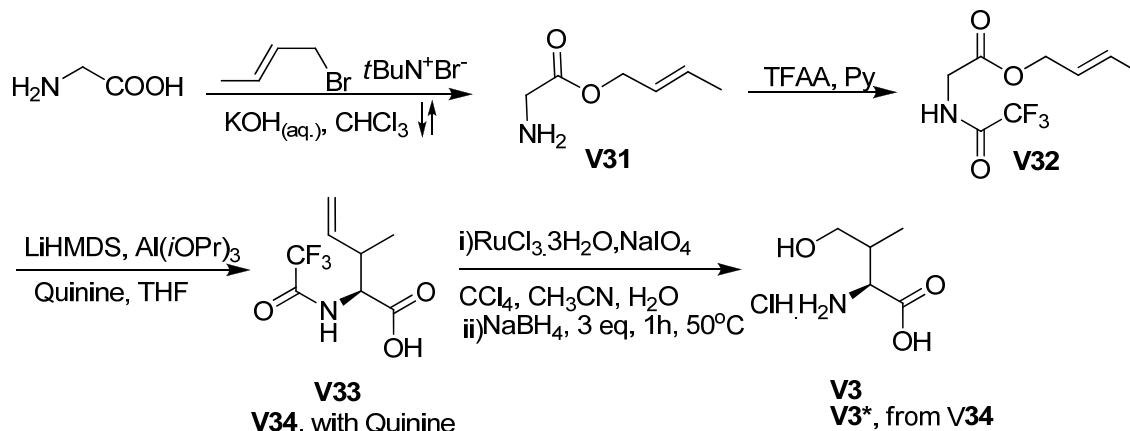
3-(hydroxymethyl)-2-oxobutanoic acid, V5

A solution of the α -ketolactone in taken in a mixture of 6N HCl and HOAc (2:1(v/v)) and the reaction mixture was refluxed gently for 4.5 hours. The reaction was allowed to cool down and filtered. The solvent was evaporated to yield the desired product **5** in near quantitative yield. ^1H NMR (CDCl_3 , 500 MHz) δ 1.79 (br, 2H), 1.97 (m, 3H), 4.65 (m, 2H), 5.82 (br, 1H); ^{13}C NMR (CDCl_3 , 300 MHz) δ 9.8, 71.0, 129.3, 137.3, 171.7; IR (NaCl, thin film) 3437.5, 2928.3, 2848.4, 1755.3, 1643.4, 1221.0 cm^{-1} . HRMS (ESI+): m/z calcd for $\text{C}_5\text{H}_8\text{O}_4(\text{M}+\text{Li})$, 139.0584 found, 139.0583.

Note 3:

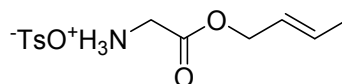
Effort was made to access γ -hydroxyvaline **V3** by subjecting intermediate **V21** to a Mitsunobu reaction to give the azide, which upon reduction could provide access to precursor **V3** (by epoxidation and regioselective ring opening of the epoxide or hydroboration of the olefin). However, the reaction afforded a mixture of products substituted at the α - or γ -position. Hydroboration of isodehydrovaline, **V10** also resulted in low yields of the product. Likewise, attempts to access γ -hydroxyvaline **V3** via condensation of acetylated acetol with the azlactone

of hippuric acid with TiCl_4/Py , [232] $\text{Pb}(\text{OAc})_4$ [233, 234] and subsequent hydrolysis generated upto only 20% of the desired product in our hands on this substrate.



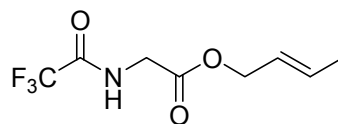
Scheme 13. Synthesis towards V3

(*E*)-But-2-enyl 2-aminoacetate, V31



A suspension of glycine (1g, 13.3 mmol), crotyl alcohol (4.75 g, 66.6 mmol) and *p*-TsOH.H₂O (2.53 g, 13.3 mmol) was refluxed in benzene using a Dean-Starks apparatus for ~ 10 h. The reaction was cooled and the solvent evaporated to yield the desired product **31** as its tosylate salt (**Scheme 13**). ¹H NMR (500 MHz, CDCl₃): δ 1.61 (d, 3H, *J*=6.5 Hz) 2.27(s, 3H), 3.61 (s, 2H), 4.33 (d, 2H, *J*= 6 Hz), 5.35 (m, 1 H), 5.63(m, 1H), 7.03(d, 2H, *J*=7 Hz), 7.64(d, 2H, *J*=7 Hz), 7.94(br, 3H). ¹³C NMR (125 MHz, CDCl₃): δ 17.9, 21.4, 40.6, 66.8, 124.3, 126.1, 129.1, 132.3, 140.5, 141.3, 167.5. IR (NaCl, thin film) 3150.3(br), 2863.2, 1750.0, 1625.7, 1223.0 cm⁻¹. HRMS (ESI+): *m/z* calcd for C₆H₁₁NO₂(M+Li), 136.0948 found, 136.0950.

(*E*)-but-2-enyl 2-(2,2,2-trifluoroacetamido)acetate, V32

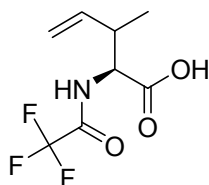


A suspension of allyl glycine ester **V31** (0.53g, 4.1 mmol) in pyridine (1.63g, 20.7 mmol) was maintained at 0 °C. Trifluoroacetic anhydride (4.35g, 20.7 mmol) was added dropwise and the

reaction allowed stirring overnight at room temperature. The reaction mixture was quenched with water and extracted with ether (3X). The organic layer was washed once with 2% HCl solution to remove traces of pyridine and provide the product as mixture of two rotamers, **V32** (**Scheme 13**). ^1H NMR (500 MHz, CDCl_3): δ 1.73 (m, 3H) 4.11(d, 2H, $J=5$ Hz), 4.61 (d, 2H, $J=5$ Hz), 5.57(m, 1H), 5.82 (m, 1H), 7.1(br, -NH). ^{13}C NMR (125 MHz, CDCl_3): δ 17.9, 41.5(42.6), (66.3)67.1, 115.1(q)(115.4 (q)), (123.8)123.9, 133.3(134.5), 157.6(q) (157.2(q)),168.4. IR (NaCl, thin film) 3339.8, 2934.2, 2851.3, 1744.1, 1720.4, 1675.9, 1554.6, 1178.6 cm^{-1} . HRMS (ESI-): m/z calcd for $\text{C}_8\text{H}_{10}\text{O}_3\text{NF}_3$ (M-H), 224.0535 found, 224.0539.

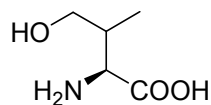
Note: values in parentheses are the chemical shifts of the rotamer

(2R,3S)-2-(2,2,2-trifluoroacetamido)-3-methylpent-4-enoic acid, V33



LiHMDS solution in THF was maintained at -78 $^{\circ}\text{C}$. The allylic ester **V32** (1g, 4.42 mmol), $\text{Al}(i\text{OPr})_3$ (0.99g, 4.86 mmol) and quinidine (2.8g, 8.84mmol) were added at -78 $^{\circ}\text{C}$ and the reaction mixture stirred. The reaction mixture was allowed to warm to room temperature for 24h. The reaction was diluted with 200 mL ether and hydrolyzed by 100 mL 1M aq. KHSO_4 . The organic layer was washed with 1M KHSO_4 again and the reaction mixture extracted with 3X 100 mL sat. NaHCO_3 . The basic solution was acidified by careful addition of solid KHSO_4 (pH=1) and extracted 3X with ether. Dried and concentrated to provide the desired product **V33** in 74% yield (0.74g) (**Scheme 13**). ^1H NMR (500 MHz, CDCl_3): δ 1.09 (d, 3H, $J=5$ Hz), 2.78(m, 1H), 4.58 (s, 1H), 5.10 (m, 2H), 5.26 (br, 1H), 5.69(m, 1H), 7.20(br, 1H). ^{13}C NMR (125 MHz, CDCl_3): δ 15.2(16.1), (39.9)40.3, (55.8)56.2, (117.7)117.8, (136.4)137.1, 157.3(q), 173.5(173.9). IR (NaCl, thin film) 3342.7(br), 2928.3, 2860.2, 1723.4, 1675.9, 1211.2 cm^{-1} . HRMS (ESI-): m/z calcd for $\text{C}_8\text{H}_{10}\text{NO}_3\text{F}$ (M-H), 224.0535 found, 224.0528.

Note: Quinine was employed to get the R-configuration amino acid V34

γ -hydroxyvaline, V3

A solution of the amino acid (300 mg, 1.32 mmol) in MeCN:H₂O (6:1, 9mL) at room temperature was mixed with RuCl₃·3H₂O (3.5 mol%) and NaIO₄ (0.56 g, 2.65 mmol) and allowed to stir for 12 minutes. The reaction was monitored by TLC for appearance of the aldehyde. NaBH₄ (0.15 mg, 3.96 mmol) was added in one lot and the reaction was stirred at 50 °C for 6h. Cooled the reaction and adjusted the pH to 5.0 and the reaction was passed through Celite to remove the white precipitate. The solvent was evaporated off to provide the product in ~85% yield (**Scheme 13**). ¹H NMR (500 MHz, CDCl₃): δ 1.26 (d, 3H, $J=6.5$ Hz), 2.37(m, 1H), 3.21(br, 1H), 3.32(dd, $J=4.5, 11.5$ Hz), 3.52(dd, $J=5.5, 11.5$ Hz), 4.57(dd, $J=7.5, 11.5$ Hz), 7.15(br, 1H). ¹H NMR (300 MHz, D₂O): δ 1.00(d, 3H, $J=6$ Hz), 2.42 (m, 1H), 3.51(m, 1H), 3.99(m,1H); ¹³C NMR (75 MHz, D₂O): δ 14.0, 37.0, 59.7, 66.7, 177.0; IR (NaCl, thin film) 3428.6(br), 3300(br), 2925.3, 2854.3, 1678.9(br), 1422.1, 1214.1 cm⁻¹. LRMS (ESI+): m/z calcd for C₅H₁₁NO₃ ((M+Li)-H), 139.08 found, 139.09.

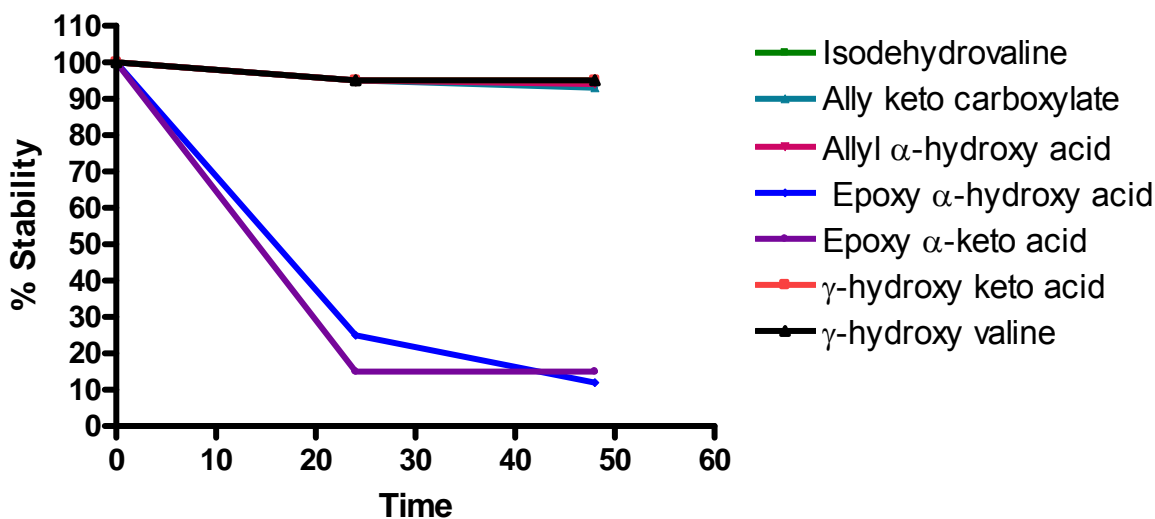


Figure 177. Stability profile of V3-12.

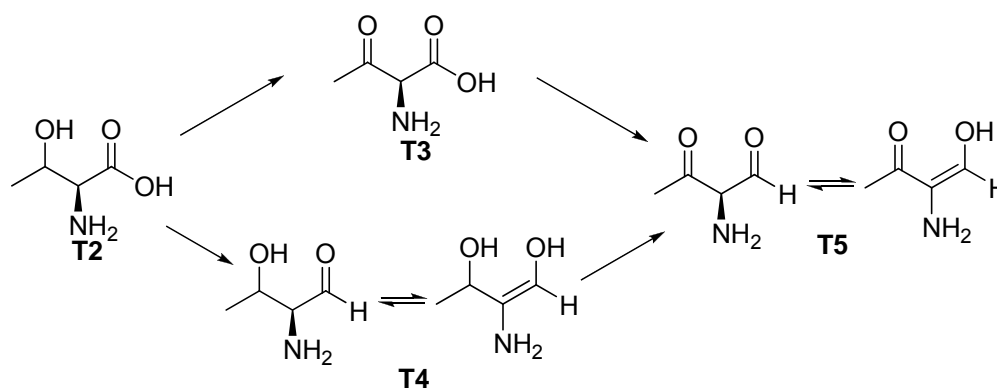
Stability tests were done by shaking samples for 48h under aqueous conditions at pH 7-7.5 at 30 °C.

SYNTHESIS INFORMATION

BIOSYNTHETIC ROUTE TO THE ENOL FRAGMENT OF AZINOMYCIN B

(SYNTHESIS BY DR. VASUDHA SHARMA)

*Reprinted with permission from “An Improved Method for Culturing *Streptomyces sahachiroi*: Biosynthetic Origin of the Enol Fragment of Azinomycin B” by Kelly, G. T., Sharma, V., and Watanabe, C. M. H., 2008. *Bioorganic Chemistry*, 36, 4-15, Copyright [2008] by Elsevier.



Scheme 14. Proposed biosynthetic routes to the enol fragment of azinomycin B

The synthetic routes were designed to allow easy and efficient preparation in high yields, selective deprotection of *O*- and *N*-functional groups and minimal chromatographic separations to afford synthesis of the molecules in a cost effective manner for the implementation of stable isotopes. The availability of synthetic routes to α -amino compounds (**T8**, **Scheme 15**), amins (**T11**, **Scheme 15**), and ketoamino alcohols (**T17**,) is of additional importance as they can serve as models for stereochemical studies [235-237] as well as serve as building blocks in the synthesis of amino-sugars [238, 239], aza-sugars [240], sphingosines [241-245], and unnatural amino acids/derivatives [246-249].

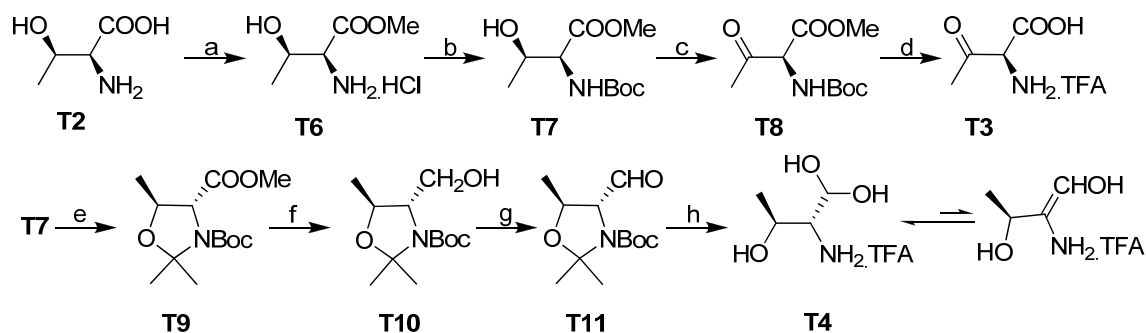
The syntheses of all three precursors **T3**, **T4** and **T5** began from commercially available (L)-threonine. Threonine, **T2** was converted into its methyl ester hydrochloride using SOCl_2 in MeOH under reflux conditions. The methyl ester **T6** was then protected with Boc-anhydride in THF in the presence of triethylamine to provide the Boc-protected methyl ester of threonine **T7** in ~88% yield. This Boc-protected methyl ester **T7** served as the common substrate for all precursors (**Scheme 15**).

β -Keto Amino Acid ((S)-2-amino-3-oxobutanoic acid), T3

Upon oxidation with Dess-Martin periodinane, Boc-protected threonine methyl ester was converted into the corresponding Boc-protected keto-ester **T8** in 91%, which when hydrolyzed with TFA/H₂O under reflux afforded the desired compound **T3** in an overall 72% yield (**Scheme 14**).

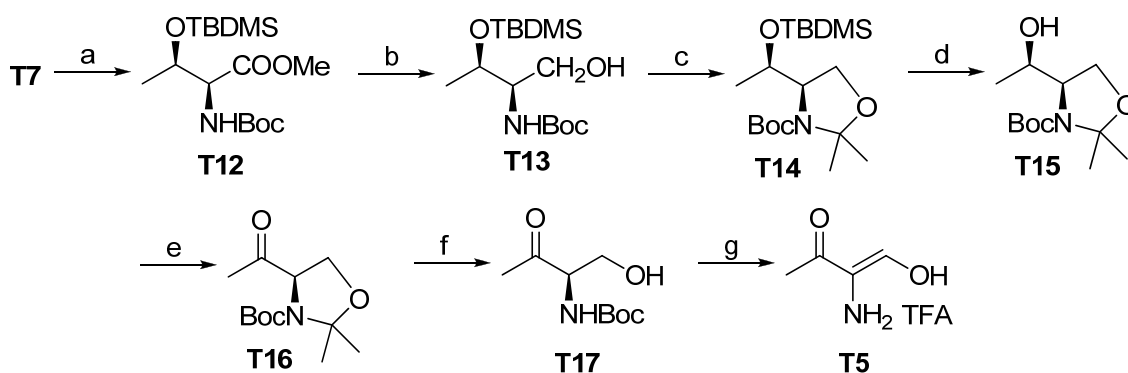
Hydroxy-aldehyde ((2S)-2-amino-3-hydroxybutanal), T4

The hydroxy-aldehyde **T4** (**Scheme 14**) was synthesized over six steps by modification of the synthesis of Garner's aldehyde. The *N*-Boc 2,2-dimethyl oxazolidine ring constituted a convenient masked modified amino acid that was expected to tolerate synthetic elaboration. Thus, Boc-protected amino acid methyl ester, **T7** was protected completely as an oxazolidine **T9** which when subjected to reduction by LiAlH₄ afforded the protected alcohol **T10** in excellent yields. The alcohol was further oxidized to the threonine analog of Garner's aldehyde **T11** in 98% yield. The protected amino-aldehyde was not stable over long periods of time and was immediately subjected to deprotection by treatment with TFA/D₂O. This TFA salt of the amino hydrate system generated was unstable to isolation and was characterized and directly utilized in feeding experiments.



Scheme 15. Synthesis of threonine derivatives

a) MeOH, HCl (dry) reflux, 2h. b) Boc₂O, Et₃N, THF, 0 °C → r.t. 14h, then 50 °C 3h. c) Dess-Martin Periodinane, CH₂Cl₂, r.t., 1h d) TFA(aq.), reflux e) 2-methoxypropene, acetone, r.t., 3h f) LiAlH₄, THF, 40' g) IBX, EtOAc, reflux, 3h h) TFA, water, 25 °C.



Scheme 16. Synthesis of threonine derivatives

a) TBDMSCl, DMAP, Et₃N, dry DMF, 0 °C → r.t., 36h. b) LiAlH₄, THF, -50 °C, 30' c) 2-methoxypropene, acetone, r.t., 2h d) TBAF, THF, 8h e) Dess-Martin Periodinane, CH₂Cl₂, r.t., 1h f) 0.5M TFA, CH₂Cl₂, r.t., 15' g) IBX, DCE, 3h, cool, filter then TFA, H₂O, 15'.

β-ketoaminoaldehyde ((R)-2-amino-3-oxobutanal), T5

We next examined a synthetic route for the preparation of β-ketoaminoaldehyde **T5**. Since the β-ketoenamine system is synthetically equivalent to the corresponding ketoaldehyde, we expected it to be directly formed via oxidation of the corresponding 1,3 diol system. Treatment with TPAP/NMO [250], PCC [251], PDC [252], Dess-Martin [253], and IBX(2-iodoxy benzoic acid) [223], however, resulted in a complex mixture of products unstable to column chromatography. Alternatively, access to the Boc-protected aminoaldehyde using reduction of Boc-protected esters or Weinreb amides [254] led to overreduction to the corresponding alcohol or complicated and tedious column chromatographic separations, not suitable for implementation of stable isotopes. Based on synthesis and stability studies of **T3**, we envisaged N-Boc-protected acetyl glycinol **T17** (Scheme 16) as a convenient moiety to undergo oxidation and subsequent deprotection. Thus, chiral acetyl oxazolidine **T16** was synthesized from the common precursor *tert*-butoxycarbonyl-protected methyl L-threoninate **T7** using a modified procedure employed by Dondoni *et al.* [255] This ester was first transformed into the alcohol **T13** by silylation (91%) of the secondary hydroxyl group with *tert*-butyldimethylsilyl chloride (TBDMSCl) and subsequent reduction of the ester group with LiAlH₄. Our earlier efforts and studies by others [255] revealed that the selective step-wise protection of the two hydroxyl groups was important. Acetonation with 2-methoxypropene (95%) and desilylation (*n*-Bu₄N⁺F⁻) converted **T13** into the (*R,R*)-hydroxyethyl oxazolidine **T15** (88%) in rotameric forms. The secondary alcohol was then subjected to oxidation with Dess-Martin periodinane to yield **T16**. Use of PCC for oxidation

gave a complex mixture of products that remained impure even after column chromatography. The oxazolidine ring was cleaved with very dilute TFA (boc group still intact) to yield the desired acetyl Boc-protected glycinol **T17**. Alternatively, the acetyl Boc-protected glycinol was also synthesized starting from N-Boc-protected serine, which was converted into its Weinreb amide. Further acetonation with 2-methoxypropene, followed by treatment with organolithium (MeLi) in presence of CH_3MgBr as the sacrificial base provided acetylation of the $\alpha\text{-C}$ [256, 257]. However, overall yields from this methodology and purification were not found to be cost-effective in our hands. This primary alcohol was now ready for oxidation and subsequent final deprotection. Heterogenous IBX oxidation [223] provided a mild method to form the aldehyde, however, all efforts to isolate the keto-aminal resulted in rapid decomposition of the product. Hence, the reaction was simply filtered and treated with TFA/ H_2O for 25 min. at room temperature to afford final deprotection, producing the desired keto-aminal **T5**.

Each of the threonine derivatives (compounds **T3**, **T4**, and **T5**) were synthesized in universally labeled form and fed individually to whole cell suspension cultures as detailed previously. Interestingly, none of these amino acid precursors gave any site-specific incorporation above background (**Figure 134**, **Figure 135**, **Figure 136**, and **Figure 137**). As a control for cellular uptake, since the majority of the amino acid derivatives were synthesized as their respective TFA salts, we fed [methyl- ^{13}C] methionine as its TFA salt and monitored its incorporation ([methyl- ^{13}C]-methionine labels specifically the methoxy group of azinomycin B, **Figure 116**). Intact incorporation was observed as reported previously, confirming that the TFA salts of amino acids are capable of penetrating the cell membrane of the producer strain, *S. sahachiroi*. As noted previously [258, 259], both of the enol systems (**T4** and **T5**) were found to be relatively unstable as compared to the corresponding acetylglycine **T3**. Figure 3 illustrates the stability analysis of the compounds. After 48 h at room temperature under aqueous conditions, only 70% of the hydroxyl-aminal **T4** and 35% of the keto-aminal **T5** were detected (**Table 31**).

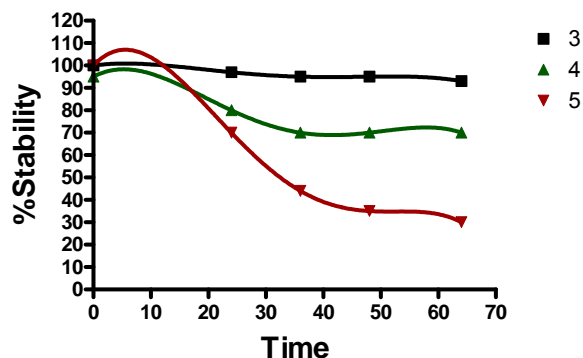


Figure 178. Stability curve as a function of time for T3, T4, T5.

Table 31. Stability of compounds T3, T4, T5 after 48 h under aqueous conditions as judged by NMR spectroscopy

Stability % observed after 48h at r.t.	
T3	93
T4	70
T5	35

Synthesis of isotopically labeled compounds T3, T4 and T5.

Threonine methyl ester hydrochloride, T6

Thionyl chloride (398.5 mg, 3.4 mmol) was added drop-wise to cold anhydrous methanol (15 mL) at 0 °C. The solution was allowed to stir at 0 °C for 10 min. Threonine, **T2** (0.4 g, 3.35 mmol) was added and the reaction mixture allowed to reflux for 1h. The reaction was allowed to cool and the solvent evaporated *in vacuo*. A 2N solution of anhydrous HCl in methanol was generated and the reaction was again refluxed for 1h. The solution was allowed to cool and the solvent evaporated *in vacuo* on a rotary evaporator. A foamy solid was obtained in quantitative yield. IR (NaCl, thin film) ν_{\max} 3375.3, 3236.2, 2960.6(br), 1744.1, 1599.0, 1516.1, 1240.9 cm^{-1} ; ^1H NMR (CD_3OD , 500 MHz) δ 1.35 (d, 3H, $J = 6.5$ Hz), 3.87 (s, 3H), 3.97(d, 1H, $J = 4.5$ Hz), 4.29 (dq, 1H, $J_1 = 6.5$ Hz, $J_2 = 4.0$ Hz), ^{13}C NMR and DEPT(CD_3OD , 500MHz) δ 20.5, 53.7, 59.7, 66.3, 169.6; HRMS (ESI+): m/z calcd for $\text{C}_5\text{H}_{12}\text{NO}_3\text{Cl}$ (M+H), 134.0818, found, 134.0812. ESI-(LRMS): m/z 34.96, 36.99.

Boc-protected Threonine methyl ester, T7

Method A: A flame dried 25 mL three-necked round-bottomed flask, equipped with a magnetic stirring bar, thermometer, reflux condenser (protected from moisture by a calcium chloride-filled drying tube), and a pressure-equalizing dropping funnel connected to a N₂-line was charged with a solution of di-tert-butyl dicarbonate (0.34 g, 1.56 mmol) in THF (2.5 mL). A suspension of methyl threoninate hydrochloride **T6** (0.27 g, 1.59 mmol) in THF (5 mL) and triethylamine (0.34 g, 3.4 mmol) was maintained at 0 °C and allowed to stir for 5 min. The solution of di-tert-butyl dicarbonate was added dropwise over a period of 1 h at 0 °C. After 10 min of additional stirring, the ice-water bath was removed and the suspension was stirred overnight (14 h) at room temperature, then warmed at 50 °C for a further 3 h. The solvent was removed under reduced pressure and the residue was partitioned between diethyl ether (20 mL) and saturated aqueous bicarbonate solution (25 mL). The aqueous phase was extracted with ether 3X15 mL. The combined organic phases were dried with anhydrous Na₂SO₄ and concentrated under reduced pressure to give 0.33 g (88% yield) of N-Boc-L-threonine methyl ester, **T7** as a thick colorless oil that was used without further purification.

Method B: Threonine methyl ester hydrochloride salt, **T6** (3.0 g, 17.7 mmol) and NaHCO₃ (4.6 g, 53.2 mmol) were dissolved in a 1:1 (v/v) mixture of water and methanol (36 mL). (Boc)₂O (5.8 g, 26.6 mmol) was added drop-wise and the solution was stirred at room temperature for 20 h. The reaction mixture was concentrated under vacuum. The reaction mixture was then acidified with aqueous citric acid (1 M) to pH 4.5. The reaction mixture was extracted with ethyl acetate (30 mL x 4). The organic layers were combined, dried with MgSO₄, filtered and concentrated *in vacuo* to obtain the product **T7** in quantitative yield and was used without further purification.

IR (NaCl, thin film) ν_{\max} 3432.1, 2982.4, 2853.2, 1753.4, 1719.9, 1510.4, 1365.2, 1172.4 cm⁻¹; ¹H NMR (CDCl₃, 500 MHz) and gCOSY δ 1.21 (d, 3H, *J* = 7 Hz), 1.45 (s, 9H), 2.23(br, 1H), 3.74 (s, 3H), 4.22 (d, 1H, *J* = 9 Hz), 4.26 (d, 1H, *J* = 6 Hz), 5.41 (d, 1H, *J* = 7 Hz). ¹³C NMR (CDCl₃, 500MHz) and gHMQC δ 19.8, 28.2, 52.5, 58.6, 68.1, 80.1, 156.1, 172.0; HRMS (ESI⁺): *m/z* calcd for C₁₀H₁₉NO₅ (M+Li), 240.1423, found, 240.1415.

tert-butyl 1-(methoxycarbonyl)-2-oxopropylcarbamate (Boc-protected β -keto-Threonine methyl ester), T8.

A solution of Boc-protected threonine methyl ester, **T7** (0.1 g, 0.43 mmol) and Dess-Martin periodinane (0.22 g, 0.52 mmol) in dichloromethane (2 mL), was stirred for 1 h at room temperature. The reaction was then quenched with 15 mL of 1:1 v/v solution of NaHCO₃ and 10% Na₂S₂O₃ and extracted with ethyl acetate (3X, 30 mL). The organic phase was collected, dried over Na₂SO₄ and concentrated *in vacuo* to afford the product (**T8**) as a low melting white solid in 91% yield (92 mg). M.P. =61 °C ; $[\alpha]_D=-3.8(c=2.5, \text{CHCl}_3)$; IR (NaCl, thin film) ν_{max} 3384.2, 2931.2, 2851.3, 1758.9, 1720.4, 1708.6, 1483.6, 1365.1, 1157.9 cm⁻¹; ¹H NMR (CDCl₃, 300MHz) δ 1.42 (s, 9H), 2.35 (s, 3H), 3.78 (s, 3H), 5.02 (d, 1H, $J= 7.2\text{Hz}$), 5.74 (br, 1H). ¹³C NMR (CDCl₃, 300MHz) δ 27.8, 28.1, 53.2, 64.2, 80.8, 154.9, 166.9, 198.8; HRMS (ESI+): m/z calcd for C₁₀H₁₇NO₅ (M+H), 232.1185, found, 232.1178.

2-amino 3-oxobutanoic acid TFA salt, T3.

A solution of tert-butyl 1-(methoxycarbonyl)-2-oxopropylcarbamate, **T8** (0.13 g, 0.56 mmol) in 5 mL TFA:H₂O (v/v 1:1) was refluxed for 8 h and allowed to stir for an additional 5 h. The solvent was evaporated *in vacuo* to give the desired triflate salt as a light yellow sticky solid, **T3**. $[\alpha]_D=-3.24(c 0.4, \text{MeOH})$; IR (NaCl, thin film) ν_{max} 3422.7, 3014.1, 2857.2, 1732.2, 1693.4, 1675.9, 1199.0 cm⁻¹; ¹H NMR (D₂O, 500MHz) δ 2.06(s, 3H), 3.89 (s, 1H); ¹³C NMR (D₂O + 1drop CD₃OD, 500MHz) δ 26.6, 47.7, 116.4 (q, $J_{\text{C-F}}= 1160 \text{ Hz}$), 162.8(q, $J_{\text{C-F}}= 141 \text{ Hz}$), 171.6, 204.03; HRMS (ESI+): m/z calcd for ¹³C₄H₇NO₃ ((M+H)-H₂O), 104.0, found, 103.99.

(4S,5R)-3-tert-butyl 4-methyl 2,2,5-trimethyloxazolidine-3,4-dicarboxylate, T9.

2-methoxypropene (0.31 g, 4.29 mmol) and camphor sulphonic acid (6.7 mg, 0.02 mmol) was added to a solution of N-Boc-L-threonine methyl ester, **T7** (0.1 g, 0.43 mmol) in acetone (2 mL). The resulting orange solution was stirred at room temperature for 3.5 h (TLC analysis indicated completion of reaction). The reaction mixture was quenched with 10 μL of triethylamine and the solvent removed under reduced pressure. The residual brown syrup was partitioned between diethyl ether (20 mL) and saturated aqueous sodium bicarbonate solution (30 mL). The aqueous layer was extracted with diethyl ether (2 \times 30 mL) and the combined organic phases were dried with anhydrous sodium sulfate and concentrated under reduced pressure to give 105 mg (90%) of oxazolidine methyl ester, **T9** as a yellow oil in both rotameric forms (3:1). IR (NaCl, thin film)

ν_{\max} 2984.5, 2928.3, 2857.2, 1755.9, 1720.4, 1376.9, 1362.2, 1258.6 cm^{-1} ; ^1H NMR & gCOSY (CDCl_3 , 300MHz) δ 1.31, 1.32(s, 9H), 1.41 (s, 3H), 1.49-1.57(m, 6H), 3.69(s, 3H), 3.83, 3.91(d, 2H, $J=7.5$ Hz) 4.05-4.09(m, 1H); ^{13}C NMR (CDCl_3 , 300MHz) & DEPT δ 18.7, 18.5, 23.9, 24.7, 26.4, 27.7, 28.1, 28.2, 52.1, 52.3, 65.9, 66.1, 73.4, 73.7, 80.2, 80.7, 94.4, 95.0, 151.2, 152.3, 171.0, 171.5; HRMS (ESI+): m/z calcd for $\text{C}_{13}\text{H}_{23}\text{NO}_5$, (M+H), 274.1654, found, 274.1645.

(4R,5R)-tert-butyl 4-(hydroxymethyl)-2,2,5-trimethyloxazolidine-3-carboxylate, T10

A 25-mL, two-necked, round-bottomed flask was equipped with a magnetic stirring bar, reflux condenser bearing a drying tube and a pressure-equalizing dropping funnel fitted with a rubber septum. The flask was charged with 10 mL of tetrahydrofuran and 20.9 mg (0.55 mmol) of lithium aluminum hydride. While the suspension in the flask was stirred, a solution of the oxazolidine ester, **T9** (100 mg, 0.37 mmol) in tetrahydrofuran (1 mL) was added dropwise over 20 min. The dropping funnel was washed with two 1-mL portions of tetrahydrofuran and the suspension stirred for an additional 20 min, when TLC analysis showed the complete formation of the alcohol. The reaction mixture was cooled with an ice-water bath while 1 mL of a 10% aqueous KOH solution was added drop-wise over 10 min. *Caution! The reaction is exothermic.* The reaction was stirred for another hour at room temperature, and filtered through a Celite pad (1 cm X 2.5 cm) that was subsequently rinsed with diethyl ether (3X, 10mL). The combined organic filtrates were washed with 25 mL of aqueous phosphate buffer (pH=7.0), and the aqueous layer extracted with diethyl ether (3 \times 30 mL). The combined organic phases were dried with anhydrous sodium sulfate, filtered and concentrated *in vacuo* to give 85.1 mg (~95%) of the desired product, **T10** as a pale yellow oil which was used without further purification. IR (NaCl, thin film) ν_{\max} 3437.5, 2978.6, 2928.3, 2875.0, 1696.7, 1670.1, 1456.9, 1406.6, 1255.6 cm^{-1} ; ^1H NMR & gCOSY (CDCl_3 +1drop D_2O), 300MHz) δ 1.32(d, 3H, $J=6$ Hz), 1.44 (s, 3H), 1.47(s, 3H), 1.55 (s, 3H), 3.49(m, 1H), 3.62(d, 2H, $J=3$ Hz) 3.71(m, 1H); ^{13}C NMR (CDCl_3 , 300MHz) & HMQC δ 18.1, 25.9, 27.8, 28.3, 64.7, 67.2, 71.9, 81.3, 94.1, 154.2; HRMS (ESI+): m/z calcd for $\text{C}_{12}\text{H}_{23}\text{NO}_4$, (M+H), 246.1705, found, 246.1699.

(4S,5R)-tert-butyl 4-formyl-2,2,5-trimethyloxazolidine-3-carboxylate, T11

Oxazolidine alcohol **T10** (85 mg, 0.35 mmol) was dissolved in ethyl acetate (2.5 mL, 0.14 M final concentration), and IBX (307.2 mg, 1.1 mmol) was added. The resulting suspension was refluxed in an oil bath set to 80 $^\circ\text{C}$ with vigorous stirring. After 2 h (TLC monitoring), the reaction was cooled to room temperature and filtered through a medium glass frit. The filter cake

was washed with ethyl acetate (3X, 2 mL), and the combined filtrates washed with pre-chilled NaHCO₃ (1X). The organic layer was collected, dried over Na₂SO₄, filtered and concentrated *in vacuo* to yield 82 mg (98% yield) of the desired product **T11** as a mixture of rotomers (2:1). *Note: the aldehydes were immediately used for deprotection. Prolonged storage in an organic solvent led to decomposition of the product.* IR (NaCl, thin film) ν_{\max} 2963.8, 2860.2, 1717.4, 1684.9, 1374.0, 1264.5 cm⁻¹; ¹H NMR & gCOSY (CDCl₃, 300MHz) δ 1.34(d, 3H, *J*=6 Hz), 1.41, 1.49 (s, 9H), 1.55-1.64(m, 6H), 4.02-4.08, 4.19-4.26(m, 1H), 3.68, 3.80 (dd, 1H, *J*=2.4, 2.7 Hz), 9.37, 9.46(d, 1H, *J*=1.8 Hz); ¹³C NMR (CDCl₃, 300MHz) & gHMQC δ 17.6, 17.7, 25.0, 25.8, 26.2, 27.3, 28.1, 28.2, 69.8, 70.0, 70.9, 71.0, 81.4, 81.5, 94.1, 94.9, 150.9, 152.5, 197.5; HRMS (ESI+): *m/z* calcd for C₁₂H₂₁NO₄ (M+H), 244.1549, found, 244.1546.

(R)-2-aminobutane-1,1,3-diol trifluoroacetate salt, T4

A solution of aldehyde **T11** (0.14g, 0.58 mmol) was stirred in deuterated acetone (15% in D₂O) at room temperature. Trifluoroacetic acid (N₂ flushed, Aldrich, 0.21g, 1.84 mmol) was added drop-wise to this solution. A brown grease-like material separated instantaneously. The slurry was stirred for 20 min to yield the product as a triflate salt, **T4** in the D₂O layer. *Note: All attempts to concentrate the product led to decomposition of the material. This adduct was used for feeding studies immediately. Stability studies indicated the presence of ~70% of the compound after 48 h in D₂O at room temperature.* IR (NaCl, thin film) ν_{\max} 3393.1, 1675.9 cm⁻¹; ¹H NMR & gCOSY(D₂O, 500MHz) δ 1.01(d, 3H, *J*=6.5 Hz), 2.76-2.80(m,1H), 3.76-3.84(m, 1H), 4.08(d,1H, *J*=5 Hz). ¹³C NMR (D₂O, 500MHz) δ 19.2, 61.1, 63.9, 86.6, 116.0 (q, *J*_{C-F} = 1153 Hz), 162.2(q, *J*_{C-F} = 139.5 Hz); HRMS (ESI+) *m/z* calcd for C₄H₁₁NO₃ (M+H), 121.0739, found 122.0819; C₄H₉NO₂ (M+H) 104.0712, found, 104.0715.

Methyl (2S,3R)-2-(tert-Butoxycarbonylamino)-3-O-(tert-butyldimethylsilyl) butanoate, T12

A mixture of Boc-protected methyl ester **T7** (1.0 g, 4.29 mmol), triethylamine (0.99 mL, 6.86 mmol), 4-*N,N*-(dimethylamino)pyridine (52.3 mg, 0.42 mmol) in anhydrous DMF (16 mL) was cooled at 0 °C. *tert*-butyldimethylsilyl chloride (0.84 g, 5.57 mmol) was added and the mixture was stirred for 1.5 h. The ice-bath was removed and the reaction mixture was stirred at room temperature for 36 h. The reaction was quenched with methanol (1mL), stirred for an additional 30 min, diluted with Et₂O (100 mL), and washed with saturated aqueous NH₄Cl (3X 25mL). The organic phase was dried (NaSO₄), filtered and concentrated *in vacuo* to give the corresponding silyl derivative, **T12** (1.35 g, 91.2%). [α]_D = -28.6(c 0.73, MeOH); IR (NaCl, thin film) ν_{\max}

2916.3, 2860.0, 1757.8, 1713.3, 1380.2, 1162.2 cm^{-1} ; ^1H NMR & gCOSY (CDCl_3 , 500MHz) δ 0.01(s, 3H), 0.06(s, 3H), 0.87(s, 9H), 1.21(d, 3H, $J=6.5$ Hz), 1.48(s, 9H), 3.74(s, 3H), 4.24(dd, 1H, $J=2, 8$ Hz), 4.44(m, 1H), 5.20(1H, $J=8$ Hz); ^{13}C NMR (CDCl_3 , 500MHz) δ -5.2, -4.3, 17.9, 20.7, 25.5, 28.3, 52.1, 59.5, 68.8, 79.7, 156.2, 171.7; HRMS (ESI+): m/z calcd for (M+H) $\text{C}_{16}\text{H}_{33}\text{NO}_5\text{Si}$, 348.2206, found, 348.2208.

(2R,3R)-2-(tert-Butoxycarbonylamino)-3-O-(tert-butyldimethylsilyl)-1,3-butandiol, T13.

A well-stirred suspension of LiAlH_4 (0.59 g, 15.5 mmol) in anhydrous THF (24 mL) was maintained at -50 °C. Boc-protected silyl derivative, **T12** (1.35g, 3.88 mmol) in anhydrous THF (2 mL) was added over a period of 20 min. The mixture was stirred at -50 °C for an additional 30 min, diluted with 1 M phosphate buffer at pH = 7 (3 mL) and EtOAc (30 mL), warmed to room temperature, and filtered through a pad of Celite. The organic layer was collected and concentrated. The residue was eluted from a column of silica gel with 4:1 cyclohexane-AcOEt to give product **T13** (0.99 g, 80 %) as a thick colorless oil. $[\alpha]_{\text{D}}=-6.9$ (c 0.8, CHCl_3) Lit. $[\alpha]_{\text{D}}=-7.5$ (c 0.8, CHCl_3); IR (NaCl, thin film) ν_{max} 3446.3, 2929.1, 2850.6, 1702.7, 1504.2, 1169.2 cm^{-1} ; ^1H NMR & gCOSY (CDCl_3 , 500MHz) δ 0.09(s, 3H, Si- CH_3), 0.1(s, 3H, Si- CH_3), 0.90(s, 9H, Si- $\text{C}(\text{CH}_3)_3$), 1.19(d, 3H, $J=6$ Hz), 1.47(s, 9H), 3.52-3.70(m, 3H), 4.06-4.11(m, 1H), 4.91(1H, $J=8$ Hz); ^{13}C NMR (CDCl_3 , 500MHz) δ -5.3, -4.3, 17.8, 20.8, 26.0, 28.3, 57.3, 64.2, 67.7, 79.7, 156.8; HRMS (ESI+): m/z calcd for (M+H) $\text{C}_{15}\text{H}_{33}\text{NO}_4\text{Si}$, 320.2257, found, 320.2260.

(4R)-4-[(R)-1-O-(tert-butyldimethylsilyl)ethyl]-2,2-dimethyl-N-(tert-butoxycarbonyl)-1,3-oxazolidine, T14

A solution of Boc-protected silyl alcohol, **T13** (0.85 g, 2.66 mmol) and 2-methoxypropene (1.73 g, 23.98 mmol) in acetone (10 mL) was maintained at 0 °C. 10-camphorsulfonic acid (61.79 mg, 0.26 mmol) was added and the mixture stirred for 1 h at 0 °C, followed by 30 min at room temperature. The reaction was quenched with Et_3N (0.2 mL, color changes from dark red to yellow) and the solvent was removed under reduced pressure. The residual brown syrup was partitioned between diethyl ether (50 mL) and saturated aqueous sodium bicarbonate solution (4 X 30mL). The organic layer was collected and washed once with brine. The organic phase was dried (Na_2SO_4) and concentrated to give the desired product **T14** as a mixture of rotamers (2:1) (0.9g, 95%). IR (NaCl, thin film) ν_{max} 2929.3, 2856.7, 1705.9, 1471.3, 1381.9, 1256.2 cm^{-1} ; ^1H NMR & gCOSY (CDCl_3 , 500MHz) δ 0.07(m, 6H), 0.88(s, 9H), 1.09(d, 3H, $J=6.5$ Hz), 1.27, 1.34(s, 3H), 1.47, 1.49(s, 9H), 1.56, 1.62(s, 3H), 3.78-3.82, 3.92-3.96(m, 1H), 3.87-

3.92, 4.14-4.19(m, 1H) 4.22-4.28, 4.31-4.37(m, 1H); ^{13}C NMR (CDCl_3 , 500MHz) δ -4.8, -4.7, 17.8, 22.6, 22.7, 25.7, 28.1, 28.3, 28.6, 28.6, 29.7, 60.6, 61.2, 62.8, 63.0, 66.2, 66.9, 79.7, 79.9, 94.6, 93.9, 152.3, 152.7; HRMS (ESI+): m/z calcd for (M+H) $\text{C}_{18}\text{H}_{37}\text{NO}_4\text{Si}$, 360.2570, found, 360.2580.

(4R)-4-[(R)-1-Hydroxyethyl]-2,2-dimethyl-N-(tert-butoxycarbonyl)-1,3-oxazolidine, T15

A solution of the silyl ether derivative (0.9 g, 2.82 mmol) in anhydrous THF (10 mL) was treated with $n\text{-Bu}_4\text{N}^+\text{F}^-\cdot 3\text{H}_2\text{O}$ (3.38 mL (1M in THF), 3.39 mmol) at room temperature for 8 h and concentrated. The residue was dissolved in CH_2Cl_2 (20 mL), washed with H_2O (2X, 20 mL), dried (Na_2SO_4), and concentrated to give the crude product as a dark yellow oil. The residue was eluted from a plug of silica gel with 4:1 hexane-AcOEt (containing 0.3% of Et_3N) to afford the product (**T15**) as a white solid (0.55 g, 88%). IR (NaCl, thin film) ν_{max} 3443.4, 2972.7, 2827.3, 1696.7, 1379.9 cm^{-1} ; ^1H NMR(CDCl_3 , 500MHz) δ 1.14(d, 3H, $J=6.5\text{Hz}$), 1.46(s, 3H), 1.47(s, 9H), 1.55 (s, 3H), 3.78-3.98, 4.11-4.19(2m, 4H); ^{13}C NMR (CDCl_3 , 500MHz) δ 24.4, 25.9, 28.2, 28.3, 28.4, 29.8, 63.2, 64.7, 70.1, 81.3, 94.0, 152.3; HRMS (ESI+): m/z calcd for (M+H) $\text{C}_{12}\text{H}_{23}\text{NO}_4$, 246.1705, found, 246.1697.

(4R)-4-Acetyl-2,2-dimethyl-N-(tert-butoxycarbonyl)-1,3-oxazolidine, T16

A mixture of alcohol **15** (0.19 g, 0.79 mmol), and Dess-Martin reagent (0.37 g, 0.88 mmol) in anhydrous CH_2Cl_2 (10 mL) was stirred at room temperature for 2 h away from light. The reaction was quenched with a 1:1 solution of cold $\text{Na}_2\text{S}_2\text{O}_3$ and NaHCO_3 (v/v) and extracted in ether (3X, 30mL). The organic layer was collected, dried over Na_2SO_4 , filtered and concentrated *in vacuo* to give crude product **T16** as mixture of rotamers as a thick yellow oil (0.17 mg, 90%). IR (NaCl, thin film) ν_{max} 2917.2, 2847.7, 1732.6, 1697.8, 1366.3 cm^{-1} ; ^1H NMR(CDCl_3 , 500MHz) δ 1.43, 1.51(s, 9H), 1.48, 1.54(s, 3H), 1.66, 1.72 (s, 3H), 2.20, 2.22(s, 3H), 3.93, 3.98(dd, 1H, $J=3.0$, 6.5 Hz), 4.10-4.18(m, 1H), 4.28, 4.42(dd, 1H, $J=3.0$, 5.5 Hz); ^{13}C NMR (CDCl_3 , 500MHz) δ 24.7, 25.6, 25.4, 25.9, 26.3, 26.5, 28.3, 28.2, 65.1, 65.5, 65.5, 65.6, 81.1, 80.7, 94.5, 95.2, 151.4, 152.4, 206.5, 207; HRMS (ESI+): m/z calcd for (M+H) $\text{C}_{12}\text{H}_{21}\text{NO}_4$, 244.1549, found, 244.1537.

Tert-butyl (S)-1-hydroxy-3-oxobutan-2-ylcarbamate, T17

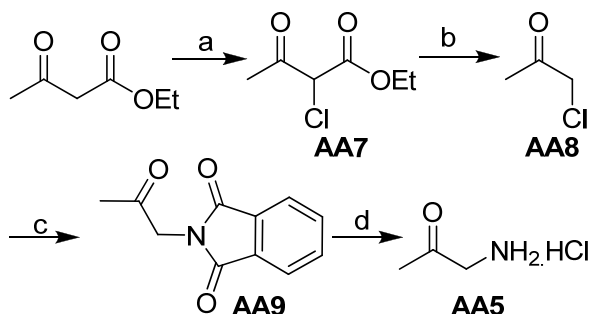
A solution of ketone **T16** (0.17 g, 0.71 mmol) in CH_2Cl_2 (1 mL) was mixed with 0.5 M TFA in anhydrous CH_2Cl_2 (15 mL) and stirred at room temperature for 15 min. The reaction was

quenched with cold NaHCO_3 (30 mL) and extracted in ether (3X, 30 mL). The organic layer was collected, dried over Na_2SO_4 , filtered and concentrated *in vacuo* to give the crude product as a thick yellow oil. The crude material was then purified by column chromatography by eluting with ethyl acetate:hexane (1:3) $R_f=0.25$ to yield acetyl glycinol **T17** (0.12g, 85%). IR (NaCl, thin film) ν_{max} 3418.4, 2919.2, 2851.1, 1711.9, 1687.7, 1366.7 cm^{-1} ; ^1H NMR(CDCl_3 , 500MHz) δ 1.46(s, 9H), 2.29(s, 3H), 3.96(ddd, $J=4, 8, 25$ Hz), 4.32(m, 1H), 5.68(br, 1H); ^{13}C NMR (CDCl_3 , 500MHz) δ 27.3, 28.2, 62.1, 62.9, 80.2, 155.9, 205.6; HRMS (ESI+): m/z calcd for (M+H) $\text{C}_9\text{H}_{17}\text{NO}_4$, 204.1236, found, 204.1239.

3-amino-4-hydroxy but-3-en-2-one trifluoroacetate salt

A suspension of ketone **T17** (0.08 g, 0.4 mmol) in dichloroethane (2 mL) was refluxed gently with IBX (0.7 g, 1.2 mmol, 45%) for 3 h. The suspension was allowed to cool to room temperature and further cooled at -20 °C for 20 min. The resulting white precipitate was filtered. The filtrate was mixed with aqueous TFA (50 mg in 1 mL water) and allowed to stir for 25 min at room temperature. The aqueous layer was collected and characterized. *Note: the keto-aldehyde and keto-aminal were found to be unstable to isolation conditions. Any attempts to concentrate this material led to extensive decomposition of the product. This precursor was used for feeding studies immediately. Stability studies indicated the presence of ~35% of the compound after 48 h in D_2O at room temperature.* ^1H NMR(D_2O , 500MHz) δ 1.69(s, 3H), 1.83 (s, 3H), 4.69 (s, 1H), 5.06(s, 1H). HRMS (ESI+): m/z calcd for (M+H) $\text{C}_4\text{H}_7\text{NO}_2$, 102.0555, found, 102.0551.

BIOSYNTHETIC ROUTE TO THE END FRAGMENT OF AZINOMYCIN A
(SYNTHESIS BY DR. VASUDHA SHARMA)



Scheme 17. Synthesis of Aminoacetone Hydrogen Chloride
(a) SO_2Cl_2 , 0 °C, 36h; (b) 2 equiv. conc. H_2SO_4 , aq. THF, reflux; (c) Potassium phthalimide, DMF, 16h; (d) conc. HCl , reflux, 7h.

Ethyl 2-Chloroacetoacetate (AA7)

Sulfuryl chloride (322 μL) was added drop-wise via a dropping funnel to ethyl acetoacetate (500 mg) maintained at 0°C. The mixture was stirred overnight at room temperature. The product, AA7 was obtained by evaporation *in vacuo* of the formed SO_2 and HCl (0.62 g, 98%) as a slightly yellow liquid (Scheme 17). Both the ^1H NMR spectrum and the ^{13}C NMR spectrum showed a keto-enol mixture of ethyl 2-chloroacetoacetate. ^1H NMR (300 MHz, CDCl_3): δ 4.76 (m, 1H), 4.18-4.27 (m, 4H (keto/enol)), 2.38 (s, 3H), 2.19 (s, 3H (enol)), 2.16 (s (br), OH, 1H (enol)), 1.30 (m, 6H (keto/enol)). ^{13}C NMR (300 MHz, CDCl_3): δ 196.8, 172.7, 169.3, 164.9, 96.6, 63.1, 61.3, 26.2, 20.1, 14.1.

Chloroacetone (AA8)

A solution of ethyl 2-chloroacetoacetate, AA7 (0.62g, 3.74 mmol) dissolved in 3mL of THF was mixed with and 0.27 mL water. Concentrated H_2SO_4 (2 eq.) was added and the reaction mixture was refluxed for 40 h. Subsequently, the mixture was cooled to room temperature followed by the addition of 15 mL of water and 25 mL of diethyl ether. The aqueous layer was extracted with 50 mL (3X) of diethyl ether. The combined organic layers were washed with saturated NaHCO_3 solution and brine. The organic layer was dried over Na_2SO_4 , filtered and diethylether was then removed via distillation at atmospheric pressure due to volatility of the product. The resulting solution of chloroacetone AA8 in THF was used in the following step (Scheme 17). ^1H NMR

(500 MHz, CDCl₃): δ 4.09 (s, 2H), 2.30 (s, 3H). ¹³C NMR (125 MHz, CDCl₃): δ 200.5, 48.9, 27.2.

N-acetyl phthalamide (AA9)

In a dried flask, to a solution of chloroacetone, **AA8** (1g, 10.8 mmol) in DMF (10 mL) was added potassium phthalimide (2.20g, 11.8 mmol) with constant stirring (potassium phthalimide was not completely soluble in the DMF). The reaction was stirred at room temperature for 16h and monitored by TLC. After the reaction was complete, the reaction mixture was poured into water (250 mL). Ivory-white colored solid (**AA9**) precipitated (2.17 g, 99.3%) which was filtered and dried (**Scheme 17**). ¹H NMR (CDCl₃, 300MHz) 2.25(s, 3H), 4.48 (s, 2H), 7.72(dd, 2H, $J_1=2.7$ Hz, $J_2=5.4$ Hz), 7.85(dd, 2H, $J_1=2.7$ Hz, $J_2=5.4$ Hz). ¹³C NMR (CDCl₃, 300MHz) δ 27.1, 47.3, 123.9, 132.2, 134.6, 167.8, 199.9. IR (NaCl, thin film) cm⁻¹: 3055.6, 2925.3, 2860.2, 1770.7, 1729.3, 1616.7, 1418.4, 1190.8. HRMS (ESI+) C₁₁H₉NO₃ (M+Li), 210.0742, found, 210.0739.

Aminoacetone hydrochloride (AA5)

A suspension of N-acetylphthalimide, **AA9** in aqueous solution (1:1) of conc. HCl was heated to reflux for 7h. The solution was allowed to cool down. The precipitated phthalic acid was filtered and washed once with cold water (2 mL). The solvent was evaporated from the filtrate to yield the desired product **AA5** in 77% yield as its hydrochloride salt. ¹H NMR (D₂O, 300MHz) 2.10 (s, 3H), 3.92 (s, 2H), 6.70 (br, NH₂, exchangeable) (**Scheme 17**). ¹³C NMR (D₂O, 300MHz) δ 26.4, 47.4, 203.3. IR (NaCl, thin film) cm⁻¹: 3422.7(br), 2919.4, 2848.3, 1729.3, 1590.1; MS (ESI+) C₃H₇NO (M+H), 74.0606, found, 74.0609. *Note: the product was freeze dried and kept at -20 °C away from light for prolonged storage.*

BIOSYNTHETIC ROUTE TO THE AZIRIDINO[1,2A]PYRROLIDINE (1-AZABICYCLO[3.1.0]HEXANE) MOIETY

(SYNTHESIS BY DR. VASUDHA SHARMA)

Serine methyl ester hydrochloride

Methanol (10 mL) was cooled to 0 °C, and thionyl chloride (0.69 mL, 9.52 mmol) was added dropwise. To the resultant solution of HCl in methanol was added L-serine (1.0 g, 9.52 mmol), and the reaction mixture was heated under reflux for 1 h. The solvent was removed *in vacuo*, another 10 mL of a 2 M solution of HCl in methanol, prepared in the same manner as before, was added, and the reaction mixture was heated under reflux for another 1 h. The solvent was removed *in vacuo* to yield the title compound (1.48 g, quant.) as a white solid. ¹H NMR (300 MHz, CDCl₃) δ 3.85(s, 3H) 3.99-4.02 (m, 2H), 4.11(m, 1H), 5.48 (br, -NHs); ¹³C NMR (500 MHz; CDCl₃) δ 53.7, 55.9, 60.9,169.3; IR (NaCl, thin film) cm⁻¹: 3428.6, 2928.3, 2848.35, 1741.1, 1476.7; HRMS (ESI+): *m/z* calcd for C₄H₁₀NO₃Cl(M+Li), 120.0661, found, 120.0662.

Boc-protected serine methyl ester

A flame dried 25 mL three-necked round-bottomed flask, equipped with a magnetic stirring bar, thermometer, reflux condenser (protected from moisture by a calcium chloride-filled drying tube), and a pressure-equalizing dropping funnel connected to a N₂-line was charged with a solution of di-tert-butyl dicarbonate (2.02 g, 9.31 mmol) in THF (30 mL). A suspension of methyl serinate hydrochloride (1.48 g, 9.5 mmol) in THF (30 mL) and triethylamine (2.07 g, 20.4 mmol) was maintained at 0 °C and allowed to stir for 5 min. The solution of di-tert-butyl dicarbonate was added drop-wise over a period of 1 h at 0 °C. After 10 min of additional stirring, the ice-water bath was removed and the suspension was stirred overnight (14 h) at room temperature, then warmed at 50 °C for a further 3 h. The solvent was removed under reduced pressure and the residue was partitioned between diethyl ether (25 mL) and saturated aqueous bicarbonate solution (25 mL). The aqueous phase was extracted with ether 3X25 mL. The combined organic phases were dried with anhydrous Na₂SO₄ and concentrated under reduced pressure to give 1.84 g (88% yield) of N-Boc-L-serine methyl ester, as a thick colorless oil that was used without further purification. ¹H NMR & gCOSY (300 MHz, CDCl₃) δ 1.42(s, 9H), 3.47(br, 1H), 3.75(s, 3H) 3.82-3.92 (m, 2H), 4.36(m, 1H), 5.66 (br, -NH); ¹³C NMR & gHMQC (300 MHz; CDCl₃) δ 52.4, 55.9, 63.2, 80.0, 155.9, 171.5; IR (NaCl, thin film) cm⁻¹: 3446.4,

3404.9, 2978.6, 2928.3, 1747.0, 1714.5, 1519.1; HRMS (ESI+): m/z calcd for $C_9H_{17}NO_5$ (M+Li), 220.1185, found, 220.1181.

(S)-3-tert-butyl 4-methyl 2,2-dimethyloxazolidine-3,4-dicarboxylate, AZ10

2-methoxypropene (3.2 g, 45 mmol) and camphor sulphonic acid (9.3 mg, 0.04 mmol) was added to a solution of N-Boc-L-serine methyl ester, (1g, 4.5 mmol) in acetone (20 mL). The resulting orange solution was stirred at room temperature for 3.5 h (TLC analysis indicated completion of reaction). The reaction mixture was quenched with 100 μ L of triethylamine and the solvent removed under reduced pressure. The residual brown syrup was partitioned between diethyl ether (50 mL) and saturated aqueous sodium bicarbonate solution (50 mL). The aqueous layer was extracted with diethyl ether (2×50 mL) and the combined organic phases were dried with anhydrous sodium sulfate and concentrated under reduced pressure to give 1.06 g (90%) of oxazolidine methyl ester as a yellow oil in both rotameric forms (3:1). IR (NaCl, thin film) ν_{\max} 2981.6, 2886.8, 1758.9, 1714.5, 1385.9, 1095.7 cm^{-1} ^1H NMR & gCOSY (CDCl_3 , 500MHz) δ 1.22, 1.31(s, 9H), 1.38, 1.40 (s, 3H), 1.54, 1.56(m, 3H), 3.69(s, 3H), 3.95-4.11(m, 2H), 4.33-4.40(m, 1H); ^{13}C NMR (CDCl_3 , 125MHz) δ 24.3, 24.9, 25.1, 25.9, 28.2, 28.3, 52.2, 52.3, 59.1, 59.2, 65.8, 66.2, 80.3, 80.9, 94.3, 95.0, 151.2, 152.1, 171.0, 171.6 HRMS (ESI+): m/z calcd for $C_{12}H_{21}NO_5$, (M+H), 266.1580, found, 266.1583.

(R)-tert-butyl 4-(hydroxymethyl)-2,2-dimethyloxazolidine-3-carboxylate

A 25-mL, two-necked, round-bottomed flask was equipped with a magnetic stirring bar, reflux condenser bearing a drying tube and a pressure-equalizing dropping funnel. The flask was charged with 10 mL of tetrahydrofuran and 20.9 mg (0.55 mmol) of LiAlH_4 . While the suspension in the flask was stirred, a solution of the oxazolidine ester (100 mg, 0.38 mmol) in tetrahydrofuran (1 mL) was added dropwise over 20 min. The dropping funnel was washed with two 1-mL portions of tetrahydrofuran and the suspension stirred for an additional 20 min, when TLC analysis showed the complete formation of the alcohol. The reaction mixture was cooled with an ice-water bath while 1 mL of a 10% aqueous KOH solution was added drop-wise over 10 min. *Caution! The reaction is exothermic.* The reaction was stirred for another hour at room temperature, and filtered through a Celite pad (1 cm X 2.5 cm) that was subsequently rinsed with diethyl ether (3X, 10mL). The combined organic filtrates were washed with 25 mL of aqueous phosphate buffer (pH=7.0), and the aqueous layer extracted with diethyl ether (3×30 mL). The combined organic phases were dried with anhydrous sodium sulfate, filtered and concentrated *in*

vacuo to give 85.1 mg (~95%) of the desired product as a pale yellow oil which was used without further purification. IR (NaCl, thin film) ν_{\max} 3446.4, 2972.7, 2872.0, 1699.7(br), 1670.1, 1462.8 cm^{-1} ^1H NMR (CDCl_3 , 500MHz) δ 1.38, 1.42 (s, 3H), 1.45, 1.46(s, 9H), 1.51,1.68 (s, 3H), 3.53(m, 1H), 3.72(m, 2H) 3.99(m, 3H) ^{13}C NMR (CDCl_3 , 125 MHz) δ 24.3, 24.4, 27.2, 28.3, 28.4, 59.3, 59.5, 64.9, 65.3, 65.4, 65.8, 81.1, 81.2, 94.1, 94.4, 153.9,154.2; LRMS (ESI+): m/z calcd for $\text{C}_{11}\text{H}_{21}\text{NO}_2$, (M+Li), 238.2, found, 238.2.

(S)-tert-butyl 4-formyl-2,2-dimethyloxazolidine-3-carboxylate, AZ11

Oxazolidine alcohol (85 mg, 0.36 mmol) was dissolved in ethyl acetate (2.5 mL, 0.14 M final concentration), and IBX (307.2 mg, 1.1 mmol) was added. The resulting suspension was refluxed in an oil bath set to 80 °C with vigorous stirring. After 2 h (TLC monitoring), the reaction was cooled to room temperature and filtered through a medium glass frit. The filter cake was washed with ethyl acetate (3X, 2 mL), and the combined filtrates washed with pre-chilled NaHCO_3 (1X). The organic layer was collected, dried over Na_2SO_4 , filtered and concentrated *in vacuo* to yield 82 mg (98% yield) of the desired product **AZ11** as a mixture of rotomers (2:1). *Note: the aldehydes were immediately used for deprotection. Prolonged storage in an organic solvent led to decomposition of the product.* IR (NaCl, thin film) ν_{\max} 2981.6, 2928.2,1739.0, 1705.6, 1684.9, 1453.9 cm^{-1} ^1H NMR(CDCl_3 , 500MHz) δ 9.33, 9.42(d, 1H, $J=1.8$ Hz), 4.03(m, 1H), 3.78-3.67(m, 2H),1.62(s, 3H),1.48, 1.56(s, 3H), 1.39(s, 9H) LRMS (ESI+): m/z calcd for $\text{C}_{11}\text{H}_{19}\text{NO}_2$ (M+Li), 236.2, found, 236.2.

Ethyl 2-(Diethyl phosphoryl)acetate

A mixture of ethyl bromoacetate (2.2g, 13.2 mmol) and triethylphosphite (2.19g, 13.2 mmol) was heated in a flame-dried flask to 130 °C for 10h. The mixture was allowed to cool down to room temperature to afford the desired product in 98% yield (2.83g) as a mixture of rotamers. ^1H NMR (CDCl_3 , 300 MHz): δ 0.94 (m, 9H), 2.57(d, 2H, $J=21.3$ Hz), 3.81(m, 6H) ^{13}C NMR (CDCl_3 , 300 MHz): δ 13.24, 15.51, 32.6, 34.3, 60.6, 61.69, 164.8, 164.9. IR (NaCl, thin film) cm^{-1} : 29371.9, 1745.3, 1468.1 HRMS (ESI+): m/z calcd for $\text{C}_8\text{H}_{17}\text{O}_5\text{P}$ (M+Li), 231.0974, found, 231.0977.

2-(tert-butoxycarbonylamino)-5-ethoxy-5-oxopentanoic acid, AZ12

Step A: N-tert-butyl 4-(3-ethoxy-3-oxoprop-1-enyl)-2,2-dimethyloxazolidine-3-carboxylate:

In a sealed tube, under a steady stream of N_2 , NaH (0.14 g, 3.59 mmol) was washed with dry hexanes. Ethyl 2-(diethylphosphoryl)acetate (0.87 g, 3.87 mmol), dissolved in dry

tetrahydrofuran (10 ml) was added at 0 °C. The mixture was stirred for 15 minutes. Garner's aldehyde (0.59 g, 2.58 mmol) was added to the reaction mixture and stirred at 0 °C for 30 min, then at room temperature for 6h. The reaction was quenched by addition of a saturated NH₄Cl solution (5 ml). The aqueous layer was extracted with diethyl ether (3X40 ml) and the organic fractions were collected, dried with Na₂SO₄, and filtered. Evaporation of the solvent *in vacuo* yielded the desired product as a mixture of cis and trans diastereomers as well as rotamers as a light-yellow oil which was used further without purification (0.46 g, 60%). ¹H NMR (300 MHz, CDCl₃): δ 1.20(m, 3H), 1.40,1.43,1.44,1.52(s,9H), 1.62, 1.66,1.69,1.70(s, 6H), 1.72, 1.73, 1.75,1.78(s, 6H),3.81-4.05(m,1H), 4.13(m, 2H), 4.31-4.49(m, 2H),5.61, 5.65, 5.77, 5.71(m, 1H),6.03, 6.066.09, 6.20 (m, 1 H). IR (NaCl, thin film) cm⁻¹: 2954.9, 2869.1, 1732.2, 1717.4, 1462.8, 1166.8. HRMS (ESI+): *m/z* calcd for C₁₅H₂₄NO₅(M+Li), 306.1893, found, 306.1886.

Step B: N-tert-butyl 4-(3-ethoxy-3-oxopropyl)-2, 2-dimethyloxazolidine-3-carboxylate:

The mixture of isomers of the alkene were dissolved in MeOH and hydrogenated at 1 atm at room temperature for 24 h in presence of 10% Pd/C as the catalyst (1:1 w/w).The reaction slurry was filtered through celite and washed with warm EtOAc twice. The solvent was evaporated off to afford the product are a dark yellow oil. ¹H NMR (300 MHz, CDCl₃) δ 4.12 (q, *J*=8.8 Hz, 2H), 3.94–3.71 (m, 2H+1H), 2.32 (m, 2H), 2.03–1.89 (m, 2H), 1.59–1.43 (m, 6H), 1.46 (s, 9H), 1.25 (t, *J*=8.8 Hz, 3H). IR (NaCl, thin film) cm⁻¹: 2960.6, 2929.7, 2867.9, 1709.9, 1703.7, 1656.3, 1374.1. HRMS (ESI+): *m/z* calcd for C₁₅H₂₆NO₅(M+Li), 308.2049, found, 308.2047.

Step C: A stirring solution of oxazolidinone ester (692 mg, 2.3 mmol) in 5 mL of acetone, was maintained at 0 °C. Jones' reagent (1.73 mL, 4.6 mmol) was added and the reaction mixture was allowed to warm to room temperature and the stirring was continued for 12 h. The mixture was then transferred to a larger flask and then Celite and isopropyl alcohol were added. The mixture was stirred for 15 min and the precipitate was filtered, washed with acetone, and made alkaline by the addition of sat. NaHCO₃(aq). The solution was concentrated to remove organic solvents and washed with Et₂O (3X25 mL). The aqueous layer was acidified to a pH=3 by the addition of solid Citric acid and extracted with CHCl₃ (5X25 mL). The combined extracts were washed with brine (1X15 mL) and dried over solid Na₂SO₄. The solvent was concentrated to afford 252 mg (40%) of a semi-solid as mixture of rotamers. ¹H NMR (300 MHz, CDCl₃) δ 5.25 (br, 1H), 4.35 (m, 1H), 4.12 (q, *J*=7.8 Hz, 2H), 2.44 (m, 2H), 2.25 (m, 1H), 2.06 (m, 1H), 1.45 (s, 9H), 1.26 (t, *J*=7.8 Hz, 3H); ¹³C NMR (75 MHz, CDCl₃) δ176.2, 175.7, 173.2, 172.9,156.9,155.8,82.1, 80.5,

60.9, 60.7, 53.9, 52.9, 30.6, 30.2, 28.4, 28.0, 27.6, 14.3. IR (NaCl, thin film) cm^{-1} : 3363.5, 2922.4, 2851.3, 1732.2, 1720.4, 1696.7, 1166.8. HRMS (ESI+): m/z calcd for $\text{C}_{12}\text{H}_{21}\text{NO}_6(\text{M}+\text{Li})$, 282.1529, found, 282.1517.

D-Glutamic acid , AZ 6

A solution of boc-protected glutamic acid ethyl ester (200 mg, 0.73 mmol) was maintained at 0 °C in ethanol (0.5 mL). NaOH (2.1 eq, 3 mL H_2O) was added and the reaction was allowed to stir at room temperature for 9h. The reaction was washed with hexanes(1X) and the aqueous layer was collected and acidified with TFA at 10 °C with constant stirring to pH~2. The solvent was removed to afford the glutamic acid as its triflate salt in 86% yield. ^1H NMR (300 MHz, D_2O) δ 3.85(m, 1H), 2.16-2.34(m, 4H); ^{13}C NMR (75 MHz, D_2O) δ 181.2, 180.8, 53.8, 32.5, 29.8. IR (NaCl, thin film) cm^{-1} : 3235.0, 2962.4, 2890.3, 1650.0, 1600.0, 1410.0.

Pyroglutamic acid, AZ17

Glutamic acid, **AZ6** (1g, 6.8 mmol) was heated in water (10 mL) for 15 hours in a sealed tube. The solvent was evaporated to afford the pure product in quantitative yields (0.876 g). ^1H NMR (500 MHz, $\text{D}_2\text{O}+2$ drops of CD_3OD) δ 1.99-2.06 (m, 1H), 2.24-2.42(m, 3H), 4.22(m, 1H); ^{13}C NMR (500 MHz, $\text{D}_2\text{O}+2$ drops pf CD_3OD) δ 25.5, 30.3, 56.9, 177.5, 182.9; HRMS (ESI+): m/z calcd. for $\text{C}_5\text{H}_7\text{NO}_3(\text{M}+\text{H})$, 130.0504, found, 130.0506.

(S)-methyl 5-oxopyrrolidine-2-carboxylate, AZ13

Acetyl chloride (0.53g, 6.82 mmol) was added drop-wise to 10 mL MeOH at 0 °C. Pyroglutamic acid, **AZ17** (800 mg, 6.2 mmol) was added in one lot and the reaction was stirred at 0 °C for 1h. The temperature was allowed to rise and the reaction was stirred at room temperature. The solvent was evaporated and the residue washed with NaHCO_3 (3X, 20 mL). The reaction was extracted with EtOAc(3X, 50 mL). The organic layer was collected, dried over Na_2SO_4 , filtered and concentrated *in vacuo* to yield the product **AZ13** as a thick colorless oil in 87% yield (0.77g). ^1H NMR (300 MHz, CDCl_3) δ 2.05-2.40 (m, 4H), 3.69(s, 3H), 4.22(m, 1H), 7.05(br, 1H, -NH); ^{13}C NMR (500 MHz, CDCl_3) δ 24.6, 29.2, 52.4, 55.3, 172.5, 178.3; LRMS (ESI+): m/z calcd for $\text{C}_6\text{H}_9\text{NO}_3(\text{M}+\text{H})$, 144.06, found, 144.06.

(S)-5-(hydroxymethyl)pyrrolidin-2-one, AZ5

A solution of methyl 5-oxopyrrolidine-2-carboxylate, **AZ13** (0.7g, 4.89 mmol) in THF:MeOH (3:2) was maintained at 0°C. NaBH₄ (0.55g, 14.67mmol) was added in small lots and allowed to stir for 2h. The slurry was allowed to warm up to room temperature after which conc. HCl was added drop-wise such that the pH=4. The reaction was stirred for 1h at room temperature after which it was neutralized to pH=7 with solid NaHCO₃. Filtered the slurry through celite and extracted the aqueous layer with EtOAc(2X). The organic layer was collected, dried over Na₂SO₄, filtered and concentrated *in vacuo* to yield the product **AZ5** as a thick colorless oil in 85% yield (0.48g). ¹H NMR (300 MHz, CD₃OD) δ 1.86-1.88 (m, 1H), 2.18-2.37(m, 3H), 3.46-3.59(m, 2H), 3.72-3.76(m,1H); ¹³C NMR (500 MHz, CD₃OD) δ 23.7, 31.03, 57.6, 65.9,181.3; HRMS (ESI+): *m/z* calcd for C₅H₉NO₂ (M+H), 116.0711, found, 116.0700.

(R)-(5-oxopyrrolidin-2-yl)methyl 4-methylbenzenesulfonate, AZ14

A solution of (R)-5-(hydroxymethyl)pyrrolidin-2-one **AZ5** (0.1g, 0.87 mmol) and TEA (0.093 g, 0.91 mmol) in CH₂Cl₂ (10 mL) was maintained at 0 °C. TsCl(0.17 g, 0.91 mmol) was added and allowed to stir overnight. The slurry was allowed to warm up to room temperature after which the solution was washed with dil. HCl (2X, 20 mL) and then with sat. NaHCO₃ (1X, 15 mL). The organic layer was collected, dried over Na₂SO₄, filtered and concentrated *in vacuo* to yield the product as a white solid in 80% yield (0.19g). ¹H NMR & gCOSY (500 MHz, CDCl₃) δ 1.77-1.80 (m, 1H), 2.22-2.37(m, 3H), 2.47(s, 3H), 3.89(dd, *J*₁=7.5Hz, *J*₂= 9.5 Hz) 3.91-3.94(m,1H), 4.05 (dd, *J*₁=4Hz, *J*₂= 9.5 Hz), 6.22(s, br, -NH), 7.37(d, 2H, *J*=7.2Hz), 7.79(d, 2H, *J*=7.2Hz); ¹³C NMR (500 MHz, CDCl₃) δ 21.6, 22.7, 29.2, 52.5, 71.9, 127.9, 130.0, 132.3, 145.3,177.8; HRMS (ESI+): *m/z* calcd for C₁₂H₁₅NO₄S (M+H), 270.0800, found, 270.0786.

(3S,7aR)-3-phenyltetrahydropyrrolo[1,2-c]oxazol-5(1H)-one, AZ18

A mixture of 0.4g (3.4 mmol) of alcohol **5**, 0.54 g (4.5 mmol) of benzaldehyde, and 1.6 g (0.003 mmol) of p-TsOH in toluene (10 mL) was refluxed under a Dean-Stark water separator with vigorous stirring in an oil bath. After 9 h the reaction was stopped and cooled. The reaction mixture was washed with 5% NaHCO₃ solution (2 X 5 mL), saturated NaHSO₃ solution (4 X 5 mL), water (2 X 5 mL), and brine (1 X 5 mL). The organic layer was dried over Na₂SO₄ and concentrated to afford a yellow oil, which on distillation afforded 0.23 g (33%) of **AZ9** as a colorless liquid. ¹H NMR (CDCl₃) 7.66-7.61 (2 H, m), 7.46-7.23 (3 H, m), 6.34 (1 H, s), 4.22 (1 H, dd, *J* = 8.0 and 6.4 Hz), 4.2-4.12 (1 H, m), 3.48 (1 H, t, *J* = 8.0 Hz), 2.85-2.76 (1 H, m), 2.58-

2.50 (1 H, m), 2.41-2.32 (1 H, m) and 1.98-1.88 (1 H, m); ^{13}C NMR (500 MHz, CDCl_3) δ 178.3, 139.1, 128.8, 126.3, 88.6, 71.8, 58.9, 33.7, 23.1; IR (neat) 1702 cm^{-1} . LRMS (ESI+): m/z calcd for $\text{C}_{12}\text{H}_{13}\text{NO}_2$ (M+Li), 210.1114 found, 210.1106. *Note: characterization matches the data reported by Thottahil et al. [187].*

(3R,4R)-1-(4-methoxybenzyl)-3,4-dihydroxypyrrolidine-2,5-dione, AZ20. A suspension of L-tartaric acid (2g, 13.4 mmol) and p-methoxybenzylamine (2.09g, 15.3 mmol) was taken in 50% MeOH(aq.)(10 mL) and warmed to $50\text{ }^\circ\text{C}$. The reaction was mildly exothermic. The solvent was removed *in vacuo* and replaced with xylene (50 mL) and the reaction mixture was heated to reflux for 14h. The reaction was cooled and solvent removed *in vacuo* to isolate the product as a white solid in 74%. ^1H NMR (300 MHz, DMSO-*d*6) δ 3.70(s, 3H), 4.33(s, 2H), 4.45(d, $J=3\text{ Hz}$, 2H), 6.24 (br, -OH) 6.86(d, $J=1.5\text{ Hz}$, 2H), 7.17(d, $J=1.5\text{ Hz}$, 2H); ^{13}C NMR (300 MHz, DMSO-*d*6) δ 40.7, 55.1, 74.6, 113.9, 128.0, 129.2, 158.7, 174.6; IR (NaCl, thin film) cm^{-1} : 3286.5, 2925.3, 1700.0, 1646.4; LRMS (ESI+): m/z calcd for $\text{C}_{12}\text{H}_{13}\text{NO}_5\text{Cl}$ (M+Li-H), 257.1, found, 257.1.

(3R,4R)-1-(4-methoxybenzyl)-3,4-diacetoxypyrrolidine-2,5-dione

A suspension of pyrrolidinone **AZ20** (0.8 g, 3.18 mmol) in pyridine (3 mL) was stirred with acetic anhydride (0.68 g, 6.69 mmol) for 10h. The solvent was removed *in vacuo*. The reaction mixture was taken up in dichloromethane and was successively washed with 1N HCl and saturated NaHCO_3 (aq.). The organic layer was collected, dried and solvent was evaporated to provide the product in 94% yield ^1H NMR (300 MHz, CDCl_3) δ 2.13(s, 6H), 4.61(dd, $J_1=6\text{ Hz}$, $J_2=19.6\text{ Hz}$, 2H), 5.48 (s, 2H), 6.86(d, $J=3\text{ Hz}$, 2H), 7.27(d, $J=3\text{ Hz}$, 2H); ^{13}C NMR (300 MHz, CDCl_3) δ 15.3, 20.4(20.0), 42.6(42.4), 55.3, 66.1(65.9), 72.7(72.4), 114.1(114.0), 126.8, 130.4(130.5), 159.5(159.1), 166.3(166.0), 169.0(169.2), 169.9(170.2); IR (NaCl, thin film) cm^{-1} : 2940.1, 2833.6, 1755.9, 1729.3, 1510.2, 1246.7; HRMS (ESI+): m/z calcd. for $\text{C}_{16}\text{H}_{17}\text{NO}_7$ (M+Li), 342.1165, found, 342.1163. *Note: values in parentheses belong to the rotamers.*

(3S,4S)-3, 4, 5-Triacetoxy-1-(4-methoxybenzyl)-2- pyrrolidinone, AZ21

A solution of (3S, 4S)-3, 4-diacetoxy- 1-(4-methoxybenzyl)-2,5-pyrrolidinedione (2.6 g, 7.76 mmol), in methanol (50 mL) was maintained at $0\text{ }^\circ\text{C}$. NaBH_4 (1.47 g, 38.8 mmol) was added and the reaction was stirred for 1 h. The reaction mixture was then quenched with saturated aqueous NaHCO_3 and extracted with dichloromethane (2X). The organic layer was dried over Na_2SO_4 and evaporated to dryness to give the hydroxylactam as a white solid. This solid was then taken in

pyridine (5 mL) and acetic anhydride (3.9g, 38.8 mmol) was added, and the reaction mixture was stirred at room temperature overnight. After evaporation of the solvent, the residue was extracted with chloroform (1X). The organic layer was washed successively with 1 M HCl and saturated aqueous NaHCO₃, dried over Na₂SO₄, filtered and evaporated. The crude product was purified by column chromatography on silica gel (hexane/EtOAc=1:1) to give the desired compound **21**(mixture of diastereomers) in 94% yield as a colorless oil. ¹H NMR (CDCl₃) δ 1.86 (s, 3H), 1.97 (s, 3H), 2.08 (s, 3H), 3.70 (s, 3H), 4.14 (d, *J*=15 Hz, 1H), 4.57 (d, *J*=15 Hz, 1H), 5.11 (dd, *J*=4, 2 Hz, 1H), 5.25 (d, *J*=4 Hz, 1H), 5.95 (d, *J*=2 Hz, 1H), 6.73 (m, 2H), 7.08 (m, 2H). ¹³C NMR (CDCl₃) δ 20.8 (2 C), 21.4, 44.5, 55.5, 73.5, 76.2, 83.5, 114.3, 127.4, 129.9, 159.5, 167.9, 169.8, 169.9, 170.0. LRMS (ESI⁺): *m/z* calcd. for C₁₈H₂₁NO₈(M+H), 380.1, found, 380.1.

(3S, 4S)-3, 4, -Diacetoxy-3-cyano-1-(4-methoxybenzyl)-2- pyrrolidinone, AZ22

A solution of acetoxylactam **AZ21** (0.6 g, 1.6 mmol) and trimethylsilyl cyanide (0.23 g, 2.38 mmol) in dichloromethane (3 mL) was maintained at 0 °C added a solution of boron trifluoride etherate (0.44 g, 3.1 mmol) in dichloromethane (5 mL) under an argon atmosphere, and stirred for 5 min. Allowed to temperature to rise upto room temperature and stirred for 1 h, after which the reaction mixture was quenched with saturated aqueous Na₂CO₃ and extracted with dichloromethane. The organic layer was dried over Na₂SO₄ and concentrated *in vacuo*. The crude product was purified by column chromatography on silica gel (hexane:EtOAc=1:1) to give the desired compound **AZ22** as a mixture of diastereomers in 92% yield. ¹H NMR (CDCl₃) δ 2.03 (s, 3H), 2.12 (s, 3H) (2.07 (s, 6H)), (3.68), 3.74 (s, 3H), 3.97(3.99) (d, *J*=15 Hz, 1H), 4.00 (4.60) (d, *J*=5 Hz, 1H), (4.84) 5.11 (d, *J*=15 Hz, 1H), (5.22) 5.28 (m, 1H), 5.42 (5.47) (m, 1H), 6.79-6.84 (m, 2H), 7.13- 7.17 (m, 2H). ¹³C NMR (CDCl₃) δ 20.1(20.3), 20.2(20.4), 42.9(43.8), 44.5(44.9), 55.5(55.6), 71.1(71.7), 72.4(73.2), 114.2(114.3), 114.6(114.7), 125.5 (125.8), 129.3(129.4), 159.4 (159.9), 166.8 (167.4), 169.8 (170.2), 170.6(170.8).

Note: ¹³C labeled TMSCN was generated by reacting ¹³C labeled KCN with TMSCl in catalytic amounts of KI at room temperature for 20 hours.

3, 4 dihydroxy glutamic acid, AZ15a/b

A suspension of cyanolactam **AZ22** (0.48 g, 1.1 mmol) and ceric ammonium nitrate (1.2 g, 2.2 mmol) in acetonitrile/ water mixture (3:1, 4.4 mL) at room temperature, and the resulting mixture was stirred for 4 h. The reaction mixture was then diluted with ethyl acetate, washed with water, and dried over Na₂SO₄. After removal of the solvent, the residue was hydrolyzed in refluxing 6

M HCl (30 mL) overnight. The cooled aqueous solution was washed with chloroform and concentrated to dryness. The residue was submitted to ion exchange column chromatography by stirring with Dowex 50W-X8 to furnish the mixture of diastereomers **AZ15b** (0.18 g, 71%) as off-white powder $^1\text{H NMR}$ (D_2O) δ 3.96(4.05) (m, 1H), 4.2 (4.24) (m, 1H), 4.51(4.60) (m, 1H). LRMS (ESI-): m/z calcd. for $\text{C}_5\text{H}_9\text{NO}_6$ (M- H_2O), 161.0, found, 161.0. *Note: According to the procedure for the preparation of compound AZ15b, deprotection and hydrolysis of cyanolactam gave the title compound AZ15a (~53%) as white powder. The spectral data of compound was identical to AZ15a and previously published [189, 190].*

(3R,4S)-3,4-dihydroxy-5-(hydroxymethyl)pyrrolidin-2-one, AZ16a/b.

A solution of the cyanolactam **AZ22** (0.4g, 1.1 mmol) in methanol and maintained at 0 °C. SOCl_2 (1.1 eq.) was added dropwise and the reaction was refluxed overnight. The solvent was evaporated and the solvent / SOCl_2 replenished. The reaction mixture was again refluxed for 10h. The solvent was evaporated and the residue was treated with ceric ammonium nitrate (2 eq.). The reaction was stirred for 4 h at room temperature after which the reaction was diluted with ethyl acetate and washed with water (3X, 20 mL). The organic solvent was evaporated and the residue was dissolved in THF. NaBH_4 was added and the reaction allowed to stir for 3 h at room temperature after which conc. HCl was added drop-wise such that the pH=4. The reaction was stirred for 1h at room temperature after which it was neutralized to pH=7 with solid NaHCO_3 . Filtered the slurry through celite and extracted the aqueous layer with EtOAc(2X). The organic layer was collected, dried over Na_2SO_4 , filtered and concentrated *in vacuo* to yield the product as buff colored solid in (0.11g) ~70% yield. $^1\text{H NMR}$ (CD_3COCD_3 , 500 Hz) δ 7.88(br, 1H), 5.90(br, 1H), 4.35(m, 2H), 3.25(d, $J=11.5$ Hz, 1H), 2.9(br, 1H) 2.60(br, 1H), 2.53(m, 1H), 1.52(m, 1H). *Note: According to the procedure for the preparation of compound AZ16a, methaolysis, deprotection and reduction of cyanolactam gave the title compound AZ16b (~43%) as buff-white powder. The spectral data of compound was identical to AZ16a.*

VITA

Name: Gilbert Thomson Kelly

Education: B.S. Chemistry, Biochemistry & Molecular Biology,
Centre College, 2002

Ph.D. Chemistry, Texas A&M University, 2009

Permanent Address: Department of Chemistry
M.S. 3255
Texas A&M University
College Station, TX 77843

Publications:

Liu, C.M., Kelly, G.T., and Watanabe, C.M.H. (2006). *In vitro* biosynthesis of the antitumor agent azinomycin B. *Org. Lett.* **8**, 1065-1068.

Kelly, G.T., Liu, C., Smith, R., 3rd, Coleman, R.S., and Watanabe, C.M.H. (2006). Cellular effects induced by the antitumor agent azinomycin B. *Chem. Biol.* **13**, 485-492.

Kelly, G.T., Sharma, V., and Watanabe, C.M.H. (2008). An improved method for culturing *Streptomyces sahachiroi*: Biosynthetic origin of the enol fragment of azinomycin B. *Bioorg. Chem.* **36**, 4-15.

Sharma, V., Kelly, G.T., and Watanabe, C.M.H. (2008). Exploration of the molecular origin of the azinomycin epoxide: Timing of the biosynthesis revealed. *Org. Lett.* **10**, 4815-4818.

Sharma, V., Kelly, G.T., Foulke-Abel, J., and Watanabe, C.M.H. (2009). Aminoacetone as the penultimate precursor to the DNA crosslinker azinomycin A. *J. Am. Chem. Soc.*, Manuscript submitted.

Kelly, G.T., Sharma, V., and Watanabe, C.M.H. (2009). Exploration of the biosynthetic construction of the aziridinopyrrolidine moiety of the azinomycins: Incorporation of molecular oxygen and glutamic acid. Manuscript in preparation.